R D SANDERSON
E IMMELMAN

RESEACH ON THE INHIBITION OF BACTERIAL OXIDATION OF PYRITE AND THE CONCOMITANT ACID MINE DRAINAGE: PART 3. DEVELOPMENT AND TESTING OF SLOW RELEASE SYSTEMS

Report to the
WATER RESEARCH COMMISSION
by the Institute for Polymer Science
UNIVERSITY OF STELLENBOSCH

WRC Report No 132/3/90
ISBN 1 874858 03 9
ISBN SET 1 874858 04 7

RESEARCH ON THE INHIBITION OF BACTERIAL OXIDATION OF PYRITE AND THE CONCOMITANT ACID MINE DRAINAGE

This project was funded by the Water Research Commission and carried out in terms of a tripartite agreement between the Water Research Commission, the Chamber of Mines and the University of Stellenbosch.

The report is presented in three parts:

Part 1. Investigations on gold mine sand dumps by MA Loos, JM Conradie, PA Whillier, J Maré and C Bosch (Department of Microbiology)

Part 2. Investigations on coal waste dumps by MA Loos, C Bosch and J Maré (Department of Microbiology)

Part 3. Development and testing of slow release systems by RD Sanderson and E Immelman (Institute of Polymer Science)

ACKNOWLEDGEMENT

The Steering Comittee and referees for this project consisted of the following persons:

Dr MJ Pieterse	Water Research Commission	(Chairman)
Dr TC Erasmus	Water Research Commission	
Mr PW Weideman	Water Research Commission	(Secretary)
Mr DJ Bosman	Anglo American Corporation	
Mr J Easton	Chamber of Mines	
Dr HNS Wiechers	Chamber of Mines	
Prof FDI Hodgson	University of the Orange Free State	
Prof MA Loos	University of Stellenbosch	
Prof RD Sanderson	University of Stellenbosch	

The following persons also served for certain periods on the Steering Committee or the Technical Subcommittee:

Mr PE Odendaal	Water Research Commission
Mr JW Funke	Water Research Commission
Mr DD Marsden	Chamber of Mines
Mr DB Gaynor	Chamber of Mines
Dr JD Greig	Chamber of Mines
Mr JD Wells	Rand Mines
Mr MH Pitcher	BTR Sarmcol
Mr TI Cannon	BTR Sarmcol
Dr L Bednarik	Cape Technikon

The financing of the project by the Water Research Commission, the contributions and collaboration of the Chamber of Mines and the contributions by the members of the Steering Committee are acknowledged gratefully.

EXECUTIVE SUMMARY

The goal of the investigation was to be able to establish a delivery system for Thiobacillus ferrooxidans inhibitors that would be active for three to five years on coal mine dumps.

Initial work was centered around the use of rubber pellets. These pellets were the newest delivery system available in the USA. They were extruded by B.F.Goodridge and superceded the rubber sheet technique. These sheets were buried under the ground at various intervals in the mine dumps surfaces and in the state of Pennsylvania gave very favourable inhibition results.

The work centered around two facets. One to improve the pellet release device and secondly to minimize the amount of rubber matrix used by forming sachet devices. (Concentrated solution of inhibitor held in a sachet where the walls are slow release membranes.)

The work proved the following:

1. Monolithic elastomeric pellets containing various loadings of dissolved/dispersed SLS can be prepared satisfactorily.

2. Novel membrane devices, which release SLS at constant rates, can be prepared and the use of such devices for the long-term inhibition of the bacterial oxidation of pyrite in mine dumps give such promising laboratory results as to warrant protection being sought.

3. It is possible to determine the solubility limits of SLS in the various elastomers by means of differential scanning calorimetry (DSC), which show that phase separation occurs when the solubility limit of SLS in a particular rubber is exceeded. The onset of phase separation is characterized by an endotherm that appeared at 115°C. The solubility limits of SLS in the different elastomers vary. The solubility limits of SLS in natural rubber and in synthetic polyisoprene are 4% and 3%, respectively, when formulations are stored at °C before analysis. Storage of the natural-rubber formulations at room temperature for six months causes the solubility limit of SLS to increase to 9%.

4. High loadings of SLS in the various elastomers interfere seriously with the vulcanization process. The Borchardt & Daniels DSC Kinetics Data Analysis software, used to study the effects of the SLS loadings on the vulcanization of elastomers, can be used to analyze curing exotherms.

5. Mathematical models, given in the literature, give poor correlation between experimental data and theoretically-predicted values, which indicates that the release of SLS does not follow $t^{1/2}$ order kinetics.

6. Investigation of the effects of various factors on the rate of release of SLS from monolithic elastomeric pellets shows the following:

   6.1 The initial SLS loading in elastomeric pellets affects the release rate dramatically, but the relationship between the release rate and the SLS loading is non-linear. Loadings of up to 25% SLS have very little effect on the release rate, whereas loadings of 35% and more cause a dramatic increase in the release rate. This indicates that a second mechanism of release operates at SLS loadings of 35%

and more. This mechanism is postulated and to be the result of the creation of pores in the elastomeric matrices.

6.2 The addition of release promotors ($CaCO_3$ and $(NH_4)_2SO_4$) has virtually no effect on the rate of release of SLS from the particular formulations.

6.3 The pH of the eluent affects the release rate, especially when the matrices contain $CaCO_3$, but the effect is not significant enough to outweigh the effects of the other variables.

6.4 The base elastomer (NR, SBR, NR/SBR blend or IR) influences the release rate of SLS, with the release rates being the highest from the elastomer which displays the greatest solvation power for SLS.

6.5 **The most effective method for attaining a desirable rate of release of SLS is by varying the surface area to volume ratios of elastomeric pellets.**

7. An existing mathematical model to determine the effective diffusion coefficients of SLS in natural and synthetic rubbers gives a poor fit to the experimental data, probably due to the invalidity of the assumption that diffusion coefficients are independent of SLS concentration.

8. The values of the diffusion coefficients depend on the SLS loadings in the elastomeric pellets. It is suggested that the amount of porosity created in elastomeric pellets is a function of the SLS loading, and the concept of a concentration-dependent diffusion coefficient supports the argument for the dependence of the release rate on porosity.

9. A new model has been developed, based on a numerical method commonly used for predicting processes such as heat transfer and fluid flow. This model, which incorporates the effect of porosity development on the rate of release of SLS by employing a concentration-dependent diffusion coefficient, can be used as the basis of further investigation of the relationship between the diffusion coefficient and the concentration of SLS in rubber pellets.

10. An iterative procedure, which involves the use of the tri-diagonal matrix algorithm (Thomas algorithm), can be used to predict numerically the rate of release of SLS from cylindrical pellets. This procedure can be implemented by a FORTRAN program written for the purpose.

11. When it was assumed that the relationship between the diffusion coefficient and the concentration of SLS in the pellet is as follows:

$$\text{For } C > C_\alpha \qquad D = D_0$$

$$\text{For } C \leq C_\alpha \qquad D = (D_t - D_0)\left[\frac{C_\alpha - C}{C_\alpha - 0}\right]^1 + D_0$$

$$= (C_k * D_0 - D_0)\left[\frac{C_\alpha - C}{C_\alpha}\right] + D_0$$

where $D_t = C_k.D_o$, a much-improved correlation between experimentally-determined and theoretically-predicted data could be obtained for elastomeric pellets containing 35% to 55% SLS.

12. The research findings on monolithic elastomeric pellets have been used by the Chamber of Mines in investigations on simulated coal dumps at the Wolwekrans mine near Witbank, Transvaal.

13. The release of SLS, from a saturated reservoir, through membranes containing no SLS, as well as through those containing 10% SLS, follows zero-order kinetics. It is apparent that when the membranes contain 35% SLS, two release mechanisms are involved. Membranes containing 35% SLS initially appear to function as monolithic devices, but during the last half of the test period the release rate is constant.

14. The high steady-state release rates obtained with elastomeric membranes containing 35% SLS strongly support the theory of a leakage flow, such as would be caused by porosity. Scanning electron microscopy studies on cross-section of leached NR/35% SLS membranes indicate that the membranes were porous. The studies on elastomeric membranes confirm the dependence of the release rate of SLS on the type of rubber used.

15. Contrary to generalized findings in the literature, the flux of SLS does not vary significantly with membrane thickness. The presence of a surface phenomenon (boundary-layer effect), occuring as the result of the micellar structure of SLS molecules, is proposed to explain these findings.

16. **The elastomeric membrane sachet reservoir is the most economic use of carrier (rubber) the time scale of release is predictable and can be extended to a number of years.**

17. **The reservoir release devices can also be used in inhibiting corrosion in mine cooling water where there is a need to inhibit Thiobacillus ferrooxidans.**

18. **The program has been fully successful in the creation of a useable dosing system for inhibitor, namely the sachet.**

CONTENTS

CHAPTER 3: MATERIALS AND METHODS

CHAPTER 5: CONCLUSIONS AND SUGGESTIONS FOR FUTURE WORK

LIST OF TABLES

CHAPTER 2: HISTORICAL BACKGROUND

TABLES

CHAPTER 3: MATERIALS AND METHODS

CHAPTER 4 : RESULTS AND DISCUSSION

APPENDIX 1A: COMPOSITIONS OF RUBBER-SLS FORMULATIONS: SERIES B TO G

APPENDIX 1B :COMPOSITIONS AND DIMENSIONS OF RUBBER-SLS PELLETS USED IN EXPERIMENTS 2 TO 17

APPENDIX 3C : LINEAR EXPANSION COEFFICIENTS OF RUBBER-SLS FORMULATIONS

APPENDIX 3D : DSC ANALYSIS OF RUBBER-SLS FORMULATIONS

APPENDIX 4A : DATA OBTAINED FROM ELUTION EXPERIMENTS

APPENDIX 4C : STANDARD DEVIATIONS AND CORRELATION COEFFICIENTS

LIST OF FIGURES

CHAPTER 2: HISTORICAL BACKGROUND

CHAPTER 3: MATERIALS AND METHODS

CHAPTER 4: RESULTS AND DISCUSSION

APPENDIX 2A: ^{13}C NMR SPECTRA

APPENDIX 3A: THE CHEMISTRY OF ACCELERATED SULPHUR VULCANIZATION OF RUBBERS

APPENDIX 3B: MONSANTO RHEOGRAPHS

APPENDIX 5A: PLOTS OF THE FRACTION OF SLS RELEASED AS A FUNCTION OF TIME

APPENDIX 7D: CONCENTRATION DISTRIBUTION OF SLS IN A STYRENE- BUTADIENE-RUBBER PELLET

APPENDIX 8A: THE BEHAVIOUR OF SURFACTANTS IN SOLUTION

CHAPTER 1

INTRODUCTION

1.1 AN OVERVIEW OF THE PROBLEM

Acid mine drainage causes a pollution problem which is associated with the mining of coal and sulphide-containing minerals. The oxidation of fine-grained, reactive pyrite exposed during the mining process results in the production of acid and the solubilization of heavy metals. Acid-contaminated waters are found wherever pyritic materials come into contact with air and water.

A bacterium, **Thiobacillus ferrooxidans**, accelerates the acidification of pyritic materials and increases the eventual level of acid production by catalyzing the oxidation of pyrite (FeS_2) to ferric sulphate [$Fe_2(SO_4)_3$] and sulphuric acid (H_2SO_4).

The release of acid mine drainage from working and abandoned mines into associated water systems affects the water quality adversely by increasing acidity, hardness, metal ion concentrations and levels of suspended solids. These changes in the physical and chemical characteristics of the water often necessitate additional water treatment and water quality monitoring. In addition, pollution by acid mine drainage has serious detrimental effects on the ecology of streams and rivers.

1.2 CONVENTIONAL CONTROL MEASURES

Acid mine drainage is controlled either by treating the water as it leaves the mines or by taking steps to reduce the oxidation of pyrite at the site of acid production. Control measures include neutralizing the acid water by treatment with lime before it is discharged into rivers, preventing the seepage of water into mine workings, hydraulic sealing of abandoned mines by flooding them to reduce the amount of oxygen available for the oxidation of pyrite, and the regrading and revegetation of mine dumps. Such control measures are effective but expensive.

1.3 THE USE OF CONTROLLED-RELEASE TECHNOLOGY

A more recent approach to dealing with the problem of acid mine drainage is to reduce pyrite oxidation by the inhibition of **Thiobacillus ferrooxidans**. Anionic surfactants, and in particular sodium lauryl sulphate at low concentrations, are capable of inhibiting the activity of **Thiobacillus ferrooxidans**. However, the biodegradability and solubility of most anionic surfactants preclude the long-term control of bacterial activity by a single application as, for example, spraying of a surfactant solution onto mine dumps. Inhibitory concentrations of the surfactant will be sustained only until the next major rainfall when most of the surfactant will be flushed away by infiltrating rainwater. Therefore, the application of surfactant solutions, although effective in reducing acid formation, cannot be regarded as a long-term control measure.

In order to prevent repopulation by **Thiobacillus ferrooxidans**, the bactericidal treatment must be repeated frequently or, alternatively, a continuous supply of the inhibitor must be available. The latter can be accomplished by using controlled-release technology. The inhibitor is incorporated into a polymeric matrix from which it is released slowly into the aqueous environment by diffusion through the polymer matrix and dissolution from the surface of the controlled-release device. The continuous release of an inhibitor from a controlled-release matrix makes possible the effective treatment of **Thiobacillus ferrooxidans** for extended periods of time.

In studies conducted at the United States Bureau of Mines, sodium lauryl sulphate (SLS) and other anionic surfactants were incorporated into various natural and synthetic rubber formulations, as well as into a high-melting-point wax. Laboratory tests were conducted to determine the release rates of the surfactants from the various controlled-release formulations. Those formulations which showed the optimum combination of a desirable release rate and inhibitory effect on **Thiobacillus ferrooxidans** were selected for use in field tests. Considerable success was achieved with the inhibition of **Thiobacillus ferrooxidans** under field conditions by the application of controlled-release rubber-SLS formulations to fresh coal refuse and abandoned, unreclaimed surface mines. These field tests demonstrated that the inhibition of **Thiobacillus ferrooxidans** by controlled release of anionic surfactants from rubbers can reduce pyrite oxidation and acid formation inexpensively.

1.4 SCOPE OF THE PRESENT STUDY

Various methods for attaining the controlled-release of active agents from polymeric materials have been developed over the years. The different controlled-release technologies and their numerous applications, in particular in the administration of pharmacologically active agents and

in the application of pest-control chemicals, have been well documented in the literature. The mechanisms and the kinetics of the release of active agents from controlled-release polymeric devices have been studied and theoretical models which describe the kinetics of release of agents from the more commonly known controlled-release systems have been developed. Although a vast amount of work has been done on the controlled release of relatively simple organic molecules from polymers, the release of surfactants from rubbers has received virtually no attention.

In work done in the United States on the development of monolithic rubber-SLS formulations for the long-term control of the bacterial oxidation of pyrite, the emphasis has been on the field testing of such formulations. In spite of this, some laboratory tests have also been conducted and the effects of variables, such as the SLS loading, the type of rubber matrix used and the surface area of the controlled-release device, on the release rate of SLS have been investigated qualitatively. However, insufficient data have been made available to illustrate the importance of these variables in altering the rate of release of SLS from matrix-controlled devices. It is well known that the solubility limit and the diffusion coefficient of an agent in a polymer are the major factors in determining the rate of transport of the agent through the polymeric matrix. So far neither the solubility limits nor the effective diffusion coefficients of SLS in natural and synthetic rubbers have been determined.

The kinetics of release of SLS from monolithic matrix devices has not been studied in any detail. It has generally been assumed that the release of SLS from these devices will follow square-root-of-time-order kinetics, as suggested in the literature, but no attempt has been made to fit theoretical models to experimental data in order to confirm that this assumption is valid for rubber-SLS systems.

For monolithic devices in which an active agent is physically dispersed in a polymeric matrix, it has been suggested in the literature that the mechanism of release of the agent is by a combination of diffusion through the matrix phase and dissolution from the surface of the controlled-release device. It has been assumed that, regardless of the SLS loading, such a diffusion-dissolution mechanism applies to the release of SLS from rubber matrices. The development of porosity in rubber matrices which contain high loadings of SLS and the possibility that transport of the SLS molecules occurs by diffusion through pores within the matrix structure, rather than diffusion through the matrix phase itself, has not been considered.

It is therefore obvious that, although previous studies have provided useful basic information regarding some of the factors which will influence the rate of release of SLS from monolithic elastomeric devices, many questions remain unanswered and there is still much to be learned about

the mechanism of release of SLS and the kinetics involved, as well as about the various factors which will influence the rate of release of SLS from such devices.

Finally, only monolithic matrix devices have thus far been considered for attaining controlled release of SLS. The release of SLS from membrane-controlled devices, that is, devices which consist of a reservoir of SLS surrounded by a rate-controlling elastomeric membrane, has not been investigated.

The studies reported here form part of an investigation, sponsored by the Water Research Commission, of possible ways to inhibit the bacterial oxidation of pyrite and the concomitant production of acid mine drainage in South African gold and coal mine dumps. The objective of the research was to gain a better understanding of the mechanisms and kinetics involved in the release of SLS from both matrix-controlled and membrane-controlled elastomeric devices, since it is believed that a thorough knowledge of these aspects will assist in the design and development of controlled-release rubber-SLS devices.

The research approach was to prepare such controlled-release devices, using natural and synthetic rubbers as binding matrices and as rate-controlling membranes, and to determine, under laboratory conditions, the rate of release of SLS from these devices. At the same time, the influence of various factors on the rate of release of SLS from elastomeric matrices and through elastomeric membranes was investigated. Theoretical equations were fitted to experimental data, using computer programs, in order to determine whether the release of SLS followed square-root-of-time-order kinetics for monolithic matrix devices and zero-order kinetics for membrane-controlled devices, as suggested in the literature on controlled-release technologies, not involving SLS. Finally, the solubility limits and effective diffusion coefficients of SLS in natural and synthetic rubbers were determined and the use of a numerical method for predicting the rate of release of SLS from cylindrical rubber-SLS composite pellets was investigated.

In Chapter 2, the various controlled-release systems, as well as their release characteristics and applications, are discussed. The theoretical principles of controlled release are reviewed with emphasis on monolithic devices and membrane-controlled devices. A description of the materials and methods used in the preparation and testing of controlled-release devices is presented in Chapter 3. The results of experimental investigations are discussed in Chapter 4. Additional information, computer programs and much of the raw and processed data are given in appendices at the end of this document. The conclusions reached from this study and suggestions for future work are discussed in Chapter 5.

CHAPTER 2

HISTORICAL BACKGROUND

2.1 INTRODUCTION

Controlled release may be defined as the permeation-moderated transfer of an active agent from a reservoir to a target surface to maintain a predetermined concentration or emission level for a specified period of time.

During the last few decades, controlled-release technology has received increasing attention because of a growing awareness that substances such as drugs and agricultural chemicals are frequently excessively toxic and sometimes ineffective when administered or applied by conventional means.

Drugs which are administered by conventional means, i.e., in the form of pills, capsules, injections and ointments, are introduced into the body as pulses which usually produce large fluctuations of drug concentrations in the bloodstream and tissues and, consequently, unfavourable patterns of efficiency and toxicity. Conventional application of agricultural chemicals, i.e., by spraying and broadcasting, similarly provides an initial concentration far in excess of that required for immediate results in order to ensure the presence of sufficient chemical for a practical period of time. Such overdosing wastes much of the potential of the chemical and often causes toxicity problems for non-target organisms.

The advantages of controlled release, when compared with those of conventional delivery of active agents, have been discussed for both drug-delivery and pesticide-delivery systems[1].

The process of molecular diffusion through polymer matrices and membranes has been used as an effective and reliable means for attaining the controlled release of not only drugs and pharmacologically active agents, but also of pesticides.

The various controlled-release technologies which have been developed over the years are reviewed briefly in Section 2.2, with emphasis on the more commonly known physical and chemical methods of controlling the release of active agents from polymeric systems.

The release characteristics of the most common controlled-release systems are reviewed briefly in Section 2.3.

Monolithic devices provide the simplest means for delivering substances at controlled rates of release. The solute is incorporated into a polymeric matrix and then migrates to the surface of the polymer either by diffusion through pores within the matrix or by diffusion through the polymeric phase itself. Monolithic plastic and elastomeric devices are discussed in detail in Section 2.4. The methods which are used for the preparation of monolithic devices and the various mechanisms by which agents can be released from these devices are reviewed. The theoretical principles of controlled release from monolithic devices are discussed with special emphasis on the use of the physical-model approach to describe the kinetics of solute transport. Tractable mathematical expressions are presented by which monolithic systems can be designed and evaluated.

The factors which influence the kinetics of release of solutes from monolithic devices are discussed with reference to both solute-dependent and solute-independent variables. The release lifetime of monolithic devices depends on several factors. These are discussed with emphasis on monolithic elastomeric devices which rely upon a diffusion-dissolution mechanism for agent release.

Membrane-controlled systems are discussed in Section 2.5. These systems function by the movement of active molecules from a reservoir to a sink through a polymeric film membrane which offers a predetermined resistance to this movement. The driving force for such systems is the concentration gradient of active molecules between reservoir and sink. The mechanism of movement is diffusion, and the medium may be either the polymer itself or a fluid entrapped in a polymer network.

In Section 2.5, the principles of membrane permeation are reviewed and special consideration is given to aspects such as the application of Fick's law to membranes, factors which influence diffusivity and partition, and the kinetics of solute release from membrane-controlled devices. Important design considerations for membrane-controlled devices are also pointed out in Section 2.5. Only dense polymer membranes are considered and the discussions do not include hydrophilic (hydrogel) membranes and hydrophobic microporous membranes.

A brief overview of the major applications of monolithic devices and membrane-controlled devices is presented in Section 2.6. The discussions focus on the administration of pharmaceutical agents and the application of pest-control chemicals, such as insecticides, molluscicides and herbicides. A discussion of acid mine drainage problems, and the use of controlled-release technology as a means of controlling or preventing these problems is included in Section 2.6.

2.2 POLYMER SYSTEMS FOR CONTROLLED RELEASE

Once an application has been thoroughly investigated and found suitable, it is important to select that controlled-release technology which best fits the application, as well as the basic physical form of the device, the rate-controlling polymer matrix, and the active agent to be used.

2.2.1 Brief Descriptions of Controlled-Release Technologies

Table 2.1[1] categorizes the various controlled-release systems broadly as either physical or chemical. Brief descriptions of the technologies by category are given in Sections 2.2.1.1 to 2.2.1.6.

2.2.1.1 Reservoir systems with a rate-controlling membrane

2.2.1.1.1 Micro- and macrocapsules

Microencapsulation (for forming microcapsules) is a procedure that reproducibly applies a uniformly thin polymeric coating (the rate-controlling membrane) around small solid particles, droplets of liquid, or dispersions of solids in liquids, with the size of the resulting capsules ranging from a few tenths of a micrometre to several thousand micrometres. Capsules of diameter greater than 2 000 to 3 000 μm are called macrocapsules.

There are no real differences between micro- and macrocapsules with respect to the release characteristics or type of active agent that can be encapsulated. Many methods for microencapsulation of active agents have been developed and these have been discussed by several authors[2-8].

Although many of the microencapsulated products are released by permeation through the walls, other mechanisms are also important, such as breakdown or dissolution of the walls and osmotic bursting[1].

TABLE 2.1. Categorization of polymeric systems for controlled release[1]

I. PHYSICAL SYSTEMS

A. Reservoir systems with rate-controlling membrane

1. Microencapsulation
2. Macroencapsulation
3. Membrane systems

B. Reservoir systems without rate-controlling membrane

1. Hollow fibres
2. Poroplastic® and Sustrelle® Ultramicroporous Cellulose Triacetate
3. Porous polymeric substrates and foams

C. Monolithic systems

1. Physically dissolved in non-porous, plastic or elastomeric matrix

    1. Non-erodible
    2. Erodible
    3. Environmental agent ingression
    4. Degradable

2. Physically dispersed in non-porous, plastic or elastomeric matrix

    1. Non-erodible
    2. Erodible
    3. Environmental agent ingression
    4. Degradable

D. Laminated Structures

1. Reservoir layer chemically similar to outer control layers
2. Reservoir layer chemically dissimilar to outer control layers

E. Other physical methods

1. Osmotic pumps
2. Adsorption onto ion-exchange resins

II. CHEMICAL SYSTEMS

A. Chemical erosion of polymer matrix

1. Heterogeneous
2. Homogeneous

B. Biological erosion of polymer matrix

1. Heterogeneous
2. Homogeneous

2.2.1.1.2 Membrane systems

A controlled-release device in this category is the polymeric film membrane. These devices function by the diffusion of active agent from a reservoir to the environment. The membrane provides a predetermined resistance to the outflow of chemicals; this resistance is a function of film thickness, film composition, the migrating species, and the given environment. A thorough discussion of membrane systems for controlled release of active agents has been presented by O'Neill[9]. Membrane-controlled devices are discussed in more detail in Section 2.5.

2.2.1.2 Reservoir systems without a rate-controlling membrane

These systems include filled hollow fibres[10-12], impregnated porous plastics such as porous polyvinyl chloride sheet, Millipore[R] filters, Celgard[R] porous polypropylene[9,11,13], foams, and possibly hydrogels[8,9,11,14] and ultramicroporous cellulose triacetate[11,15-17].

The simplest example is perhaps the hollow fibres, which hold the active agent in tiny open tubes, from which it escapes to the outside by diffusion through the air layer above the agent. Systems in which impregnated porous plastics[9,11] are used are more complex, but in all of them the active agent is retained by capillary action or it is physically embedded in the pores. It is also released by diffusion through the air layer above the liquid that fills the pores. Strictly speaking, most of these systems may be regarded as monolithic matrix systems, except that interaction of the active agent and the polymer is minimal.

2.2.1.3 Monolithic systems

The simplest and least expensive means of controlling the release of an active agent is to disperse it in an inert thermoplastic matrix. Generally, the active agent is physically blended with the thermoplastic powder and the mixture is then fused by compression moulding, injection moulding, screw extrusion, calendering, or casting[18], all operations which are common processes in the plastics industry. This system of controlled release has been discussed by Zeoli et al.[11], R. seman[19], and Cardarelli[20].

Alternatively, the active agent is blended with elastomeric materials in the compounding step, as is done with the other additives, such as accelerators, reinforcing pigments, stabilizers, and processing aids[21]. Controlled-release elastomeric systems have been discussed by Cardarelli[22].

In both of the abovementioned cases, the active agent dissolves in the plastic or elastomeric matrix until saturation is reached. Any additional active agent remains dispersed within the polymer matrix and the system is physically dispersed. As the agent is removed from the surface of the monolithic device, more of the agent diffuses from the interior to the surface in response to the decrease in the concentration gradient between the interior and the interface[1,11].

If the polymer used is soluble or if it is degraded during use, the monolithic device is erodible. In this case, the active agent is released by a combination of diffusion and liberation due to matrix erosion. A distinction should be made between pure degradable and erodible systems. Degradable systems can be defined as systems that release their contents by diffusion, osmotic bursting, leaching, and any other controlled-release mechanism, but in addition have the very desirable property of becoming chemically or biologically degraded after the useful life of the device has expired[1]. Contamination of the environment into which a degradable device is placed is thus minimal. Degradable systems have been discussed by Allan et al.[23] and Zweig[24].

Erodible systems can be regarded as a subdivision of degradable systems. They release their contents only by the liberation of the active agent due to the chemical or biological erosion of the matrix[1,11,25].

If the polymer is plasticizable or swellable by an environmental agent such as water, the system involves ingress of an environmental agent into the device. This causes plasticization of the polymeric matrix, thereby allowing physically-bound active ingredient to diffuse out. This system, which differs from the erodible one in that the matrix remains physically intact, includes the starch xanthate systems[26], hydrogels[8,9,11], and some of the lignin-modified controlled-release systems[27].

2.2.1.4 Laminated structures

This type of controlled-release system involves the lamination of at least two, and usually three, polymeric films. The centre layer of a three-layer laminate is the reservoir layer. It contains a large amount of active agent and may be made of porous or non-porous polymeric material. The outer layers control the rate of release of the agent and are usually fabricated from a polymer more rigid than that from which the reservoir is made. Should both the reservoir layer and the outer films be made of the same polymer, it is apparent that the system will in time revert to a monolithic matrix system[1,11]. Discussion of its ramifications, as they relate to pharmaceutical and pesticidal systems, has been presented by O'Neill[9] and Kydonieus et al[28-30].

2.2.1.5 Other physical methods

Osmotic pumps comprise another system that is both novel and useful. In its simplest and most elegant design, the pump consists of a tablet containing the active agent and an osmotic "attractant", such as NaCl, surrounded by a semipermeable membrane in which is a small orifice. When the pump is placed in an aqueous environment, the osmotic pressure of the NaCl solution draws water to the device through the semipermeable membrane. Because the membrane coating is non-extensible, the NaCl-saturated solution and active agent inside the device are pumped out through the orifice as water is osmotically imbibed[11,31,32].

Attempts have also been made to produce controlled-release devices consisting of ion-exchange resins onto which active agents have been adsorbed[1,11].

2.2.1.6 Retrograde chemical reaction systems

Controlled release of active agents may be achieved by a variety of chemical methods. The active agent may be bound by means of covalent or ionic bonds to a preformed polymer, in accordance with the equation:

$$\text{Preformed polymer} + \text{pesticide} \underset{\text{Environment}}{\overset{\text{Synthesis}}{\rightleftharpoons}} \text{Polymeric pesticide}$$

This approach requires the use of macromolecules with pendent functional groups capable of reacting with the active ingredients or their derivatives.

Another approach involves the polymerization of difunctional monomeric pesticides. In these materials, the pesticide is incorporated directly into the polymer backbone. The pesticide is released by the chemical or biological depolymerization of the system in accordance with the equation:

$$\text{Monomer} + \text{pesticide} \underset{\text{Environment}}{\overset{\text{Synthesis}}{\rightleftharpoons}} \text{Polymeric pesticide}$$

The depolymerization reaction can be purely homogeneous, purely heterogeneous (i.e., surface reactions), or some combination of the two. Chemical methods for controlled release of active agents have been discussed by several authors[23,33-36].

2.2.2 Basic Components of Controlled-Release Devices

A controlled-release product consists of the active agent and the polymer matrix or matrices that regulate its release.

Advances in controlled-release technology have been rapid because polymer science has become sophisticated enough to enable tailor-made properties for each controlled-release application to be incorporated in polymers. The selection of the type of polymer to be used in a specific application is very important and different design criteria must be satisfied[1,11].

The large number of polymers which have been used in controlled-release formulations has been listed by Kydonieus[1]. Controlled-release technologies have been considered for a wide variety of applications, but the major effort in applying these technologies has been in the administration of pharmaceutical agents and the application of pest-control chemicals. Broad product-areas in which controlled-release technology has been applied to pharmaceutical, agricultural, and veterinary active agents have been summarized by Kydonieus[1], Zeoli et al.[11], and Paul[37].

2.3 RELEASE CHARACTERISTICS OF CONTROLLED-RELEASE SYSTEMS

Considering the different technologies listed in Table 2.1 (Section 2.2.1), all the physical processes are in some way controlled by diffusion. Possibly the only systems that are not controlled by diffusion are the "pure" erodible devices and some heterogeneous retrograde chemical reaction devices, but even in these systems release is generally achieved by a combination of diffusion and erosion.

In the absence of pores or holes the active agent passes through the polymeric barrier by a process of absorption, solution, and diffusion down a gradient of thermodynamic activity until it is desorbed or removed. The transport of the active agent is governed by Fick's first law:

$$J = \frac{dM_t}{Adt} = -D\frac{dC_m}{dx} \qquad (2.1)$$

where J is the flux in $g.cm^{-2}\,sec^{-1}$, A is the surface area through which diffusion takes place in cm^2, M_t is the mass of agent released in g, dM_t/dt is the steady-state release rate at time t, C_m is the concentration of the active agent in the polymeric membrane in $g.cm^{-3}$, dC_m/d_x is the concentration gradient, and D is the diffusion coefficient of the active agent in the polymeric membrane in $cm^2.sec^{-1}$.

Equation (2.1) can be integrated under the proper boundary conditions for most of the systems listed in Table 2.1 to obtain an equation to give the amount of agent released as a function of time. In many situations the mathematics become rather complicated, and no explicit equations can be derived. The mathematics of diffusion have been discussed by several authors[38-42]. However, release characteristics of the most common controlled-release systems are described in Sections 2.3.1 to 2.3.6.

2.3.1 Reservoir Systems with a Rate-Controlling Membrane

When applied to these systems, Fick's law predicts that a steady state will be established, with the release rate being constant and independent of time, if an active agent is enclosed within an inert polymer membrane and if the concentration of the agent is maintained constant within the enclosure[1,11,41,42].

The amount of agent released per day, M_t, is therefore constant for the life of the device:

$$M_t = kt \qquad (2.2)$$

where k is a constant.

The above equation applies to all geometries of the device, e.g., spheres. slabs, etc[42]. This type of release is referred to as "zero-order", and is shown as Curve I in Figure 2.1.

Micro- and macrocapsules are the major controlled-release reservoir systems with rate-controlling membranes (Section 2.2.1.1.1). Microcapsules are made with very thin polymer walls[2,3], and where the polymer phase is not homogeneous, these devices follow a " $t^{1/2}$-order" release[1], as described in Section 2.3.2.

2.3.2 Reservoir Systems without a Rate-Controlling Membrane

With these systems, a large amount of the agent is released initially, and substantially smaller and decreasing amounts are released during the last half of the life of the device[1,10,11]. It can be shown that, for these devices, the amount of agent released is proportional to $t^{1/2}$ ($t^{1/2}$-order), as given by the equation:

$$M_t = kt^{1/2} \qquad (2.3)$$

This equation gives a parabolic curve, as shown by Curve II in Figure 2.1.

The rate of release is then proportional to the inverse square root of time, $t^{-1/2}$, and is given by the equation:

$$\frac{dM_t}{dt} = \tfrac{1}{2}kt^{1/2} \qquad (2.4)$$

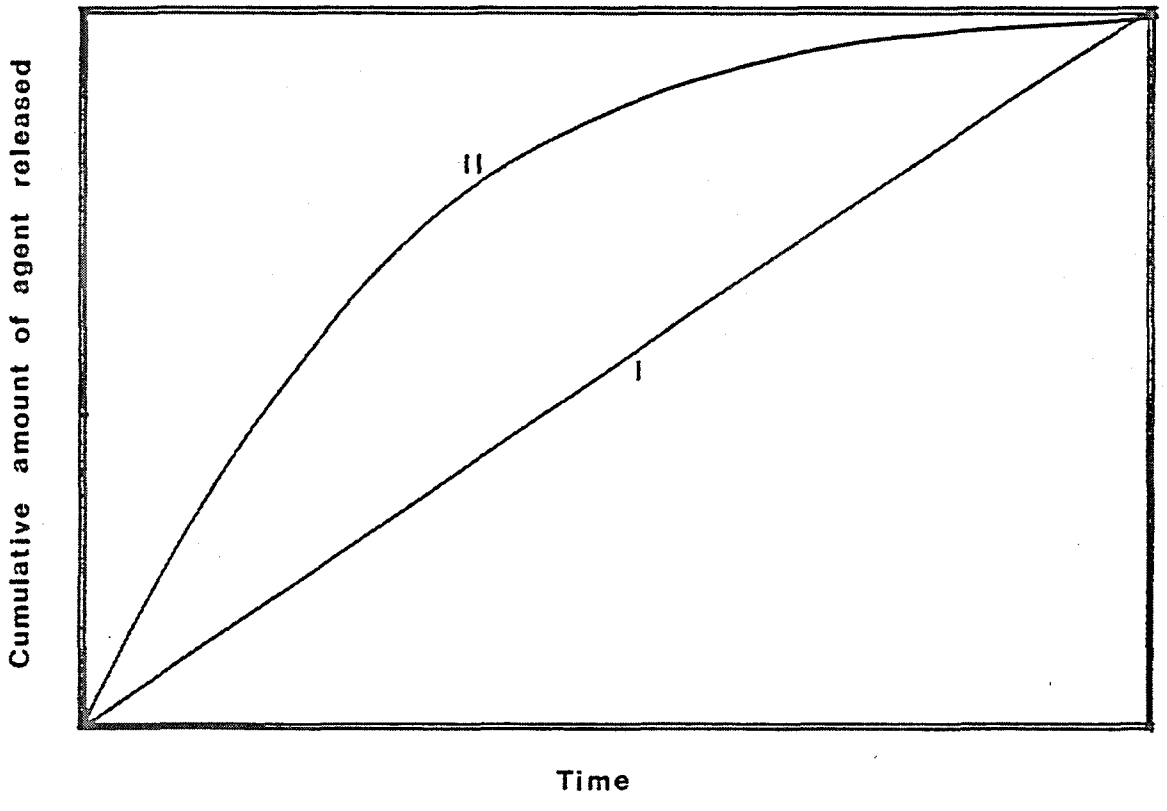

FIGURE 2.1 Representation of "zero-order" and " $t^{1/2}$-order" release

2.3.3 Monolithic Systems

2.3.3.1 Physically dissolved, non-erodible plastic or elastomeric matrix

The release rate in this system is proportional to $t^{1/2}$ (same as Equation 2.4), until about 60% of the active agent is released. The release rate thereafter is related exponentially to time[11,19,41,42]:

$$\frac{dM_t}{dt} = k_1 e^{-k_2 t} \qquad (2.5)$$

where k_1 and k_2 are constants.

This type of release, which is called "first-order", is also observed in reservoir systems in which the solution of active agent within the enclosure is less than saturated[41].

2.3.3.2 Physically dispersed, non-erodible plastic or elastomeric matrix

For these systems, the amount of agent released is proportional to $t^{1/2}$ (Equation 2.3), as long as the concentration of the active agent present (dissolved and dispersed) is higher than the solubility of the agent in the matrix[11,19,41,42]. The dispersed systems are, therefore, similar to the dissolved systems (discussed in the previous section), except that instead of a decreased release rate after 60% of the chemical has been emitted, the relationship holds almost over the complete release curve[41].

2.3.3.3 Monolithic erodible systems

If it is assumed that release of the active agent by diffusion is negligible in this system, the speed of erosion will control the release rate[1,11]. Release by erosion is a surface-area-dependent phenomenon, and the release will be constant (zero-order) as long as the surface area does not change during the erosion process. This is true for slab-shaped devices[43]. Erodible cylinders and spheres give delivery rates that decrease with time (owing to decreasing surface area), even though the kinetic process providing the rate-determining step is, in fact, zero-order[43].

2.3.4 Laminated Structures

If the distribution coefficient of the active agent between the reservoir layer and the barrier membrane is much smaller than unity, the system approximates zero-order release (reservoir system with rate-controlling membrane, Section 2.3.1), and the amount released per day is independent of time[28].

If the distribution coefficient is close to unity, the system approximates the $t^{1/2}$-order release (monolithic, physically dispersed system, Section 2.3.3.2).

2.3.5 Other Physical Methods - Osmotic Pumps

The mechanism of release is based on the osmotic pressure generated by the diffusion of water through the semipermeable membrane to form a saturated aqueous solution of the agent inside the device. The delivery rate of the solute by the pump is constant (zero-order release) as long as excess solid is present inside the pump to form a saturated solution. The rate declines exponentially (first-order release) as soon as the concentration of the solution inside the device drops below saturation[31,32,42,44].

2.3.6 Retrograde Chemical Reaction Systems

The kinetic expressions that describe the rate of release of an active agent from these systems vary depending on whether the hydrolysis reaction is purely homogeneous, purely heterogeneous (surface reactions), or some combination of the two[33,34,42,45]. The observed release rate is determined by the reaction kinetics and by the diffusion rate of liberated agent through the polymer[42].

The purely heterogeneous systems are similar to the erodible matrix systems (Section 2.3.3.3), and zero-order release is obtained for slabs. Because of geometry, i.e., change in surface area as the reaction proceeds, spherical and cylindrical systems show non-linear release characteristics with time[33,34,42].

For a water-soluble polymer undergoing homogeneous hydrolysis in the absence of boundary-layer effects, the rate of release follows conventional first-order kinetics if the liberated agent diffuses rapidly through the polymer. In this case, the release rate is limited by the reaction rate, because the diffusion time is very short compared with the reaction time[33,34]. For homogeneous systems

where diffusion and reaction times are comparable ("limited diffusion" case), the situation becomes much more complicated[42].

2.4 MONOLITHIC PLASTIC AND ELASTOMERIC DEVICES

2.4.1 The Preparation of Monolithic Devices

2.4.1.1 Monolithic plastic devices

Monolithic plastic devices are usually prepared by incorporating the solute within the monomeric material before polymerization and subsequent compression moulding, extrusion, injection moulding or film casting[46-54]. Granular or porous matrices are manufactured utilizing tableting technology, and have been prepared by direct compression of the mixture of the solute in a plastic matrix or by adding the solute to melted wax, followed by granulation and then compression[55-58]. The geometry of the device is controlled by the dimensions of the mould, die, or film.

2.4.1.2 Compounding of monolithic elastomeric materials

Elastomers in their raw state generally lack useful properties. In order to use them in practical applications, it is necessary to crosslink the molecules into networks and, usually, to develop environmental resistance, etc., by the addition of various agents. This process is termed "compounding"[22].

The initial step in processing the raw elastomer, often referred to as "gum stock", consists of softening the elastomer by mechanical working on a two-roll rubber mill[59]. Once in the softened state, additives can be homogeneously blended into the elastomer. The materials added serve distinct purposes and create desirable properties in the elastomer[60,61]. The active agent to be released from the elastomeric matrix is also blended into the elastomer during this initial processing step.

Typical compounding ingredients, with examples of each[22], are listed in Table 2.2.

TABLE 2.2. Typical compounding ingredients

Category	Examples
Vulcanization agents	Sulphur, zinc oxide, various peroxides
Accelerators (increase cure rate)	Mercaptobenzothiazole, tetramethylthiuram disulphide
Activators (enhance acceleration)	Stearic acid, zinc oxide
Antioxidants	Various secondary amines, substituted phenols
Non-reinforcing fillers	Kaolinite, chalk
Reinforcing fillers	Carbon black, precipitated silica
Softening agents	Paraffin oils and waxes, fatty acids

Carbon black or finely-powdered silicas are used to impart strength; clays may be added to extend volume; antioxidants offer protection against oxidation; various oils or fatty acids assist in the dispersion of other additives or increase processibility through what is essentially a lubrication process; vulcanization agents perform crosslinking during later processing[22].

After the compounding process, the material, now designated as "batch stock", is heated at elevated temperatures for a determined period of time in order to effect crosslinking and the creation of a network. This so-called "curing" step can be performed through compression moulding or extrusion at elevated temperatures[59].

2.4.2 Release Mechanisms

2.4.2.1 General considerations

The solubility of a material in a polymer is determined by intermolecular forces. Where such forces are weak, as with the elastomers, a wide variety of substances will dissolve in the polymer[20]. The degree of solubility will depend upon the respective solubility parameters (discussed in Section 2.4.4.4). On the other hand, the stronger interchain forces characteristic of many plastics generally reduce the possibility of a desired agent being dissolved in a particular type of matrix. Consequently, a diffusion-dissolution mode of agent release, as discussed in Section 2.4.2.3, probably cannot be developed in the case of plastics[20].

In order to establish a uniform and continuous release of agent molecules from the surface of a given plastic dispenser, the agent must be capable of being incorporated into the plastic and the agent molecules must in some manner migrate through the matrix towards a depleting surface[20]. Migration of a solid through a solid or of a liquid through a solid can occur by an interstitial or vacancy mechanism[62,63].

Polymeric materials contain unoccupied space, a free volume, within the matrix. The amount and the nature of this free volume have been used extensively in the interpretation of polymer properties, including small-molecule diffusion[64,65]. An increase in free volume in a given material increases the mobility of polymer chain-segments, which gives rise to an increase in the diffusion coefficient, at least for relatively small molecules.

Processed plastics contain voids of various magnitudes, which are dependent upon processing conditions and additives[20]. These voids are dimensionally larger than, and not to be confused with, free volume. The larger voids and their interconnecting channels are commonly termed "pores", while the network is termed "porosity"[20]. Free volume is basically a thermodynamic or kinetic quantity, whereas porosity is not. The effects of free volume and micropore structure on transport dynamics have been elucidated by Rogers[66], Kumins et al.[67], and Barrer[68].

2.4.2.2 Release from plastic matrices

Agent release from a plastic material can be effected by several processes[20]. One such process is leaching, whereby the ingress of a liquid element, such as water, partitions the agent which then migrates outward following the pore structure. Another process is volatilization, whereby the agent molecule in the gaseous state moves in a random motion, making interstitial jumps, or follows a free-volume network until it reaches the surface of the device, from where it passes into the external medium. A third process is matrix degradation caused by chemical, biological or physical stresses.

Leaching as a mechanism of agent release is tenable only in an aqueous situation, i.e., water and moist soil, but even so, special methods may be required to provide effective, continuous, long-term release of agent. Both the degree of porosity and the associated tortuosity of the pore structure are controlling factors[20].

In general, plastics are not particularly permeable to water, the thermoplastic elastomers[69] being slightly more permeable, and even where transmission does occur, the agent molecule, which will

be considerably larger than the water molecule, may not be accommodated by pores of the size developed. If agent loading is adequately high, pore growth can be realized by gradual partition and by loss of the agent. This method is used with the major class of antifouling paints, where cuprous oxide is mechanically bound by an elastomeric or plastic film-forming polymer[70].

In those plastic matrices where no degree of agent solubility is present, the use of a coleachant or "porosigen"[71] to enhance porosity generation and growth is essential.

Release by means of a volatility mechanism can take one of several forms[20]. If the incorporated agent is volatile and the plastic is permeable to the vapour phase, then diffusion to the plastic surface will occur with concomitant loss into the surrounding medium. This mode of release does not lend itself readily to practical use, since very volatile agents are not capable of being incorporated into plastics because of the necessary high processing temperatures. Conversely, agents stable under processing conditions are almost always insufficiently volatile to be released effectively[20].

The solution to the problems associated with a volatility mechanism lies in the utilization of an additive which serves as a transmission path for the agent molecule[20]. In such systems, the additive is dispersed at a relatively high concentration throughout the matrix. The agent, which usually displays some degree of solubility within the additive, moves through it via solution forces and reaches the surface of the device where vaporization occurs.

2.4.2.3 Release from elastomeric matrices

A material that is soluble in an elastomeric matrix will disperse evenly through the batch stock during processing, so that a uniform condition of solution equilibrium exists. Upon immersion of the device in water, agent molecules on or very near the elastomer surface will pass slowly into the interface through dissolution processes. As the surface layer of the device depletes, a localized solution disequilibrium results and internal solute molecules, driven by the concentration gradient of the solution, diffuse outward towards the depleting zone. A continuous process is thus activated and the mechanism is appropriately termed "diffusion-dissolution"[22].

The kinetics of solute release will depend upon whether diffusion or dissolution is the rate-controlling process. Release-rate expressions have been presented by Cardarelli[22], and Ayres et al.[72,73] for both these situations.

When solubility of the agent in the elastomeric matrix is lacking, reliance must be placed upon other processes for release of the agent. In antifouling paints[70,74], matrix-insoluble inorganic or organic chemicals are usually compounded with a polymeric material. Release is achieved by either a leaching process or exfoliation[22]. In the former case, the rate of development of porosity and its tortuosity are rate-controlling together with water solubility. To achieve the required porosity, relatively high agent loadings are necessary[22]. In an exfoliating-type surface, the polymeric matrix either undergoes slow solvation or degrades through chemical processes, thereby releasing the mechanically-held active agent into the interfacial zone.

2.4.3 Theoretical Principles of Controlled Release from Monolithic Devices

The derivation of mathematical expressions which describe the release of solutes from matrix systems is based upon Fick's laws of diffusion[38-40]. Fick's first law states that the flux (J) or rate of solute transfer across a plane of unit area is

$$J\ (\text{Rate}) = -D\frac{dC}{dx} \qquad (2.6)$$

where dC/dx is the concentration gradient or the change in concentration (C) with respect to distance (x), and D is the diffusion coefficient. Fick's second law is given by

$$\frac{\partial C}{\partial t} = D\frac{\partial^2 C}{\partial x^2} \qquad (2.7)$$

where the rate of change of concentration (C) with time (t) at a particular level is proportional to the rate of change of the concentration gradient at that level[39a].

Two different variations of the diffusional process in which an active agent migrates through and from an enveloping, homogeneous polymer matrix will be considered. In the first system (discussed in Section 2.4.3.1), the active agent is completely dissolved in the surrounding polymer. In the second system (discussed in Section 2.4.3.3), the active agent is dispersed in the matrix at a concentration which greatly exceeds its equilibrium solubility in the matrix. The kinetics associated with the two systems are quite different.

2.4.3.1 Homogeneous monolithic devices containing only dissolved solute

Two valid expressions for the fraction of dissolved active agent released as a function of time from slab geometries have been obtained using error functions and separation of variables[75,76]. These series are:

$$\frac{M_t}{M_\infty} = 4\left[\frac{Dt}{h^2}\right]^{1/2}\left[\pi^{-1/2} + 2\sum_{n=1}^{\infty}(-1)^n \text{ ierfc } \frac{nh}{2(Dt)^{1/2}}\right] \qquad (2.8)$$

and

$$\frac{M_t}{M_\infty} = 1 - \sum_{n=0}^{\infty}\frac{8\exp\left[-D(2n+1)^2\pi^2 t/h^2\right]}{(2n+1)^2\pi^2} \qquad (2.9)$$

where D is the diffusion coefficient, h is the thickness of the device, M_t is the amount of agent released at time t, and M_∞ is the amount desorbed at infinite time.

A form of Equation (2.9) has been deduced by Higuchi[77] to be applicable to the release of drugs from ointment vehicles[78].

Equations (2.8) and (2.9) are not easily handled, but fortunately they reduce to two approximations which are valid for different portions of the desorption curve. The early-time approximation, which holds over the initial portion of the curve, is derived from Equation (2.8). The late-time approximation, which holds over the final portion of the desorption curve, is derived from Equation (2.9). Early- and late-time approximations are summarized in Table 2.3 (from Baker and Lonsdale[41]) for both the fraction of solute released and the release rate as a function of time. Consideration is given to three geometries of general interest, namely, the slab, cylinder and sphere of radius r.

Mathematical solutions for desorption of solutes from cylindrical and spherical devices can be found in standard sources[79,80].

For the slab, the release pattern is characterized by a square-root-of-time dependence at early times, and an exponential dependence on time during the terminal phase of solute release. The initial release period for the slab is analogous to the desorption kinetics from a semi-infinite medium where[81]

$$\text{(Amount Released)} \quad M_t = 2C_o\left[\frac{Dt}{\pi}\right]^{1/2} \qquad (2.10)$$

and

$$\text{(Rate)} \quad \frac{dM_t}{dt} = C_o\left[\frac{D}{\pi t}\right]^{1/2} \qquad (2.11)$$

TABLE 2.3 Equations describing the release kinetics of a solute dissolved in a monolithic device.

Device	Early-time approximation		Late time approximation	
	Fraction released[a]	Release rate[b]	Fraction released[a]	Release rate[b]
Slab[c]	$\left\{4\left(\frac{Dt}{\pi h^2}\right)^{1/2}\right\}$	$\left\{2\left(\frac{D}{\pi h^2 t}\right)^{1/2}\right\}$	$\left\{1-\frac{8}{\pi^2}\exp\left(\frac{-\pi^2 Dt}{h^2}\right)\right\}$	$\left\{\frac{8D}{h^2}\exp\left(\frac{-\pi^2 Dt}{h^2}\right)\right\}$
Cylinder[d,e]	$\left\{4\left(\frac{Dt}{r^2\pi}\right)^{1/2}-\frac{Dt}{r^2}\right\}$	$\left\{2\left(\frac{D}{r^2\pi t}\right)^{1/2}-\frac{D}{r^2}\right\}$	$\left\{1-\frac{4}{(2.405)^2}\exp\left(\frac{-(2.405)^2 Dt}{r^2}\right)\right\}$	$\left\{\frac{4D}{r^2}\exp\left(\frac{-(2.405)^2 Dt}{r^2}\right)\right\}$
Sphere[d,e]	$\left\{6\left(\frac{Dt}{r^2\pi}\right)^{1/2}-\frac{3Dt}{r^2}\right\}$	$\left\{3\left(\frac{D}{r^2\pi t}\right)^{1/2}-\frac{3D}{r^2}\right\}$	$\left\{1-\frac{6}{\pi^2}\exp\left(\frac{-\pi^2 Dt}{r^2}\right)\right\}$	$\left\{\frac{6Dt}{r^2}\exp\left(\frac{-\pi^2 Dt}{r^2}\right)\right\}$

a. Fraction released equals M_t/M_∞
b. Release rate equasls $d(M_t/M_\infty)/dt$
c. Short-time approximation is valid for $0 < M_t/M_\infty < 0.6$, while long-time approximation is valid for $0.4 < M_t/M_\infty < 1.0$.
d. Short-time approximation is valid for $0 < M_t/M_\infty < 0.4$, while long-time approximation is valid for $0.6 < M_t/M_\infty < 1.0$.
e. In the case of the cylinder and sphere, surface area changes with time. To obtain the cumulative amount released (M_t) or the release rate (dM_t/dt), allow M_∞ to be the total amount released at infinite time.

where C_o is the initial concentration. Figures 2.2 and 2.3 illustrate the early- and late-time approximations, as given by Equations (2.10) and (2.11), for the slab.

In the analysis by Baker and Lonsdale[41], it has been assumed that the height of the cylinder is large compared with its radius, i.e., negligible longitudinal diffusion, and that for the slab, edge effects are negligible. When this is not the situation, more complex mathematical expressions are required[46,82,83].

Many attempts have been made to develop mathematical models which could be used to estimate the rates of release of active agents from controlled-release capsules, tablets, or pellets which comprise agents distributed homogeneously in polymer matrices. Apart from the equations presented by Baker and Lonsdale[41] (as summarized in Table 2.3), some of the more frequently cited theoretical calculations are given in papers by Higuchi[84,85], Roseman and Higuchi[47], Garrett and Chemburkar[86], and Flynn[87].

Most of these models are based on a simplified version of the diffusion equation involving one space variable, for example, the spherical shape and the slab. Fu et al.[46] have presented a more sophisticated mathematical model for the release of an active agent from a finite cylinder for which the diffusion from both the end and lateral surfaces are not negligible. This model is described in some detail below, but for a comprehensive discussion of the mathematics involved, the reader is referred to Fu et al.[46] and to the references therein.

2.4.3.2 Mathematical model for diffusion from cylindrical monolithic devices

This model represents a solid tablet or pellet with the active agent distributed homogeneously throughout the polymer matrix. The dimensions of the pellet are represented in cylindrical coordinates with radius a and length 2ℓ. The model applies to pellets that range in shape from that of a flat disk (radius > thickness) to that of a cylindrical rod (radius small compared with length). This model also takes into consideration the diffusion from all surfaces, in contrast to previously proposed models for a cylinder[41], in which diffusion from the top and bottom surfaces of the cylinder has been neglected.

In the diffusion of active agent from a pellet to its surrounding medium, the change in the concentration of the agent within the agent-polymer matrix is related to several factors. Among these are the dimensions of the pellet, i.e., the radius a and the length 2ℓ, as well as the time t over

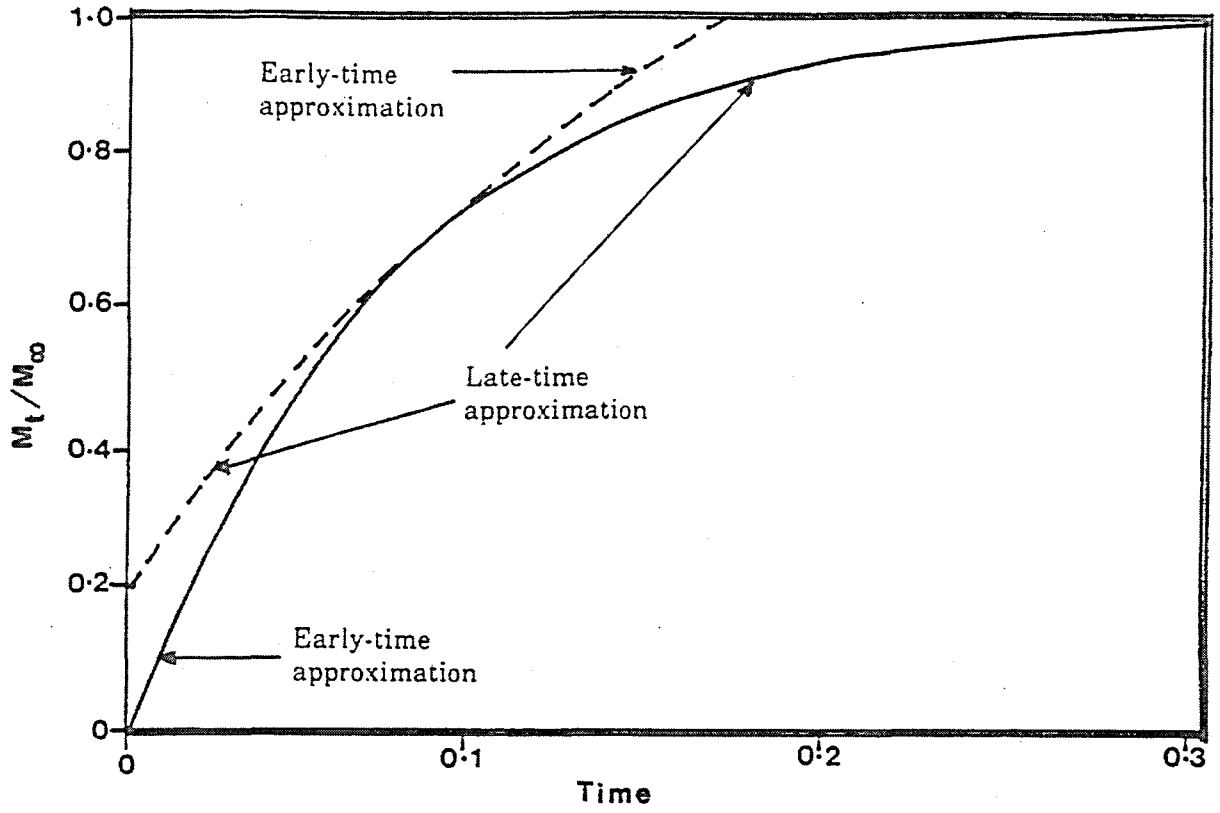

FIGURE 2.2 Plots of the fraction of drug desorbed from a slab as a function of time, using the early-time and late-time approximations. The full line shows the portion of the curve over which the approximations are valid.

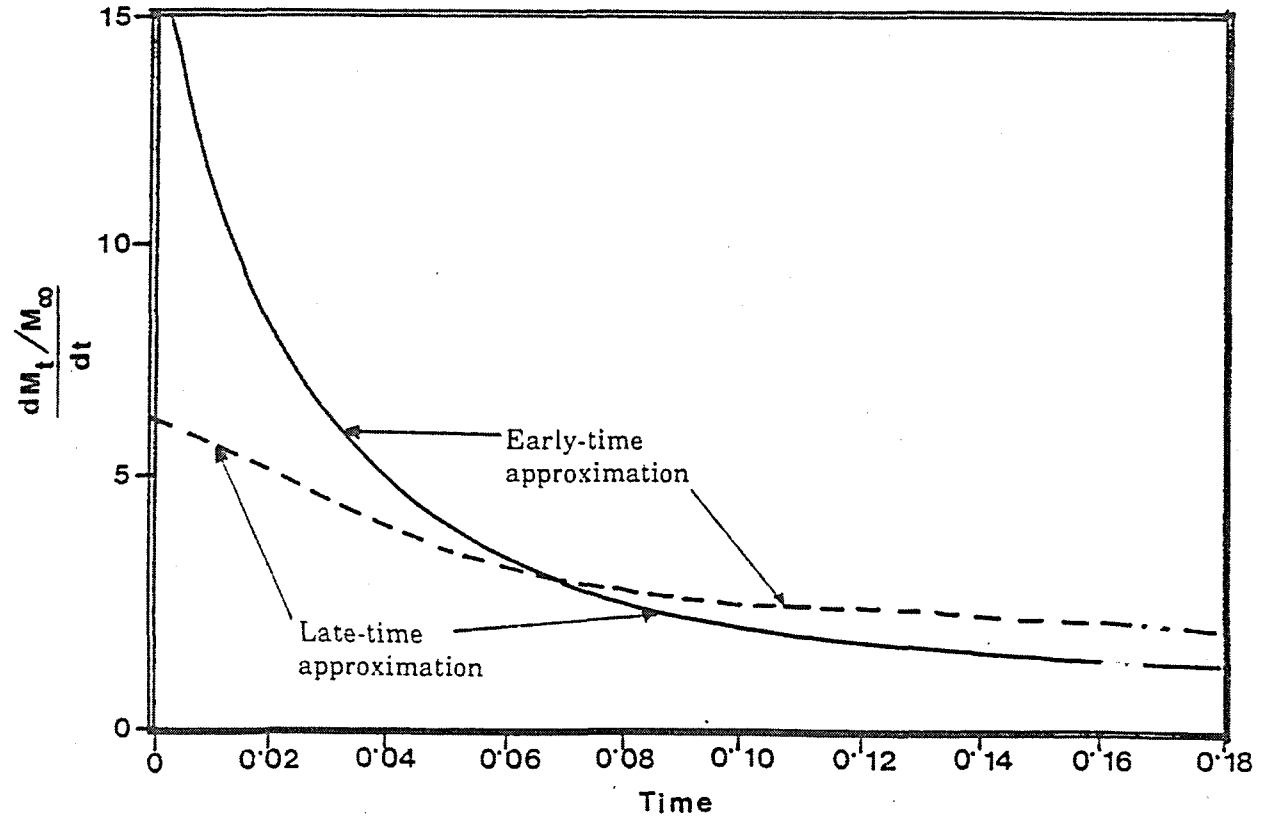

FIGURE 2.3 Plots of the release rate of drug initially dissolved in a slab as a function of time, using the early-time and late-time approximations. The full line shows the portion of the curve over which the approximations are valid.

which the agent has been diffusing into the eluent. The situation is best described by a time-dependent diffusion equation involving the two space variables r and z:

$$\frac{\partial C}{\partial t} = D\left[\frac{\partial^2 C}{\partial r^2} + \frac{1}{r}\frac{\partial C}{\partial r} + \frac{\partial^2 C}{\partial z^2}\right] \qquad 0 \le r \le a\ ;\ -l \le z \le l \qquad (2.12)$$

It is assumed that at time t=o the agent concentration inside the matrix is C_o, and that in the eluent the concentration of the agent is zero. At t>o, the concentrations of agent in the eluent and at the matrix-eluent interface are zero (i.e., continuous replacement of fresh eluent is implied). From the assumptions that the movement of the agent is governed by the concentration gradient and that the concentration at the pellet surface is zero, it follows that C tends to zero over the whole pellet as t tends to infinity. The rate of release of agent from the pellet at any point is clearly proportional to the concentration gradient perpendicular to the outer surface.

It can be shown that for the above boundary conditions, a solution for Equation (2.12) must be of the form[88]:

$$C = C_o \psi\,(z, l, t)\ X\ (r, a, t) \qquad (2.13)$$

The solution can be written as the product of a Fourier series in z, Ψ in Equation (2.13), and a Bessel series in r, X in Equation (2.13), such that

$$\psi\,(z,l,t) = \frac{4}{\pi}\sum_{n=0}^{\infty}\frac{(-1)^n}{(2n+1)}\exp\left[\frac{-D\,(2n+1)^2\pi^2 t}{4l^2}\right]\cos\left[\frac{(2n+1)\pi z}{2l}\right] \qquad (2.14)$$

and

$$X\,(r,a,t) = \frac{2}{a}\sum_{m=1}^{\infty}\exp\left[-D\alpha_m^2 t\right]\frac{J_o\,(r\alpha_m)}{\alpha_m J_1(a\alpha_m)} \qquad (2.15)$$

where J_o and J_1 are the zero-th and first Bessel functions and α_i is the i-th root of the zero-th Bessel function. The flux of agent out of the pellet is obtained by calculating the concentration gradients normal to the lateral and end surfaces of the pellet and integrating over the whole pellet.

Since the total amount of agent in the pellet at the beginning is known ($C_o . 2l . \pi a^2$), it is convenient to express the amount of agent released at time t, M(t), as a function of the total amount of agent released as time approaches infinity, $M(\infty)$. By integrating over time, it can be shown that the total amount of agent released at time t, M(t), is given by:

$$\frac{M(t)}{M(\infty)} = 1 - \frac{8}{l^2 a^2} \sum_{m=1}^{\infty} \frac{\exp(-D\alpha_m^2 t)}{\alpha_m^2} \sum_{n=0}^{\infty} \frac{\exp(-D\beta_n^2 t)}{\beta_n^2} \quad (2.16)$$

where $M(t)/M(\infty)$ is the fraction of agent released at time t

and

$$\beta_n = \frac{(2n+1).\pi}{2l} \quad (2.17)$$

It is obviously impractical to calculate each term in the infinite series in Equation (2.16). Usually ten terms in each series X (Equation 2.15) and Ψ (Equation 2.14) are sufficient for the purpose.

This model can be used to test against experimental data in several ways. First, for a pellet of a given size and specific polymer whose diffusion coefficient is known, the model can be applied to the prediction of agent release rate at any time. Second, it can be used to find the value of the diffusion coefficient for a particular formulation of pellet. Third, it can be applied to calculate the optimal combination of geometric (size) and material (diffusion coefficient) variables in order to design a device with a desired rate of agent release[46].

2.4.3.3 Homogeneous monolithic devices containing dispersed solute

Monolithic devices of this type contain finely divided solute particles which are uniformly dispersed or suspended within the matrix phase. The dispersed solute is in equilibrium with the dissolved solute, and the total concentration is designated as C_s.

As with monolithic devices containing only dissolved solute, diffusion occurs only through the matrix phase. The derivation of the release-rate expression, however, relies on Fick's first law (Equation 2.6), and therefore the kinetics of solute release is different. The analysis of this system was originally presented by Higuchi for the release of drugs dispersed in a stationary matrix, e.g., semi-solid ointment[84].

A schematic illustration of the physical model is shown in Figure 2.4, depicting the dependence of the concentration gradient on time.

In this model, it is assumed that solid active agent first dissolves from the surface layer of the device and when this layer becomes exhausted of agent the next layer begins to be depleted. The interface between the region containing only dissolved agent and the region containing dispersed

agent thus moves into the interior as a front. The movement of the dissolving agent front has been monitored under the microscope by Roseman and Higuchi[47].

Assuming that (1) a pseudo-steady state exists, (2) the agent particles are small compared with the average distance of diffusion, (3) the diffusion coefficient, D, is constant, and (4) that a perfect sink condition exists in the external medium (i.e., concentration of agent equals zero), the following equations have been derived for the slab[19,41,47]:

$$M_t = A\left[DC_s(2C_o - C_s)t\right]^{1/2} \qquad (2.18)$$

and

$$M_t \simeq A\left[2DC_sC_ot\right]^{1/2} \text{ for } C_o >> C_s \qquad (2.19)$$

where M_t is the amount of agent released at time t, A is the surface area, D is the diffusion coefficient, C_o is the total concentration of agent in the matrix, and C_s is the solubility of the agent in the matrix phase.

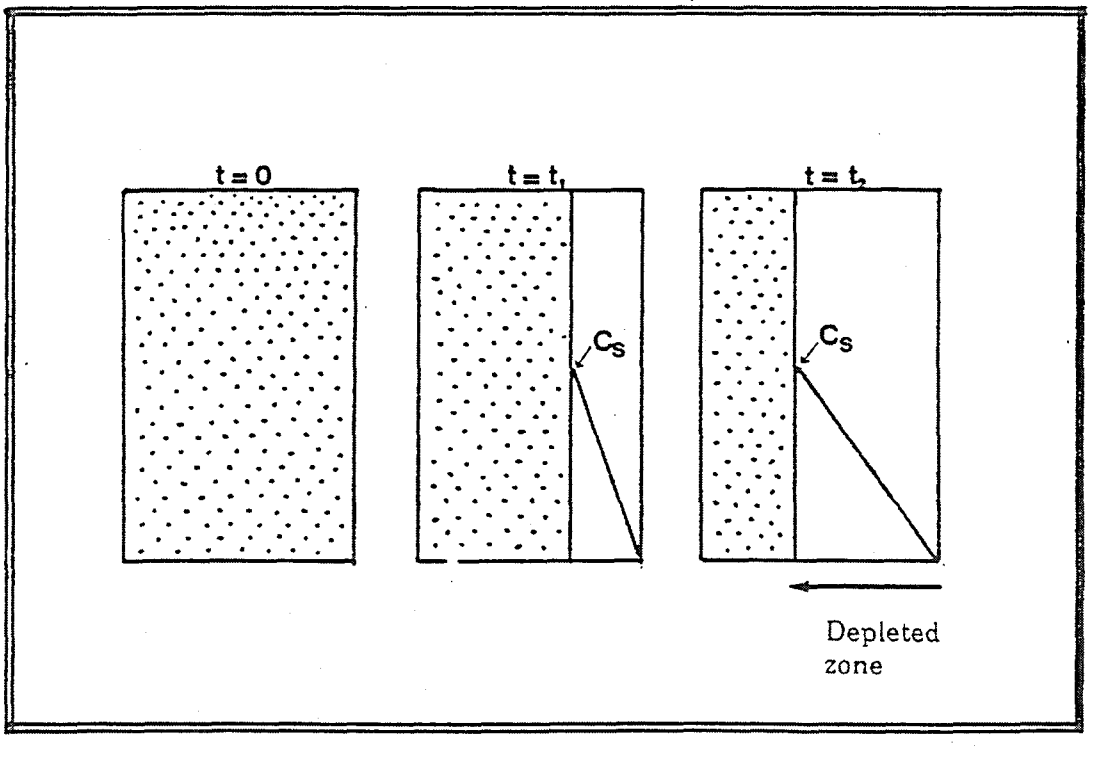

FIGURE 2.4 Schematic representation of the pseudo-steady state concentration profiles for the release of solute from a single face of a monolithic device containing dispersed drug. The lines are drawn for three times such that $t_2 > t_1$.

The release rate at any time, dM_t/dt, is then given by:

$$\frac{dM_t}{dt} = \frac{A}{2}\left[\frac{DC_s(2C_o - C_s)}{t}\right]^{1/2} \qquad (2.20)$$

and

$$\frac{dM_t}{dt} \simeq \frac{A}{2}\left[\frac{2DC_sC_o}{t}\right]^{1/2} \quad \text{for } C_o >> C_s \qquad (2.21)$$

The form of these equations is almost the same as that of the equations for the initial release of agent from monolithic devices containing only dissolved active agent (Equations (1) and (2), Table 2.3). However, instead of tailing off at late times, the $t^{-1/2}$ relationship holds over almost the complete release curve, i.e., until the agent concentration in the centre of the matrix falls below the saturation level[41].

From Equation (2.21) it follows that the release rate is proportional to the square root of the agent loading and, therefore, the release rate can be varied by incorporating different amounts of agent.

The solution for the release kinetics for cylindrical geometries when $C_o >> C_s$ has been given by Roseman and Higuchi[47], and Roseman[48]. An example of the release of a dispersed drug from a cylindrical Silastic^R device has been given in the work of Cornette and Duncan[89]. The solution for a spherical geometry is similar to that for the slab and the cylinder, and has been discussed by Baker and Lonsdale[41] and Higuchi[85].

Equations describing the fraction of agent released and the release rate as a function of time for monolithic slabs, cylinders and spheres containing dispersed solute are summarized in Table 2.4 (from Baker and Lonsdale[41]).

The pseudo-steady-state approximation in the development of Equation (2.18) requires that C_o must be greater than C_s. Paul and McSpadden[90] have provided a rigorous derivation which relies on Fick's second law. Starting with Equation (2.7), they derived the following expression:

$$M_t \simeq [2DC_s(C_o - C_s)t]^{1/2} \qquad (2.22)$$

which was the limiting form of an error function series expansion for $C_o >> C_s$. Equations (2.18) and (2.22) differ only in that the coefficient of C_s in Equation (2.22) is unity instead of one half. However, when $C_o >> C_s$, Equations (2.18) and (2.22) both reduce to the same result, which supports the validity of the pseudo-steady-state assumption.

TABLE 2.4 Equations describing the release kinetics of a solute dispersed in a monolithic device

Device	Fraction released[a]	Release rate[b]
Slab	$\left\{\left(\frac{M_t}{M_\infty}\right)^{1/2} = \frac{8C_s Dt}{C_0 l^2}\right\}$	$\left\{\frac{dM_t/M_\infty}{dt} = \frac{4C_s D}{l^2 C_0} \cdot \frac{1}{M_t/M_\infty}\right\}$
Cylinder	$\left\{\left(1 - \frac{M_t}{M_\infty}\right)\left(\ln\left[1 - \frac{M_t}{M_\infty}\right]\right) + \frac{M_t}{M_\infty} = \frac{4C_s Dt}{C_0 r_0^2}\right\}$	$\left\{\frac{dM_t/M_\infty}{dt} = \frac{-4C_s D}{r_0^2 C_0 \ln(1 - M_t/M_\infty)}\right\}$
Sphere	$\left\{\frac{3}{2}\left(1 - \left[1 - \frac{M_t}{M_\infty}\right]^{2/3}\right) - \frac{M_t}{M_\infty} = \frac{3DC_s t}{r_0^2 C_0}\right\}$	$\left\{\frac{dM_t/M_\infty}{dt} = \frac{3C_s D}{r_0^2 C_0}\left(\frac{[1 - M_t/M_\infty]^{1/3}}{1 - [1 - M_t/M_\infty]^{1/3}}\right)\right\}$

a. Fraction released equals M_t/M_∞
b. Release rate equals $d(M_t/M_\infty)/dt$

Comparison of the expressions for the release during early times for dissolved solute (Equations 2.10 and 2.11) and dispersed solute (Equations 2.19 and 2.21) in a matrix shows certain similarities and differences. Identical dependences on time and diffusivity are predicted, but there is a different relationship of concentration. When only dissolved solute is present, release is proportional to the initial concentration, while release is dependent on the square root of the total concentration when dispersed solute is present.

2.4.3.4 Granular or porous monolithic devices

Release of a solute from a granular matrix occurs through connecting capillaries or pores. The steps in the derivation of the release-rate expression are identical to those presented in the preceding section[47] for the homogeneous monolithic device containing dispersed solute. The resulting terms in the equation, however, refer to values in the elution medium rather than to the matrix phase. From Equation (2.18):

$$M_t = \left[C_a D_a \frac{\epsilon}{\tau} (2C_o - \epsilon C_a) t \right]^{1/2} \qquad (2.23)$$

where C_a and D_a are the solubility and diffusion coefficient, respectively, in the leaching solvent ϵ is the porosity, and τ is the tortuosity of the matrix.

Specific cases have been considered and equations have been derived which account for equilibrium solute binding to the matrix phase[91], release of two non-interacting solutes[92], and release of mutually interacting solutes[93].

When the initial porosity of the matrix is small or when the fraction of the matrix volume occupied by the solute is relatively large, i.e., $\epsilon = C_o/\rho$ where ρ is the density of the solute, Equation (2.23) yields:

$$M_t = C_o \left\{ \frac{D_a C_a}{\tau \rho} \left[2 - \frac{C_a}{\rho} \right] t \right\}^{1/2} \qquad (2.24)$$

In contrast to the homogeneous monolithic device containing dispersed solute, the release from a porous monolithic device is expected to be linearly dependent upon C_o.

2.4.3.5 Monolithic devices and the effects of boundary layers

In Section 2.4.3.3 it has been assumed that the rate of agent release is determined solely by the rate of diffusion of the agent to the surface of the device. It has also been assumed that the concentration of the agent at the surface of the device is maintained at zero, i.e., a perfect sink exists in the external medium. This situation is sometimes not attained in practice because of the slow transport of agent away from the surface of the device.

It is argued that diffusion of an agent from the surface of a solid monolithic device into the surrounding medium involves transport across a region adjacent to the solid. The concentration of the agent at the surface is maintained at saturation level, and diffusion occurs across an unstirred region termed the boundary diffusion layer[47,94]. This diffusion layer offers an additional resistance to mass transfer and can influence the kinetics of solute release from monolithic devices. A schematic representation of a diffusion layer, h_a, in series with a monolithic device containing dispersed solute is depicted in Figure 2.5.

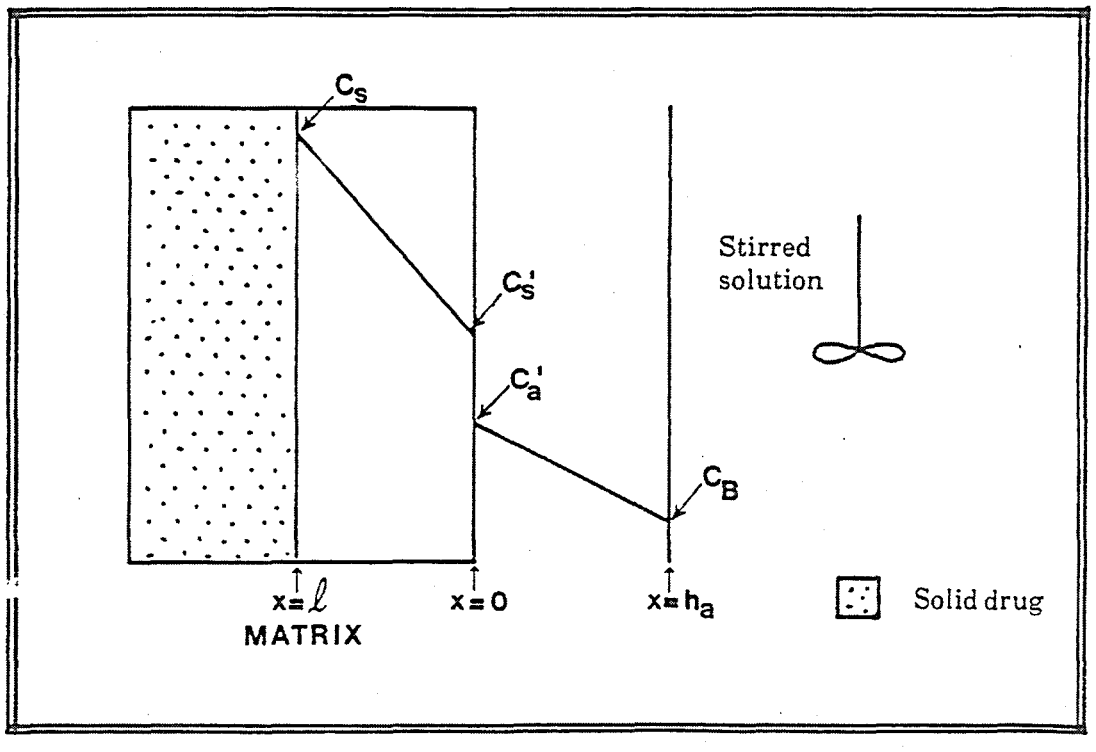

FIGURE 2.5 Hypothetical diagram for the matrix-diffusion layer model.

The rate of transport across a plane of unit area according to Equation (2.6) is:

$$\frac{dM_t}{dt} = \frac{D}{l}\left[C_s - C_s'\right] \qquad (2.25)$$

where C_s and D are the solubility and effective diffusion coefficient, respectively, in the matrix phase, C_s' is the concentration in the matrix at $x = 0$, and ℓ is the diffusional distance (zone of depletion). The rate of transport across the diffusion layer (h_a) is given by:

$$\frac{dM_t}{dt} = \frac{D_a}{h_a}\left[C_a' - C_B\right] \qquad (2.26)$$

where D_a is the diffusion coefficient in the aqueous phase, C_a' is the concentration in water at $x=0$, and C_B is the concentration at $x = h_a$. The solute must pass from the matrix phase to the eluting solvent, and the concentrations on either side of $x = 0$ are related by the partition coefficient, K[19,47]:

$$K = \frac{C_s}{C_a} = \frac{C_s'}{C_a'} \qquad (2.27)$$

where C_a is the solubility in the aqueous phase.

Equating Equations (2.25) and (2.26) and solving for the unknown C_s yield:

$$\frac{dM_t}{dt} = \frac{D}{l}\left[C_s - \frac{C_s D h_a + D_a l C_B}{\frac{D_a l}{K} + D h_a}\right] \qquad (2.28)$$

Equation (2.28) relates the rate of release to the time-dependent zone of depletion (ℓ). However, the rate of release per unit area is also[19]:

$$\frac{dM_t}{dt} = C_o \frac{dl}{dt} - \frac{C_s\, dl}{2\, dt} \qquad (2.29)$$

Equating Equations (2.28) and (2.29), and integrating and assuming perfect sink conditions, i.e., $C_B = 0$, give:

$$l^2 + \frac{2 D h_a K l}{D_a} = \frac{2 D C_s t}{C_o - \frac{1}{2} C_s} \qquad (2.30)$$

When $C_o >> C_s$, the cumulative amount released per unit area is[19]:

$$M_t = \frac{-Dh_aKC_o}{D_a} + \left\{ \left[\frac{Dh_aKC_o}{D_a} \right]^2 + 2C_oDC_st \right\}^{1/2} \qquad (2.31)$$

and the rate becomes[19]:

$$\frac{dM_t}{dt} = \frac{\alpha C_s}{2(\beta^2K^2 + \alpha C_st)^{1/2}} \qquad (2.32)$$

where $\alpha = 2C_oD$ and $\beta = Dh_aC_o/D_a$. For small values of β^2K^2, Equations (2.31) and (2.32) reduce to the previously derived equations, i.e., Equations (2.19) and (2.21) which follow square-root-of-time relationships. This is commonly referred to as matrix-controlled kinetics[19,47]. A linear dependence of M_t on time results when β^2K^2 is large:

$$M_t = \frac{C_aD_a}{h_a}t \qquad (2.33)$$

and the corresponding rate expression is zero-order:

$$\frac{dM_t}{dt} = \frac{C_aD_a}{h_a} \qquad (2.34)$$

This is referred to as boundary-layer-controlled kinetics[19]. Regardless of the value of β^2K^2, Equations (2.33) and (2.34) will apply at early times[19].

The matrix - boundary diffusion layer model represents a generalized description of the kinetics of solute release from monolithic devices when diffusion from the surface offers a significant resistance to the mass transport process.

2.4.4 Factors which Influence the Kinetics of Solute Release from Monolithic Devices

The factors which influence the release profiles of solutes from monolithic devices are summarized in Table 2.5. These are categorized as solute-dependent or solute-independent variables. The former are related to the physical-chemical nature of the solute in the polymer, and the latter are system variables. Either set can be varied to optimize the release rate. The following sections describe how these factors influence solute release.

TABLE 2.5. Variables which influence the kinetics of solute release from monolithic devices

Dependent upon solute	Independent of solute
Solubility	Concentration
Partition coefficient	Geometry
Diffusion coefficient	Tortuosity
	Porosity
	Volume fraction
	Diffusion layer

2.4.4.1 Concentration of solute in polymer matrix

The influence of concentration on the release profiles of steroids from silicone rubber has been widely studied[47,48,54,95,96]. For monolithic devices containing dispersed solute, release rates are proportional to the square root of the total concentration ($C_o^{1/2}$). This dependence is in agreement with the prediction by Equation (2.21). It has been observed that the shape of M_t vs. $t^{1/2}$ plots is also dependent upon C_o. As concentration increases, greater periods of non-linearity occur at early times[54]. Initial curvature has also been noted for a series of progestins[48], ethynodiol diacetate[97], and esters of p-aminobenzoic acids[98].

It has been shown that because of the relatively high partition coefficients for these compounds, the boundary diffusion layer influences the kinetics of solute release. The higher values of C_o result in smaller zones of depletion at any given time and hence the boundary layer exhibits a larger resistance to diffusion.

Release profiles are expected to be independent of C_o, as shown in Equations (2.33) and (2.34), when there is diffusion-layer control.

The effect of concentration on matrix permeability (DC_s) has been analyzed by Baker and Lonsdale[41]. It has been postulated that at high loadings, there is diffusion through the polymer phase, as well as through the pores which result from the dissolution of dispersed particles.

Release of solute from monolithic devices containing only dissolved solute is generally shown to be linearly related to the initial concentration, C_o. The concept has been employed in topical drug-delivery[77, 78, 99] and in pesticide-delivery systems[100].

The relationship between drug release and total concentration (C_o) for porous monolithic devices has been studied using plastics[55,101,102], waxes[56,103], methyl acrylate - methyl methacrylate copolymers[58], and hydroxypropyl methyl cellulose[57,104]. Release increases with concentration, but there is not always a linear dependence as predicted by Equation (2.24). This finding suggests that porosity may not be a direct function of C_o or that another variable has been altered in the equation when concentration has been changed[55].

2.4.4.2 Diffusion coefficients

The magnitude of the diffusion coefficient is dictated by the energy as well as the geometry of the system[19]. The size and shape of the diffusing molecule, the degree of polymer crystallinity, and polymer chain-chain interactions and flexibility will affect the polymer's ability to form a hole large enough to accommodate the penetrating molecule[38,105,106].

The diffusion coefficients of solutes in liquids are given by the Stokes-Einstein equation[107,108]. Diffusion coefficients of solutes in polymers are difficult to predict, but can be empirically related to molecular size or mass[19,63]. Diffusion coefficients of solutes in polymers can be determined by the lag-time method[109]. Diffusion coefficients of some selected compounds are given in Reference 19. The wide range of values indicates that the diffusion coefficient is a major factor in determining the rate of solute release.

On the basis of the derivations presented in Sections 2.4.3.1 and 2.4.3.3, release rates are expected to be proportional to the square root of the diffusion coefficient. Concentration-dependent diffusion coefficients have been considered by Crank[39].

2.4.4.3 Partition coefficients

The polymer-water partition coefficient comes into play when transfer from the polymer phase to the eluting solvent occurs. With membrane transport, the product of the partition coefficient and the diffusion coefficient defines the permeability constant (Section 2.5.6.2). The partition coefficient is an additive property of the functional groups present in a molecule[110], and in contrast with the diffusion coefficient it is extremely sensitive to slight changes in molecular structure.

The effect of the partition coefficient on the mass transport of steroids and a homologous series of esters of p-aminobenzoic acid from monolithic devices containing dispersed solute has been investigated[47,48,97,98,111-114]. Employing Equation (2.31) or (2.32), Roseman and Yalkowsky[98] have demonstrated that the overall release kinetics are biphasic, with the early portion being invariant with time (zero-order), and the later phase being dependent upon the square root of time. The magnitude of the partition coefficient (K) is a controlling factor in determining the duration of the zero-order period, as seen in Equations (2.33) and (2.34) when K^2 is large, and in Equations (2.19) and (2.21) when K^2 is small.

2.4.4.4 Solubility of the solute

The solubility of the solute in the polymer or elution medium depends upon the intermolecular forces between the solute and solvent. Relative extents of solubility can be estimated from the solubility parameter (δ), which is a measure of the cohesive energy densities of the same molecules[115,116]. The smaller the difference between the δ's of a solute and the solvent, the greater the solubility of the solute. Release rates of solutes from monolithic devices containing excess solute are expected to be proportional to the square root of their solubilities in the polymer, i.e., $C_s^{1/2}$, as seen in Equations (2.19) and (2.21).

Chien[117] has presented the thermodynamic relationships for the dependence of the solute's solubility in the polymer on its melting point, T_m. Michaels et al.[118] have applied the thermodynamic approach presented by Chien to the prediction of steroid permeability rates across polymer membranes as a function of melting point. This has been expressed by the following equation:

$$J_{max}\, h \exp(1+\chi) = \frac{-\Delta S_f}{R}\left[\frac{T_m}{T} - 1\right] + \ln \rho_d D_s \qquad (2.35)$$

where J_{max} is the flux from a saturated solution across a membrane of thickness h, χ is a solute-polymer interaction constant, ΔS_f is the entropy of fusion, R is the gas constant, T_m is the melting point of the solute, ρ_d is the density of the solute, and D_s is the diffusion coefficient of the solute in the polymer.

The interaction constant, χ, depends upon the solubility parameters and is given by:

$$\chi = \frac{V}{RT}\left[\delta_d - \delta_p\right]^2 \qquad (2.36)$$

where δ is the solubility parameter and the subscripts d and p refer to the solute and polymer, respectively, and V_d is the volume fraction of the solute.

2.4.4.5 Additional factors

Filler materials, such as silica, zinc oxide, carbon black, etc., are incorporated into elastomers to modify physical properties and to improve handling characteristics[119]. Assuming that the filler is inert with regard to solute transport, its presence in monolithic devices reduces the volume fraction for diffusion and increases tortuosity[19]. Diffusion coefficients determined by the lag-time method[109] will be decreased if the solute adsorbs onto filler particles. The degree to which this occurs depends upon the binding capacity and the extent of adsorption[108]. Adsorption effects have been observed during the transport of organic solutes across silicone-rubber membranes[48, 120, 121].

Surfactants increase solute release from porous monolithic devices by the wetting of channels for subsequent diffusion, thereby effectively increasing the porosity[101,122,123]. The effect of tortuosity in altering the release kinetics has been shown for the release of sulfanilamide from a wax matrix, for which extremely large values of tortuosity have been reported[103]. Increases in tortuosity values have also been related to the slower release of drugs from a methyl acrylate - methyl methacrylate copolymer which has been exposed to acetone vapour[124].

The use of hydrophobic polymers with highly water-soluble compounds or macromolecules is limited. Monolithic devices have been prepared using hydrophilic polymers, such as crosslinked polyacrylamide and polyvinylpyrrolidone, hydroxyethylmethacrylate, polyvinyl alcohol, and ethylene vinyl acetate copolymers to release proteins and hormones[125, 126]. Release has been dependent upon the molecular mass of the solute as well as on the design of the monolithic device. Hydrophilic polymers have also been used to deliver smaller organic molecules, such as the narcotic antagonist cyclazocine[127], and steroids[53].

The equations discussed in the Theoretical Principles Section (Section 2.4.3) have been developed for situations where the controlling step is in the matrix or boundary diffusion layer (h_a). In the latter situation, transport rates will be inversely related to the thickness of this unstirred region. In biological systems where in vivo release is slower than in vitro release, diffusion layers have been

purported to be a major factor in explaining the differences[128]. The degree to which this influences the release profile, however, is also a function of the solute concentration, diffusion coefficient, and partition coefficient which have been discussed in Section 2.4.3.5. Because the kinetics of solute release is affected by the magnitude of the diffusion-layer resistance, it is an important consideration in the design and evaluation of controlled-release systems.

In general, micronized solute is incorporated into the matrix to ensure rapid dissolution of solute, as well as uniformity of content and reproducible release patterns. The agreement of theory and data is supportive of a rapid dissolution step under these conditions[19]. Increasing particle size has been shown to reduce the release rates of chlormadinone acetate from silicone rubber[54] and other solutes from ointments[129]. A mathematical model which includes dissolution-controlled kinetics has been derived by Ayres and Lindstrom[72,73].

2.4.5 Factors which Influence the Release Lifetime of Monolithic Elastomeric Devices

The release lifetime of a given diffusion-dissolution formulation (Section 2.4.2.3) is basically dependent upon the polymer used, the type and amount of regulator used, such as carbon black, the vulcanization or curing conditions, the geometry of the device, and the agent loading[22].

2.4.5.1 The choice of the base polymer

Controlled-release formulations of the monolithic elastomeric type may rely either upon a diffusion-dissolution or a leaching-release mechanism (Section 2.4.2.3). The diffusion-dissolution systems will provide extremely long release duration, whereas leaching systems are much shorter-lived[22]. Generally, inorganic substances are insoluble in elastomers, and no choice exists except to create a leaching-type of system.

Since the establishment of a diffusion-dissolution mechanism of agent release is dependent upon solubility parameters (discussed in Section 2.4.4.4), the choice of base polymers is limited to those displaying solvation power for a given agent.

Solubility of an active agent in an elastomer can be measured by several techniques[22]. If the agent is a liquid, then the gum rubber or a non-filled, cured rubber can be immersed in the agent and periodically weighed after wiping excess agent from the surface. The elastomer will absorb the agent until the solute concentration reaches the solubility limit.

Determination of the solubility of a solid in an elastomer requires considerably greater effort. One technique used by Cardarelli[22] consists of preparing two smooth, thin panels, one of the masterbatch formulation and the other of the masterbatch with a known excess concentration of the agent. Both panels are cured, weighed and pressed firmly together. If the agent is soluble in the loaded panel, there will be a constant migration under solution pressure into the non-loaded panel. This process continues until the blank panel reaches an equilibrium weight which represents the solubility limit.

Another method of determining solubility is by observing certain physical properties of loaded panels. Usually, properties such as tensile strength and modulus show little change with agent loading until the solubility limit is reached. At that point there may be dramatic variation, though not always[22].

The presence or absence of solubility can also be determined by microtoming the sheet stock into very thin sections and examining each section by SEM techniques or X-ray fluorescence[22].

In general, high molecular mass and/or high crosslink-density materials show lower agent solubilities than low molecular mass and/or lower crosslink-density materials of the same general monomeric structure[11, 22].

A high degree of agent solubility does not in itself produce a long biological life. Usually, the higher the agent loading, the greater the loss rate. In contrast, conditions of very low agent solubility have always been inefficient[22].

In leaching-type systems where agent loadings must of necessity be high (Section 2.4.2.3) elastomer selection is usually based upon the ability of the given matrix to mechanically hold large concentrations of the agent without unacceptable loss in physical properties. Ethylene-propylene-diene terpolymers, natural rubber, cis-polybutadiene and moderate molecular mass styrene-butadiene copolymers have been found by Cardarelli[22] to be capable of retaining 70% or more by mass of fillers such as copper sulphate monohydrate.

2.4.5.2 The effect of fillers

Highly-structured carbon blacks[130], petroleum waxes, and various finely-powdered substances such as kaolinite, calcium carbonate, etc., when added to a given elastomer/active agent system, will influence the agent loss-rate. Both the amount of carbon black used and its structural type[130] must

be considered. The greater the absorptive surface area present, the greater the effective diffusion path-length in diffusion-dissolution systems and, therefore, the slower the release of the agent to the depleting surface. Since a minimal amount of the active agent must undergo dissolution in order to maintain the required biological dosage, the agent delivery-rate is critical to both efficiency and lifetime of the device[22].

The effect of carbon black structure and particle size has been studied by Cardarelli[22] for the release of bis (tri-n-butyltin) oxide from chloroprene rubber.

In leaching-type systems, carbon black loading, regardless of the type of carbon black used, affects the agent loss-rate. The cumulative one-month loss of copper ion from a compound with various carbon black contents has been reported as 40% (10 part carbon black loading), 9% (20 part carbon black loading), 8% (30 part carbon black loading), and 7% (50 part carbon black loading)[22].

2.4.5.3 The effect of vulcanization conditions

Vulcanization time and temperature affect the release rate of an agent in a diffusion-dissolution-type formulation. The particular cure system used, if it is appropriate to the elastomer in question, does not seem to greatly influence loss rates[22]. Higher curing temperatures and longer curing times increase crosslink-density and, consequently, the diffusion coefficient of the agent in the elastomer decreases.

2.4.5.4 The effect of device geometry

The effective release lifetime of a given diffusion-dissolution-type formulation can be related to the ratio of the surface area to the volume of the controlled-release device. Increasing this ratio increases the agent loss-rate[22,131].

2.4.5.5 The effect of agent loading

In studies with elastomers in antifouling applications it has been observed that excellent fouling protection is achieved with organotin concentrations of 6% or less in chloroprene rubber, compared with the 40% or greater organotin and 85% or greater cuprous oxide loadings necessary in paint preparations[70]. This contrast is startling and illustrates one favourable aspect of diffusion-dissolution systems when they are compared with leaching- or exfoliating-release systems.

Although in many instances it is possible to achieve agent loadings exceeding the solubility limit, without drastic deterioration in physical properties, high agent loadings do not guarantee a longer release lifetime. The higher the agent loading, the faster will be the release rate, due to more rapid development of porosity[22]. Consequently, the release lifetime of the device will be shorter.

2.5 MEMBRANE-CONTROLLED DEVICES

The most important class of membranes in controlled-release devices is the non-porous, homogeneous polymeric film through which transport occurs by a process of dissolution of the permeating species in the polymer at one interface and diffusion down a gradient of thermodynamic activity. These membranes are usually referred to as diffusion-dissolution membranes.

2.5.1 Fick's Law Applied to Membranes

If a fluid mixture is brought into contact with one surface of a membrane under conditions where the other surface of the membrane is in contact with another fluid mixture, and the chemical potentials of the components common to both fluids differ across the barrier, there will generally be a transfer of components through the membrane in the direction of declining chemical potential.

If a homogeneous film of uniform thickness separates two fluid phases of different composition, and the boundary conditions on both sides of the membrane are maintained constant, a steady-state flux of one or more components through the membrane will ultimately be established, as is given by Fick's first law of diffusion:

$$J = -D \frac{dC_m}{dx} \qquad (2.37)$$

where J is the mass flux in $g.cm^{-2}sec^{-1}$, C_m is the concentration of permeant in the membrane in $g.cm^{-3}$, dC_m/dx is the concentration gradient in $g.cm^{-1}$, and D is the diffusion coefficient of the permeant in the membrane in $cm^2.sec^{-1}$. The minus sign reflects the fact that the direction of flow is down the concentration gradient.

When the permeating component on either side of the membrane is in equilibrium with the respective surface layers of the membrane, the concentration of permeant just inside the membrane surface can be related to the concentration of permeant in the solution contacting the membrane by the following expressions:

$$C_{m(o)} = KC_{(o)} \quad \text{at the upstream surface } (x = 0) \qquad (2.38)$$

$$C_{m(\ell)} = KC_{(\ell)} \quad \text{at the downstream surface } (x = \ell) \qquad (2.39)$$

where K is defined as the partition coefficient (discussed in Section 2.5.4).

A schematic representation of the concentration profile through a membrane is presented in Figure 2.6, where, for purposes of illustration, it has been assumed that the partition coefficient is less than unity.

If it is assumed that the diffusion and partition coefficients are constant under steady-state conditions, Equation (2.37) can be integrated to give[41]:

$$J = D \frac{C_{m(0)} - C_{m(\ell)}}{\ell} = D \frac{\Delta C_m}{\ell} \qquad (2.40)$$

where ℓ is the membrane thickness.

Since the concentration of permeant within the membrane is usually not known, Equation (2.40) is frequently written:

$$J = D \frac{K\Delta C}{\ell} \qquad (2.41)$$

where K is the partition coefficient and ΔC is the difference in concentration between the solutions on either side of the membrane, i.e.,:

$$\Delta C = C_{(o)} - C_{(\ell)} \qquad (2.42)$$

Fick's law, presented in Equation (2.37) is a phenomenological relationship which has been found experimentally to have broad-ranging validity[41]. However, from irreversible thermodynamics[132], it can be shown that the flux is really proportional to the gradient in the thermodynamic activity, rather than the concentration gradient. Fick's law is a simplification of the more general statement, and it is valid because in most cases the activity coefficient is approximately unity and

concentration and activity are essentially identical[41]. The distinction between activity and concentration becomes important when different solvents are compared[9].

The implications of Fick's law for many controlled-release systems, including the membrane situations of interest here, have been the subject of detailed treatments by Baker and Lonsdale[41], Flynn et al.[87,108], and by Rogers[66] who elaborated the principles articulated by Barrer, Crank, and Park in their texts on diffusion[38,39,39a]. The general topic of polymeric membrane permeation has been surveyed by Michaels et al.[105] and Hopfenberg[133].

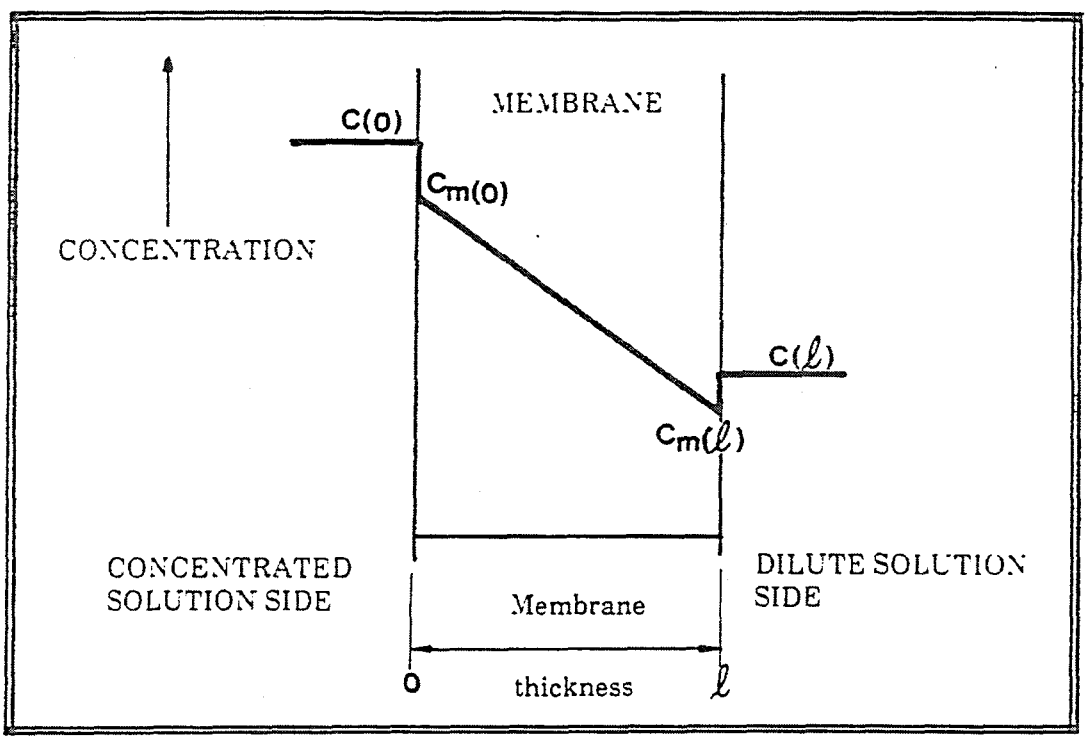

FIGURE 2.6 Schematic representation of the concentration gradient across a membrane.

2.5.2 Measurement of Diffusion Coefficients

Techniques for the measurement of diffusion coefficients in polymers have been well discussed by Crank and Park[134]. The commonly used methods for the determination of diffusivity include the measurement of permeation rates[135] and sorption/desorption kinetics[136]. For steady-state permeation through a membrane of thickness ℓ, the diffusion coefficient can be deduced from a single observation of the flux by using Equation (2.41), provided the solubility in the membrane is known[9]. In the case of transient permeation measurements, the diffusion coefficient can be deduced from the time lag[137] by using the equation[9]:

$$D = \frac{l^2}{6 t_{lag}} \qquad (2.43)$$

2.5.3 Factors which Influence the Diffusivity

The medium for diffusion in a homogeneous polymer membrane is its amorphous phase. The diffusion of a solute molecule within an amorphous polymer matrix is an activated process involving the cooperative movements of the penetrant and of the polymer-chain segments that surround it. In effect, thermal fluctuations of chain segments must allow sufficient local separation of adjacent chains to permit the passage of a penetrant molecule[9]. The frequency with which a diffusion step will occur depends upon the size and shape of the diffusing molecule, the tightness of packing and force of attraction between adjacent polymer chains, and the stiffness of the polymer chains.

Diffusion in polymers is more sensitive to the molecular mass of the diffusing species than is diffusion in liquids such as water. The difference between the diffusivity in liquids and polymers increases with increasing size of the penetrant molecule. This is because diffusion of a molecule in a polymer requires the cooperative movement of several polymer-backbone segments for each molecular jump. The larger the molecule, the larger the movement required. The stiffer the polymer backbone, the greater the energy required for movement of polymer-chain segments, and the lower will be the diffusion coefficient. The variation of diffusion coefficients with molecular mass for solutes diffusing in water, natural rubber and polystyrene has been discussed by Baker and Lonsdale[41].

Mathematical expressions which relate the diffusivity and activation energy for diffusion of simple molecules within polymer matrices to the molecular dimensions of the penetrant and the

configuration of the polymer chains have been derived[105]. Diffusivity relates to the free volume of the amorphous phase, which for a given polymer decreases with increasing molecular mass, but is best appreciated in terms of the glass transition temperature, T_g[9,138,139].

Most polymers undergo discontinuous changes in several second-order thermodynamic properties at their glass transition temperature, T_g. Such polymers in membrane form display corresponding changes in properties that govern transport, e.g., heats of solution and diffusion activation energy, at or near T_g[105]. Apparently, below the T_g there are regions of virtually immobilized chains through which activated diffusion is impossible[138]. In general, the further below its T_g a polymer is employed as a diffusion barrier, the less its free volume, and the less permeable will be its amorphous phase. Since T_g increases with polymer molecular mass[139], diffusion coefficients are inversely related to the degree of polymerization.

Plasticizers increase the free volume, promote polymer-segment mobility, and lower the T_g[139]. Therefore, the diffusivity generally increases with the amount of plasticizer incorporated[66]. Diffusivity, together with other properties, can also be modified by copolymerization[139] and grafting[66]. Crosslinking reduces chain mobility and diffusivity and, therefore, can be used to modify membrane characteristics of polymers[9]. Generally, fillers simply decrease the volume fraction of membrane available for diffusion, but well-dispersed reinforcing fillers[119] may decrease diffusivity further by reason of their crosslinking activity[87].

By definition, thermoplastics do not contain permanent crosslinks. However, there are two important sources of chain constraint in such polymers, namely, crystallinity and strain-induced orientation. The influence of crystallinity on diffusivity has been discussed by Michaels et al.[105]. The effect of the thermal history of a semicrystalline polymer membrane on its permeability has been investigated by Michaels et al.[105], Barrer[68], and Klein and Briscoe[140,141].

Vulcanization of rubber, which involves formation of crosslinks and introduction of combined-sulphur groups, decreases permeability markedly[142].

2.5.4 Factors which Influence Partition

Permeation is a consequence of not only diffusivity, but also of the distribution of the solute between the polymer and the medium surrounding it. The partition coefficient (K) is the ratio of the solubility of the permeant in the membrane to its solubility in a given liquid solvent[110].

When a liquid containing a solute is brought into contact with a polymer, the extent to which the polymer will absorb the solute will be governed primarily by the similarity of chemical constitutions of the solute and the polymer[9]. A convenient measure of compatibility of a given solute in a polymer is the difference in the solubility parameters of the solute and polymer (discussed in Section 2.4.4.4).

2.5.5 Kinetics of Solute Release from Membrane Devices

If an agent is enclosed within an inert membrane, and if the thermodynamic activity of the agent is maintained constant within the enclosure, then a steady state will be established during which the release rate will be constant. This is commonly referred to in the literature as zero-order release.

If the agent is initially present within the enclosure as an unsaturated solution, or as a saturated solution with no excess solid phase present, the thermodynamic activity, and hence the release rate, will fall exponentially. This is referred to as first-order release.

2.5.5.1 Agent release from a constant-activity source

The release rate from a membrane-controlled device is determined by the membrane permeability and the configuration of the device. For a slab or sandwich geometry illustrated in Figure 2.7(a)[41], Fick's law can be restated:

$$\frac{dM_t}{dt} = \frac{ADK\Delta C}{l} \qquad (2.44)$$

where M_t is the mass of agent released, dM_t/dt is the steady-state release rate at time t, A is the surface area of the device (both surfaces; edge effects are ignored), DK is the membrane permeability, ΔC is the difference between the internal and external agent concentrations, and ℓ is the thickness of the membrane. The total amount of agent released up to any time t, is obtained by integrating Equation (2.44).

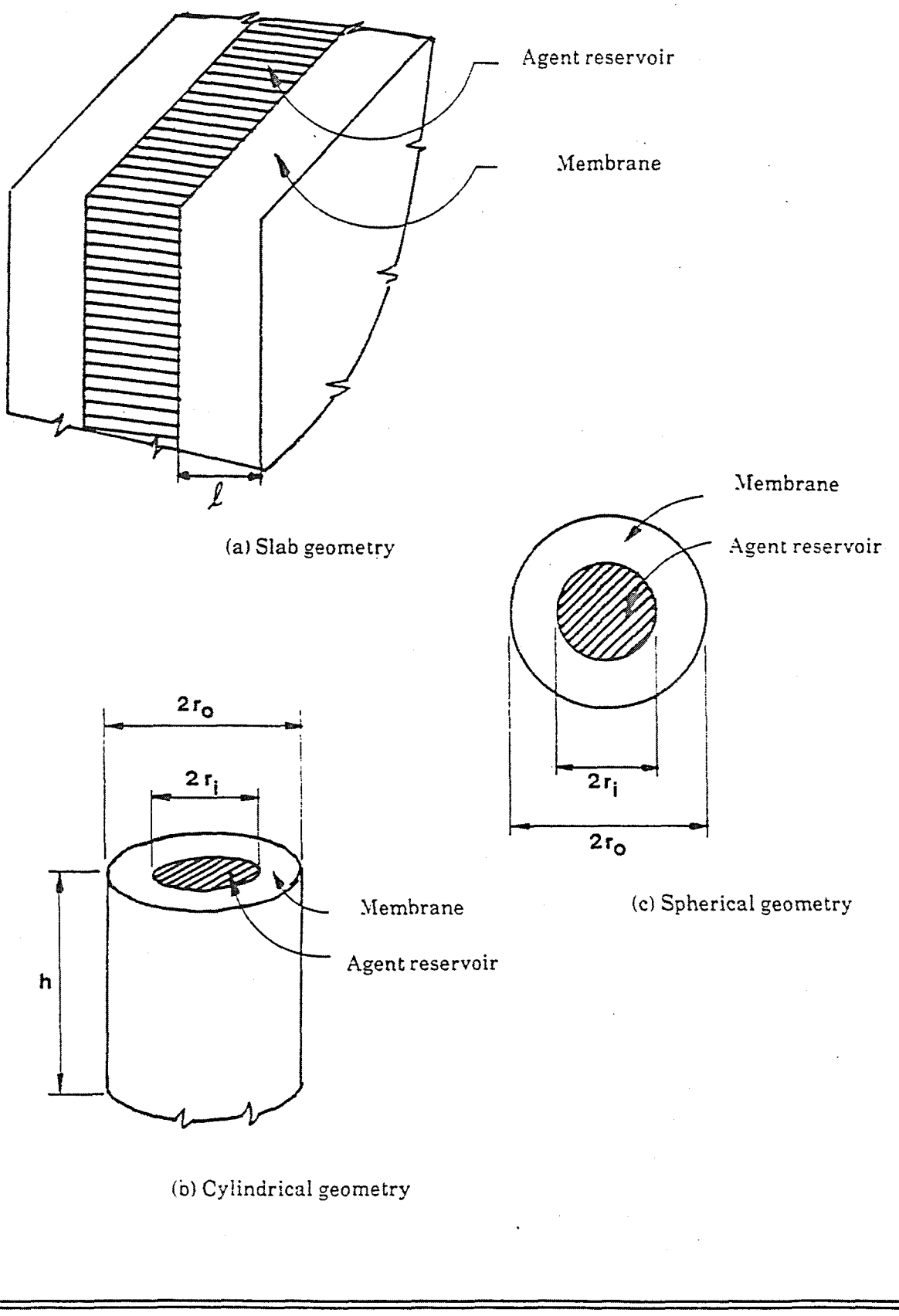

FIGURE 2.7 Schematic representation of (a) the slab geometry, (b) the cylindrical geometry and (c) the spherical geometry

For several other geometries, the appropriate statement of Fick's law is presented in the classic texts in the field[79,80]. For a cylinder, the steady-state release rate (ignoring end effects) is given by[41]:

$$\frac{dM_t}{dt} = \frac{2\pi hDK\Delta C}{\ln (r_o / r_i)} \qquad (2.45)$$

where r_o and r_i are the outside and inside radii, respectively, and h is the height of the cylinder, as shown in Figure 2.7(b).

For the sphere, shown in Figure 2.7(c), the steady-state release rate is given by[41]:

$$\frac{dM_t}{dt} = 4\pi DK\Delta C \frac{r_o r_i}{r_o - r_i} \qquad (2.46)$$

Examples of zero-order release from constant-activity-source reservoir devices of sandwich geometry, and release from spherical intrauterine devices have been presented by Baker and Lonsdale[41].

2.5.5.2 Agent release from a non-constant-activity source

For several reasons, it may not be practical to maintain constant thermodynamic activity of the agent within the reservoir. Even where constant activity is initially established, continuous loss of agent can eventually produce a situation in which the activity of the agent decreases with time. An example of the mathematical treatment of such problems has been presented by Baker and Lonsdale[41], who gave the following expressions:

$$M_{1_t} = \frac{M_\infty}{V_2 + V_1} \left\{ V_2 \exp \left[\frac{-ADK(V_1 + V_2)t}{\ell V_1 V_2} \right] + V_1 \right\} \qquad (2.47)$$

$$\frac{dM_{1_t}}{dt} = \frac{-M_\infty ADK}{V_1 \ell} \exp \left[\frac{-ADK(V_1 + V_2)t}{\ell V_1 V_2} \right] \qquad (2.48)$$

where M_{1_t} is the amount of agent remaining in the device at time t (and not the amount released as in previous equations), M_∞ is the total amount of agent, V_1 is the volume of the reservoir, V_2 is the volume of the receiving fluid, A is the surface area of the device, DK is the membrane permeability, and ℓ is the membrane thickness.

2.5.6 Design Considerations for Membrane-Controlled Devices

2.5.6.1 Membrane variables

The total rate of solute transport through a membrane composed of a specific polymeric material is controlled by adjusting the area and thickness of the membrane and/or the activity or chemical potential gradient across the membrane. The mechanical properties of the rate-controlling membrane create specific limitations to which the overall design must respond[9]. The effects of geometry on release kinetics in membrane-moderated systems have been analyzed[41], and theoretical patterns can be predicted for spherical, cylindrical, and laminated, sandwich-type devices (discussed in Section 2.5.5.1).

2.5.6.2 Reservoir variables

In most instances, since infinite sink conditions of negligible diffusant activity are maintained in the receiving fluid, i.e., the downstream side of the membrane, all other things being equal, the delivery rate is determined by the thermodynamic activity of the diffusant maintained in the reservoir, i.e., the upstream side of the membrane. For these conditions, Equation (2.41) can be modified to[9]:

$$J = \frac{DKC^*}{l} \qquad (2.49)$$

where C^* is the concentration or activity maintained in the reservoir. If this activity is maintained constant, the release rate from the system will also remain constant.

Change in the volume of the reservoir as a function of time can vary the area of contact between the reservoir medium and the membrane, which will modify the overall release rate of the device. This is of concern especially when a solid agent is used in the reservoir. Employment of a liquid medium in the reservoir makes possible continuous contact between the supply of agent and the entire membrane and will, therefore, ensure a constant releas rate[9].

The permeability constant, P, defined as the product of the flux through the membrane times the membrane thickness divided by the concentration difference across the membrane, is commonly used to describe membrane permeation[143]. Rearranging Equation (2.44) gives:

$$\frac{1}{A}\frac{dM}{dt} = \frac{DK\Delta C}{l} \qquad (2.50)$$

Here A is the membrane area, dM/dt is the mass transported per unit time, D is the solute diffusion coefficient, K is the membrane-solvent partition coefficient, ΔC is the difference in concentration between the solutions on either side of the membrane, and l is the membrane thickness.

The product DK is termed the permeability, P, and hence:

$$\frac{1}{A}\frac{dM}{dt} = \frac{P\Delta C}{l} \qquad (2.51)$$

Membranes may also be characterized by a term, $\overline{T}$, defined by Equation (2.52) as the transference[143]:

$$T = \frac{l}{A}\left[\frac{dM}{dt}\right]_{sat} = J_{sat}\, l = PC^{s} = DC_{m}^{s} \qquad (2.52)$$

The transference is the product of the membrane thickness, l, and the solute flux, J_{sat}, through the membrane from a saturated solution to the pure solvent. It is also given by the product of the permeability coefficient, P, and the solubility in the reservoir solvent, C^s, or the product of the diffusion coefficient of the solute in the membrane, D, and the solubility of the solute in the membrane, C^s_m. The quantity Jl is referred to as the normalized mass flux[9]. The transference, $\overline{T}$, is the normalized mass flux at the specified boundary conditions, namely, a saturated solution on one side of the membrane, and pure solvent, i.e., zero concentration of solute, on the other side of the membrane.

Transference, $\overline{T}$, completely describes the permeation process, and agent solubilities in the reservoir solvent are not required to compute fluxes through the membrane. Transference is a reproducible intensive property of the solute/membrane system, and is independent of the solvent used[143].

The pattern of release of a membrane-controlled system could be made to vary in a predictable manner by employing two or more co-solvents in the reservoir[144].

2.5.6.3 Issues related to the recipient environment

When transport of agent away from the membrane surface is relatively slow, agent concentration can reach appreciable levels at the surface and in the fluid immediately surrounding the device. Should the concentration in the boundary layer exceed the solubility of the agent, delivery will actually cease[9]. This has frequently caused poor agreement between the results of **in vitro** and **in vivo** tests, especially with agents of low water solubility in devices that release at high rates[9]. Baker and Lonsdale[41] have analyzed boundary-layer effects on transmembrane diffusion rates and have shown that release rates are dependent on the quotient J_{max}/C_{rc}, where J_{max} is the maximum flux under infinite sink conditions, and C_{rc} is the solubility of the agent in the recipient compartment. Boundary-layer effects have also been discussed in Section 2.4.3.5.

Membrane-controlled release is quite temperature-sensitive, so that the temperature of the operating environment is an important element of design[9]. Rogers[66] has reported that over a reasonable temperature range the temperature-dependence of permeability can be represented by an Arrhenius-type equation.

2.5.6.4 The time lag and the burst effect

During early release periods, devices may exhibit release rates higher or lower than the steady-state value, depending on the history of the device. When devices are used immediately after fabrication, they will require a certain time period to establish the steady-state concentration gradient within the membrane. This time period is termed the "time lag". On the other hand, when devices are stored before use, the solute will saturate the membrane, and the release rate will initially be higher than the steady-state value. This phenomenon is termed the "burst effect". The magnitude of these two effects depends upon the solute diffusivity in the membrane, the membrane thickness, and the relative temperatures of storage and use[9].

Mathematical equations have been derived by Crank et al.[38, 39] and Baker et al.[41] to quantify these phenomena at constant temperatures. For the burst effect, the equation describing the phenomenon is:

$$\frac{J_B}{J_{max}} = 1 + 2e^{-D\pi^2 t / l^2} \qquad (2.53)$$

where J_{max} is the steady-state flux, and J_B is the flux during the burst period.

For time lag, the following equation has been given:

$$\frac{J_T}{J_{max}} = 1 - 2e^{-D\pi^2 t / l^2} \qquad (2.54)$$

where J_T is the flux during the time-lag period.

2.6 SOME APPLICATIONS OF CONTROLLED-RELEASE TECHNOLOGY

As already noted, the major effort in applying controlled-release principles has been in the administration of pharmaceutical agents and the application of pest-control chemicals. An extensive literature has developed over the years describing the theory, formulation, evaluation and efficiency of a vast number of experimental and commercial controlled-release products. Reference 70 and References 145 to 150 are convenient sources for review of this subject. Some of the more frequently cited applications of monolithic devices and membrane-controlled devices are briefly discussed below.

2.6.1 Monolithic Devices

2.6.1.1 Administration of pharmaceutical agents

Monolithic devices have been used for the administration of a variety of drugs. These are summarized in Table 2.6.

A vaginal ring containing the contraceptive agent medroxyprogesterone acetate supports the concept of a continuous dosing pattern from a monolithic device[19]. An example of a monolithic matrix containing norgestrel attached to an intrauterine device has been discussed by Nilsson et al.[151].

P· ·ous or granular monolithic devices which require a leaching solvent to penetrate the matrix are mployed in the development of sustained-release tablets. Drugs administered with this dosage form include methamphetamine hydrochloride, ferrous sulphate, hexocyclium methylsulphate, lithium, alprenolol, potassium chloride, prednisolone, and hyoscyamine[19].

TABLE 2.6. Drugs which have been released from monolithic matrices

DRUG	MONOLITHIC MATRIX	SOURCE
Pyrimethamine	Silicone rubber	Fu et al.[46]
Hydrocortisone	Ethylene vinyl acetate	Fu et al.[46]
Hydrocortisone	Polycaprolactone	Fu et al.[46]
Medroxyprogesterone acetate	Silastic[R] silicone rubber	Roseman and Higuchi[47]
Progesterone	Silastic[R] silicone rubber	Roseman[48]
6α-Methyl-11β-hydroxy-progesterone	Silastic[R] silicone rubber	Roseman[48]
17α-Hydroxyprogesterone	Silastic[R] silicone rubber	Roseman[48]
Salicylic acid	Ethylcellulose	Donbrow and Friedman[50]
Caffeine	Ethylcellulose	Donbrow and Friedman[50]
Pentobarbital	Hydroxypropyl cellulose	Borodkin and Tucker[51]
Methapyrilene	Hydroxypropyl cellulose	Borodkin and Tucker[51]
Salicylic acid	Hydroxypropyl cellulose	Borodkin and Tucker[51]
Benzocaine	Ethylcellulose	Sciarra and Patel[52]
Cyclomethycaine	Ethylcellulose or polyamide	Sciarra and Patel[52]
Methapyrilene hydrochloride	Polyamide	Sciarra and Patel[52]
Norgestomet	Poly (hydroxyethyl methacrylate)	Chien and Lau[53]
Chlormadinone acetate	Silicone rubber	Haleblian et al.[54]
Sodium salicylate	Polyvinyl chloride	Desai et al.[55]
Sodium salicylate	Polyethylene	Desai et al.[55]
Chlorpheniramine maleate	Hydroxypropyl methylcellulose ether	Lapidus and Lordi[57]
Sodium pentobarbital	Methyl acrylate-co-methyl methacrylate	Farhadieh et al.[58]
Methapyrilene hydrochloride	Methyl acrylate-co-methyl methacrylate	Farhadieh et al.[58]
Ephedrine hydrochloride	Methyl acrylate-co-methyl methacrylate	Farhadieh et al.[58]
Dextromethorphan hydrobromide	Methyl acrylate-co-methyl methacrylate	Farhadieh et al[58]
Salicylic acid	Stearyl alcohol and polyvinylpyrrolidone	Cobby et al.[83]
Ephedrine	Stearyl alcohol and polyvinylpyrrolidone	Cobby et al.[83]
Estradiol	Silicone rubber	Cornette and Duncan[89]
Ethynodiol diacetate	Silicone rubber	Chien et al.[95]
Esters of p-aminobenzoic acid	Silicone rubber	Roseman and Yalkowsky[98]
Caffeine	Polyethylene	Desai et al.[101]
Sulfanilamide	Polyethylene	Desai et al.[101]
Potassium acid phthalate	Polyethylene	Desai et al.[101]
Hydrocortisone	Silicone rubber	Flynn et al.[113]
Cyclazocine	Poly (hydroxyethyl methacrylate)	Abrahams and Ronel[127]
d-Norgestrel	Silicone rubber	Nilsson et al.[151]
Desoxycorticosterone acetate	Silicone rubber	Ormsbee and Ryan[152]
Testosterone	Silicone rubber	Shippy et al.[153]

2.6.1.2 Application of pest-control chemicals

2.6.1.2.1 Controlled release of pesticides from plasticized polyvinyl chloride matrices

The first known product based on the monolithic dispersal of an insecticide in plasticized polyvinyl chloride (PVC) is the Shell No-Pest® strip[154]. The active agent, dichlorvos (dimethyl-2,2-dichlorovinyl phosphate), is released by diffusion and the emitted vapours are insecticidal. Only PVC compounds containing a plasticizing element have shown long-term controlled emission of dichlorvos at efficient rates[154]. Emission of the active agent varies with the type and amount of plasticizer used.

In work conducted at the Environmental Management Laboratory of the University of Akron, Ohio, a number of insecticides has been incorporated in PVC formulations having the following general composition[155]:

PVC	40 to 60%
Plasticizer	20 to 35%
Active agent	20 to 40%
Stabilizer	0 to 2%

The pesticides examined are summarized in Table 2.7.

2.6.1.2.2 Controlled release of pesticides from non-plasticized plastic matrices

So far as is known, only a few products consisting of a pesticide monolithically dispersed in a non-plasticized plastic dispenser have reached the commercial market. These products are summarized in Table 2.8[156].

TABLE 2.7 Pesticides incorporated in plasticized PVC formulations[155]

Sevin[R]	:	1-Naphthyl methylcarbamate
Dimethoate	:	O,O-dimethyl-S-(N-methylcarbamoylmethyl) phosphorodithioate
Ethyl trithion	:	S-[(p-chlorophenyl thio) methyl] O,O-diethyl phosphorodithioate
Methyl trithion	:	S-[(p-chlorophenyl thio) methyl] O,O-dimethyl phosphorodithioate
Diazinon[R]	:	O,O-diethyl-0-(2-isopropyl-6-methyl-5-pyrimidinyl) phosphorothioate
Naled[R]	:	1,2-dibromo-2,2-dichloroethyl dimethyl phosphate
Malathion[R]	:	O,O-dimethyl dithiophosphate of diethylmercaptosuccinate
Temephos	:	O,O,O',O'-tetramethyl-O,O-thiodi-p-phenylene
Chlorpyrifos	:	O,O-diethyl-O-3,5,6-trichloro-2-pyridyl phosphorothioate

TABLE 2.8. Commercially available non-plasticized pesticide emittors[156]

Designation	Agent	Polymer matrix	Manufacturer
Dursban[R] 10 CR	Chlorpyrifos[a] (mosquito larvicide)	Chlorinated polyethylene	Dow Chemical Co.
Ecopro[TM] 1700	Temephos[b] (insecticide)	EPM/LDPE[c]	Environmental Chemicals, Inc.
Ecopro[TM] 1000	Copper sulphate (molluscicide)	EVA/PE[d]	Environmental Chemicals, Inc.
Ecopro[TM] 1330	Tributyltin fluoride (molluscicide)	EVA/PE[d]	Environmental Chemicals, Inc.

a. O,O-diethyl-O-3, 5,6-trichloro-2-pyridyl phosphorothioate
b. O,O,O',O'-tetramethyl-O,O-thiodi-p-phenylene
c. Ethylene-propylene copolymer modified with low-density polyethylene
d. Ethylene vinyl acetate copolymer modified with polyethylene

2.6.1.2.3 Controlled release of trace nutrients from non-plasticized plastic matrices

In a programme sponsored by Environmental Chemicals, Inc., nine trace elements, namely, zinc, copper, iron, manganese, selenium, boron, cobalt, molybdenum and magnesium, have been monolithically incorporated into several plastic matrices[157].

The key to continuous long-term emission of inorganic ions from a plastic matrix lies in either the use of a porosity-enhancing coleachant or in the use of a mixture of plastic materials. Polymers investigated as binding matrices have included EPM modified with LDPE, and EVA modified with LDPE[157].

2.6.1.2.4 Antifouling elastomers

Antifouling rubber, available from B.F. Goodrich Co., Akron, Ohio, was the first controlled-release elastomer. This material is a solid-sheet formulation that releases its antifoulant by a diffusion-dissolution mechanism[158]. Known as Nofoul[R], it is used in the rubber covering of sonar domes where extremely long-term antifouling activity has been noted. Nofoul[R] sheet rubber is also used on ship hulls and other objects subjected to a marine environment, where it provides long-term protection against the attachment and growth of sessile organisms, such as barnacles, and also prevents damage by "ship worm" and **Limnoria** (the so-called "marine termite")[159]. Nofoul[R] is an organotin-loaded elastomer with chloroprene rubber (tradename Neoprene[R]) as the binding matrix. Active agents found effective in antifouling-rubber formulations are the specific trialkyl and triaryl organotins[160] listed in Table 2.9.

TABLE 2.9. Elastomer-soluble organotin agents for use in antifouling-rubber formulations[160]

TBTO	:	bis (tri-n-butyltin) oxide
TBTS	:	bis (tri-n-butyltin) sulphide
TBTA	:	tributyltin acetate
TBTF	:	tributyltin fluoride
TPTA	:	triphenyltin acetate
TPTC	:	triphenyltin chloride

2.6.1.2.5 Controlled release of molluscicides from elastomeric matrices

Both diffusion-dissolution- and leaching-type controlled-release molluscicides have been developed. Commercial controlled-release molluscicides are summarized in Table 2.10[161].

Monolithic elastomeric materials have been used for the controlled release of molluscicides such as organotins[161], e.g., TBTO and TBTF (Table 2.9), organoleads[162], e.g., triphenyllead acetate (TPLA) and tributyllead acetate (TBLA), ethanolamine niclosamide[163], and the mono- and pentahydrate of copper sulphate[164]. Several non-metallic organic chemicals have also been found to be effective against snails at relatively low concentrations[165]. These chemicals include 2,4,5,6-tetrachloroisophthalonitrile and 3,3,4,4-tetrachlorotetrahydrothiophene-1,1-dioxide.

TABLE 2.10. Commercial controlled-release molluscicides of the monolithic elastomeric type[161]

Designation	Agent	Elastomer	Manufacturer
BioMet SRM™	TBTO	Natural rubber	M & T Chemicals, Inc.
CBL-9B	TBTF	Natural rubber	Creative Biology Laboratory
Ecopro™ 1330	TBTF	Ethylene-propylene copolymer	Environmental Chemicals, Inc.
Ecopro™ 1043	$CuSO_4.H_2O$	Ethylene-propylene copolymer	Environmental Chemicals, Inc.
Intracide E-51®	$CuSO_4.H_2O$	Ethylene-propylene-diene terpolymer	International Copper Research Assoc.

2.6.1.2.6 Elastomer-based schistolarvicides

Many chemicals which have been found to be effective as molluscicides are also effective as schistolarvicides[166]. Laboratory investigations have demonstrated that TBTO, TBTF and TBTA (Table 2.9), as well as triphenyllead acetate and tributyllead acetate, are effective as schistolarvicides at very low concentrations[166]. The elastomer products CBL-9B, BioMet SRM™ and Ecopro™ 1330 (Table 2.10) have been shown to be extremely effective against **Schistosoma mansoni** cercaria, with CBL-9B being the superior product[167].

2.6.1.2.7 Controlled release of herbicides from elastomeric materials

The development and evaluation of controlled-release herbicidal materials for aquatic weeds has been a natural outgrowth of the work which has been done on antifouling and molluscicidal elastomeric materials.

Initial work has been based on the use of the butoxyethanol ester of 2,4-dichlorophenoxyacetic acid (2,4-D BEE) and the dimethylamine (2,4-D DMA) in monolithic elastomeric dispensers[168]. 2,4-D BEE has been found to be highly soluble in natural rubber, ethylene-propylene elastomers, and several styrene-butadiene copolymers. Field tests conducted against **Eichornia crassipes** (water hyacinth) and **Myriophyllum spicatum** (Eurasian watermilfoil) using controlled release of 2,4-D BEE from natural rubber matrices have been successful[169].

Although most of the known tests with herbicide/elastomer systems have concentrated on 2,4-D, several other agents have also been examined. Herbicides which have been incorporated in elastomeric formulations are listed in Table 2.11[169].

TABLE 2.11. Herbicides incorporated into elastomeric matrices[169]

2,4-D acid	:	2,4-dichlorophenoxyacetic acid
Diquat	:	6,7-dihydrodipyrido (1,2-a:2',1'-c) pyrazidium dibromide
Fenac^R	:	sodium salt of 2,3,6-trichlorophenylacetic acid
Fenuron^R	:	3-phenyl-1,1-dimethylurea
Endothall	:	7-oxabicyclo (2,2,1) heptane-2,3-dicarboxylic acid
Silvex^R	:	2-(2,4,5-trichlorophenoxy) propionic acid

Comparatively little work has been done in the application of controlled-release herbicides to soil as a means of controlling weeds of agricultural importance. The rate of release of the toxic agent from the binding matrix will depend on the amount of moisture present in the soil, the pH, and adsorption properties of the soil[170].

2.6.1.2.8 Control of acid mine drainage formation by inhibition of Thiobacillus ferrooxidans

Strip mining of coal has resulted in serious water-pollution problems in the United States of America[171,172]. In South Africa, acid drainage from active and abandoned gold, coal and other mines also constitutes a water-pollution problem[173-175]. Acid mine waters are found wherever pyritic materials come into contact with air and water[173]. Sulphur-bearing minerals, such as pyrite (FeS_2), are commonly associated with coal deposits[172]. In addition, South African gold-bearing ores always contain iron pyrite[176]. Exposure and oxidation of these pyritic materials result in acid production and solubilization of heavy metals. A bacterium, **Thiobacillus ferrooxidans**, is important in the acidification of mine drainage water, as it catalyzes the oxidation of pyrite (FeS_2) to $Fe_2(SO_4)_3$ and H_2SO_4[171,173,177].

Acid drainage may enter and pollute streams and rivers in two ways: as surface run-off from min dumps, or with the groundwater as it percolates through mineral spoils and waste dumps[172]. The release of acid drainage from working and abandoned mines into associated water systems limits the possible use of the water by increasing acidity, hardness, metal ion concentrations, and suspended solids. These changes in physical and chemical characteristics of the water result in changes in aquatic life. The economic impact of acid mine drainage can be immense as chemical and

physical changes, which affect water quality adversely, necessitate additional water treatment and water quality monitoring[175,177].

The nature and source of water pollutants created by mining operations in South Africa have been summarized by Henzen et al.[175], and water-pollution problems in the South African mining industry have been reviewed by Thompson[173] and Kempe[174]. Mine-water pollution in the United States and the United Kingdom have been discussed by Lovell[178] and Glover[179], respectively.

There are different approaches to dealing with the problem of acid mine drainage. Since the oxidation of pyrite is a function of time and availability of air and water, any approach to reducing pollution requires that one or more of these factors must be controlled. On active mines, prevention of the infiltration of water into mine workings is the obvious solution[175]. The acid water can be neutralized by treatment with lime before it is discharged into rivers[173,175,176,180]. Other methods that have shown promise include hydraulically sealing abandoned mines by flooding to restrict the availability of oxygen for pyrite oxidation[172], impoundment of mine drainage[172,175], and compaction of mine refuse piles[172]. In strip mines, the acid mine drainage can be effectively controlled by spreading topsoil over the mine dumps and by establishing a vegetation cover[175,177].

Treatment of acid mine drainage by processes such as reverse osmosis[181,182], ion exchange[182,183], charged-membrane ultrafiltration[184,185], and electrochemical treatment[186,187] have been reported, but economic constraints have effectively prevented their use on any large scale.

The role of **Thiobacillus ferrooxidans** in pyrite oxidation and the production of acid mine drainage has been well discussed by Kleinmann[171] and Conradie[177]. The inhibition of **Thiobacillus ferrooxidans** as a means of slowing pyrite oxidation has also been discussed by Kleinmann[171]. A variety of chemicals have been evaluated as possible inhibitors for **Thiobacillus ferrooxidans**[171,177], and it has been established that sodium lauryl sulphate (SLS), a biodegradable anionic surfactant, can effectively inhibit the oxidation of pyrite by **Thiobacillus ferrooxidans** at low concentrations[188]. Anionic detergents have the additional advantage of being bactericidal only at low pH.

The high solubility and biodegradability of most anionic surfactants precludes the long-term control of bacterial activity by a single application, e.g., spraying of a surfactant solution. To prevent repopulation by **Thiobacillus ferrooxidans**, the bactericidal treatment must be repeated frequently. To accomplish this at low cost, Kleinmann[188] and Kleinmann et al.[189] have added SLS to various elastomers in order to obtain controlled release of the inhibitor for extended periods of time. They have had considerable success with the inhibition of **Thiobacillus ferrooxidans** under field

conditions by application of these controlled-release rubber-SLS formulations to fresh coal refuse and abandoned, unreclaimed surface mines. In their field tests, they have used an unvulcanized rubber formulation shown in Table 2.12[189].

TABLE 2.12. Sodium lauryl sulphate (SLS) - rubber formulation used in field tests[189]

50 parts by mass natural rubber
50 parts thermoplastic styrene-butadiene rubber
30 parts sodium lauryl sulphate
10 parts carbon black

Adsorption limits the amount of surfactant that reaches the acid-producing environment. Coal and fine-grained particles, such as clay, retain the surfactant. To counteract this, before or during the application of the controlled-release rubber formulation, the surfactant must be applied as a solution in order to saturate the adsorptive capacity of the site.

The control of acid mine drainage by application of surfactant solutions, organic acids, and controlled-release formulations, as well as several other techniques, has been thoroughly discussed in a U.S. Bureau of Mines information circular[190].

Although successful trials have been carried out in the United States of America, there has been no detailed investigation of the mechanisms and kinetics of release of SLS from elastomeric devices.

2.6.2 Membrane-Controlled Devices

2.6.2.1 Silicone-rubber membranes

Polydimethylsiloxane (PDMS) was the first synthetic polymer studied as a rate-controlling membrane. Its use in controlled-release devices has been encouraged by the evidence of the biocompatibility of this polymer. For several years, Dow Corning Corporation was the only source of silicone polymers. As a result, much of the work reported in the literature refers to the tradename Silastic® medical-grade silicone rubber.

The development of controlled-release technology has motivated a series of studies on PDMS tubing for the release of anesthetics, thyroid hormone, and certain cardiovascular agents in animals[191-196]. This work has encouraged further studies in many areas of pharmacology.

The principal developments in the use of silicone-rubber membranes have involved the controlled release of steroid hormones, primarily for contraception[153,197-206]. The transport properties and characteristics of PDMS membranes have been extensively studied[48,120,207-213] and the variable of polymer-backbone modification in the polysiloxane series has been explored[214]. Numerous examples of the controlled release of a wide variety of steroids from silicone-rubber devices have been discussed by O'Neill[9], and in the references quoted by him.

Release of agents other than steroids from silicone-rubber devices has also been investigated. These agents have included anesthetics, tranquilizers, sedatives, stimulants, cardioregulatory agents, anti-inflammatory agents, prostaglandins, antimicrobial agents, etc.[215]

2.6.2.2 Ethylene vinyl acetate copolymer membranes

Careful study of the performance characteristics of the many polymeric materials that are available has led to recognition by the ALZA Corporation of the ethylene vinyl acetate (EVA) copolymers as a family of materials with a number of promising advantages[216]. For certain applications, these thermoplastic materials have been found to be far superior to silicone rubber in terms of both membrane function and formability.

EVA is attractive because it can be used in high-speed thermoplastic processes, such as extrusion and injection moulding. Certain members of the EVA-copolymer family are flexible without plasticizers, and because of this, they have been considered as candidates for the replacement of plasticized polyvinyl chloride in blood containers and tubing[9].

Utilization of copolymer materials enables membrane properties to be varied by small changes in the monomer ratios. The introduction of the vinyl acetate comonomer into the basic polyethylene structure reduces the crystallinity of the polymer, which has several consequences. As the vinyl acetate concentration is increased, the stiffness, tensile strength, and softening point decrease, while toughness, permeability, and flexibility increase. A thorough review of the structure/property relationships of general interest within the EVA series has been presented by Salyer et al.[217]

Clinical studies conducted by the ALZA Corporation have led to the commercial introduction of an ethylene vinyl acetate membrane-controlled intrauterine progesterone contraceptive system with the tradename PROGESTASERT[R][9]. Another membrane-controlled therapeutic system employing an EVA copolymer is the OCUSERT[R] system, also developed and commercialized by the ALZA Corporation. The OCUSERT[R] therapeutic system is used for the controlled release of pilocarpine for the treatment of the elevated intraocular pressure associated with chronic glaucoma[9]. The OCUSERT[R] systems are thin, flexible, lamillar ellipses that deliver pilocarpine to the tear fluid continuously for a week after placement behind the upper or lower eyelid.

2.6.2.3 Polyurethane membranes

The family of polyurethanes comprises a diverse variety of compositions with a wide range of physical characteristics. Both crosslinked and soluble forms are available from many manufacturers, and various isocyanate (hard-segment) and polyether or polyester (soft-segment) combinations are offered[9,218].

Lyman et al.[219] have done a good deal of work with copolyether-urethane membranes directed towards creating artificial-kidney elements that would separate molecules on the basis of chemical structure as well as physical size. Studies involving the permeation of steroids through polyurethane membranes have also been reported by Michaels et al.[118], Zentner et al.[220], and Lee et al.[221]

2.6.2.4 Other dense polymer membranes

Other hydrophobic polymers which have been found to be useful as rate-moderating membranes are polyethylene[9,222,223], polyamide[144,224-226], polymethyl methacrylate, and poly-n-butyl methacrylate[227].

CHAPTER 3

MATERIALS AND METHODS

3.1 INTRODUCTION

In this chapter, the materials and methods which were used in the preparation and evaluation of controlled-release systems are described. Two types of controlled-release technologies were investigated, namely, monolithic systems and membrane systems.

Sodium lauryl sulphate (SLS), an anionic surfactant, was used as the active agent which was to be released from controlled-release devices because its ability to inhibit the activity of **Thiobacillus ferrooxidans** at low concentrations had been verified experimentally by both local and overseas researchers (Chapter 2, Section 2.6.1.2.8).

Elastomers were used as binding matrices and as rate-controlling membranes because, when compared with plastics, elastomeric materials generally display greater solvation power for a wide variety of chemicals, as discussed in Chapter 2, Section 2.4.2.1.

Another characteristic of elastomers, which makes their use in controlled-release formulations very attractive, is their ability to mechanically hold large quantities of filler materials, as discussed in Chapter 2, Section 2.4.5.1.

3.2 APPARATUS

The instruments which were used for the preparation and testing of controlled-release formulations, together with the purpose for which they were used, are given in Table 3.1.

The Monsanto 100 Rheometer and the Carter two-roll rubber mill were made available by Karbochem in Sasolburg and by Rubber Products and Mouldings in Maitland, respectively. The remaining instruments were available at the Institute for Polymer Science and at the Departments of Physics and Chemistry at the University of Stellenbosch.

TABLE 3.1. Instruments used for the preparation and testing of controlled-release formulations

Instrument	Purpose for which it was used
Monsanto 100 Rheometer	Study of the curing kinetics of rubber masterbatch formulations.
Carter laboratory-size two-roll rubber mill	Compounding of rubber- SLS formulations which were used for production of monolithic pellets
Brabender Plasti-Corder® PLE 651 and Brabender two-roll mill	Compounding of rubber-SLS formulations which were used for production of membranes
ACL Hydraulic press (capacity 10 tons)	Compression moulding and vulcanization of rubber-SLS formulations
Varian 1275 single-beam atomic absorption spectrophotometer	Determination of sodium concentrations in eluates
Du Pont 9900 Computer/Thermal Analyzer and its Du Pont 910 Differential Scanning Calorimeter module	Determination of the solubility limits of SLS in rubbers Study of the effect of SLS loading on the curing kinetics of rubbers
Du Pont 9900 Computer/Thermal Analyzer and its Du Pont 942 Thermomechanical Analyzer module	Study of the effect of SLS loading on the curing kinetics of rubbers
Du Pont 9900 Computer/Thermal Analyzer and its Du Pont 951 Thermogravimetric Analyzer module	Determination of the degradation temperature of SLS
Hitachi S-405A scanning electron microscope	Study of the microstructure of rubber-SLS membranes
Nikon Optiphot light microscope and Nikon stereomicroscope	Study of the microstructure of rubber-SLS pellets and membranes
Varian nuclear magnetic resonance spectrometer	Determination of the solubility limit of SLS in natural rubber

3.3 MATERIALS

a. Natural rubber (SMR 20), styrene-butadiene rubber (AFPOL 1502) and synthetic cis-1,4-polyisoprene (IR-80) were supplied by Karbochem.

b. The following elastomer additives were also supplied by Karbochem:

Carbon black N220
Zinc oxide
Stearic acid
N-cyclohexyl-2-benzothiazole sulphenamide (ORAC CS)
Tetramethylthiuram disulphide (TMTD)
Styrenated phenol antioxidant (OROX SP)

c. Sublimed sulphur (BDH Laboratory Reagents)

d. Ammonium sulphate ($(NH_4)_2SO_4$), 99% (Riedel-de Haën)

e. Sodium chloride (NaCl), 99.5% (Riedel-de Haën)

f. Concentrated sulphuric acid, 98% (AECI)

g. Sodium lauryl sulphate (Texapon K12) was obtained from Henkel South Africa (Pty) Limited.

h. The following grades of untreated and treated calcium carbonate were supplied by Lewis & Everitt:

Kulubrite 2 ($CaCO_3$ content 95%; mean particle size 2,25 μm)
Kulubrite 5 ($CaCO_3$ content 95%; mean particle size 5 μm)
Kulubrite 10 ($CaCO_3$ content 95%; mean particle size 10 μm)
Omyalite 95T (surface-treated; $CaCO_3$ content 98.5%; mean particle size 1 μm)
Omya EX-H1 (surface-treated; $CaCO_3$ content 98.5%; mean particle size 1,5 μm)
Omya BSH (surface-treated; $CaCO_3$ content 98.5%; mean particle size 2 μm)

All the materials were used as-received from the suppliers, without purification.

3.4 EXPERIMENTAL TECHNIQUES

3.4.1 Preparation of Rubber Masterbatch Formulations

Four types of rubber masterbatch formulations were prepared, namely, natural rubber (NR), styrene-butadiene rubber (SBR), a 50:50 blend of natural rubber and styrene-butadiene rubber (NR/SBR), and synthetic cis-1,4-polyisoprene (IR).

The raw rubber ("gum stock") was softened by mechanical working on a two-roll rubber mill. Once it was in the softened state, vulcanization additives, carbon black, and an antioxidant were incorporated into the elastomer by further processing on the two-roll mill. The compositions of the four masterbatch formulations are given in Table 3.2.

3.4.2 Preparation of Rubber-SLS Formulations

Controlled-release formulations were prepared by stepwise addition of SLS to the rubber masterbatch formulations (Table 3.2), during processing on a two-roll mill. Some of the controlled-release formulations contained porosity-enhancing materials, namely, $CaCO_3$ and $(NH_4)_2SO_4$. These materials were added with the SLS. An accelerated sulphur vulcanization system was used and, therefore, the necessary amounts of sulphur were also added to masterbatch formulations at that stage of the mixing process. After the addition of SLS and other additives, the mixing process was continued for approximately two minutes to ensure good dispersion of the SLS in the rubber matrices.

Several series of rubber-SLS formulations were prepared. The compositions of rubber-SLS formulations which comprised Series A are given in Table 3.3. The compositions of the remaining rubber-SLS formulations, i.e., Series B to G, are given in Appendix 1A.

3.4.3 Compression Moulding of Rubber-SLS Formulations to Effect Curing (Vulcanization)

In order to study the curing kinetics of the masterbatch formulations shown in Table 3.2, a mass of sulphur equivalent to 2 phr was blended with 400g of each of the four formulations. The curing rates of these formulations were determined by using a Monsanto rheometer. This instrument is used to measure the increase in the modulus of the elastomer, caused by the introduction of crosslinks, as a function of time. The rheographs which were obtained were used to calculate the time required to achieve maximum crosslink-density. Optimum time and temperature conditions for vulcanization were selected for subsequent sample preparations.

The rubber-SLS formulations given in Table 3.3 and in Appendix 1A were vulcanized by compression moulding in a heated hydraulic press. Two moulds were designed and made for the production of cylindrical rubber-SLS composite pellets of different surface area/volume ratios. The moulds were made of gauge plate into which holes of different diameters were drilled.

TABLE 3.2. Compositions of rubber masterbatch formulations

Component	Formulation number			
	A	B	C	D
Natural rubber (SMR 20)	100 parts		50 parts	
Styrene-butadiene rubber (AFPOL 1502)		100 parts	50 parts	
Synthetic cis-1,4-polyisoprene (IR-80)				100 parts
Carbon black N220	9 phr[a)]	9 phr	9 phr	9 phr
Zinc oxide	5 phr	5 phr	5 phr	5 phr
Stearic acid	1 phr	1 phr	1 phr	1 phr
ORAC CS[b)]	1,5 phr	1,5 phr	1,5 phr	1,5 phr
TMTD[c)]	0,5 phr	0,5 phr	0,5 phr	0,5 phr
OROX SP[d)]	2 phr	2 phr	2 phr	2 phr

a) Parts per hundred parts of rubber.
b) N-cyclohexyl-2-benzothiazole sulphenamide (accelerator).
c) Tetramethylthiuram disulphide (accelerator).
d) Styrenated phenol (antioxidant).

TABLE 3.3. Compositions of natural rubber-SLS formulations: Series A

	Formulation number							
Constituent	A.1	A.2	A.3	A.4	A.5	A.6	A.7	A.8
Natural rubber (g)	200	200	200	200	200	200	200	200
Carbon black (g)	18	18	18	18	18	18	18	18
Zinc oxide (g)	10	10	10	10	10	10	10	10
Stearic acid (g)	2	2	2	2	2	2	2	2
ORAC CS (g)	3	3	3	3	3	3	3	3
TMTD (g)	1	1	1	1	1	1	1	1
OROX SP (g)	4	4	4	4	4	4	4	4
Sulphur (g)	4	4	4	4	4	4	4	4
SLS (g)	0	12,7	26,[illegible]	42,7	80,7	130,3	198,0	295,8
Mass % SLS	0	5	10	15	25	35	45	55

The cavity dimensions of Mould I (10 mm-thick plate) and Mould II (5 mm-thick plate) are given in Tables 3.4 and 3.5, respectively. Schematic representations of the two moulds are shown in Figures 3.1 and 3.2.

Samples were moulded at 433°K and a mould pressure of 2,9 MPa. The vulcanization times were either 12 or 24 minutes, depending on the information which was obtained from the Monsanto rheographs. The temperature of the press was maintained constant at 433°K $\pm$ 0,5°K by means of temperature controllers and probes. The vulcanized rubber pellets were cooled at room temperature and the flashings were removed by hand trimming.

3.4.4 Laboratory Determination of the Release Rates of SLS from Monolithic Rubber Pellets

Vulcanized rubber-SLS composite pellets were weighed before elution in distilled water. The pellets were placed in 0,200 dm^3 glass bottles, and 50 ml of the eluent, i.e., distilled water, was added by means of an automatic water dispenser. The bottles were sealed with screw caps in order to prevent evaporation of the eluent. All the elution experiments were conducted at room temperature under stationary conditions, i.e., no shaking. At regular intervals, 20 ml of the eluate was collected for analysis. After being sampled, the remaining eluate was discarded; the container and pellets were rinsed with eluent; 50 ml of fresh eluent was added; and the elution process was continued. The rubber-SLS pellets were eluted for a period of 56 days and samples of the eluates were collected after 24, 72, 120 and 168 hours during the first week, and once a week thereafter, i.e., after 14, 21, 28, 35, 42, 49 and 56 days of elution.

The objective of Experiment 1 was to study the effect of the agent loading on the release rate of SLS from natural-rubber matrices. The compositions and dimensions of the pellets which were used in Experiment 1 are given in Table 3.6.

Several other experiments were also conducted. The compositions and dimensions of rubber-SLS pellets which were used in Experiments 2 to 17, together with a description of the objective of each experiment, are given in Appendix 1B. With Experiments 13 to 17, the pH of the eluent (distilled water) was adjusted by addition of 0,1M H_2SO_4. Eluents with pH values which ranged between 1,5 and 4,5 were used in these experiments.

TABLE 3.4. Dimensions of Mould I (10 mm-thick plate)

Number of cavities	Hole diameter (mm)	Volume (mm^3)	Area (mm^2)	Area:Volume ratio (mm^{-1})
2	18	2545	1074	0,42
4	12	1131	603	0,53
6	10	785	471	0,60
10	8	503	352	0,70

TABLE 3.5. Dimensions of Mould II (5 mm-thick plate)

Number of cavities	Hole diameter (mm)	Volume (mm^3)	Area (mm^2)	Area:Volume ratio(mm^{-1})
10	8	251	226	0,90
18	6	141	151	1,07

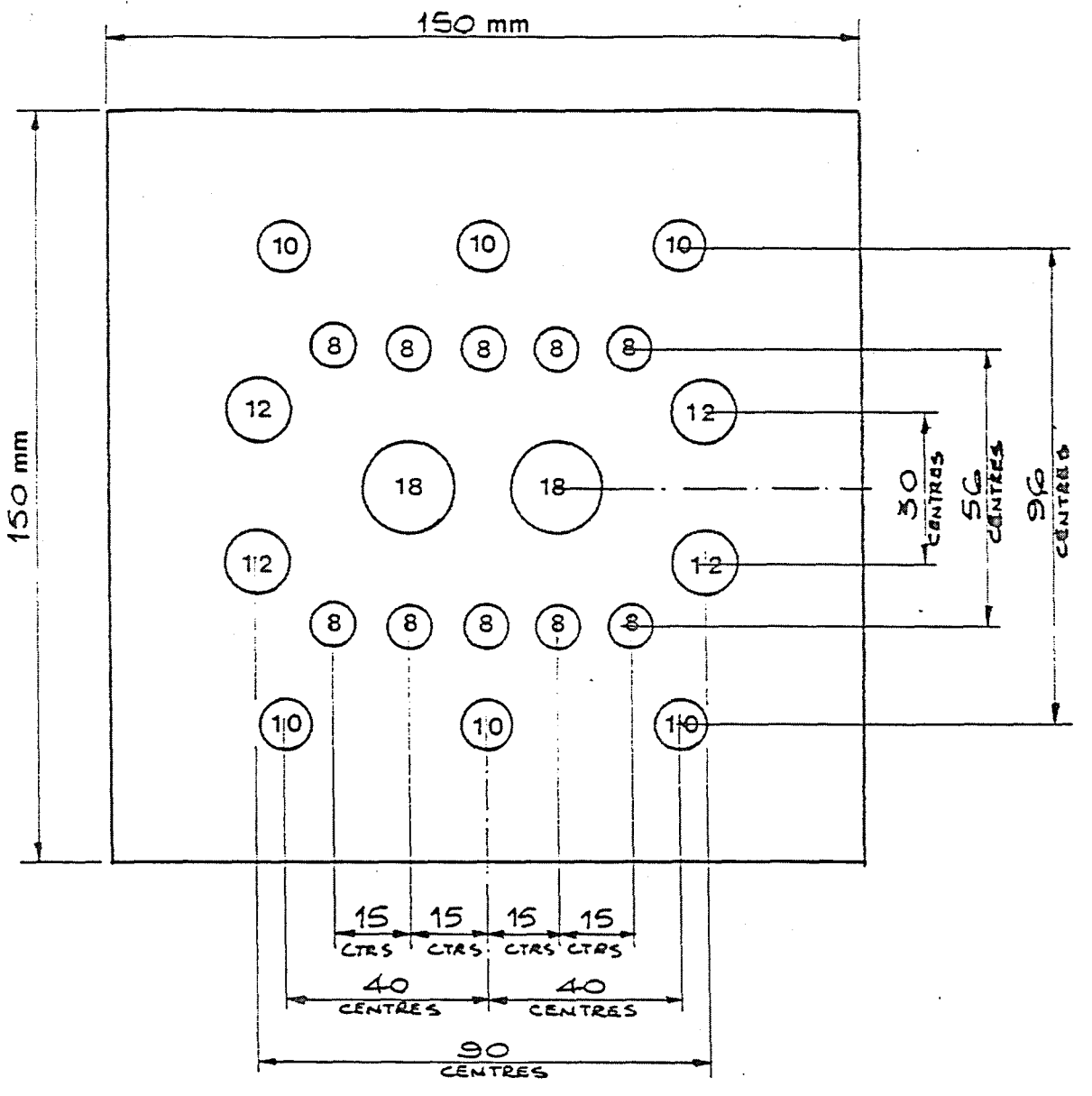

10 mm GAUGE PLATE, GROUND BOTH SIDES, WITH HOLES DRILLED AND REAMED 8, 10, 12 & 18 mm DIAMETER, AS SHOWN.

FIGURE 3.1 Schematic representation of Mould I.

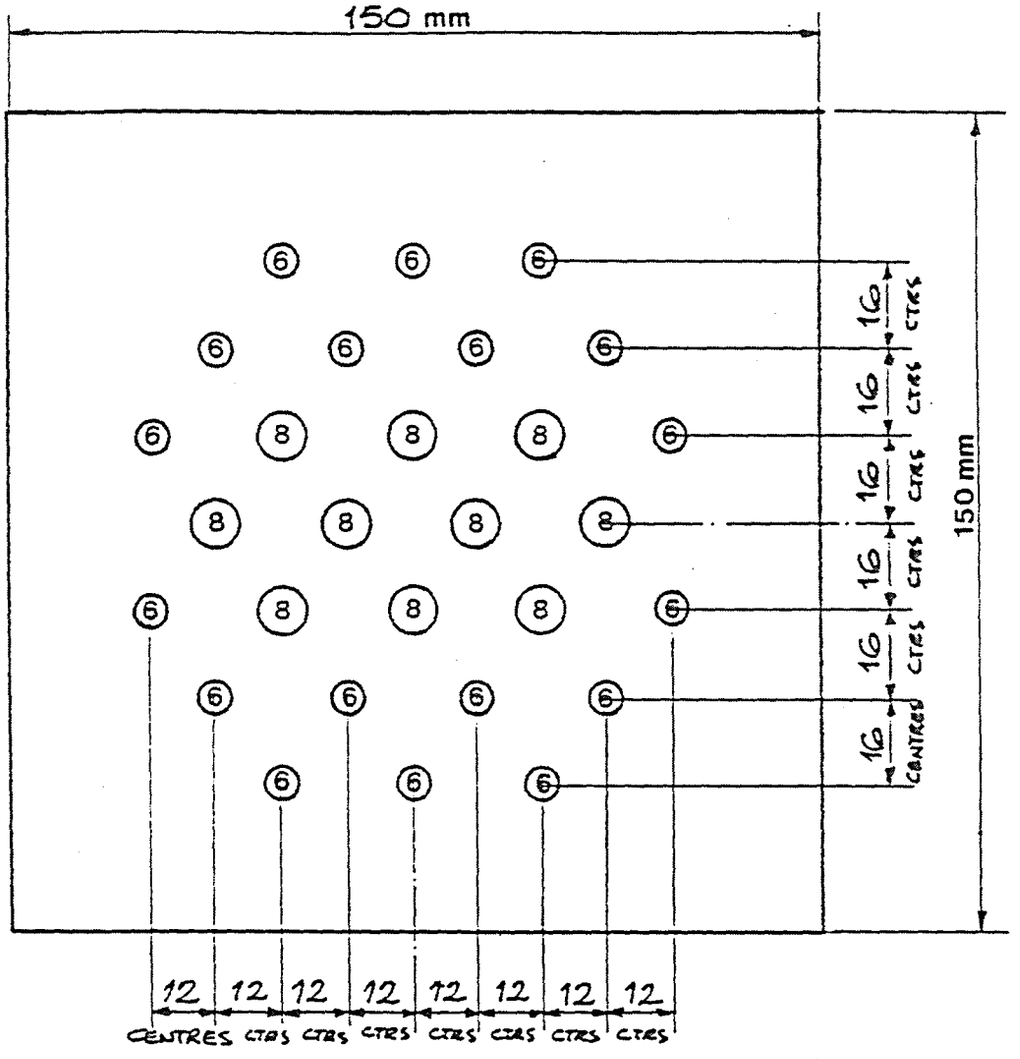

5mm GAUGE PLATE, GROUND BOTH SIDES, WITH HOLES DRILLED AND REAMED 6 & 8 mm DIAMETER, AS SHOWN

FIGURE 3.2 Schematic representation of Mould II.

3.4.5 Analysis of Eluates to Determine SLS Concentrations

Because of the large number of analyses, samples of the eluates were analyzed by means of atomic absorption and/or atomic emission spectroscopy, in order to determine the concentrations of sodium in them. Sodium concentrations less than 5 ppm were determined in the absorption mode, while sodium concentrations exceeding 5 ppm were determined in the emission mode.

A Varian 1275 single-beam atomic absorption spectrophotometer was used for analysis of the samples. A sodium hollow cathode lamp was used for atomic absorption determinations. The instrument was calibrated according to the specifications in the Varian 1275 Operating Manual. Distilled water was used as a blank in calibrations. A series of standard solutions with sodium concentrations which ranged between 1 ppm and 100 ppm was prepared from a NaCl stock solution which contained 1000 ppm of sodium. The stock solution was prepared by dissolving 2,542g of NaCl (purity, 99.5%) in distilled water in a 1 dm^3 volumetric flask.

The operating conditions were:

Atomic absorption

Wavelength	:	589 nm
Lamp current	:	3 mA
Fuel	:	acetylene
Support	:	air

Flame emission

Wavelength	:	589 nm
Fuel	:	acetylene
Support	:	air

On the assumption that one $CH_3(CH_2)_{11}SO_4^-$ ion was present for every Na^+ ion, the concentration of sodium lauryl sulphate in the eluate was calculated by multiplying the measured value by a factor of 288,49/22,99 (i.e., molecular mass of SLS/atomic mass of sodium).

3.4.6 Preparation of Controlled-Release Membranes

Two types of rubber masterbatch formulations, namely, natural rubber (NR) and synthetic polyisoprene (IR), were used for the preparation of controlled-release membranes. These

masterbatch formulations were identical to Formulations A and D, which are presented in Table 3.2.

The masterbatch formulations were blended with SLS and sulphur, as described in Section 3.4.2. The smaller quantities of controlled-release rubber-SLS formulations which were prepared for the production of membranes made possible the use of a smaller, adjustable-speed two-roll mill which could be handled easily. The rubber-SLS formulations used for the production of controlled-release membranes were prepared by using a Model PLE 651 Brabender Plasti-Corder and a Brabender two-roll mill. The compositions of these rubber-SLS formulations are shown in Table 3.7.

The rubber-SLS formulations given in Table 3.7 were vulcanized by compression moulding for 12 minutes at 433°K and a mould pressure of 2,9 MPa. Frames made of stainless steel plate of external dimensions 130 mm x 130 mm and internal dimensions 110 mm x 110 mm, and 0,65 mm, 0,90 mm and 1,20 mm thick were used to prepare three membranes of different thicknesses from each of the six rubber-SLS formulations shown in Table 3.7.

Two control experiments were also run, for which purpose two thin, SLS-free membranes, one based on natural rubber and the other based on synthetic polyisoprene, were prepared. The vulcanization conditions were the same as those for the membranes prepared from blends AMD1 to AMD6. The thicknesses of the vulcanized rubber membranes were measured with a dial micrometer.

The compositions and dimensions of the membranes which were prepared for evaluation in subsequent diffusion experiments are given in Table 3.8.

3.4.7 Determination of the Flux of SLS through Rubber Membranes

Referring to Figures 3.3(a) and 3.3(b), the testing apparatus 1 comprised two flanged glass containers, 2 and 3, of inside diameter 5,8 cm. The volume of each container was approximately 0,300 dm^3. The testing apparatus 1 also comprised a membrane, 4, sandwiched between the flanges 2.1 and 3.1 of the containers, i.e., located between the open ends of the containers. The membrane and containers were held together by means of holding plates, 5 and 6, which were bolted together (not shown). These plates exerted a uniform pressure on both flanges and thereby eliminated the possibility of leakage.

TABLE 3.6. Compositions and dimensions of rubber-SLS pellets used in Experiment 1

Sample number	Formulation number[a]	Mass of pellet (g)	Mass % SLS	Mass of SLS (g)	d[b] (mm)	h[c] (mm)	S/V[d] ratio
1	A.4	2,499	15	0,375	18	10	0,42
2	A.5	2,556	25	0,639	18	10	0,42
3	A.6	2,598	35	0,909	18	10	0,42
4	A.7	2,627	45	1,182	18	10	0,42
5	A.8	2,677	55	1,472	18	10	0,42

a) Given in Table 3.2.
b) Diameter of pellet.
c) Thickness of pellet.
d) Surface area: volume ratio of pellet.

TABLE 3.7. Compositions of controlled-release rubber-SLS formulations which were used for the production of membranes

	Formulation number					
Constituent	AMD1	AMD2	AMD3	AMD4	AMD5	AMD6
Natural rubber (g)	100	100	100			
Synthetic polyisoprene (g)				100	100	100
Carbon black (g)	9	9	9	9	9	9
Zinc oxide (g)	5	5	5	5	5	5
Stearic acid (g)	1	1	1	1	1	1
ORAC CS (g)	1,5	1,5	1,5	1,5	1,5	1,5
TMTD (g)	0,5	0,5	0,5	0,5	0,5	0,5
OROX SP (g)	2	2	2	2	2	2
Sulphur (g)	2	2	4	2	2	4
SLS (g)	0	13,44	65,15	0	13,44	65,15
Mass % SLS	0	10	35	0	10	35

TABLE 3.8. The compositions and dimensions of membranes evaluated in diffusion experiments

Membrane number	Type of rubber	Mass % SLS	Membrane thickness (mm)[g]	Membrane area (mm^2)
1	NR[a]	0	1,40	2642
2	NR[a]	0	1,14	2642
3	NR[a]	0	0,90	2642
4	NR[b]	10	1,35	2642
5	NR[b]	10	1,11	2642
6	NR[b]	10	0,88	2642
7	NR[c]	35	1,25	2642
8	NR[c]	35	0,92	2642
9	NR[c]	35	0,70	2642
10	IR[d]	0	1,54	2642
11	IR[d]	0	1,17	2642
12	IR[d]	0	0,88	2642
13	IR[e]	10	1,36	2642
14	IR[e]	10	1,11	2642
15	IR[e]	10	0,92	2642
16	IR[f]	35	1,23	2642
17	IR[f]	35	0,94	2642
18	IR[f]	35	0,72	2642
Control A	NR[a]	0	0,37	2642
Control B	IR[d]	0	0,39	2642

a) Formulation AMD1 (Table 3.6).
b) Formulation AMD2 (Table 3.6).
c) Formulation AMD3 (Table 3.6).
d) Formulation AMD4 (Table 3.6).
e) Formulation AMD5 (Table 3.6).
f) Formulation AMD6 (Table 3.6).
g) Average of ten measured values.

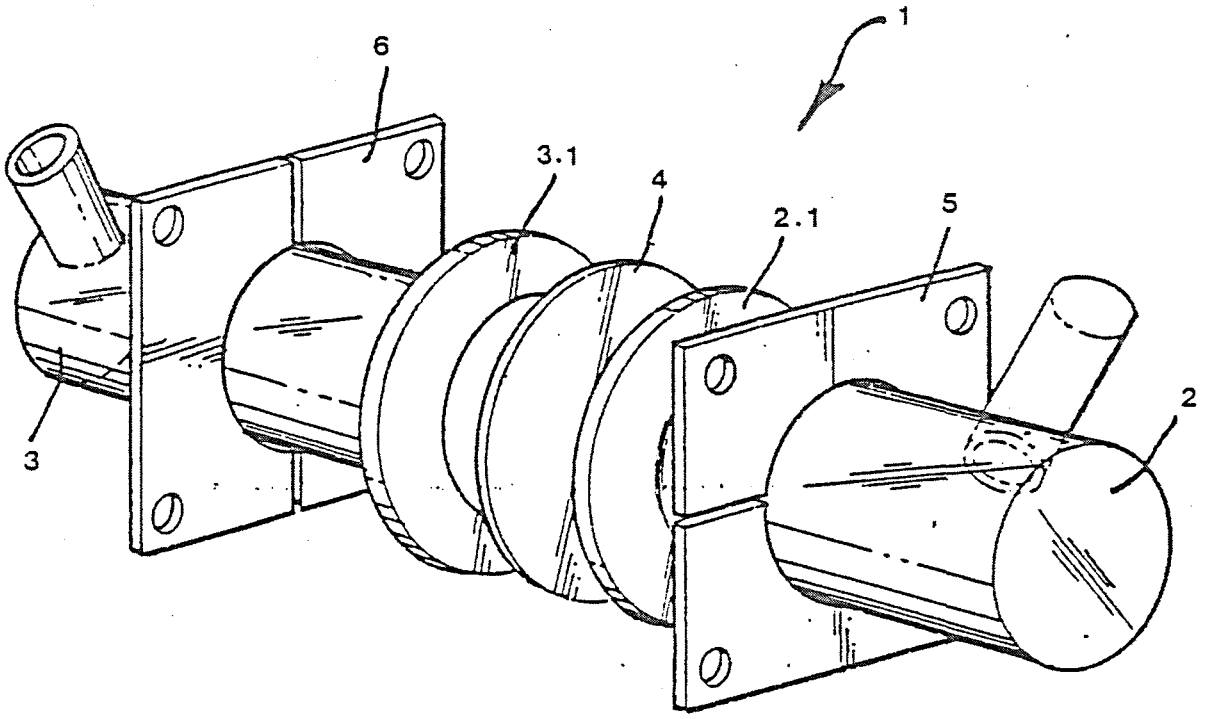

(a)

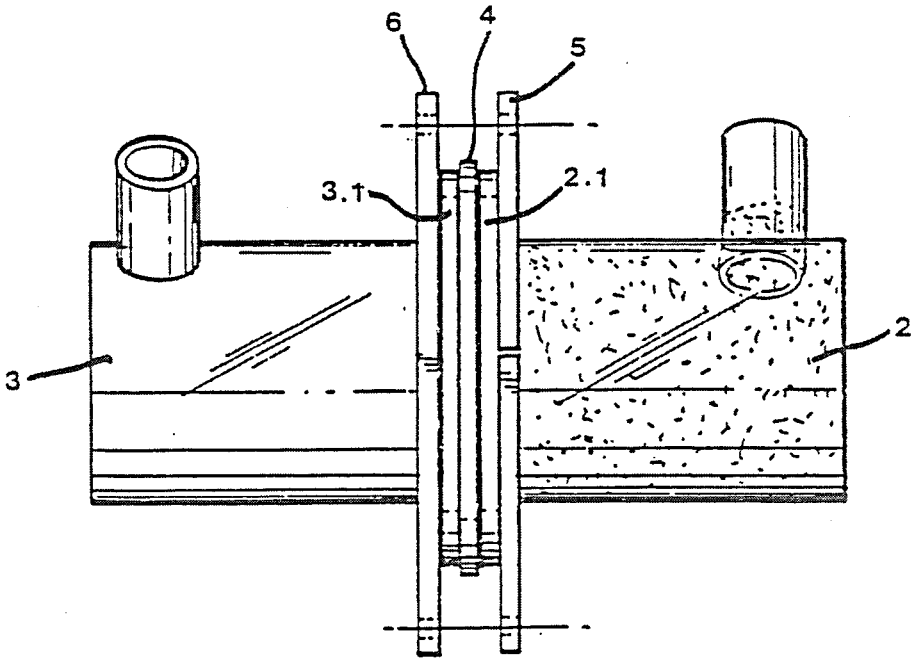

(b)

FIGURE 3.3 Schematic representation of the testing apparatus used for the determination of the flux of SLS through rubber membranes.

The reservoir compartment, or container 2, was filled with 270 ml of a saturated SLS solution, and the receiving compartment, or container 3, located on the downstream side of the membrane, contained 270 ml of freshly distilled water. The water in the receiving compartment was collected for analysis every 24 hours, after which the receiving compartment was rinsed with distilled water, and 270 ml of freshly distilled water added. This procedure was repeated for 80 days for each experimental run.

The laboratory temperature was maintained at 294°K $\pm$ 2°K for the duration of the test period, and was monitored continuously by means of a thermohygrometer.

Two control experiments, namely, with Control Membrane A and Control Membrane B (see Table 3.8), were set up in a temperature-controlled room, the temperature of which was maintained at 294°K. The reservoir sides contained saturated SLS solutions and were stirred continuously. The receiving sides contained 320 ml of distilled water. The solutions on the receiving sides were collected for analysis at 24-hour intervals, after which the receiving sides were rinsed and 320 ml of freshly distilled water added. The experiments continued for a period of 30 days.

3.4.8 SLS Solutions Used in the Reservoir Compartment

For each experimental run, an 8% (m/v) SLS solution was initially used in the reservoir compartment. This solution was replaced by a 10% solution on day 25, and by a 20% solution on day 40. The SLS solutions were stirred for a period of 24 hours in order to dissolve all the SLS before the reservoirs were filled. Excess SLS crystallized out of all three of these solutions after a few hours. Since excess solids were present for the entire duration of the experiments, all three solutions could hence be regarded as saturated at the temperature of use.

3.4.9 Analysis of Solutions which were Collected from the Receiving Compartments

The concentrations of sodium in the receiving fluids (distilled water) were determined by atomic absorption spectroscopy, as described in Section 3.4.5.

3.4.10 Determination of the Solubility Limits of SLS in Rubbers

3.4.10.1 Thermal analysis

The solubility limits of SLS in natural rubber and in synthetic polyisoprene were investigated by means of differential scanning calorimetry (DSC), using a Du Pont 9900 Thermal Analyzer and its Model 910 Differential Scanning Calorimeter module. DSC scans were done on SLS (Texapon K12) in order to determine its melting temperature. This was followed by DSC scans on natural rubber and synthetic polyisoprene formulations which contained different loadings of SLS. The compositions of the formulations which were analyzed by DSC are given in Table 3.9. The objective of this investigation was to determine the level of SLS at which phase separation started, i.e., the level at which the solubility limit of the SLS in the rubber was exceeded. In addition to DSC analyses, the degradation temperature of SLS was determined by thermogravimetric analysis (TGA). This was done by using a Du Pont Model 951 Thermogravimetric Analyzer.

3.4.10.2 Nuclear magnetic resonance (NMR) spectroscopy

Samples of natural rubber which contained different loadings of SLS were analyzed by ^{13}C NMR to determine whether any absorption peaks would appear in the spectrum when the solubility limit of the SLS in the rubber was exceeded and, hence, to investigate the feasibility of this technique as a means for determining the solubility limits of SLS in natural and synthetic rubbers. Disks of diameter 8 mm were cut from flat sheets of unvulcanized rubber-SLS formulations using a hollow punch. The disks were stacked to a height of approximately 30 mm in an NMR tube of 10 mm diameter, and were then compacted. Unvulcanized natural rubber - SLS formulations which contained 0, 5, 10 and 15% SLS (Formulations A.1, A.2, A.3 and A.4, respectively; Table 3.3) were analyzed by this means.

3.4.11 Investigation of the Effect of SLS Loading on the Curing Kinetics of Rubber-SLS Formulations

3.4.11.1 Thermomechanical analysis (TMA)

The amount of crosslinking (degree of cure) of rubber-SLS formulations was investigated by thermomechanical analysis, using a Du Pont 9900 Thermal Analyzer and its Model 942 Thermomechanical Analyzer module. The TMA method involved the determination of the coefficient of linear expansion, α , which is a measure of the degree of cure of an elastomer.

Generally, a lower coefficient of expansion indicates a higher degree of cure, whereas a higher coefficient of expansion indicates incomplete or a lower degree of cure. Formulations DS1 to DS12 and formulations DS17 to DS19, given in Table 3.9, were analyzed by TMA.

3.4.11.2 Differential scanning calorimetry (DSC)

As an alternative to the TMA method described above, DSC was used for determining the effect of the SLS loading on the curing kinetics of rubber-SLS formulations. The curing exotherms were analyzed by using the Borchardt & Daniels DSC Kinetics Data Analysis software. This software permits activation energy (E), pre-exponential factor (Z), heat of reaction (ΔH) and order of reaction (n) to be calculated from a single DSC scan of a reaction exotherm. This method was used for the analysis of the curing exotherms of the formulations given in Table 3.9.

3.4.12 Light Microscopy

The microstructure of rubber-SLS composite pellets and membranes which contained various loadings of SLS were studied by light microscopy. Cross-sections of rubber-SLS pellets were investigated by using a Nikon stereomicroscope. Membranes which contained different loadings of SLS were studied by using a Nikon Optiphot microscope. Cross-sections of membranes, as well as membrane surfaces, were investigated by means of both reflected light Differential Interference Contrast (DIC) and reflected light Dark Field (DF) microscopy.

3.4.13 Scanning Electron Microscopy (SEM)

The microstructure and composition of rubber-SLS membranes which contained 0, 10 and 35% SLS were studied before and after the release of SLS using SEM. Samples of the membranes were frozen with liquid nitrogen, cut with a knife, mounted on aluminium stubs, and sputter-coated with a thin layer of gold. The surfaces and cross-sections of membrane samples were observed using an Hitachi S-405A scanning electron microscope.

TABLE 3.9. Compositions of the rubber-SLS formulations which were analyzed by DSC

Formulation number	Type of rubber	Mass % SLS
DS1	NR	0
DS2	NR	0,5
DS3	NR	1
DS4	NR	2
DS5	NR	3
DS6	NR	4
DS7	NR	5
DS8	NR	6
DS9	NR	7
DS10	NR	8
DS11	NR	9
DS12	NR	10
DS13	NR	11
DS14	NR	12
DS15	NR	13
DS16	NR	14
DS17	NR	15
DS18	NR	25
DS19	NR	35
DS20	IR	0
DS21	IR	2
DS22	IR	3
DS23	IR	4
DS24	IR	6
DS25	IR	8
DS26	IR	10
DS27	IR	11
DS28	IR	12
DS29	IR	13
DS30	IR	14
DS31	IR	15
DS32	IR	25
DS33	IR	35

CHAPTER 4

RESULTS AND DISCUSSION

4.1 INTRODUCTION

As was mentioned in the introductory chapter, not much is known about the mechanisms and kinetics of release of SLS from monolithic devices. In addition, the use of membrane devices for attaining controlled release of SLS has not been investigated.

The studies reported in this chapter involve monolithic elastomeric pellets and elastomeric membrane devices for attaining controlled release of SLS.

4.2 THE SOLUBILITY LIMITS OF SLS IN NATURAL RUBBER (NR) AND SYNTHETIC POLYISOPRENE (IR)

The rate of release of an agent from a polymeric matrix will depend on the agent's solubility in that matrix, as discussed in Chapter 2, Sections 2.4.4.4 and 2.4.5.1. It seems that no data on the solubility limits of SLS in natural and synthetic rubbers have been published. It was, therefore, necessary to investigate techniques which would be suitable for determining these solubility values. The techniques which are frequently used for determining the solubility of solids in elastomers were discussed in Chapter 2, Section 2.4.5.1. Some of these techniques are time-consuming, while others are suitable for determining the presence or absence of solubility, rather than the solubility limit, of a solid agent in an elastomer. Two techniques for determining the solubility limit of SLS in elastomers were investigated. These techniques, together with the results obtained, are discussed in Sections 4.2.1 and 4.2.2.

4.2.1 ^{13}C NMR Analysis of Rubber-SLS Formulations

Attempts were made to determine the solubility limit of SLS in natural rubber (SMR 20) by ^{13}C NMR analysis of rubber-SLS composite formulations. Samples were prepared and analyzed as described in Chapter 3, Section 3.4.10.2. The ^{13}C NMR spectra which were obtained provided no information about the solubility of SLS in NR , since the spectra for samples of NR which contained

0, 5, 10 and 15% SLS were identical. The ^{13}C NMR spectra of NR which contained 0% and 15% SLS are shown in Figures 2A.1 and 2A.2, respectively, in Appendix 2A. These spectra showed the expected absorption peaks for the rubber hydrocarbons, but none for SLS.

4.2.2 Differential Scanning Calorimetry (DSC) Analysis of Rubber-SLS Formulations

As an alternative to the technique discussed in Section 4.2.1 above, DSC was investigated as a method for determining the solubility limits of SLS in elastomers. Samples of NR and IR with SLS loadings which ranged from 0 to 35% were analyzed. The preparation and analysis of these samples were discussed in Chapter 3, Section 3.4.10.1.

A DSC scan of SLS (Texapon K12) showed a sharp endotherm at about 115°C, as shown in Figure 4.1. Values for the melting point of SLS were difficult to trace, and reliance had to be placed upon values given in chemical catalogs. According to the Aldrich Chemical Catalog[228], the melting point of SLS is 204-207°C. Thermogravimetric analysis (TGA) of SLS showed that a weight loss of about 56% occurred at 227°C. This temperature was not much higher than the melting point of SLS and indicated that SLS started to decompose soon after it melted. Heating of the SLS in an open oven to 230°C did not lead to melting, but only to a charring of the surface. A TGA scan of SLS is shown in Figure 4.2.

A possible explanation for the appearance of a sharp endotherm at about 115°C (Figure 4.1), instead of at about 204°C, is that at 115°C there was an apparent crystalline phase transition. As Figure 4.1 shows, a small endotherm also appeared at about 205°C, with a peak temperature at 208°C. However, the heat of fusion for this endotherm was 6.94 J/g, compared with 25.58 J/g for the endotherm at 115°C.

Subsequent DSC scans of NR samples with SLS contents which ranged from 0 to 35% showed the appearance of an endotherm at approximately 115°C for NR which contained 5% SLS. A sample of NR with an SLS content of 4% showed no sign of a melting endotherm at that temperature.

These results, therefore, indicated that at a level of 4% all the SLS was present as dissolved surfactant, whereas when the SLS was at a level of 5%, the solubility limit of SLS in NR was exceeded and some SLS was present as dispersed, solid particles. Phase separation therefore occurred at an SLS level of 5%, i.e., the SLS was not compatible with the rubber at this level so that a separate SLS phase was formed. The endotherm observed at about 115°C for NR which contained

5% SLS was the result of the phase transition in the dispersed, solid SLS particles. DSC scans of NR which contained 4% and 5% SLS are shown in Figure 4.3.

The appearance of an endotherm at about 115°C was more pronounced in NR which contained 6% and 10% SLS, as shown in Figure 4.4. An increase in the SLS content of rubber-SLS formulations resulted in an increase in the area of the endotherm, as can be seen in Figure 4.5. Samples which contained 25% and 35% SLS (Curves I and II, respectively, in Figure 4.5), showed that most of the SLS was obviously present as a separate phase, i.e., as dispersed, solid surfactant particles. The broad endotherms observed for these samples, as opposed to the sharp endotherm for SLS, could be attributed to interference with the phase transition due to dispersion of the SLS in the rubber.

DSC scans of IR with SLS contents which ranged from 0 to 35% showed that phase separation started at a level of 4% SLS, which suggests that the solubility limit of SLS in IR was 3%. This is illustrated in Figure 4.6. As with NR, an increase in the SLS content of IR samples resulted in an increase in the area of the endotherm. This is illustrated in Figure 4.7 for IR samples which contained 4%, 6%, 8% and 10% SLS.

All the NR and IR samples referred to above were stored at 0°C. Before they were analyzed, these samples were removed from the freezer and allowed to equilibrate at room temperature for a period of approximately 24 hours. DSC analysis of NR samples which contained different loadings of SLS was repeated after they had been stored at room temperature for 6 months. DSC scans of these samples showed a marked increase in the solubility limit of SLS in NR. Phase separation, i.e., the appearance of an endotherm, occurred when the level of SLS was 10%, as shown in Figure 4.8. These results illustrated the importance of storage temperature and time in the determination of the solubility limit of SLS in elastomers.

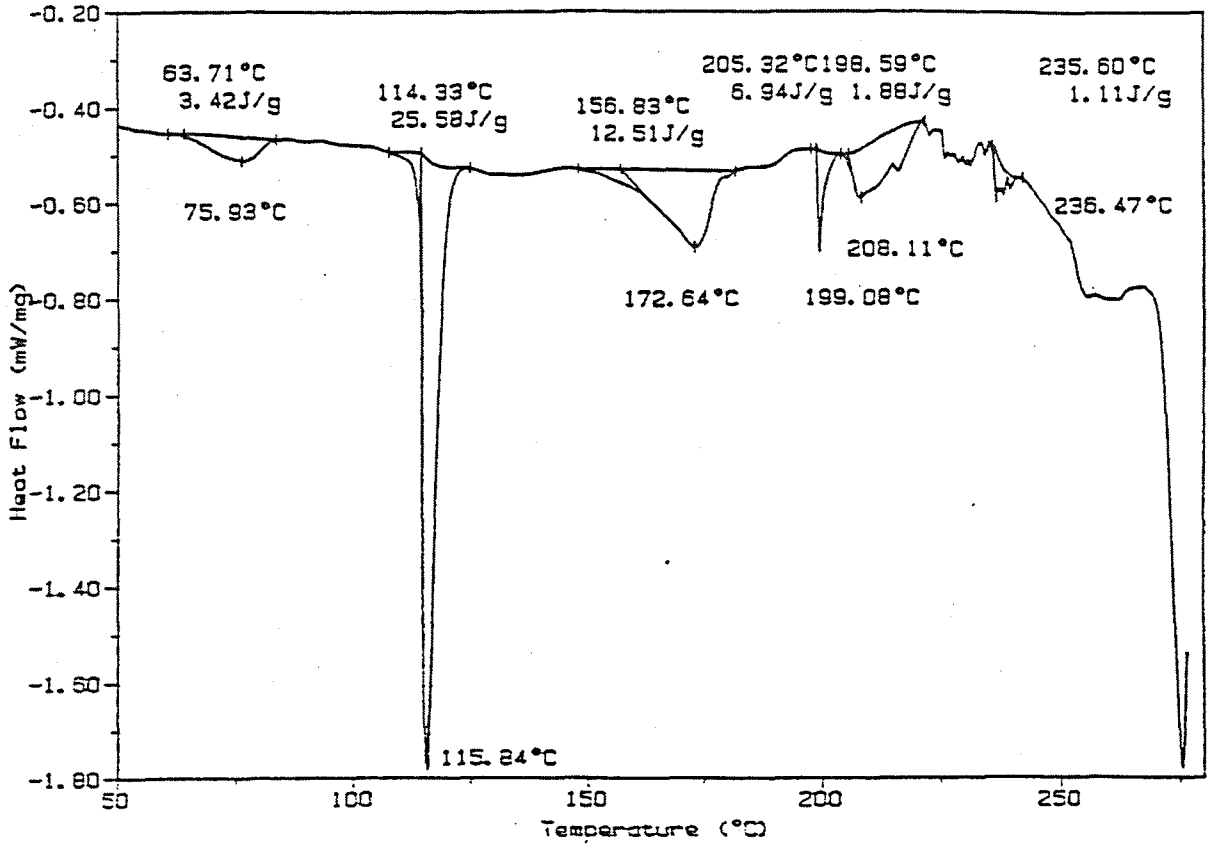

FIGURE 4.1 DSC scan of sodium lauryl sulphate (Texapon K12), showing the endotherm at about 115°C.

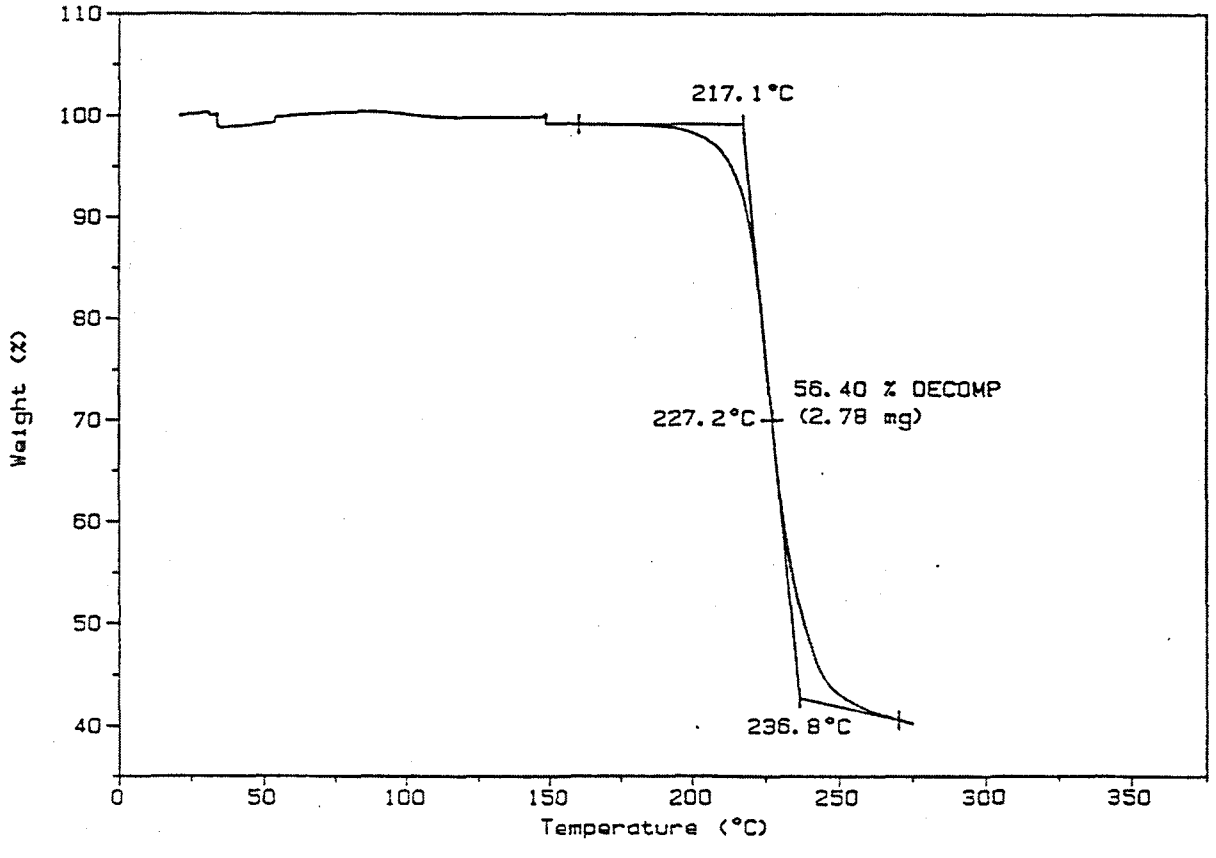

FIGURE 4.2 TGA scan of sodium lauryl sulphate (Texapon K12).

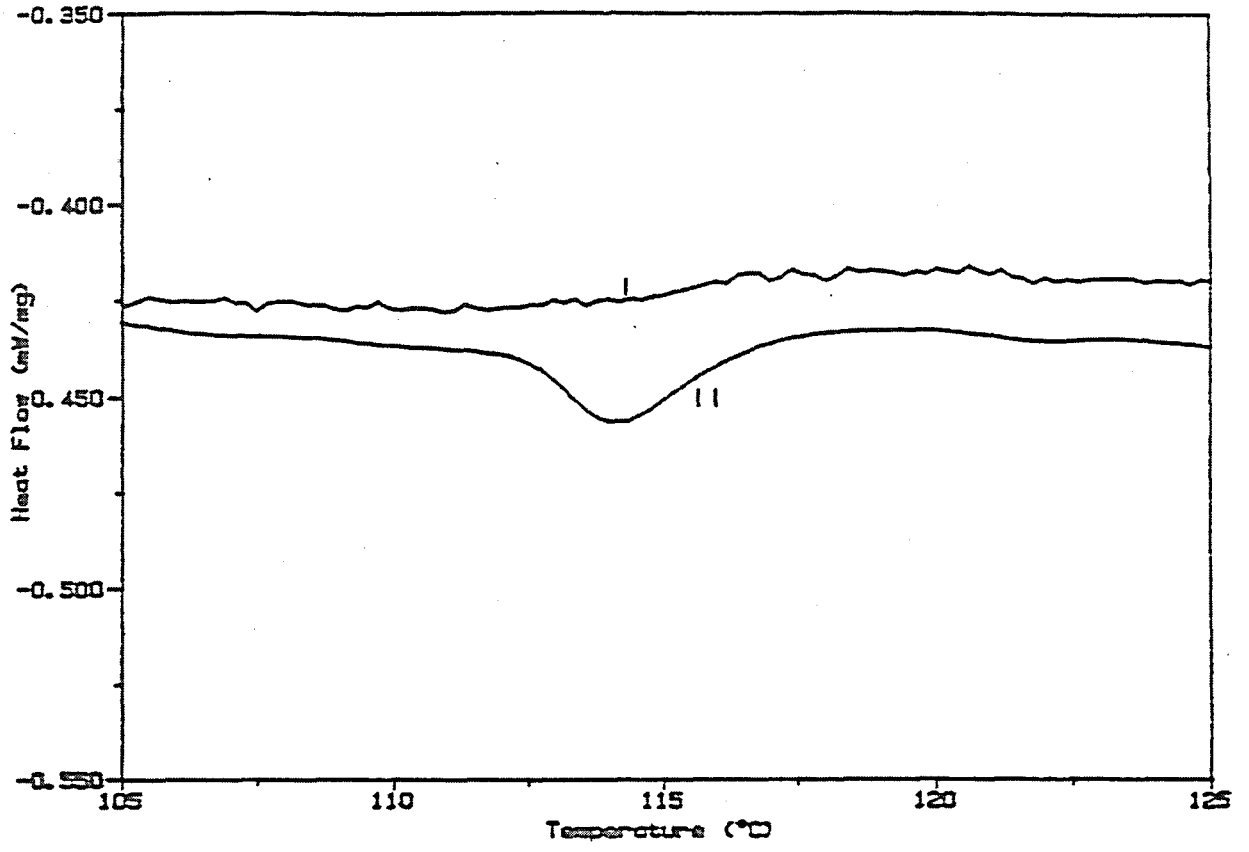

FIGURE 4.3 DSC scans of natural rubber containing 4% SLS (Curve I) and 5% SLS (Curve II).

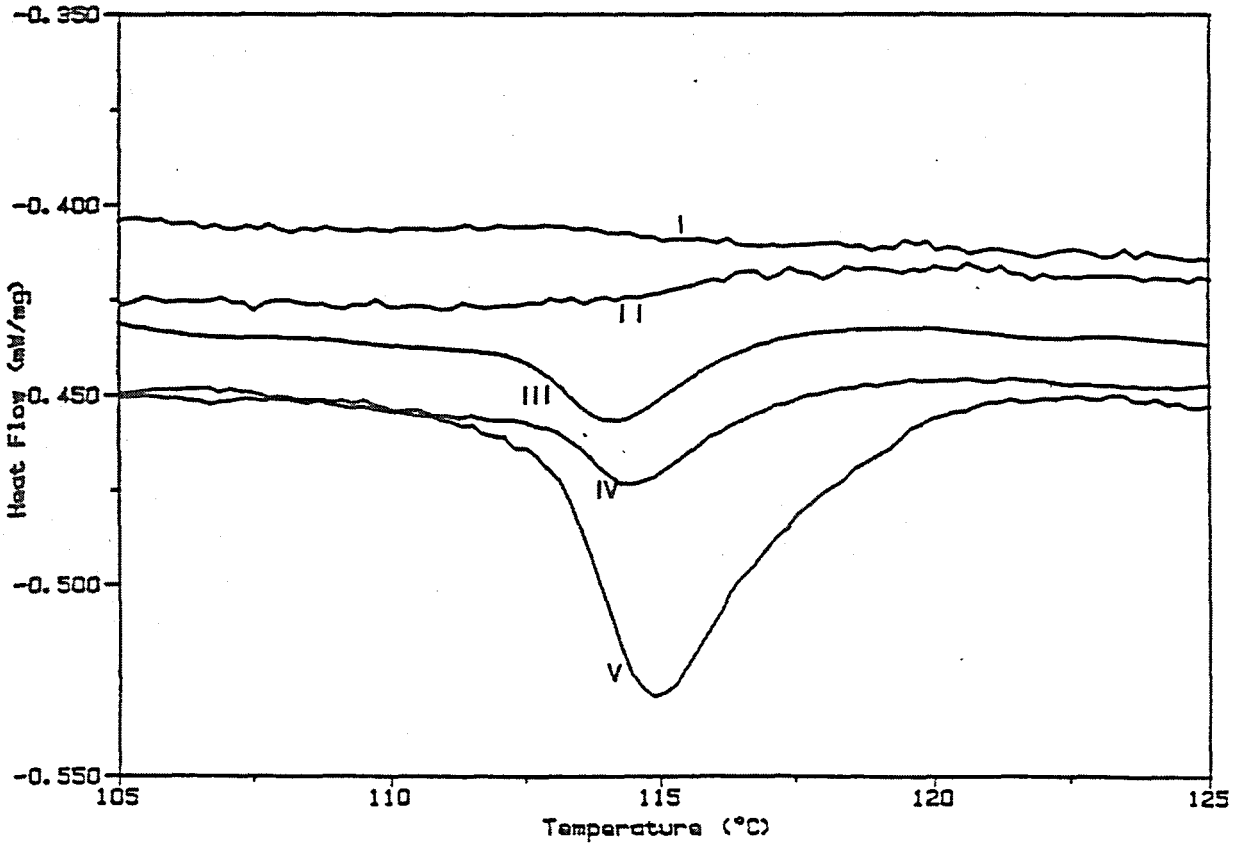

FIGURE 4.4 DSC scans of natural rubber containing 0% SLS (Curve I), 4% SLS (Curve II), 5% SLS (Curve III), 6% SLS (Curve IV) and 10% SLS (Curve V).

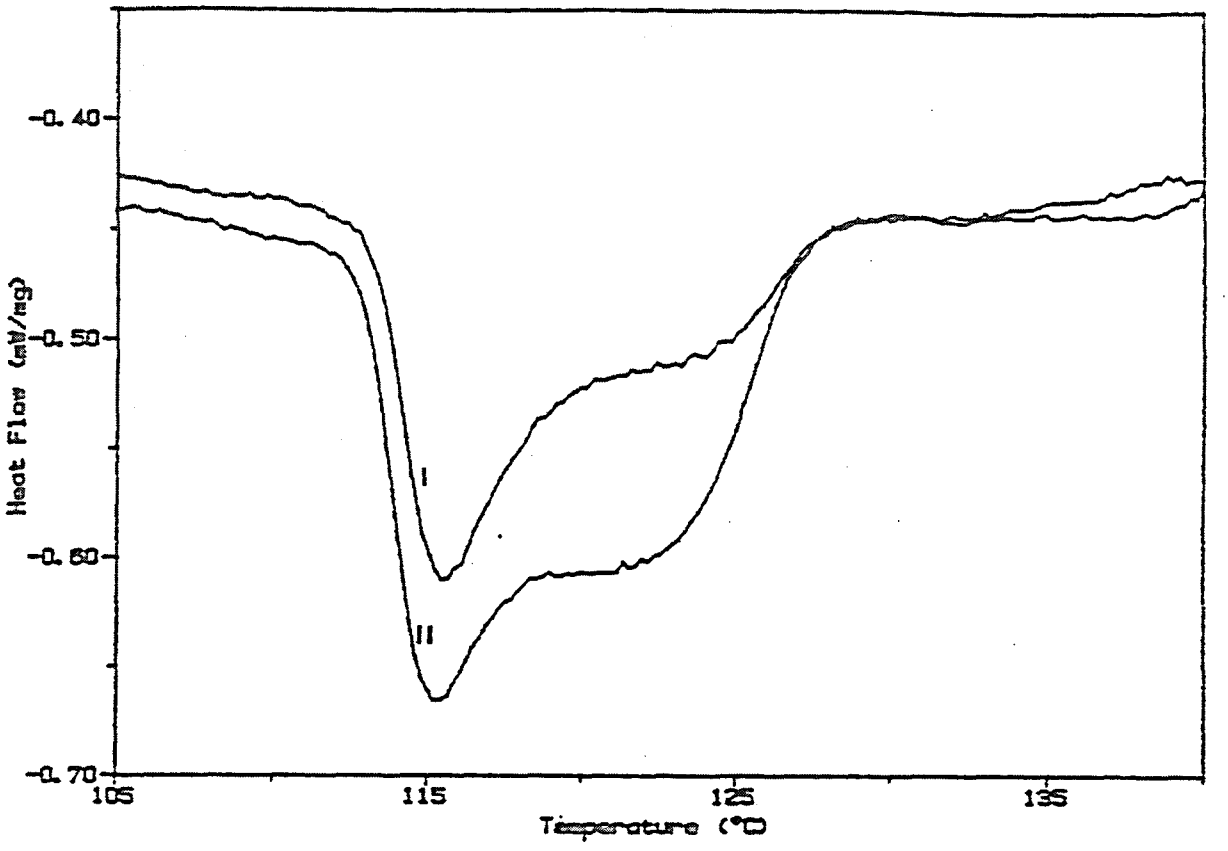

FIGURE 4.5 DSC scans of natural rubber containing 25% SLS (Curve I) and 35% SLS (Curve II).

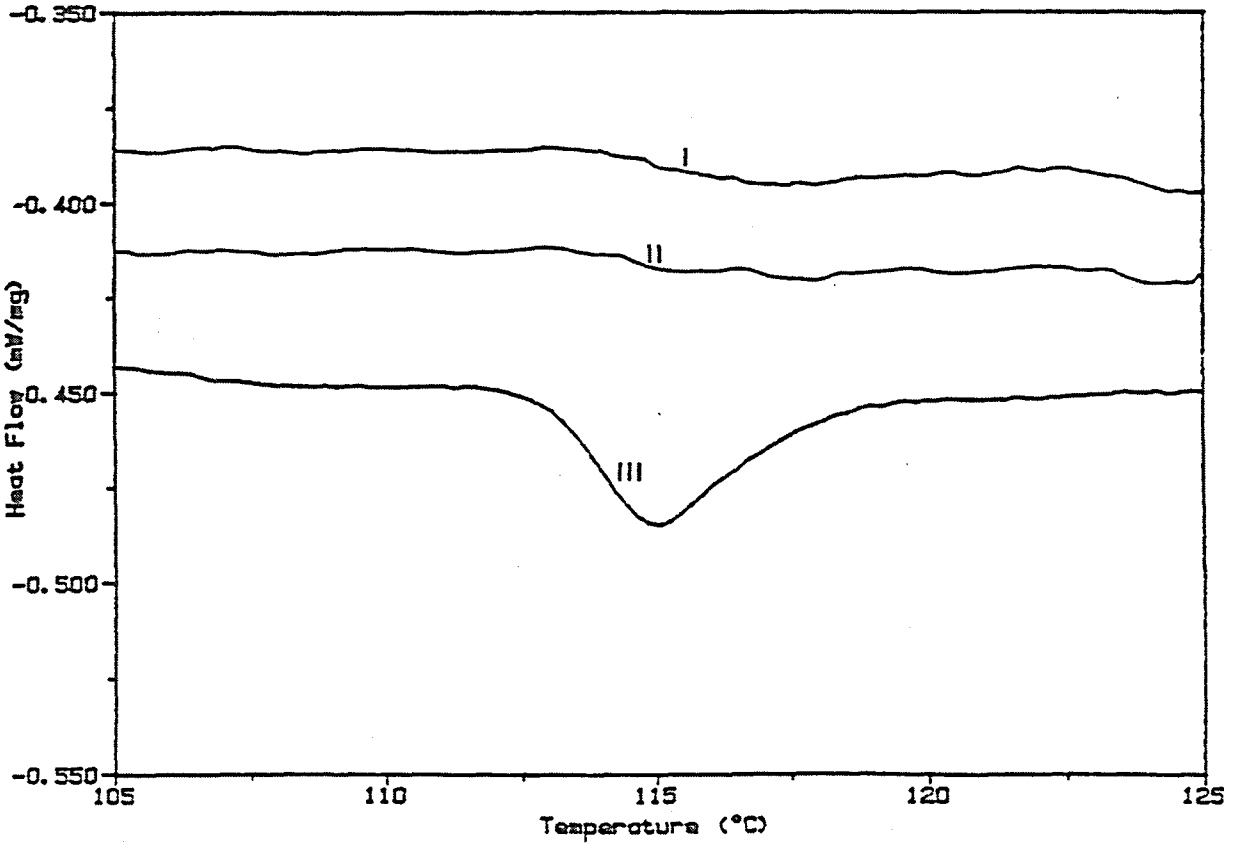

FIGURE 4.6 DSC scans of synthetic polyisoprene containing 0% SLS (Curve I), 3% SLS (Curve II) and 4% SLS (Curve III).

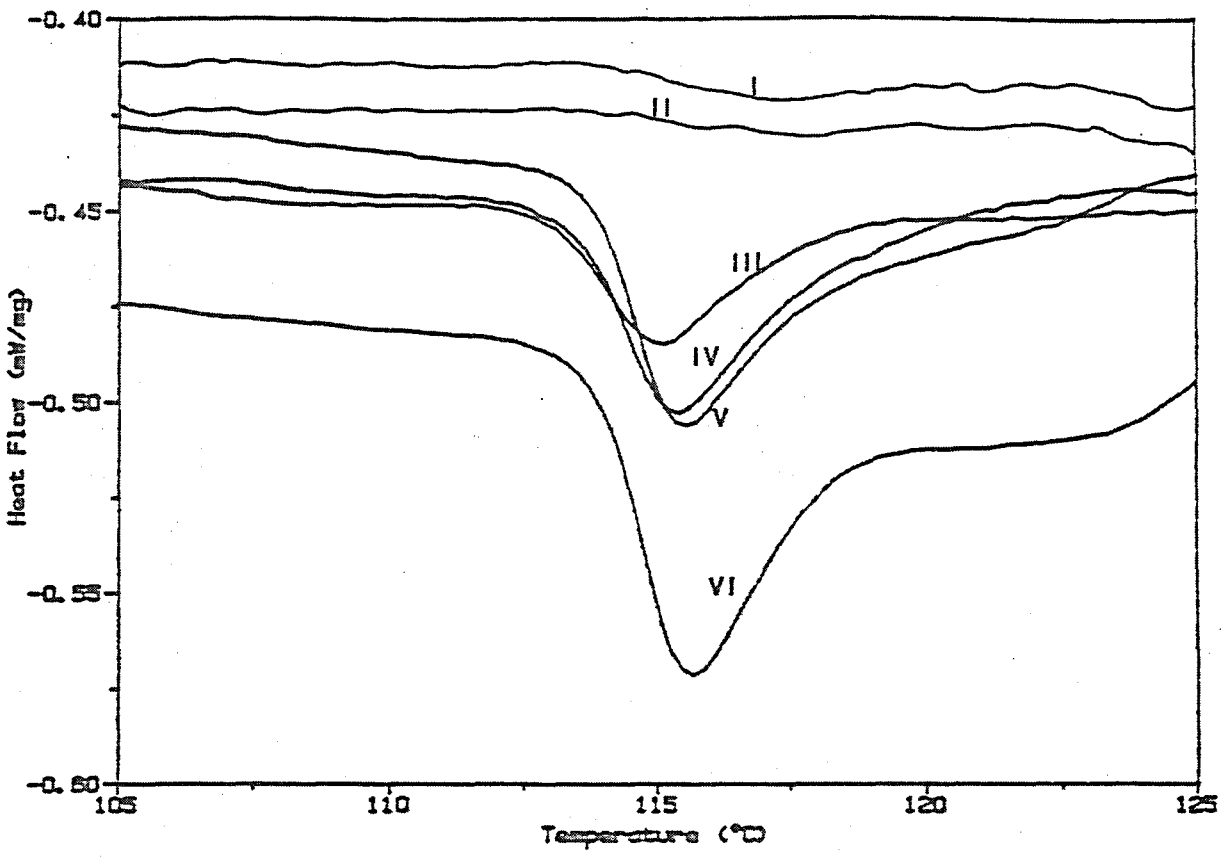

FIGURE 4.7 DSC scans of synthetic polyisoprene containing 0% SLS (Curve I), 3% SLS (Curve II), 4% SLS (Curve III), 6% SLS (Curve IV), 8% SLS (Curve V) and 10% SLS (Curve VI)

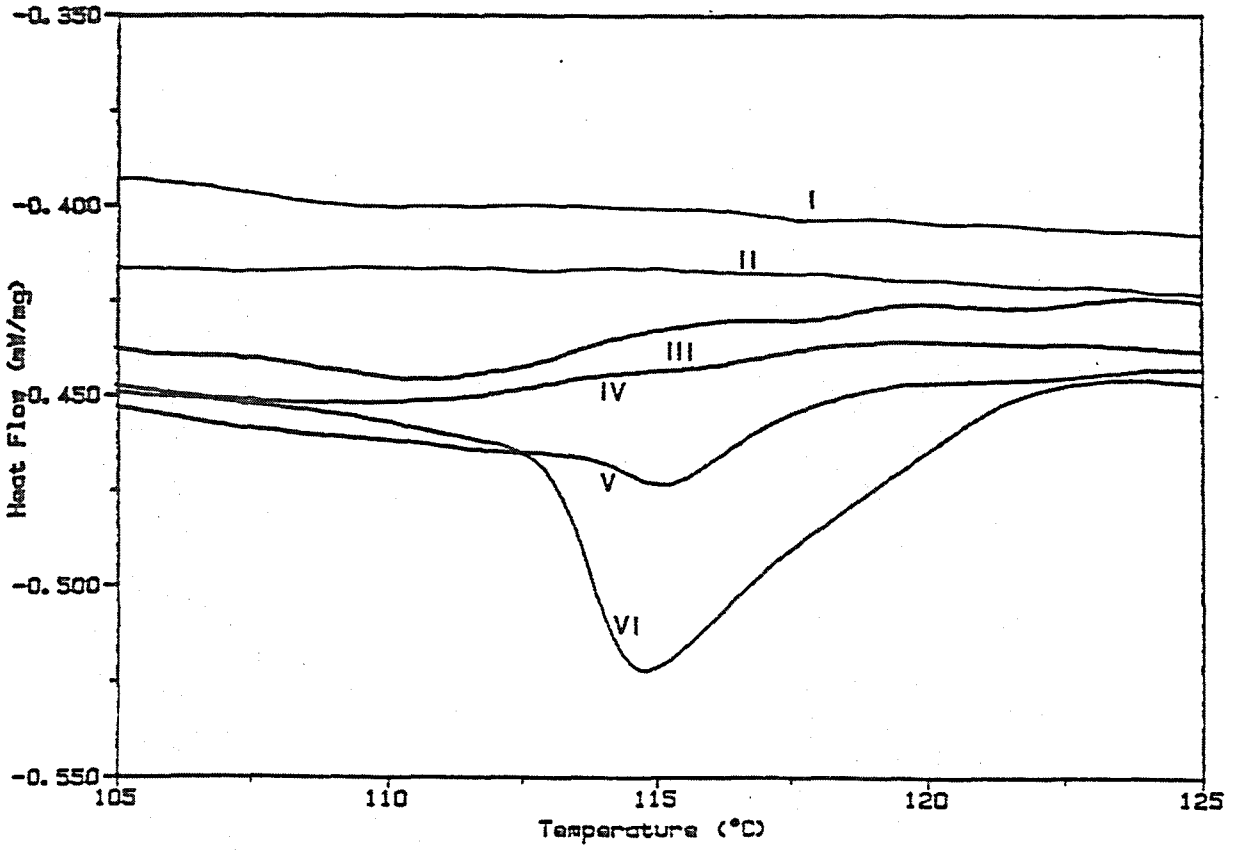

FIGURE 4.8 DSC scans of natural rubber containing 0% SLS (Curve I), 4% SLS (Curve II), 8% SLS (Curve III), 9% SLS (Curve IV), 10% SLS (Curve V) and 15% SLS (Curve VI). These samples were stored at room temperature for 6 months before they were analyzed.

4.3 THE EFFECT OF THE SLS LOADING ON THE VULCANIZATION (CURING) OF CONTROLLED-RELEASE ELASTOMERIC FORMULATIONS

For the benefit of the reader who is not familiar with the chemistry of accelerated sulphur vulcanization, a brief overview of this subject is presented in Appendix 3A.

4.3.1 Determination of the Cure Rates of Rubber Masterbatch Formulations

The cure rates of the four masterbatch formulations which were used for the preparation of controlled-release samples were determined by Monsanto rheometer studies, as discussed in Chapter 3, Section 3.4.3. The compositions of these masterbatch formulations were given in Chapter 3, Table 3.2. The rheographs, together with the information they provided regarding the cure rates of masterbatch formulations, are given in Appendix 3B.

The rheographs showed that at 150°C $t_c(90)$, i.e., the time required to achieve a crosslink-density of 90%, was 4,1 minutes for Formulation A (NR), 10,8 minutes for Formulation B (SBR), 7,4 minutes for Formulation C (NR/SBR 50:50 blend), and 7,0 minutes for Formulation D (IR), while $t_c(98)$ was 6,8, 18,0, 13,6 and 13,6 minutes for Formulations A, B, C and D, respectively. Initially, controlled-release rubber-SLS samples based on Formulation A were vulcanized at 150°C for 12 minutes, and those based on Formulations B, C and D were vulcanized at 150°C for 24 minutes to ensure maximum crosslink-density. However, during the preparation of controlled-release samples it was found that samples which contained high loadings of SLS were insufficiently vulcanized. In order to solve this problem, the vulcanization temperature was increased to 160°C during all subsequent sample preparations, but this did not improve the crosslinking of rubber formulations which contained high loadings of SLS. It was, therefore, apparent that high SLS loadings had had a detrimental effect on the vulcanization process. In order to determine the level at which the SLS started to interfere with the vulcanization reaction, samples of NR and IR which contained different loadings of SLS were analyzed by TMA and DSC, as discussed in Chapter 3, Sections 3.4.11.1 and 3.4.11.2, respectively. The results of these analyses are discussed in the following sections.

4.3.2 Thermomechanical Analysis (TMA) of Rubber-SLS Formulations

The use of TMA for studying the degree of cure of elastomers is well known[229]. The method involved the determination of the coefficient of linear expansion, α, which is a measure of the degree of cure of an elastomer, as discussed in Chapter 3, Section 3.4.11.1. Vulcanized NR formulations which contained 0 to 55% SLS (Chapter 3, Table 3.9) were analyzed by TMA.

A typical TMA scan is shown in Figure 4.9. This figure shows that α was calculated from the linear portion of the scan over the temperature range 80°C - 120°C. The α values obtained for a series of NR samples with different SLS contents are given in Appendix 3C. Figure 4.10 shows a plot of the coefficient of linear expansion, α , as a function of the SLS loading. As mentioned in Chapter 3, Section 3.4.11.1, a lower α value indicates a higher degree of cure, whereas a higher α value indicates a lower degree of cure. Figure 4.10 shows that at SLS loadings of 0 - 15% the α values decreased markedly. This suggests that the degree of cure increased with an increase in the SLS loading, which was, of course, impossible. An explanation for these results could be that the scattering of α values was caused by a mechanical defect of the probe which was used to measure these values. However, since an increase in the SLS content resulted in a decrease in the volume fraction of rubber per test specimen, the possibility must be considered that this technique is not suitable for determining the degree of cure of elastomers which contain high loadings of foreign chemicals such as SLS.

4.3.3 Vulcanization Kinetics of Rubber-SLS Formulations by Differential Scanning Calorimetry (DSC)

DSC scans were done on unvulcanized NR and IR samples which contained 0 to 35% SLS (Chapter 3, Table 3.9). Curing exotherms were observed for all these samples, except for NR and IR samples which contained 35% SLS. The curing exotherms were analyzed by means of the Borchardt & Daniels DSC Kinetics Data Analysis software.

The use of the DSC kinetics method for obtaining reaction kinetics information has been discussed by Kah et al.[230]. This method is based on the assumption that the rate of evolution of heat from a reaction is proportional to the rate of the chemical reaction and, therefore, the total amount of heat evolved up to any stage of the reaction is proportional to the amount of reactants consumed up till then.

If it is assumed that the reagents are present in stoichiometric proportions and that there is only one slow step in the reaction mechanism, the general n'th-order rate expression can be written in terms of concentration in logarithmic form as follows:

$$\ln k(T) = \ln \left\{ \frac{1}{C_o} \left[\frac{dC}{dt} \right] \quad \left[\frac{C_o - C}{C_o} \right]^n \right\} \qquad (4.1)$$

where C_o is the initial concentration, C is the amount reacted at time t, dC/dt is the rate of disappearance of reactants, n is the order of the reaction and k(T) is the temperature-dependent rate constant.

Rewriting Equation (4.1) in terms of the observable variables obtained from the DSC scan, gives the following equation:

$$\ln k(T) = \ln \left\{ \frac{1}{\Delta H_o} \left[\frac{dH(t,T)}{dt} \right] \left[\frac{\Delta H_o - H(t,T)}{\Delta H_o} \right]^n \right\} \qquad (4.2)$$

where ΔH_o is the total heat of reaction, H(t, T) is the amount of heat evolved up to time t and temperature T, and dH(t, T)/dt is the time- and temperature-dependent heat flow.

By substituting the Arrhenius expression

$$\ln k(T) = \ln Z - \frac{E}{RT} \qquad (4.3)$$

into Equation (4.2) and rearranging, the following equation is obtained:

$$\left\{ \ln \frac{1}{\Delta H_o} \left[\frac{dH(t,T)}{dt} \right] \right\} = \ln Z - \frac{E}{RT} + n \left\{ \ln \left[\frac{\Delta H_o - H(t,T)}{\Delta H_o} \right] \right\} \qquad (4.4)$$

which is of the form

$$P = a + bx + cy \qquad (4.5)$$

The data are fitted to this expression by a multiple-regression technique. The DSC kinetics method, therefore, permits the calculation of the activation energy (E) and the pre-exponential factor (Z) in the Arrhenius expression (Equation 4.3), as well as the calculation of the heat of reaction (ΔH) and the order of the reaction (n)[210].

It was not the intention of this investigation to obtain quantitative reaction-kinetics information for the accelerated-sulphur-vulcanization reaction used for the curing of rubber-SLS formulations. The objectives were to determine a pattern which would illustrate how the SLS loading influenced the vulcanization of rubber formulations and also to determine at which level of SLS content the inhibition of the vulcanization process became significant.

The information obtained from the analysis of the curing exotherms for NR-SLS and IR-SLS formulations is given in Tables 3D.1 and 3D.2, respectively, in Appendix 3D. A typical curing exotherm is shown in Figure 4.11. Figure 4.12 shows the curing exotherms for NR formulations which contained 0, 5, 13 and 15% SLS, and Figure 4.13 gives the curing exotherms for IR formulations which contained 0, 11 and 15% SLS. These figures show that the area of the exothermic peak (as given by the ΔH values), the onset temperature, and the peak temperature were influenced by the SLS content of the formulation.

Figures 4.14, 4.15 and 4.16 illustrate the effect of the SLS content on the curing of natural-rubber formulations. The heat of reaction (ΔH) is a measure of the area of the exothermic peak and is, therefore, an indication of the extent to which curing occurred. Figure 4.14 shows that ΔH increased with an increase in the SLS content until an SLS level of 5% was reached. Above this 5% level, ΔH started to decrease and at an SLS level of 25% the peak area decreased considerably. Figure 4.14 suggests that at levels of up to 5% the SLS actually played a positive role in the curing process. At SLS levels of 6-15%, the peak areas (i.e., ΔH values) decreased slightly. This was probably because the SLS which existed as a separate phase dissolved some of the sulphur, or other vulcanization additives, and thereby inhibited the curing reaction to a certain extent. At SLS levels of 25% and more, the SLS interfered seriously with the curing reaction, since most of the SLS was present as a dispersed phase. It is also important to realize that at increasing SLS levels, the volume fraction of rubber available for crosslinking was reduced. Corrections for this did not alter the trend and uncorrected values are used in Figures 4.14 and 4.17.

When the onset and peak temperatures were plotted against the SLS loading, as in Figures 4.15 and 4.16, respectively, the same trend was observed. Initially, both the onset and the peak temperature increased until an SLS level of 6% was reached. At SLS levels above 6%, the onset temperature, as well as the peak temperature, decreased slightly. At SLS levels of 25% and more, both the onset and the peak temperatures dropped markedly. The reasons for this are unclear.

Figure 4.17 shows the effect of the SLS loading on the curing of synthetic polyisoprene (IR). At SLS levels up to 3%, which represented the solubility limit of SLS in IR, as discussed in Section 4.2, the SLS loading had little effect on the area of the curing exotherm, as shown by the ΔH values. At SLS levels above 3%, however, the ΔH values decreased markedly. This was, in particular, the case for IR formulations which contained 25% SLS.

From this investigation, it is evident that if rubber-SLS formulations with different SLS contents are vulcanized at the same temperature for the same period of time, the degree of curing of such formulations will vary as a function of the SLS content. For NR and IR formulations which

contained 35% SLS, no curing exotherms were observed. It was, therefore, apparent that rubber formulations which contained 35% or more SLS could be regarded essentially as unvulcanized.

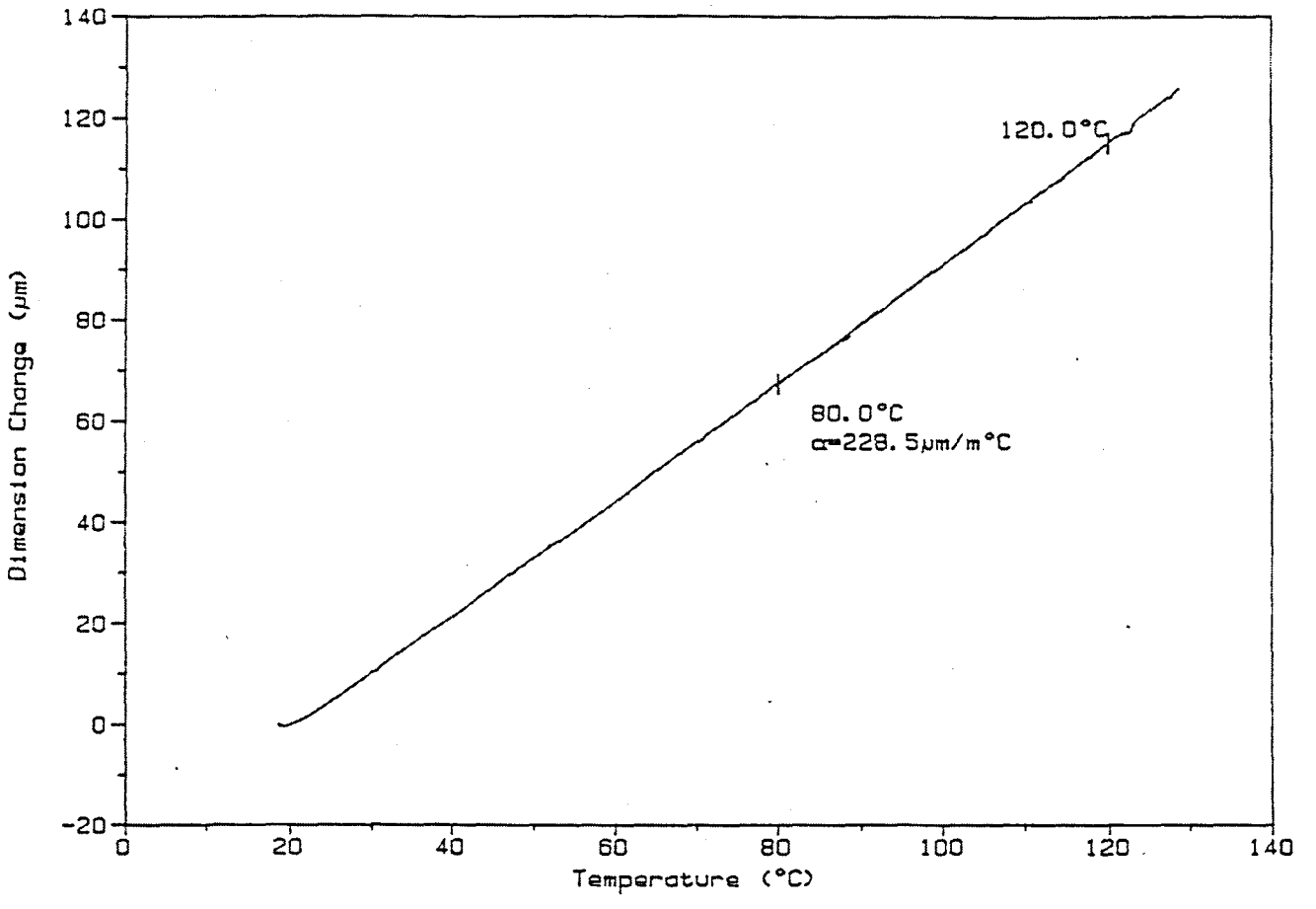

FIGURE 4.9 TMA scan of natural rubber which contained no SLS.

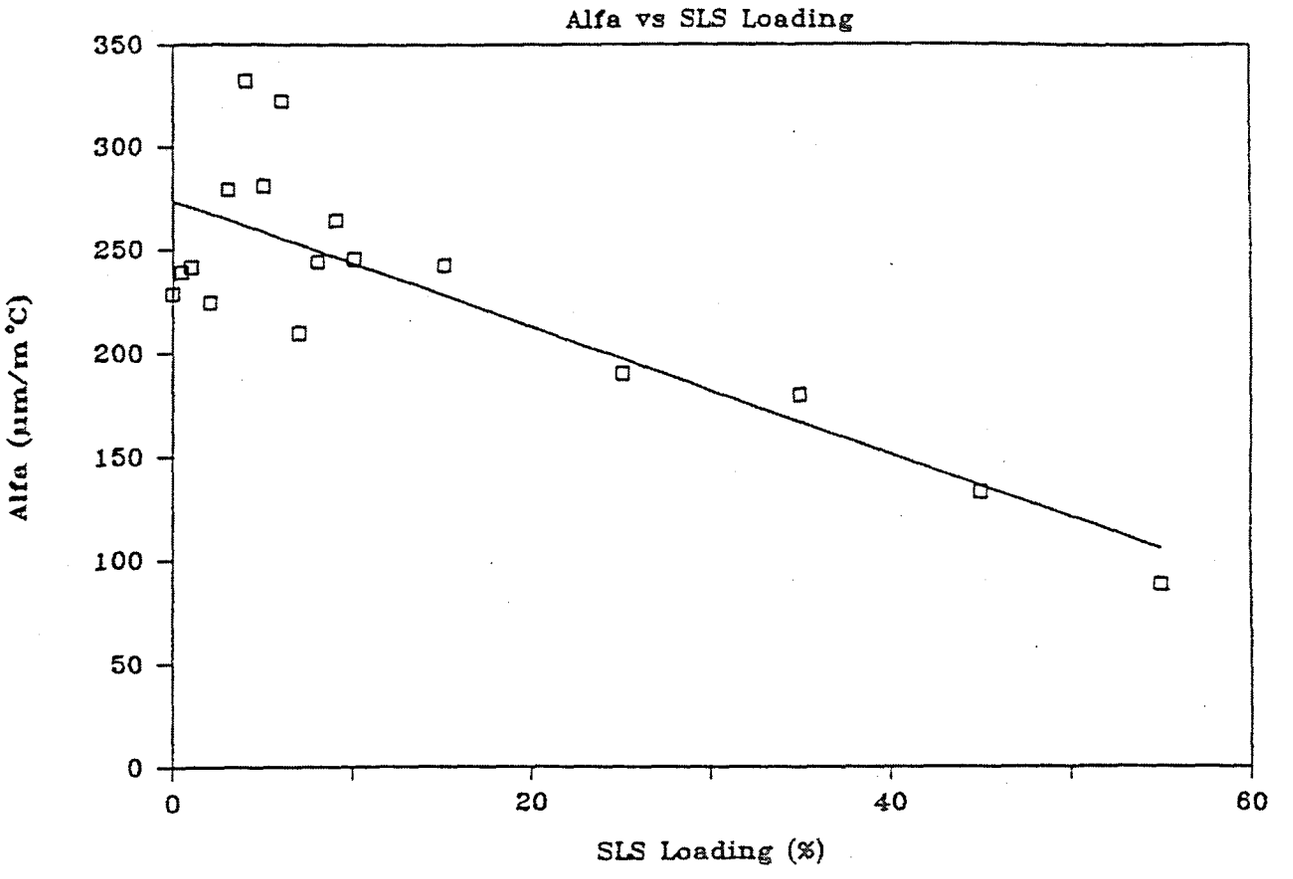

FIGURE 4.10 Variation of the coefficient of linear expansion, α , with SLS loading for a series of natural-rubber samples which contained 0 to 55% SLS.

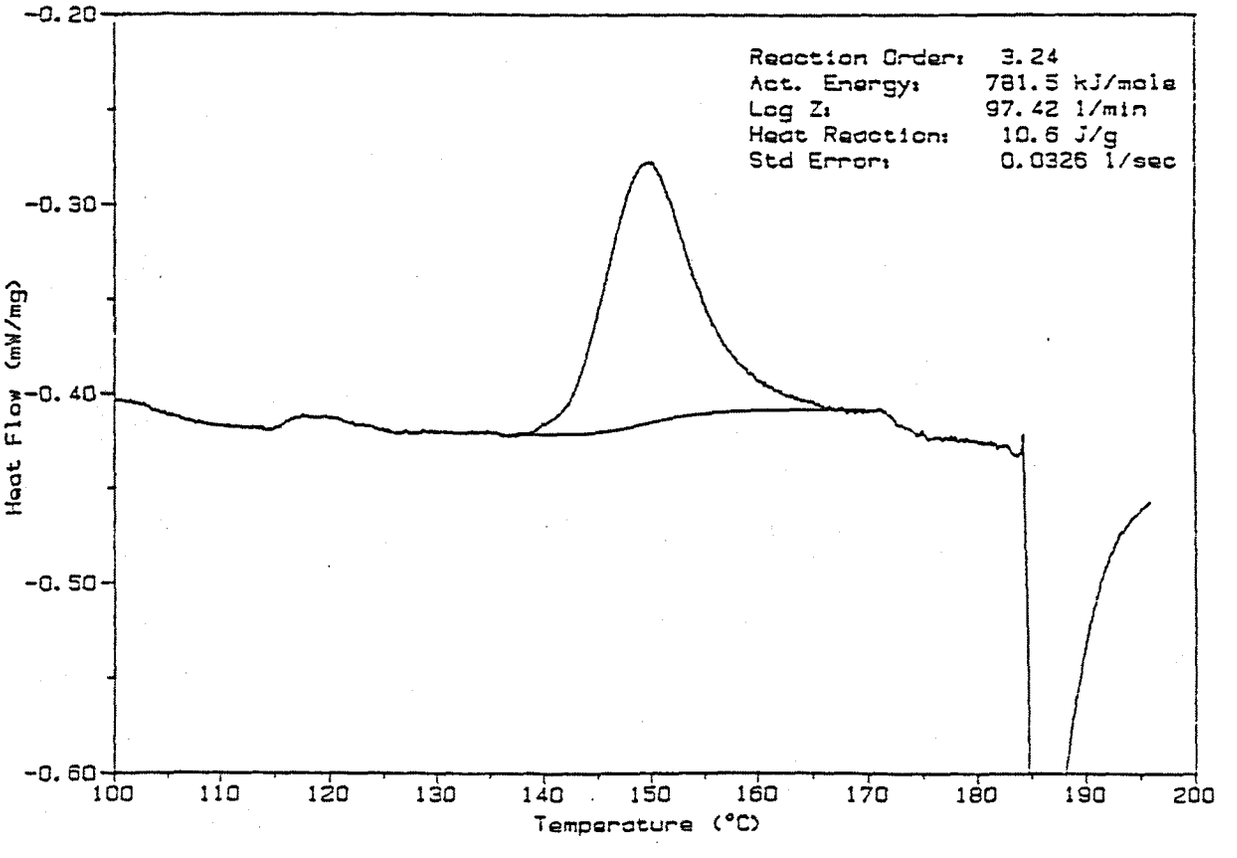

FIGURE 4.11 Curing exotherm for a natural-rubber sample which contained 4% SLS

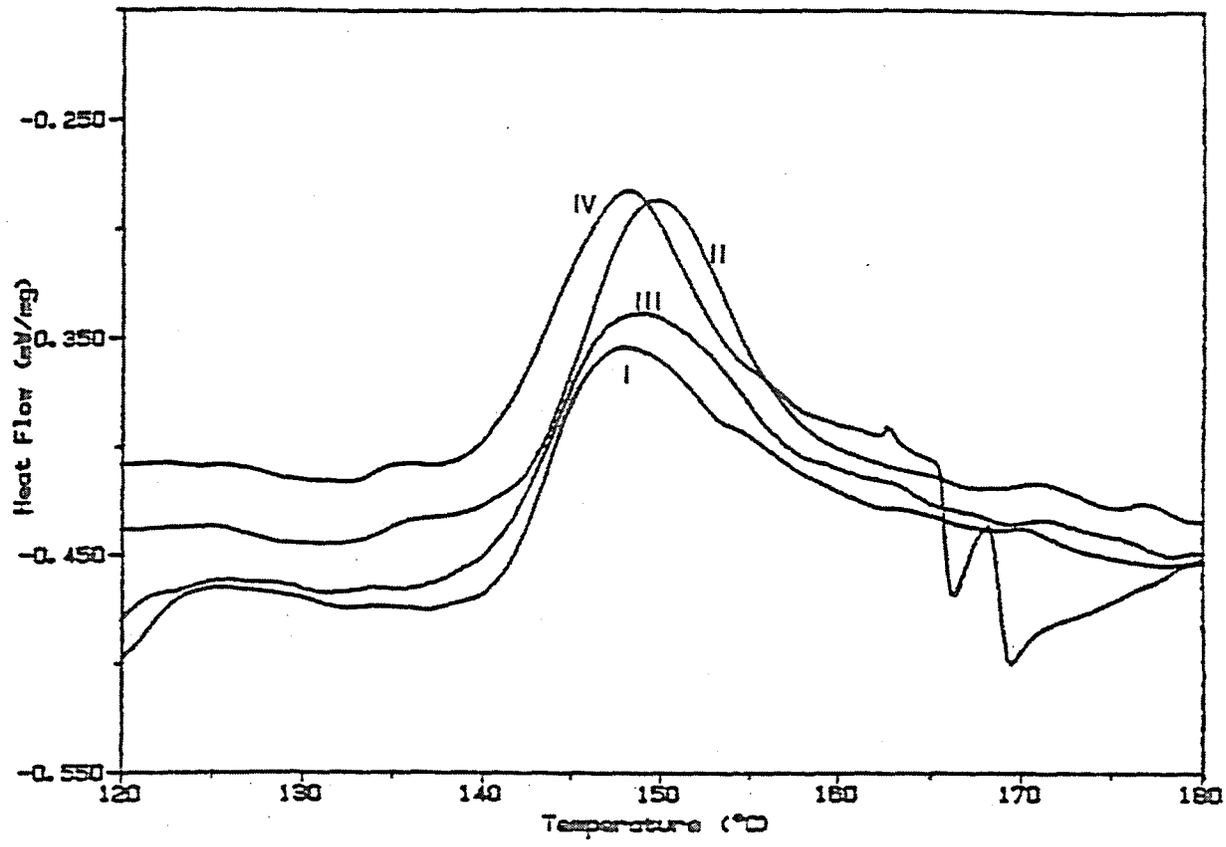

FIGURE 4.12 Curing exotherms for natural-rubber samples which contained 0% SLS (Curve I), 5% SLS (Curve II), 13% SLS (Curve III) and 15% SLS (Curve IV)

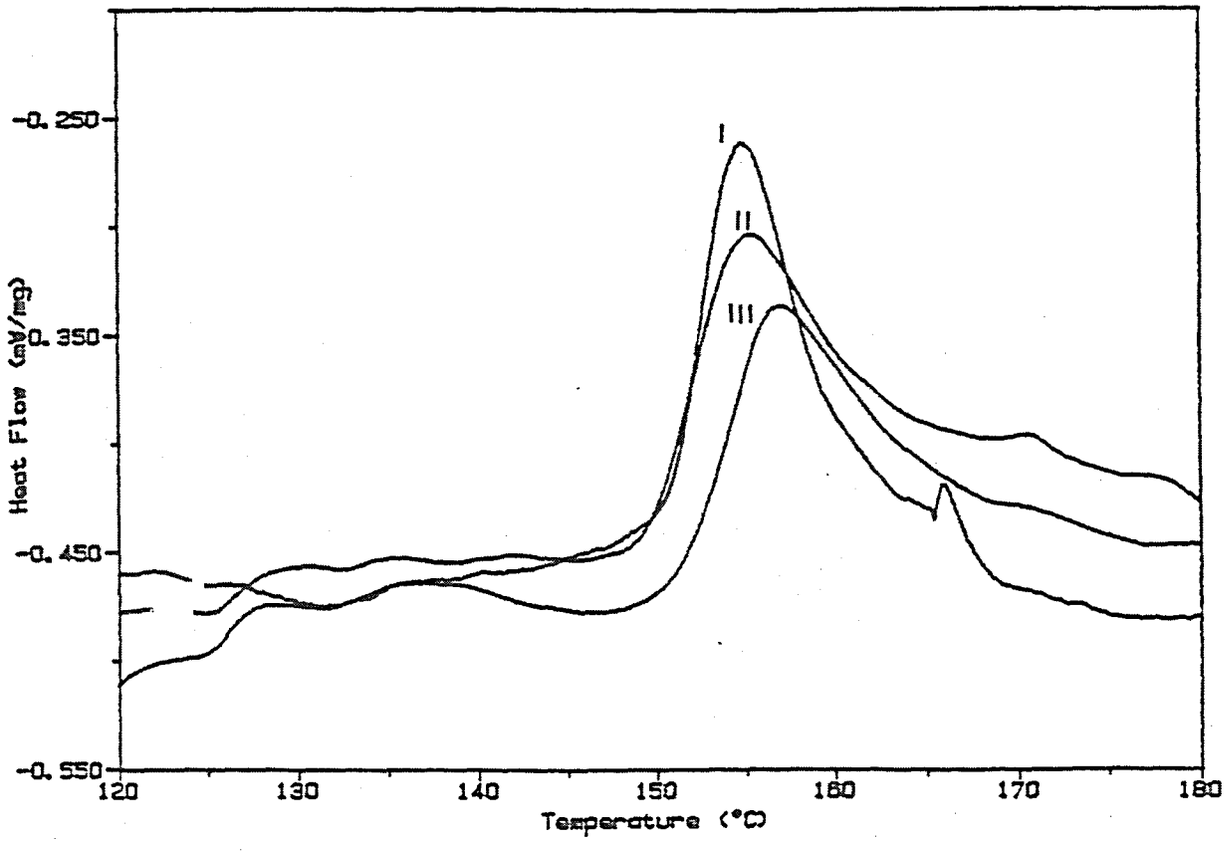

FIGURE 4.13 Curing exotherms for synthetic polyisoprene samples which contained 0% SLS (Curve I), 11% SLS (Curve II) and 15% SLS (Curve III).

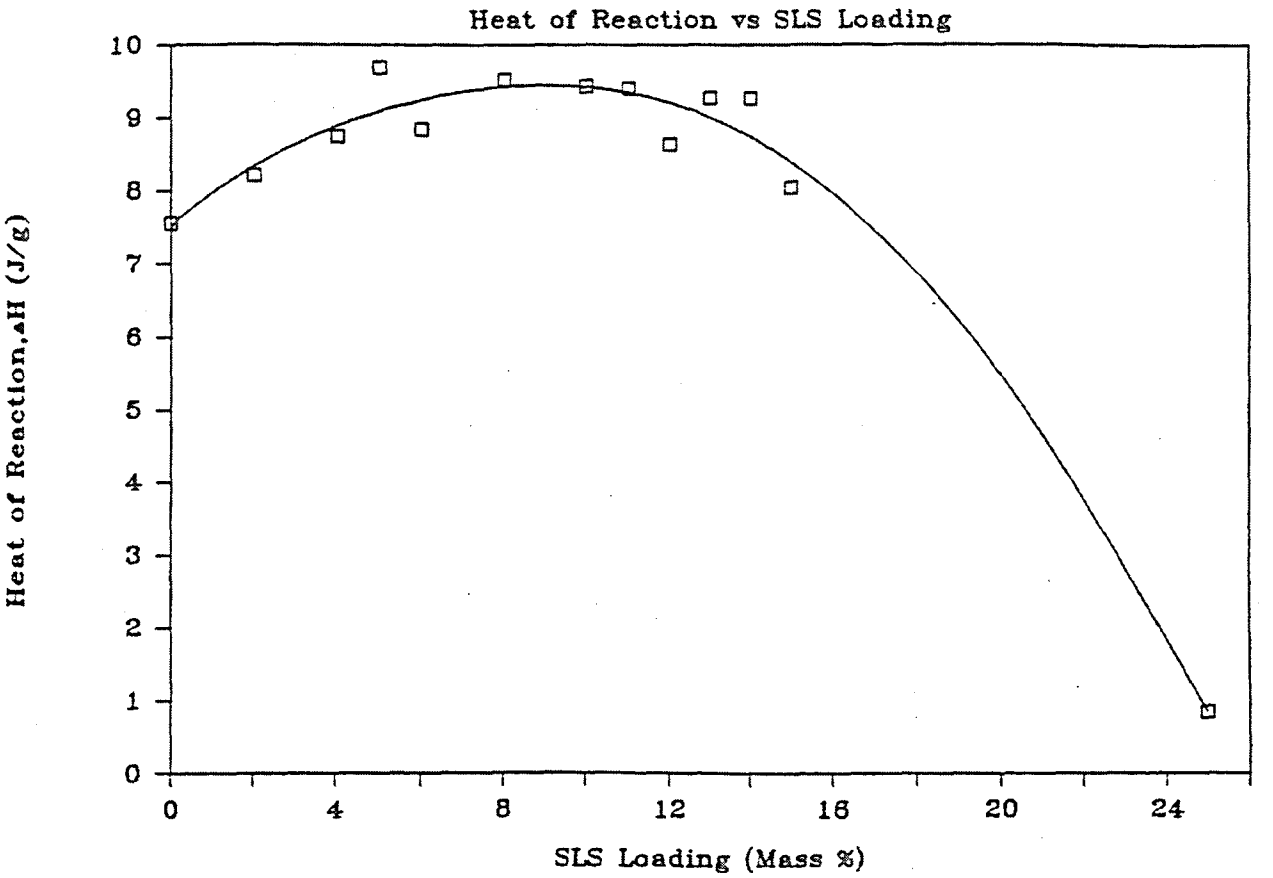

FIGURE 4.14 The change in the heat of reaction, ΔH, as a function of the SLS loading for a series of natural-rubber formulations which contained 0 to 25% SLS.

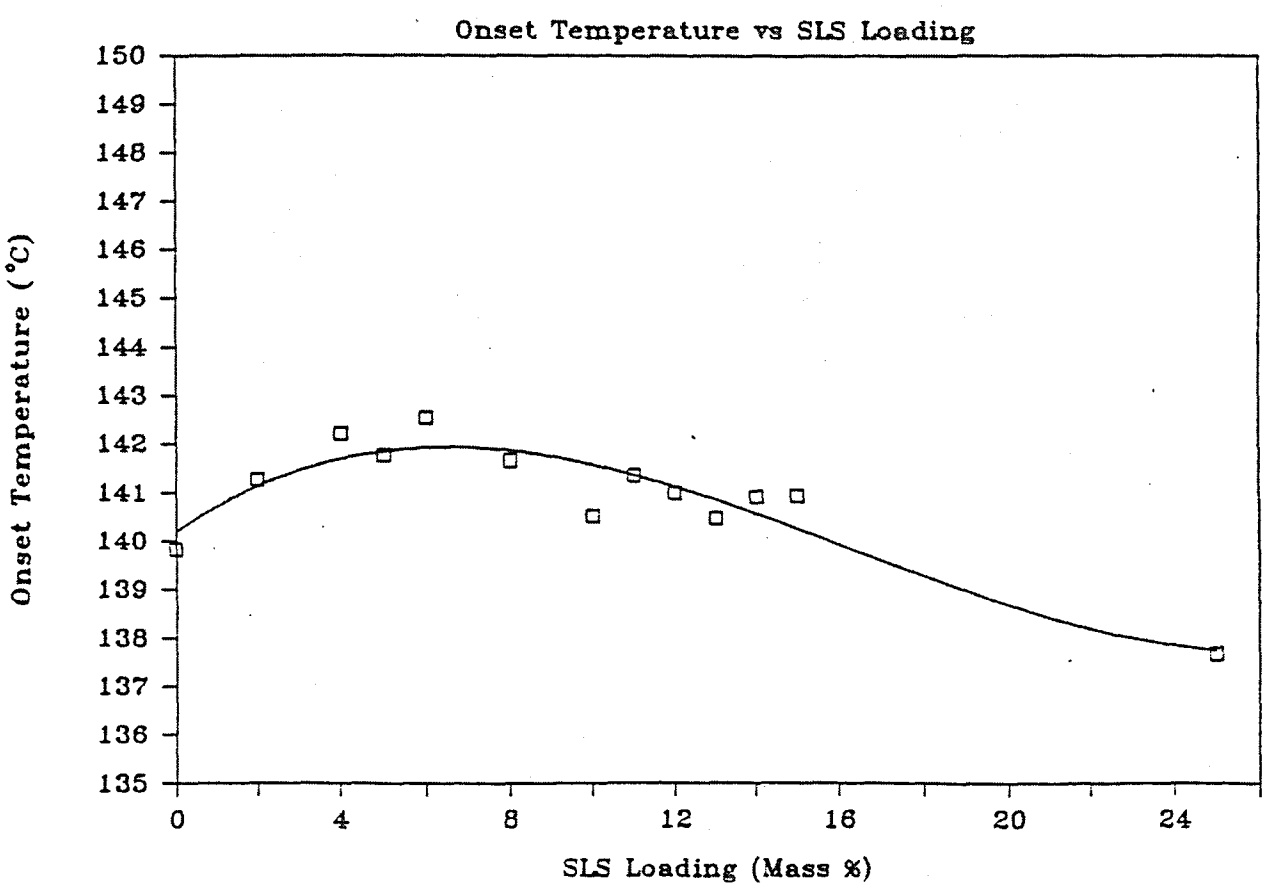

FIGURE 4.15 The change in the onset temperature as a function of the SLS loading for a series of natural-rubber formulations which contained 0 to 25% SLS.

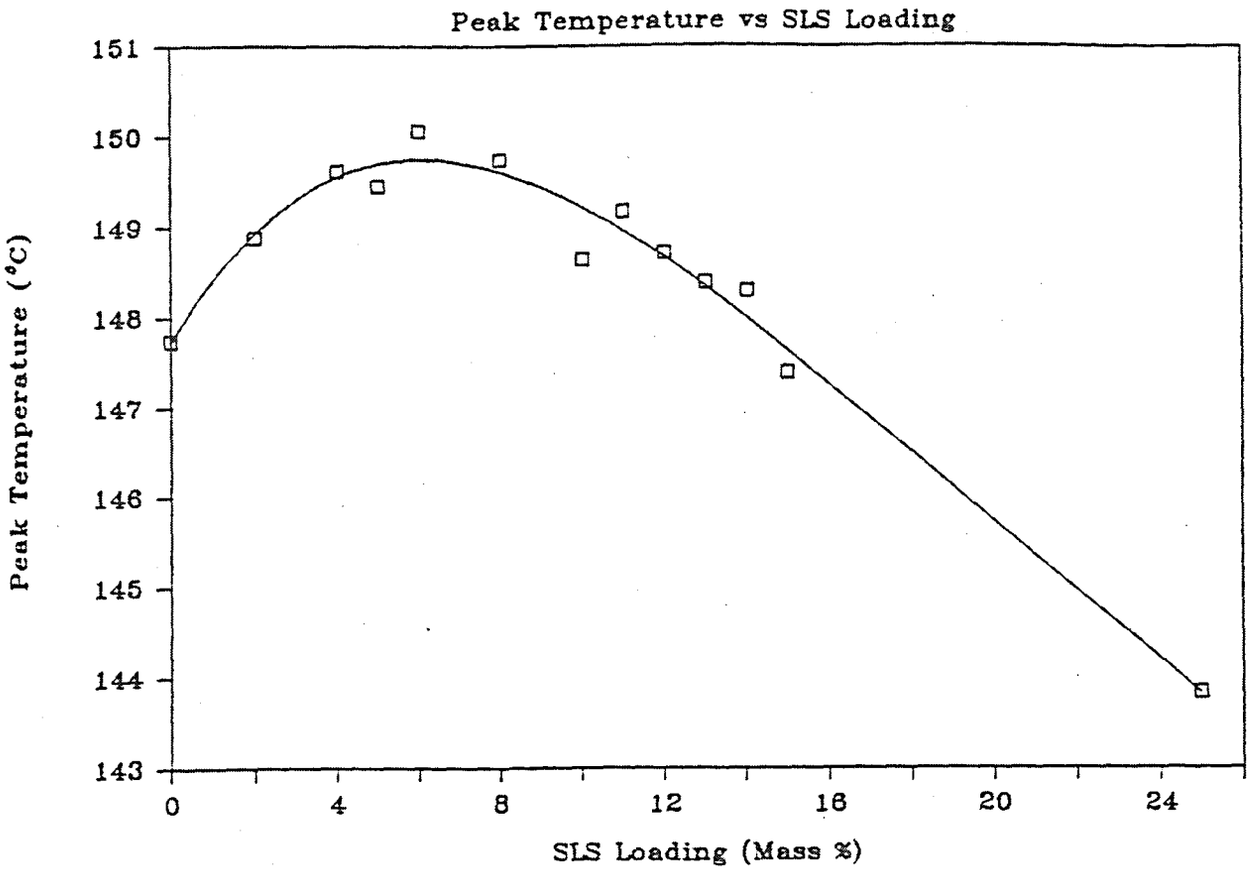

FIGURE 4.16 The change in the peak temperature as a function of the SLS loading for a series of natural-rubber formulations which contained 0 to 25% SLS.

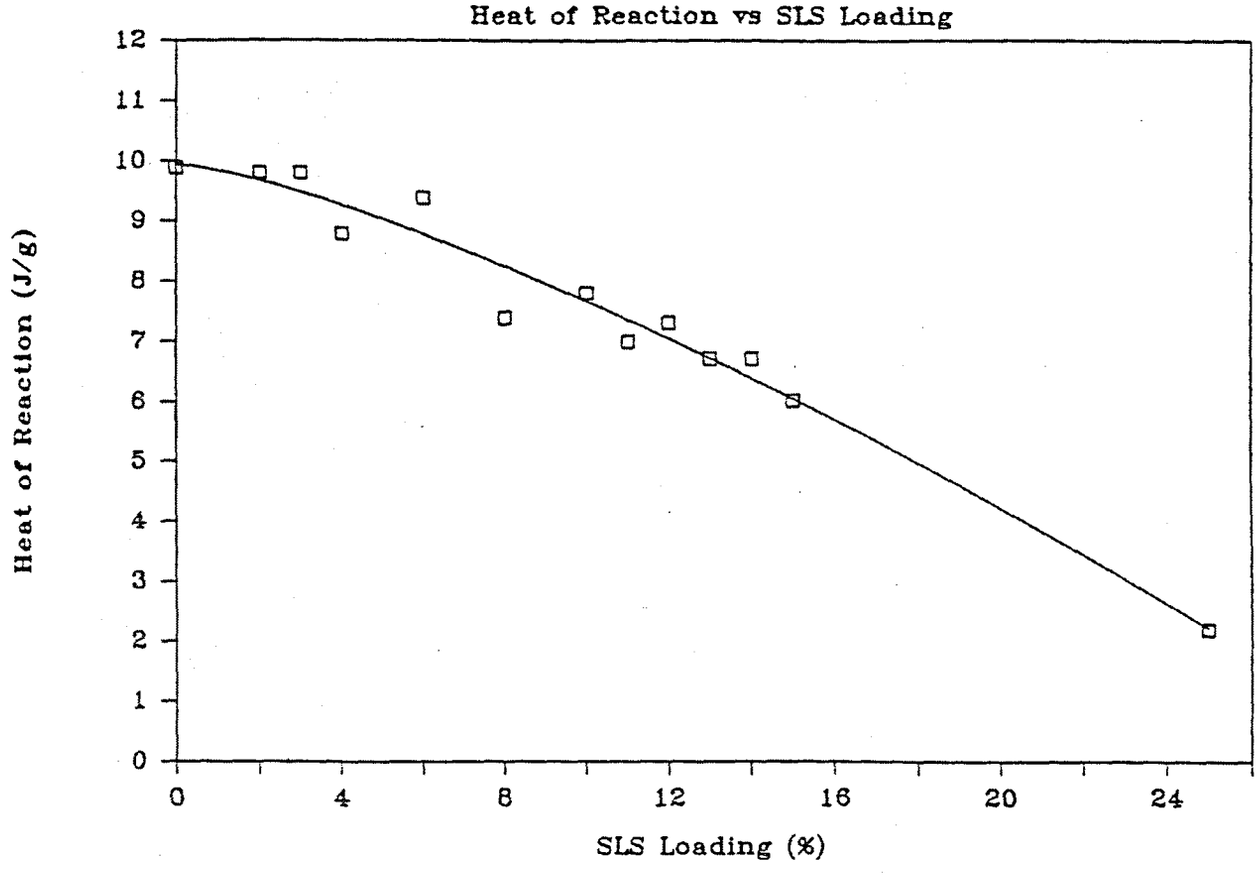

FIGURE 4.17 The change in the heat of reaction, ΔH , as a function of the SLS loading for a series of synthetic polyisoprene formulations which contained 0 to 25% SLS.

4.4 THE KINETICS OF THE RELEASE OF SLS FROM MONOLITHIC ELASTOMERIC PELLETS

Elution experiments were conducted as described in Chapter 3, Section 3.4.4. The concentrations of sodium in the eluates were determined by atomic absorption spectroscopy (see Chapter 3, Section 3.4.5). From these results, the concentrations of SLS in the eluates and the total amounts of SLS released from the various rubber-SLS pellets were calculated. Data were processed by means of an IBM Personal Computer and the LOTUS 1-2-3 software package. The processed data were represented graphically as the released cumulative concentration of SLS, cumulative amount of SLS, fraction or percentage of SLS, or as release rate of SLS, all as a function of time. The data obtained from elution experiments, as well as the processed data, are given in Appendix 4A.

Equations which describe the release kinetics of a solute dispersed in a monolithic device were discussed in Chapter 2, Sections 2.3.3 and 2.4.3.3. For monolithic systems in which the agent is physically dispersed in the matrix phase at a concentration which greatly exceeds its solubility in the matrix, the amount of agent released, M_t, as a function of time, t, is given by:

$$M_t = k_1 t^{1/2} \qquad (4.6)$$

and the release rate of the agent is given by:

$$\frac{dM_t}{dt} = k_2 t^{-1/2} \qquad (4.7)$$

where k_1 and k_2 are constants, as discussed in Chapter 2, Section 2.3.3. The amount released is, therefore, proportional to the square root of time, while the release rate is proportional to the inverse square root of time. In the discussion of his work on rubber-SLS systems, Kleinmann[171] assumed that these relationships were valid, but he did not present any results to prove that this was, in fact, so. It was, therefore, of interest to determine whether the release of SLS from rubber pellets followed $t^{1/2}$-order kinetics, as suggested in the literature on controlled-release systems.

A Turbo Pascal program (code POLI) was used to fit various theoretical equations to the experimental data. These equations were:

$$\sum [SLS] = a_1 t^{1/2} \qquad (4.8)$$

$$\sum [SLS] = a_2 t^{1/2} + c \qquad (4.9)$$

$$\sum [SLS] = a_3 t^{b} \qquad (4.10)$$

where $\sum$[SLS] is the cumulative concentration of SLS released and a_1, a_2, a_3, b and c are constants. The program POLI.PAS is given in Appendix 4B. This program was written for use on an IBM Personal Computer with a Hercules Graphics Card. It read experimental data from an input data file and fitted the theoretical equations given above (i.e., Equations 4.8, 4.9 and 4.10) to experimental data points. The data points obtained experimentally, together with the generated data which represented the line of best fit through these points for each of the three theoretical models, were written in print files. The LOTUS 1-2-3 / FILE IMPORT NUMBERS command was used to import these print files into LOTUS worksheet files. Graphs were created by using the LOTUS 1-2-3 / GRAPH command.

For the purpose of discussion, Equation (4.8) is referred to as the "AVERAGE MODEL", Equation (4.9) is referred to as the "SQUARE-ROOT MODEL", and Equation (4.10) is referred to as the "LOGARITHMIC MODEL". These models were fitted to data obtained from 17 elution experiments (refer to Appendix 1B). The standard deviations (for the AVERAGE MODEL) and correlation coefficients (for the SQUARE-ROOT and LOGARITHMIC MODELS), as well as the values of the constants a_1, a_2, a_3, b and c, for the 113 rubber-SLS samples (cylindrical pellets) which were evaluated, are given in Appendix 4C.

According to the literature, the AVERAGE MODEL should fit the experimental data. However, it was found that, with a few exceptions, this model did not do so. In general, better fits were obtained by using the SQUARE-ROOT and LOGARITHMIC MODELS. Examples of the fits which were obtained are shown in Figures 4.18 to 4.23. Figures 4.18 and 4.19 show plots of the cumulative concentration of SLS released against time for NR which contained 35% SLS (Sample 3) and SBR which contained 35% SLS (Sample 8), respectively. It can be seen that, for these specific samples, all three models fitted the experimental data fairly well (refer to Appendix 4C for correlation coefficients). The correlation coefficients (R) are also given on the graphs which follow.

In general, fairly good fits of the AVERAGE MODEL were obtained only for samples which contained 35% SLS and for natural-rubber samples which contained 45% SLS and 10 phr surface-treated $CaCO_3$. The LOGARITHMIC MODEL fitted most of the experimental data fairly well, as

shown in Figures 4.20 and 4.21 for Sample 7 (SBR which contained 25% SLS) and Sample 13 (NR/SBR blend which contained 35% SLS), respectively. However, the value of the constant b in Equation (4.10) ranged between 0,117 and 0,610. Although the SQUARE-ROOT MODEL fitted some sets of experimental data well, as shown in Figure 4.22 for Sample 61 (IR which contained 35% SLS), it is of little practical use. This model suggests that at time t = 0, some of the SLS has been released already, which is impossible. None of these models fitted the experimental data obtained from elution of samples which contained 45% and 55% SLS, with the exception of Samples 108 to 113 (NR which contained 45% SLS and 10 phr surface-treated $CaCO_3$). Examples of the poor fits obtained for samples with SLS loadings of 45% and higher are shown in Figure 4.23 for SBR which contained 55% SLS.

For most of the samples tested, in particular those which contained 35% and more SLS, release patterns were characterized by an initial release rate which was much higher than expected. Large amounts of SLS were released during the first week of elution. This was followed by the release of substantially smaller and decreasing amounts of SLS during the remaining portion of the test period. With rubber-SLS pellets which contained 45% and 55% SLS, most of the SLS was released during the first two weeks of elution, after which period the release curves reached a plateau, as shown in Figure 4.24.

The release patterns observed for these samples were attributed to the development of porosity in the rubber matrices. In subsequent experiments with rubber-SLS membranes (discussed in Section 4.9), the development of porosity in the rubbers was verified experimentally by scanning electron microscopy (SEM) studies on cross-sections of leached membranes. The effect of the initial SLS loading on the amount as well as the rate of development of porosity and, consequently, on its rate of release from elastomeric pellets, is discussed in detail in Section 4.5.1.

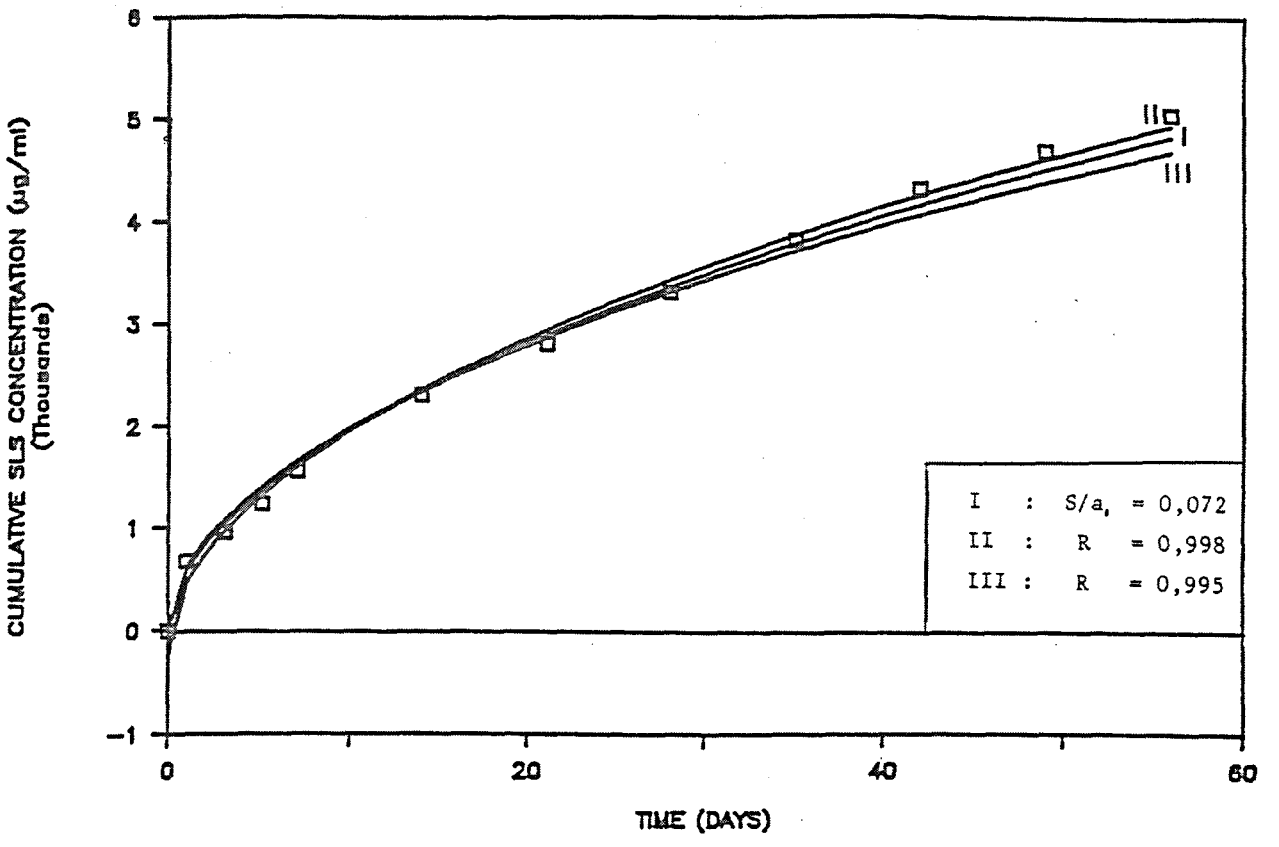

FIGURE 4.18 Agreement between experimental and theoretical data, as predicted by the AVERAGE MODEL (Curve I), the SQUARE-ROOT MODEL (Curve II) and the LOGARITHMIC MODEL (Curve III), for a natural-rubber sample which contained 35% SLS (Sample 3).

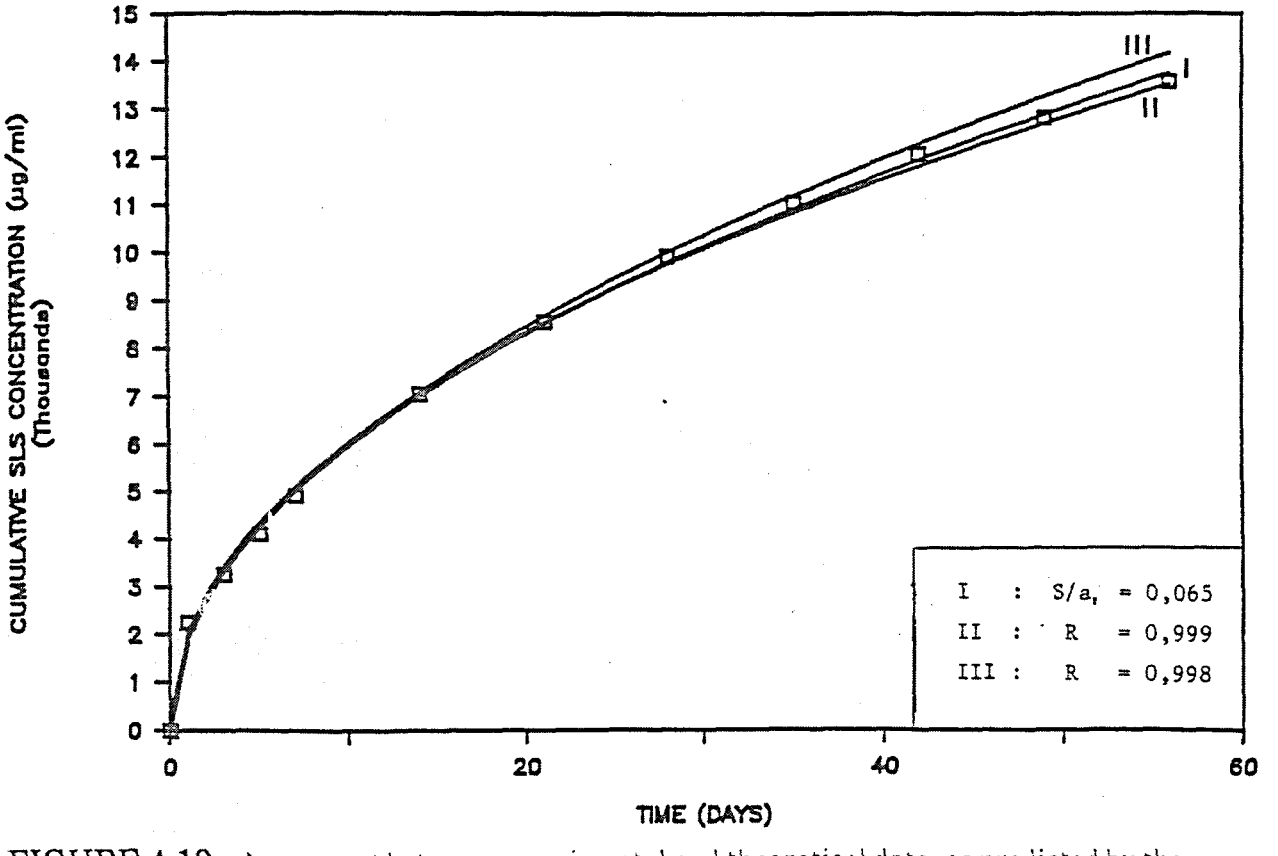

FIGURE 4.19 Agreement between experimental and theoretical data, as predicted by the AVERAGE MODEL (Curve I), the SQUARE-ROOT MODEL (Curve II) and the LOGARITHMIC MODEL (Curve III), for a styrene-butadiene rubber sample which contained 35% SLS (Sample 8).

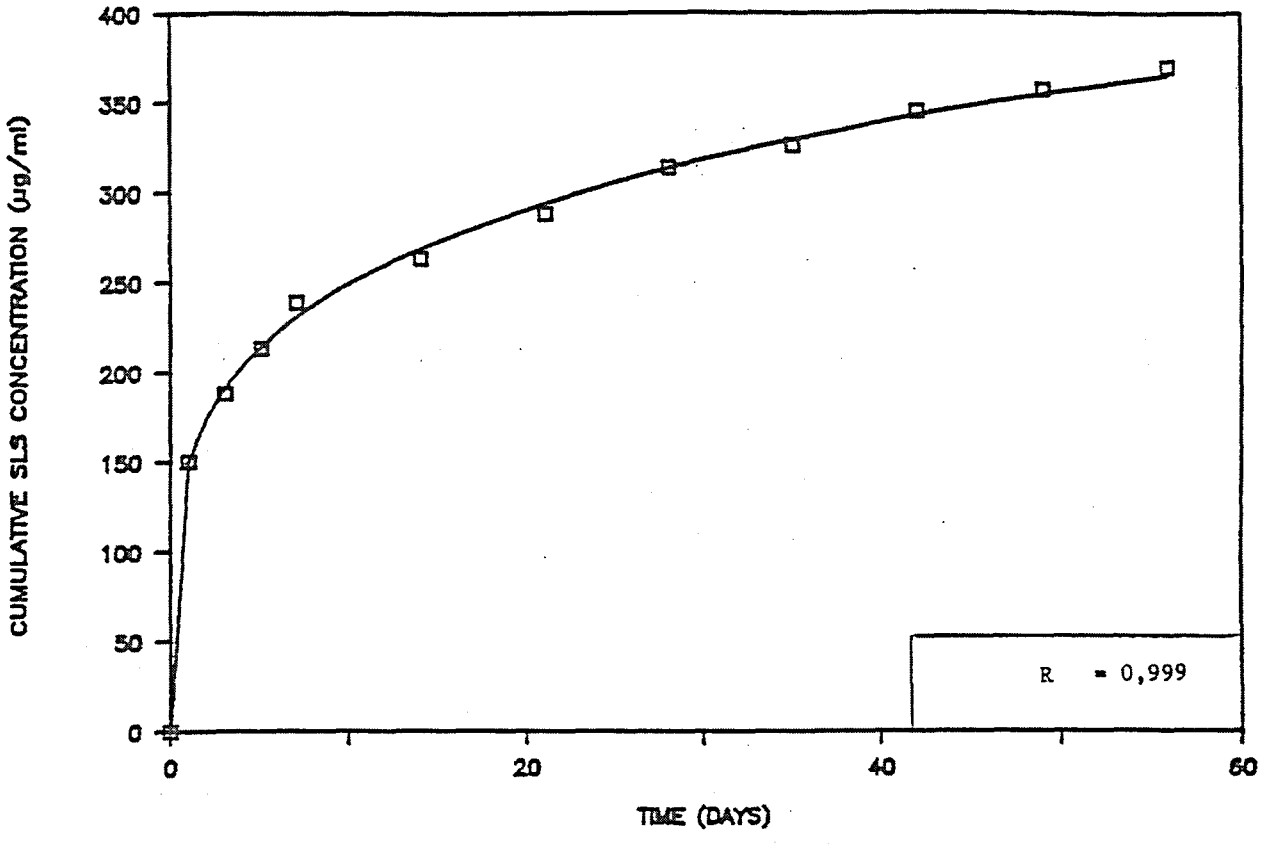

FIGURE 4.20 Agreement between experimental and theoretical data, as predicted by the LOGARITHMIC MODEL, for a styrene-butadiene rubber sample which contained 25% SLS (Sample 7).

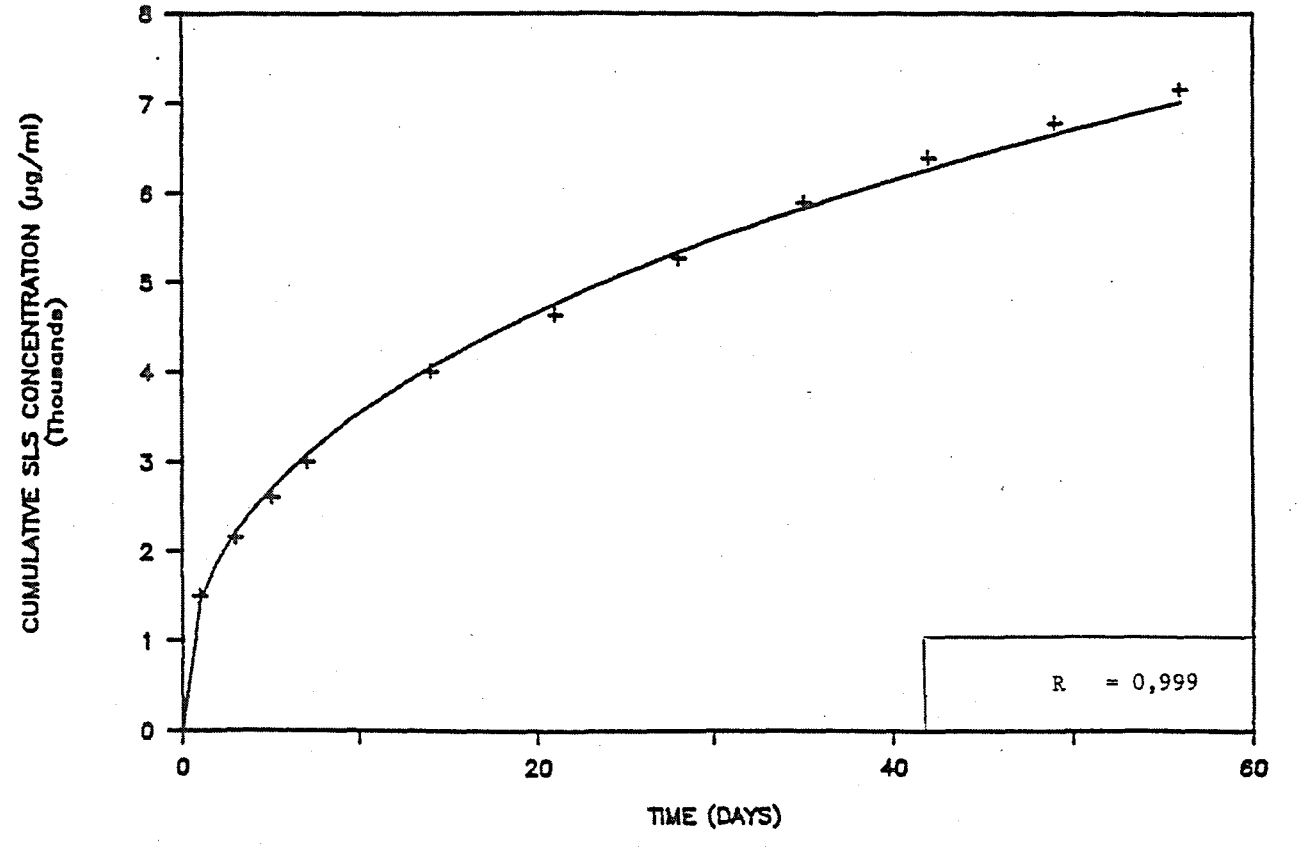

FIGURE 4.21 Agreement between experimental and theoretical data, as predicted by the LOGARITHMIC MODEL, for an NR/SBR blend which contained 35% SLS (Sample 13).

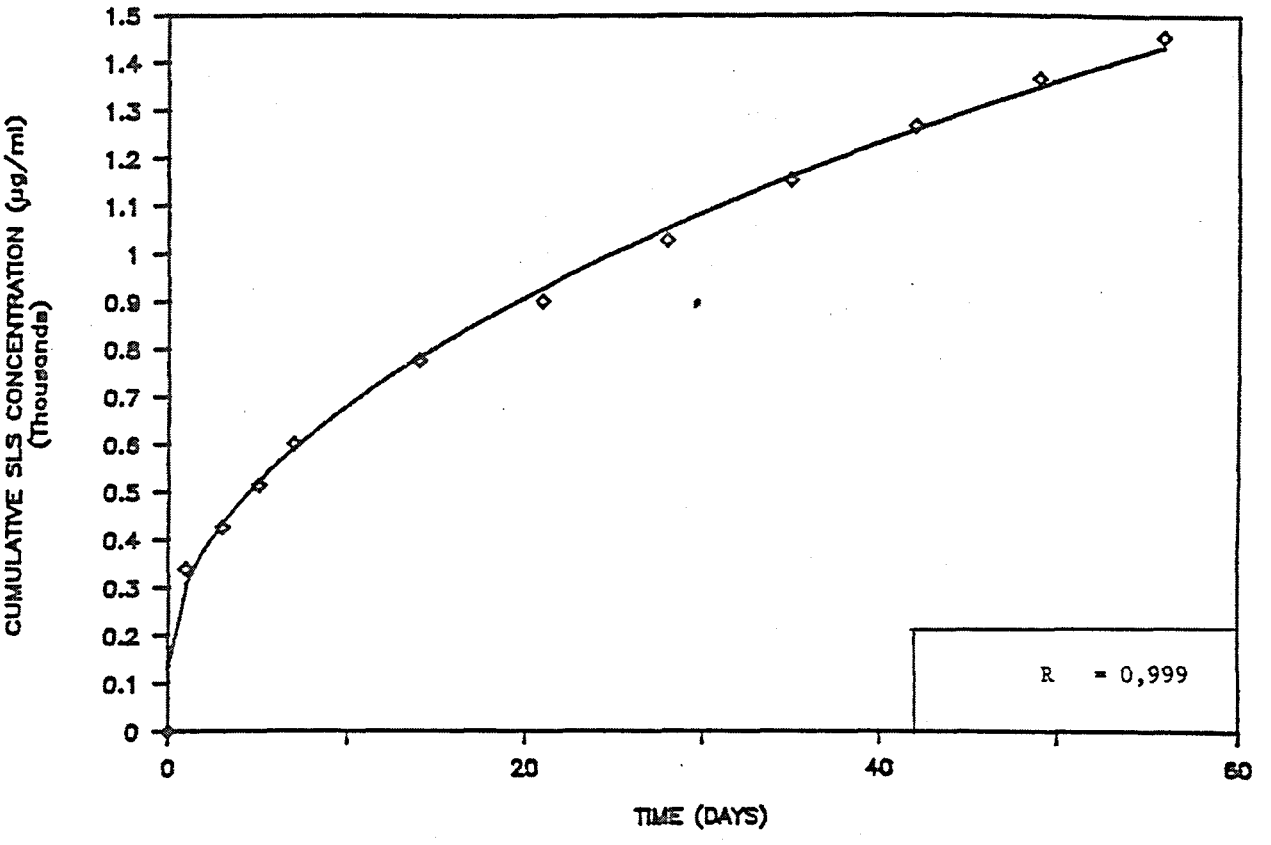

FIGURE 4.22 Agreement between experimental and theoretical data, as predicted by the SQUARE-ROOT MODEL, for a synthetic polyisoprene sample which contained 35% SLS (Sample 61).

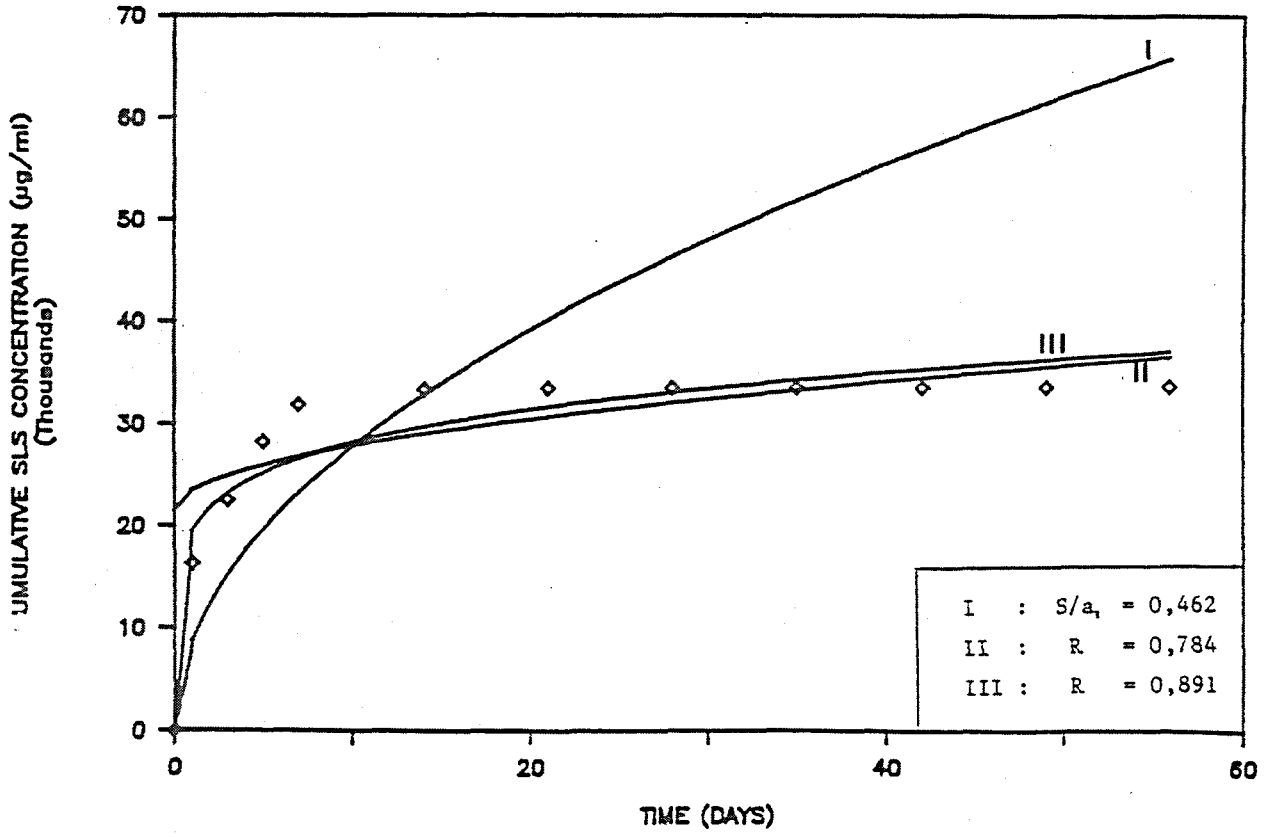

FIGURE 4.23 Poor agreement between experimental and theoretical data, as predicted by the AVERAGE MODEL (Curve I), the SQUARE-ROOT MODEL (Curve II) and the LOGARITHMIC MODEL (Curve III), for a styrene-butadiene rubber sample which contained 55% SLS (Sample 10).

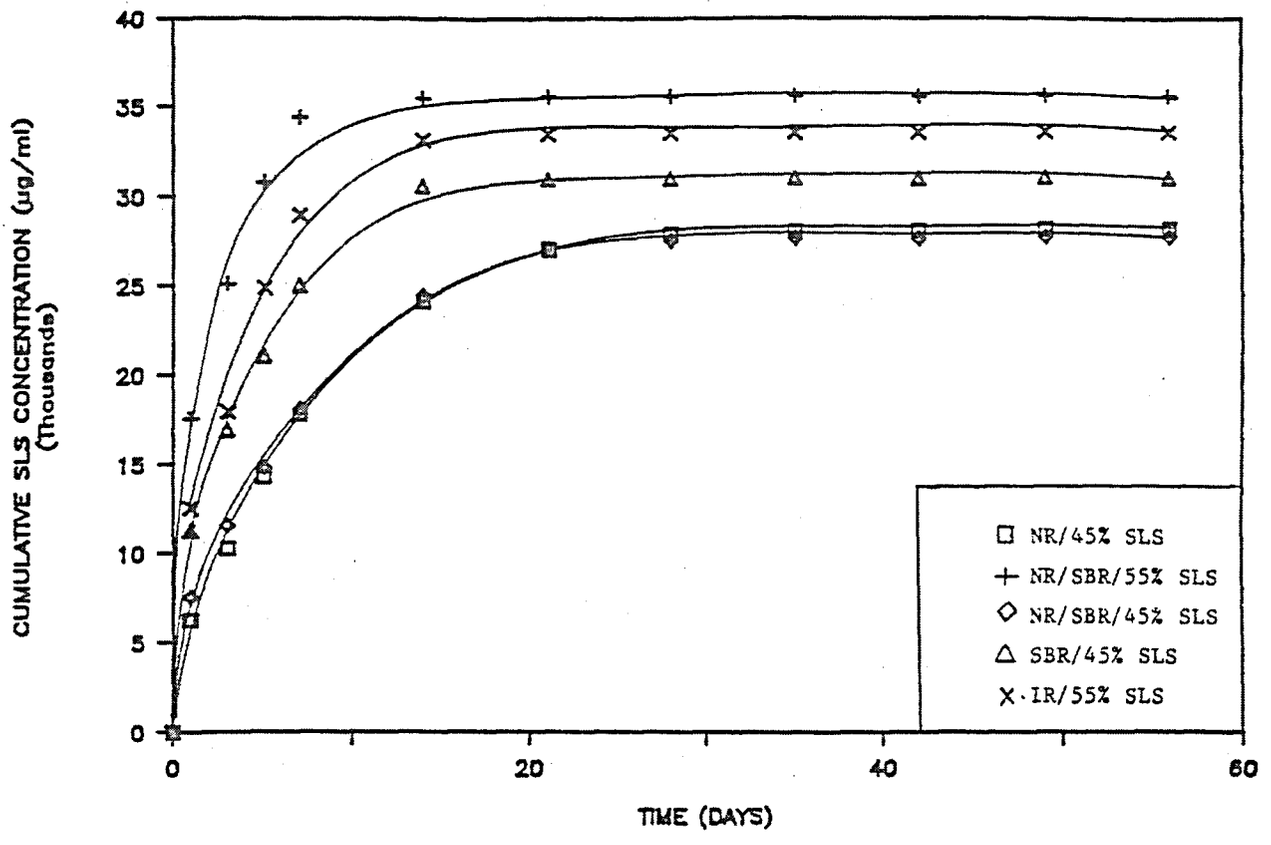

FIGURE 4.24 Release patterns of rubber formulations which contained 45% and 55% SLS.

4.5 FACTORS WHICH INFLUENCED THE RATE OF RELEASE OF SLS FROM MONOLITHIC ELASTOMERIC PELLETS

4.5.1 The Effect of the Initial SLS Loading

Natural rubber appeared to be a very useful material in terms of its ability to mix well with SLS. However, the release rates of SLS from NR pellets which contained from 5 to 25% SLS were very low. When the loading was 35%, the release rate of SLS increased markedly, and when it was 45% and 55%, the initial release rates were extremely high. Plots of the fraction of SLS released against time, as shown in Figures 4.25 and 4.26, illustrate the effect of the initial loading of SLS on its release rate from NR pellets. Figure 4.25 shows that there was no significant increase in the release rate for NR pellets which contained 5% to 25% SLS. However, at levels of 35% and 45% SLS, there was a dramatic increase in the release rate, as shown in Figure 4.26.

Similar release patterns were obtained for IR, a 50:50 blend of NR and SBR, and SBR pellets which contained 15 to 55% SLS. The effect of the SLS loading on the release rate is shown in Figure 4.27 for IR pellets which contained different loadings of SLS. Graphs which illustrate this effect for SBR and NR/SBR pellets are shown in Appendix 5A.

For monolithic elastomeric pellets containing dispersed SLS, the release rates were expected to be proportional to the square root of the total SLS loading, as discussed in Chapter 2, Section 2.4.4.1. However, when the percentages of SLS released after certain times were plotted against the initial SLS loading, S-shaped curves were obtained. These curves are shown in Figures 4.28 and 4.29 for samples of NR/SBR and SBR, respectively, at different intervals during the elution period. S-shaped curves were also obtained when the release rates at certain times during the test period were plotted against the SLS loading, as shown in Figure 4.30 for NR samples which contained different loadings of SLS. Figures 4.28 to 4.30 show very clearly that the release rate was neither a linear function of the SLS loading, nor proportional to the square root of the SLS loading. It can be seen from these figures that there was a large increase in the release rate for SLS levels of 25% to 35%, and an even bigger jump for levels of 35% to 45%. The shape of the curves shown in Figures 4.28 to 4.30 suggests that different mechanisms were involved in the release of SLS from elastomeric matrices which contained different loadings of SLS.

Several factors might have contributed to this non-linear variation of the release rate with initial SLS loading. The most important of these factors is considered to be the difference between the degrees of cure of rubber-SLS formulations which contained different loadings of SLS and the development of porosity in the rubber matrices as the release process continued.

The effect of the SLS loading on the degree of cure of rubber-SLS formulations was discussed in Section 4.3.3. It was shown that, for both NR and IR formulations, an increase in the SLS loading affected the degree of cure of these formulations. This effect became significant when the SLS loading was 15%. At levels of 25% SLS, the degree of cure decreased markedly, while at levels of 35% SLS no curing exotherm was observed. These results suggested that, while rubber formulations which contained 15% and 25% SLS were vulcanized to a certain extent, formulations which contained 35% and more SLS were essentially unvulcanized. This clearly contributed to the increase in the release rate between the SLS levels of 25% to 35%, but did not account for the extremely large increase when levels of SLS were 35% to 45%. The latter can best be explained in terms of the development of porosity in rubber matrices which contained a large excess of SLS.

In all the rubber-SLS pellets which were evaluated, the concentration of SLS exceeded its solubility limit in the rubbers. Large amounts of SLS were, therefore, present as dispersed particles. Because of the high concentrations of SLS at the surfaces of these pellets, as well as in the layers near the surface, it could be expected that the initial release period would be dominated by dissolution of SLS at the pellet-eluent interface. As more of the SLS was dissolved from the surface and from the layers immediately below the surface, the effective surface area of the pellet in contact with the eluent was increased because of the formation of pores, which resulted from the dissolution of dispersed SLS particles. As the release process continued, this porous structure extended further into the pellet. Obviously, a highly porous structure would result in not only a faster overall release rate of SLS, but also in a shorter effective release lifetime of the controlled-release device. This explained the "plateau effect" observed for the final portion of the release curves obtained for rubber-SLS pellets which contained 45% and 55% SLS, as shown in Figure 4.24 in Section 4.4.

From the above discussion, it is clear that the rate of development of porosity will depend on the initial SLS loading, and that the release rate of SLS at any time will be a function of the amount of porosity developed in the rubber matrix up to that time. The mechanism of release of SLS will, therefore, also depend on the initial loading of SLS in the matrix. For rubber pellets which contained up to 25% SLS, the release rates were very low. This indicated that the amount of porosity in such pellets was negligible. It can, therefore, be assumed that release of SLS from these pellets occurred by a combination of dissolution of SLS at the surface of the pellet and diffusion of SLS through the matrix phase. The effect of porosity on the release rate of SLS became significant in rubber pellets which contained 35% SLS. For such pellets, the release mechanism initially involved dissolution of dispersed SLS particles from the surface of the pellet, which was then followed by diffusion of SLS through the matrix phase, as well as diffusion through pores which developed as a result of dissolution of the large excess of dispersed SLS particles. In rubber pellets which contained 45% and 55% SLS, dissolution of the extremely large amounts of SLS resulted in

highly porous matrices and, consequently, in very fast initial release rates. It is suggested that in such systems the initial period of release was dominated by dissolution of dispersed SLS particles, while the release mechanism which operated after this period involved diffusion of SLS through pores within the matrix structure. Because of the very large amounts of SLS which were initially released from rubber matrices which contained more than 45% SLS, it was assumed that the contribution of diffusion through the matrix phase itself to the overall release mechanism was negligible in such systems.

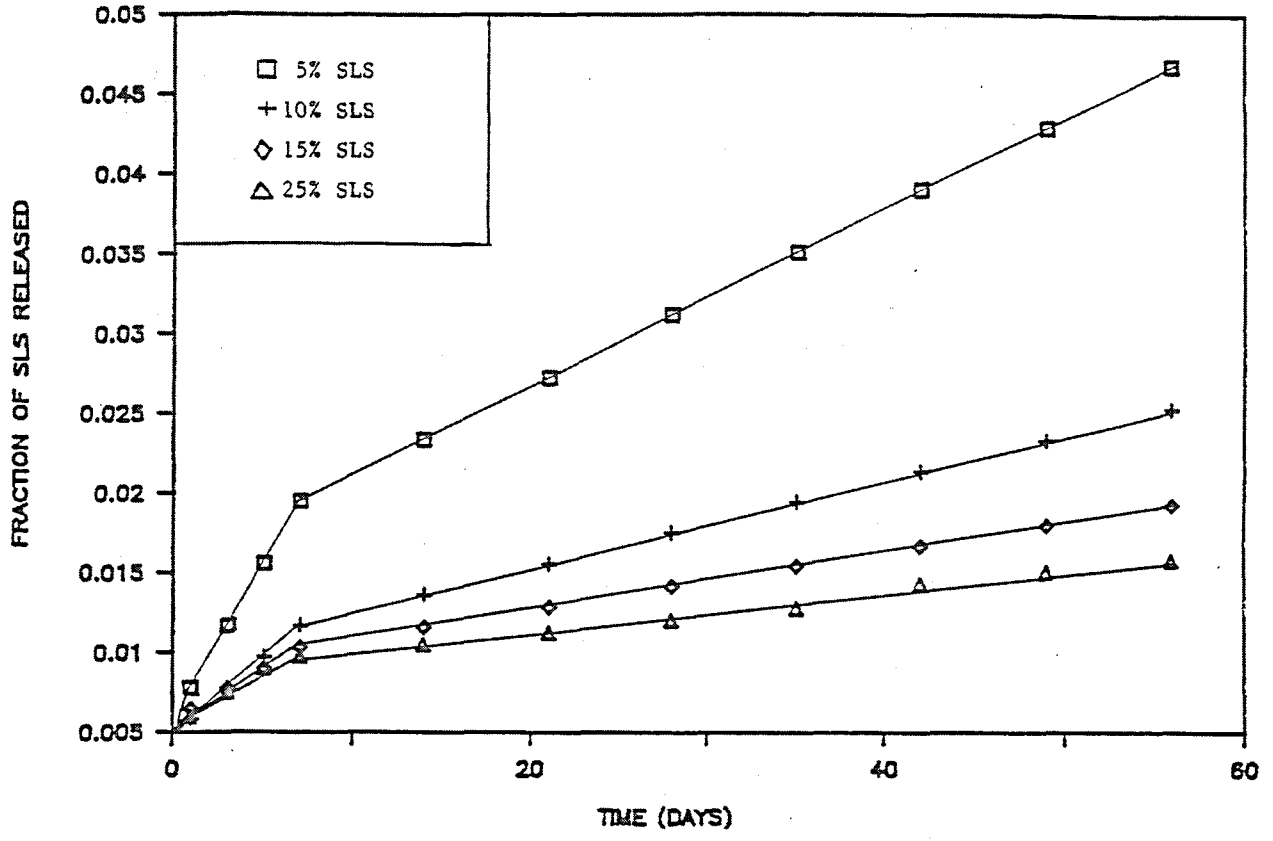

FIGURE 4.25 The effect of the initial SLS loading on the release of SLS from natural-rubber matrices.

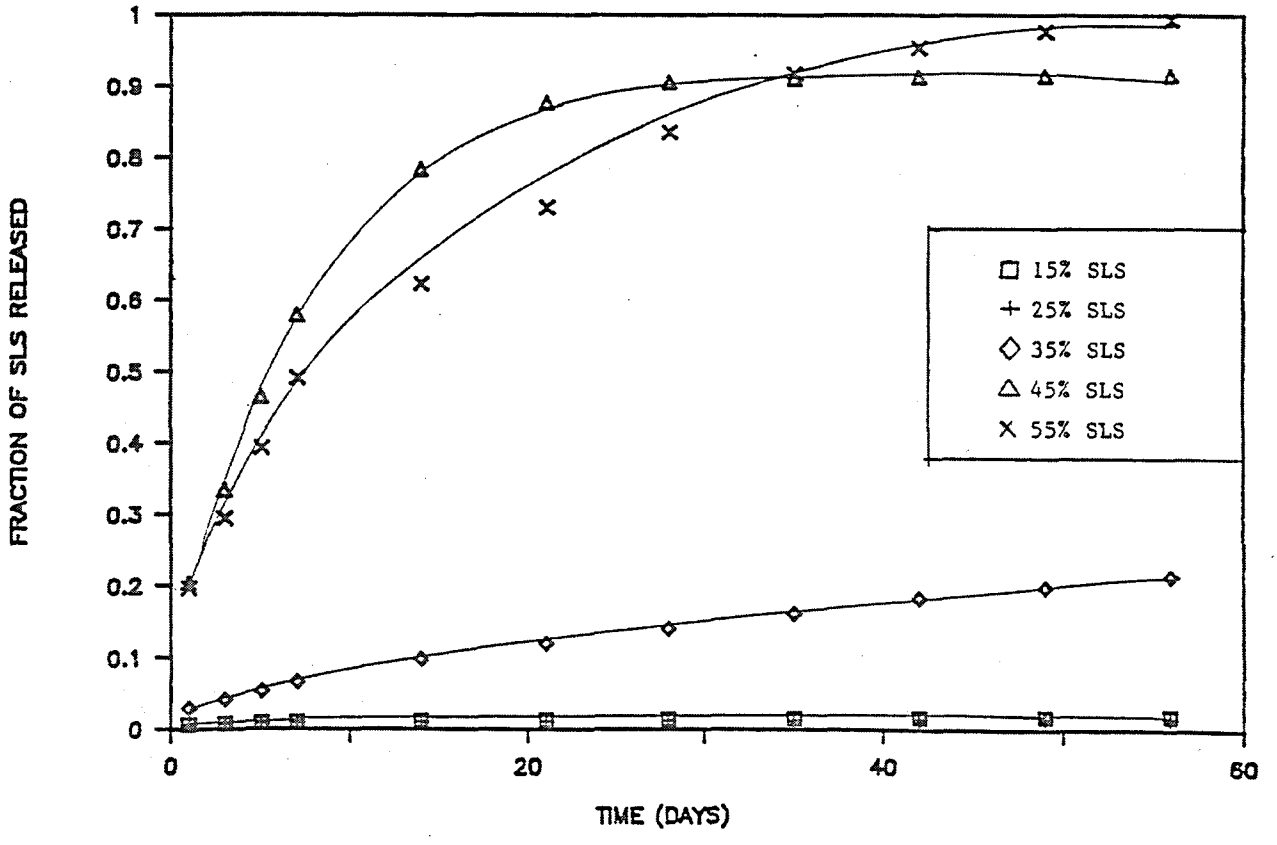

FIGURE 4.26 The effect of the initial SLS loading on the release of SLS from natural-rubber matrices.

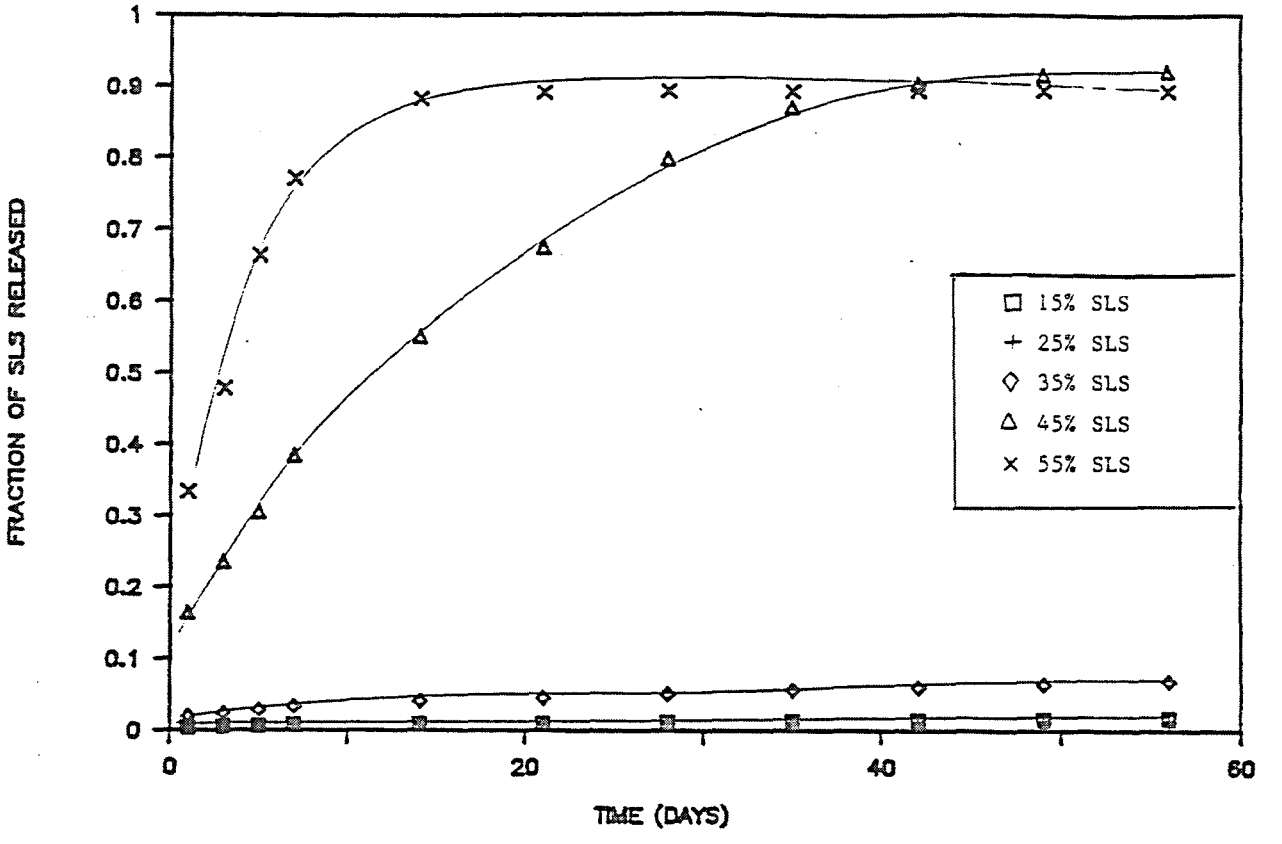

FIGURE 4.27 The effect of the initial SLS loading on the release of SLS from synthetic polyisoprene matrices.

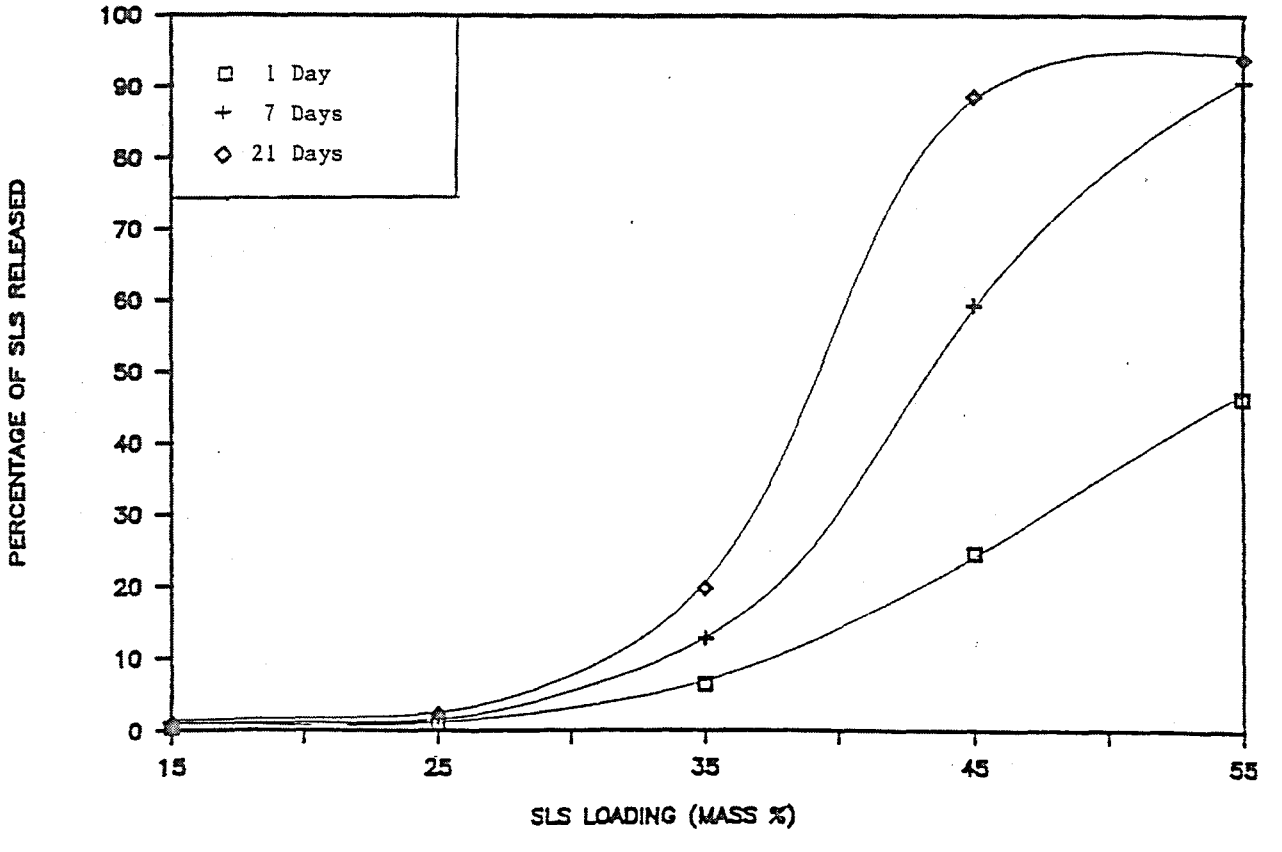

FIGURE 4.28 Plots of the percentage SLS released as a function of the initial SLS loading for NR/SBR matrices at different intervals during the elution period.

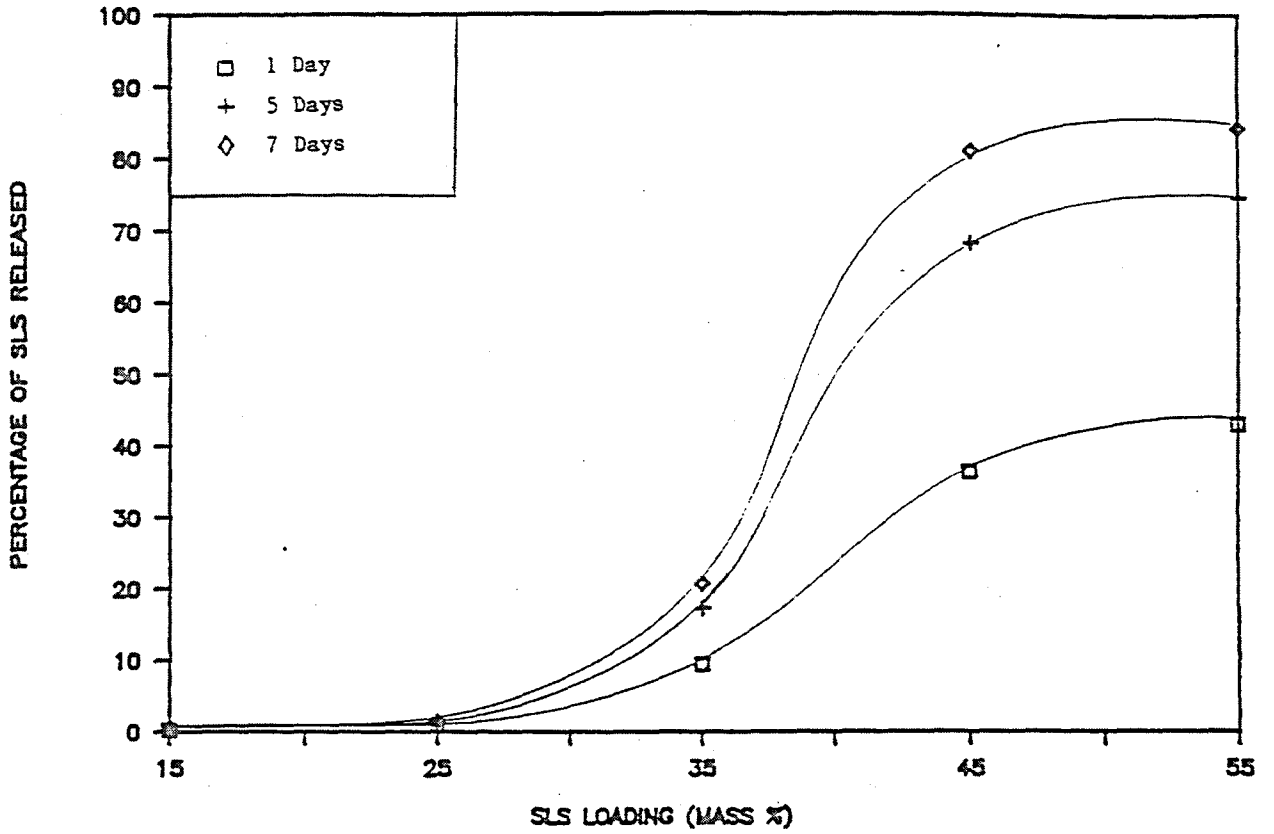

FIGURE 4.29 Plots of the percentage SLS released as a function of the initial SLS loading for SBR matrices at different intervals during the elution period.

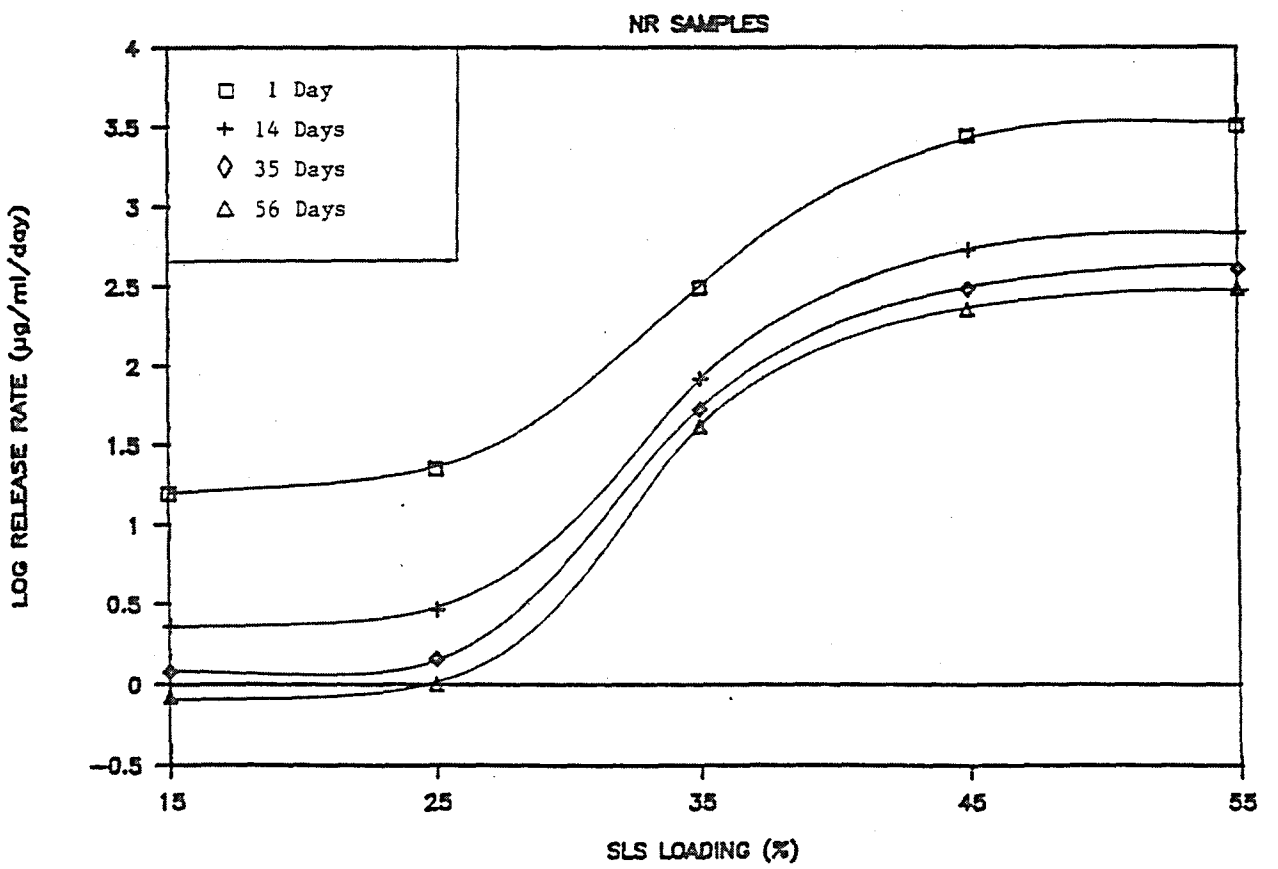

FIGURE 4.30 Plots of the release rate of SLS as a function of the initial SLS loading for NR matrices at different intervals during the elution period.

4.5.2 The Effect of the Addition of Release Promotors

It is known that the incorporation of certain chemicals (the so-called "porosigens") into a controlled-release matrix will enhance the development of porosity and will thereby increase the release rate of an active agent from such a matrix. Ammonium sulphate and sodium bicarbonate are considered to be "fast" porosigens, while calcium carbonate and silica function as "slow" porosity-enhancing materials.[71]

Some of the controlled-release formulations which were evaluated in elution experiments contained such porosity-enhancing materials. The effect of the addition of ammonium sulphate and calcium carbonate on the release rate of SLS from NR matrices was investigated. The sample numbers, compositions and dimensions of NR pellets which contained different grades (including different particle sizes), as well as different amounts, of $CaCO_3$ are given in Tables B3 and B10 in Appendix 1B, while Table B11 in Appendix 1B gives the sample numbers, compositions and dimensions of NR pellets which contained different amounts of $(NH_4)_2SO_4$. The release-rate data obtained from elution of these pellets are given in Appendix 4A.

Figure 4.31 shows the effect of the addition of different amounts of an untreated $CaCO_3$ (Kulubrite 2; mean particle size 2,25 μm) on the release rate of SLS from NR which contained 45% SLS. This figure shows that samples which contained $CaCO_3$ showed a moderate increase in the initial rate of release of SLS. However, the amounts of $CaCO_3$ added (i.e., 3 phr, 6 phr and 10 phr) did not seem to have a significant influence on the release rate. Similar results were obtained for formulations which contained other grades of untreated $CaCO_3$. The addition of various amounts of a surface-treated $CaCO_3$ (Omya BSH; mean particle size 2 μm) to an NR formulation which contained 45% SLS, had virtually no effect on the rate of release of SLS, as shown in Figure 4.32.

The particle size of the $CaCO_3$ used had little effect on the release rate of SLS, as illustrated in Figure 4.33 for NR formulations which contained 45% SLS and 6 phr $CaCO_3$. The particle sizes of the three different grades of untreated $CaCO_3$ which were added to NR formulations were 2,25 μm, 5 μm, and 10 μm.

With NR formulations which contained low loadings of SLS, the addition of various amounts of $CaCO_3$ (grade Omya BSH) to these formulations caused only a slight increase in the initial rate of release of SLS. This is illustrated in Figure 4.34 for NR formulations which contained 5% SLS.

The addition of various amounts of $(NH_4)_2SO_4$ to NR formulations which contained 5% SLS had no effect on the release rate of SLS from these formulations. as shown in Figure 4.35. These results illustrated clearly that there was essentially nothing to be gained by the addition of $CaCO_3$ and $(NH_4)_2SO_4$ to natural-rubber formulations which contained low loadings of SLS.

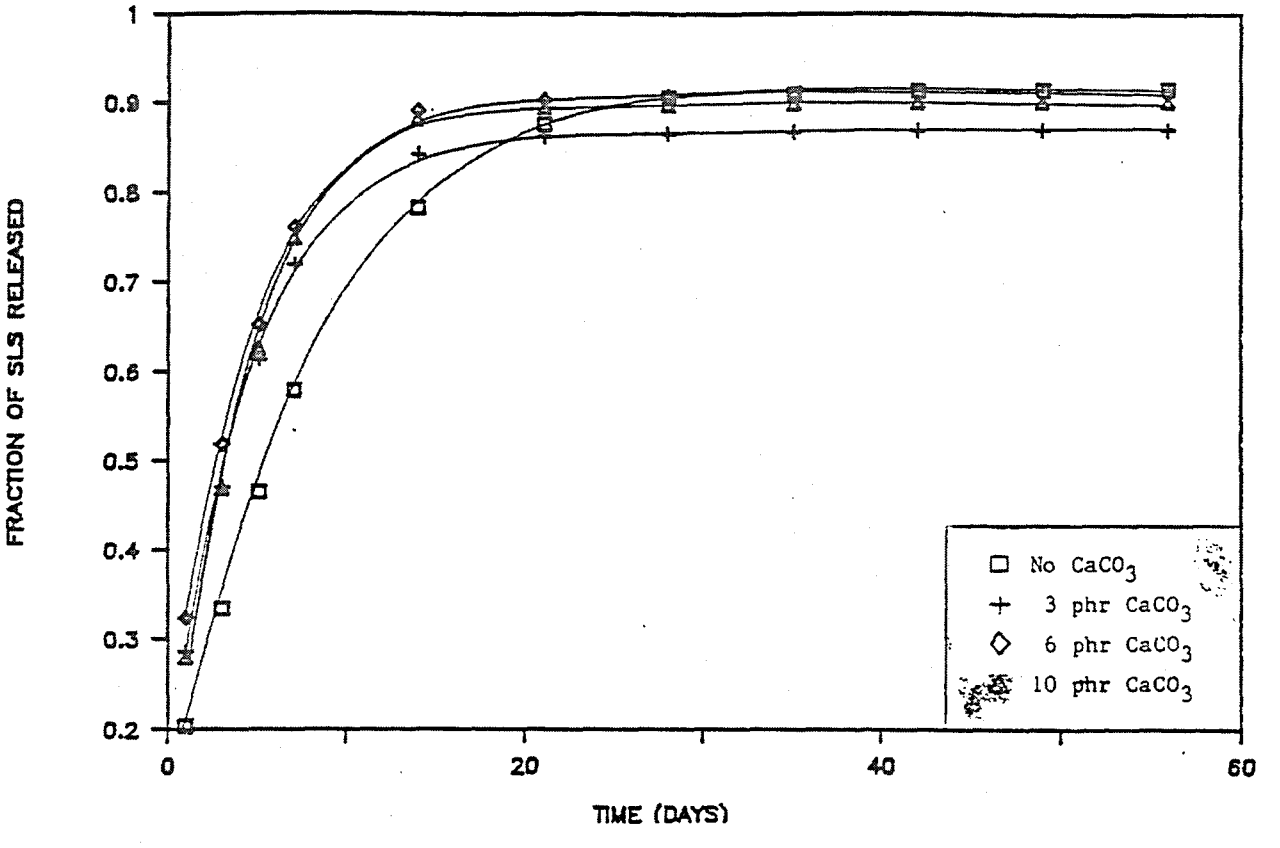

FIGURE 4.31 The effect of the addition of various amounts of an untreated $CaCO_3$ (Kulubrite 2) on the release of SLS from a natural-rubber formulation which contained 45% SLS.

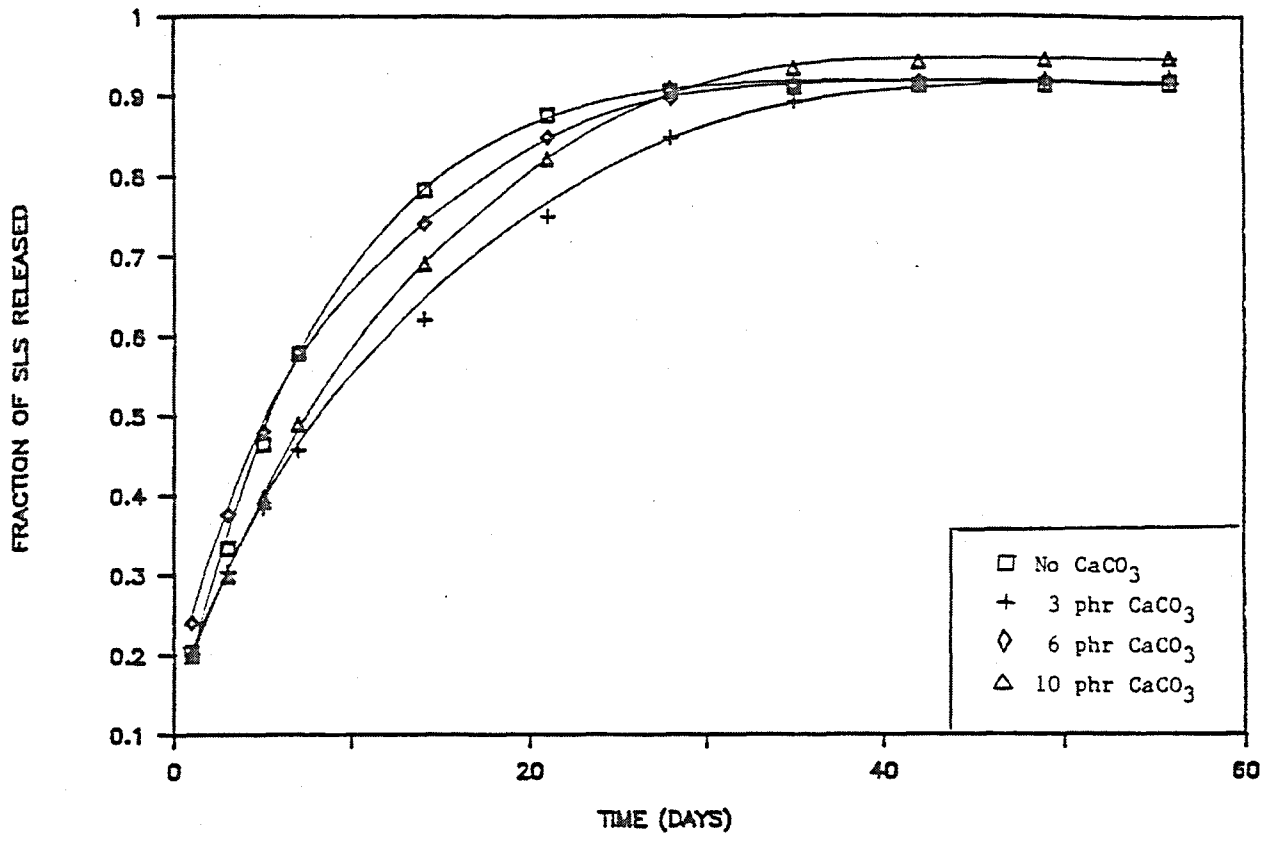

FIGURE 4.32 The effect of the addition of various amounts of a surface-treated $CaCO_3$ (Omya BSH) on the release of SLS from a natural-rubber formulation which contained 45% SLS.

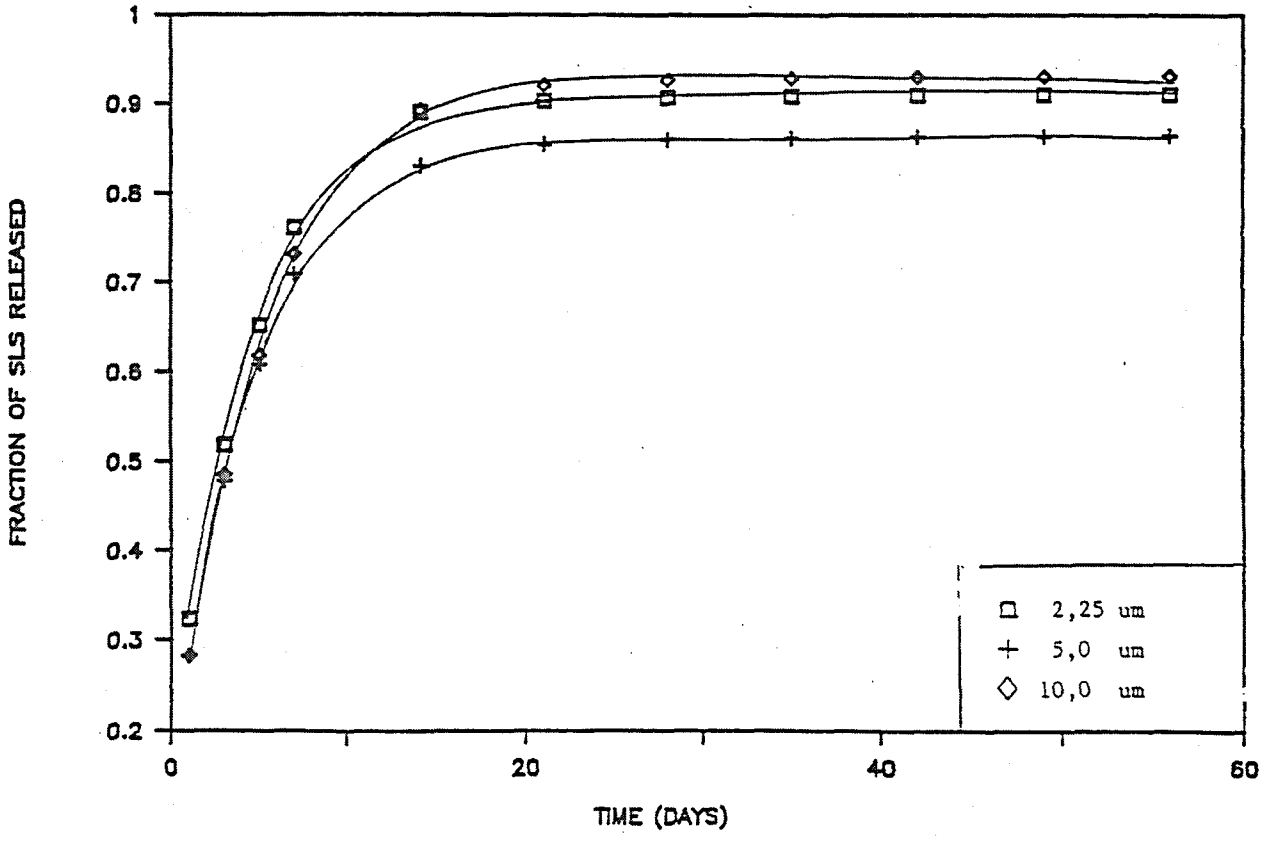

FIGURE 4.33 The effect of the particle size of $CaCO_3$ on the release of SLS from natural-rubber formulations which contained 45% SLS and 6 phr $CaCO_3$.

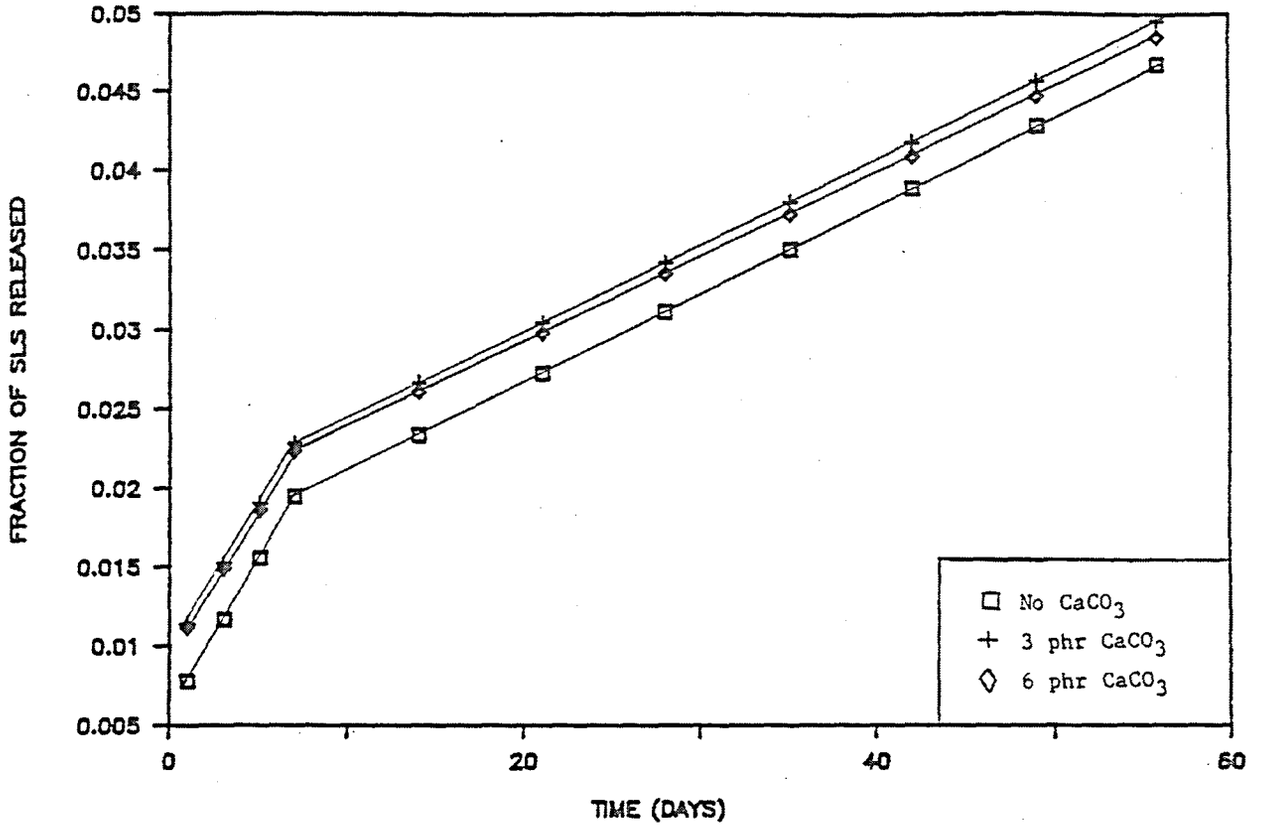

FIGURE 4.34 The effect of the addition of various amounts of $CaCO_3$ (Omya BSH) on the release of SLS from natural-rubber formulations which contained 5% SLS.

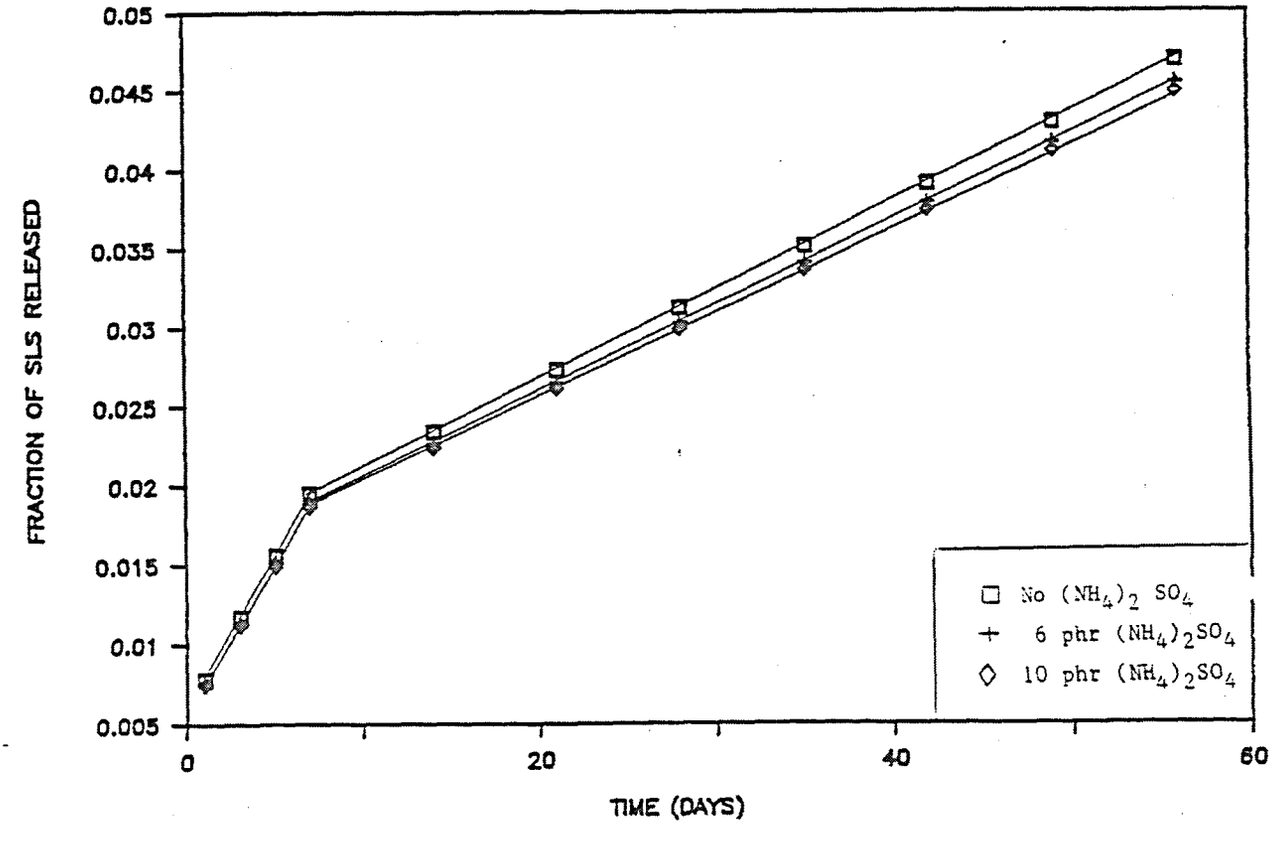

FIGURE 4.35 The effect of the addition of various amounts of $(NH_4)_2SO_4$ on the release of SLS from natural-rubber formulations which contained 5% SLS.

4.5.3 The Effect of the pH of the Eluent

In the application of controlled-release rubber-SLS pellets to mine dumps for the long-term inhibition of the bacterial oxidation of pyrite (discussed in Chapter 2, Section 2.6.1.2.8) such pellets will be exposed to acid mine water the pH of which may be as low as 1,5. It was, therefore, thought important that the effect of the pH of the eluent (distilled water) on the release rate of SLS from rubber pellets should be investigated.

The effect of the pH of the eluent on the release rate of SLS is shown in Figures 4.36 and 4.37 for an NR formulation which contained 25% SLS and an IR formulation which contained 25% SLS, respectively. Figure 4.36 shows that a decrease in the pH of the eluent caused a slight increase in the release rate of SLS. The most significant increase in the release rate occurred at a pH of 2,0. For the IR formulation which contained 25% SLS, the effect of the pH of the eluent on the release rate of SLS was less noticeable, as shown in Figure 4.37. Again, the highest release rate was obtained at pH 2,0. Although the release rate of SLS increased slightly below the pH of distilled water, this effect was too small to be of any importance in the application of controlled-release pellets to mine dumps.

The effect of the pH of the eluent on the release rate of SLS was also investigated for NR formulations which contained 45% SLS and different grades of $CaCO_3$. The results of these investigations are shown in Figures 4.38 and 4.39. For NR formulations which contained 45% SLS and 10 phr of an untreated $CaCO_3$, the pH of the eluent had no significant effect on the release rate of SLS, as shown in Figure 4.38. For NR formulations which contained 45% SLS and 10 phr of a surface-treated $CaCO_3$, an increase in the rate of release of SLS occurred at pH 4,5. However, at lower pH values an unusual effect was observed, since a decrease in the pH of the eluent from 4.0 to 2,5 resulted in a decrease in the rate of release of SLS, as illustrated in Figure 4.39. A possible explanation for these results is that at a low pH there was interaction between the SLS and the surface-treated $CaCO_3$. Unfortunately, no evidence to support this suggestion was obtained.

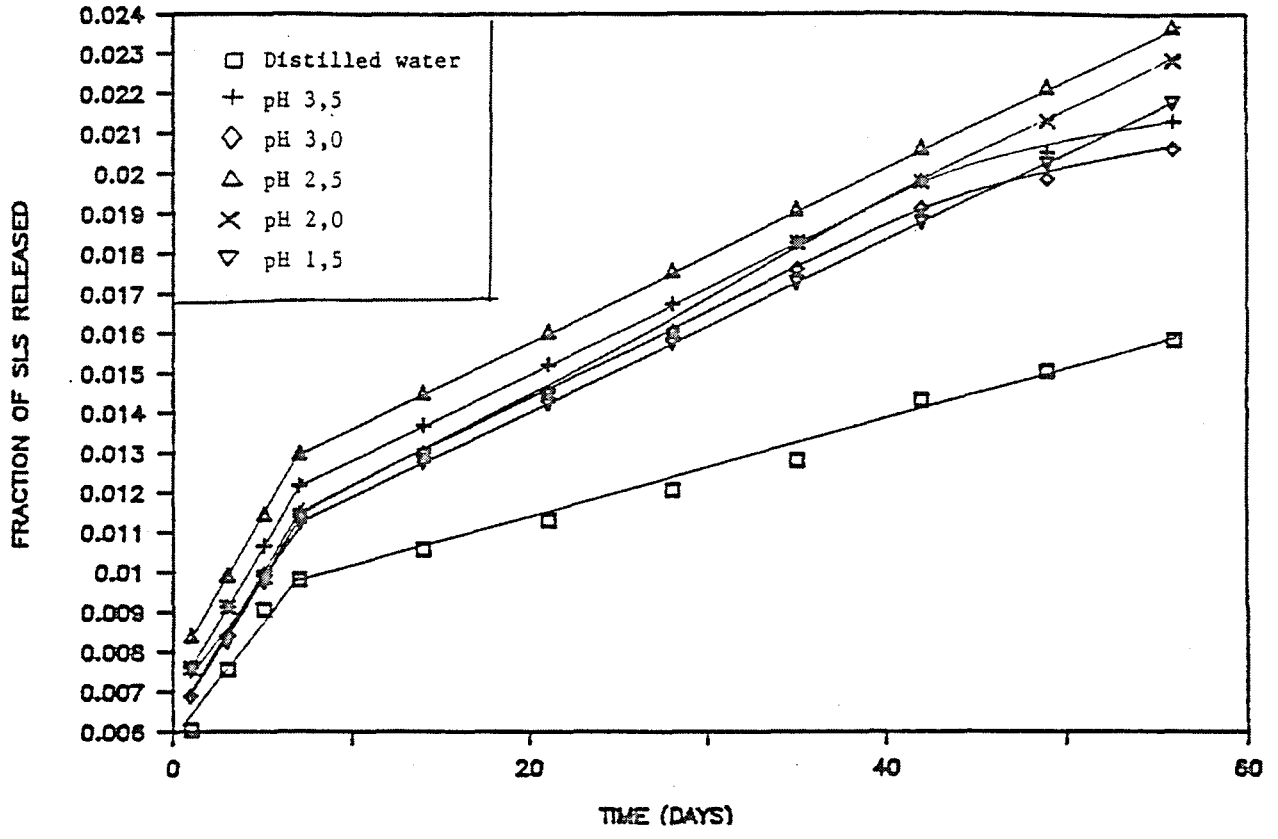

FIGURE 4.36 The effect of the pH of the eluent on the release of SLS from a natural-rubber formulation which contained 25% SLS.

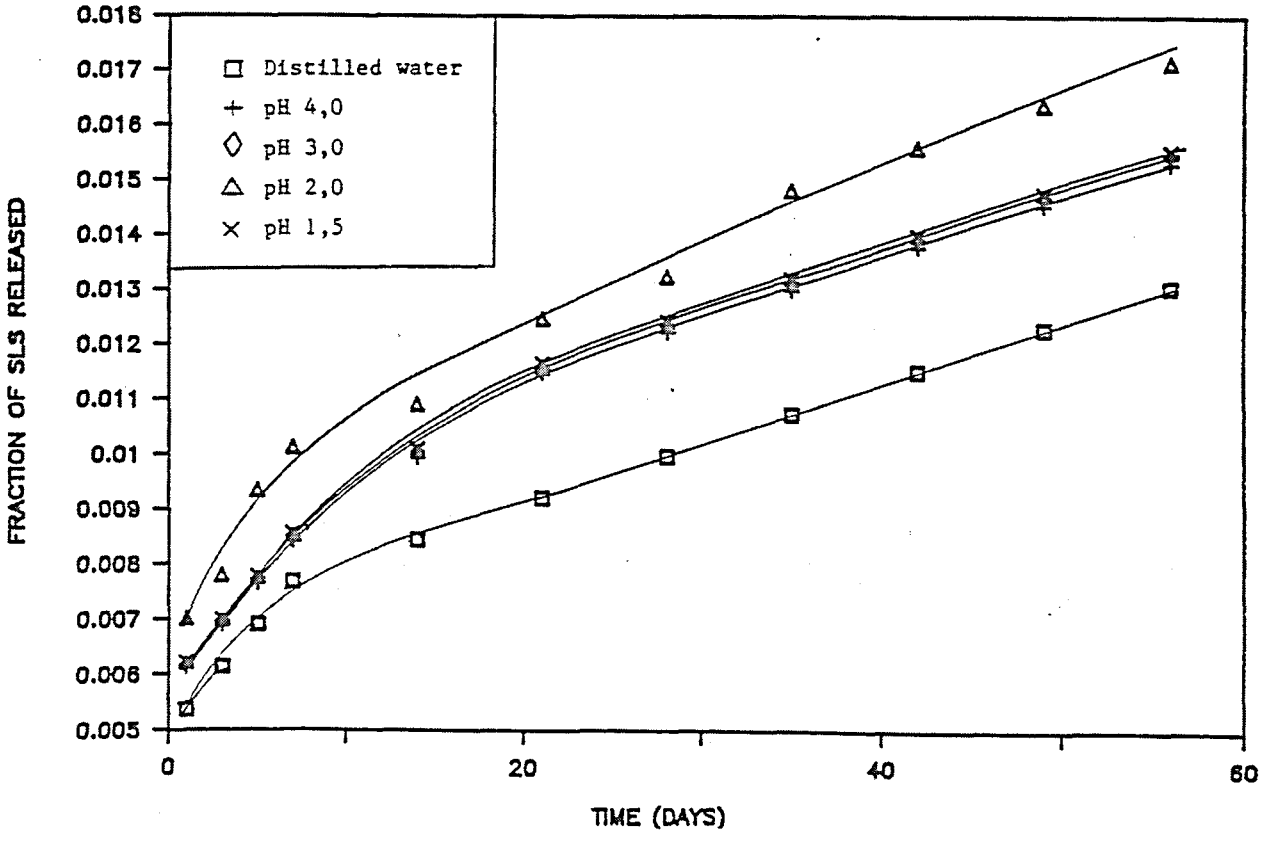

FIGURE 4.37 The effect of the pH of the eluent on the release of SLS from a synthetic polyisoprene formulation which contained 25% SLS.

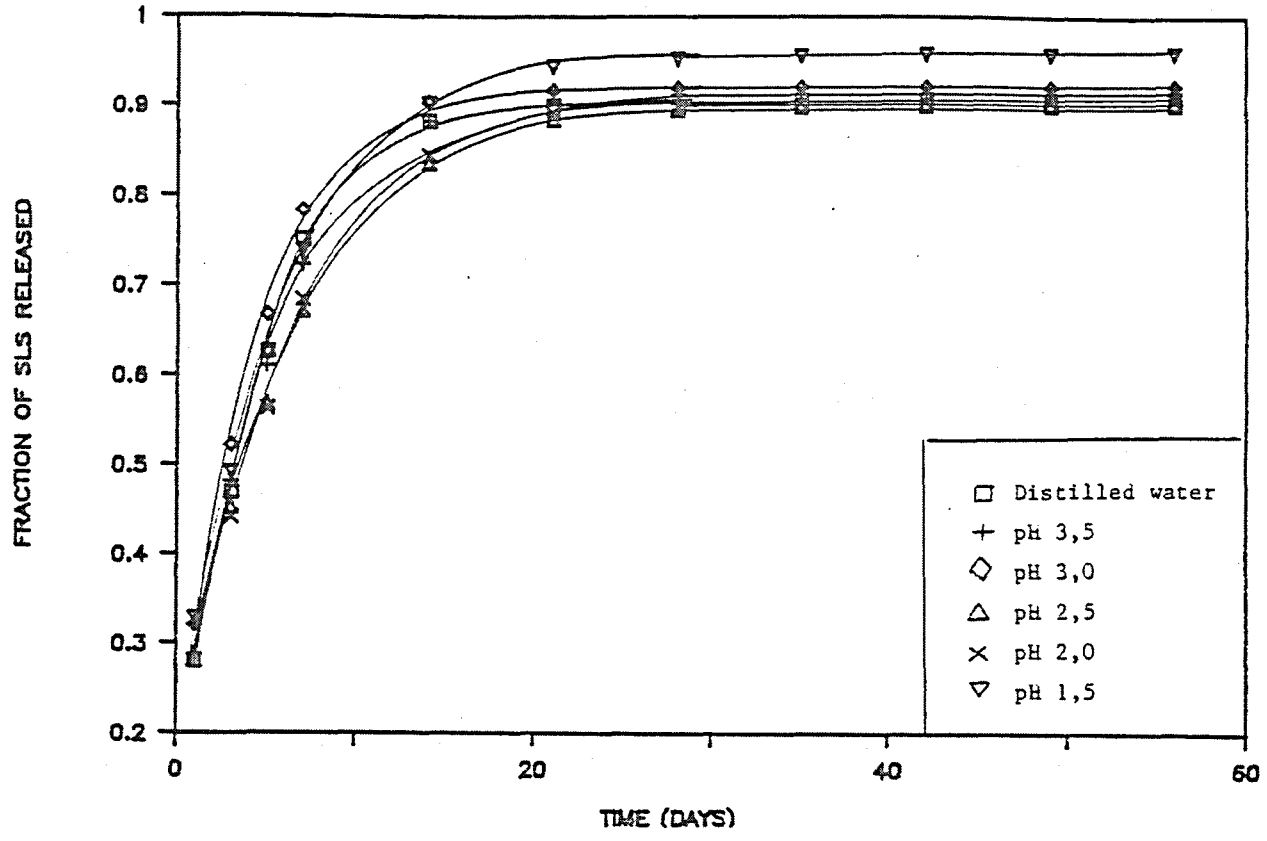

FIGURE 4.38 The effect of the pH of the eluent on the release of SLS from a natural-rubber formulation which contained 45% SLS and 10 phr of an untreated $CaCO_3$.

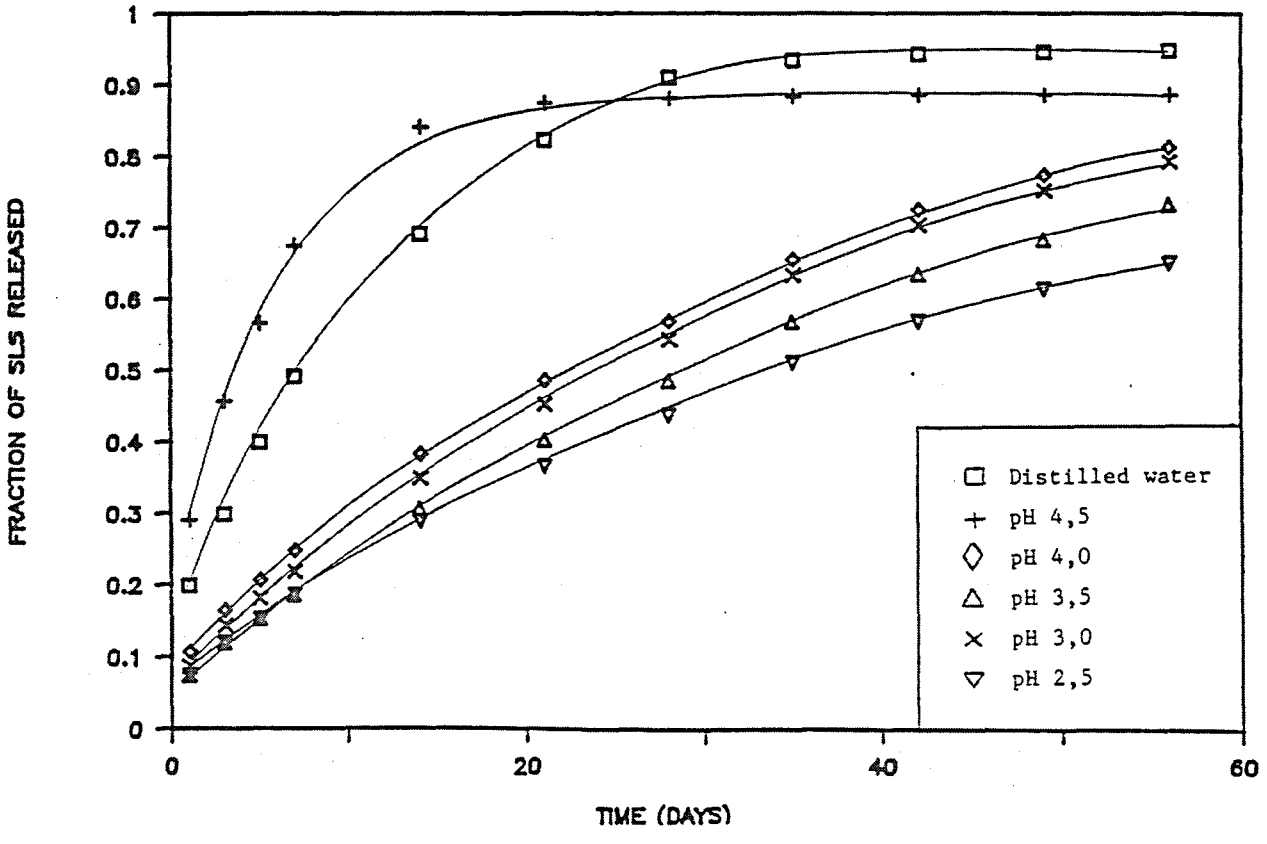

FIGURE 4.39 The effect of the pH of the eluent on the release of SLS from a natural-rubber formulation which contained 45% SLS and 10 phr of a surface-treated $CaCO_3$.

4.5.4 The Effect of the Base Polymer

Natural rubber (NR), styrene-butadiene rubber (SBR), a 50:50 blend of NR and SBR (NR/SBR) and synthetic polyisoprene (IR) were used as binding matrices in controlled-release formulations.

The effect of the rubber type on the release rate of SLS from formulations which contained 25%, 35% and 45% SLS is shown in Figures 4.40 to 4.42. As was to be expected, the release rate of SLS was influenced by the type of rubber used. At SLS loadings of 25%, the highest release rate was obtained from NR/SBR matrices, while IR matrices showed the lowest rate of release, as illustrated in Figure 4.40. It is clear that at SLS levels of 25%, the difference in the release rates of SLS from the various rubber matrices was noticeable, but the absolute values were very low.

At SLS levels of 35% and 45%, the highest initial release rate was obtained from SBR matrices, followed by NR/SBR, NR and IR matrices, as illustrated in Figures 4.41 and 4.42. The marked increase in the rate of release of SLS from rubber matrices which contained 35% or more SLS was attributed to the development of porosity in such matrices, as discussed in Section 4.5.1. Figures 4.41 and 4.42 suggest that the rate of development of porosity was the fastest in SBR matrices and slowest in IR matrices.

At all levels of SLS, the rate of release of SLS from NR matrices was higher than that from IR matrices. Apart from the possibility that porosity developed at a higher rate in NR matrices, as suggested by the graphs in Figures 4.41 and 4.42, the solubility limits of SLS in these two rubbers also differed. DSC studies (discussed in Section 4.2.2) showed that the solubility limit of SLS in NR was 4%, while that in IR was 3%.

Since the rate of transport of SLS through the rubber matrices depends on the solubility of the SLS in the respective rubbers, it is obvious that the higher solubility limit of SLS in NR matrices would result in a higher rate of release. It can be assumed that the influence of the solubility limit of SLS on its rate of transport through rubber matrices was more important in rubber formulations which contained less than 35% SLS, since at the 35% level the rubbers became porous and release of the SLS from such matrices was expected to occur mainly through pores within the matrix structures.

It was obvious from these findings that the rate of release of SLS from controlled-release rubber-SLS pellets, as well as the effective release lifetime of such pellets, can be varied, not only by incorporating different amounts of SLS into the pellets, but also by employing mixtures of different types of rubber pellets.

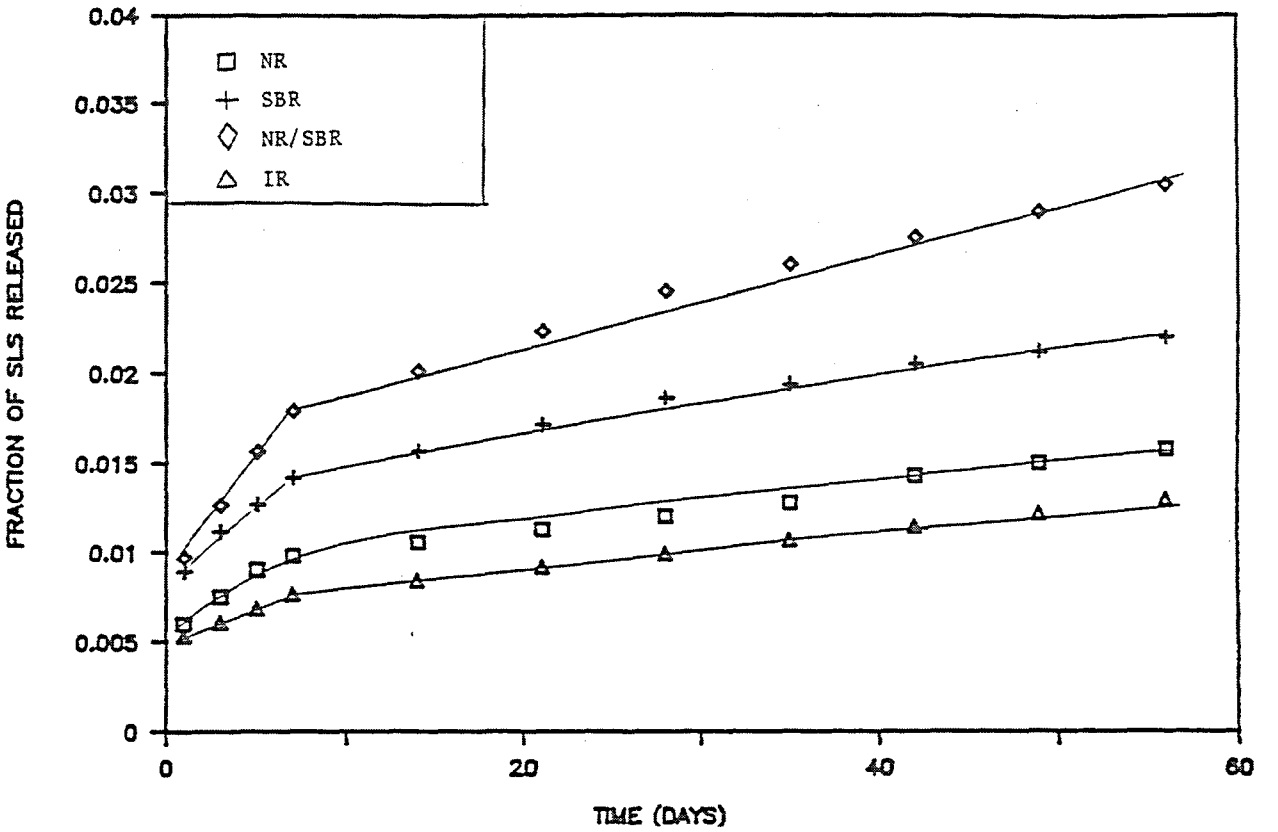

FIGURE 4.40 The effect of the type of rubber used on the release of SLS from controlled-release rubber-SLS formulations which contained 25% SLS.

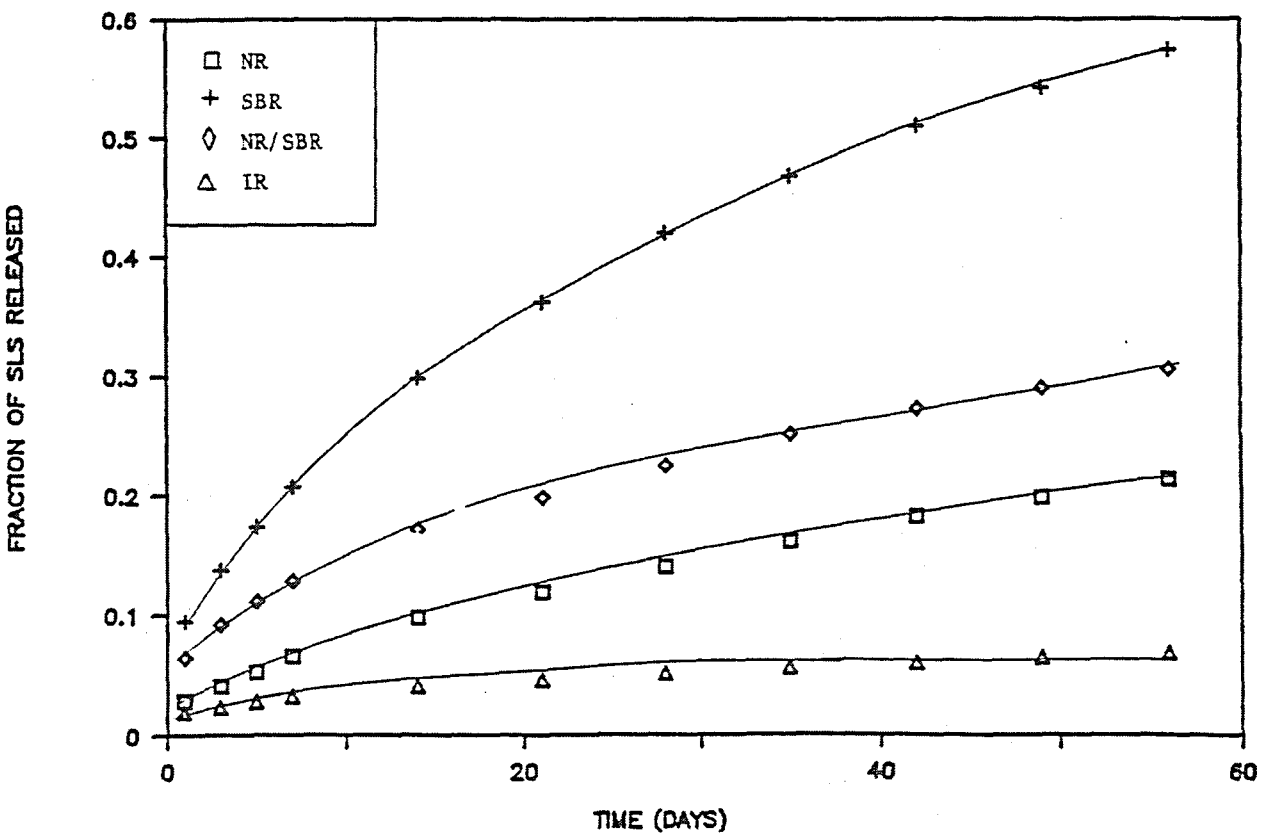

FIGURE 4.41 The effect of the type of rubber used on the release of SLS from controlled-release rubber-SLS formulations which contained 35% SLS.

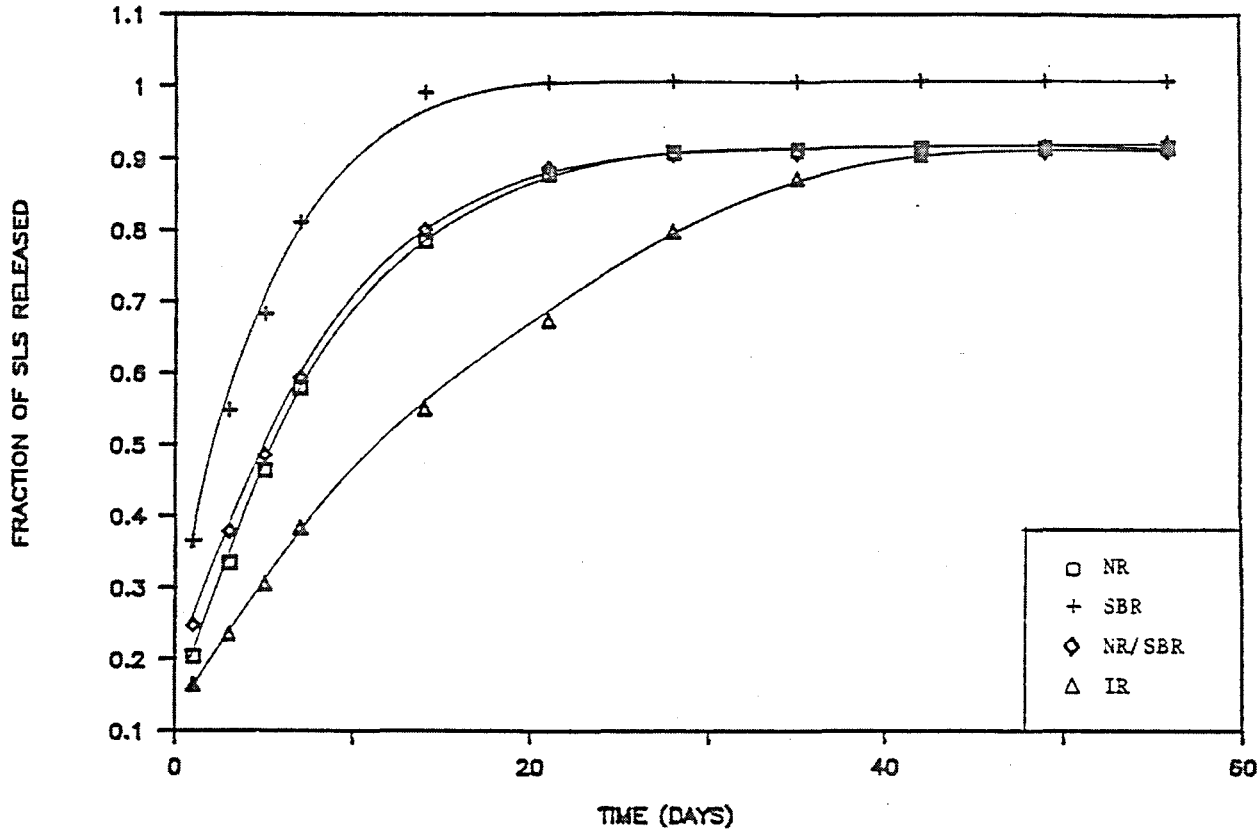

FIGURE 4.42 The effect of the type of rubber used on the release of SLS from controlled-release rubber-SLS formulations which contained 45% SLS.

4.5.5 The Effect of the Surface Area: Volume Ratio of Controlled-Release Pellets

The most convenient method of attaining a desirable rate of release of an agent from a monolithic matrix is by changing the surface area/volume ratio of the controlled-release device. It is obvious that by increasing the surface area of the device in contact with the elution medium, a higher rate of release of the active ingredient can be achieved.

The effect of the ratio of the surface area/volume of rubber-SLS pellets on the release rate of SLS was investigated for different types of rubbers which contained various loadings of SLS.

Cylindrical pellets were used in this investigation and the surface area/volume ratios were varied by changing the radii and thicknesses of the pellets, as discussed in Chapter 3, Section 3.4.3.

The effects of the surface area/volume (S/V) ratios of rubber-SLS composite pellets on the rate of release of SLS from NR pellets which contained 35% SLS (Samples 43 - 48, Table B6, Appendix 1B), SBR pellets which contained 25% SLS (Samples 49 - 54, Table B7, Appendix 1B), and IR pellets which contained 35% SLS (Samples 61 - 66, Table B9, Appendix 1B) are shown in Figures 4.43, 4.44 and 4.45, respectively.

As was to be expected, the amount of SLS released increased markedly when the S/V ratio of the pellets was increased. However, these figures show that the increase in the amount of SLS released with an increase in the S/V ratio of the pellets occurred mainly as a result of higher initial rates of release of SLS from pellets with larger S/V ratios. This was because the initial period of release of SLS involved the dissolution of dispersed SLS particles and, therefore, an increase in the surface area of the pellet in contact with the eluent resulted in the dissolution of larger amounts of dispersed SLS.

Figures 4.46 to 4.48 show plots of the percentages of SLS released as functions of the S/V ratios of the pellets for different intervals during the elution period. These figures suggest that the increase in the amount of SLS released was not a linear function of the S/V ratio of the pellets.

It is obvious from these results that the rate of release of SLS can be varied by changing the surface area with respect to the volume of the rubber-SLS composite pellets. Further, it is clear that by using a mixture of pellets which have different surface area/volume ratios, an optimum combination of desirable amounts of SLS released and effective release lifetimes of controlled-release pellets can be obtained.

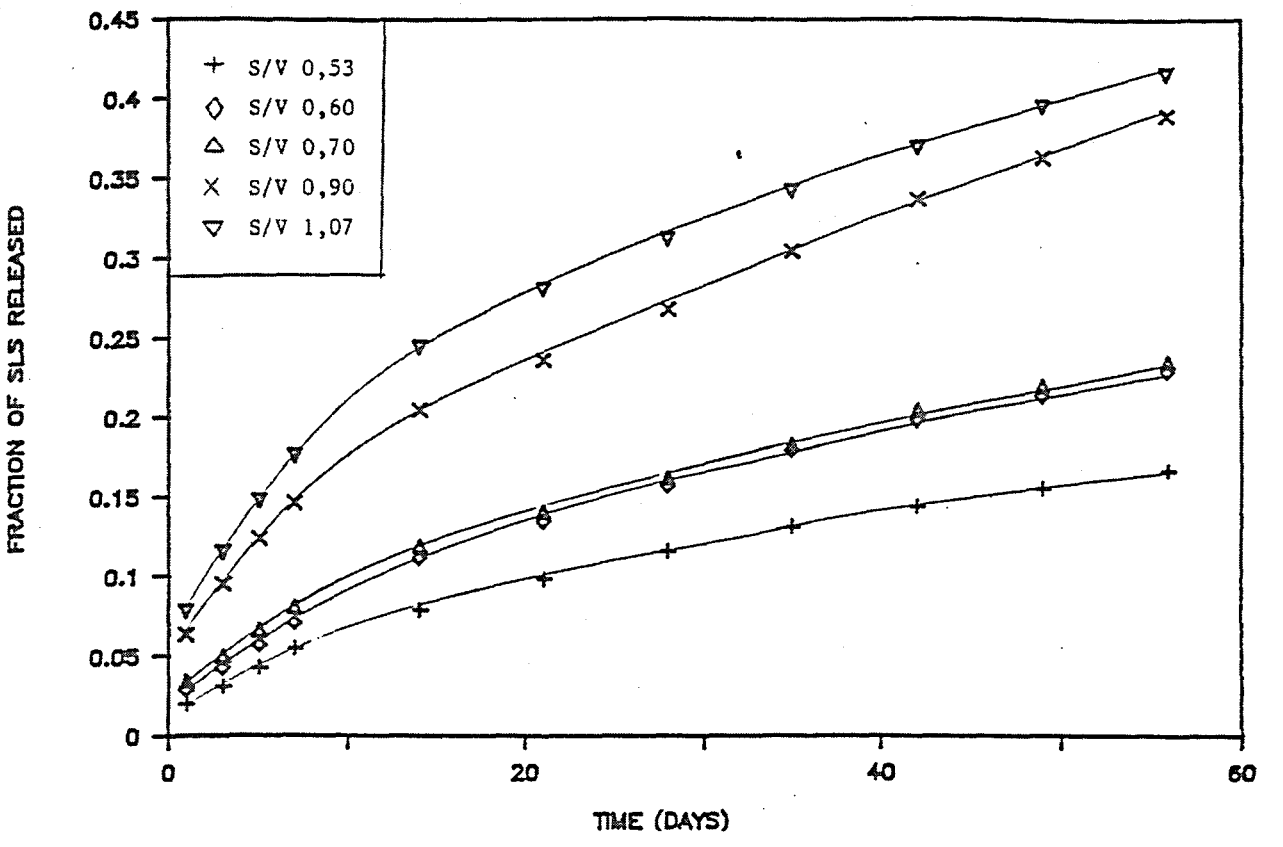

FIGURE 4.43 The effect of the surface area/volume ratio of rubber-SLS composite pellets on the release of SLS from natural-rubber pellets which contained 35% SLS.

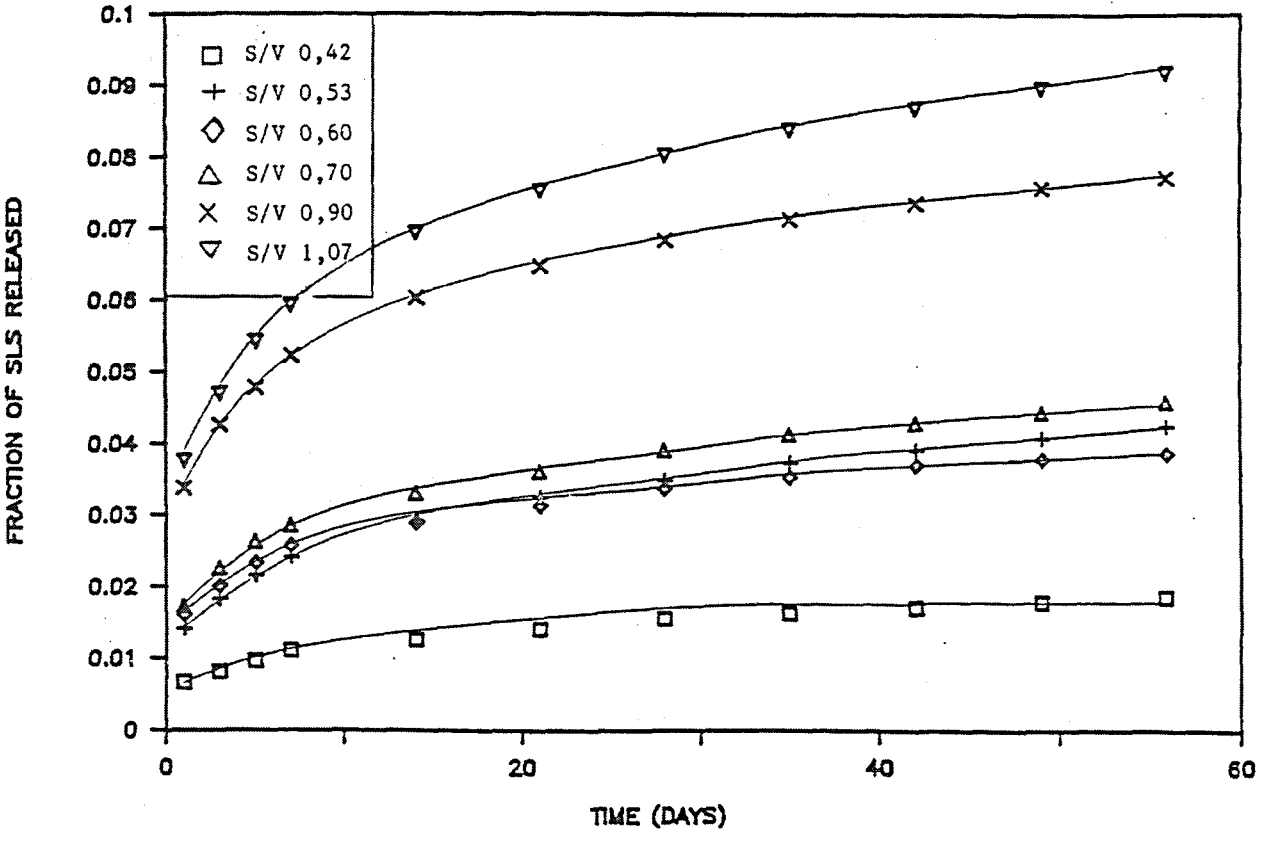

FIGURE 4.44 The effect of the surface area/volume ratio of rubber-SLS composite pellets on the release of SLS from styrene-butadiene rubber pellets which contained 25% SLS.

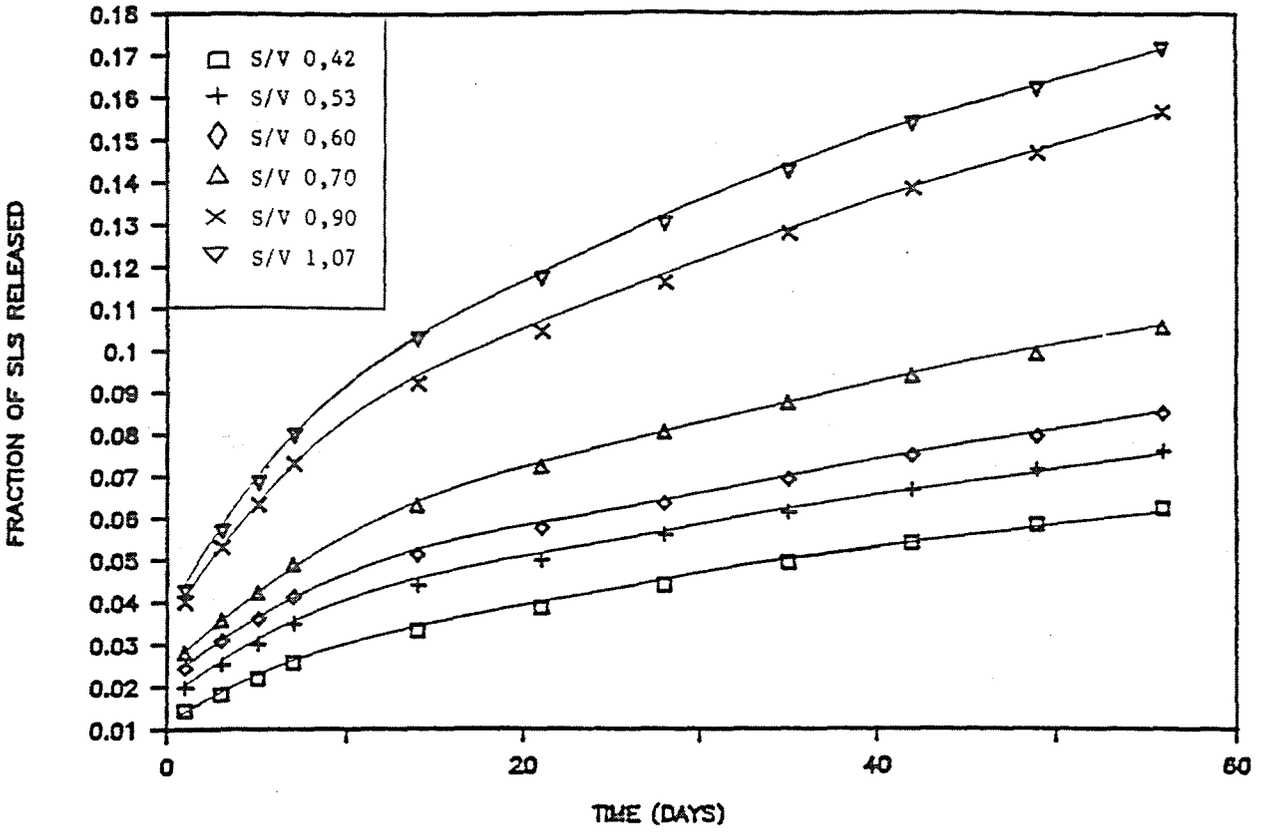

FIGURE 4.45 The effect of the surface area/volume ratio of rubber-SLS composite pellets on the release of SLS from synthetic polyisoprene pellets which contained 35% SLS.

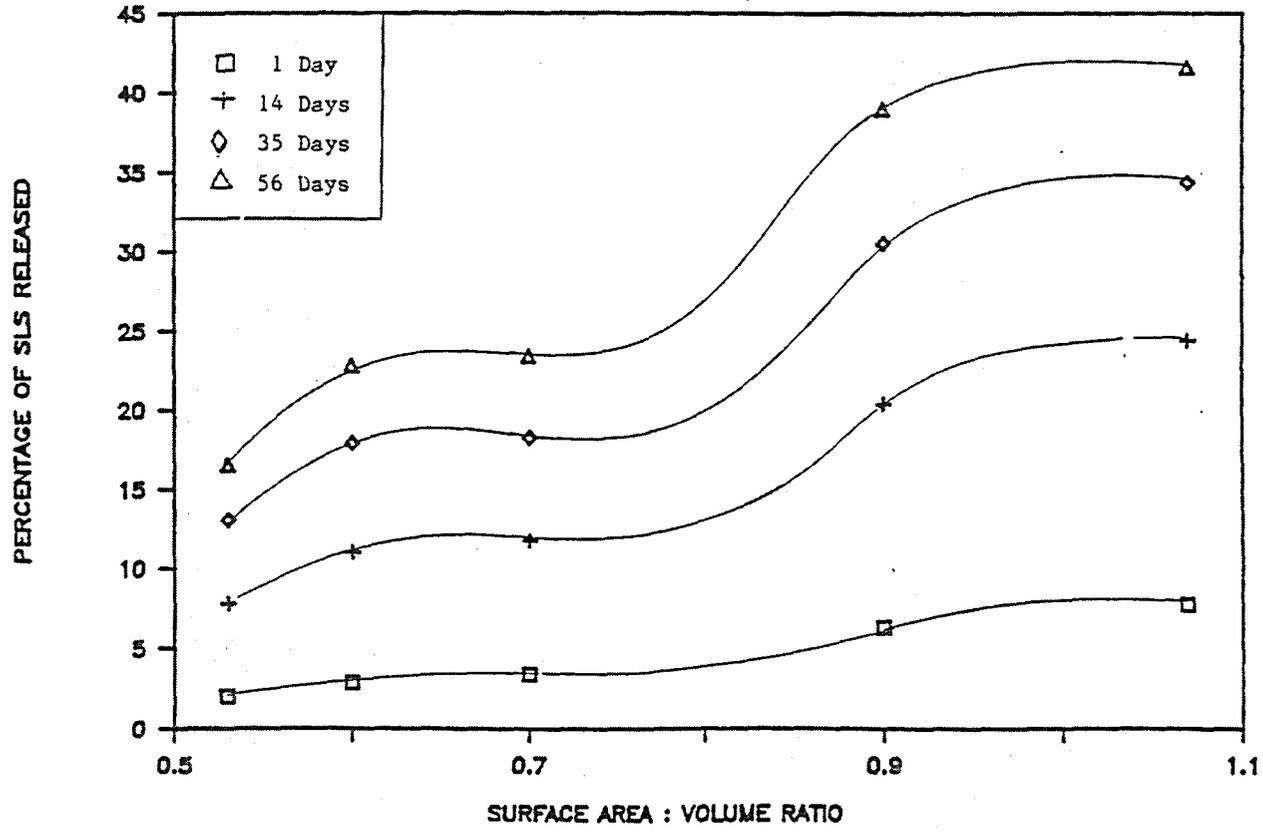

FIGURE 4.46 Plots of the percentages of SLS released as functions of the surface area/volume ratios of natural-rubber pellets which contained 35% SLS. The plots are shown for different intervals during the elution period.

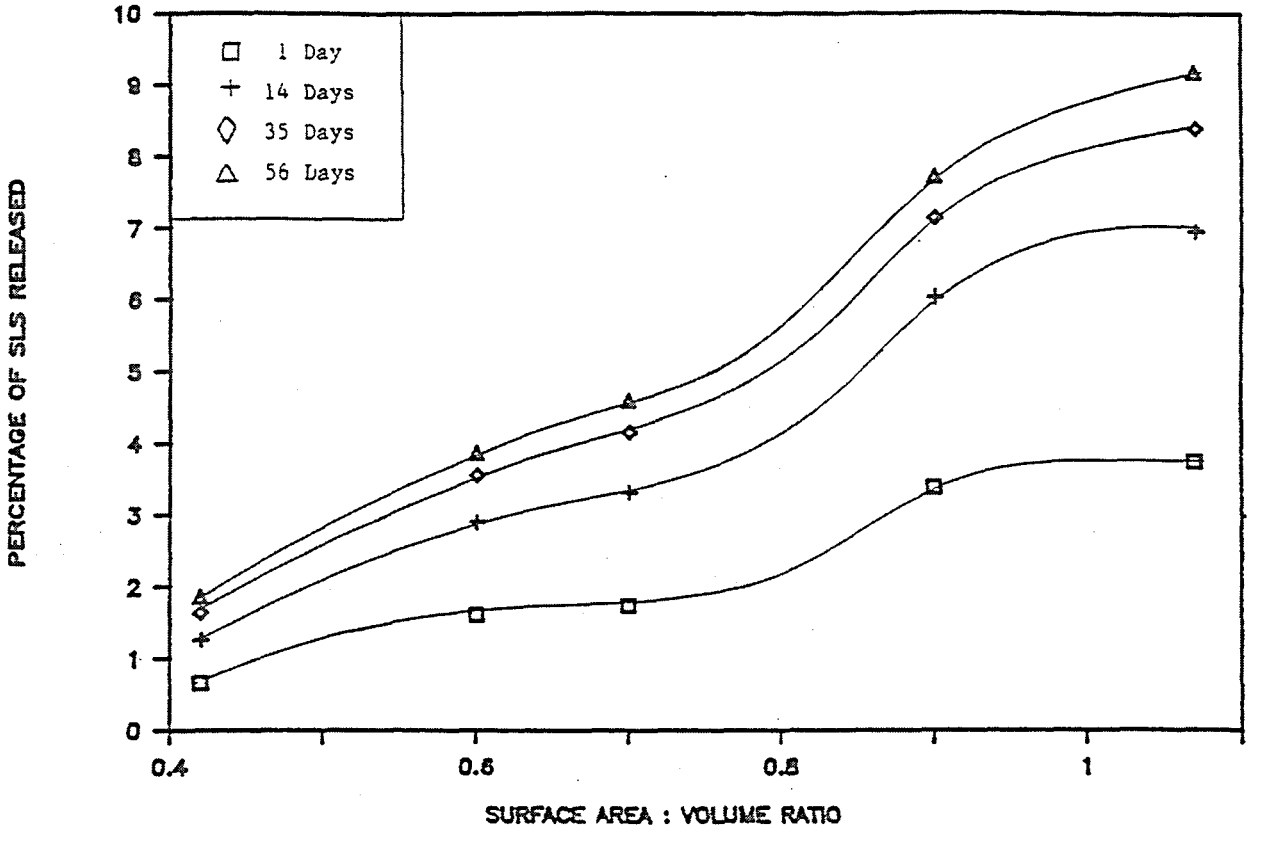

FIGURE 4.47 Plots of the percentages of SLS released as functions of the surface area/volume ratios of styrene-butadiene rubber pellets which contained 25% SLS. The plots are shown for different intervals during the elution period.

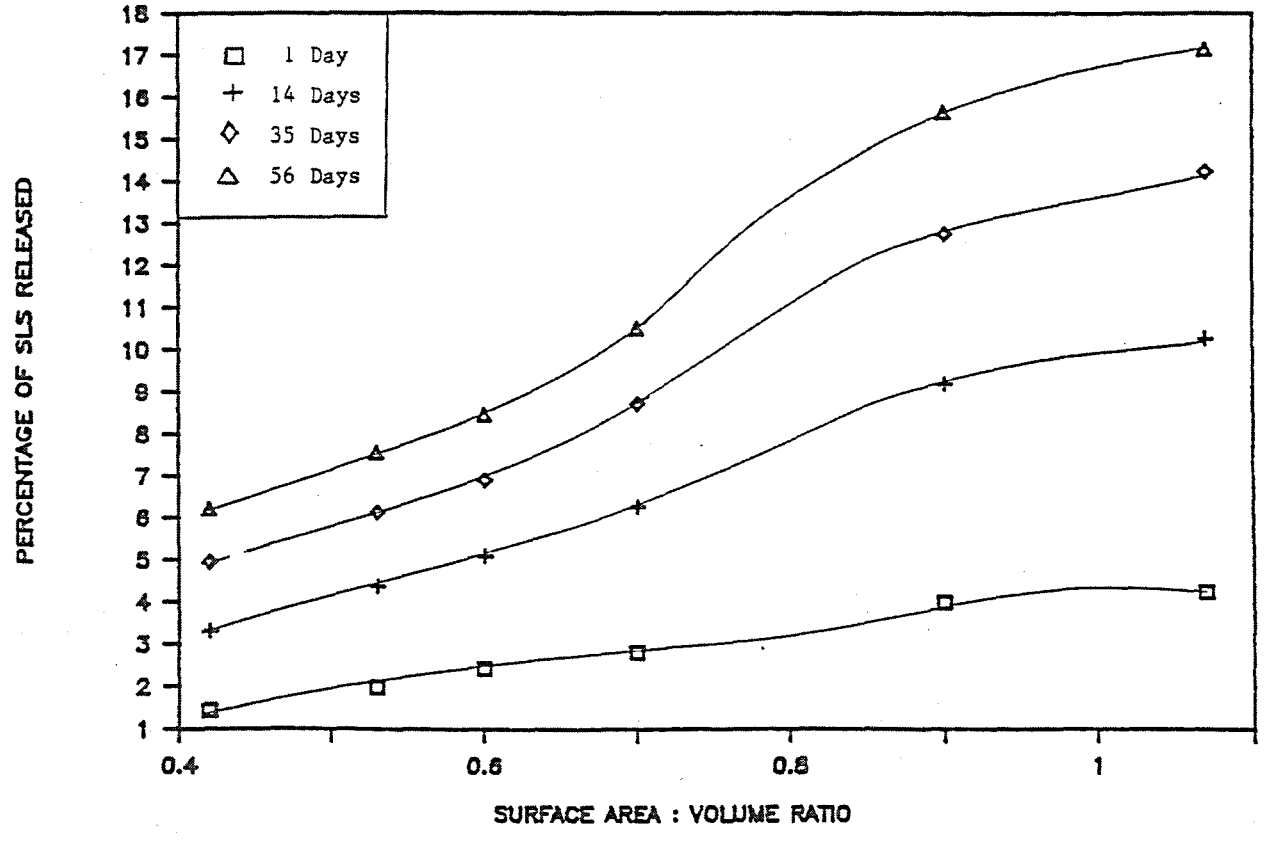

FIGURE 4.48 Plots of the percentages of SLS released as functions of the surface area/volume ratios of synthetic polyisoprene pellets which contained 35% SLS. The plots are shown for different intervals during the elution period.

4.6 THE EFFECTIVE DIFFUSION COEFFICIENTS OF SLS IN NATURAL AND SYNTHETIC RUBBERS

As discussed in Chapter 2, Section 2.4.3.1, most of the mathematical models which have been developed to estimate the rates of release of active agents from monolithic devices are based on a simplified version of the diffusion equation, involving only one space variable. For cylindrical devices, it has been assumed that the height of the cylinder is large compared with its radius, i.e., diffusion from the end surfaces can be neglected, and for slab-shaped devices it has been assumed that edge effects are negligible[41]. Models which describe the release of an active agent from a finite cylinder for which the diffusion from both the end and lateral surfaces is not negligible, require considerably more complex mathematical expressions. Such a mathematical model has been developed by Fu et al.[46]

For the cylindrical rubber-SLS composite pellets used in the experimental investigations reported here, it is obvious that diffusion from both the end and lateral surfaces must be considered. The model developed by Fu et al.[46] was fitted to experimental data for different sets of rubber SLS composite pellets to determine the diffusion coefficients of SLS in natural and synthetic rubbers. The numerical method used to solve the problem, as well as a computer program which has been developed, is discussed in the following sections.

4.6.1 Numerical Method Used for the Calculation of Diffusion Coefficients

The mathematical background of the Fu model was discussed in Chapter 2, Section 2.4.3.2. It was shown that the general solution for the fraction of agent released at time t, according to this model, is:

$$\frac{M(t)}{M(\infty)} \simeq 1 - \frac{8}{l^2 a^2} \sum_{m=1}^{\infty} \frac{\exp(-D\alpha_m^2 t)}{\alpha_m^2} \cdot \sum_{n=0}^{\infty} \frac{\exp(-D\beta_n^2 t)}{\beta_n^2} \qquad (4.11)$$

where M(t)/M(D) is the fraction of agent released at time t, ℓ is half the length of the pellet (i.e., the length is 2ℓ), a is the radius of the pellet, D is the diffusion coefficient, α_m are the roots of $J_o(a\alpha) = 0$, where J_o is a zero-order Bessel function, and $\beta_n = (2n+1)\,\pi/2\,\ell$ From Equation (4.11), it is clear that there is no direct method for determining the value of D. A least-squares technique is therefore followed.

Let y_i be the experimental fractions of SLS released at times t_i, so that the error function S is defined as:

$$S = \sum_i \left[y_i - f(t_i) \right] \tag{4.12}$$

where $f(t_i)$ is the theoretical fraction of SLS released at time t_i. To minimize S with respect to D, it is required that

$$\frac{\partial S}{\partial D} = 0 \tag{4.13}$$

Since this cannot be obtained directly, Newton's method is applied to the problem[211], setting

$$D_{k+1} = D_k - \left[\frac{\partial S}{\partial D} \right] \left[\frac{\partial^2 S}{\partial D^2} \right] \tag{4.14}$$

where D_k is the k-th and D_{k+1} the (k + 1)-th guess of the value of D. It can be shown that

$$\frac{\partial S}{\partial D} = \sum_i - 2 \left[y_i - f(t_i) \right] \frac{\partial f}{\partial D} \tag{4.15}$$

and that

$$\frac{\partial^2 S}{\partial D^2} = \sum_i - 2 \left\{ - \left[\frac{\partial f}{\partial D} \right]^2 + \left[y_i - f(t_i) \right] \frac{\partial^2 f}{\partial D^2} \right\} \tag{4.16}$$

Since

$$\frac{\partial f}{\partial D} \simeq \frac{8t}{l^2 a^2} \left[\sum_{m=1}^{60} \exp\left(-D\alpha_m^2 t\right) \sum_{n=0}^{60} \frac{\exp\left(-D\beta_n^2 t\right)}{\beta_n^2} + \sum_{m=1}^{60} \frac{\exp\left(-D\alpha_m^2 t\right)}{\alpha_m^2} \sum_{n=0}^{60} \exp\left(-D\beta_n^2 t\right) \right] \tag{4.17}$$

and

$$\frac{\partial^2 f}{\partial D^2} \simeq \frac{-8t^2}{l^2 a^2}\left[\sum_{m=1}^{60} \alpha_m^2 \exp(-D\alpha_m^2 t) \sum_{n=0}^{60} \frac{\exp(-D\beta_n^2 t)}{\beta_n^2}\right.$$

$$+ 2\sum_{m=1}^{60} \exp(-D\alpha_m^2 t) \sum_{n=0}^{60} \exp(-D\beta_n^2 t) \qquad (4.18)$$

$$\left.+ \sum_{m=1}^{60} \frac{\exp(-D\alpha_m^2 t)}{\alpha_m^2} \sum_{n=0}^{60} \beta_n^2 \exp(-D\beta_n^2 t)\right]$$

all the unknowns in Equation (4.14) are specified and a close approximation of D can be obtained by successive substitution. The iteration process is stopped when S reaches a value smaller than a constant specified by the analyst. A Turbo Pascal program (code DIFFCALC) which performs this task is given in Appendix 6A.

4.6.2 Procedure Followed for Calculating the Values of D

In order to calculate the diffusion coefficient, D, of SLS in natural and synthetic rubbers and to fit the model developed by Fu et al.[46] to experimental data, an IBM PC and a disk containing the following files were used:

ALSLS.WK1	LOTUS 1-2-3 worksheet file containing experimental data.
ALSLS.PRN	Print file containing raw data from worksheet file.
DIFFCALC.PAS	Pascal source code of the processing program.
DIFFCALC.COM	Executable processing program.
DIFFC87.COM	8087 Version of DIFFCALC program (for use with a PC which is equiped with an 8087 mathematical co-processor).

DIFFSLS.PRN	Print file containing processed data.
DIFFSLS.WK1	LOTUS 1-2-3 worksheet file containing processed data.

The sequence of steps required to calculate the values of D are as follows:

A. Enter the LOTUS 1-2-3 system disk and load ALSLS.WK1. This file contains originally measured data and the mass of each of the rubber-SLS pellets used in experimental investigations in one table and the dimensions and SLS contents of the pellets, as well as the fractions of the total SLS contents released, in another table. The format of this table is sample number, a (the radius of the pellet), ℓ (half the length of the pellet) and then experimental points. The LOTUS 1-2-3 worksheet file ALSLS.WK1 is given in Appendix 6B.

Create a print file containing the fractions of SLS released for those samples which must be read by the DIFFCALC program. This is done by using the LOTUS 1-2-3 / PRINT FILE command. An example of such a print file is ALSLS.PRN. There must be no blank lines in this print file and, therefore, none of the LINE, PAGE, etc., commands must be used. The last line in the print file must be a data line and may not be followed by a blank line.

B. Run DIFFCALC or DIFFC87. The program will prompt the user for the input filename (eg. ALSLS.PRN) and the output filename (eg. DIFFSLS.PRN). The program requires the data in the format of ALSLS.WK1, as printed into the print file. It will read and process the data one sample at a time and will stop automatically when all the samples have been read. After a sample has been read, the sample number, a and ℓ will be displayed, followed by the 11 experimental points read. It is assumed that the times at which the points were measured are 1, 3, 5, 7, 14, 21, 28, 35, 42, 49 and 56 days (as mentioned in Chapter 3, Section 3.4.4). The message "Hit ESC to interrupt and modify D for the next iteration" is then displayed, after which a pause will follow while the program initializes itself for the new sample. From this point on, hitting the ESC button will interrupt the program (after the pause) and request the user to input a new value for D. Normally, the program will select its own initial value for D as 0,5 for the first sample, or the value of D obtained for the previous sample. If it is found that this does not give a satisfactory value for D, a value of 1/10 times the previous D value is used. If D becomes too small or too large, the program will request the user to input a new value for

D. By just hitting RETURN, the program will use the same D value. If the user gives D as 0, the program will give up trying to find D for this sample and will proceed to the next sample. If the user gives D as <0, the program will stop.

When calculating the next D value, the program displays the experimental point number, followed by a dash, followed by another number. This second number is the number of terms evaluated in the power series (discussed in Section 4.6.3). For example, 4-867 would mean that 867 terms were evaluated to find point 4 of the present example. The maximum number of terms is 1 000. Hitting ESC at any time during the calculation of D will abort the calculation at the end of the present point and will prompt the user for a new D value. For a PC without an 8087 mathematical co-processor, the determination of 1 000 terms is quite a time-consuming process. The smaller the value of D multiplied by the time, the more terms must be evaluated. Once an accurate value of D has been found, the program writes the value of D, the experimental points and the theoretical points for the curve to the output file and proceeds to the next sample. If the user aborts the calculation by entering D as less than or equal to zero, the sample is not written to the output file.

C. The output file of the DIFFCALC program is a print file (eg. DIFFSLS.PRN) ready to be read using the LOTUS 1-2-3 / FILE IMPORT NUMBERS command.

The first line of this print file contains headings for the columns, as well as the time for each point. The samples then follow this. Each sample consists of a blank line followed by two data lines. The first data line contains, sequentially, the sample number, the value of a, the value of D, and then the word "Experimental", followed by the experimental data points, starting with zero. The second data line contains a spacer (empty string), the value of ℓ, a measure of the "goodness of fit" called e, the word "Theoretical", and then the theoretically predicted values for the fractions of SLS released at times corresponding to the experimental points, again starting with zero. The file DIFFSLS.WK1 is a LOTUS 1-2-3 worksheet file containing such an imported print file, and is given in Appendix 6C. The LOTUS 1-2-3 / GRAPH command can then be used to display the results of the DIFFCALC program. It will be noted that even the very few theoretical points given produce a reasonably smooth curve, as shown in Section 4.6.4. As a result of the excessive computation time involved in solving the very long power series, it was deemed undesirable to provide more theoretical points. The worksheet file DIFFSLS.WK1 can be used to prepare all the graphs for display purposes.

4.6.3 The Power Series

When the DIFFCALC program is run, it will be noted that most of the computation time goes into the calculation of the power series. Referring to DIFFCALC.PAS (i.e., the Pascal source code of the processing program) in Appendix 6A, it can be seen that the series contains terms such as

```
exp  ( - D * alfa2 * t)  /  alfa2
```

and

```
exp ( - D * beta2 * t)  /  beta2
```

Here, exp represents exponentiation, alfa is a short phonetic spelling for alpha, and alfa2 and beta2 represent the squares of alfa and beta. Alfa is a root of the zero-th Bessel function and beta is a number originating from a Fourier series[46]. Both alfa and beta depend on i, that is, the number of the term. What is important to note is that both alfa and beta increase linearly and, therefore, the difference between alfa in one term and alfa in the next term is a constant. The same argument applies to the beta values. This is especially true after about 20 terms. The reason for this is apparent from the formula of beta, namely, $\beta = (2n+1)\,\pi\,/2\ell$, and the result that for large i, the i-th and (i + 1)-th roots of the zero-th Bessel function is pi (3,14159 ...) apart[212].

When D*t is large (say larger than 10^{-3}), the value inside the exponent is relatively large and negative, so that the exponent becomes very small (or even zero due to the finite capacity of the digital computer storage) for moderate values of alfa2 and beta2. However, if D*t is very small, the exponent is approximately 1, and very large values of alfa2 and beta2 are required to decrease this value significantly. Assuming that the exponent term is approximately 1, the terms in the power series are approximately 1/alfa2 and 1/beta2. These terms converge very slowly, since alfa and beta increase only linearly. Referring to Equation (4.11), it can be shown that for a=1 and $\ell = 1$, the sum over an infinite number of terms of 1/alfa2 should equal 0,25[213]. Since alfa increases only linearly, the value after 1 000 terms is only about 0,2485. This is understandable since all the alfas are positive, so there must be "enough space" between this number and 0,25 to fit the sum of all the terms up to infinity. A similar argument can be advanced for beta.

The problem, however, which arises for small values of D*t, is that one is interested in the fraction of SLS released. The fraction, f, is given by one minus the product of the two power series. For small fractions, it is clear that the product of the two power series would be close to 1, so that a small error

in either of the power series would result in a relatively large change in the difference between one and the product of the two power series. Since this case corresponds to the very small values of D, where the terms in the power series diminish very slowly, it is clear that a large number of terms are required in each of the power series to obtain an accurate result.

The values of beta are obtained from an algebraic expression and as many terms as are required can be generated without problems. The values of alfa, however, must be obtained from the zeros of the zero-th Bessel function. The first sixty of these zeros were taken from the literature[234]. More digits of precision are used for terms 1 to 20 than for terms 21 to 40, which have more digits of precision than terms 41 to 60 have. This is because the relative importance of precision diminishes for the higher terms. For terms 61 to 1 000, the result that two zeros are approximately pi (3.141 ...) apart was used to approximate the values of the zeros. It is estimated that the resulting error in D because of this approximation would be less than D/100, which is approximately what the error would be from the truncation of the power series after 1 000 terms for the smallest values of D found with the present experiments[235].

Using the present version of the DIFFCALC program, the theoretical curves obtained, as given in Figures 4.49 to 4.54, show qualitatively that the agreement of experimental and theoretical data is such that the numerical error in determining D is negligible in comparison with experimental errors, and it would be prudent to give D to one or two significant digits only.

The above approach was thorough enough to ensure that the D values, as presented in the file DIFFSLS.WK1 (Appendix 6C) and in Table 4.1, were obtained with a mathematical model of sufficient sophistication and to sufficient numerical accuracy to be representative of the effective diffusion coefficients of SLS in natural and synthetic rubbers, allowing for experimental error.

4.6.4 Agreement Between Experimental and Theoretically-Predicted Data

Figures 4.49 to 4.54 show comparisons of the experimentally-determined fraction of SLS released as a function of time with the theoretical fractions released, as predicted by the mathematical model of Fu et al.[16] The symbols in these figures represent the measured values, whereas the curves represent the theoretically-predicted fractions of SLS released.

In general, good fits of the model to experimental data were obtained for rubbers which contained 5, 10, 35 and 45% SLS, whereas the agreement between theoretical and experimental values was less satisfactory for rubbers which contained 15, 25 and 55% SLS. Figures 4.49 and 4.50 show the

agreement between theoretical and experimental data for NR which contained 5% SLS and IR which contained 5% SLS, respectively. The agreement between the theoretically-predicted and experimentally-measured values of the fractions of SLS released was very satisfactory for these samples. The same was true for SBR which contained 35% SLS and NR/SBR which contained 35% SLS, as shown in Figures 4.51 and 4.52, respectively. However, for SLS levels of 25% and 55%, the model did not fit the experimental data very well. This is shown in Figures 4.53 and 4.54, respectively, for IR which contained 25% SLS and SBR which contained 55% SLS.

These poor fits, as shown in Figures 4.53 and 4.54, are unlikely to be the result of a substantial experimental error in the determination of the fractions of SLS released. It was shown in Section 4.5.1 that the rate of release of SLS was a non-linear function of the initial SLS loading. Since it was suggested that this non-linear increase in the release rate with an increase in the SLS loading occurred because of the development of porosity in the rubbers, it seems reasonable to assume that the poor correlation of theoretical data with experimental points is the result of the development of porosity in the rubber matrices. The assumption is made in the mathematical model of Fu et al.[46] that diffusion of an agent occurs through a homogeneous polymer matrix. It is, therefore, obvious that poor fits of this model to experimental data will result when the polymer matrices are highly porous. The poor fits obtained for rubbers which contained 25% SLS are difficult to explain. It is possible that at levels of 25% SLS a transition from a diffusion-controlled to a porosity-controlled release mechanism occurred.

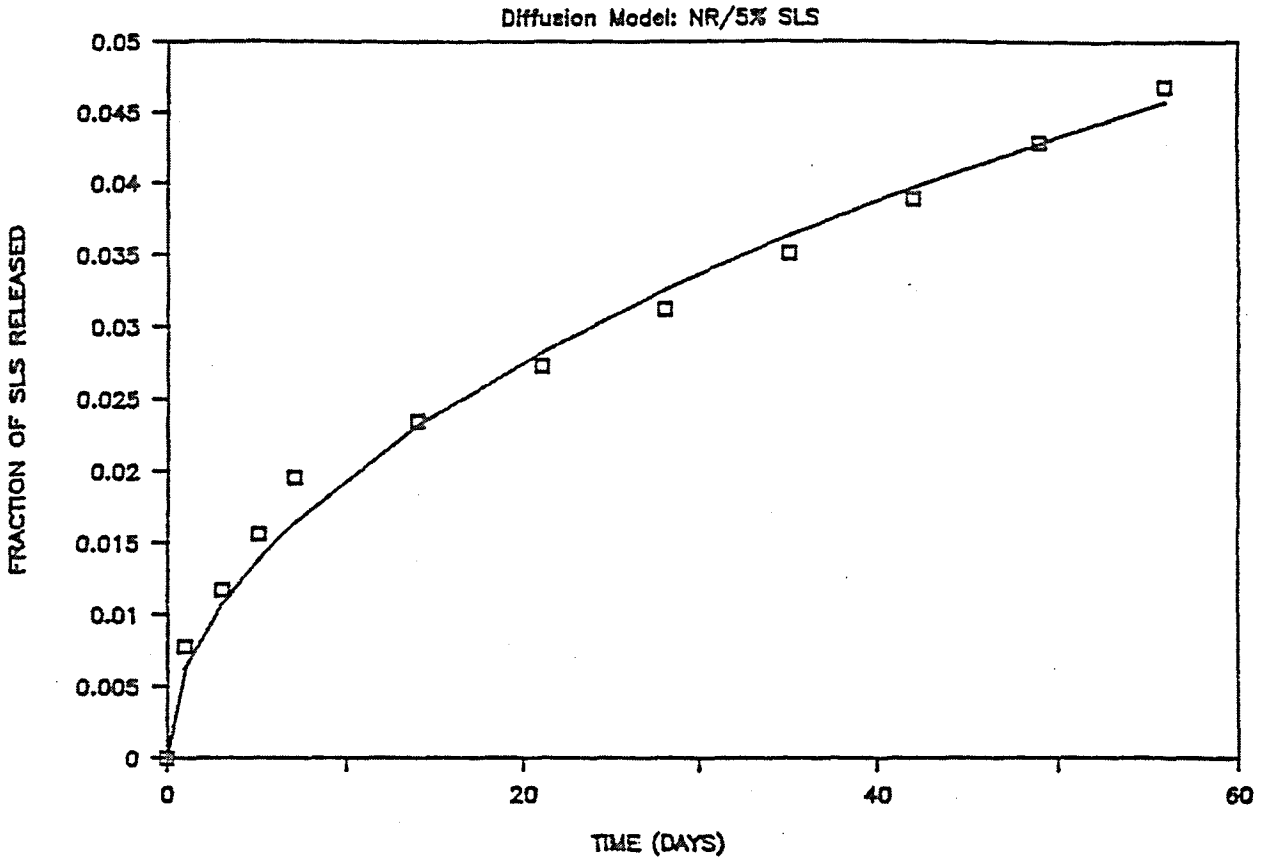

FIGURE 4.49 Comparison of the experimentally-determined fraction of SLS released as a function of time with the theoretical fractions released (as predicted by the mathematical model developed by Fu et al.[46]) for a natural-rubber formulation which contained 5% SLS.

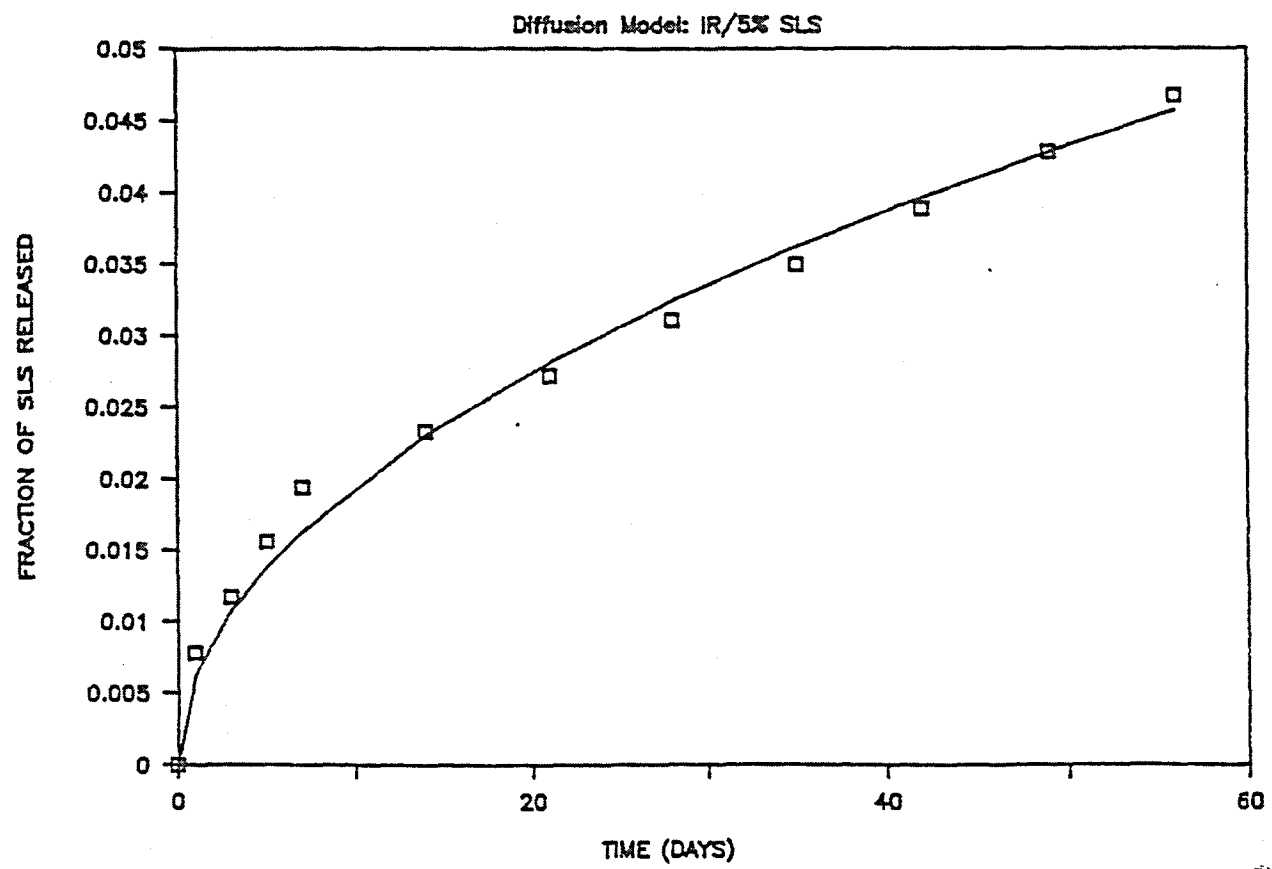

FIGURE 4.50 Comparison of the experimentally-determined fraction of SLS released as a function of time with the theoretical fractions released (as predicted by the mathematical model developed by Fu et al.[46]) for a synthetic polyisoprene formulation which contained 5% SLS.

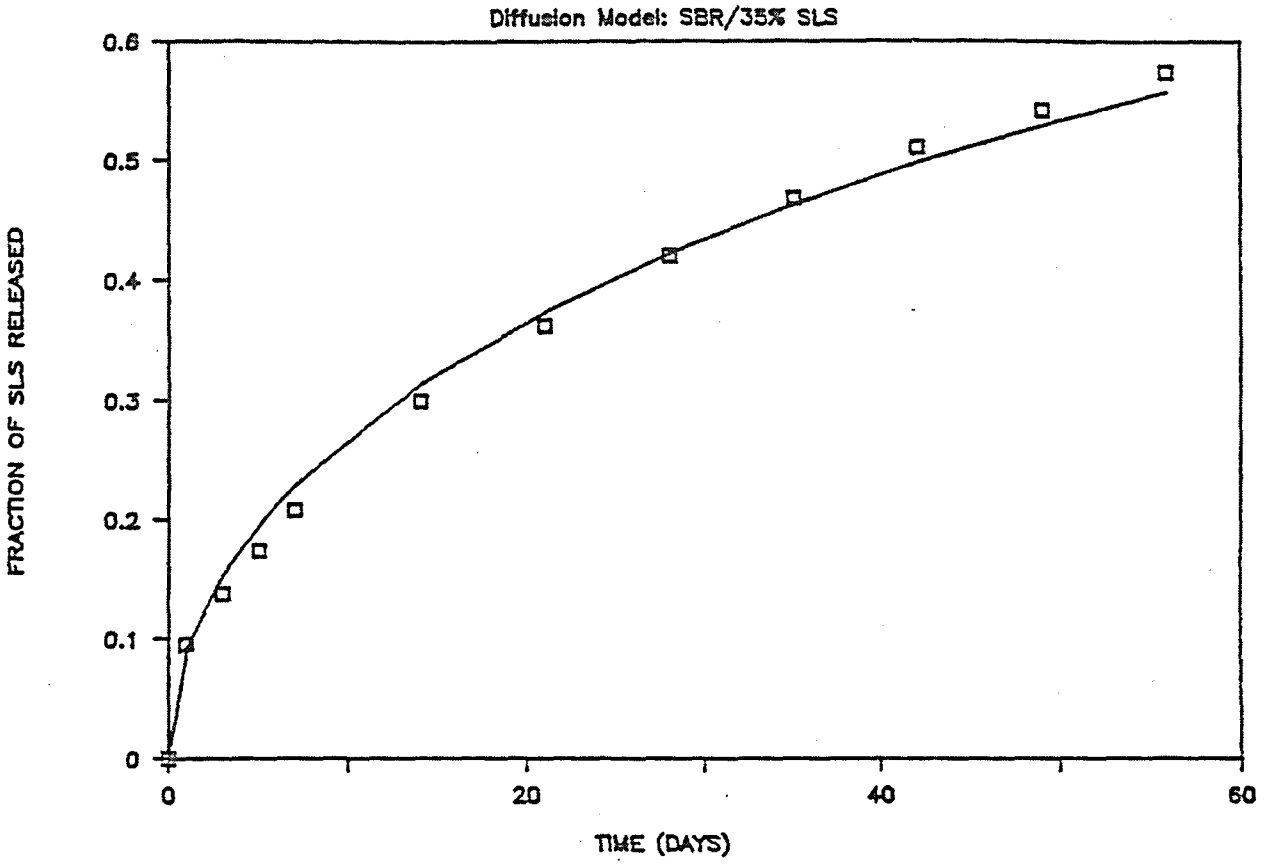

FIGURE 4.51 Comparison of the experimentally-determined fraction of SLS released as a function of time with the theoretical fractions released (as predicted by the mathematical model developed by Fu et al.[46]) for a styrene-butadiene rubber formulation which contained 35% SLS.

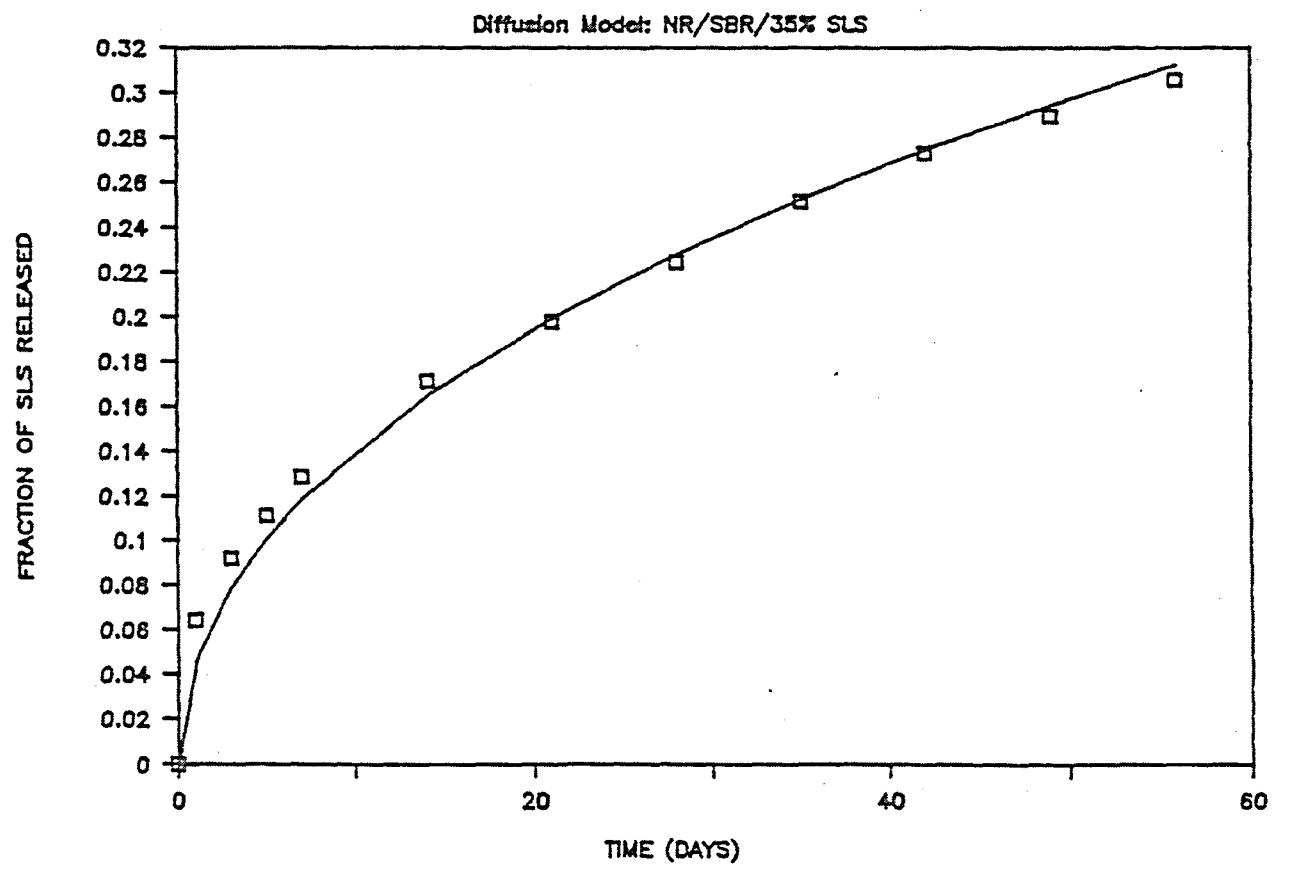

FIGURE 4.52 Comparison of the experimentally-determined fraction of SLS released as a function of time with the theoretical fractions released (as predicted by the mathematical model developed by Fu et al.[46]) for a 50:50 blend of natural rubber and styrene-butadiene rubber which contained 35% SLS.

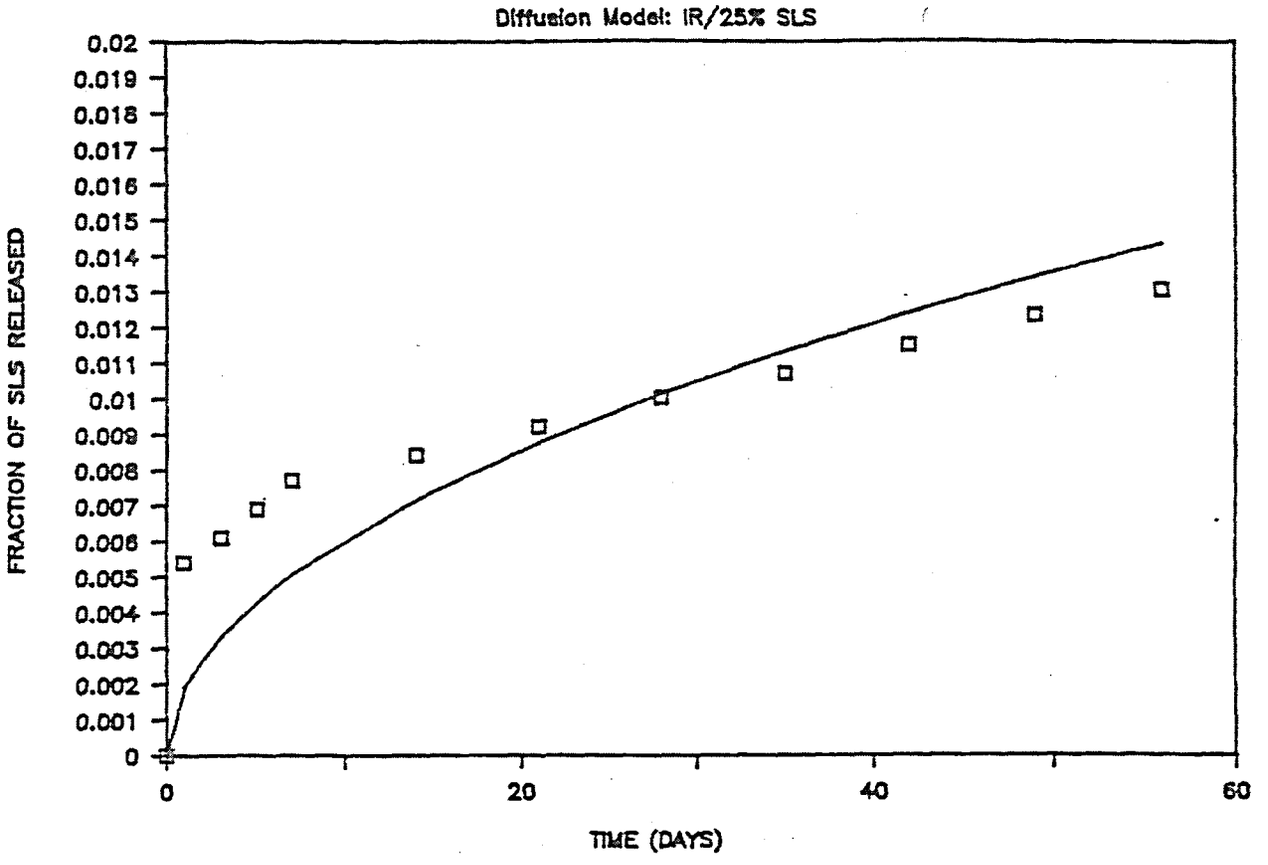

FIGURE 4.53 Comparison of the experimentally-determined fraction of SLS released as a function of time with the theoretical fractions released (as predicted by the mathematical model developed by Fu et al.[46]) for a synthetic polyisoprene formulation which contained 25% SLS.

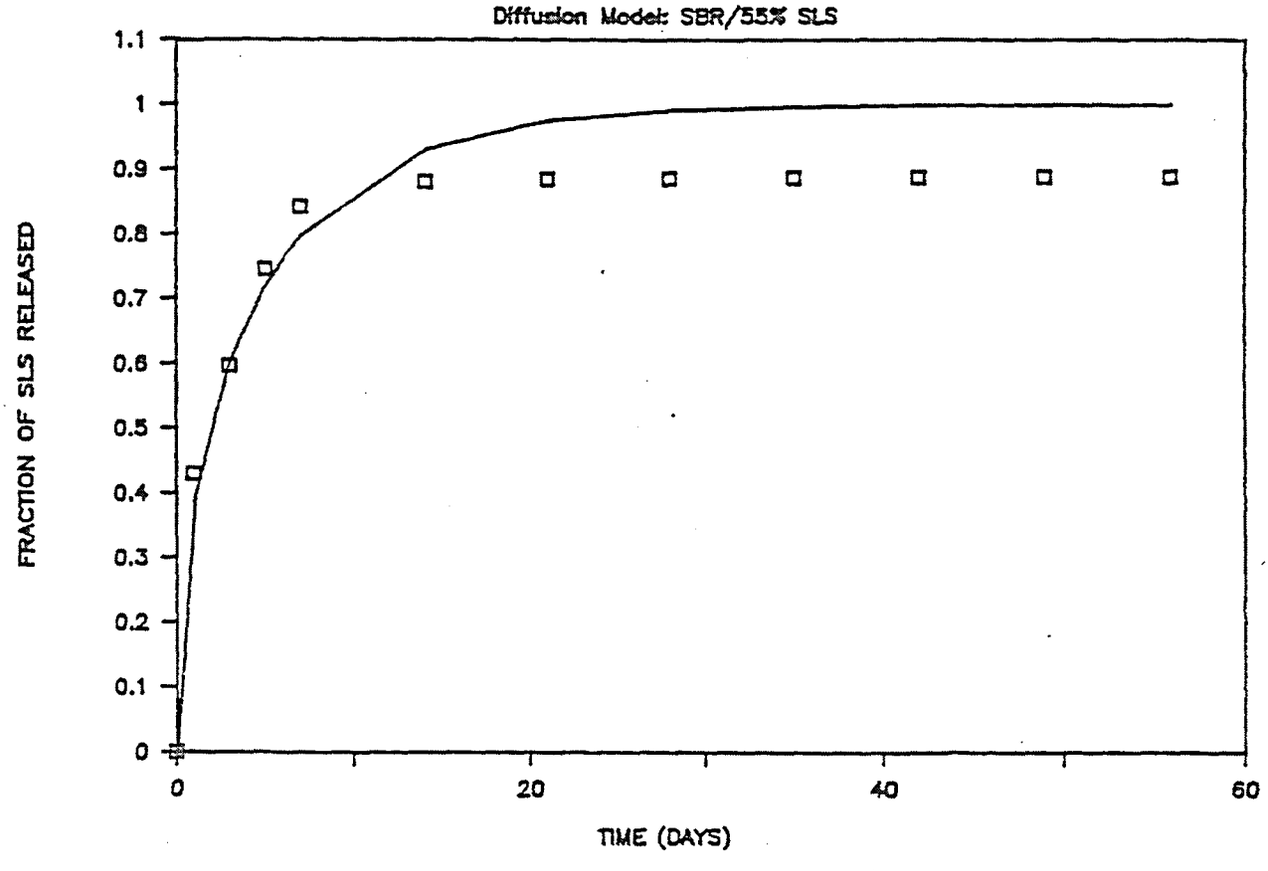

FIGURE 4.54 Comparison of the experimentally-determined fraction of SLS released as a function of time with the theoretical fractions released (as predicted by the mathematical model developed by Fu et al.[46]) for a styrene-butadiene rubber formulation which contained 55% SLS.

4.6.5 Concentration-Dependent Diffusion Coefficients

The values obtained for the effective diffusion coefficients (D) of SLS in elastomeric pellets, as given in Table 4.1 and in Appendix 6C, showed that for a particular type of elastomer, the value of D depended on the initial loading of SLS in that elastomer. For a series of natural-rubber pellets which contained 15 to 55% SLS, there was a four-orders-of-magnitude increase in the value of D when the SLS loading was increased from 15 to 55%. Similar increases in the value of D with an increase in the SLS loading were obtained for other elastomeric formulations.

Figures 4.55 and 4.56 show plots of log D as a function of the SLS loading. These figures show clearly that D increased with an increase in the SLS loading and that, for a particular elastomer, the relationship between D and the SLS loading was non-linear. As discussed previously (Sections 4.5.1 and 4.6.4), porosity developed in rubber matrices which contained 35% or more SLS. As the release process continued, the degree of porosity in a specific rubber-SLS pellet increased. It is, therefore, obvious that at any given time during the release process, the value of D will depend on the degree of porosity created in the rubber matrix up to that time. For rubber pellets which contained 10, 15 and 55% SLS, the calculated values of D are expected to be incorrect.

The model developed by Fu et al.[46], which was used to calculate the values of D, assumed that D was a constant, as given by the equation[46]:

$$\frac{\partial C}{\partial t} = D\left[\frac{\partial^2 C}{\partial r^2} + \frac{1}{r}\frac{\partial C}{\partial r} + \frac{\partial^2 C}{\partial z^2}\right] \qquad (4.19)$$

where D was written outside the differential. However, the values obtained for D (Table 4.1) showed that, for a given series of rubber-SLS formulations, D was not a constant.

Attempts were, therefore, made to develop a mathematical model which would express D as a function of the SLS loading. A numerical method was used to predict the rate of release of SLS, according to this model, from cylindrical rubber-SLS composite pellets. This numerical method is discussed in Section 4.7.

TABLE 4.1 The effective diffusion coefficients of SLS in cylindrical rubber-SLS composite pellets

Sample number	a[a] (mm)	ℓ[b] (mm)	Type of rubber	Mass % SLS	D ($cm^2.sec^{-1}$)
1	9	5	NR	15	$3,86 \times 10^{-12}$
2	9	5	NR	25	$2,85 \times 10^{-12}$
3	9	5	NR	35	$4,27 \times 10^{-10}$
4	9	5	NR	45	$3,69 \times 10^{-8}$
5	9	5	NR	55	$2,80 \times 10^{-8}$
6	9	5	SBR	15	$2,01 \times 10^{-12}$
7	9	5	SBR	25	$6,06 \times 10^{-12}$
8	9	5	SBR	35	$4,43 \times 10^{-9}$
9	9	5	SBR	45	$9,78 \times 10^{-8}$
10	9	5	SBR	55	$1,02 \times 10^{-7}$
11	9	5	NR/SBR	15	$2,53 \times 10^{-12}$
12	9	5	NR/SBR	25	$1,08 \times 10^{-11}$
13	9	5	NR/SBR	35	$1,11 \times 10^{-9}$
14	9	5	NR/SBR	45	$3,95 \times 10^{-8}$
15	9	5	NR/SBR	55	$1,46 \times 10^{-7}$
34	9	5	IR	15	$2,62 \times 10^{-12}$
35	9	5	IR	25	$1,88 \times 10^{-12}$
36	9	5	IR	35	$4,97 \times 10^{-11}$
37	9	5	IR	45	$2,08 \times 10^{-8}$
38	9	5	IR	55	$6,66 \times 10^{-8}$

a. Radius of the pellet
b. Half the length of the pellet

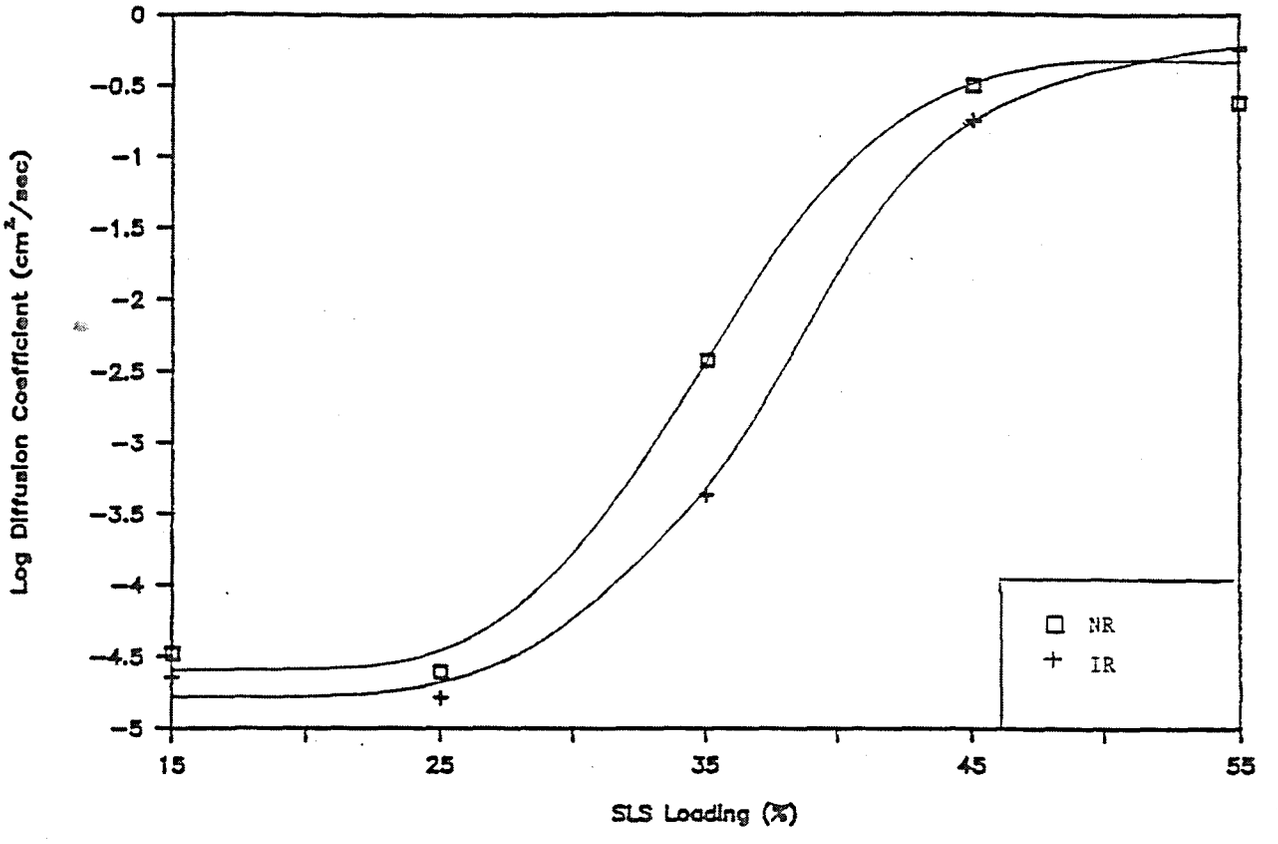

FIGURE 4.55 Plots of log D as a function of the SLS loading for natural rubber and synthetic polyisoprene.

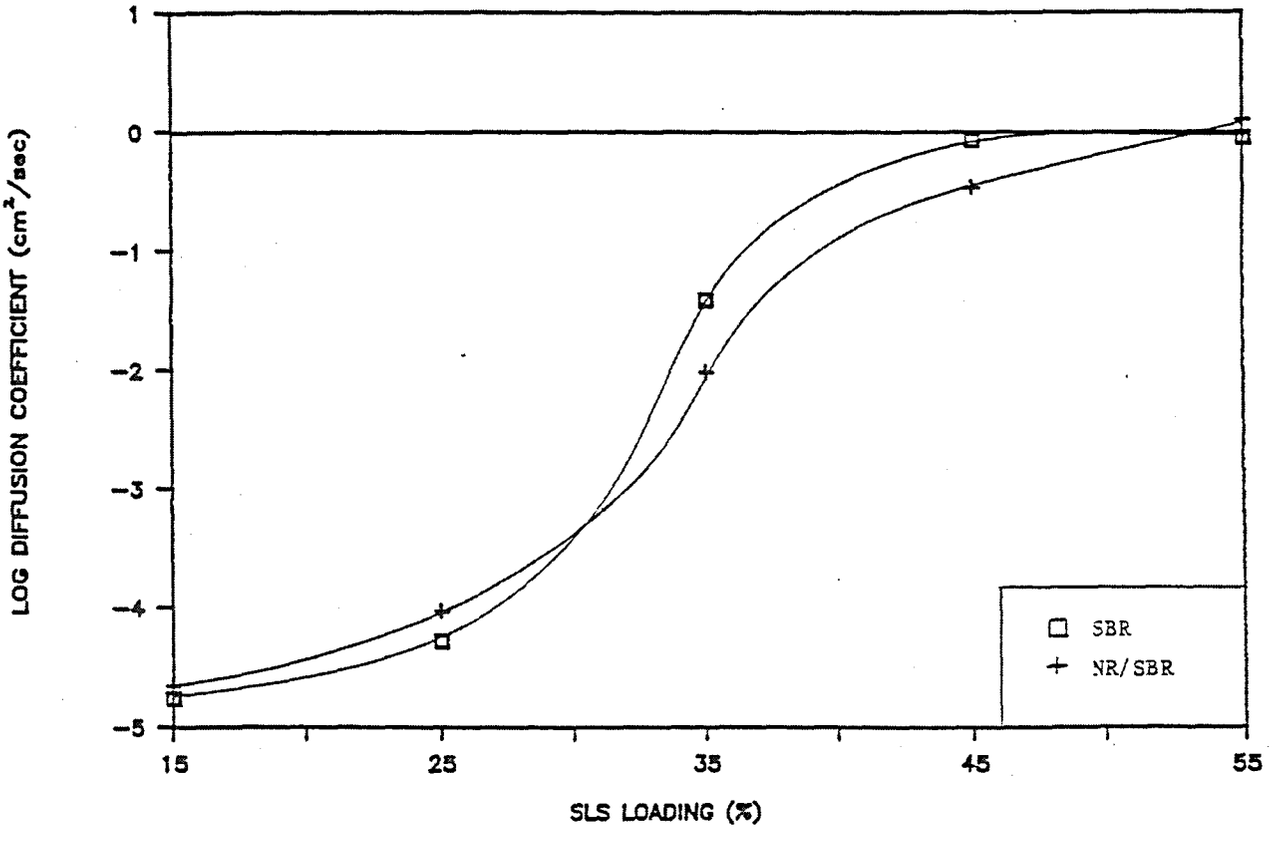

FIGURE 4.56 Plots of log D as a function of the SLS loading for styrene-butadiene rubber and a 50:50 blend of styrene-butadiene rubber and natural rubber.

4.7 NUMERICAL PREDICTION OF THE RATE OF RELEASE OF SLS FROM CYLINDRICAL RUBBER-SLS COMPOSITE PELLETS

4.7.1 General Background

The numerical method used for predicting the rates of release of SLS from cylindrical rubber-SLS composite pellets is based on a general method of prediction for heat and mass transfer, fluid flow, and related processes. The construction of numerical methods for predicting these processes has been discussed thoroughly by Patankar[216]. An important characteristic of these methods is that they are strongly based on physical considerations, not just on mathematical manipulations.

4.7.1.1 Mathematical description of physical phenomena

The numerical solution of processes such as heat transfer, mass transfer and fluid flow can begin when the laws governing these processes have been expressed in mathematical form, generally in terms of differential equations. The individual differential equations express a certain conservation principle. Each equation employs a certain physical quantity as its dependent variable and implies that there must be a balance among the various factors which influence this variable. The dependent variables of these equations are usually specific properties, i.e., quantities expressed on a unit-mass basis. Examples are mass fraction, velocity, and specific enthalpy[217].

The terms in a differential equation of this type denote influences on a unit-volume basis. For example, if J denotes a flux influencing a typical dependent variable Φ, consider the control volume of dimensions dx, dy, dz, as shown in Figure 4.57.

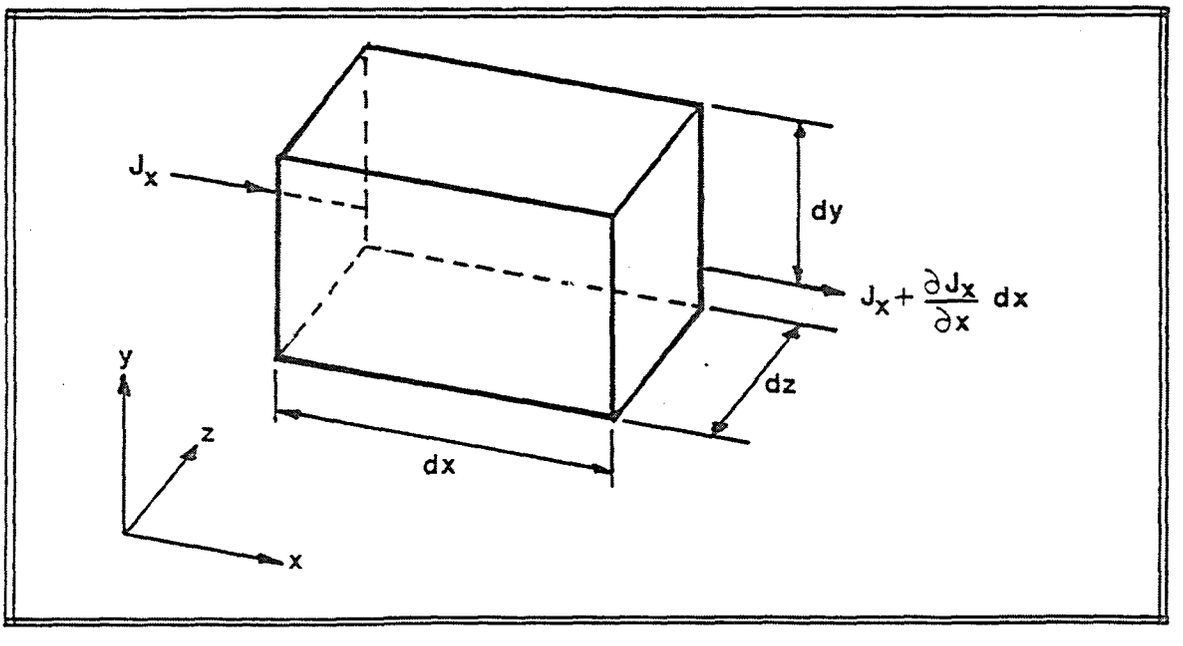

FIGURE 4.57 Flux balance over a control volume.

The flux J_x (which is the x-direction component of J) is shown entering one face of area dy dz, while the flux leaving the opposite face is shown as $J_x + (\partial J_x / \partial x)\,dx$. Thus, the net efflux is $(\partial J_x / \partial x)\,dx\,dy\,dz$ over the area of the face. Considering the contributions of the y and z directions as well, and noting that dx dy dz is the volume of the region considered, it is clear that:

$$\text{Net efflux per unit volume} = \frac{\partial J_x}{\partial x} + \frac{\partial J_y}{\partial y} + \frac{\partial J_z}{\partial z} = \text{div } J \qquad (4.20)$$

The numerical methods developed by Patankar have been constructed by performing a balance over a control volume.

Examples of standard differential equations have been presented for the conservation of chemical species, the energy equation, the momentum equation, the turbulence-kinetic-energy equation, etc. For these differential equations, it has been shown that all the dependent variables of interest seemed to obey a generalized conservation principle. If the dependent variable is denoted by Φ, the general differential equation is:[218]

$$\frac{\partial}{\partial t}(\rho\Phi) + \text{div}(\rho u\Phi) = \text{div}(\Gamma\ \text{grad}\ \Phi) + S \qquad (4.21)$$

where u is the velocity field, ρ is the density, Γ is the diffusion coefficient, and S is a source term. The quantities Γ and S are specific to a particular meaning of Φ.

Equation (4.21) is written in vector form. Another useful representation is the Cartesian-tensor form:[219]

$$\frac{\partial}{\partial t}(\rho\Phi) + \frac{\partial}{\partial x_j}(\rho u_j \Phi) = \frac{\partial}{\partial x_j}\left(\Gamma \frac{\partial \Phi}{\partial x_j}\right) + S \qquad (4.22)$$

where the subscript j can take the values 1, 2 and 3, denoting the three space coordinates. When a subscript is repeated in a term, a summation of three terms is implied, for example:

$$\frac{\partial}{\partial x_j}(\rho u_j) = \frac{\partial}{\partial x_1}(\rho u_1) + \frac{\partial}{\partial x_2}(\rho u_2) + \frac{\partial}{\partial x_3}(\rho u_3) \qquad (4.23)$$

The dependent variable $\bar{\Phi}$ (Equation 4.21) would, in general, be a function of three space coordinates and time. Thus:

$$\Phi = \Phi (x, y, z, t) \qquad (4.24)$$

where x, y, z and t are the **independent** variables. In a numerical solution, the values of the independent variables at which the values of $\bar{\Phi}$ are to be calculated are **chosen**. Independent variables and the proper choice of coordinates have been discussed by Patankar[240]

4.7.1.2 Discretization of differential equations

The numerical method of interest here treats as its basic unknowns the values of the dependent variable ($\bar{\Phi}$) at a finite number of locations (called the **grid points**) in the calculation domain. The method includes the tasks of providing a set of algebraic equations for these unknowns and of prescribing an algorithm for solving these equations. In focusing attention on the values of the grid points, the continuous information, contained in the exact solution of the differential equation, is replaced by discrete values. The distribution of $\bar{\Phi}$ is thus discretized, and it is appropriate to refer to this class of numerical methods as discretization methods.

The algebraic equations involving the unknown values of $\bar{\Phi}$ at chosen grid points are referred to as discretization equations. These equations are derived from the differential equation governing $\bar{\Phi}$. In this derivation, some assumptions about how $\bar{\Phi}$ varies between grid points must be employed. This "profile" of $\bar{\Phi}$ could be chosen such that a single algebraic expression suffices for the whole calculation domain. However, it is often more practical to use **piecewise** profiles[241], such that a given segment describes the variation of $\bar{\Phi}$ over only a small region in terms of the $\bar{\Phi}$ values at the grid points within and around that region. Thus, it is common to subdivide the calculation domain into a number of subdomains such that a separate profile assumption can be associated with each subdomain.

The structure of discretization equations and methods of deriving such equations have been well discussed[242]. Common methods of deriving these equations include the Taylor-Series Formulation, the Method of Weighted Residuals, and the Control-Volume Formulation[243]. The latter method has certain definite advantages and, therefore, it has been employed in the numerical method developed by Patankar[236].

So far as known, the discretization method has not been applied to the prediction of the rates of release of active agents from controlled-release matrix devices. In the following sections, the application of this method to the prediction of the rate of release of SLS from cylindrical rubber-SLS pellets is discussed.

4.7.2 Discretization of the Fundamental Diffusion Equation for the Axisymmetric Problem

Patankar[244] has presented the discretized equations for a two-dimensional flat plane. The equations derived in this section refer to the cylindrical or so-called "axisymmetric", form.

The fundamental diffusion equation (presented in cylindrical coordinates) is given by:

$$\frac{\partial C}{\partial t} = \frac{\partial}{\partial x}\left[D\frac{\partial C}{\partial x}\right] + \frac{1}{y}\frac{\partial}{\partial y}\left[yD\frac{\partial C}{\partial y}\right] + S \qquad (4.25)$$

S in Equation (4.25) is a source term. If the substance, of which the concentration C is measured, is produced by a chemical reaction, $S>0$. If the substance is destroyed (or converted) chemically, $S<0$. If the substance does not react but just diffuses through a medium, $S=0$. For the problem discussed here, the term S is equivalent to zero and it can, therefore, be ignored.

A schematic representation of a segment of a cylindrical pellet, showing side and front views of the segment, is given in Figure 4.58. This figure shows that the segment can be subdivided into cells. The side and top views of one such a cell is shown in Figure 4.59. A general cell is shown in Figure 4.60. The areas and volumes referred to in these figures appear "naturally" in the discretization equations and the formulas are derived only to physically interpret the terms which will be used in these equations.

The general cell, shown in Figure 4.60, will be used to discretize Equation (4.25). The assumptions made are as follows:[245]

(i) On walls east and west, C is constant, D is constant and $\frac{\partial C}{\partial x}$ is constant. However, this only applies to on the walls and it holds for all time, but is not constant with respect to time.

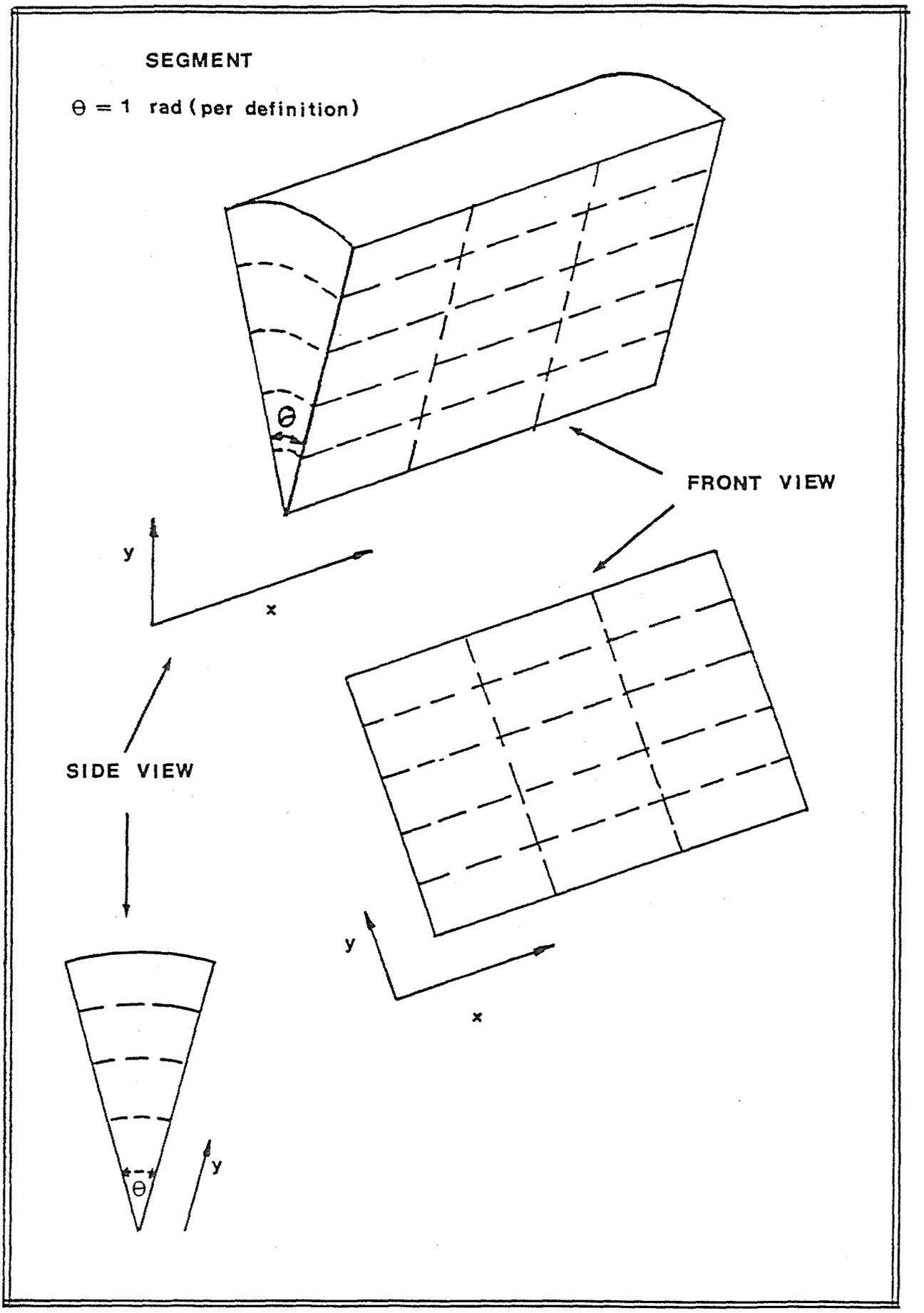

FIGURE 4.58 Schematic representation of a segment (Θ = 1 rad) of a cylindrical pellet.

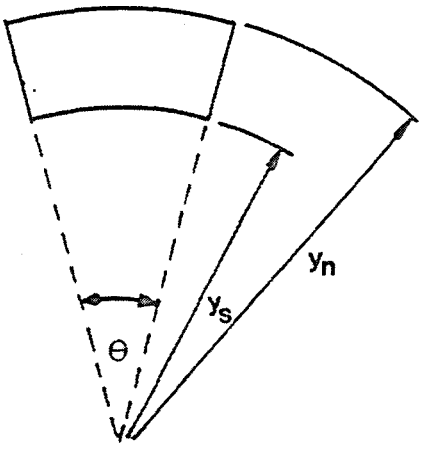

SIDE VIEW OF CELL

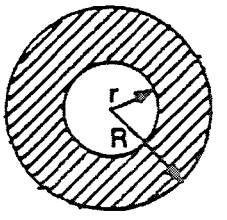

For circle:

coloured area is $\pi R^2 - \pi r^2$

$= \pi(R^2 - r^2)$

Since $\theta = 1$, per definition, the area of the side view of the cell is only $\frac{1}{2\pi}$ of that of the ring shown above.

Therefore:

$$\text{Area} = \frac{1}{2\pi}\pi(R^2 - r^2)$$
$$= \frac{1}{2}(y_n^2 - y_s^2)$$

where the small n and s refer to the northern and southern walls of the cell.

TOP VIEW OF CELL

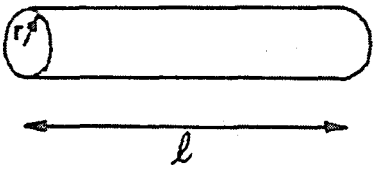

For cylinder:

Area = $2\pi r\ell$

Perspective:

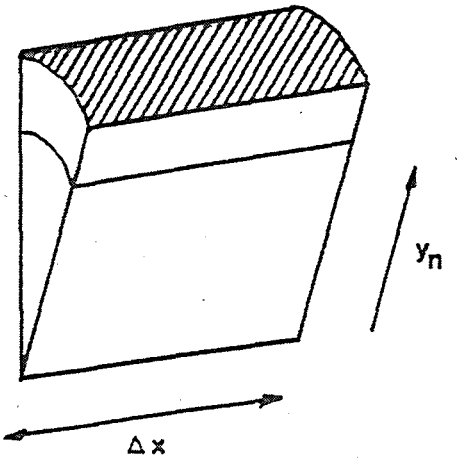

Since $\theta = 1$, per definition, the area of the top of the cell is $\frac{1}{2\pi}$ of that of the cylinder shown above. If the length is Δx, then:

$$\text{Area} = \Delta x . y_n$$

(Similar for bottom of cell:

$$\text{Area} = \Delta x . y_s$$)

FIGURE 4.59 Side and top views of a cell.

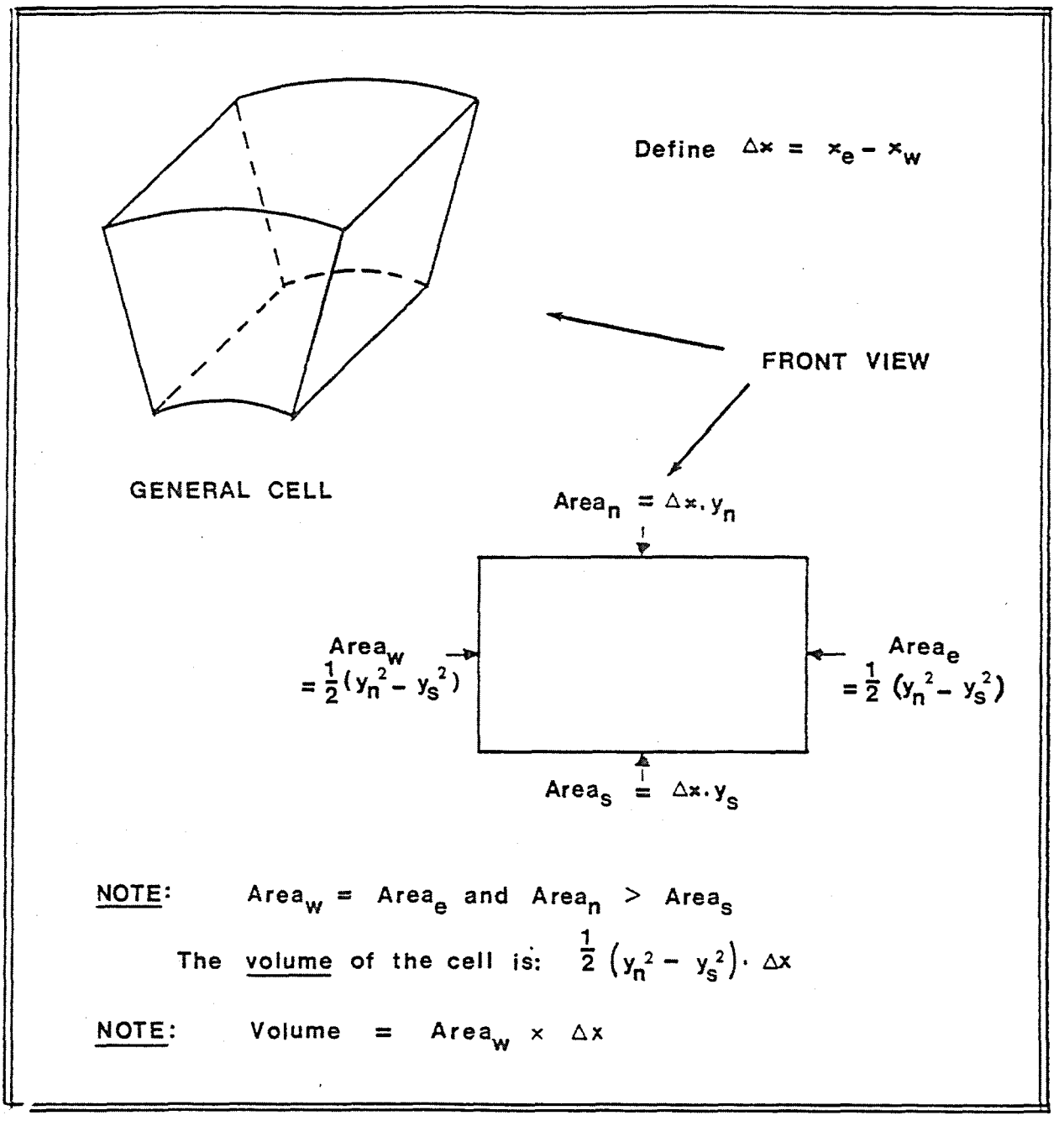

FIGURE 4.60 Schematic representation of a general cell.

(ii) Similarly to (i), on walls north and south, C is constant, D is constant and $\frac{\partial C}{\partial y}$ is constant.

(iii) Generally, at the NE, SW, NW and SE corners a discontinuity is assumed, since an averaged value of C and D on each wall is assumed.

(iv) In the θ direction all variables are constant, per definition, from the axially symmetric assumption.

(v) Assume that time progresses from t to $t + \Delta t$.

(vi) Assume that $C\big|_t$ and $C\big|_{t+\Delta t}$ are averaged values of C over the whole cell (These are "time walls" similar to (i) and (ii)).

(vii) For any quantity ψ, assume that $\psi(t)$ goes as $\psi\big|_t = \psi^o$ and $\psi_{t \in [t, t+\Delta t]} = \psi$ where ψ^o is the value of ψ at the beginning of the time interval. It is assumed that for the rest of the interval the value of ψ is the same as that at the end of the interval. Therefore, $\int_t^{t+\Delta t} \psi \, dt = \psi \cdot \Delta t$. This is known as the fully implicit method. (See Patankar[245] for a motivation for this method, as opposed to the fully explicit and Crank-Nicholson methods).

Finally, it is assumed that C is a "well-behaved" function so that the order of integration may be changed at will.

Integration of Equation (4.25) gives:

$$\int_t^{t+\Delta t}\int_{x_w}^{x_e}\int_{y_s}^{y_n} \frac{\partial C}{\partial t}\, y\, dy\, dx\, dt = \int_t^{t+\Delta t}\int_{x_w}^{x_e}\int_{y_s}^{y_n} \frac{\partial}{\partial x}\left[D\frac{\partial C}{\partial x}\right] y\, dy\, dx\, dt$$

(I) (II)

$$+ \int_t^{t+\Delta t}\int_{x_w}^{x_e}\int_{y_s}^{y_n} \frac{1}{y}\frac{\partial}{\partial y}\left[yD\frac{\partial C}{\partial y}\right] y\, dy\, dx\, dt \qquad (4.26)$$

(III)

Change the order of integration of I:

$$I = \int_{x_w}^{x_e} \int_{y_s}^{y_n} \left(\int_{t}^{t+\Delta t} \frac{\partial C}{\partial t} dt \right) y \, dy \, dx$$

$$= \int_{x_w}^{x_e} \int_{y_s}^{y_n} C \Big|_{t}^{t+\Delta t} y \, dy \, dx$$

$$= C \Big|_{t}^{t+\Delta t} \int_{x_w}^{x_e} \int_{y_s}^{y_n} y \, dy \, dx \quad \text{(from assumption 6)}$$

$$= C \Big|_{t}^{t+\Delta t} \cdot \frac{1}{2} \left(y_n^2 - y_s^2 \right) \cdot \Delta x \qquad (4.27)$$

Note that $\frac{1}{2}(y_n^2 - y_s^2) \cdot \Delta x$ is the volume of the cell (since the integral of $\int_{x_w}^{x_e} \int_{y_s}^{y_n} y \, dy \, dx$ gives the volume).

Therefore:

$$I = C \Big|_{t}^{t+\Delta t} \cdot \text{Vol}, \quad \text{where Vol} = \frac{1}{2} \left(y_n^2 - y_s^2 \right) \Delta x \qquad (4.28)$$

Now denote $C\Big|_t$ by C^o, so that:

$$I = C \cdot \text{Vol} - C^o \cdot \text{Vol} \qquad (4.29)$$

The quantities at $t + \Delta t$ (which is considered to be "now", i.e., the end of the interval) are written without any special designators, as they will be used to calculate a value "now" and, therefore, to approximate that value by the numerical value.

Change the order of integration of II:

$$II = \int_t^{t+\Delta t} \int_{y_s}^{y_n} \int_{x_w}^{x_e} \frac{\partial}{\partial x} \left(D \frac{\partial C}{\partial x} \right) dx\, y\, dy\, dt$$

$$= \int_t^{t+\Delta t} \int_{y_s}^{y_n} \left(D \frac{\partial C}{\partial x} \right) \Bigg|_{x_w}^{x_e} y\, dy\, dt \qquad (4.30)$$

Since, from assumption (i), $D\big|_{x_e}$, $D\big|_{x_w}$, $\frac{\partial C}{\partial x}\big|_{x_e}$ and $\frac{\partial C}{\partial x}\big|_{x_w}$ are constants, it follows that:

$$II = \int_t^{t+\Delta t} D \frac{\partial C}{\partial x} \Bigg|_{x_w}^{x_e} \cdot \frac{1}{2} \left(y_n^2 - y_s^2 \right) dt$$

$$= D \frac{\partial C}{\partial x} \Bigg|_{x_w}^{x_e} \cdot \frac{1}{2} \left(y_n^2 - y_s^2 \right) \Delta t \qquad (4.31)$$

Note that all the values are at time $t + \Delta t$. Note also that $\frac{1}{2}(y_n^2 - y_s^2)$ is the area of the eastern and western walls of the cell, so that:

$$II = D \frac{\partial C}{\partial x} \Bigg|_{x_e} \cdot \text{Area}_e \cdot \Delta t - D \frac{\partial C}{\partial x} \Bigg|_{x_w} \cdot \text{Area}_w \cdot \Delta t \qquad (4.32)$$

For III in Equation (4.26):

$$III = \int_t^{t+\Delta t} \int_{x_w}^{x_e} \int_{y_s}^{y_n} \frac{1}{y} \frac{\partial}{\partial y} \left(y D \frac{\partial C}{\partial y} \right) y\, dy\, dx\, dt$$

$$= \int_t^{t+\Delta t} \int_{x_w}^{x_e} \left(y D \frac{\partial C}{\partial y} \right) \Big|_{y_s}^{y_n} \, dx \, dt$$

$$= \int_t^{t+\Delta t} \left(y D \frac{\partial C}{\partial y} \right) \Big|_{y_s}^{y_n} . \Delta x . dt \quad \text{(from assumption (ii))}$$

$$= \left(y D \frac{\partial C}{\partial y} \right) \Big|_{y_s}^{y_n} . \Delta x . \Delta t \quad \text{(from assumption (vii))} \qquad (4.33)$$

Therefore:

$$III = \left(y_n . \Delta x \right) . \left(D \frac{\partial C}{\partial y} \right) \Big|_{y_n} . \Delta t - \left(y_s . \Delta x \right) . \left(D \frac{\partial C}{\partial y} \right) \Big|_{y_s} . \Delta t \qquad (4.34)$$

Note that all the variables are at time $t + \Delta t$ and that $y_n . \Delta x = Area_n$ and $y_s . \Delta x = Area_s$.

It follows that:

$$III = \left(D \frac{\partial C}{\partial y} \right) \Big|_{y_n} . Area_n . \Delta t - \left(D \frac{\partial C}{\partial y} \right) \Big|_{y_s} . Area_s . \Delta t \qquad (4.35)$$

Since I = II + III, and since $\Delta t > 0$, I, II and III can be divided by Δt to give:

$$C . \frac{Vol}{\Delta t} = \left(D \frac{\partial C}{\partial x} \right) \Big|_{x_e} . Area_e - \left(D \frac{\partial C}{\partial x} \right) \Big|_{x_w} . Area_w$$

$$+ \left[D \frac{\partial C}{\partial y} \right]\Big|_{y_n} . \text{Area}_n - \left[D \frac{\partial C}{\partial y} \right]\Big|_{y_s} . \text{Area}_s \qquad (4.36)$$

$$+ C^o . \frac{\text{Vol}}{\Delta t}$$

It now remains to determine $\left(D \frac{\partial C}{\partial x}\right)\Big|_{x_e}$, $\left(D \frac{\partial C}{\partial x}\right)\Big|_{x_w}$, $\left(D \frac{\partial C}{\partial y}\right)\Big|_{y_n}$ and $\left(D \frac{\partial C}{\partial y}\right)\Big|_{y_s}$. The values of $D|_{x_e}$, $D|_{x_w}$, D_{y_n} and $D|_{y_s}$ are usually determined by interpolation (see Schreuder[247], "Harmonic Interpolation").

Equation (4.25) can be simplified by dropping the time-dependence and by making D constant.

Consider the one-dimensional version of Equation (4.25) in x, so that:

$$D \frac{\partial^2 C}{\partial x^2} = 0 \qquad (4.37)$$

This implies a linear function of C in the x-direction. A one-dimensional version of Equation (4.25) in y gives:

$$D \frac{\partial^2 C}{\partial y^2} + \frac{1}{y} \frac{\partial C}{\partial y} = 0 \qquad (4.38)$$

which implies that $C = C_1 \ln y + C_2$ and $\frac{\partial C}{\partial y} = \frac{C_1}{y}$, where c_1 and c_2 are constants.

Therefore, in the x-direction a linear approximation of C is highly accurate, whereas in the y-direction it is probably a good approximation[248]. Because of the lack of better knowledge, it is assumed that:

$$\left.\frac{\partial C}{\partial x}\right|_e = \frac{C_E - C_P}{\delta\zeta_E} \quad ;$$

$$\left.\frac{\partial C}{\partial x}\right|_w = \frac{C_P - C_W}{\delta\zeta_W} \quad ; \qquad (4.39)$$

$$\left.\frac{\partial C}{\partial y}\right|_n = \frac{C_N - C_P}{\delta\eta_N} \quad ;$$

$$\left.\frac{\partial C}{\partial y}\right|_s = \frac{C_P - C_S}{\delta\eta_S} \quad .$$

where the notations are illustrated by Figure 4.61.

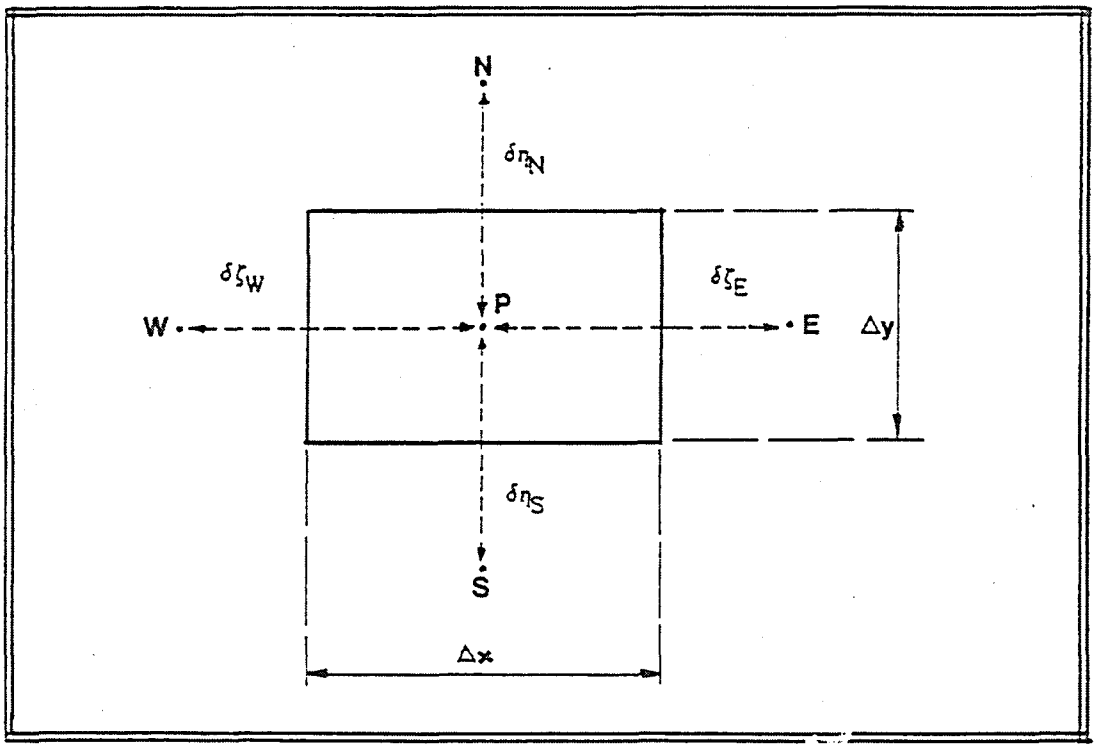

FIGURE 4.61 Schematic representation of a control volume for the two-dimensional situation.

In Figure 4.61, it can be seen that $\delta\zeta$ is the x inter-nodal distance and $\delta\eta$ is the y inter-nodal distance.

Substitution of Equation (4.39) into (4.36) gives:

$$C \cdot \frac{Vol}{\Delta t} = D_e \frac{C_E - C_P}{\delta\zeta_E} Area_e - D_w \frac{C_P - C_W}{\delta\zeta_W} Area_w + D_n \frac{C_N - C_P}{\delta\eta_N} Area_n - D_s \frac{C_P - C_S}{\delta\eta_S} Area_s \quad (4.40)$$

Set $C = C_P$. It follows that $C^o = C_P{}^o$ (since C^o is $C = C_P$ for the previous time step).

Now define:

$$A_E = D_e \frac{Area_e}{\delta\zeta_E}$$

$$A_W = D_w \frac{Area_w}{\delta\zeta_W}$$

$$A_N = D_n \frac{Area_n}{\delta\eta_N}$$

$$A_S = D_s \frac{Area_s}{\delta\eta_S} \quad (4.41)$$

$$A_P{}^o = \frac{Vol}{\Delta t}$$

and

$$A_P = A_E + A_W + A_N + A_S + A_P{}^o$$

Using Equation (4.41), Equation (4.40) can be written as:

$$C_P A_P = C_E A_E + C_W A_W + C_N A_N + C_S A_S + C_P^{\circ} A_P^{\circ}$$

$$= \sum_{nb} A_{nb} C_{nb} \qquad (4.42)$$

where the subscript nb denotes a neighbour point. In Equation (4.42), C_P° is treated as a neighbour, since it is a neighbour in time.

4.7.3 Iterative Solution Procedure

Methods which may be used to solve the set of discretized equations derived in the previous section (Equation 4.42) have been discussed by Schreüder[249]. Due to the complex nature of the equations, the methods are all of an iterative nature and special techniques are required to let the iterative procedure converge at an acceptable rate.

A disadvantage of iterative procedures is that they produce one approximation of the solution from a previous approximation of the solution. The first approximation is supplied by the numerical analyst, either by guessing the solution or using the solution of a similar problem. It is required that the solution procedure should produce successive approximations of the solution until the approximation is sufficiently close to the actual solution.

The fundamental problem of iterative procedures, however, is that they may diverge and give no solution or may stagnate and give a false solution. Convergence criteria are defined to guard against false solutions, but divergence is a more serious problem. The reason for divergence could be a natural instability in the problem, which would probably cause the problem not to have a solution at all, or possibly several solutions. Divergence, however, is also found in well-behaved problems with unique, stable solutions. The divergence then is the result of an approximation of the problem that is so poor that the next approximation is even worse. The first bad approximation could be the result of a poor initial guess of the solution as supplied by the analyst, or it could be the result of inaccuracies in the procedure. To lessen the effect of these inaccuracies in the procedure, relaxation[249] is often used.

One of the most commonly used iterative procedures in fluid mechanics is the tri-diagonal matrix algorithm (TDMA) or Thomas algorithm. A thorough discussion of the TDMA has been presented by Schreüder[249]. The TDMA was used to solve the discretization equations derived in Section 4.7.2.

A FORTRAN program (PELLET.FOR) was written to implement the iterative procedure. This program is given in Appendix 7A. A brief description of the program is given in the next section.

4.7.4 The FORTRAN Code PELLET

The program was written in FORTRAN using the VAX-11 FORTRAN compiler version 4.2. The program was developed for the DEC VAX-11 series computers and was finally used on the

VAX 11/785 of the University of Stellenbosch. The operating system presently used at Stellenbosch is VAX/VMS 4.3. The utilities supported by VAX/VMS include a powerful full-screen editor called EDIT/EDT, which provides easy access to all text information on the machine.

All the user input to the program is through a data file in which all the relevant variables (including the grid and numerical control variables) are specified. The input is free format, but must be in a fixed sequence and all variables must be supplied. On starting up, the program requests the name of the input data file. The input data are then read from the input data file. The output from the program comes in two forms, namely, print files presenting tabular fields of the variable values and plot files (restart files) which contain the same data, but in a compact format which is difficult for the user to decipher. The plot file is intended to be the link between PELLET and an optional graphics post-processor program UNIPLOT (Appendix 7B), and as restart information for PELLET itself.

The program consists of a main program, 13 subroutines and 2 functions. Functions are used to compute values that are too complex to specify as single-line functions inside the subroutines, or to implement functions that are widely used throughout the program. Subroutines are used to perform sections of the procedure that logically belong together, for example, to compute the A coefficients (see Equation 4.42) for a certain variable. A brief description of the program structure is as follows:

Main program. The main program is a driver which calls the subroutines and controls the program flow. It also does the time increments, solves the transport equations and controls the input/output files.

Subroutine INPUT: This subroutine reads the input data file name and all input data. It also initializes some data variables and does limited data checking.

Subroutine GRID: This subroutine generates the grid from the data supplied by the user and initializes grid variables.

Subroutine INIT: This subroutine initializes all the variables that are not supplied by the user, either from standard values or by reading values from a result file.

Subroutine HEAD: This subroutine writes the print file heading to the given file.

Subroutine BOUND: This subroutine sets the boundary conditions for the relevant variables according to the problem modelled.

Subroutine TPREP: This subroutine prepares for the next time step.

Subroutine CPREP: This subroutine sets up the coefficients of the transport equation which must be solved.

Subroutine DPREP: This subroutine calculates the value of the diffusion coefficient (D).

Function DNS: This function calculates D at the northern and southern cell boundaries, using harmonic interpolation.

Function DEW: This function calculates D at the eastern and western cell boundaries, using harmonic interpolation.

Subroutine TDMANS: This subroutine performs the TDMA in a north-south direction.

Subroutine TDMAEW: This subroutine performs the TDMA in a east-west direction

Subroutine OVACON: This subroutine calculates the overall contents of the pellet.

Subroutine OUTPUT: This subroutine writes the values of the variables to the given print file. It also supplies data such as, for example, the convergence criteria and minimum and maximum values of the variables.

Subroutine PLTDAT: This subroutine writes the values of the variables to the given result file. It also writes information, such as some of the grid variables and other dimensional variables, to the result file for plotting purposes.

4.7.5 The Relationship between the Diffusion Coefficient (D) and the Concentration of SLS in the Pellet (C)

In Section 4.6.5, it was mentioned that in the mathematical model developed by Fu et al.[16], it was assumed that D was a constant. The values obtained for D, as given in Table 4.1, showed that D was not a constant, but that it was dependent on the concentration of SLS in the rubber pellet. It was suggested that the degree of porosity developed in the pellet was a function of the initial SLS loading, and that the formation of porosity was the single most important factor leading to the increase in D. One of the main objectives in the development of the PELLET program was, therefore, to express D as a function of the SLS concentration in the pellet.

To find D as a function of the concentration, the following assumptions were made:[250]

(i) Assume a diffusion coefficient for the rubber-SLS pellet and call this diffusion coefficient D_o.

(ii) Consider a second diffusion coefficient for the same pellet, but with all the SLS released and, consequently, with the maximum degree of porosity in the rubber pellet. Call this diffusion coefficient D_t.

(iii) Assume that the major factor affecting D is the formation of porosity. Obviously, $D_t = D_o(C_o-C)$, where C_o is the initial SLS concentration and C is the present SLS concentration. Therefore, D depends only on the amount of SLS already released.

(iv) Assume that D varies linearly from D_o to D_t with the amount of SLS released. If the amount of SLS which is not released, even after an infinite time, is C_t (normally, C_t would be zero), then the D-C relationship can be written as:

$$D = D_o + (D_t - D_o)\left(\frac{C_o - C}{C_o - C_t}\right) \qquad (4.43)$$

It can also be assumed that, instead of a variation of D with C for all values of C, for some values of C (say C_α) the following relationship holds:

$$D = \begin{cases} D_0 & \text{for } C > C_\alpha \\ D_0 + (D_1 - D_0)\left[\dfrac{C_\alpha - C}{C_\alpha - C_1}\right]^n & \text{for } C_1 \le C \le C_\alpha \end{cases} \qquad (4.44)$$

For $n = 1$ in Equation (4.43), the variation of the diffusion coefficient, D, with concentration, C, is shown in Figure 4.62(a). Similarly, for $n \neq 0$, the variation of D with C is illustrated by Figure 4.62(b).

In subroutine DPREP of the present version of the FORTRAN program PELLET (Appendix 7A), where the relationship between the diffusion coefficient and concentration was specified, it was assumed that:

$$D_1 = C_k * D_0 \quad (\text{where } C_k \text{ is a constant})$$
$$C_1 = 0$$
$$n = 1$$

Therefore:

$$\text{For } C > C_\alpha \qquad D = D_0 \qquad (4.45)$$

$$\text{For } C \le C_\alpha \qquad D = (D_1 - D_0)\left[\frac{C_\alpha - C}{C_\alpha - 0}\right]^1 + D_0$$

$$= (C_k * D_0 - D_0)\left[\frac{C_\alpha - C}{C_\alpha}\right] + D_0$$

$$= \left\{(C_k - 1)\left[1 - \frac{C}{C_\alpha}\right] + 1\right\} D_0 \qquad (4.46)$$

The results obtained by using Equations (4.45) and (4.46) were encouraging. It is, however, believed that improved results can be obtained by using the following equation:

$$D = D_0 + (D_1 - D_0)\left[\frac{C_0 - C}{C_0 - C_1}\right]^n \qquad (4.47)$$

For $n > 0$ in the above equation, the variation of D with C is shown in Figure 4.62(c).

Although only the D-C relationships given by Equations (4.45) and (4.46) were used, modification of the PELLET program to incorporate other D-C relationships is possible.

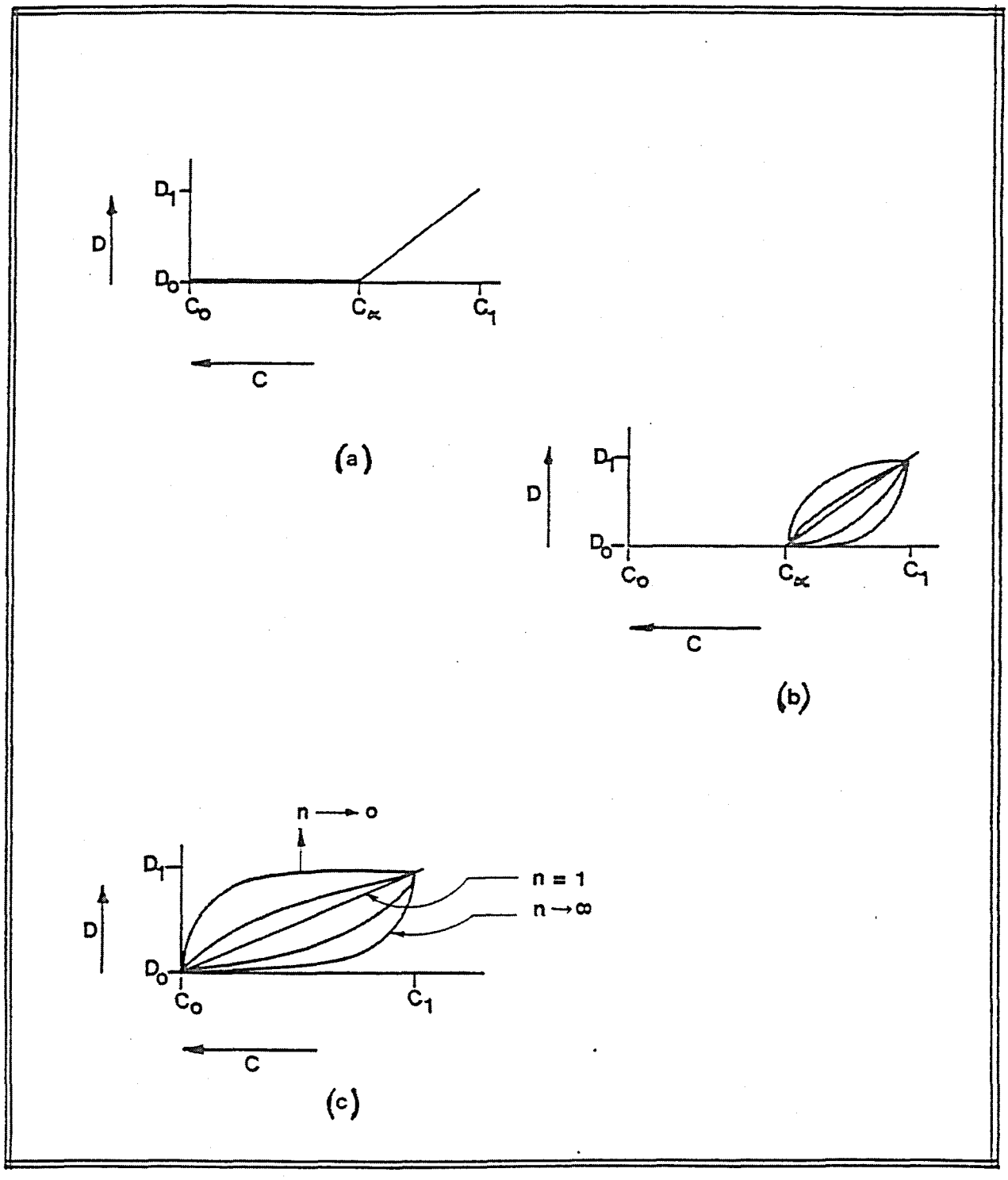

FIGURE 4.62 Variation of the diffusion coefficient (D) with concentration (C).

4.7.6 COMPARISON OF EXPERIMENTAL DATA WITH THEORETICAL DATA PREDICTED BY THE DISCRETIZATION MODEL

Although the FORTRAN program PELLET has reached only the first stage of development, the theoretical data obtained by using the present version of this program already show a remarkably close fit to experimental data. Examples of the agreement between experimental and theoretical data are shown in Figures 4.63 to 4.66.

The fits obtained by using the discretization model were better than those obtained with the mathematical model developed by Fu et al.[46] (DIFFCALC program, Section 4.6). This was so, particularly for rubber pellets which contained 45% or 55% SLS. The advantage of the PELLET program is that it incorporates the effect of porosity development by employing a variable diffusion coefficient (D) as a function of SLS concentration (C).

The discretization method developed by Patankar has not been applied to the prediction of the release rates of active agents from controlled-release matrices. The development of the PELLET program represents an initial attempt to apply this numerical method to the prediction of the rate of release of SLS from cylindrical elastomeric pellets. Refinement of the PELLET program, e.g. by using other D-C relationships and by changing the grid variables, is possible, but it is clear that a considerable amount of computer work will be required before a final, reliable program can be developed.

As discussed in Section 4.7.4, the subroutine PLTDAT in the PELLET program writes the values of the variables to a given result file for plotting purposes. The graphics post-processor program UNIPLOT (Appendix 7B) was used to read the data from result files and to create two-dimensional plots showing the change in the concentration of SLS in a rubber pellet as the release process continued. Figure 4.67 (a) - (h) shows the concentration distribution of SLS in a natural-rubber pellet (SLS content 55%) at eight different intervals during the elution period. The FORTRAN data file giving the percentages of SLS released from this particular pellet at different intervals during the elution period (as predicted by the PELLET PROGRAM) is given in Appendix 7C. Two-dimensional plots showing the concentration distribution of SLS in a styrene-butadiene-rubber pellet (SLS content 35%) at different intervals during the elution period are given in Appendix 7D. The FORTRAN data file giving the percentages of SLS released from the SBR/35% SLS pellet at different intervals during the elution period is given in Appendix 7C.

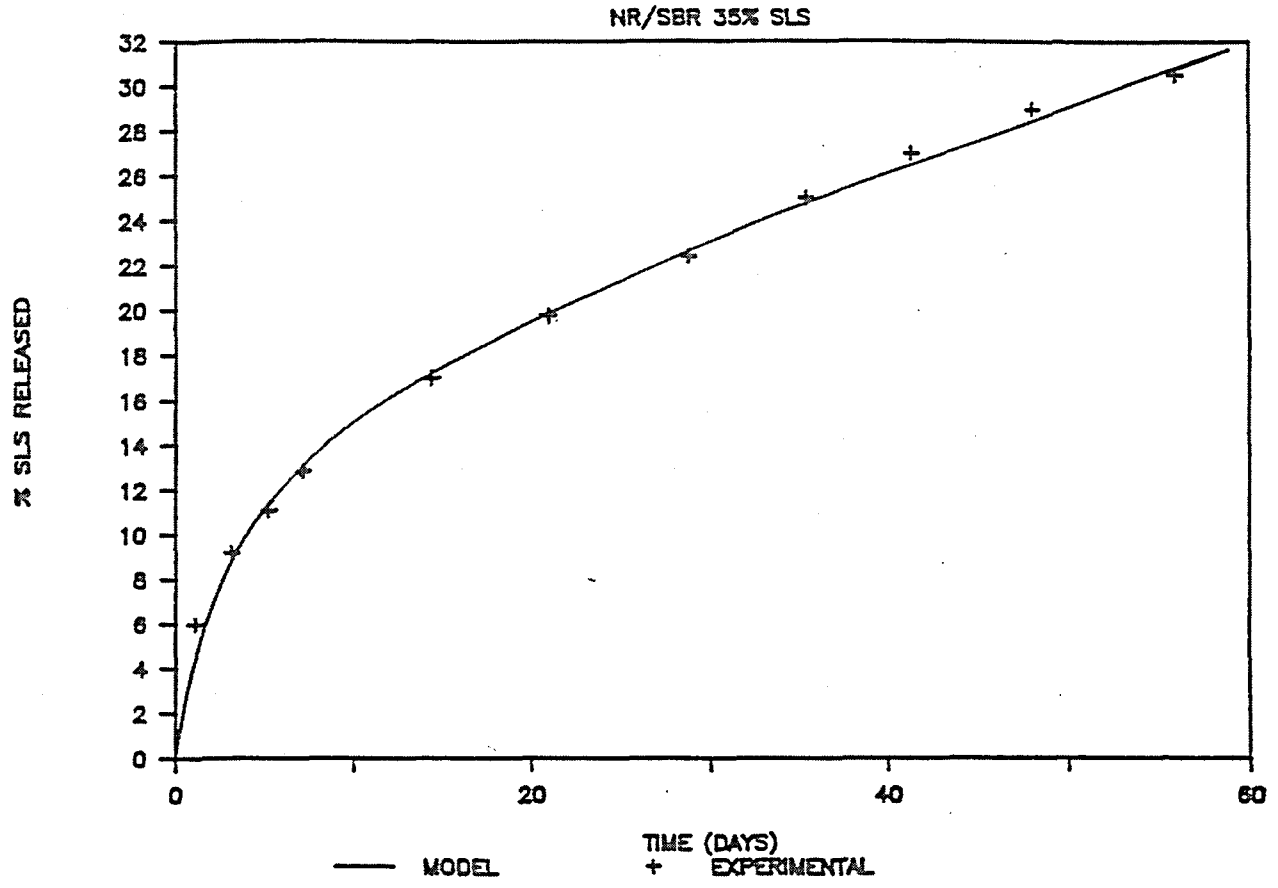

FIGURE 4.63 Agreement between experimental data and theoretical data, predicted by the discretization model, for an NR/SBR/35% SLS pellet.

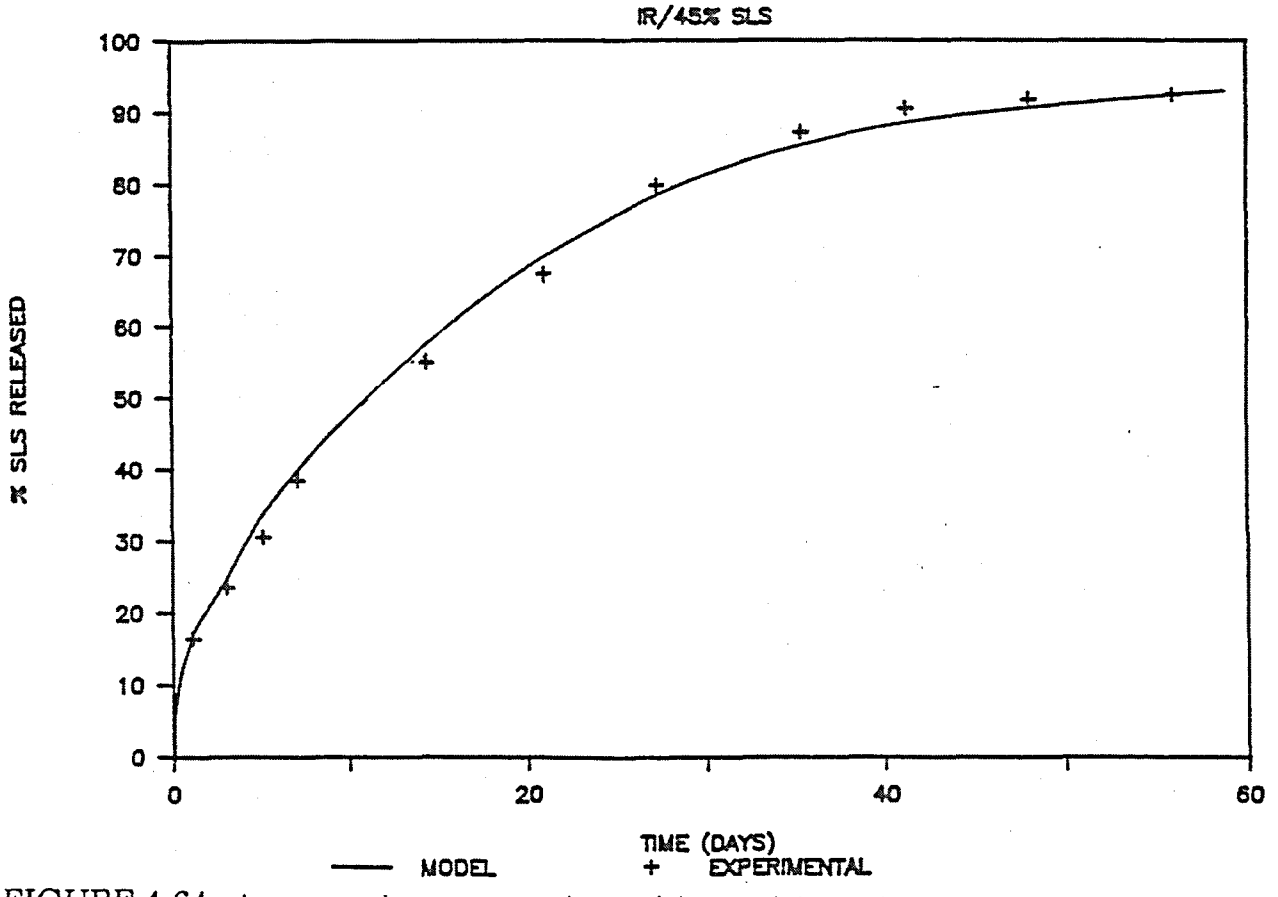

FIGURE 4.64 Agreement between experimental data and theoretical data, predicted by the discretization model, for an IR/45% SLS pellet.

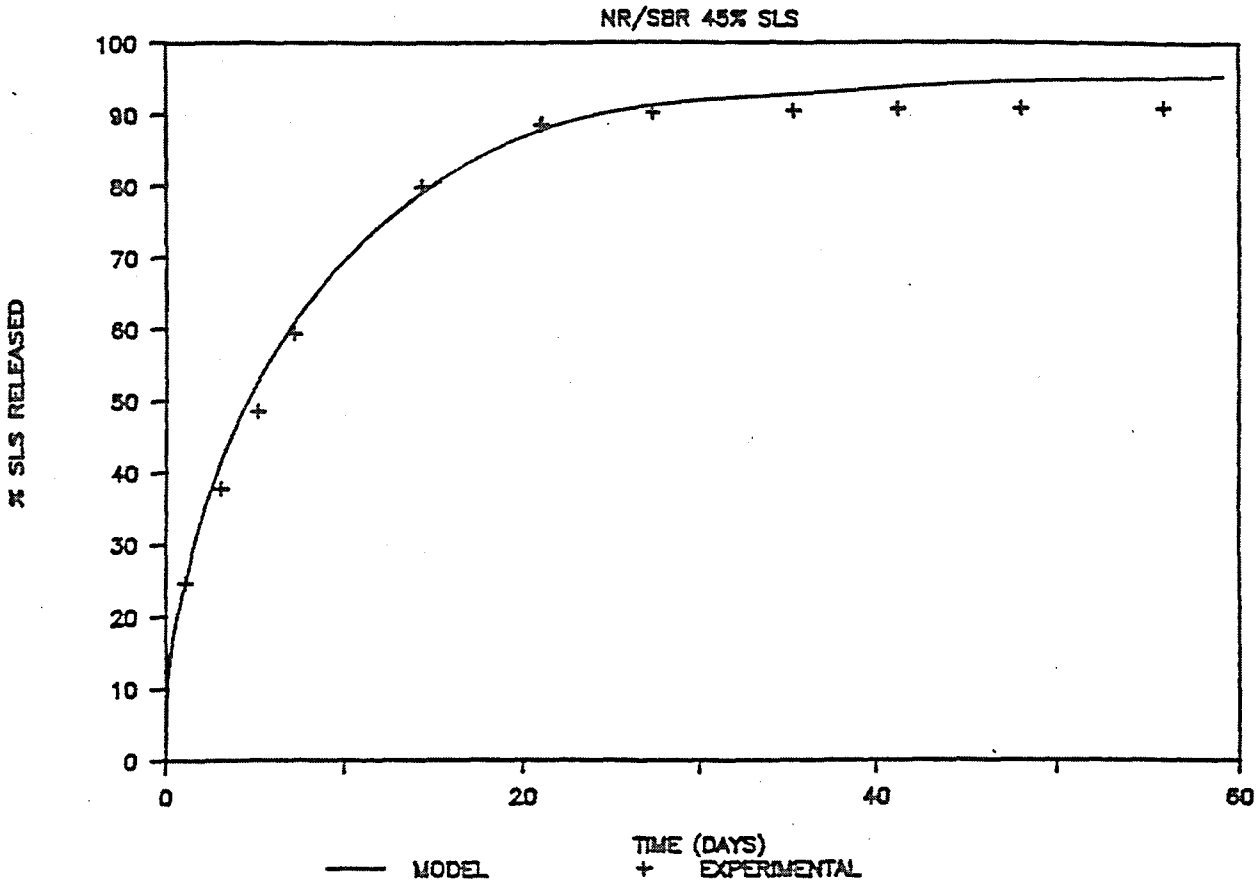

FIGURE 4.65 Agreement between experimental data and theoretical data, predicted by the discretization model, for an NR/SBR/45% SLS pellet.

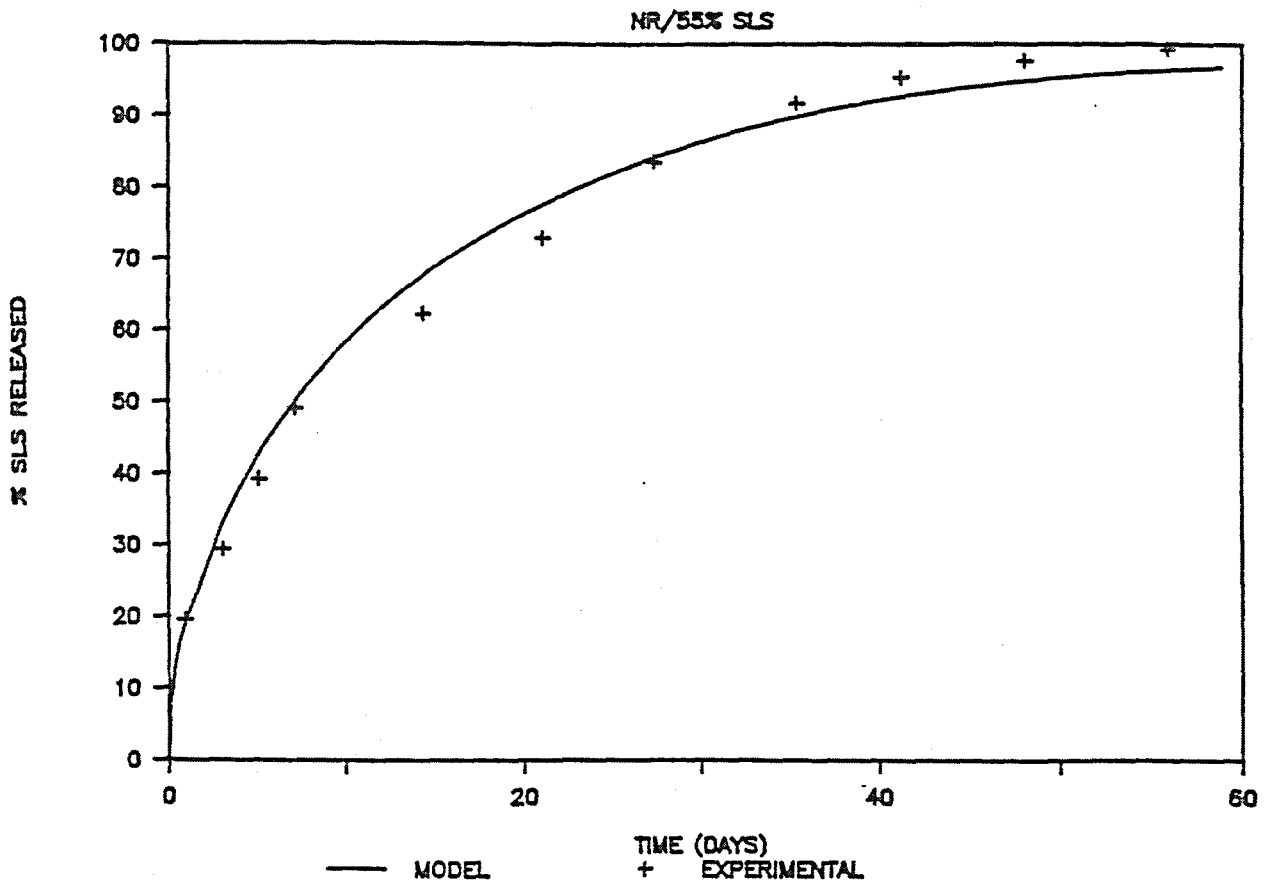

FIGURE 4.66 Agreement between experimental data and theoretical data, predicted by the discretization model, for an NR/55% SLS pellet.

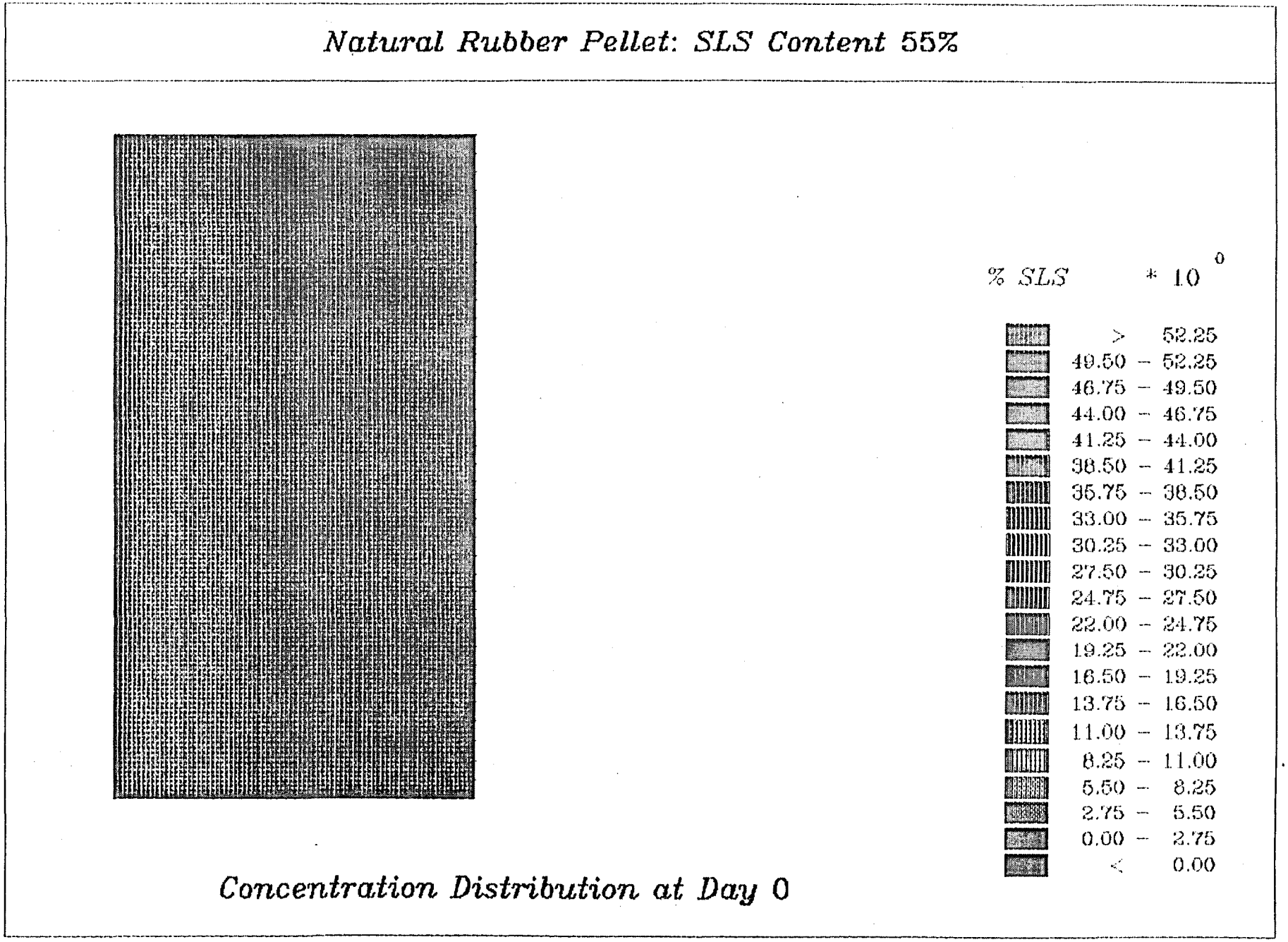

FIGURE 4.67(a). Concentration distribution of SLS in a natural-rubber pellet before elution

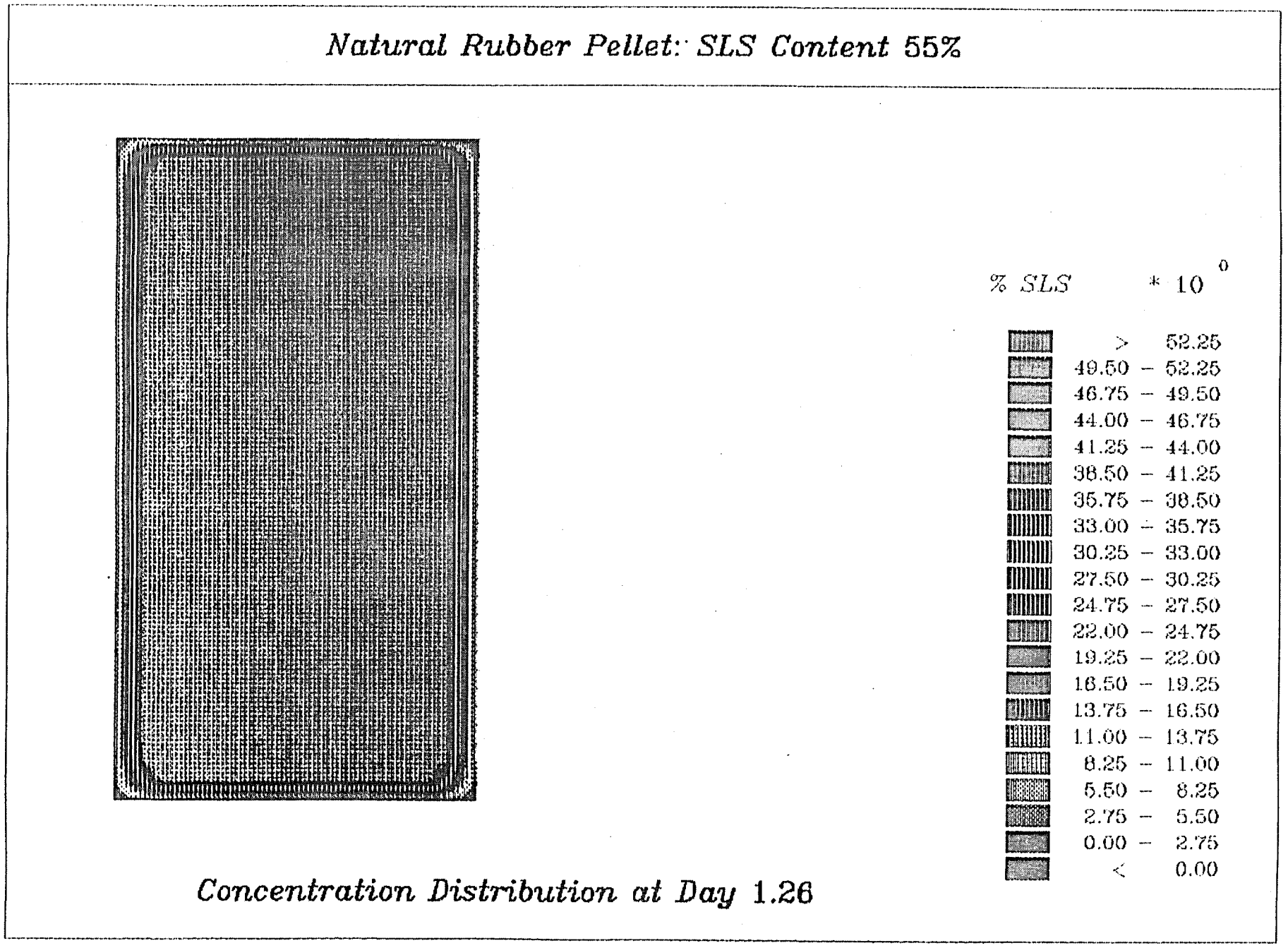

FIGURE 4.67(b). Concentration distribution of SLS in a natural-rubber pellet after 1,26 days elution

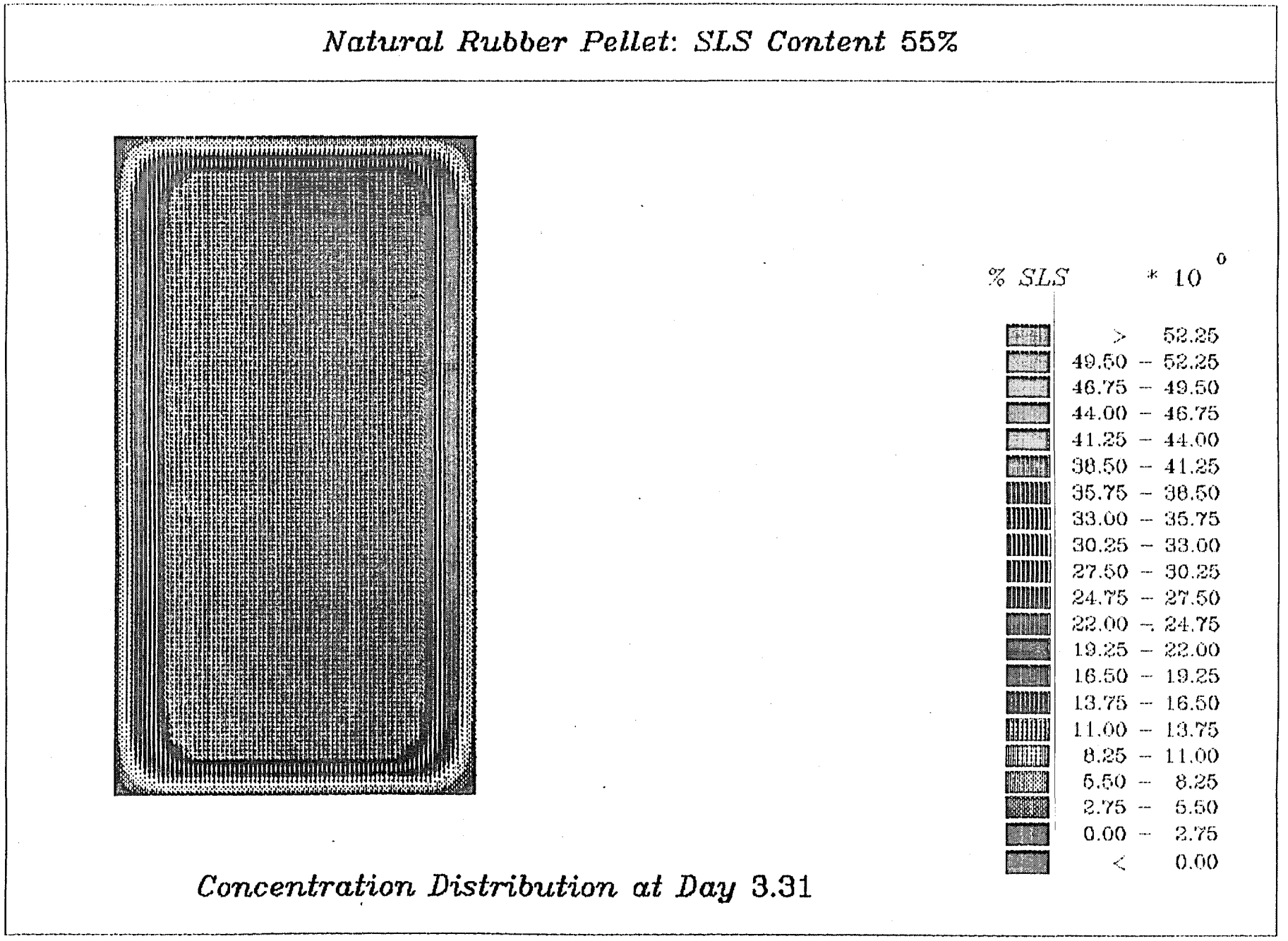

FIGURE 4.67(c). Concentration distribution of SLS in a natural-rubber pellet after 3,31 days elution

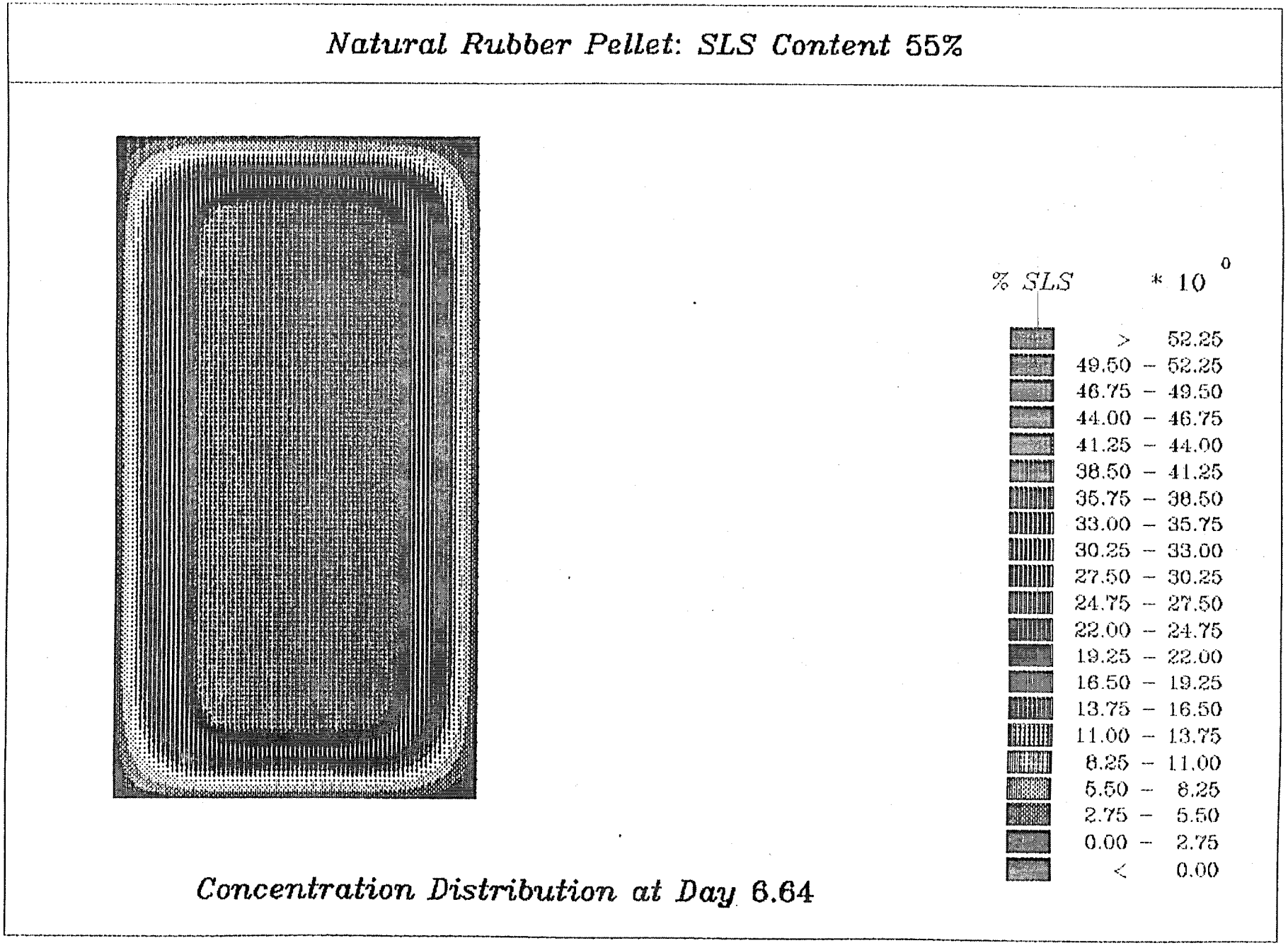

FIGURE 4.67(d). Concentration distribution of SLS in a natural-rubber pellet after 6,64 days elution

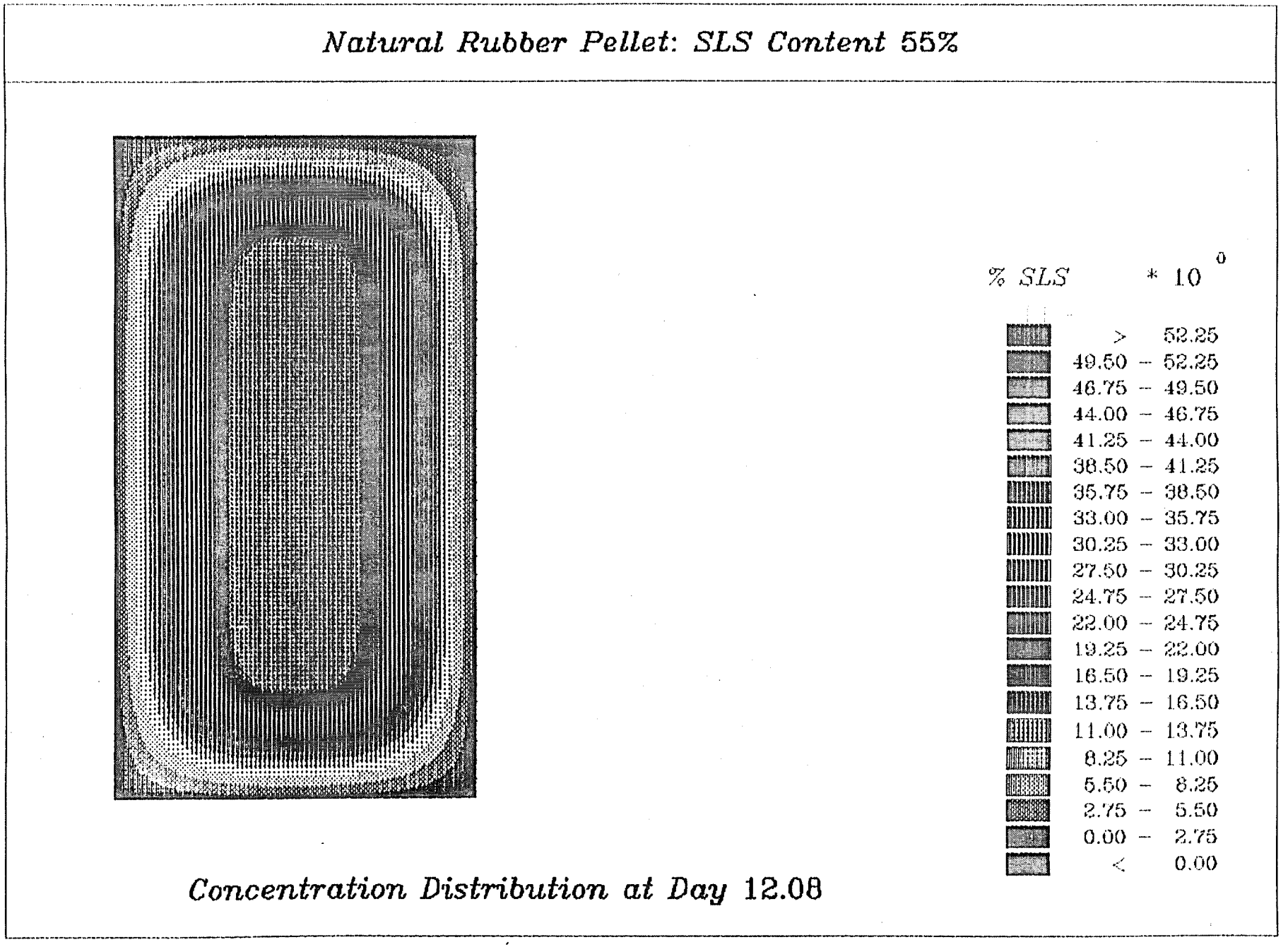

FIGURE 4.67(e). Concentration distribution of SLS in a natural-rubber pellet after 12,08 days elution

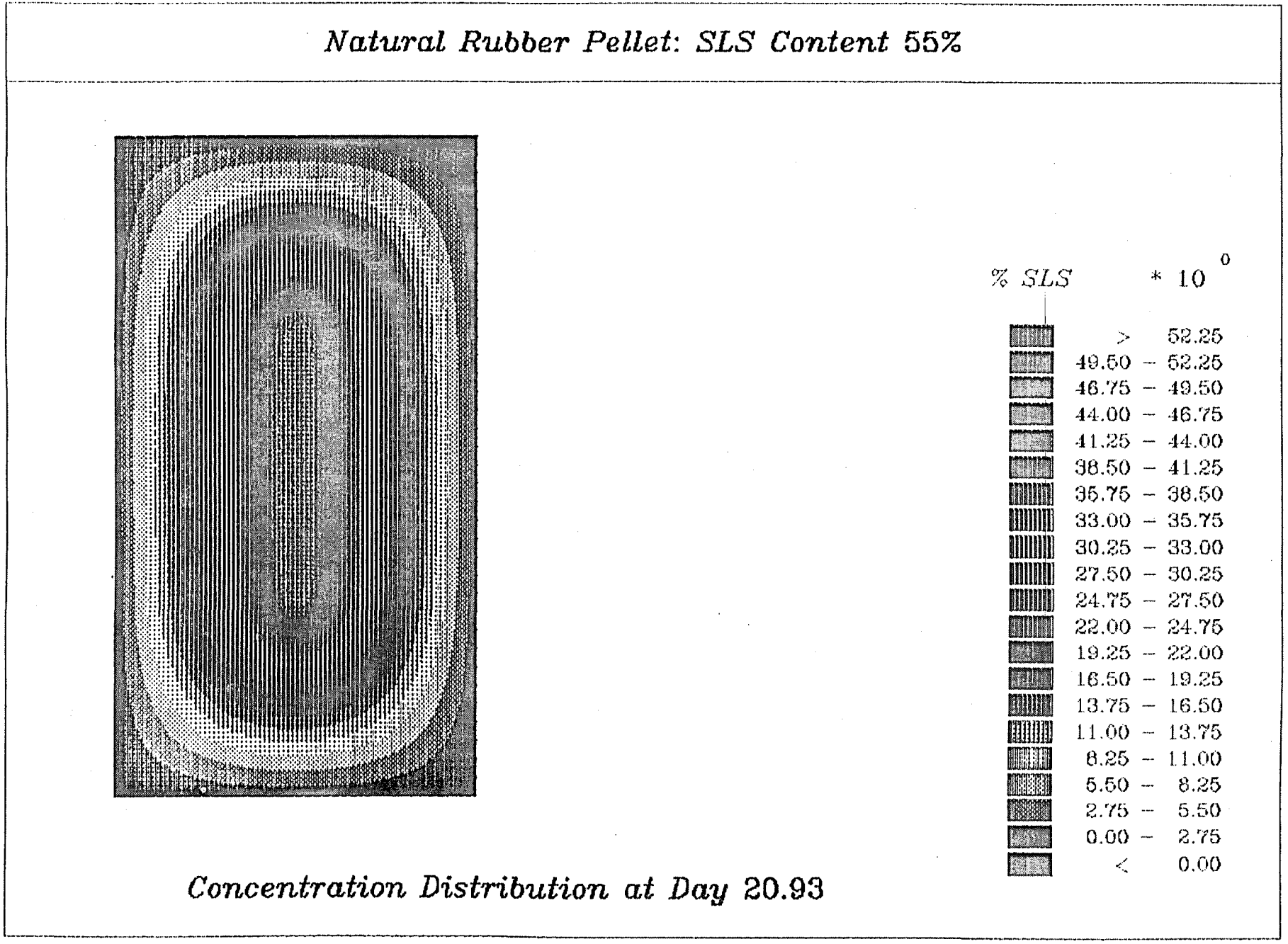

FIGURE 4.67(f). Concentration distribution of SLS in a natural-rubber pellet after 20,93 days elution

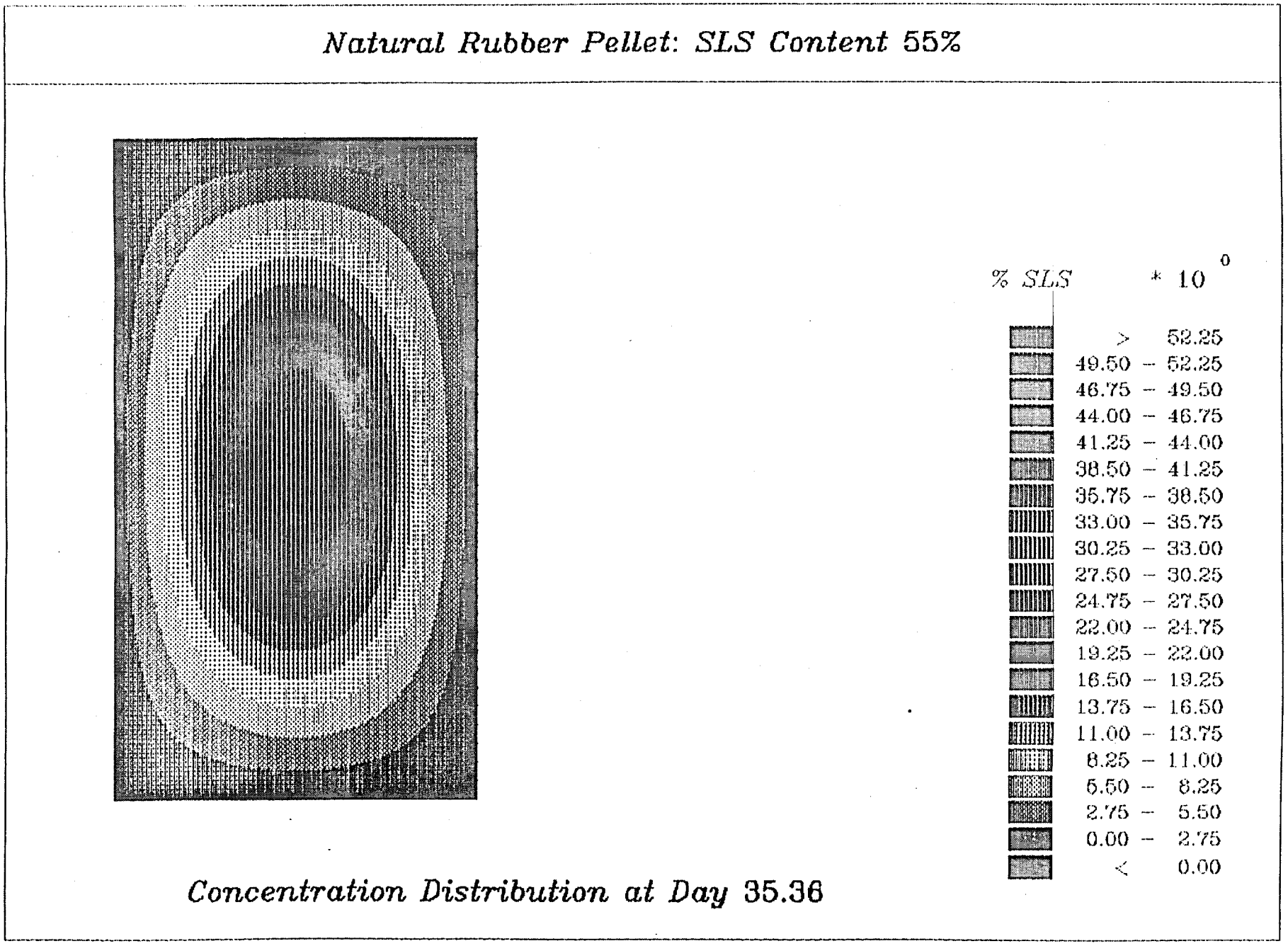

FIGURE 4.67(g). Concentration distribution of SLS in a natural-rubber pellet after 35,36 days elution

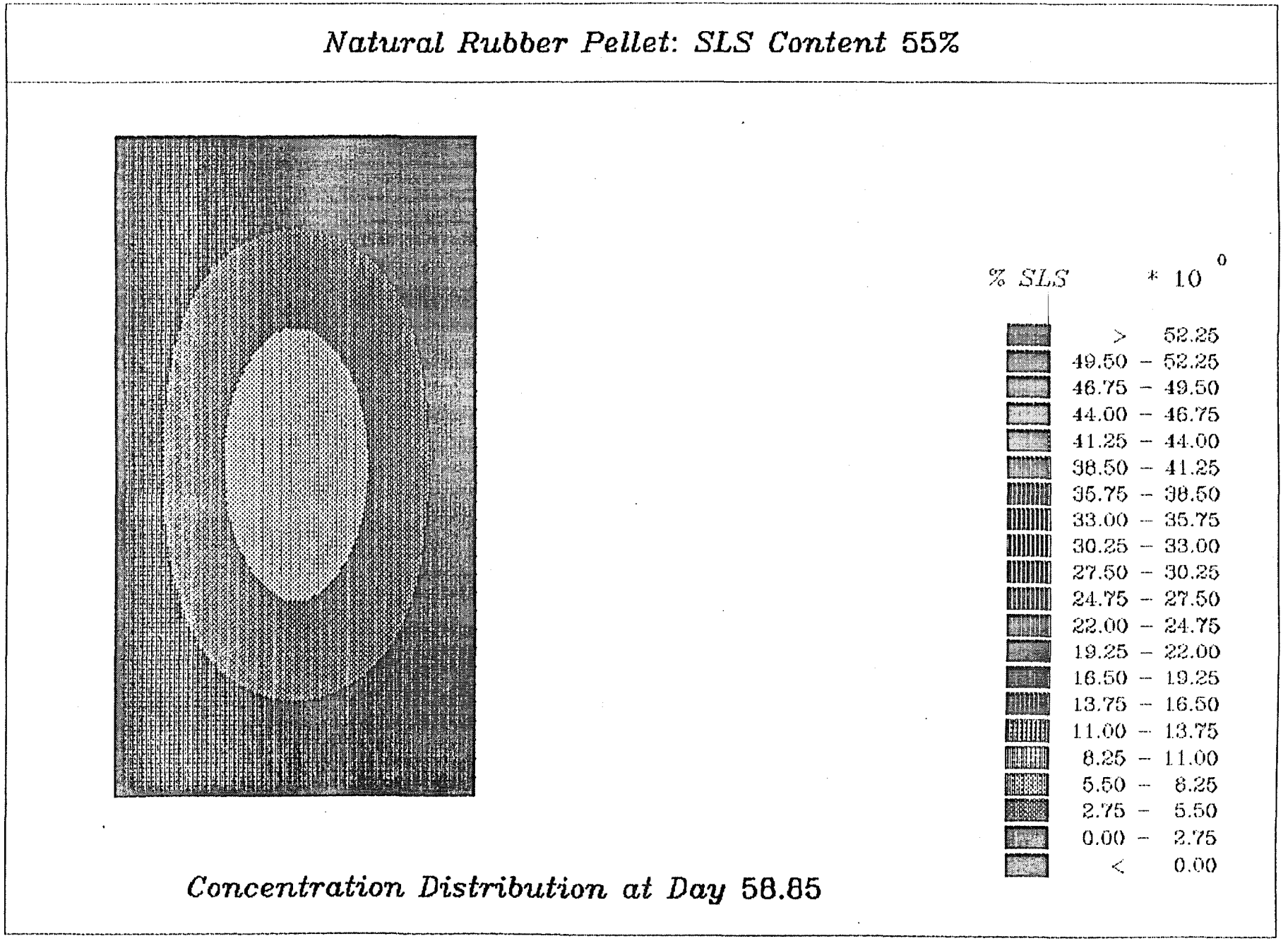

FIGURE 4.67(h). Concentration distribution of SLS in a natural-rubber pellet after 58,85 days elution

4.8 PILOT-SCALE STUDIES

Since that studies reported here was done under a sponsorship, it was felt that not only the preparation and characterization of monolithic devices, the study of release kinetics, and the study of predictive mathematical models was necessary, but that the devices under study should have practical significance. This aspect of the entire study did not wait for the scientific investigation to be completed, but pre-empted the optimum choice of materials for a pilot-scale study.

Natural rubber and synthetic polyisoprene pellets containing 35% (by mass) SLS showed a satisfactory long-term slow release of SLS under conditions of continuous immersion at a temperature of 21 $\pm$ 3°C. However, the crucial problem of how effectively the SLS could move to the target bacteria in gold- or coal-mine dumps had to be assessed. The reduced effectiveness of inhibitors in the presence of mine dump material, as discussed by Bosch and Loos[251], suggested that interactions such as adsorption might be a serious problem. This was of concern, particularly where the acid-producing **Thiobacillus ferrooxidans** bacteria were situated deep within the dumps, as seemed probable in the case of gold mine sand dumps.

It was, therefore, clear that the laboratory experiments would have to be followed by pilot-scale experiments to test the inhibitory effect of SLS under field conditions, where temperature and moisture would fluctuate greatly with season and where dump material in the case of coal was not restricted to coal of small, defined sizes. Since coal dumps could still create acid drainage problems long after the gold mine sand dumps have been removed for reprocessing, it was decided that pilot-scale studies should be concentrated on coal. During the summer of 1985 an inhibition study, involving various SLS treatments, was undertaken on pilot-scale coal dumps at the Wolwekrans mine near Witbank, Transvaal. These treatments included controlled-release SLS-containing rubber formulations.

The study involved ten dumps (test heaps) 7.5 m in length and 4,5 m wide, with a slope of 1:40. Each dump contained 55 tons of layered, compacted waste coal. Six of the dumps were treated with rubber pellets containing SLS for slow release. Two types of rubber pellets, namely, natural rubber and synthetic polyisoprene pellets, each containing 35% (by mass) SLS, were compared. Three concentrations (5, 10 and 15 kg/dump) of each pellet type were spread evenly over dumps compacted to a height of 1.05 m. The pellets were covered with a 0,5 m layer of waste coal. In order to saturate the adsorptive capacity of the coal, each of the six dumps was treated with 1 kg SLS in 20 dm^3 water. Test heap 7 was treated only with 1 kg SLS in 20 dm^3 water, and test heap 8 received no SLS treatment. Two further heaps (9 and 10), which received no SLS treatment, were inoculated with 200 dm^3 mine dump effluent as a source of **Thiobacillus ferrooxidans**.

During the rainy season, effluents from the test dumps were collected in rubber bins. These effluents were analyzed monthly to follow the progress of acidification and the leaching of SLS from the dumps. The chemical and bacteriological monitoring of effluents was conducted by staff of the Department of Microbiology, University of Stellenbosch, and by staff of the Chamber of Mines.

The preliminary results of pilot-scale studies were discussed by Maré and Loos[252]. Wrong information in the planning stage on the amount of coal to be used in the test heaps resulted in the dose of dissolved SLS (1 kg per heap) being too small to saturate the adsorptive capacity of the 55 tons of coal. The very low concentration of SLS in the effluents suggested that much of the SLS leached from the rubber pellets in test heaps 1 to 6 had been adsorbed by the coal. These low SLS concentrations in the effluents were inadequate to inhibit the growth of **Thiobacillus ferrooxidans**.

The cumulative amounts of SLS leached from the test heaps showed that the dumps treated with 15 kg of controlled-release pellets released the highest quantities of SLS, followed by heaps treated with 10 kg of pellets and those treated with 5 kg of pellets. The rate of release of SLS from the natural-rubber pellets was slightly higher than that from the synthetic polyisoprene pellets.

The results of these preliminary studies indicated clearly that more SLS in solution should have been added to the dumps to saturate the adsorptive capacity of the coal and to provide an excess of SLS for inhibition of **Thiobacillus ferrooxidans**. Such an excess would be provided by an amount of SLS greater than 2,47 kg[253].

It was decided that, during the summer of 1986/87, a second dose of dissolved SLS should be applied as a "shock dose" (for example, 5 kg SLS per heap, which is about twice the amount calculated for saturation of the coal) to see whether the established acidification could be stopped and subsequently held in check by SLS leaching from the rubber pellets. In addition, it was decided to increase the amounts of rubber pellets added to the respective waste coal dumps.

4.9 THE KINETICS AND THE MECHANISMS OF RELEASE OF SLS THROUGH ELASTOMERIC MEMBRANES

As discussed in Chapter 2, membrane-controlled devices have the distinct advantages of a constant-release rate and an extended release lifetime ("reservoir effect"). These devices also permit better control of the amount of agent released, since the release rate is less dependent on the geometry of the device. The total rate of transport of an agent through a membrane can normally be controlled by adjusting the thickness of the membrane, as well as the area of the membrane in contact with the recipient environment. Membrane-controlled devices may also be more cost- effective in the long term.

The release of SLS from membrane-controlled devices for attaining long-term inhibition of the bacterial oxidation of pyrite has not been investigated. Membrane-controlled devices should, therefore, form an interesting study in their own right in this context. Since the selection of membranes is a problem, an advantage of the study on monolithic devices is that it has formed a background for the selection of membrane materials.

Elastomeric membranes were prepared and tested as described in Chapter 3, Sections 3.4.6 to 3.4.9. The composition and thickness of each of the 20 membranes which were evaluated in diffusion experiments were given in Table 3.8 in Chapter 3.

4.9.1 Vulcanized NR and IR Membranes which Contained no SLS

When applied to membrane systems, Fick's law (discussed in Chapter 2, Section 2.5.1) predicts that a steady state will be established, with the release rate being constant and independent of time, if an active agent is enclosed within an inert polymer membrane and if the thermodynamic activity of the agent is maintained constant within the enclosure (Chapter 2, Section 2.5.5). The amount of agent released is, therefore, proportional to time:

$$M_t = k\,t \qquad (4.48)$$

and the release rate is independent of time:

$$\frac{dM_t}{dt} = k \qquad (4.49)$$

This is referred to in the literature as zero-order release (Chapter 2, Section 2.5.5). A plot of the cumulative amount of agent released as a function of time, therefore, gives a straight line through the origin, and the slope of that line gives the value of the steady-state release rate.

For the elastomeric membrane systems of interest here, the thermodynamic activity of the SLS was maintained constant by using a saturated SLS solution, with excess solid phase present, in the reservoir compartment (Chapter 3, Section 3.4.8). This ensured a constant concentration gradient across the membranes.

The release of SLS through membranes which consisted of vulcanized NR and IR followed zero-order kinetics, as discussed above (Equations (4.48) and (4.49). The fluxes of SLS through these membranes were constant for the entire test period. The flux of SLS, i.e., the amount of SLS released per day per unit area of membrane, was calculated by using the following equation:

$$J = \frac{1}{A}\frac{dM}{dt} \qquad (4.50)$$

where J is the mass flux, A is the area of the membrane and dM/dt is the mass transported per unit time.

Examples of plots of the cumulative mass flux against time are shown in Figures 4.68 and 4.69 for Membrane 1 (NR; $\ell = 1{,}40$ mm) and Membrane 10 (IR; $\ell = 1{,}54$ mm), respectively. Plots of the daily flux against time for these membranes are given in Figures 4.70 and 4.71, respectively.

The steady-state fluxes of SLS through NR and IR membranes, as well as the standard deviations, are given in Table 4.2.

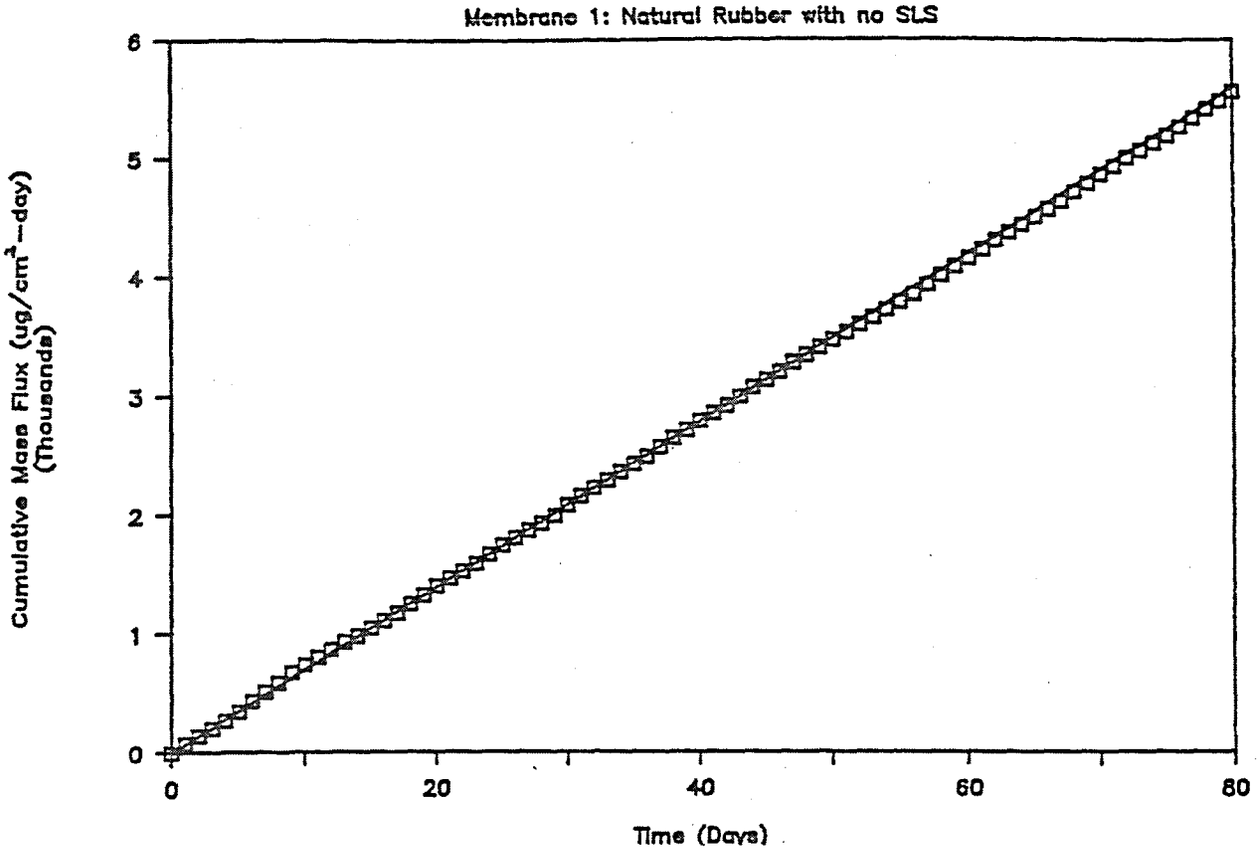

FIGURE 4.68 Plot of cumulative mass flux of SLS as a function of time through a natural-rubber membrane which contained no SLS.

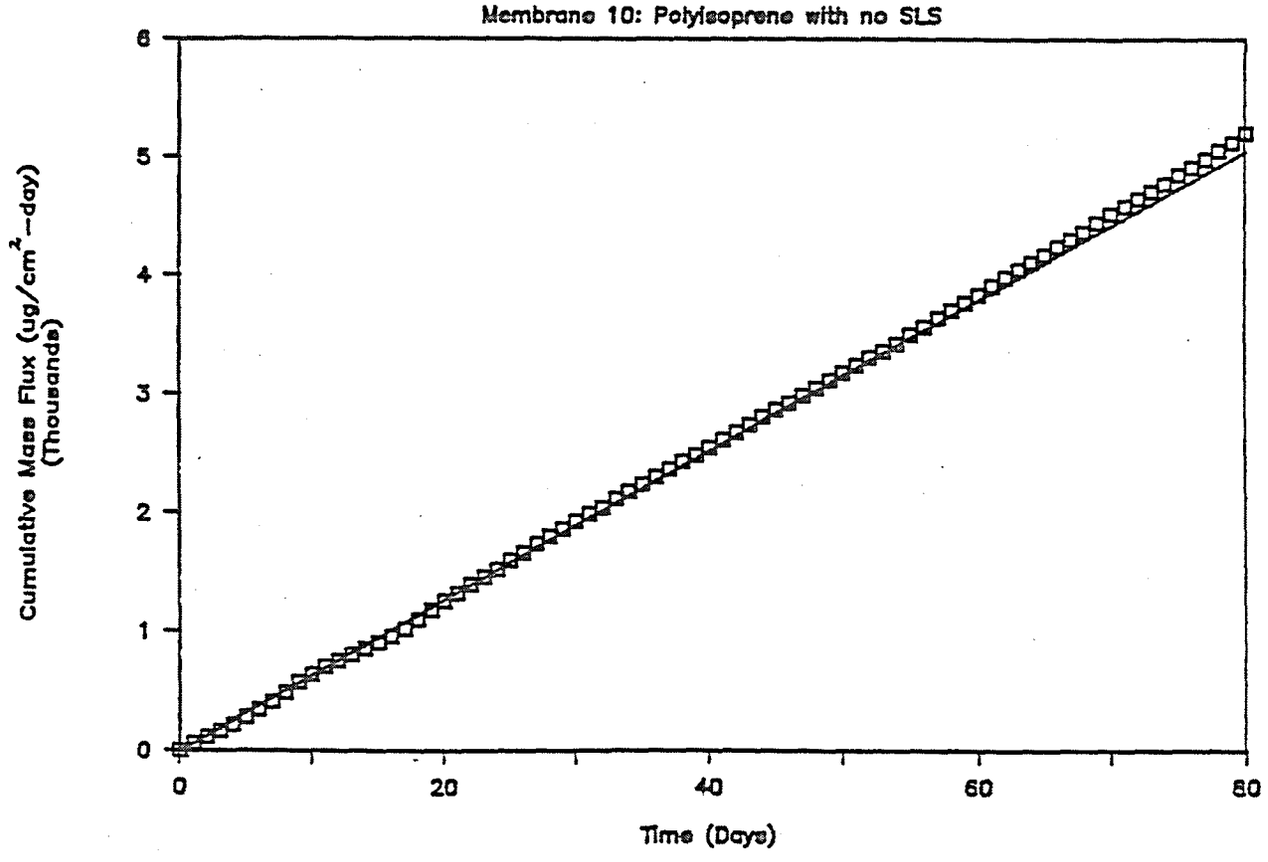

FIGURE 4.69 Plot of cumulative mass flux of SLS as a function of time through a synthetic polyisoprene membrane which contained no SLS.

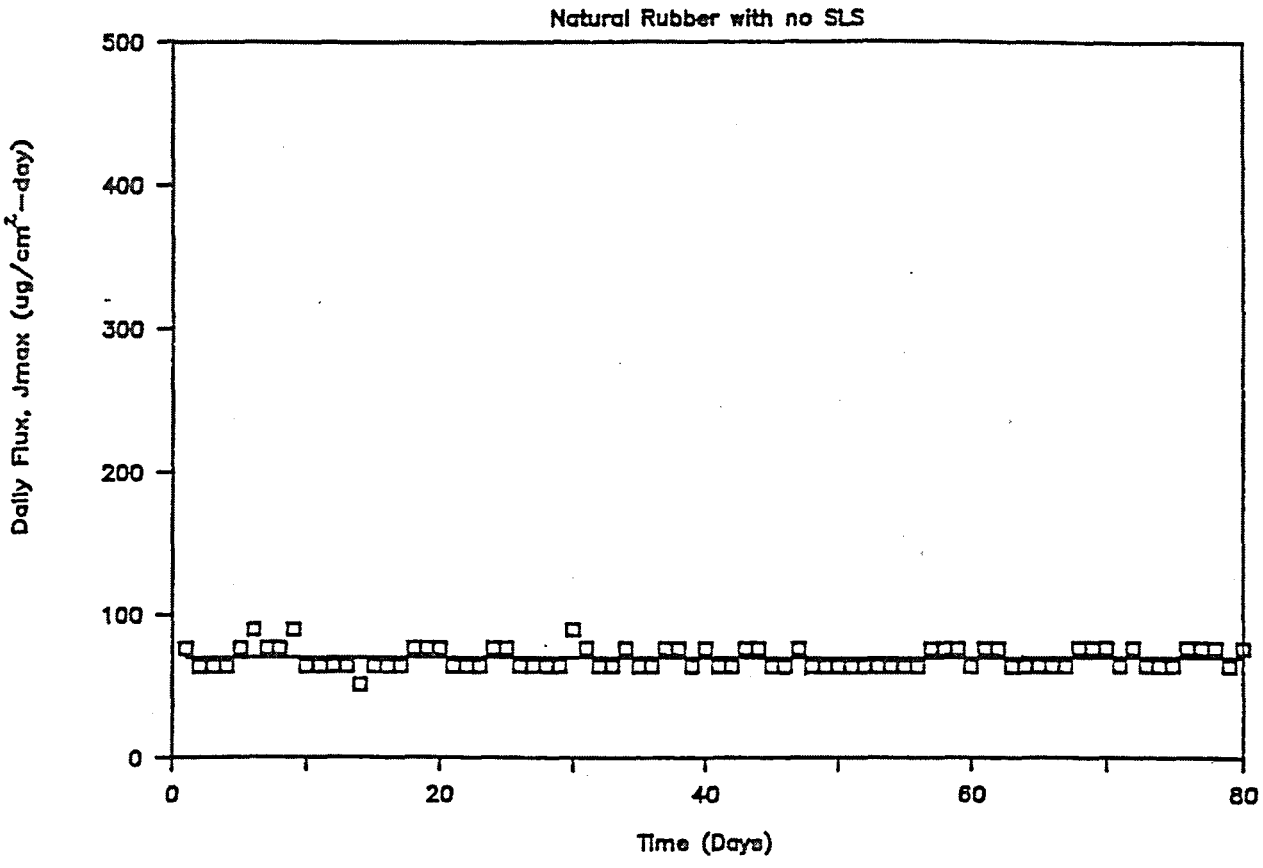

FIGURE 4.70 Plot of the daily flux of SLS as a function of time through a natural-rubber membrane which contained no SLS.

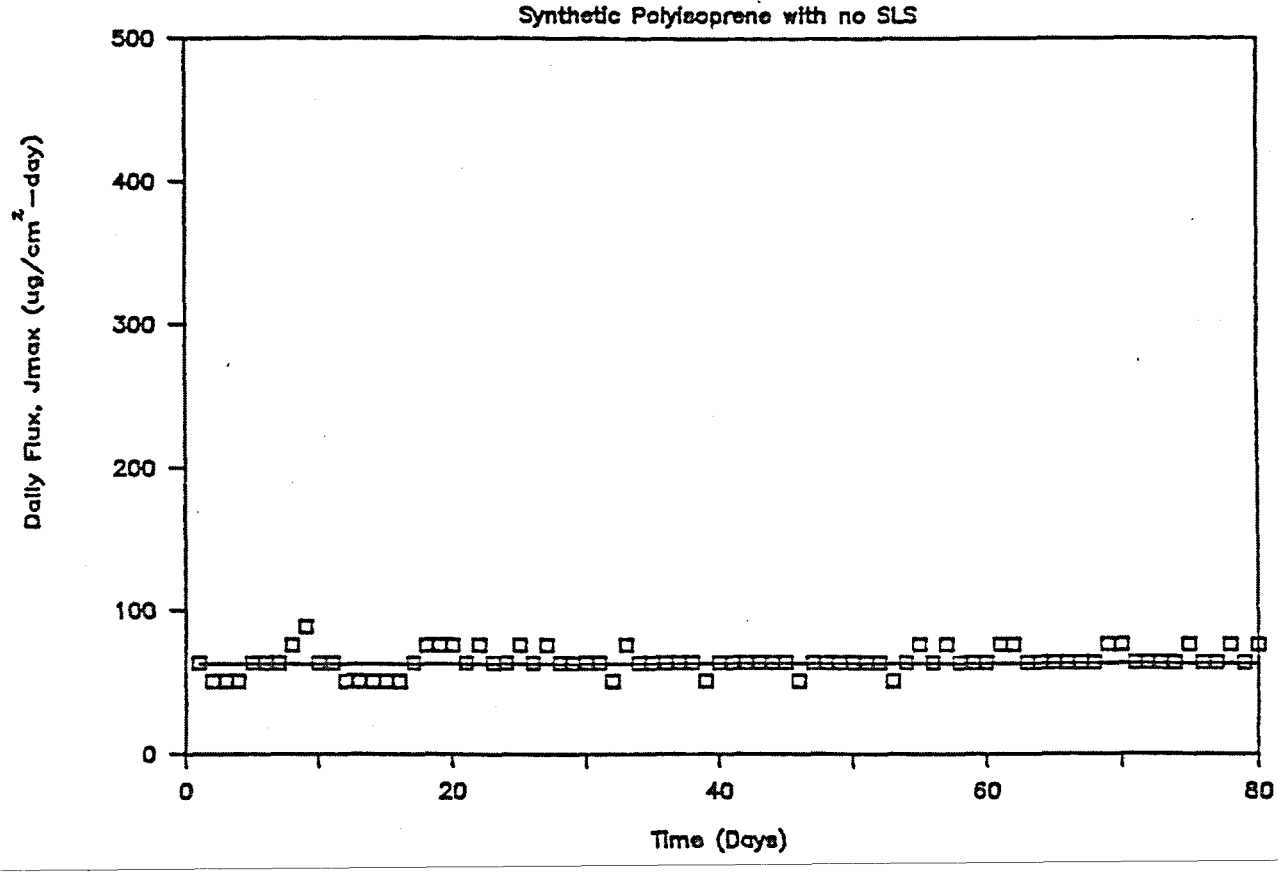

FIGURE 4.71 Plot of the daily flux of SLS as a function of time through a synthetic polyisoprene membrane which contained no SLS.

TABLE 4.2. Steady-state fluxes of SLS through NR and IR membranes

Membrane number	Type of rubber	Membrane thickness, ℓ (mm)	Steady-state flux, J (μg/cm^2-day)	Standard deviation (%)
1	NR	1,40	69,98	2,09
2	NR	1,14	70,79	3,07
3	NR	0,90	71,85	3,35
10	IR	1,54	63,18	3,49
11	IR	1,17	66,20	2,62
12	IR	0,88	68,09	3,24
Control A	NR	0,37	89,80	1,17
Control B	IR	0,39	89,18	1,20

The steady-state fluxes of SLS through these membranes suggested that the transport of SLS through these membranes occurred by diffusion through the membrane phase only. Since no SLS was incorporated into the membranes themselves, transport of SLS through pores within the membrane structures did not occur. It is, therefore, suggested that the mechanism of transport of SLS consisted of absorption of SLS at the upstream surface of the membrane, i.e., the surface of the membrane in contact with the saturated SLS solution, solution of SLS in the elastomeric membrane, diffusion down a gradient of thermodynamic activity and desorption of the SLS at the downstream surface of the membrane, i.e., the surface of the membrane in contact with pure distilled water. Since the gradient of thermodynamic activity across the membranes was maintained constant by means of a saturated SLS solution, with excess solid SLS present, in the reservoir compartment, the rate of diffusion of SLS through these membranes remained constant. It is clear that the rate of release of SLS through elastomeric membranes will depend on the solubility limit of the SLS in the respective elastomers (as discussed in Section 4.2), as well as on the thicknesses of the elastomeric membranes. This is discussed in Section 4.10.

4.9.2 NR and IR Membranes which Contained 10% SLS

The release of SLS through these membranes also followed zero-order kinetics. The amounts of SLS released per day through these membranes were only slightly higher than those released through membranes which contained no SLS (Section 4.9.1).

Plots of the cumulative mass flux of SLS as a function of time are shown in Figures 4.72 and 4.73 for Membrane 6 (NR/10% SLS; ℓ = 0,88 mm) and Membrane 15 (IR/10% SLS; ℓ = 0,92 mm),

respectively. Plots of the maximum daily flux against time for these two membranes are shown in Figures 4.74 and 4.75, respectively. Similar plots were obtained for other NR and IR membranes which contained 10% SLS. The steady-state fluxes of SLS through NR and IR membranes which contained 10% SLS, as well as the standard deviations, are given in Table 4.3.

TABLE 4.3. Steady-state fluxes of SLS through NR and IR membranes which contained 10% SLS

Membrane number	Type of rubber	Membrane thickness, ℓ (mm)	Steady-state flux, J ($\mu g/cm^2$-day)	Standard deviation (%)
4	NR	1,35	72,64	2,55
5	NR	1,11	73,14	2,35
6	NR	0,88	72,57	1,72
13	IR	1,36	69,80	5,81
14	IR	1,11	66,97	3,09
15	IR	0,92	68,40	4,36

It is believed that the release of SLS through membranes which contained 10% SLS was a two-stage process. The initial stage involved the release of SLS present in the elastomeric membrane by diffusion through the membrane and dissolution at the surface of the membrane contacting the pure distilled water in the receiving compartment. As more and more of the SLS diffused outward into the distilled water, the concentration of SLS in the membrane fell below the saturation level and stage two was initiated. During stage two, the elastomer absorbed SLS from the reservoir compartment until the membrane became saturated with SLS. The release of SLS during stage two also occurred by a diffusion-dissolution mechanism. The process of absorption, diffusion and dissolution will continue for as long as SLS is available from the reservoir. Provided that unit activity is maintained in the fluid in the reservoir, the rate of release of SLS through membranes which initially contained 10% SLS will remain constant.

The steady-state release rates (or fluxes) obtained for membranes which contained 10% SLS were only slightly higher than those obtained for membranes which contained no SLS, as shown in Tables 4.2 and 4.3. This indicated that the initial SLS loading of 10% was close to the solubility limit of SLS in the elastomers. If this 10% loading was much higher than the solubility limit of the SLS in the respective elastomers, the rate of release of SLS through these membranes would decrease after the release of the SLS which was initially present in the membranes.

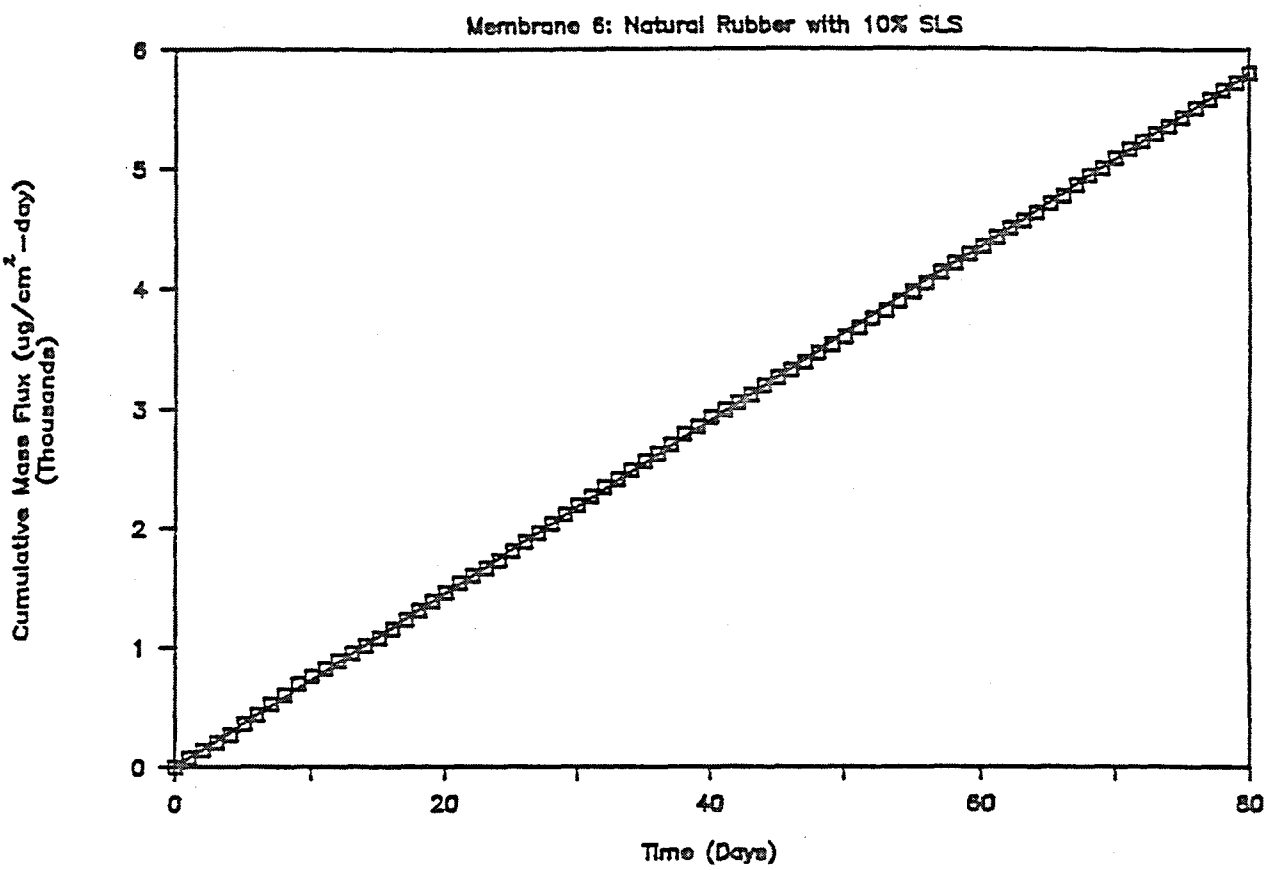

FIGURE 4.72 Plot of cumulative mass flux of SLS as a function of time through a natural-rubber membrane which contained 10% SLS.

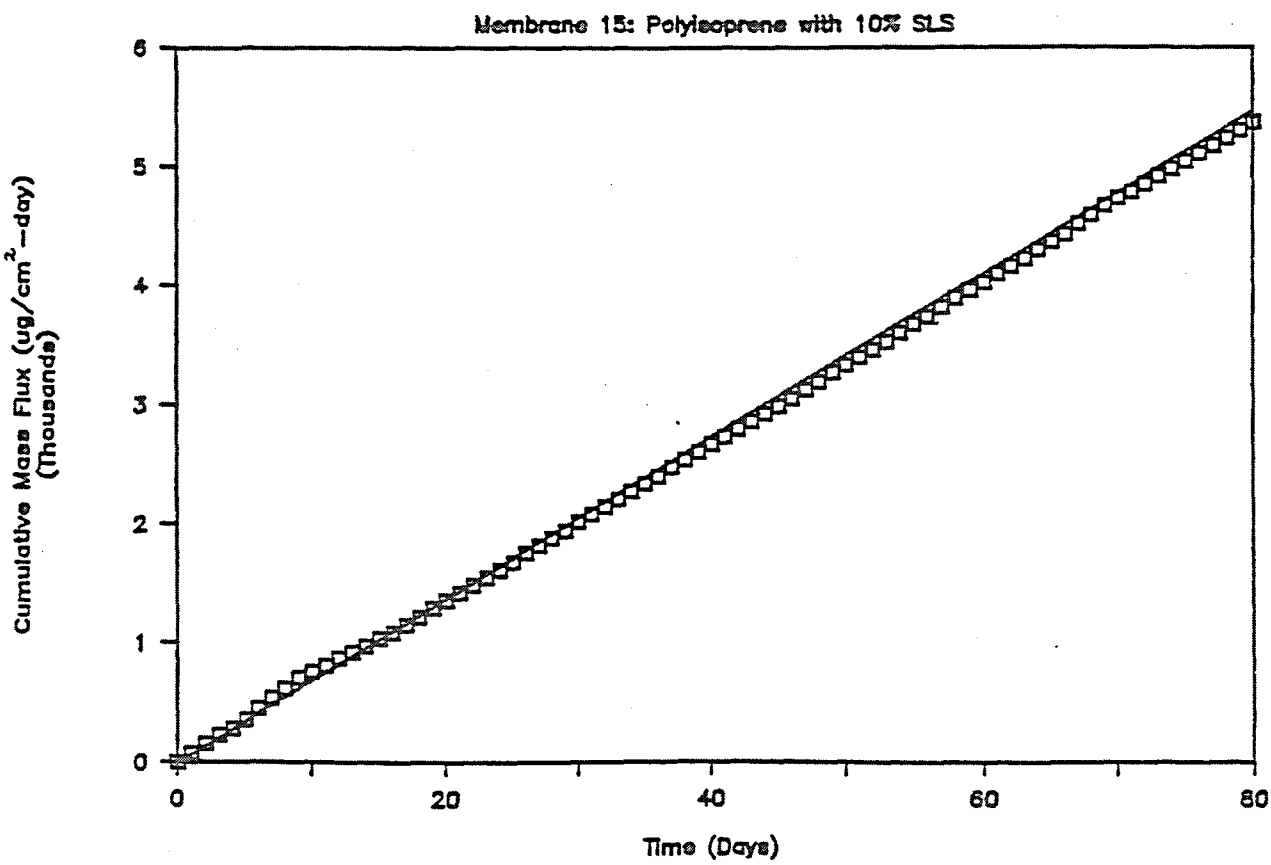

FIGURE 4.73 Plot of cumulative mass flux of SLS as a function of time through a synthetic polyisoprene membrane which contained 10% SLS.

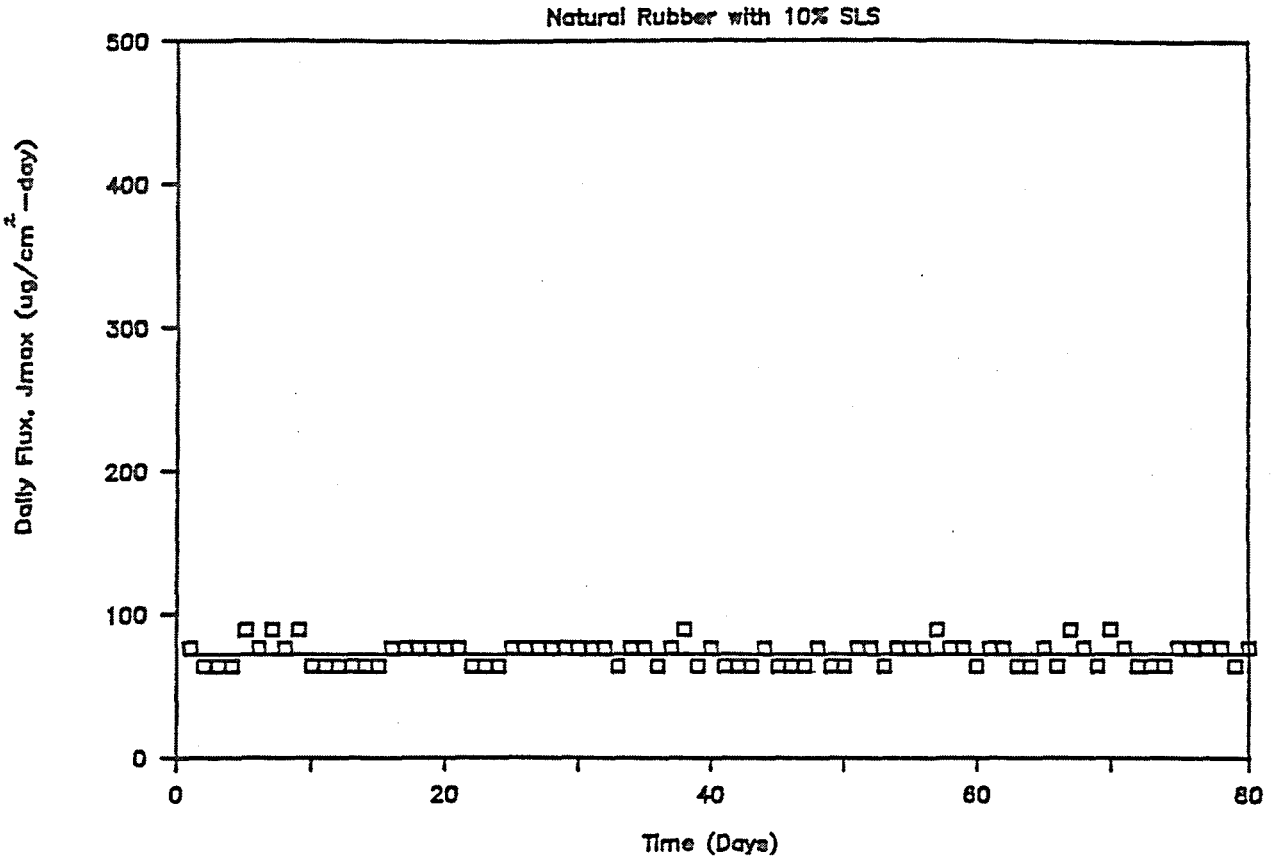

FIGURE 4.74 Plot of the daily flux of SLS as a function of time through a natural-rubber membrane which contained 10% SLS.

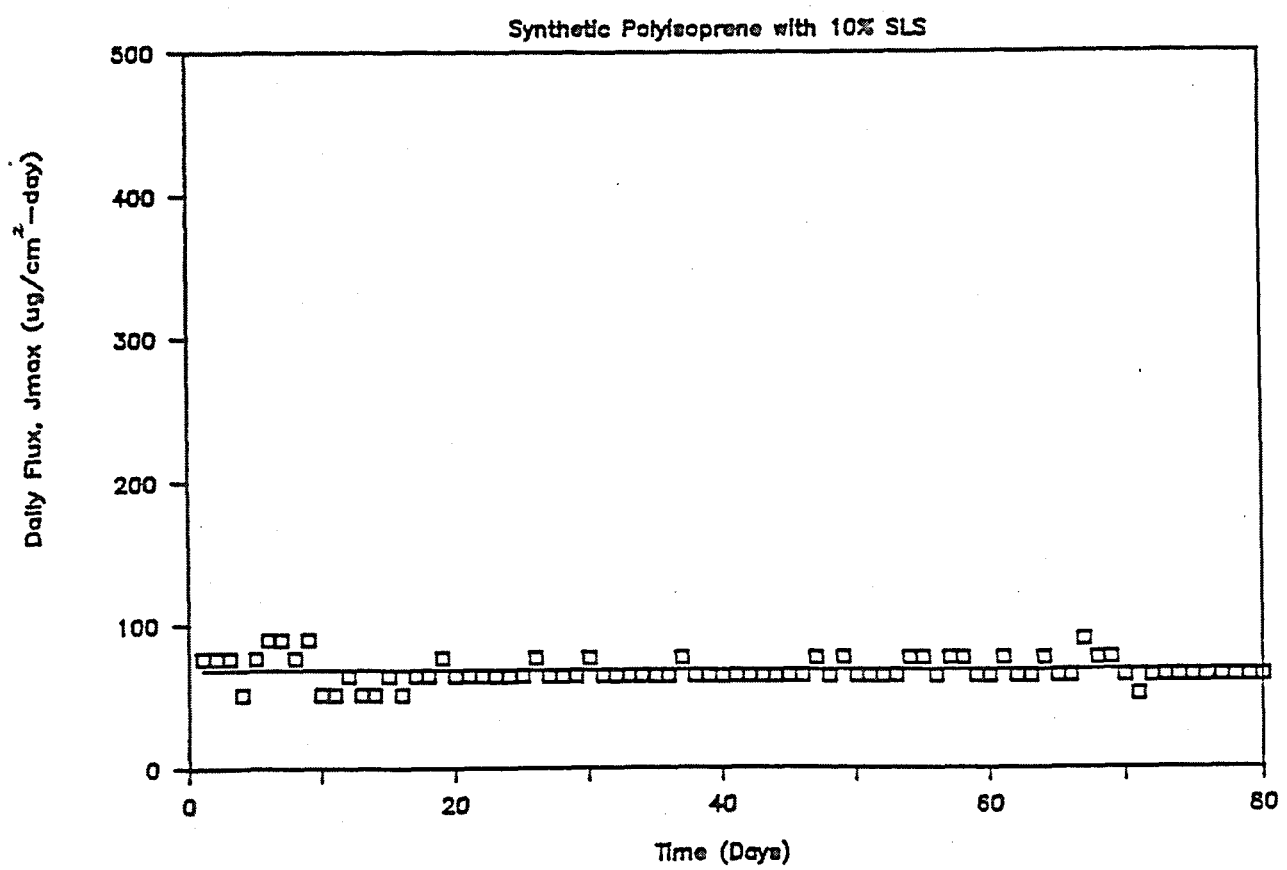

FIGURE 4.75 Plot of the daily flux of SLS as a function of time through a synthetic polyisoprene membrane which contained 10% SLS.

In Section 4.2, it was shown that the solubility limit of SLS in NR was about 4% when the rubber-SLS formulations were stored at 0°C before they were analyzed by DSC. It was also shown that the solubility limit of SLS in NR increased from 4% to 9% when the rubber-SLS formulations were stored at room temperature for six months before they were analyzed. This suggested that the solution of solid SLS in elastomers was time- and temperature-dependent. The apparently higher degree of solubility of SLS in elastomeric membranes, as suggested by the results shown in Tables 4.2 and 4.3, was understandable since the elastomers would easily dissolve the SLS from the solution contacting the membrane.

4.9.3 NR and IR Membranes which Contained 35% SLS

The release characteristics of these membranes were much more complicated, as shown in Figures 4.76 and 4.77 for Membrane 7 (NR/35% SLS) and Membrane 17 (IR/35% SLS), respectively.

It is suggested that the flux of SLS through these membranes was a combination of release of SLS present in the membrane and transport of SLS from the reservoir through the membrane into the pure water, which comprised the receiving compartment. It is important to bear in mind that, because of the large amounts of SLS which were initially dispersed in the elastomers, these systems should be regarded as monolithic slabs, rather than as membranes.

Membranes which contained 35% SLS did indeed function as monolithic devices during the first half of the test period. Figures 4.76 and 4.77 show that large amounts of SLS were released initially, but as time passed, smaller and decreasing amounts of SLS were released. At a certain stage (day 43 of the test period), the amounts of SLS released increased again and a steady-state release rate was established.

Although membrane systems which contained 35% SLS functioned as monolithic devices during the first half of the test period, the release of SLS from these devices did not follow square-root-of-time-order kinetics (as discussed in Section 4.4) during that period. Figure 4.78 shows a comparison of the experimentally-determined amounts of SLS released through an NR membrane which contained 35% SLS (Membrane 7) with the theoretical amounts released, as predicted by Equation (4.8) in Section 4.4. This figure shows clearly that the amounts of SLS released during the first half of the test period was much higher than the values predicted by Equation (4.8).

The establishment of a steady-state flux of SLS through membranes which contained 35% SLS is shown in Figure 4.79 for Membrane 7 (NR/35% SLS; ℓ = 1,25 mm). This figure shows that a steady-state flux was obtained from day 43 until day 80 of the test period.

The steady-state fluxes of SLS through membranes which contained 35% SLS are given in Table 4.4.

TABLE 4.4. Steady-state fluxes of SLS through membranes which contained 35% SLS

Membrane number	Type of rubber	Membrane thickness, ℓ (mm)	Steady-state flux, J^a ($\mu g/cm^2$-day)
7	NR	1,25	512,6
8	NR	0,92	337,2
9	NR	0,70	356,5
16	IR	1,23	140,0
17	IR	0,94	175,4
18	IR	0,72	164,6

a. Steady-state fluxes were obtained from day 43 to day 80.

The unusual shapes of the release curves obtained for NR and IR membranes which contained 35% SLS, as shown in Figures 4.76 and 4.77, respectively, were attributed to the development of porosity in such membranes. The dissolution of dispersed SLS particles, which were incorporated into the rubber formulations during processing, resulted in the formation of pores in the surface layers of these membranes. As the release of dispersed SLS continued, the degree of porosity increased until the entire membrane eventually became porous.

Scanning electron microscopy studies (discussed in Chapter 3, Section 3.4.13) on cross-sections of leached membranes confirmed such porous structures in membranes which initially contained 35% SLS. Scanning electron micrographs of cross-sections of NR/35% SLS membranes are shown in Figures 4.80 to 4.84. Figures 4.80 and 4.81 show cross-sections of an NR/35% SLS membrane before it was leached. The large number of dispersed SLS particles are clearly visible. Figures 4.82 and 4.83 show cross-sections of the same membrane after it was leached for a period of 80 days. These figures show the porosity which was formed in the membrane after large amounts of dispersed SLS

was released. Figure 4.84 shows a cross-section of a leached NR/35% SLS membrane which was fractured after immersion in liquid nitrogen.

These pores, or channels, in the membrane structures, as shown in Figures 4.82 to 4.84, permitted the transport of some SLS from the reservoir compartment. The steady-state flux of SLS through these membranes from day 43 until day 80 of the test period (see Table 4.4) could, therefore, be regarded as a combination of release of the SLS dispersed in the membrane by diffusion through the membrane phase, as well as through pores, and transport of SLS from the reservoir compartment through the pores within the membrane structure. If the porosity proceeds from one surface of the membrane to the other surface, it will cause a flow channel, which will give an unhanced release. This explanation would account for the higher release rate measured after about 40 days. This point is also borne out by Figure 4.84, which shows that even after 80 days of release (when the porosity proceeded throughout the membrane), there were still SLS crystals remaining in the membrane. This would mean that the reservoir maintained a saturated concentration within the rubber medium and that an enhanced release rate must be due to a structural change within the membrane.

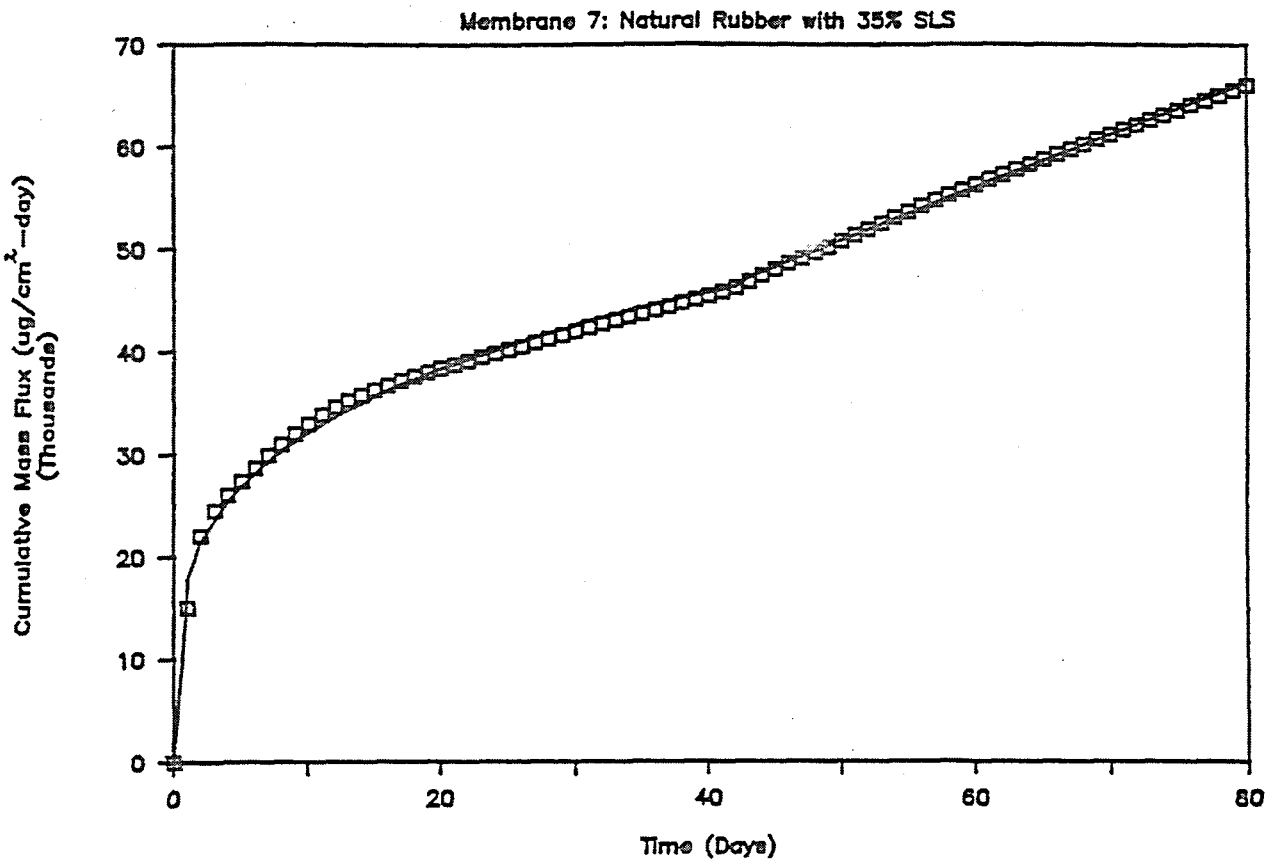

FIGURE 4.76 Plot of the cumulative mass flux of SLS as a function of time through a natural-rubber membrane which contained 35% SLS.

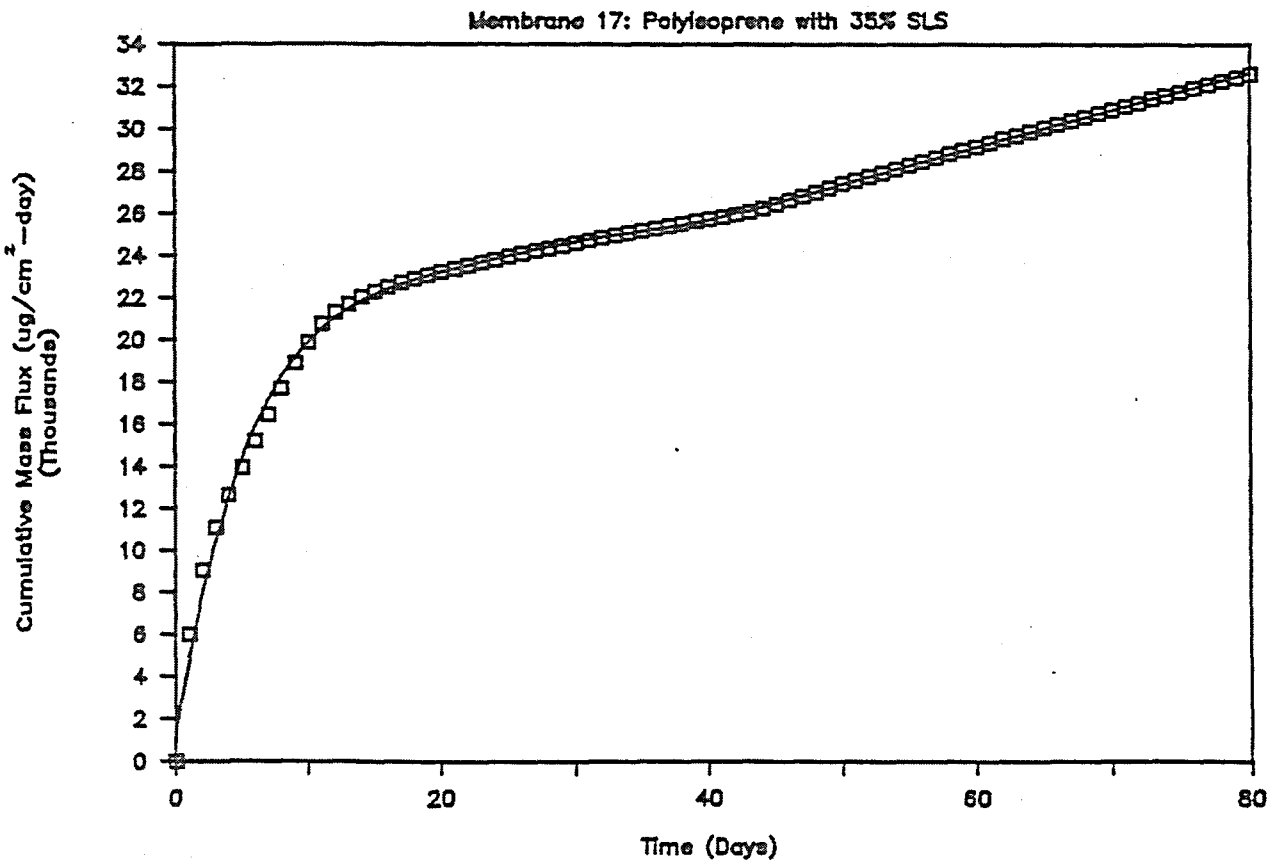

FIGURE 4.77 Plot of the cumulative mass flux of SLS as a function of time through a synthetic polyisoprene membrane which contained 35% SLS.

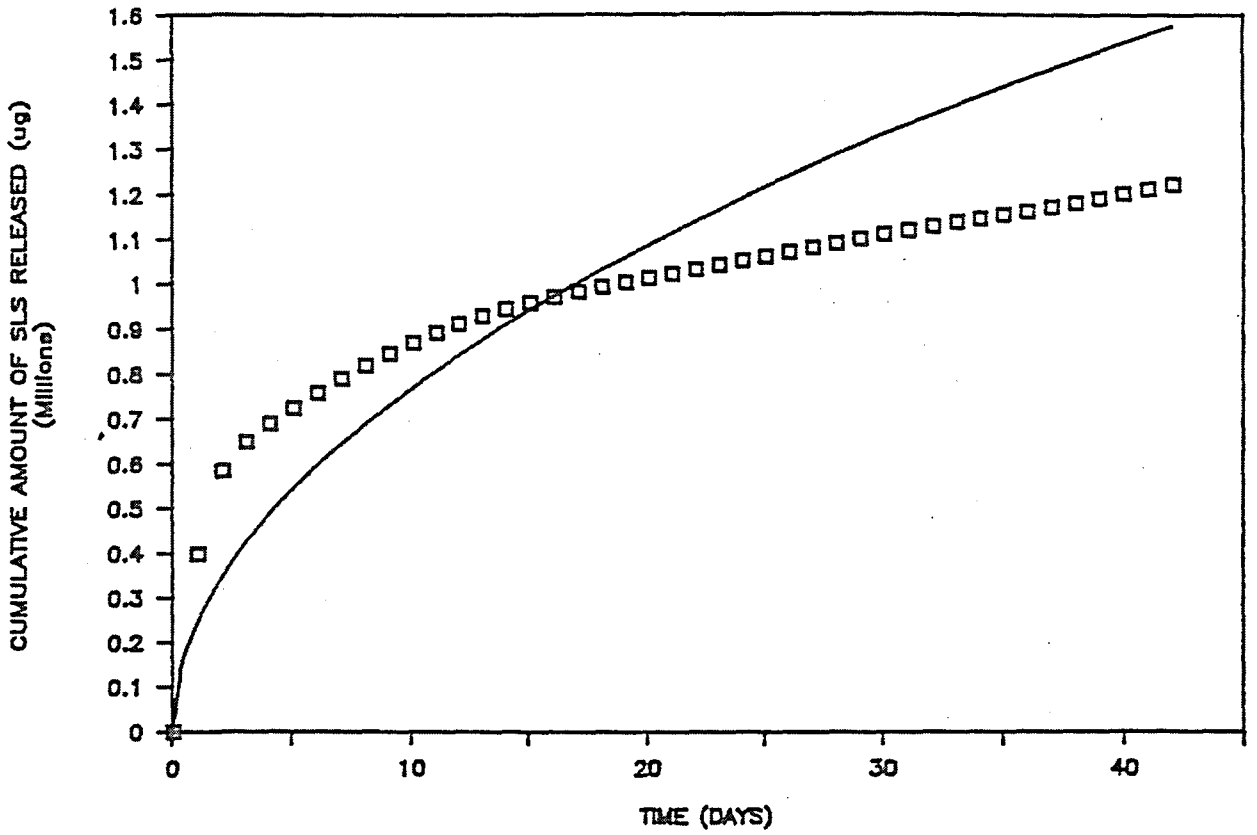

FIGURE 4.78 Comparison of the experimentally-determined amounts of SLS released through a natural-rubber membrane which contained 35% SLS with the theoretical values, as predicted by Equation (4.8).

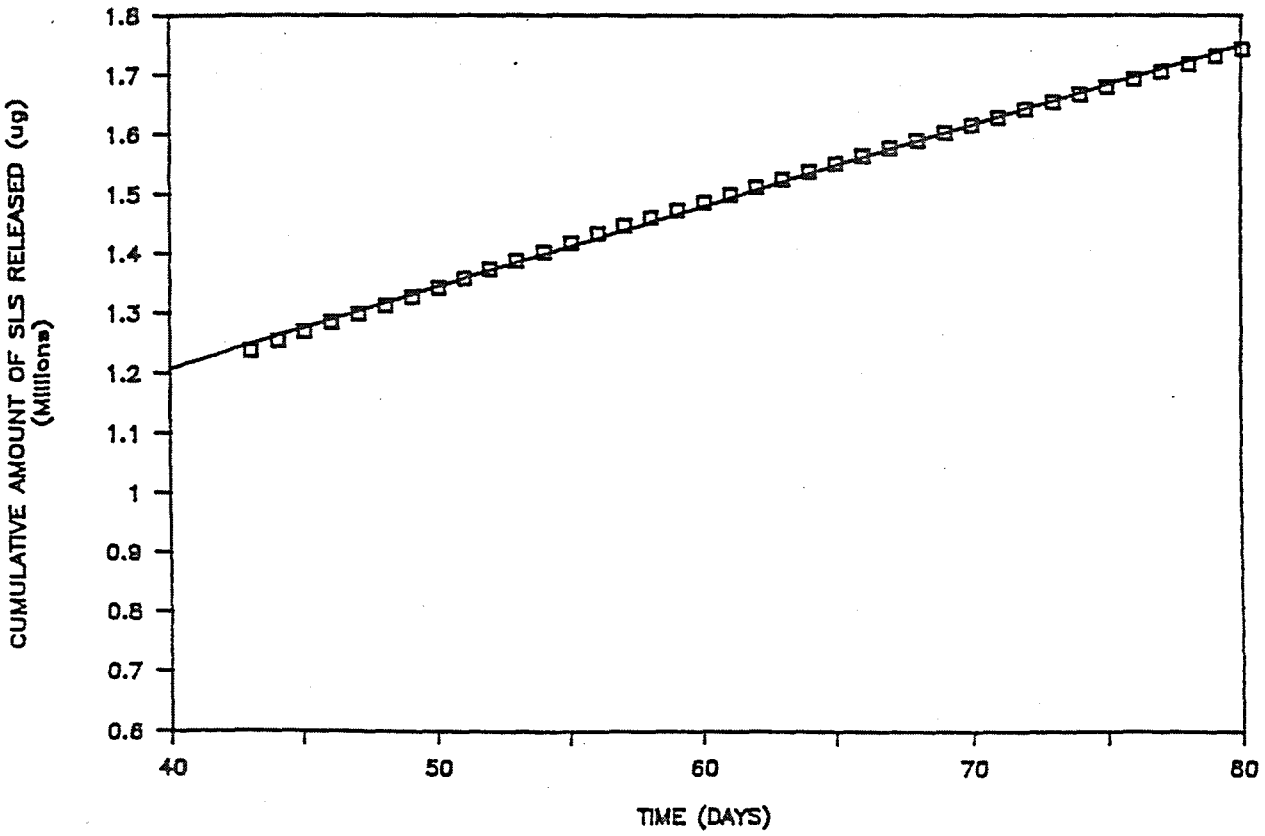

FIGURE 4.79 Plot of the amount of SLS released as a function of time through a natural-rubber membrane which contained 35% SLS. The plot shows that a steady-state release rate was established from day 43 until day 80 of the test period.

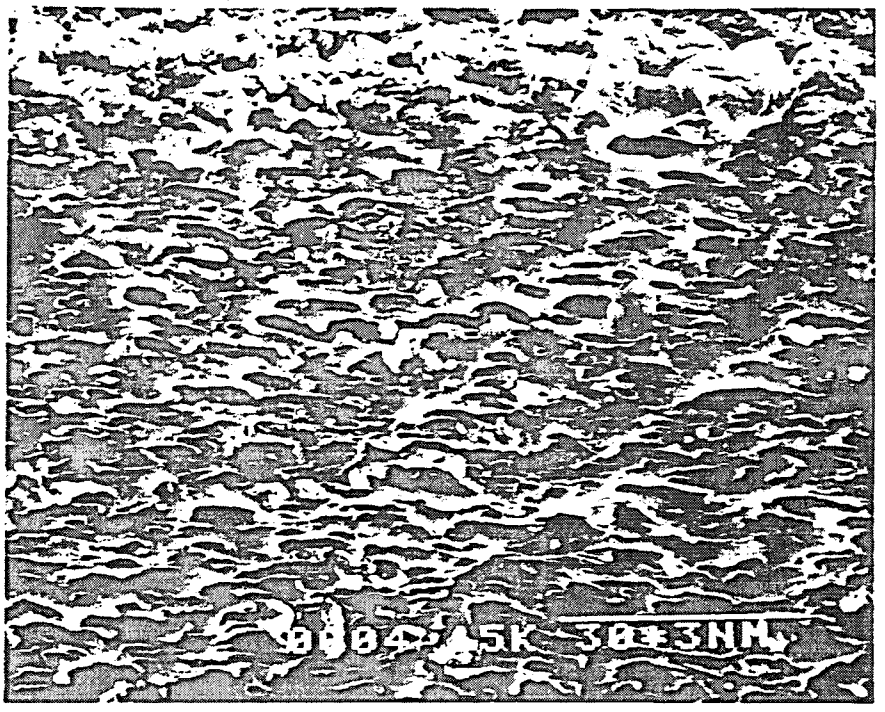

FIGURE 4.82 Scanning electron micrograph of a cross-section of a natural-rubber membrane which initially contained 35% SLS, showing the porosity which was formed in the membrane after the release of large amounts of dispersed SLS.

FIGURE 4.83 Scanning electron micrograph of a cross-section of a natural-rubber membrane which initially contained 35% SLS, showing the porosity which was formed in the membrane after the release of large amounts of dispersed SLS.

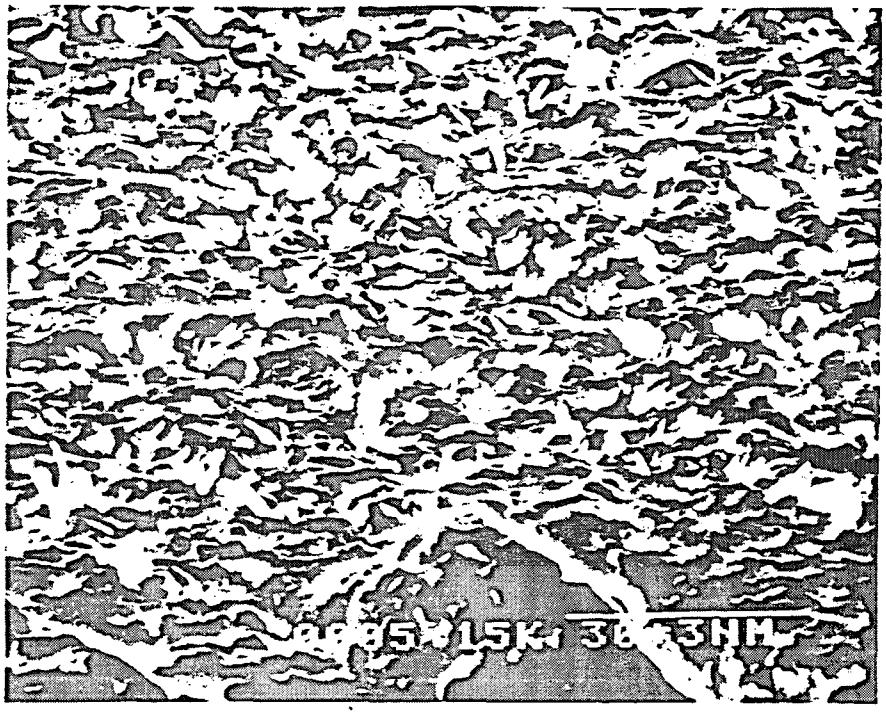

FIGURE 4.80 Scanning electron micrograph of a cross-section of a natural-rubber membrane which contained 35% SLS, showing the large amounts of dispersed SLS particles.

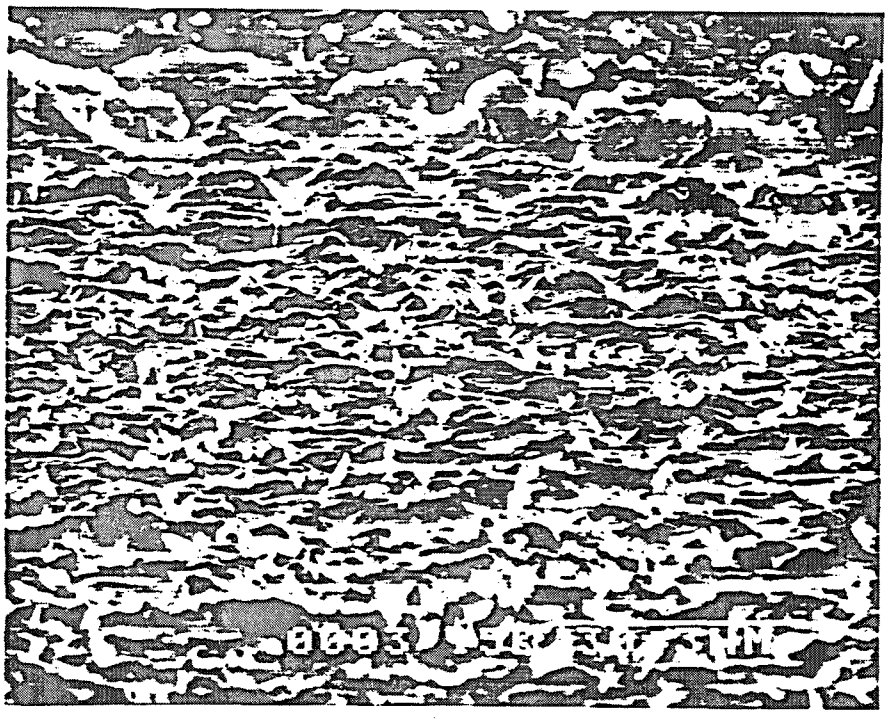

FIGURE 4.81 Scanning electron micrograph of a cross-section of a natural-rubber membrane which contained 35% SLS, showing the dispersed SLS particles in the membrane, as well as the SLS particles at the surface of the membrane.

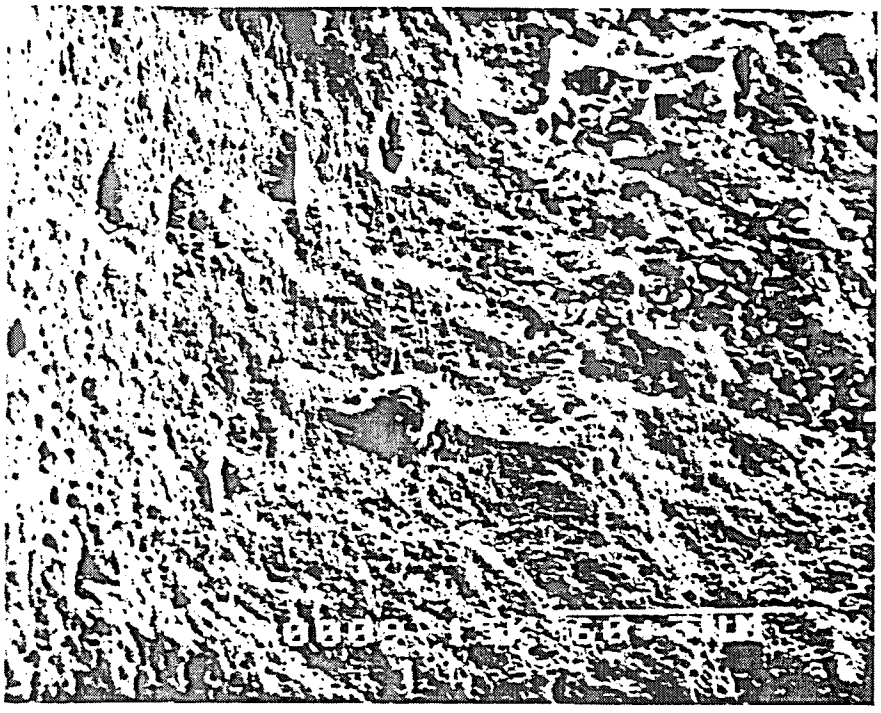

FIGURE 4.84 Scanning electron micrograph of a cross-section of a leached NR/35% SLS membrane which was fractured after immersion in liquid nitrogen. The porosity formed in the membrane is clearly visible (left). The micrograph also shows the SLS particles remaining in the centre of the membrane (right) after 80 days of leaching.

4.10 FACTORS WHICH INFLUENCED THE RATE OF RELEASE OF SLS THROUGH ELASTOMERIC MEMBRANES

4.10.1 The Effect of the SLS Loading in the Membrane on Mass Flux

Figures 4.85 and 4.86 illustrate the effect of the SLS loading in the membrane on mass flux through NR and IR membranes, respectively. In both these figures, membranes of approximately the same thicknesses were compared. It is apparent that there was no significant increase in the flux when NR and IR membranes which contained 10% SLS were used instead of NR and IR membranes which contained no SLS (see Figures 4.85 and 4.86). All the membranes containing no SLS, as well as all those which contained 10% SLS, showed release rates which were constant and independent of time (as discussed in Sections 4.9.1 and 4.9.2). This would indicate that the membranes which initially contained 0% SLS reached their saturation limit rapidly. This saturation limit was determined as 9%, which was close to the loading of the 10% SLS membrane.

With membranes which contained 35% SLS, there was a dramatic increase in the initial release rate, as well as in the release rate during the steady-state period (compare the steady-state fluxes given in Tables 4.2 and 4.3 with those given in Table 4.4). Membranes which contained 35% SLS showed complex release profiles (as shown in Figures 4.76 and 4.77) because of porosity development, which was discussed in Section 4.9.3.

4.10.2 The Effect of the Type of Rubber Used on the Mass Flux of SLS

All membranes based on NR released SLS more rapidly than the membranes based on IR. This is illustrated by Figures 4.87 to 4.90. In Figure 4.87, NR and IR membranes of approximately the same thicknesses are compared. The flux of SLS through the NR membrane (Membrane 1; $\ell = 1{,}40$ mm) was higher than that through the IR membrane (Membrane 10; $\ell = 1{,}54$ mm). The same trend was observed when thinner NR and IR membranes were compared.

In the case of the two control experiments, namely, Control A and Control B, very thin membranes were tested. Control A consisted of a pure NR membrane ($\ell = 0{,}37$ mm), whereas Control B consisted of a pure IR membrane ($\ell = 0{,}39$ mm). There was no significant difference between steady-state flux values for these two membranes, although the cumulative mass flux through the NR membrane was slightly higher, as shown in Figure 4.88. It therefore appeared as though the effect of type of rubber on the mass flux of SLS became less important when thinner membranes were used.

Figure 4.89 shows the effect of type of rubber on mass flux for NR and IR membranes which contained 10% SLS. The thickness of Membrane 4 (NR/10% SLS) was 1,35 mm, and that of Membrane 13 (IR/10% SLS) 1,36 mm. Again, the flux through the NR membrane was slightly higher than that through the IR membrane. The trend was the same when thinner membranes were compared.

When NR and IR membranes which contained 35% SLS were compared, there was a much greater dependence of the release rate of SLS on the type of rubber used. NR membranes released the SLS at considerably higher rates than IR membranes did. This confirmed the previous findings for monolithic matrix devices, SLS being released more rapidly from NR pellets than from IR pellets (see Section 4.5.4).

Figure 4.90 illustrates the effect of type of rubber on the release rates of SLS through membranes which contained 35% SLS. The membranes compared in Figure 4.90 are Membrane 8 (NR/35% SLS; ℓ = 0,92 mm) and Membrane 17 (IR/35% SLS; ℓ = 0,94 mm). All these findings are consistent with the concept of the higher solubility limit of SLS in NR, as compared with that in IR.

4.10.3 The Effect of Membrane Thickness on the Mass Flux of SLS

The flux of an agent through a membrane was expected to increase as the membrane thickness decreased. This effect is illustrated by Figure 4.91 for pure vulcanized NR membranes (i.e., Membranes 1, 2 and 3, given in Table 3.8, Chapter 3). There was only a slight increase in the mass flux with a decrease in membrane thickness for the three different thicknesses tested (ℓ = 1,40 mm for Membrane 1, 1,14 mm for Membrane 2 and 0,90 mm for Membrane 3). The same effect of membrane thickness on flux was observed for pure vulcanized IR membranes (i.e., Membranes 10, 11 and 12, given in Table 3.8, Chapter 3). The increase in the mass flux of SLS with a decrease in the membrane thickness was, however, more significant for IR membranes, as shown in Figure 4.92.

Figures 4.93 and 4.94 show the effect of membrane thickness on the flux of SLS through NR membranes which contained 10% SLS and IR membranes which contained 10% SLS, respectively. The fluxes through the NR/10% SLS membranes of three different thicknesses (Figure 4.93) were almost identical. With IR/10% SLS at three different membrane thicknesses (Figure 4.94), the steady-state fluxes increased slightly with an increase in membrane thickness. This trend was, of course, exactly the opposite to what was expected on the basis of a simple diffusion model.

A possible explanation is that when 10% SLS was incorporated into rubber formulations during processing, these membrane systems would function essentially as monolithic slab devices, at least during the initial period of release of SLS. It is, therefore, clear that membrane systems which contained 10% SLS could not be regarded as membranes in the true sense of the word. It was expected that with a monolithic slab the total amount of SLS released would increase as the thickness of the slab increased, because a larger amount of SLS was present in a thicker slab. This explains the effect of membrane thickness on flux for IR membranes which contained 10% SLS (Figure 4.94). A further explanation for the insensitivity to thickness follows from the presence of undissolved SLS remaining in leached membranes, which ensures that the rubber remains saturated with SLS (or close to saturation) and thereby makes the diffusion rate less critical.

With Membranes 7, 8 and 9 (NR which contained 35% SLS) and Membranes 16, 17 and 18 (IR which contained 35% SLS), the effect of membrane thickness on flux was contrary to that expected for the simple diffusion model. The increase in the rate of release of SLS with an increase in the membrane thickness was more pronounced for membranes which contained 35% SLS. This is shown in Figures 4.95 and 4.96 for NR/35% SLS membranes and IR/35% SLS membranes, respectively.

It was mentioned in Section 4.9.3 that these controlled-release systems should be regarded as monolithic slabs, rather than as membranes. It was, therefore, obvious that release of SLS from the rubbers themselves would dominate the overall release process for a considerable time. It is believed that the development of porosity, as well as the fact that the membrane contained a large excess of SLS, caused these complex effects.

Two thin membranes, namely, Control A (NR; $\ell = 0{,}37$ mm) and Control B (IR; $\ell = 0{,}39$ mm) were also evaluated. The steady-state fluxes through these two membranes, as given in Table 4.2, were considerably higher than those through the pure NR and IR membranes discussed earlier. The general effect of membrane thickness on flux, as suggested by the results of the studies reported here, is shown in Figures 4.97 and 4.98 for pure NR and IR membranes, respectively. Membranes which contained 10% and 35% SLS are not included in this discussion, since they could not be regarded as "true membranes". Figures 4.97 and 4.98 show clearly that there was not a linear relationship between membrane thickness and flux. These results were unusual, since the flux was expected to vary linearly with membrane thickness. It was, therefore, considered important to analyze the thickness-flux relationship by fitting various mathematical equations to experimental data. This analysis of the thickness-flux relationship is discussed in the next section.

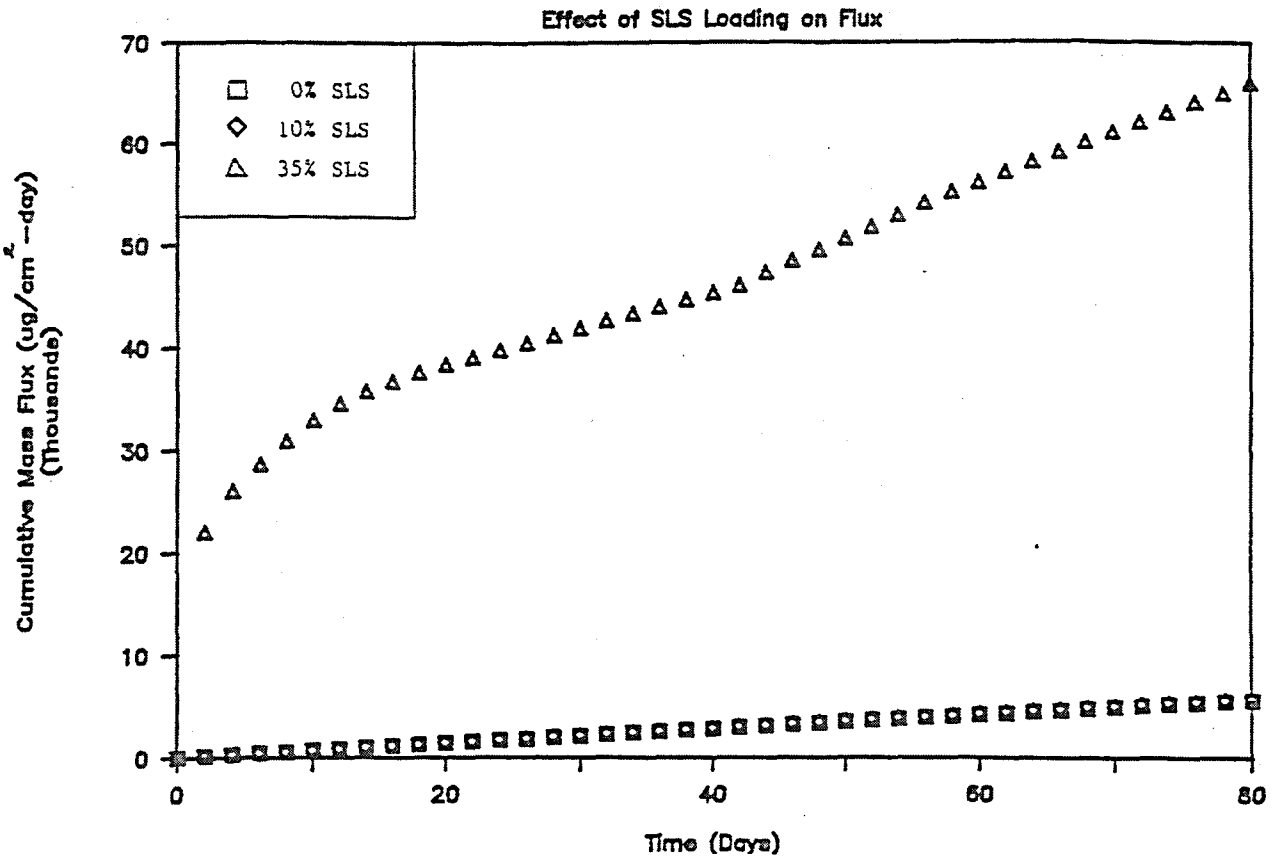

FIGURE 4.85 Plots of cumulative mass flux against time, illustrating the effect of the SLS loading on mass flux through natural-rubber membranes.

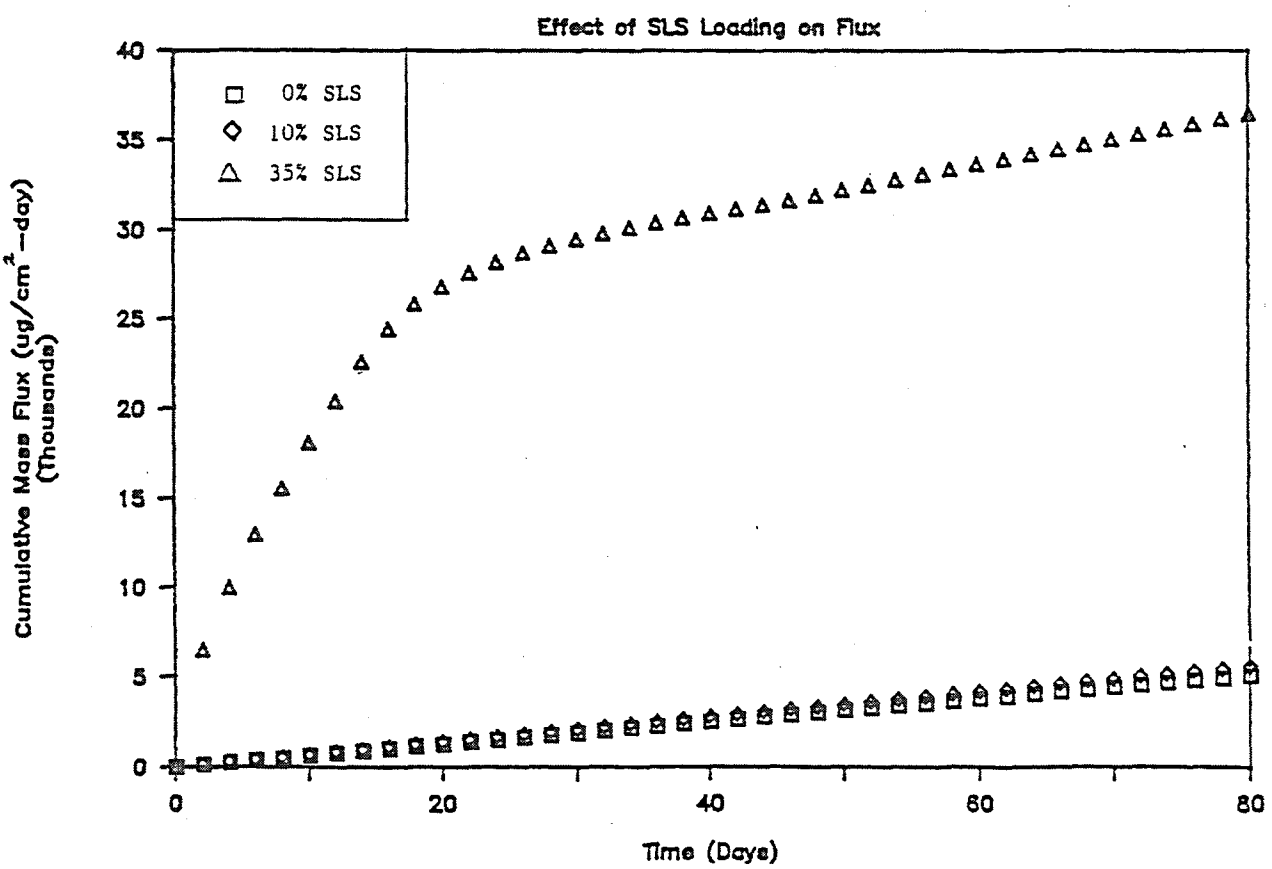

FIGURE 4.86 Plots of cumulative mass flux against time, illustrating the effect of the SLS loading on mass flux through synthetic polyisoprene membranes.

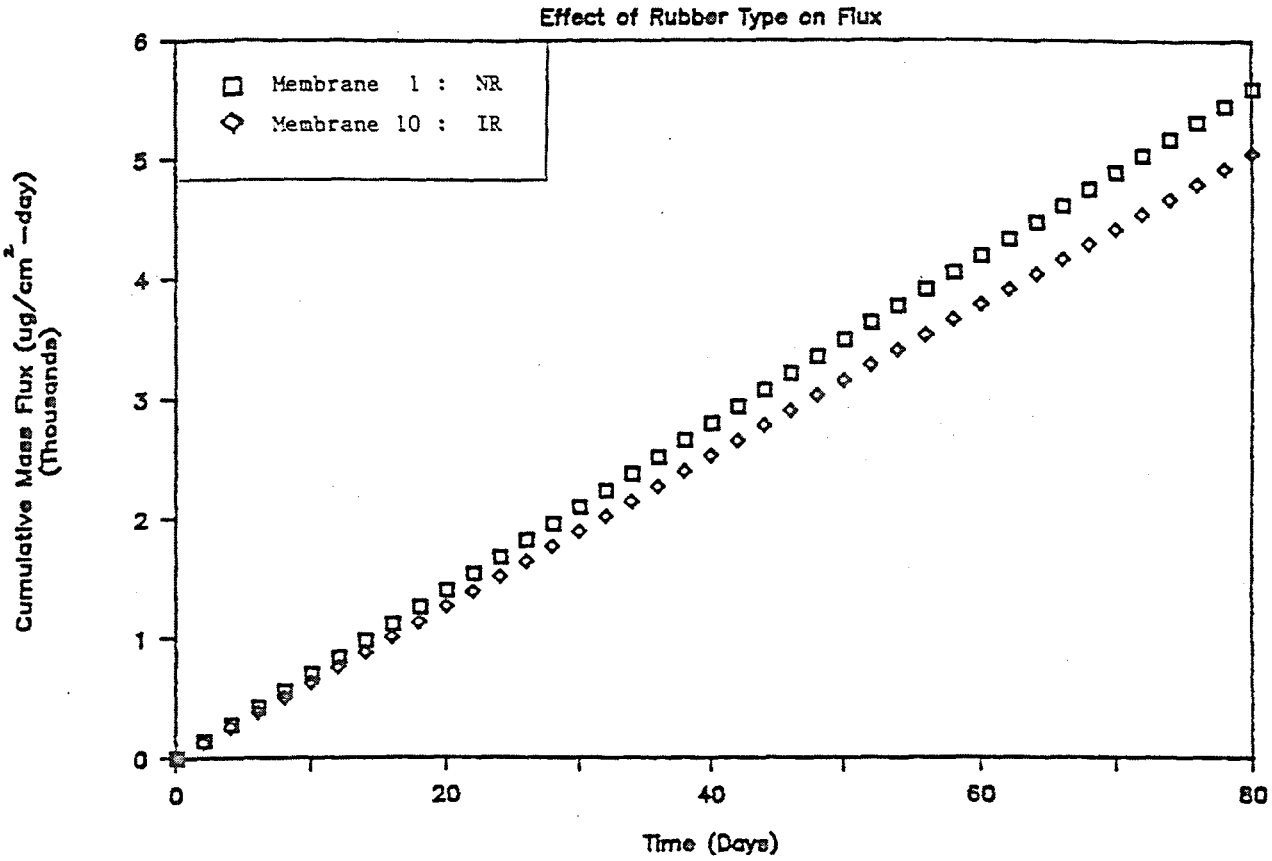

FIGURE 4.87 Plots of cumulative mass flux against time, illustrating the effect of the type of rubber used on the mass flux of SLS through rubber membranes which initially contained no SLS.

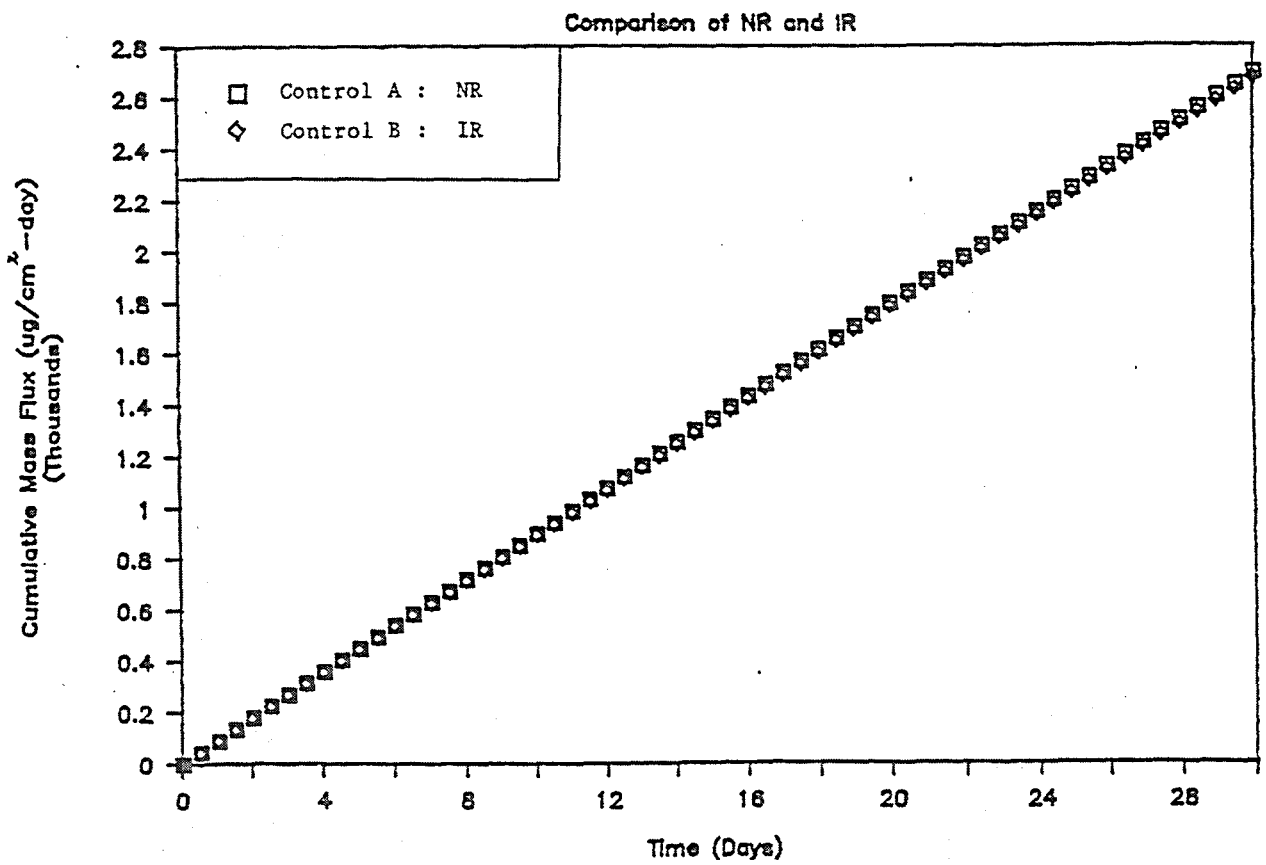

FIGURE 4.88 Plots of cumulative mass flux against time, illustrating the effect of the type of rubber used on the mass flux of SLS through rubber membranes which initially contained no SLS.

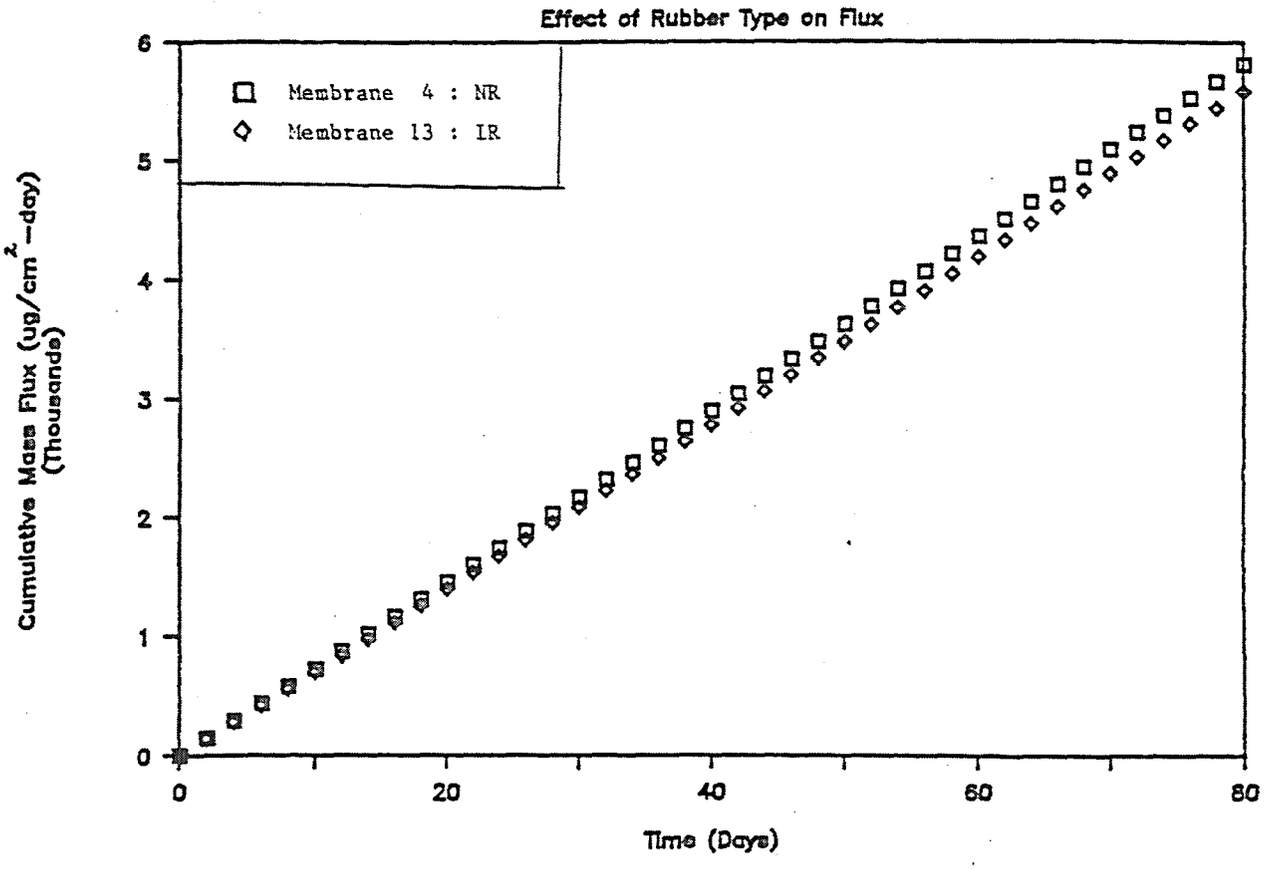

FIGURE 4.89 Plots of cumulative mass flux against time, illustrating the effect of the type of rubber used on the mass flux of SLS through rubber membranes which initially contained 10% SLS.

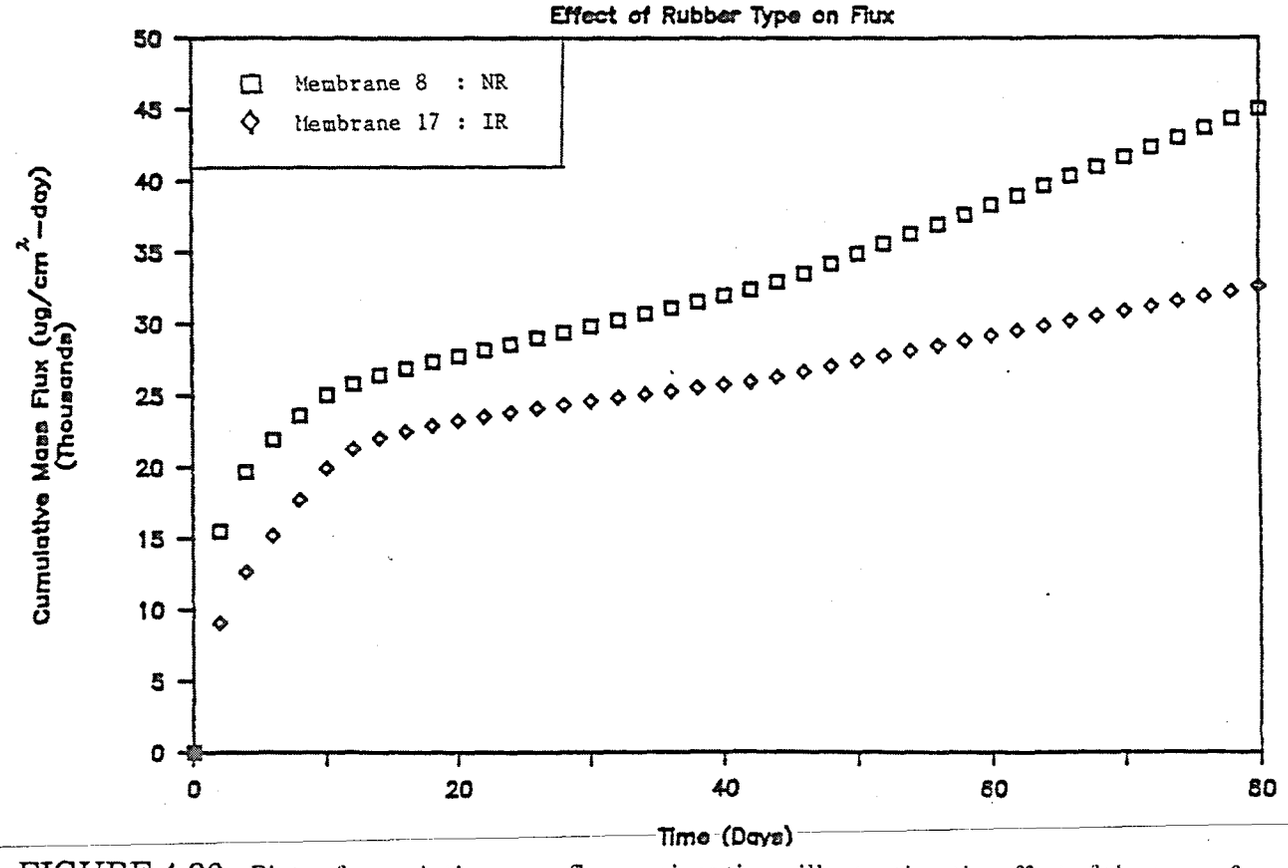

FIGURE 4.90 Plots of cumulative mass flux against time, illustrating the effect of the type of rubber used on the mass flux of SLS through rubber membranes which initially contained 35% SLS.

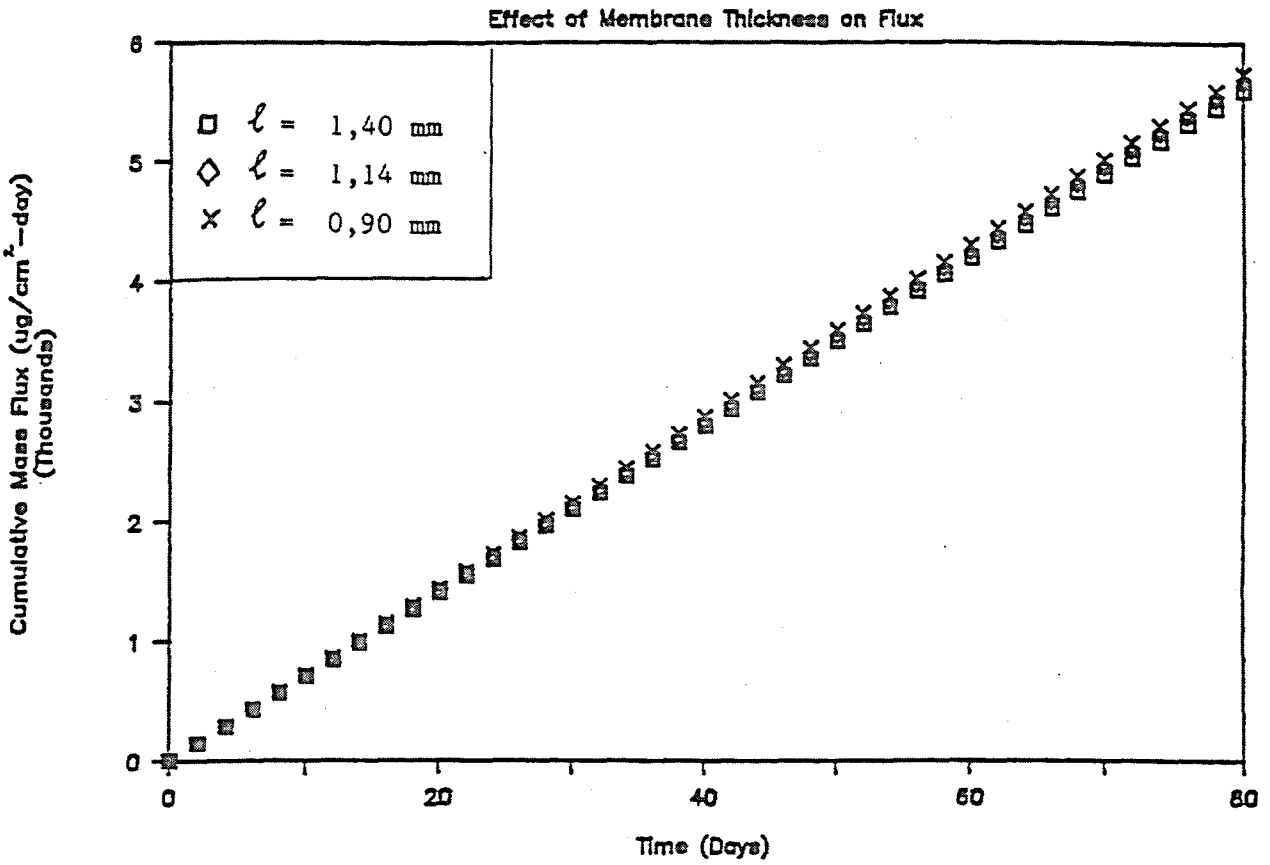

FIGURE 4.91 Plots of cumulative mass flux against time, showing the effect of membrane thickness on the mass flux of SLS through natural-rubber membranes which initially contained no SLS.

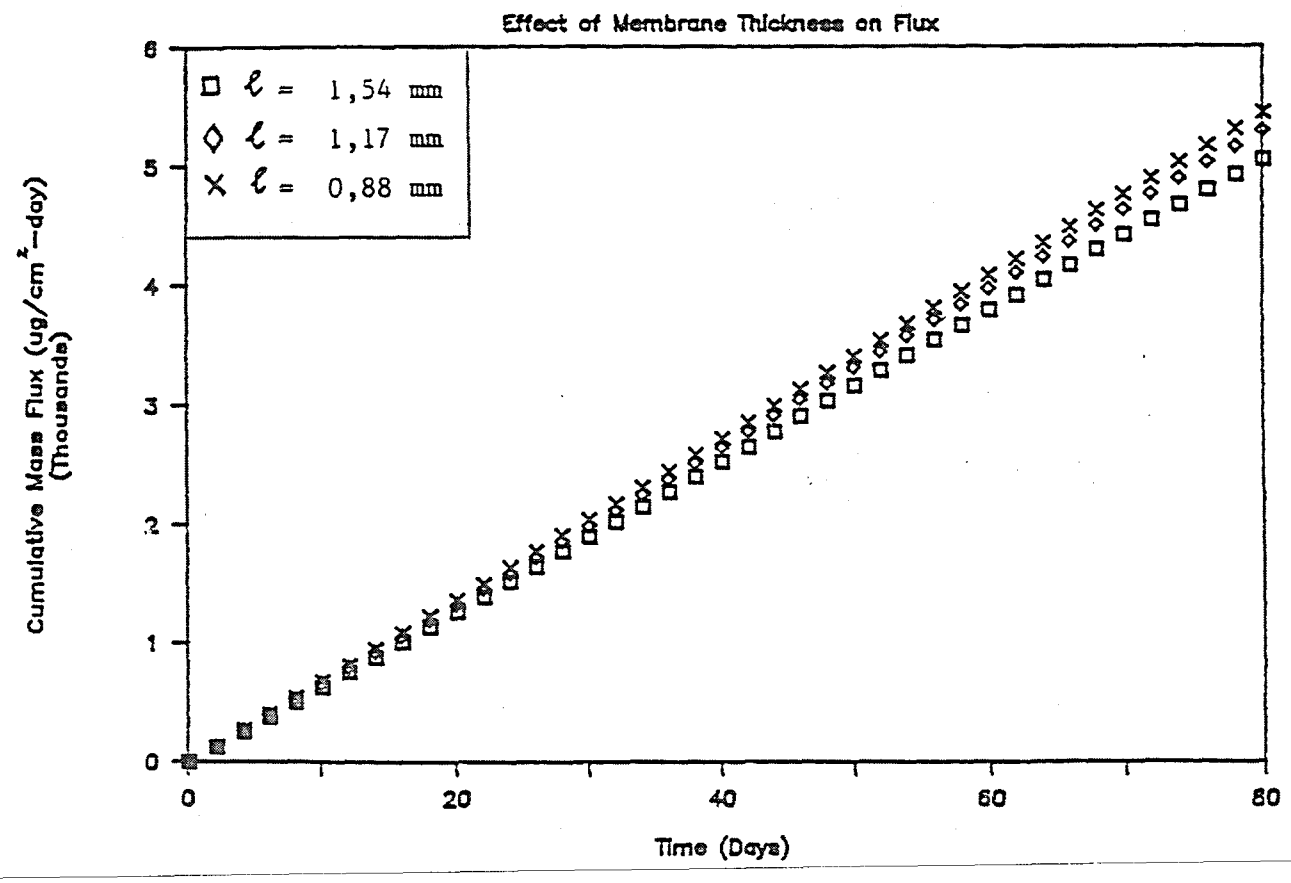

FIGURE 4.92 Plots of cumulative mass flux against time, showing the effect of membrane thickness on the mass flux of SLS through synthetic polyisoprene membranes which initially contained no SLS.

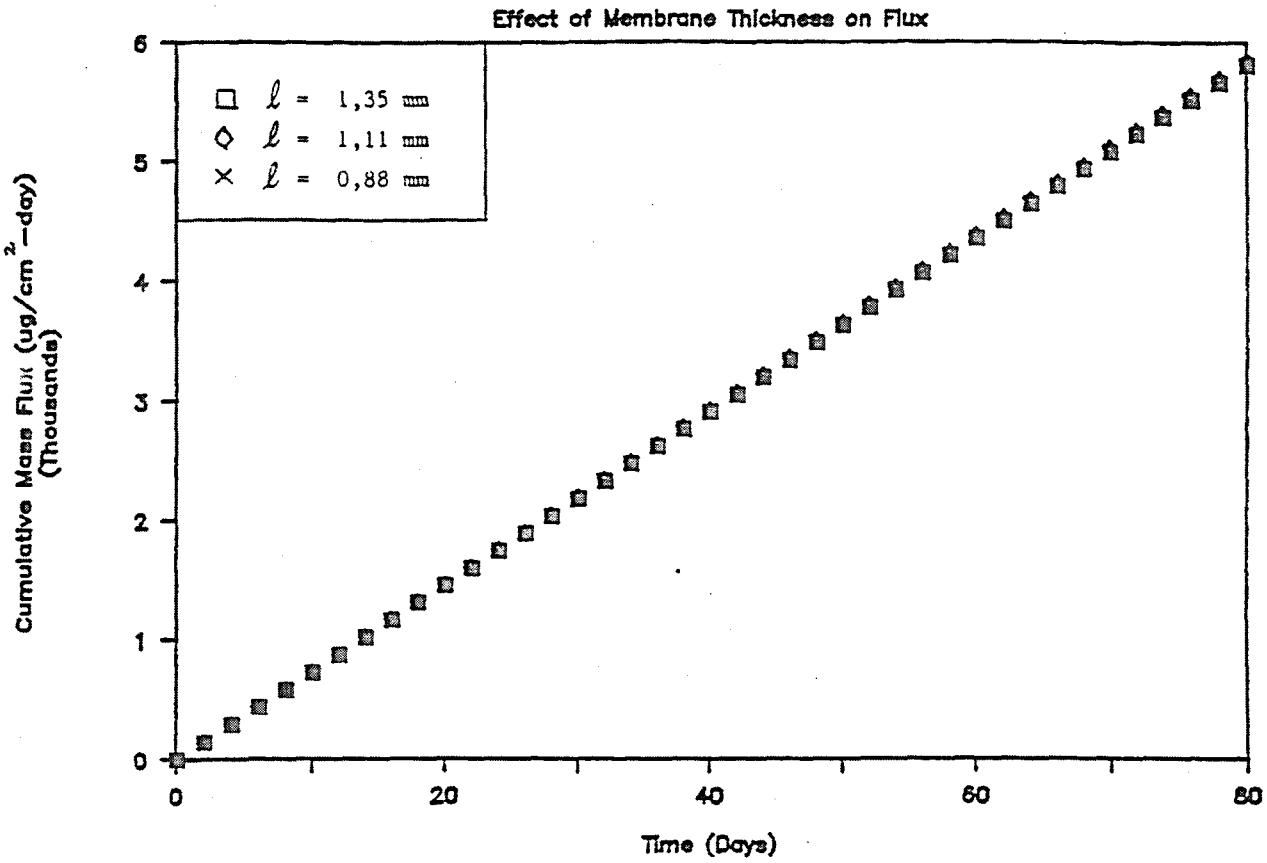

FIGURE 4.93 Plots of cumulative mass flux against time, showing the effect of membrane thickness on the mass flux of SLS through natural-rubber membranes which initially contained 10% SLS.

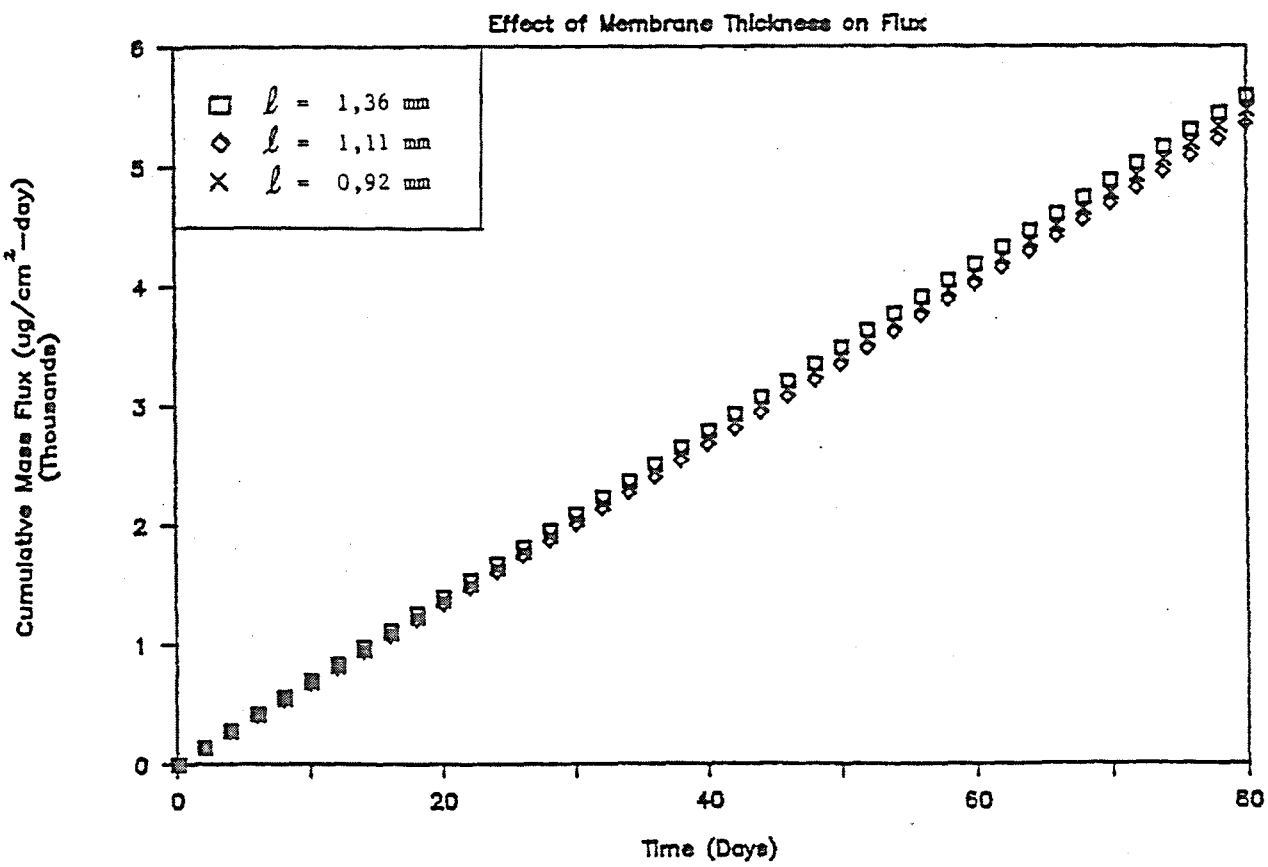

FIGURE 4.94 Plots of cumulative mass flux against time, showing the effect of membrane thickness on the mass flux of SLS through synthetic polyisoprene membranes which initially contained 10% SLS.

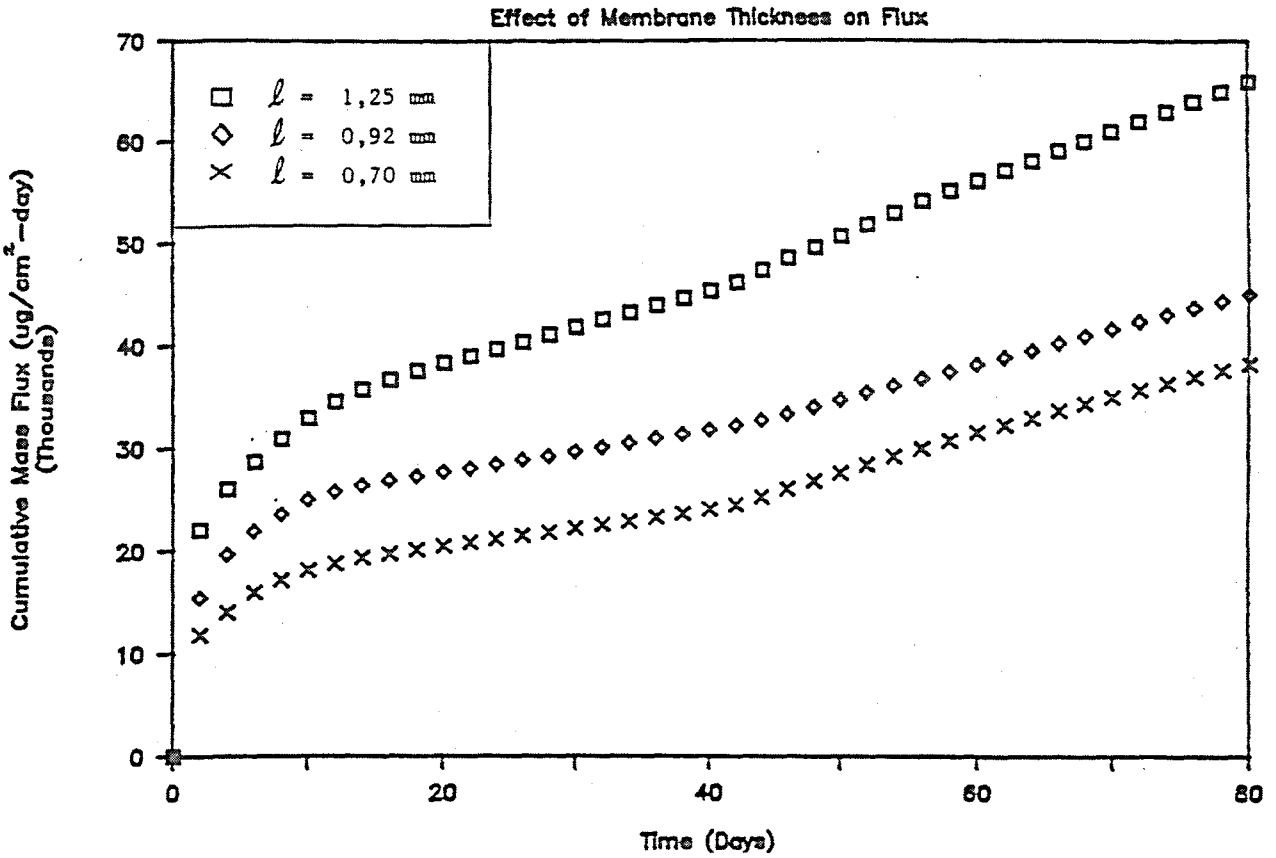

FIGURE 4.95 Plots of cumulative mass flux against time, showing the effect of membrane thickness on the mass flux of SLS through natural-rubber membranes which initially contained 35% SLS.

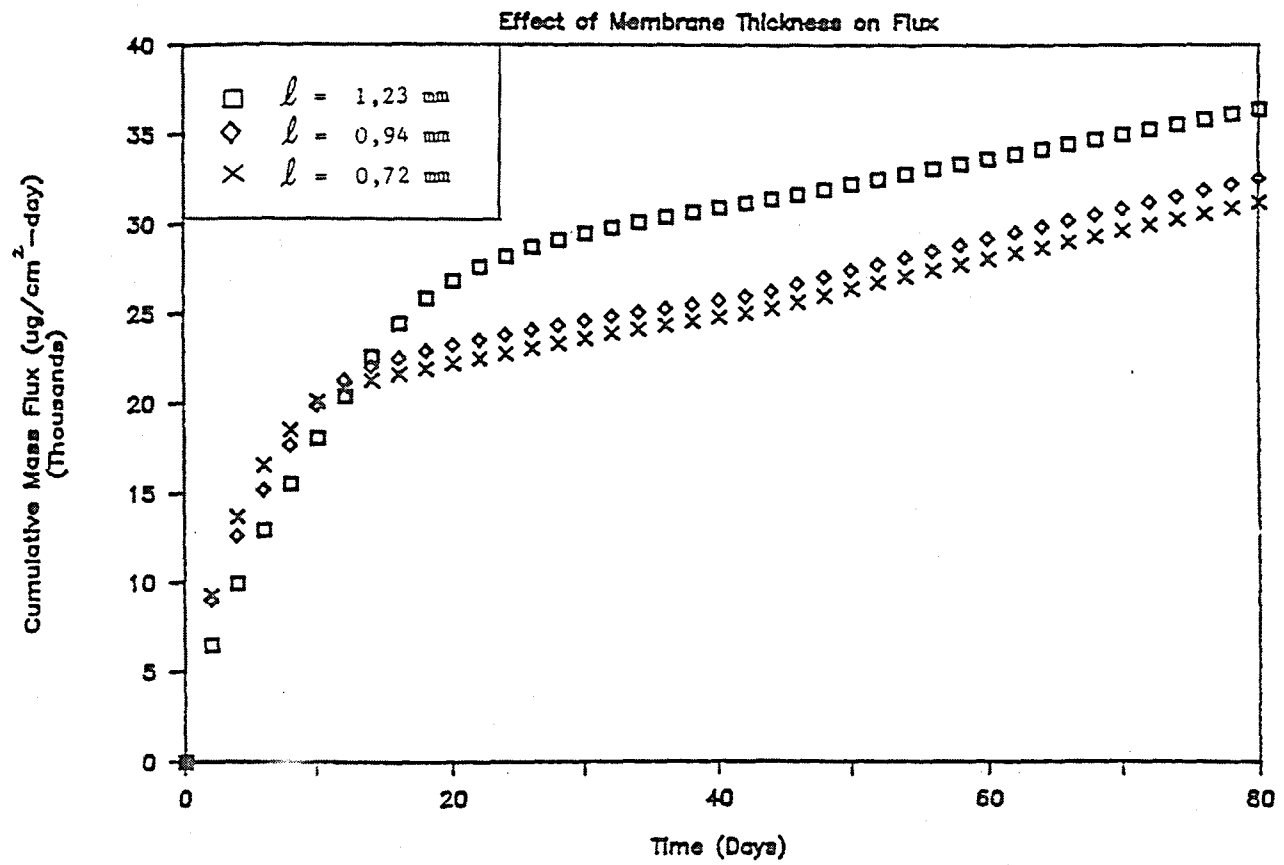

FIGURE 4.96 Plots of cumulative mass flux against time, showing the effect of membrane thickness on the mass flux of SLS through synthetic polyisoprene membranes which initially contained 35% SLS.

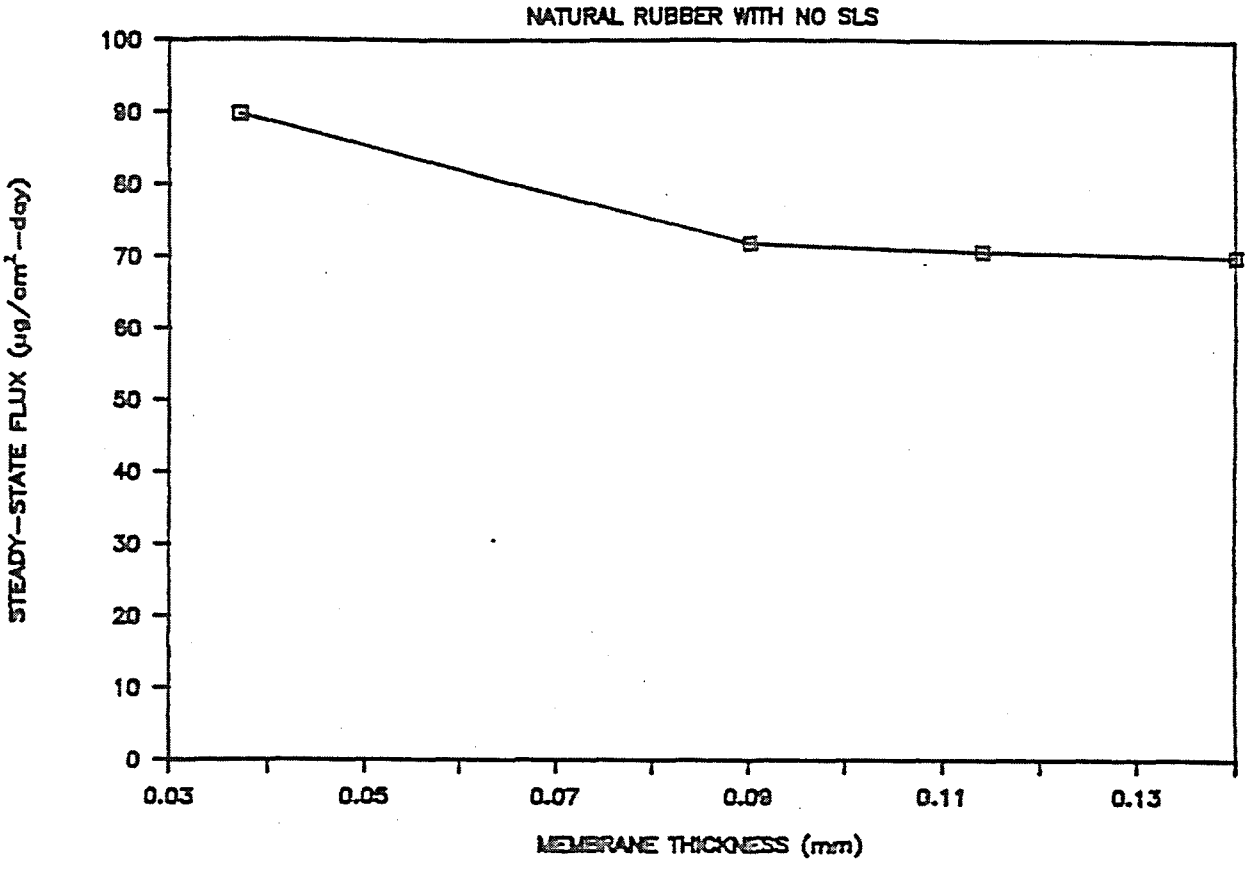

FIGURE 4.97 Plot showing the non-linear increase in the steady-state flux of SLS with a decrease in membrane thickness for natural-rubber membranes which contained no SLS.

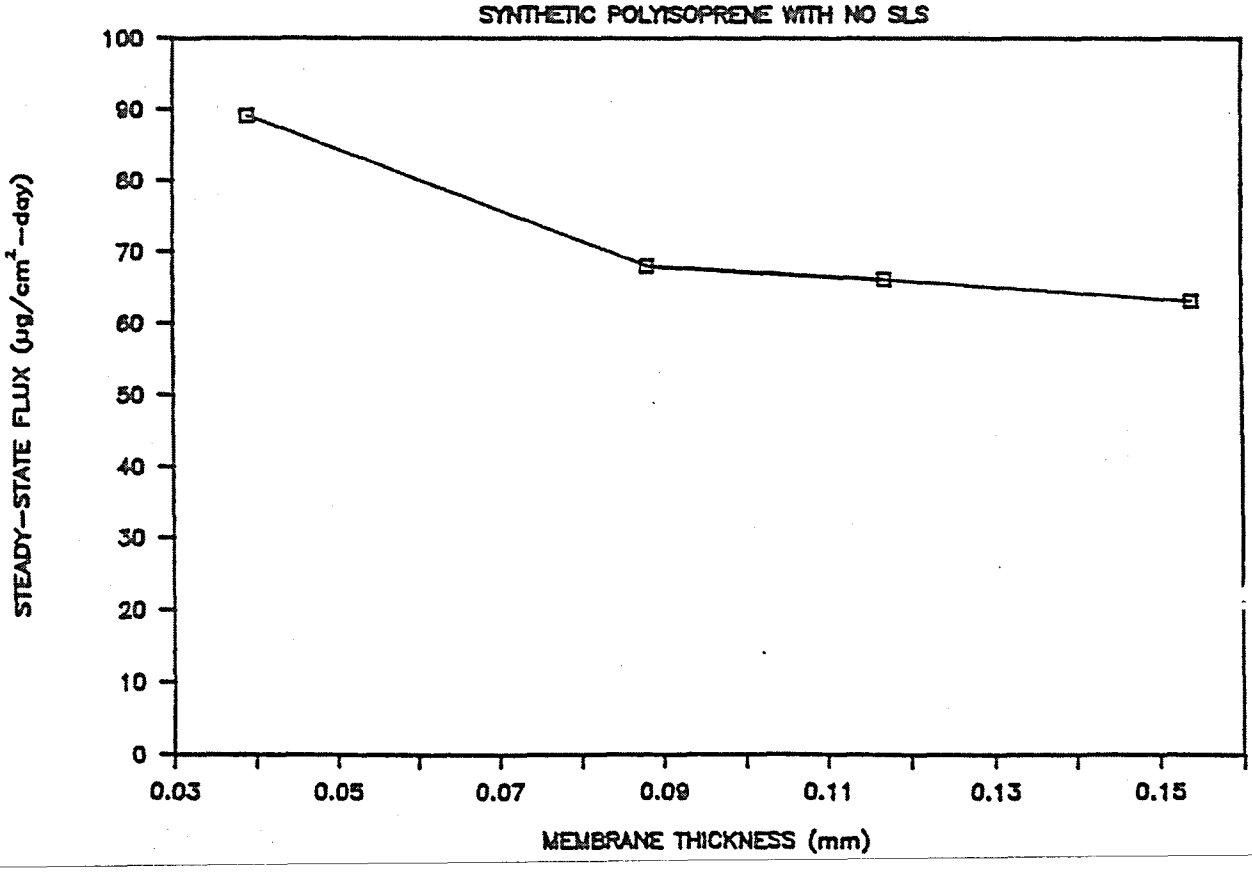

FIGURE 4.98 Plot showing the non-linear increase in the steady-state flux of SLS with a decrease in membrane thickness for synthetic polyisoprene membranes which contained no SLS.

4.10.4 Analysis of the Relationships between Mass Flux, Transference and Membrane Thickness

The normalized mass flux is the product of the membrane thickness, ℓ, and the solute flux, J. The transference, $\overline{T}$, is the normalized flux at the specified boundary conditions, namely, a saturated solution on one side of the membrane and zero concentration of solute on the other. (Chapter 2, Section 2.5.6.2)

The transference, $\overline{T}$, was calculated for membranes which contained no SLS, as well as for those which contained 10% SLS. The values obtained are given in Table 4.5.

Figures 4.99 and 4.100 show plots of the transference as a function of membrane thickness for NR and IR membranes respectively. A linear relationship is apparent between $\overline{T}$ and ℓ,

$$\overline{T} = J\ell \qquad (4.51)$$

where J is a constant. Transference was expected, in terms of Fickian diffusion theory, to be a constant. As this is not so, it is apparent that the system is not diffusion controlled and transference values have no meaning.

TABLE 4.5. Transference ($\overline{T}$) of SLS through NR and IR membranes

Membrane number	Type of rubber	Mass% SLS	Flux, J (μg/cm²-day)	Thickness ℓ (cm)	Transference, $\overline{T}$ (Jℓ) (μgcm/cm²-day)
1	NR	0	69,98	0,140	9,80
2	NR	0	0,79	0,114	8,07
3	NR	0	71,85	0,090	6,47
4	NR	10	72,64	0,135	9,81
5	NR	10	73,14	0,111	8,12
6	NR	10	72,57	0,088	6,39
10	IR	0	63,18	0,154	9,73
11	IR	0	66,20	0,117	7,75
12	IR	0	68,09	0,088	5,99
13	IR	10	69,80	0,136	9,49
14	IR	10	66,97	0,111	7,43
15	IR	10	68,40	0,092	6,29
Control A	NR	0	89,80	0,037	3,32
Control B	IR	0	89,18	0,039	3,47

Figures 4.101 and 4.102 show the variation of the flux (J) with membrane thickness (ℓ) for NR and IR membranes, respectively.

These figures suggest that the flux is almost independent of the membrane thickness (except at small values of ℓ). This would suggest that some sort of "surface effect" is rate determining. This effect may be the result of a surface-layer effect at the upstream surface of the membrane, where absorption of SLS by the rubber membrane could be the rate-controlling step in the mass- transport process. However, it may also be the result of a boundary-layer effect at the downstream surface of the membrane, where the dissolution of SLS could be the rate-controlling step.

Another possible explanation is that the "surface effect" was the result of the complex behaviour of surfactant molecules in solution, i.e., of their tendency to form micellar aggregates in solution when the critical micelle concentration (CMC) is exceeded. A brief discussion of the behaviour of surfactants in solution is presented in Appendix 8A.

In a polar medium, such as water, the surfactant molecules form micelles, with the hydrocarbon chains forming the inner core and the ionic heads exposed to the water. During the absorption of SLS by the rubber membrane, reorientation of these micellar structures is probably required. The SLS molecules are expected to be adsorbed onto the membrane by their hydrocarbon chains, with their ionic heads directed towards the water. The formation of reverse micelles in apolar media, such as hydrocarbon solvents, has been studied (see Appendix 8A). It is, therefore, possible that reverse micelles may also form in the hydrocarbon- rubber medium. In this case, the ionic heads of the SLS molecules will be protected and their hydrocarbon chains will be directed towards the rubber medium. It is very unlikely that true reverse micellar aggregates, consisting of a large number of surfactant molecules, will exist in the rubber medium. It is possible, however, that dimers and trimers of surfactant molecules could form.

It is expected that, during the dissolution of SLS molecules at the downstream surface of the membrane, the ionic heads of these molecules will be directed towards the water and that their hydrocarbon chains will remain in the rubber. This would mean that reorientation of the SLS molecules is once again required at the rubber-water interface. Either absorption or dissolution of surfactant molecules, or probably both these processes, may be the rate-controlling step or steps in the transport of SLS through rubber membranes.

It is believed that the unusual relationship between mass flux and membrane thickness is the result of the dual nature of SLS molecules and the fact that such molecules behave differently from

ordinary organic molecules. All previous studies and theories relate to ordinary organic molecules which behave rather more predictably. There is therefore very little evidence in any investigation, prior to this study, of the mechanism of diffusion of soap-type molecules.

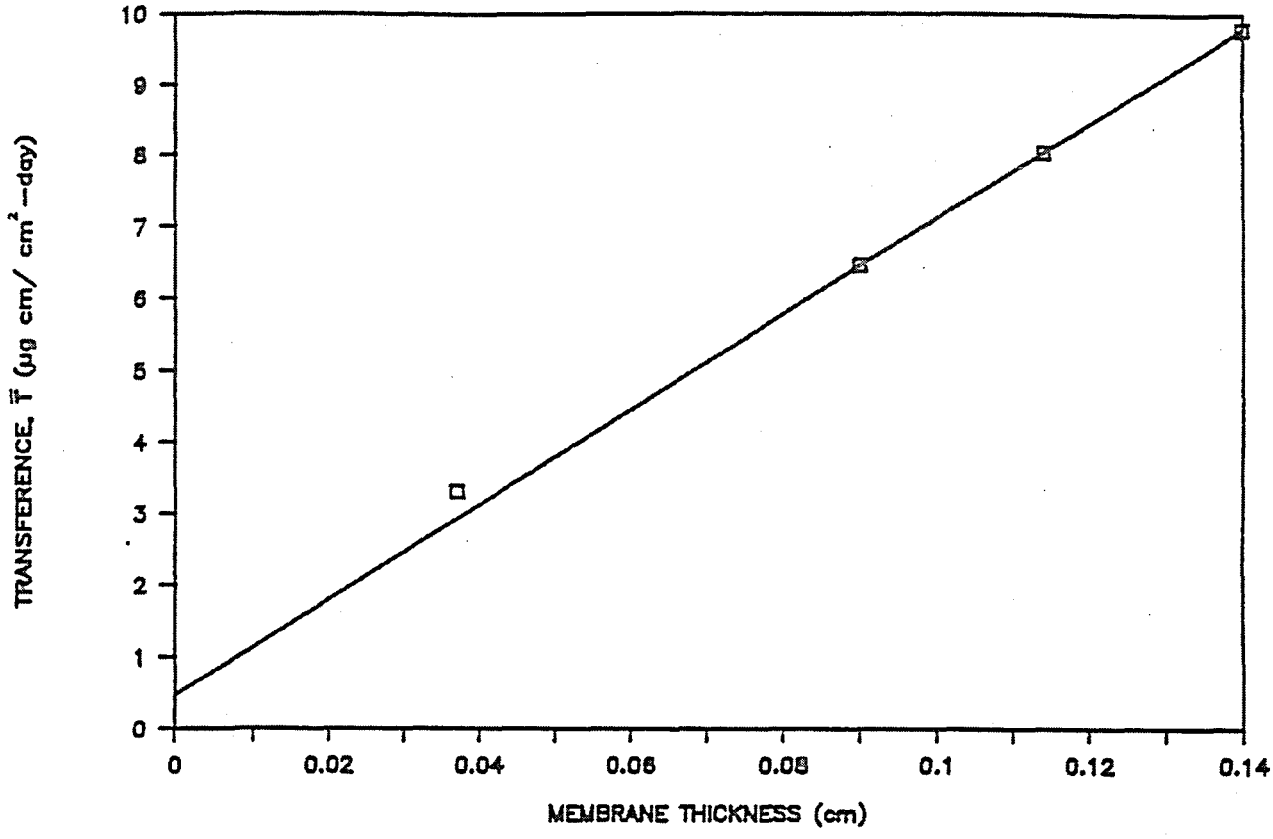

FIGURE 4.99 Plot of the transference ($\overline{T}$) as a function of membrane thickness (ℓ) for NR membranes which contained no SLS.

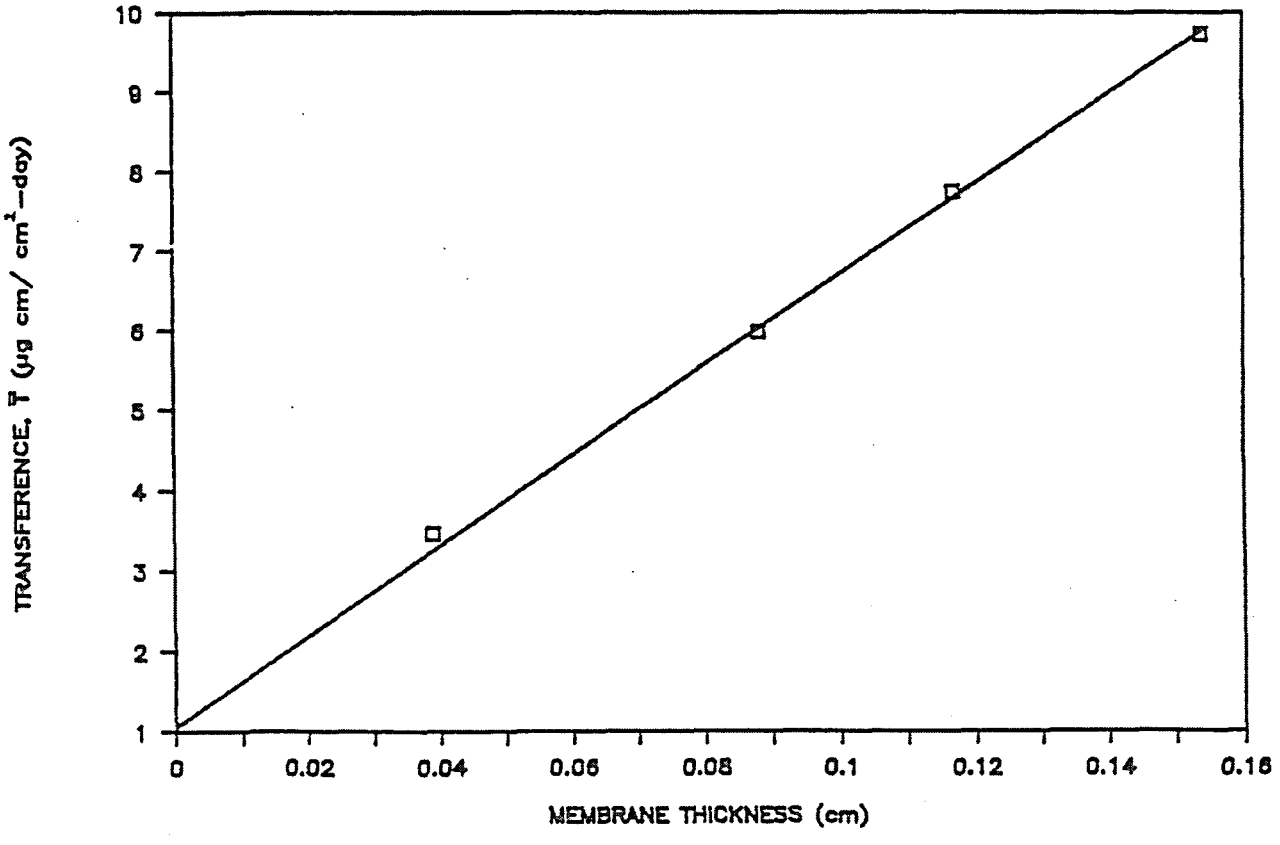

FIGURE 4.100 Plot of the transference ($\overline{T}$) as a function of membrane thickness (ℓ) for IR membranes which contained no SLS.

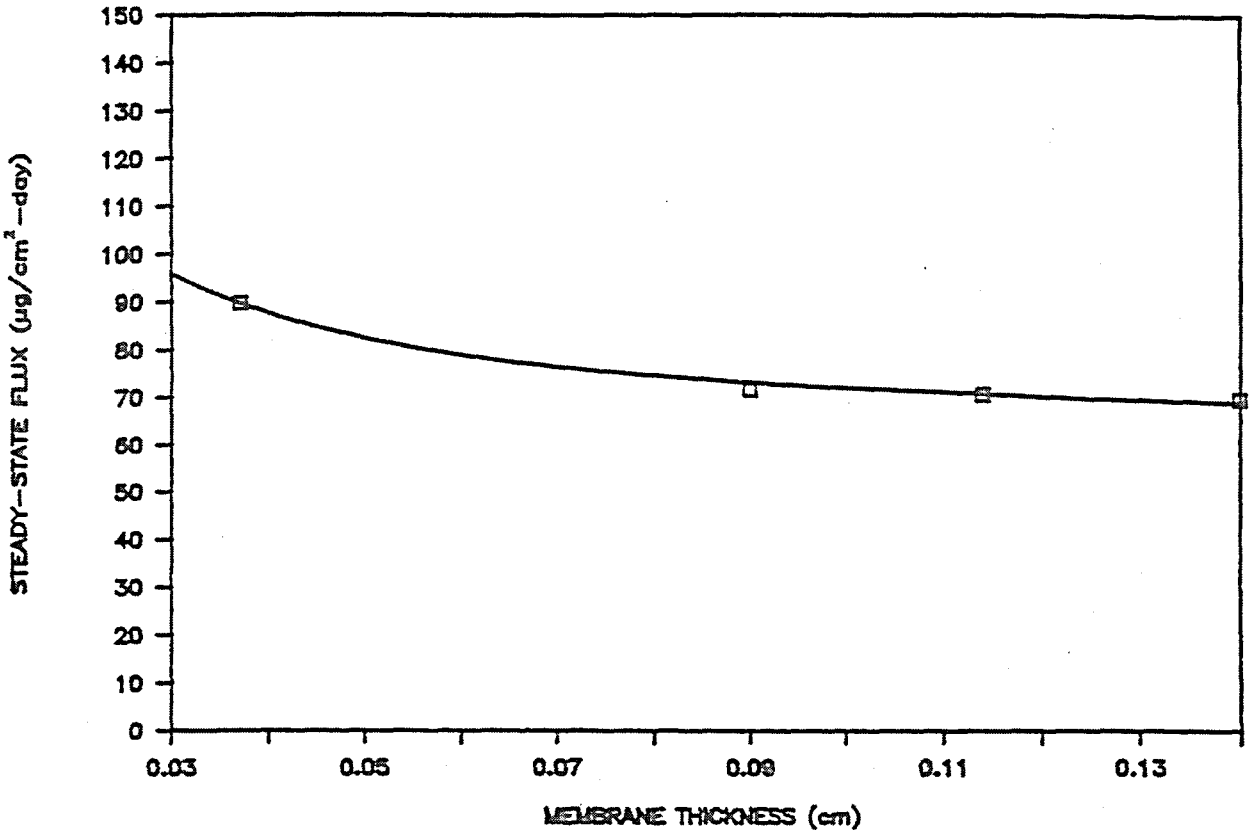

FIGURE 4.101 Plot of the steady-state flux of SLS as a function of membrane thickness for NR/0% SLS membranes.

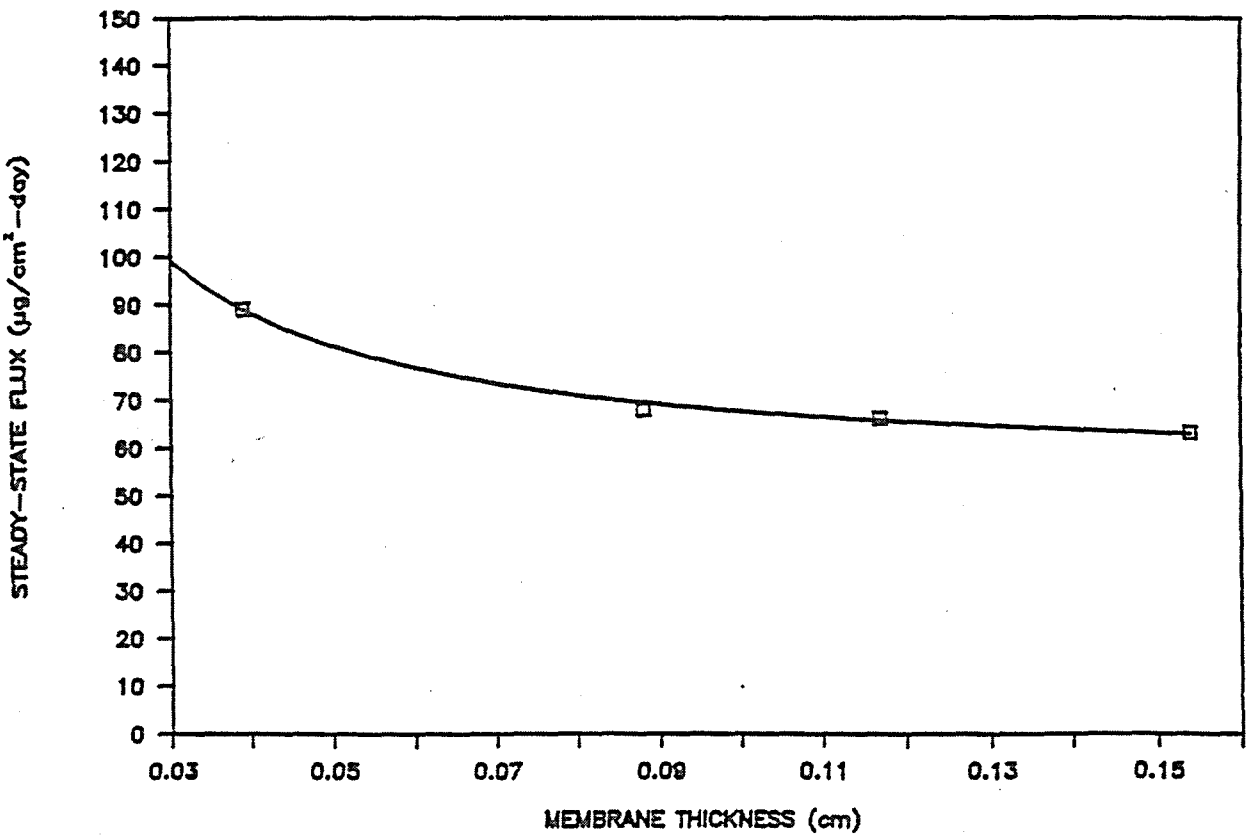

FIGURE 4.102 Plot of the steady-state flux of SLS as a function of membrane thickness for ENR/0% SLS membranes.

CHAPTER 5

CONCLUSIONS AND SUGGESTIONS FOR FUTURE WORK

5.1 CONCLUSIONS

The conclusions reached from the studies reported here were:

1. Monolithic elastomeric devices containing various loadings of dissolved/dispersed SLS can be prepared satisfactorily.

2. Novel membrane devices, which release SLS at constant rates, can be prepared and the use of such devices for the long- term inhibition of the bacterial oxidation of pyrite in mine dumps give such promising laboratory results as to warrant patent protection being sought.

3. It is possible to determine the solubility limits of SLS in the various elastomers by means of differential scanning calorimetry (DSC), which show that phase separation occurs when the solubility limit of SLS in a particular rubber is exceeded. The onset of phase separation is characterized by an endotherm that appeared at 115°C.

4. The solubility limits of SLS in the different elastomers vary. The solubility limits of SLS in natural rubber and in synthetic polyisoprene are 4% and 3%, respectively, when formulations are stored at 0°C before analysis. Storage of the natural-rubber formulations at room temperature for six months causes the solubility limit of SLS to increase to 9%.

5. High loadings of SLS in the various elastomers interfere seriously with the vulcanization process. The Borchardt & Daniels DSC Kinetics Data Analysis software, used to study the effects of the SLS loadings on the vulcanization of elastomers, can be used to analyze curing exotherms.

6. Mathematical models, given in the literature, give poor correlation between experimental data and theoretically- predicted values, which indicates that the release of SLS does not follow $t^{1/2}$-order kinetics.

7. Investigation of the effects of various factors on the rate of release of SLS from monolithic elastomeric pellets shows the following:

7.1 The initial SLS loading in elastomeric pellets affects the release rate dramatically, but the relationship between the release rate and the SLS loading is non- linear. Loadings of up to 25% SLS have very little effect on the release rate, whereas loadings of 35% and more cause a dramatic increase in the release rate. This indicates that a second mechanism of release operates at SLS loadings of 35% and more. This mechanism is postulated to be the result of the creation of pores in the elastomeric matrices.

7.2 The addition of release promotors ($CaCO_3$ and $(NH_4)_2SO_4$) has virtually no effect on the rate of release of SLS from the particular formulations.

7.3 The pH of the eluent affects the release rate, especially when the matrices contain $CaCO_3$, but the effect is not significant enough to outweigh the effects of the other variables.

7.4 The base elastomer (NR, SBR, NR/SBR blend or IR) influences the release rate of SLS, with the release rates being the highest from the elastomer which displays the greatest solvation power for SLS.

7.5 The most effective method for attaining a desirable rate of release of SLS is by varying the surface area to volume ratios of elastomeric pellets.

8. An existing mathematical model to determine the effective diffusion coefficients of SLS in natural and synthetic rubbers gives a poor fit to the experimental data, probably due to the invalidity of the assumption that diffusion coefficients are independent of SLS concentration.

9. The values of the diffusion coefficients depend on the SLS loadings in the elastomeric pellets. It is suggested that the amount of porosity created in elastomeric pellets is a function of the SLS loading, and the concept of a concentration-dependent diffusion coefficient supports the argument for the dependence of the release rate on porosity.

10. A new model has been developed, based on a numerical method commonly used for predicting processes such as heat transfer and fluid flow. This model, which incorporates the effect of porosity development on the rate of release of SLS by employing a concentration-dependent diffusion coefficient, can be used as the basis of further investigations of the relationship between the diffusion coefficient and the concentration of SLS in rubber pellets.

11. An iterative procedure, which involves the use of the tri- diagonal matrix algorithm (Thomas algorithm), can be used to predict numerically the rate of release of SLS from cylindrical pellets. This procedure can be implemented by a FORTRAN program written for the purpose.

12. When it was assumed that the relationship between the diffusion coefficient and the concentration of SLS in the pellet is as follows:

For $C > C_\alpha$ $\qquad D = D_0$

For $C \leq C_\alpha$ $\qquad D = (D_1 - D_0)\left(\dfrac{C_\alpha - C}{C_\alpha - 0}\right)^1 + D_0$

$$= (C_k * D_0 - D_0)\left(\frac{C_\alpha - C}{C_\alpha}\right) + D_0$$

where $D_1 = C_k.D_o$, a much-improved correlation between experimentally-determined and theoretically-predicted data could be obtained for elastomeric pellets containing 35% to 55% SLS.

13. The research findings on monolithic elastomeric pellets could be used by the Chamber of Mines in investigations on simulated coal dumps at the Wolwekrans mine near Witbank, Transvaal.

14. The release of SLS, from a saturated reservoir, through membranes containing no SLS, as well as through those containing 10% SLS, follows zero-order kinetics. It is apparent that when the membranes contain 35% SLS, two release mechanisms are involved. Membranes containing 35% SLS initially appear to function as monolithic devices, but during the last half of the test period the release rate is constant.

15. The high steady-state release rates obtained with elastomeric membranes containing 35% SLS strongly support the theory of a leakage flow, such as would be caused by porosity.

16. Scanning electron microscopy studies on cross-sections of leached NR/35% SLS membranes indicate that the membranes were porous.

17. The studies on elastomeric membranes confirm the dependence of the release rate of SLS on the type of rubber used.

18. Contrary to generalized findings in the literature, the flux of SLS does not vary significantly with membrane thickness. The presence of a surface phenomenon (boundary-layer effect), occurring as the result of the micellar structure of SLS molecules, is proposed to explain these findings.

5.2 SUGGESTIONS FOR FUTURE WORK

The following aspects require further investigation:

1. The further refinement of the numerical prediction model and the PELLET program to make these applicable to a wider range of porosity-promoting solutes in both elastomeric and thermoplastic pellets.

2. A study of the release of surfactant-type molecules at hydrocarbon matrix/water interfaces to shed light on the rate-determining release mechanism and to enable the reverse micelle/normal micelle concept to be confirmed or rejected.

REFERENCES

1. Kydonieus, A.F., Fundamental concepts of controlled release, in Kydonieus, A.F., Ed., Controlled Release Technologies: Methods, Theory, and Applications, Vol I, CRC Press, Boca Raton, Florida, 1980, 1.

2. Patwardhan, S.A. and Das, K.G., Microencapsulation, in Das, K.G., Ed., Controlled-Release Technology: Bioengineering Aspects, John Wiley & Sons, New York, 1983, 121.

3. Bakan, J.A., Microencapsulation using coacervation / phase separation techniques, in Kydonieus, A.F., Ed., Controlled Release Technologies: Methods, Theory, and Applications, Vol. II, CRC Press, Boca Raton, Florida, 1980, 83.

4. Calanchi, M. and Maccari, M., Pharmaceutical applications of microencapsulation using coacervation / phase separation techniques, in Kydonieus, A.F., Ed., Controlled Release Technologies: Methods, Theory, and Applications, Vol. II, CRC Press, Boca Raton, Florida, 1980, 107.

5. Koestler, R.C., Microencapsulation by interfacial polymerization techniques - agricultural applications, in Kydonieus, A.F., Ed., Controlled Release Technologies: Methods, Theory, and Applications, Vol. II, CRC Press, Boca Raton, Florida, 1980, 117.

6. Hall, H.S. and Pondell, R.E., The Wurster Process, in Kydonieus, A.F., Ed., Controlled Release Technologies: Methods, Theory, and Applications, Vol. II, CRC Press, Boca Raton, Florida, 1980, 133.

7. Somerville, G.R. and Goodwin, J.T., Microencapsulation using physical methods, in Kydonieus, A.F., Ed., Controlled Release Technologies: Methods, Theory, and Applications, Vol. II, CRC Press, Boca Raton, Florida, 1980, 155.

8. Kydonieus, A.F., Other controlled release technologies and applications, in Kydonieus, A.F., Ed., Controlled Release Technologies: Methods, Theory, and Applications, Vol. II, CRC Press, Boca Raton, Florida, 1980, 235.

9. **O'Neill, W.P.**, Membrane systems, in Kydonieus A.F., Ed., **Controlled Release Technologies: Methods, Theory, and Applications**, Vol. I, CRC Press, Boca Raton, Florida, 1980, 129.

10. **Brooks, T.W.**, Controlled vapor release from hollow fibers: Theory and applications with insect pheromones, in Kydonieus, A.F., Ed., **Controlled Release Technologies: Methods, Theory, and Applications**, Vol. II, CRC Press, Boca Raton, Florida, 1980, 165.

11. **Zeoli, L.T. and Kydonieus, A.F.**, Physical methods of controlled release, in Das, K.G., Ed., **Controlled-Release Technology: Bioengineering Aspects**, John Wiley & Sons, New York, 1983, 61.

12. **Ashare, E., Brooks, T.W., and Swenson, D.W.**, Controlled release from hollow fibers, in Paul, D.R. and Harris, F.W., Eds., **Controlled Release Polymeric Formulations**, ACS Symposium Series 33, American Chemical Society, Washington, D.C., 1976, 273.

13. **Michaels, A.S.**, Therapeutic systems for controlled administration of drugs: A new application of membrane science, in Hopfenberg, H.B., Ed., **Permeability of Plastic Films and Coatings to Gases, Vapors, and Liquids**, Polymer Science and Technology, Vol. 6, Plenum Press, New York, 1974, 409.

14. **Akkapeddi, M.K., Halpern, B.D., Davis, R.H., and Balin, H.**, Cervical hydrogel dilator: A new delivery system for prostaglandins, in Tanquary, A.C. and Lacey, R.E., Eds., **Controlled Release of Biologically Active Agents**, Advances in Experimental Medicine and Biology, Vol. 47, Plenum Press, New York, 1974, 165.

15. **Obermayer, A.S.**, Controlled release from ultramicroporous triacetate, in Kydonieus, A.F., Ed., **Controlled Release Technologies: Methods, Theory, and Applications**, Vol. I, CRC Press, Boca Raton, Florida, 1980, 239.

16. **Obermayer, A.S. and Nichols, L.D.**, Controlled release from ultramicroporous cellulose triacetate, in Paul, D.R. and Harris, F.W., Eds., **Controlled Release Polymeric Formulations**, ACS Symposium Series 33, American Chemical Society, Washington, D.C., 1976, 303.

17. **Nichols, L.D.**, Poroplastic and Sustrelle: Controlled release vehicles having broad compatibility with dissolved and precipitated pesticides, in Harris, F.W., Ed., **Proceedings of Controlled Release Pesticide Symposium**, Wright State University, Dayton, Ohio, 1975, 95.

18. **Harris, F.W.**, Preparation of plastic controlled release pesticide formulations, in Cardarelli, N.F., Ed., **Proceedings of Controlled Release Pesticide Symposium**, University of Akron, Akron, Ohio, 1976, 1.33.

19. **Roseman, T.J.**, Monolithic polymer devices - Section 1, in Kydonieus, A.F., Ed., **Controlled Release Technologies: Methods, Theory, and Applications**, Vol. I, CRC Press, Boca Raton, Florida, 1980, 21.

20. **Cardarelli, N.F.**, Monolithic polymer devices - Section 2, in Kydonieus, A.F., Ed., **Controlled Release Technologies: Methods, Theory, and Applications**, Vol. I, CRC Press, Boca Raton, Florida, 1980, 55.

21. **Cardarelli, N.F.**, Compounding methods for controlled release elastomers, in Cardarelli, N.F., Ed., **Proceedings of Controlled Release Pesticide Symposium**, University of Akron, Akron, Ohio, 1976, 1.44.

22. **Cardarelli, N.F.**, Monolithic elastomeric materials, in Kydonieus, A.F., Ed., **Controlled Release Technologies: Methods, Theory, and Applications**, Vol. I, CRC Press, Boca Raton, Florida, 1980, 73.

23. **Allan, G.G., Beer, J.W., Cousin, M.J., and Mikels, R.A.**, The biodegradative controlled release of pesticides from polymeric substrates, in Kydonieus, A.F., Ed., **Controlled Release Technologies: Methods, Theory, and Applications**, Vol. II, CRC Press, Boca Raton, Florida, 1980, 7.

24. **Zweig, G.**, Environmental aspects of controlled-release pesticides, in Das, K.G., Ed., **Controlled-Release Technology: Bioengineering Aspects**, John Wiley & Sons, New York, 1983, 179.

25. **Yolles, S. and Sartori, M.F.**, Erodible matrices, in Kydonieus, A.F., Ed., **Controlled Release Technologies: Methods, Theory, and Applications**, Vol. II, CRC Press, Boca Raton, Florida, 1980, 1.

26. **Shasda, B.S.**, Starch and other polyols as encapsulating matrices for pesticides, in Kydonieus, A.F., Ed., **Controlled Release Technologies: Methods, Theory, and Applications**, Vol. II, CRC Press, Boca Raton, Florida, 1980, 207.

27. **DelliColli, H.T.**, Pine kraft lignin as a pesticide delivery system, in Kydonieus, A.F., Ed., **Controlled Release Technologies: Methods, Theory, and Applications**, Vol. II, CRC Press, Boca Raton, Florida, 1980, 225.

28. **Kydonieus, A.F. and Quisumbing, A.R.**, Multilayered laminated structures, in Kydonieus, A.F., Ed., **Controlled Release Technologies: Methods, Theory, and Applications**, Vol. I, CRC Press, Boca Raton, Florida, 1980, 183.

29. **Kydonieus, A.F., Smith, I.K., and Beroza, M.**, Controlled release of pheromones through multilayered polymeric dispensers, in Paul, D.R. and Harris, F.W., Eds., **Controlled Release Polymeric Formulations**, ACS Symposium Series 33, American Chemical Society, Washington, D.C., 1976, 283.

30. **Kydonieus, A.F., Quisumbing, A.R., and Hyman, S.**, Application of a new controlled release concept in household products, in Paul, D.R. and Harris, F.W., Eds., **Controlled Release Polymeric Formulations**, ACS Symposium Series 33, American Chemical Society, Washington, D.C., 1976, 295.

31. **Theeuwes, F.**, Delivery of active agents by osmosis, in Kydonieus, A.F., Ed., **Controlled Release Technologies: Methods, Theory, and Applications**, Vol. II, CRC Press, Boca Raton, Florida, 1980, 195.

32. **Theeuwes, F. and Yum, S.I.**, Principles of the design and operation of generic osmotic pumps for the delivery of semisolid or liquid drug formulations, **Annals of Biomedical Engineering**, 4, 1976, 343.

33. **Harris, F.W.**, Polymers containing pendent pesticide substituents, in Kydonieus, A.F., Ed., **Controlled Release Technologies: Methods, Theory, and Applications**, Vol. II, CRC Press, Boca Raton, Florida, 1980, 63.

34. **Patwardhan, S.A. and Das, K.G.**, Chemical methods of controlled release, in Das, K.G., Ed., **Controlled-Release Technology: Bioengineering Aspects**, John Wiley & Sons, New York, 1983, 23.

35. **Harris, F.W., Aulabaugh, A.E., Case, R.D., Dykes, M.K., and Feld, W.A.**, Polymers containing pendent herbicide substituents: Preliminary hydrolysis studies, in Paul, D.R. and Harris, F.W., Eds., **Controlled Release Polymeric Formulations**, ACS Symposium Series 33, American Chemical Society, Washington, D.C., 1976, 222.

36. **Harris, F.W. and Post, L.K.**, Synthesis of polymers containing aquatic herbicides as pendent substituents, in Cardarelli, N.F., Ed., **Proceedings of Controlled Release Pesticide Symposium**, University of Akron, Akron, Ohio, 1974, 17.1.

37. **Paul, D.R.**, Polymers in controlled release technology, in Paul, D.R. and Harris, F.W., Eds., **Controlled Release Polymeric Formulations**, ACS Symposium Series 33, American Chemical Society, Washington, D.C., 1976, 1.

38. **Crank, J. and Park, G.S., Eds., Diffusion in Polymers**, Academic Press, London, 1968.

39. **Crank, J., The Mathematics of Diffusion**, Second Edition, Clarendon Press, Oxford, 1975.

39.a **Barrer, R.M., Diffusion in and through Solids**, Cambridge University Press, London, 1941.

39.b **Jost, W., Diffusion in Solids, Liquids, Gases**, Academic Press, New York, 1960.

40. **Jacobs, M.H., Diffusion Processes**, Springer-Verlag, New York, 1967.

41. **Baker, R.W. and Lonsdale, H.K.**, Controlled release: Mechanisms and rates, in Tanquary, A.C. and Lacey, R.E., Eds., **Controlled Release of Biologically Active Agents**,

Advances in Experimental Medicine and Biology, Vol. 47, Plenum Press, New York, 1974, 15.

42. **Baker, R.W. and Lonsdale, H.K.**, Principles of controlled release, in Harris, F.W., Ed., **Proceedings of Controlled Release Pesticide Symposium**, Wright State University, Dayton, Ohio, 1975, 10.

43. **Hopfenberg, H.B.**, Controlled release from erodible slabs, cylinders and spheres, in Paul, D.R. and Harris, F.W., Eds., **Controlled Release Polymeric Formulations**, ACS Symposium Series 33, American Chemical Society, Washington, D.C., 1976, 26.

44. **Eckenhoff, B.**, Osmotically driven pumps for rate-controlled delivery of solutions and viscous suspensions, in Chandrasekaran, S.K., Ed., **Controlled Release Systems**, AIChE Symposium Series, Vol. 77, No. 206, American Institute of Chemical Engineers, New York, 1981, 1.

45. **Neogi, A.N. and Allan, G.G.**, Controlled-release pesticides: Concepts and realization, in Tanquary, A.C. and Lacey, R.E., Eds., **Controlled Release of Biologically Active Agents**, Advances in Experimental Medicine and Biology, Vol. 47, Plenum Press, New York, 1974, 195.

46. **Fu, J.C., Hagemeir, C., Moyer, D.L., and Ng, E.W.**, A unified mathematical model for diffusion from drug-polymer composite tablets, **J. Biomed. Mater. Res.**, 10, 1976, 743.

47. **Roseman, T.J. and Higuchi, W.I.**, Release of medroxyprogesterone acetate from a silicone polymer, **J. Pharm. Sci.**, 59, 1970, 353.

48. **Roseman, T.J.**, Release of steroids from a silicone polymer, **J. Pharm. Sci.**, 61, 1972, 46.

49. **Fites, A.J., Banker, G.S., and Smolen, V.F.**, Controlled drug release through polymeric films, **J. Pharm. Sci.**, 59, 1970, 610.

50. **Donbrow, M. and Friedman, M.**, Timed release from polymeric films containing drugs and kinetics of drug release, **J. Pharm. Sci.**, 64, 1975, 76.

51. **Borodkin, S. and Tucker, F.E.**, Linear drug release from laminated hydroxypropyl cellulose - polyvinyl acetate films. **J. Pharm. Sci.**, 64, 1975, 1289.

52. **Sciarra, J.J. and Patel, S.P.**, In vitro release of therapeutically active ingredients from polymer matrices, **J. Pharm. Sci.**, 65, 1976, 1519.

53. **Chien, Y.W. and Lau, E.P.K.**, Controlled drug release from polymeric delivery devices. IV. In vitro - in vivo correlation of subcutaneous release of Norgestomet from hydrophilic implants, **J. Pharm. Sci.**, 65, 1976, 488.

54. **Haleblian, J., Runkel, R., Mueller, N., Christopherson, J., and Ng, K.**, Steroid release from silicone elastomer containing excess drug in suspension, **J. Pharm. Sci.**, 60, 1971, 541.

55. **Desai, S.J., Simonelli, A.P., and Higuchi, W.I.**, Investigation of factors influencing release of solid drug dispersed in inert matrices, **J. Pharm. Sci.**, 54, 1965, 1459.

56. **Schwartz, J.B., Simonelli, A.P., and Higuchi, W.I.**, Drug release from wax matrices. I. Analysis of data with first-order kinetics and with the diffusion-controlled model, **J. Pharm. Sci.**, 57, 1968, 274.

57. **Lapidus, H. and Lordi, N.G.**, Some factors affecting the release of a water-soluble drug from a compressed hydrophilic matrix, **J. Pharm. Sci.**, 55, 1966, 840.

58. **Farhadieh, B., Borodkin, S., and Buddenhagen, J.D.**, Drug release from methyl acrylate - methyl methacrylate copolymer matrix. I. Kinetics of release, **J. Pharm. Sci.**, 60, 1971, 209.

59. **Crowther, B.G. and Edmondson, H.M.**, Processing technology, in Blow, C.M., Ed., **Rubber Technology and Manufacture**, Newnes-Butterworths, London, 1978, Chapter 8.

60. **Horn, J.B.**, Materials for compounding and reinforcement, in Blow, C.M., Ed., **Rubber Technology and Manufacture**, Newnes-Butterworths, London, 1978, Chapter 6.

61. Jacques, J.E., Principles of compounding, in Blow, C.M., Ed., **Rubber Technology and Manufacture**, Newnes-Butterworths, London, 1978, Chapter 9.

62. Philibert, J., Diffusion in solids, **Sci. Technol. (N.Y.)**, 47, 1968.

63. Jost, W., **Diffusion in Solids, Liquids, Gases**, Academic Press, New York, 1960, 135.

64. Ferry, J.D., **Viscoelastic Properties of Polymers**, Third Edition, John Wiley & Sons, New York, 1980.

65. Bueche, F., **Physical Properties of Polymers**, Robert E. Krieger Publishing Co., New York, 1979.

66. Rogers, C.E., Structural factors governing controlled release, in Paul, D.R. and Harris, F.W., Eds., **Controlled Release Polymeric Formulations**, ACS Symposium Series 33, American Chemical Society, Washington, D.C., 1976, 15.

67. Kumins, C.A. and Kwei, T.K., Free volume and other theories, in Crank, J. and Park, G.S., Eds., **Diffusion in Polymers**, Academic Press, London, 1968, 107.

68. Barrer, R.M., Diffusion and permeation in heterogeneous media, in Crank, J. and Park, G.S., Eds., **Diffusion in Polymers**, Academic Press, London, 1968, 165.

69. Walker, B.M., Ed., **Handbook of Thermoplastic Elastomers**, Van Nostrand Reinhold, New York, 1979.

70. Cardarelli, N.F., **Controlled Release Pesticides Formulations**, CRC Press, Cleveland, 1976.

71. Cardarelli, N.F., Monolithic polymer devices - Section 2, in Kydonieus, A.F., Ed., **Controlled Release Technologies: Methods, Theory, and Applications**, Vol. I, CRC Press, Boca Raton, Florida, 1980, 65 & 66.

72. Ayres, J.W. and Lindstrom, F.T., Diffusion model for drug release from suspensions. I. Theoretical considerations, J. Pharm. Sci., 66, 1977, 654.

73. Lindstrom, F.T. and Ayres, J.W., Diffusion model for drug release from suspensions. II. Release to a perfect sink, J. Pharm. Sci., 66, 1977, 662.

74. Morgans, W.M., Outlines of Paint Technology, CRC Press, Cleveland, 1969.

75. Crank, J., The Mathematics of Diffusion, Second Edition, Clarendon Press, Oxford, 1975, Chapter 4.

76. Harris, F.W., Theoretical aspects of controlled release, in Cardarelli, N.F., Ed., Proceedings of Controlled Release Pesticide Symposium, University of Akron, Akron, Ohio, 1974, 8.1.

77. Higuchi, T., Physical chemical analysis of percutaneous absorption process from creams and ointments, J. Soc. Cosmet. Chem., 11, 1960, 85.

78. Higuchi, W.I., Analysis of data on the medicament release from ointments, J. Pharm. Sci., 51, 1962, 802.

79 Carslaw, H.S. and Jaeger, J.C., Conduction of Heat in Solids, Second Edition, Oxford University Press, London, 1959, Chapters 7, 8 and 9.

80. Crank, J., The Mathematics of Diffusion, Second Edition, Clarendon Press, Oxford, 1975, Chapters 5 and 6.

81. Ibid., Chapter 3.

82. Cobby, J., Mayersohn, M., and Walker, G.C., Influence of shape factors on kinetics of drug release from matrix tablets. I. Theoretical, J. Pharm. Sci., 63, 1974, 725.

83. Cobby, J., Mayersohn, M., and Walker, G.C., Influence of shape factors on kinetics of drug release from matrix tablets. II. Experimental, J. Pharm. Sci., 63, 1974, 732.

84. **Higuchi, T.**, Rate of release of medicaments from ointment bases containing drugs in suspension, **J. Pharm. Sci.**, 50, 1961, 874.

85. **Higuchi, T.**, Mechanism of sustained-action medication: Theoretical analysis of rate of release of solid drugs dispersed in solid matrices, **J. Pharm. Sci.**, 52, 1963, 1145.

86. **Garrett, E.R. and Chemburkar, P.B.**, Evaluation, control and prediction of drug diffusion through polymeric membranes. I. Methods and reproducibility of steady-state diffusion studies, **J. Pharm. Sci.**, 57, 1968, 944.

87. **Flynn, G.L.**, Influence of physico-chemical properties of drug and system on release of drugs from inert matrices, in Tanquary, A.C. and Lacey, R.E., Eds., **Controlled Release of Biologically Active Agents**, Advances in Experimental Medicine and Biology, Vol. 47, Plenum Press, New York, 1974, 73.

88. **Carslaw, H.S. and Jaeger, J.C., Conduction of Heat in Solids**, Second Edition, Oxford University Press, London, 1959, 225.

89. **Cornette, J.C. and Duncan, G.W.**, Release, excretion, tissue uptake and biological effectiveness of estradiol from Silastic devices implanted in rats, **Contraception**, 1, 1970, 339.

90. **Paul, D.R. and McSpadden, S.K.**, Diffusional release of a solute from a polymer matrix, **J. Membr. Sci.**, 1, 1976, 33.

91. **Desai, S.J., Singh, P., Simonelli, A.P., and Higuchi, W.I.**, Investigation of factors influencing release of solid drug dispersed in inert matrices. II. Quantitation of procedures, **J. Pharm. Sci.**, 55, 1966, 1224.

92. **Singh, P., Desai, S.J., Simonelli, A.P., and Higuchi, W.I.**, Release rates of solid drug mixtures dispersed in inert matrices. I. Non-interacting drug mixtures, **J. Pharm. Sci.**, 56, 1967, 1542.

93. **Singh, P., Desai, S.J., Simonelli, A.P., and Higuchi, W.I.**, Release rates of solid drug mixtures dispersed in inert matrices. II. Mutually interacting drug mixtures, **J. Pharm. Sci.**, 56, 1967, 1548.

94. **Roseman, T.J.**, Boundary layer considerations in the evaluation of controlled release delivery systems, in Goulding, R.L., Ed., **Proceedings of Controlled Release Pesticide Symposium**, Oregon State University, Corvallis, 1977, 403.

95. **Chien, Y.W., Lambert, H.J., and Grant, D.E.**, Controlled drug release from polymeric devices. I. Technique for rapid in vitro release studies, **J. Pharm. Sci.**, 63, 1974, 365.

96. **Winkler, V.W., Borodkin, S., Webel, S.K., and Mannebach, J.T.**, In vitro and in vivo considerations of a novel matrix-controlled bovine progesterone-releasing intravaginal device, **J. Pharm. Sci.**, 66, 1977, 816.

97. **Chien, Y.W. and Lambert, H.J.**, Controlled drug release from polymeric delivery devices. II. Differentiation between partition-controlled and matrix-controlled drug release mechanisms, **J. Pharm. Sci.**, 63, 1974, 515.

98. **Roseman, T.J. and Yalkowsky, S.H.**, Importance of solute partitioning on the kinetics of drug release from matrix systems, in Paul, D.R. and Harris, F.W., Eds., **Controlled Release Polymeric Formulations**, ACS Symposium Series 33, American Chemical Society, Washington, D.C., 1976, 33.

99. **Ayres, J.W. and Laskar, P.A.**, Evaluation of mathematical models for diffusion from semisolids, **J. Pharm. Sci.**, 63, 1974, 351.

100. **Baker, R.W. and Lonsdale, H.K.**, Controlled delivery - an emerging use for membranes, **Chem. Technol.**, 5, 1975, 668.

101. **Desai, S.J., Singh, P., Simonelli, A.P., and Higuchi, W.I.**, Investigation of factors influencing release of solid drug dispersed in inert matrices. III. Quantitative studies involving the polyethylene plastic matrix, **J. Pharm. Sci.**, 55, 1966, 1230.

102. **Desai, S.J., Singh, P., Simonelli, A.P., and Higuchi, W.I.**, Investigation of factors influencing release of solid drug dispersed in inert matrices. IV. Some studies involving the polyvinyl chloride matrix, **J. Pharm. Sci.**, 55, 1966, 1235.

103. **Schwartz, J.B., Simonelli, A.P., and Higuchi, W.I.**, Drug release from wax matrices. II. Application of a mixture theory to the sulfanilamide-wax system, **J. Pharm. Sci.**, 57, 1968, 278.

104. **Lapidus, H. and Lordi, N.G.**, Drug release from compressed hydrophilic matrices, **J. Pharm. Sci.**, 57, 1968, 1292.

105. **Michaels, A.S. and Bixler, H.J.**, Membrane permeation: Theory and practice, in Perry, E.S., Ed., **Progress in Separation and Purification**, Vol. 1, Interscience, New York, 1968, 143.

106. **Tuwiner, S.B.**, **Diffusion and Membrane Technology**, Van Nostrand Reinhold, New York, 1962.

107. **Edward, J.T.**, Molecular volumes and the Stokes-Einstein equation, **J. Chem. Educ.**, 47, 1970, 261.

108. **Flynn, G.L., Yalkowsky, S.H., and Roseman, T.J.**, Mass transport phenomena and models: Theoretical concepts, **J. Pharm. Sci.**, 63, 1974, 479.

109. **Crank, J. and Park, G.S.**, Methods of measurement, in Crank, J. and Park, G.S., Eds., **Diffusion in Polymers**, Academic Press, London, 1968, 6.

110. **Leo, A., Hansch, C., and Elkins, D.**, Partition coefficients and their uses, **Chemical Reviews**, 71, 1971, 525.

111. **Roseman, T.J. and Yalkowsky, S.H.**, Influence of solute properties on release of p-aminobenzoic acid esters from silicone rubber: Theoretical considerations, **J. Pharm. Sci.**, 63, 1974, 1639.

112. **Chien, Y.W., Lambert, H.J., and Lin, T.K.**, Solution-solubility dependency of controlled release of drug from polymer matrix: Mathematical analysis, **J. Pharm. Sci.**, 64, 1975, 1643.

113. **Flynn, G.L., Ho, N.F.H., Hwang, S., Owada, E., Molokhia, A., Behl, C.R., Higuchi, W.I., Yotsuyanagi, T., Shah, Y., and Park, J.**, Interfacing matrix release and membrane absorption - analysis of steroid absorption from a vaginal device in the rabbit doe, in Paul, D.R. and Harris, F.W., Eds., **Controlled Release Polymeric Formulations**, ACS Symposium Series 33, American Chemical Society, Washington, D.C., 1976, 87.

114. **Yalkowsky, S.H. and Flynn, G.L.**, Transport of alkyl homologs across synthetic and biological membranes: A new model for chain length-activity relationships, **J. Pharm. Sci.**, 62, 1973, 210.

115. **Burrell, H.**, Solubility parameter values, in Brandrup, J. and Immergut, E.H., Eds., **Polymer Handbook**, John Wiley & Sons, New York, 1975, IV-337.

116. **Barton, A.F.M.**, **Handbook of Solubility Parameters and Other Cohesion Parameters**, CRC Press, Boca Raton, Florida, 1983.

117. **Chien, Y.W.**, Thermodynamics of controlled drug release from polymeric delivery devices, in Paul, D.R. and Harris, F.W., Eds., **Controlled Release Polymeric Formulations**, ACS Symposium Series 33, American Chemical Society, Washington, D.C., 1976, 53.

118. **Michaels, A.S., Wong, P.S.L., Prather, R., and Gale, R.M.**, A thermodynamic method of predicting the transport of steroids in polymer matrices, **AIChE J.**, 21, 1975, 1073.

119. **Boonstra, B.B.**, Reinforcement by fillers, in Blow, C.M., Ed., **Rubber Technology and Manufacture**, Newnes-Butterworths, London, 1978, Chapter 7.

120. **Most, C.F., Jr.**, Some filler effects on diffusion in silicone rubber, **J. Appl. Polym. Sci.**, 14, 1970, 1019.

121. **Flynn, G.L. and Roseman, T.J.**, Membrane diffusion. II. Influence of physical adsorption on molecular flux through heterogeneous dimethylpolysiloxane barriers, **J. Pharm. Sci.**, 60, 1971, 1788.

122. **Singh, P., Desai, S.J., Simonelli, A.P., and Higuchi, W.I.**, Role of wetting on the rate of drug release from inert matrices, **J. Pharm. Sci.**, 57, 1968, 217.

123. **Dakkuri, A., Schroeder, H.G., and DeLuca, P.P.**, Sustained release from inert wax matrices. II. Effect of surfactants on tripelennamine hydrochloride release. **J. Pharm. Sci.**, 67, 1978, 354.

124. **Farhadieh, B., Borodkin, S., and Buddenhagen, J.D.**, Drug release from methyl acrylate - methyl methacrylate copolymer matrix. II. Control of release rate by exposure to acetone vapor, **J. Pharm. Sci.**, 60, 1971, 212.

125. **Davis, B.K.**, Diffusion in polymer gel implants, **Proc. Nat. Acad. Sci. U.S.A.**, 71, 1974, 3120.

126. **Langer, R. and Folkman, J.**, Polymers for the sustained release of proteins and other macromolecules, **Nature**, 263, 1976, 797.

127. **Abrahams, R.A. and Ronel, S.H.**, Biocompatible implants for the sustained zero-order release of narcotic antagonists, **J. Biomed. Mater. Res.**, 9, 1975, 355.

128. **Roseman, T.J.**, Silicone rubber: A drug-delivery system for contraceptive steroids, in Tanquary, A.C. and Lacey, R.E., Eds., **Controlled Release of Biologically Active Agents**, Advances in Experimental Medicine and Biology, Vol. 47, Plenum Press, New York, 1974, 99.

129. **Konning, G.H. and Mital, H.C.**, Sheabutter V: Effect of particle size on release of medicament from ointment, **J. Pharm.Sci.**, 67, 1978, 374.

130. **Horn, J.B.**, Materials for compounding and reinforcement, in Blow, C.M., Ed., **Rubber Technology and Manufacture**, Newnes-Butterworths, London, 1978, 179.

131. **Collins, R.L.**, Design parameters, in Das, K.G., Ed., **Controlled-Release Technology: Bioengineering Aspects**, John Wiley & Sons, New York, 1983, 15.

132. **Peterlin, A.**, Steady state transport phenomena in non-ideal permeant-polymer systems, in Hopfenberg, H.B., Ed., **Permeability of Plastic Films and Coatings to Gases, Vapors, and Liquids**. Polymer Science and Technology, Vol. 6, Plenum Press, New York, 1974, 9

133. **Hopfenberg, H.B., Ed., Permeability of Plastic Films and Coatings to Gases, Vapors, and Liquids**. Polymer Science and Technology, Vol. 6, Plenum Press, New York, 1974.

134. **Crank, J. and Park, G.S.**, Methods of measurement, in Crank, J. and Park, G.S., Eds., **Diffusion in Polymers**. Academic Press, London, 1968, Chapter 1.

135. **Ibid.**, p. 4.

136. **Ibid.**, p. 15.

137. **Ibid.**, p. 6.

138. **Bueche, F., Physical Properties of Polymers**, Robert E. Krieger Publishing Company, New York, 1979, Chapter 4.

139. **Ibid.**, Chapter 5.

140. **Klein, J.**, Diffusion of long molecules through solid polyethylene. I. Topological constraints, **J. Polym. Sci. Polym. Phys. Ed.**, 15, 1977, 2057.

141. **Klein, J. and Briscoe, B.J.**, Diffusion of long molecules through solid polyethylene. II. Measurements and results, **J. Polym. Sci. Polym. Phys. Ed.**, 15, 1977, 2065.

142. **Van Amerongen, G.J.**, Diffusion in elastomers, **Rubber Chem. Technol.**, 37, 1964, 1065.

143. **Theeuwes, F., Gale, R.M., and Baker, R.W.**, Transference: A comprehensive parameter governing permeation of solutes through membranes, **J. Membr. Sci.**, 1, 1976, 3.

144. Theeuwes, F., Ashida, K., and Higuchi, T., Programmed diffusional release rate from encapsulated cosolvent system, J. Pharm. Sci., 65, 1976, 648.

145. Kydonieus, A.F., Ed., Controlled Release Technologies: Methods, Theory, and Applications, Volumes 1 and 2, CRC Press, Boca Raton, Florida, 1980.

146. Das, K.G., Ed., Controlled-Release Technology: Bioengineering Aspects, John Wiley & Sons, New York, 1983.

147. Tanquary, A.C. and Lacey, R.E., Eds., Controlled Release of Biologically Active Agents, Advances in Experimental Medicine and Biology, Vol. 47, Plenum Press, New York, 1974.

148. Paul, D.R. and Harris, F.W., Eds., Controlled Release Polymeric Formulations, ACS Symposium Series 33, American Chemical Society, Washington, D.C., 1976.

149. Cardarelli, N.F., Ed., Proceedings of Controlled Release Pesticide Symposium, University of Akron, Akron, Ohio, 1974.

150. Harris, F.W., Ed., Proceedings of Controlled Release Pesticide Symposium, Wright State University, Dayton, Ohio, 1975.

151. Nilsson, C.G., Johansson, E.D.B., and Luukkainen, T., A d-norgestrel-releasing IUD, Contraception, 13, 1976, 503.

152. Ormsbee, H.S., III, and Ryan, C.F., Production of hypertension with desoxycorticosterone acetate-impregnated silicone rubber implants, J. Pharm. Sci., 62, 1973, 255.

153. Shippy, R.L., Hwang, S.T., and Bunge, R.G., Controlled release of testosterone using silicone rubber, J. Biomed. Mater. Res., 7, 1973, 95.

154. Cardarelli, N.F., Monolithic polymer devices - Section 2, in Kydonieus, A.F., Ed., Controlled Release Technologies: Methods, Theory, and Applications, Vol. I, CRC Press, Boca Raton, Florida, 1980, 58.

155. Ibid., p. 60.

156. Ibid., p. 63.

157. Ibid., p. 65.

158. Cardarelli, N.F., Monolithic elastomeric materials, in Kydonieus, A.F., Ed., **Controlled Release Technologies: Methods, Theory, and Applications**, Vol. I, CRC Press, Boca Raton, Florida, 1980, 88.

159. Ibid., p. 90.

160. Ibid., p. 76.

161. Ibid., p. 94.

162. Ibid., p. 101.

163. Ibid., p. 104.

164. Ibid., p. 106.

165. Ibid., p. 110.

166. Ibid., p. 112.

167. Ibid., p. 113.

168. Ibid., p. 116.

169. Ibid., p. 117.

170. Ibid., p. 121.

171. **Kleinmann, R.L.P., The Biogeochemistry of Acid Mine Drainage and a Method to Control Acid Formation.** Ph.D Dissertation, Princeton University, Princeton, NJ, 1979.

172. **Kendrick, P.J.,** Acid mine drainage - an old problem with a new dimension, **Journal WPCF,** 49 (7), 1977, 1576.

173. **Thompson, J.G.,** Acid mine waters in South Africa and their amelioration, **Water SA,** 6(3), 1980, 130.

174. **Kempe, J.O.,** Review of water pollution problems and control strategies in the South African mining industry, **Wat. Sci. Technol.,** 15 (2), 1983, 27.

175. **Henzen, M.R. and Pieterse, M.J.,** Acidic mine drainage in the Republic of South Africa, **Prog. Wat. Technol.,** 9(4), 1978, 981.

176. **Van Staden, C.M.,** How ERPM uses lime to solve unique underground water problem, **Coal Gold and Base Minerals of Southern Africa,** 27(5), 1979, 100.

177. **Conradie, J.M., Growth and Inhibition of Thiobacillus ferrooxidans in Relation to Acid Drainage from Witwatersrand Gold Mine Sand Dumps,** M.Sc. Thesis, University of Stellenbosch, Stellenbosch, R.S.A., 1984.

178. **Lovell, H.L.,** Coal mine drainage in the United States - an overview, **Wat. Sci. Technol.,** 15(2), 1983, 1.

179. **Glover, H.G.,** Mine water pollution - an overview of problems and control strategies in the United Kingdom, **Wat. Sci. Technol.,** 15(2), 1983, 59.

180. **Bosman, D.J.,** Lime treatment of acid mine water and associated solids/liquid separation, **Wat. Sci. Technol.,** 15(2), 1983, 71.

181. **Wilmoth, R.C.,** Application of reverse osmosis to acid mine drainage treatment, Report No. EPA-670/2-73-100, National Environmental Research Center, U.S. Environmental Protection Agency, Cincinnati, Ohio, 1973.

182. **Wilmoth, R.C., Baugh, T.L., and Decker, D.W.**, Removal of selected trace elements from acid mine drainage using existing technology, **33rd Industrial Waste Conference Proceedings**, 1978, 886.

183. **Wilmoth, R.C., Scott, R.B., and Harris, E.F.**, Application of ion exchange to acid mine drainage treatment. **32nd Industrial Waste Conference Proceedings**, 1977, 820.

184. **Bhattacharyya, D., Shelton, S., and Grieves, R.B.**, The effective treatment of acid mine wastes by a low pressure charged membrane ultrafiltration process, **33rd Industrial Waste Conference Proceedings**, 1978, 869.

185. **Bhattacharyya, D., Shelton, S., and Grieves, R.B.**, Charged membrane ultrafiltration of multisalt systems: Application to acid mine waters, **Separation Science and Technology**, 14(3), 1979, 193.

186. **Adams, G.B., Hollandsworth, R.P., and Bennion, D.N.**, Electrochemical treatment of acid mine water, **AIChE Symposium Series**, 73(166), 1977, 99.

187. **Sisler, F.D., Senftle, F.E., and Skinner, J.**, Electrobiochemical neutralization of acid mine water, **Journal WPCF**, 49(3), 1977, 369.

188. **Kleinmann, R.L.P.**, Bactericidal control of acid problems in surface mines and coal refuse, **Symposium on Surface Mining Hydrology, Sedimentology and Reclamation**, Lexington, Kentucky, 1980, 333.

189. **Kleinmann, R.L.P., Crerar, D.A., and Pacelli, R.R.**, Biogeochemistry of acid mine drainage and a method to control acid formation, **Mining Engineering**, 33, 1981, 300.

190. **Staff of the U.S. Bureau of Mines**, Control of acid mine drainage, U.S. Bureau of Mines Information Circular 9027, **roceedings of a Technology Transfer Seminar**, Pittsburgh, Pennsylvania, 1985.

191. **Folkman, J. and Long, D.M., Jr.**, The use of silicone rubber as a carrier for prolonged drug therapy, **J. Surg. Res.**, 4, 1964, 139.

192. Folkman, J. and Long, D.M., Jr., Drug pacemakers in the treatment of heart block. Ann. N.Y. Acad. Sci., 111, 1964, 857.

193. Folkman, J., Long, D.M., Jr., and Rosenbaum, R., Silicone rubber: A new diffusion property useful for general anesthesia, Science, 154, 1966, 148.

194. Folkman, J., Winsey, S., and Moghul, T., Anesthesia by diffusion through silicone rubber, Anesthesiology, 29, 1968, 410.

195. Folkman, J., Mark, V.H., Ervin, F., Suematsu, K., and Hagiwara, R., Intracerebral gas anesthesia by diffusion through silicone rubber, Anesthesiology, 29, 1968, 419.

196. Folkman, J. and Mark, V.H., Diffusion of anesthetics and other drugs through silicone rubber: Therapeutic implications, Trans. N.Y. Acad. Sci., 30, 1968, 1187.

197. Chang, C.C. and Kincl, F.A., Sustained release hormonal preparations. III. Biological effectiveness of 6-methyl-17 α-acetoxypregna-4,6-diene-3,20-dione, Steroids, 12, 1968, 689.

198. Zbuzkova, V. and Kincl, F.A., Sustained release hormonal preparations. XII. Plasma levels of 6-methyl-17 α-acetoxy-4,6-pregnadiene-3,20-dione in hamsters, Steroids, 16, 1970, 447.

199. Croxatto, H., Diaz, S., Vera, R., Etchart, M., and Atria, P., Fertility control in women with a progestogen released in microquantities from subcutaneous capsules, Am. J. Obst. & Gynec., 105, 1969, 1135.

200. Tatum, H.J., Coutinho, E.M., Adeodato Filho, J., and Sant' Anna, A.R.S., Acceptability of longterm contraceptive steroid administration in humans by subcutaneous Silastic capsules, Am. J. Obst. & Gynec., 105, 1969, 1139.

201. Coutinho, E.M., Mattos, C.E.R., Sant'Anna, A.R.S., Adeodato Filho, J., Silva, M.C., and Tatum, H.J., Longterm contraception by subcutaneous Silastic capsules containing megestrol acetate, Contraception, 2, 1970, 313.

202. **Croxatto, H.B., Diaz, S., Atria, P., Cheviakoff, S., Rosatti, S., and Oddo, H.**. Contraceptive action of megestrol acetate implants in women, **Contraception**, 4, 1971, 155.

203. **Mishell, D.R., Jr., and Lumkin, M.E.**, Contraceptive effect of varying dosages of progestogen in Silastic vaginal rings. **Fertil. Steril.**, 21, 1970, 99.

204. **Mishell, D.R., Jr., Lumkin, M.E., and Stone, S.**, Inhibition of ovulation with cyclic use of progestogen-impregnated intravaginal devices. **Am. J. Obst. & Gynec.**, 113, 1972, 927.

205. **Scommegna, A., Pandya, G.N., Christ, M., Lee, A.W., and Cohen, M.R.**. Intrauterine administration of progesterone by a slow releasing device, **Fertil. Steril.**, 21, 1970, 201.

206. **Ewing, L.L., Schanbacher, B., Desjardins, C., and Chaffee, V.**, The effect of subdermal testosterone-filled polydimethylsiloxane implants on spermatogenesis in rhesus monkeys, **Contraception**, 13, 1976, 583.

207. **Kincl, F.A., Benagiano, G., and Angee, I.**, Sustained release hormonal preparations. I. Diffusion of various steroids through polymer membranes, **Steroids**, 11, 1968, 673.

208. **Sundaram, K. and Kincl, F.A.**, Sustained release hormonal preparations. II. Factors controlling the diffusion of steroids through dimethylpolysiloxane membranes, **Steroids**, 12, 1968, 517.

209. **Kratochvil, P., Benagiano, G., and Kincl, F.A.**, Sustained release hormonal preparations. VI. Permeability constants of various steroids, **Steroids**, 15, 1970, 505.

210. **Garrett, E.R. and Chemburkar, P.B.**, Evaluation, control, and prediction of drug diffusion through polymeric membranes. II. Diffusion of aminophenones through Silastic membranes, **J. Pharm. Sci.**, 57, 1968, 949.

211. **Garrett, E.R. and Chemburkar, P.B.**, Evaluation, control, and prediction of drug diffusion through polymeric membranes. III. Diffusion of barbiturates, phenylalkylamines, dextromethorphan, progesterone, and other drugs, **J. Pharm. Sci.**, 57, 1968, 1401.

212. **Most, C.F., Jr.**, Co-permeant enhancement of drug transmission rates through silicone rubber, **J. Biomed. Mater. Res.**, 6, 1972, 3.

213. **Lacey, R.E. and Cowsar, D.R.**, Factors affecting the release of steroids from silicones, in Tanquary, A.C. and Lacey, R.E., Eds., **Controlled Release of Biologically Active Agents**, Advances in Experimental Medicine and Biology, Vol. 47, Plenum Press, New York, 1974, 117.

214. **Friedman, S., Koide, S.S., and Kincl, F.A.**, Sustained release hormonal preparations. VII. Permeability of three types of silicone rubber to steroids, **Steroids**, 15, 1970, 679.

215. **O'Neill, W.P.**, Membrane systems, in Kydonieus, A.F., Ed., **Controlled Release Technologies: Methods, Theory, and Applications**, Vol. 1, CRC Press, Boca Raton, Florida, 1980, 152.

216. **Leeper, H. and Benson, H.**, The role of polymers in optimizing therapeutic effectiveness of drugs, **Polym. Eng. Sci.**, 17, 1977, 42.

217. **Salyer, I.O. and Kenyon, A.S.**, Structure and property relationships in ethylene-vinyl acetate copolymers, **J. Polym. Sci. Part A-1**, 9, 1971, 3083.

218. **Boretos, J.W., Detmer, D.E., and Donachy, J.H.**, Segmented polyurethane: A polyether polymer. II. Two years experience, **J. Biomed. Mater. Res.**, 5, 1971, 373.

219. **Lyman, D.J. and Kim, S.W.**, Aqueous diffusion through partition membranes, **J. Polym. Sci. Polym. Symp.**, 41, 1973, 139.

220. **Zentner, G.M., Cardinal, J.R., and Kim, S.W.**, Progestin permeation through polymer membranes. I. Diffusion studies on plasma-soaked membranes, **J. Pharm. Sci.**, 67, 1978, 1347.

221. **Lee, E.K.L., Lonsdale, H.K., Baker, R.W., Drioli, E., and Bresnahan, P.A.**, Transport of steroids in poly(etherurethane) and poly(ethylene vinyl acetate) membranes, **J. Membr. Sci.**, 24, 1985, 125.

222. **Gonzales, M.A., Nematollahi, J., Guess, W.L., and Autian, J.,** Diffusion, permeation, and solubility of selected agents in and through polyethylene, **J. Pharm. Sci.,** 56, 1967, 1288.

223. **Kalkwarf, D.R., Sikov, M.R., Smith, L., and Gordon, R.,** Release of progesterone from polyethylene devices in vitro and in experimental animals, **Contraception,** 6, 1972, 423.

224. **DeGennaro, M.D., Thompson, B.B., and Luzzi, L.A.,** Effect of cross-linking agents on the release of sodium pentobarbital from nylon microcapsules, in Paul, D.R. and Harris, F.W., Eds., **Controlled Release Polymeric Formulations,** ACS Symposium Series 33, American Chemical Society, Washington, D.C., 1976, 195.

225. **Luzzi, L.A., Zoglio, M.A., and Maulding, H.V.,** Preparation and evaluation of the prolonged release properties of nylon microcapsules, **J. Pharm. Sci.,** 59, 1970, 338.

226. **Bottari, F., Di Colo, G., Nannipieri, E., Saettone, M.F., and Serafini, M.F.,** Evaluation of a dynamic permeation technique for studying drug - macromolecule interactions, **J. Pharm. Sci.,** 64, 1975, 946.

227. **Halpern, B.D., Solomon, O., Kopec, L., Korostoff, E., and Ackerman, J.L.,** Release of inorganic fluoride ion from rigid polymer matrices, in Paul, D.R. and Harris, F.W., Eds., **Controlled Release Polymeric Formulations,** ACS Symposium Series 33, American Chemical Society, Washington, D.C., 1976, 135.

228. Aldrich Chemical Catalog, 1986/87, 594.

229. **Hassel, R.L.,** Cure of Elastomers, Du Pont Application Brief no. TA 27.

230. **Kah, A.F., Koehler, M.E., Grentzer, T.H., Niemann, T.F. and Provder, T.,** An automated thermal analysis system for reaction kinetics, in **Personal Computers in Chemistry,** Wiley Interscience, New York, 1980, 297.

231. **Schreüder, W.A.,** Department of Mathematical Sciences, Rensselaer Polytechnic Institute, Troy, NY, Personal communication.

232. Ibid.

233. Ibid.

234. Gray, A. and Mathews, G.B., A Treatise on Bessel Functions and their Application to Physics, Dover Publications, New York, 1966.

235. Schreüder, W.A., Department of Mathematical Sciences, Rensselaer Polytechnic Institute, Troy, NY, Personal communication.

236. Patankar, S.V., Numerical Heat Transfer and Fluid Flow, Hemisphere Publishing Corporation, Washington, D.C., 1980.

237. Ibid., p. 11.

238. Ibid., p. 15.

239. Ibid., p. 16.

240. Ibid., p. 17.

241. Ibid., p. 26.

242. Schreüder, W.A., Numerical Prediction of Air Flow about an Air-Cooled Heat Exchanger, Ph.D Dissertation, University of Stellenbosch, Stellenbosch, R.S.A., 1986, Chapter 5.

243. Patankar, S.V., Numerical Heat Transfer and Fluid Flow, Hemisphere Publishing Corporation, Washington, D.C., 1980, 28.

244. Ibid, p. 59.

245. Schreüder, W.A., Department of Mathematical Sciences, Rensselaer Polytechnic Institute, Troy, NY, Personal communication.

246. **Patankar, S.V., Numerical Heat Transfer and Fluid Flow**, Hemisphere Publishing Corporation, Washington, D.C., 1980, 56.

247. **Schreüder, W.A., Numerical Prediction of Air Flow about an Air-Cooled Heat Exchanger**, Ph.D Dissertation, University of Stellenbosch, Stellenbosch, R.S.A., 1986, 6.12.

248. **Schreüder, W.A.**, Department of Mathematical Sciences, Rensselaer Polytechnic Institute, Troy, NY. Personal communication.

249. **Schreüder, W.A., Numerical Prediction of Air Flow about an Air-Cooled Heat Exchanger**, Ph.D Dissertation, University of Stellenbosch, Stellenbosch, R.S.A., 1986, Chapter 7.

250. **Schreüder, W.A.**, Department of Mathematical Sciences, Rensselaer Polytechnic Institute, Troy, NY, Personal communication.

251. **Bosch, C. and Loos, M.A.**, The Inhibition of Bacterial Oxidation of Pyrite and Concomitant Acid Mine Drainage, Research Report (Part 2) for the Water Research Commission, Department of Microbiology, University of Stellenbosch, Stellenbosch, October 1986.

252. **Maré, J. and Loos, M.A.**, The Inhibition of Bacterial Oxidation of Pyrite and Concomitant Acid Mine Drainage, Research Report (Part 1) for the Water Research Commission, Department of Microbiology, University of Stellenbosch, Stellenbosch, October 1986.

253. **Ibid**, p. 10.

APPENDIX 1A

Compositions of Rubber-SLS Formulations: Series B to G

TABLE A1. Compositions of styrene-butadiene rubber-SLS formulations : Series B

Constituent	Formulation number				
	B.1	B.2	B.3	B.4	B.5
Styrene-butadiene rubber (g)	200	200	200	200	200
Carbon black (g)	18	18	18	18	18
Zinc oxide (g)	10	10	10	10	10
Stearic acid (g)	2	2	2	2	2
ORAC CS (g)	3	3	3	3	3
TMTD (g)	1	1	1	1	1
OROX SP (g)	4	4	4	4	4
Sulphur (g)	4	4	4	4	4
SLS (g)	42,7	80,7	130,3	198,0	295,8
Mass % SLS	15	25	35	45	55

TABLE A2. Compositions of controlled-release formulations consisting of SLS and a 50 : 50 blend of natural rubber and styrene-butadiene rubber : Series C

Constituent	Formulation number				
	C.1	C.2	C.3	C.4	C.5
NR/SBR (50:50 blend) (g)	200	200	200	200	200
Carbon black (g)	18	18	18	18	18
Zinc oxide (g)	10	10	10	10	10
Stearic acid (g)	2	2	2	2	2
ORAC CS (g)	3	3	3	3	3
TMTD (g)	1	1	1	1	1
OROX SP (g)	4	4	4	4	4
Sulphur (g)	4	4	4	4	4
SLS (g)	42,7	80,7	130,3	198,0	295,8
Mass % SLS	15	25	35	45	55

TABLE A3. Compositions of controlled-release formulations consisting of natural rubber, SLS, and $CaCO_3$: Series D

Constituent	Formulation number																	
	D.1	D.2	D.3	D.4	D.5	D.6	D.7	D.8	D.9	D.10	D.11	D.12	D.13	D.14	D.15	D.16	D.17	D.18
Natural rubber (g)	200	200	200	200	200	200	200	200	200	200	200	200	200	200	200	200	200	200
Carbon black (g)	18	18	18	18	18	18	18	18	18	18	18	18	18	18	18	18	18	18
Zinc oxide (g)	10	10	10	10	10	10	10	10	10	10	10	10	10	10	10	10	10	10
Stearic acid (g)	2	2	2	2	2	2	2	2	2	2	2	2	2	2	2	2	2	2
ORAC CS (g)	3	3	3	3	3	3	3	3	3	3	3	3	3	3	3	3	3	3
TMTD (g)	1	1	1	1	1	1	1	1	1	1	1	1	1	1	1	1	1	1
OROX SP (g)	4	4	4	4	4	4	4	4	4	4	4	4	4	4	4	4	4	4
Sulphur (g)	4	4	4	4	4	4	4	4	4	4	4	4	4	4	4	4	4	4
Untreated $CaCO_3$(g) (Mean Particle size 2,25 µm)	6	12	20															
Untreated $CaCO_3$(g) (Mean Particle size 5 µm)				6	12	20												
Untreated $CaCO_3$(g) (Mean Particle size 10 µm)							6	12	20									
Treated $CaCO_3$(g) (Mean Particle size 1µm)										6	12	20						
Treated $CaCO_3$(g) (Mean Particle size 1,5 µm)													6	12	20			
Treated $CaCO_3$(g) (Mean Particle size 2 µm)																6	12	20
SLS (g)	202,9	207,8	214,4	202,9	207,8	214,4	202,9	207,8	214,4	202,9	207,8	214,4	202,9	207,8	214,4	202,9	207,8	214,4
Mass % SLS	45	45	45	45	45	45	45	45	45	45	45	45	45	45	45	45	45	45

TABLE A4. Compositions of controlled-release formulations containing natural rubber, SLS and $CaCO_3$: Series E

Constituent	Formulation number								
	E.1	E.2	E.3	E.4	E.5	E.6	E.7	E.8	E.9
Natural rubber (g)	200	200	200	200	200	200	200	200	200
Carbon black (g)	18	18	18	18	18	18	18	18	18
Zinc oxide (g)	10	10	10	10	10	10	10	10	10
Stearic acid (g)	2	2	2	2	2	2	2	2	2
ORAC CS	3	3	3	3	3	3	3	3	3
TMTD (g)	1	1	1	1	1	1	1	1	1
OROX SP (g)	4	4	4	4	4	4	4	4	4
Sulphur (g)	4	4	4	4	4	4	4	4	4
Treated $CaCO_3$ (g) (Av. Particle size 1 μm)	6	12	20	6	12	20	6	12	20
SLS	0	0	0	13,1	13,4	13,8	27,6	28,2	29,1
Mass % SLS	0	0	0	5	5	5	10	10	10

TABLE A5. Compositions of synthetic polyisoprene-SLS formulations : Series F

Constituent	Formulation number							
	F.1	F.2	F.3	F.4	F.5	F.6	F.7	F.8
Synthetic polyisoprene (g)	200	200	200	200	200	200	200	200
Carbon black (g)	18	18	18	18	18	18	18	18
Zinc oxide (g)	10	10	10	10	10	10	10	10
Stearic acid (g)	2	2	2	2	2	2	2	2
ORAC CS (g)	3	3	3	3	3	3	3	3
TMTD (g)	1	1	1	1	1	1	1	1
OROX SP (g)	4	4	4	4	4	4	4	4
Sulphur (g)	4	4	4	4	4	4	4	4
SLS (g)	0	12,7	26,9	42,7	80,7	130,3	198,0	295,8
Mass % SLS	0	5	10	15	25	35	45	55

TABLE A6. Compositions of controlled-release formulations consisting of natural rubber, SLS and $(NH_4)_2SO_4$: Series G

Constituent	Formulation number								
	G.1	G.2	G.3	G.4	G.5	G.6	G.7	G.8	G.9
Natural rubber (g)	200	200	200	200	200	200	200	200	200
Carbon black (g)	18	18	18	18	18	18	18	18	18
Zinc oxide (g)	10	10	10	10	10	10	10	10	10
Stearic acid (g)	2	2	2	2	2	2	2	2	2
ORAC CS (g)	3	3	3	3	3	3	3	3	3
TMTD (g)	1	1	1	1	1	1	1	1	1
OROX SP (g)	4	4	4	4	4	4	4	4	4
Sulphur (g)	4	4	4	4	4	4	4	4	4
$(NH_4)_2SO_4$ (g)	6	12	20	6	12	20	6	12	20
SLS (g)	0	0	0	13,1	13,4	13,8	27,6	28,2	29,1
Mass % SLS	0	0	0	5	5	5	10	10	10

APPENDIX 1B

THE COMPOSITIONS AND DIMENSIONS OF RUBBER-SLS PELLETS USED IN EXPERIMENTS 2 TO 17

Number of Experiment	Objective of Experiment
2	To study the effect of the agent loading on the release rate of SLS from styrene - butadiene rubber (SBR) matrices. The compositions and dimensions of the pellets are given in Table B1.
3	To study the effect of the agent loading on the release rate of SLS from matrices which consisted of a 50 : 50 blend of natural rubber and styrene-butadiene rubber (NR/SBR). The compositions and dimensions of the pellets are given in Table B2.
4	To study the effect of the addition of various grades of calcium carbonate on the release rate of SLS from natural rubber (NR) matrices which contained 45% (by mass) SLS. Pellet compositions and dimensions are given in Table B3.
5	To study the effect of agent loading on the release rate of SLS from synthetic cis-1,4 - polyisoprene (IR) matrices. Pellet compositions and dimensions are given in Table B4.
6	To study the release rates of SLS from NR and IR matrices which contained low loadings of SLS. Pellet compositions and dimensions are given in Table B5.
7	To study the effect of pellet geometry, i.e., surface area/volume ratio, on the release rate of SLS from NR matrices which contained

35% (by mass) SLS. Pellet compositions and dimensions are given in Table B6

8 To study the effect of pellet geometry on the release rate of SLS from SBR matrices which contained 25% (by mass) SLS. The compositions and dimensions of the pellets are given in Table B7.

9 To study the effect of pellet geometry on the release rate of SLS from NR/SBR (50 : 50 blend) matrices which contained 45% (by mass) SLS. Pellet compositions and dimensions are given in Table B8.

10 To study the effect of pellet geometry on the release rate of SLS from IR matrices which contained 35% (by mass) SLS The compositions and dimensions of the pellets are given in Table B9.

11 To study the effect of the addition of various amounts of $CaCO_3$ on the release rate of SLS from NR matrices which contained low loadings of SLS. Pellet compositions and dimensions are given in Table B10.

12 To study the effect of the addition of various amounts of $(NH_4)_2SO_4$ on the release rate of SLS from NR matrices Number of Experiment Objective of Experiment which contained low loadings of SLS. Pellet compositions and dimensions are given in Table B11.

13 To study the effect of the pH of the eluent on the release rate of SLS from NR matrices which contained 25% (by mass) SLS. The compositions and dimensions of the pellets are given in Table B12.

14 To study the effect of the pH of the eluent on the release rate of SLS from NR matrices which contained 45% (by mass) SLS. The compositions and dimensions of the pellets are given in Table B13.

15 To study the effect of the pH of the eluent on the release rate of SLS from IR matrices which contained 25% (by mass) SLS. Pellet compositions and dimensions are given in Table B14.

16 To study the effect of the pH of the eluent on the release rate of SLS from NR matrices which contained 45% (by mass) SLS and 10 phr untreated $CaCO_3$. Pellet compositions and dimensions are given in Table B15.

17 To study the effect of the pH of the eluent on the release rate of SLS from NR matrices which contained 45% (by mass) SLS and 10 phr surface-treated $CaCO_3$. Pellet compositions and dimensions are given in Table B16.

TABLE B1. Compositions and dimensions of rubber-SLS pellets used in Experiment 2

Sample number	Formulation number[a]	Mass of pellet (g)	Mass % SLS	Mass of SLS (g)	d[b] (cm)	h[c] (cm)	S/V[d] ratio
6	B.1	2,558	15	0,384	1,8	1,0	0,42
7	B.2	2,582	25	0,646	1,8	1,0	0,42
8	B.3	2,598	35	0,909	1,8	1,0	0,42
9	B.4	2,635	45	1,186	1,8	1,0	0,42
10	B.5	2,649	55	1,457	1,8	1,0	0,42

a) Given in Table A1

b) Diameter of pellet

c) Thickness of pellet

d) Surface area: volume ratio of pellet

TABLE B2. Compositions and dimensions of rubber-SLS pellets used in Experiment 3

Sample number	Formulation number[a]	Mass of pellet (g)	Mass % SLS	Mass of SLS (g)	d[b] (cm)	h[c] (cm)	S/V[d] ratio
11	C.1	2,552	15	0,383	1,8	1,0	0,42
12	C.2	2,588	25	0,647	1,8	1,0	0,42
13	C.3	2,576	35	0,902	1,8	1,0	0,42
14	C.4	2,604	45	1,172	1,8	1,0	0,42
15	C.5	2,653	55	1,459	1,8	1,0	0,42

a) Given in Table A2

b) Diameter of pellet

c) Thickness of pellet

d) Surface area: volume ratio of pellet

TABLE B3. Compositions and dimensions of rubber-SLS pellets used in Experiment 4

Sample number	Formulation number[a]	Mass of pellet (g)	Mass % SLS	Mass of SLS (g)	d[b] (cm)	h[c] (cm)	S/V[d] ratio
16	D.1	2,620	45	1,179	1,8	1,0	0,42
17	D.2	2,647	45	1,191	1,8	1,0	0,42
18	D.3	2,672	45	1,202	1,8	1,0	0,42
19	D.4	2,626	45	1,182	1,8	1,0	0,42
20	D.5	2,646	45	1,191	1,8	1,0	0,42
21	D.6	2,693	45	1,212	1,8	1,0	0,42
22	D.7	2,624	45	1,181	1,8	1,0	0,42
23	D.8	2,655	45	1,195	1,8	1,0	0,42
24	D.9	2,562	45	1,153	1,8	1,0	0,42
25	D.10	2,608	45	1,174	1,8	1,0	0,42
26	D.11	2,629	45	1,183	1,8	1,0	0,42
27	D.12	2,663	45	1,198	1,8	1,0	0,42
28	D.13	2,637	45	1,187	1,8	1,0	0,42
29	D.14	2,642	45	1,189	1,8	1,0	0,42
30	D.15	2,693	45	1,212	1,8	1,0	0,42
31	D.16	2,643	45	1,189	1,8	1,0	0,42
32	D.17	2,677	45	1,205	1,8	1,0	0,42
33	D.18	2,685	45	1,208	1,8	1,0	0,42

a) Given in Table A3

b) Diameter of pellet

c) Thickness of pellet

d) Surface area: volume ratio of pellet

TABLE B4. Compositions and dimensions of rubber-SLS pellets used in Experiment 5

Sample number	Formulation number[a]	Mass of pellet (g)	Mass % SLS	Mass of SLS (g)	d[b] (cm)	h[c] (cm)	S/V[d] ratio
34	F.4	2,506	15	0,376	1,8	1,0	0,42
35	F.5	2,515	25	0,629	1,8	1,0	0,42
36	F.6	2,561	35	0,896	1,8	1,0	0,42
37	F.7	2,596	45	1,168	1,8	1,0	0,42
38	F.8	2,625	55	1,444	1,8	1,0	0,42

a) Given in Table A5

b) Diameter of pellet

c) Thickness of pellet

d) Surface area: volume ratio of pellet

TABLE B5. Compositions and dimensions of rubber-SLS pellets used in Experiment 6

Sample number	Formulation number	Mass of pellet (g)	Mass % SLS	Mass of SLS (g)	d[c] (cm)	h[d] (cm)	S/V[e] ratio
39	A.2[a]	2,472	5	0,124	1,8	1,0	0,42
40	A.3[a]	2,474	10	0,247	1,8	1,0	0,42
41	F.2[b]	2,482	5	0,124	1,8	1,0	0,42
42	F.3[b]	2,496	10	0,250	1,8	1,0	0,42

a) Given in Table 3.2

b) Given in Table A5

c) Diameter of pellet

d) Thickness of pellet

e) Surface area: volume ratio of pellet

TABLE B6. Compositions and dimensions of rubber-SLS pellets used in Experiment 7

Sample number	Formulation number[a]	Number of pellets	Mass of pellet(s) (g)	Mass % SLS	Mass of SLS (g)	d[b] (cm)	h[c] (cm)	S/V[d] ratio
43	A.6	1	2,568	35	0,899	1,8	1,0	0,42
44	A.6	2	2,314	35	0,810	1,2	1,0	0,53
45	A.6	3	2,400	35	0,840	1,0	1,0	0,60
46	A.6	5	2,561	35	0,896	0,8	1,0	0,70
47	A.6	10	2,601	35	0,910	0,8	0,5	0,90
48	A.6	18	2,644	35	0,925	0,6	0,5	1,07

a) Given in Table 3.2

b) Diameter of pellet(s)

c) Thickness of pellet(s)

d) Surface area: volume ratio of pellet(s)

TABLE B7. Compositions and dimensions of rubber-SLS pellets used in Experiment 8

Sample number	Formulation number[a]	Number of pellets	Mass of pellet(s) (g)	Mass % SLS	Mass of SLS (g)	d[b] (cm)	h[c] (cm)	S/V[d] ratio
49	B.2	1	2,585	25	0,646	1,8	1,0	0,42
50	B.2	2	2,312	25	0,578	1,2	1,0	0,53
51	B.2	3	2,396	25	0,599	1,0	1,0	0,60
52	B.2	5	2,558	25	0,640	0,8	1,0	0,70
53	B.2	10	2,621	25	0,655	0,8	0,5	0,90
54	B.2	18	2,668	25	0,667	0,6	0,5	1,07

a) Given in Table A1

b) Diameter of pellet(s)

c) Thickness of pellet(s)

d) Surface area: Volume ratio of pellet(s)

TABLE B8. Compositions and dimensions of rubber-SLS pellets used in Experiment 9

Sample number	Formulation number[a]	Number of pellets	Mass of pellet(s) (g)	Mass % SLS	Mass of SLS (g)	d[b] (cm)	h[c] (cm)	S/V[d] ratio
55	C.4	1	2,610	45	1,175	1,8	1,0	0,42
56	C.4	2	2,331	45	1,049	1,2	1,0	0,53
57	C.4	3	2,420	45	1,089	1,0	1,0	0,60
58	C.4	5	2,584	45	1,163	0,8	1,0	0,70
59	C.4	10	2,610	45	1,175	0,8	0,5	0,90
60	C.4	18	2,654	45	1,194	0,6	0,5	1,07

a) Given in Table A2

b) Diameter of pellet(s)

c) Thickness of pellet(s)

d) Surface area: volume ratio of pellet(s)

TABLE B9. Compositions and dimensions of rubber-SLS pellets used in Experiment 10

Sample number	Formulation number[a]	Number of pellets	Mass of pellet(s) (g)	Mass % SLS	Mass of SLS (g)	d[b] (cm)	h[c] (cm)	S/V[d] ratio
61	F.6	1	2,565	35	0,898	1,8	1,0	0,42
62	F.6	2	2,287	35	0,801	1,2	1,0	0,53
63	F.6	3	2,372	35	0,830	1,0	1,0	0,60
64	F.6	5	2,536	35	0,888	0,8	1,0	0,70
65	F.6	10	2,548	35	0,892	0,8	0,5	0,90
66	F.6	18	2,595	35	0,908	0,6	0,5	1,07

a) Given in Table A5

b) Diameter of pellet(s)

c) Thickness of pellet(s)

d) Surface area: volume ratio of pellet(s)

TABLE B10. Compositions and dimensions of rubber-SLS pellets used in Experiment 11

Sample number	Formulation number[a]	Mass of pellet (g)	Mass % SLS	Mass of SLS (g)	d[b] (cm)	h[c] (cm)	S/V[d] ratio
67	E.4	2,530	5	0,127	1,8	1,0	0,42
68	E.5	2,585	5	0,129	1,8	1,0	0,42
69	E.6	2,594	5	0,130	1,8	1,0	0,42
70	E.7	2,565	10	0,257	1,8	1,0	0,42
71	E.8	2,597	10	0,260	1,8	1,0	0,42
72	E.9	2,603	10	0,260	1,8	1,0	0,42

a) Given in Table A4

b) Diameter of pellet

c) Thickness of pellet

d) Surface area: volume ratio of pellet

TABLE B11. Compositions and dimensions of rubber-SLS pellets used in Experiment 12

Sample number	Formulation number[a]	Mass of pellet (g)	Mass % SLS	Mass of SLS (g)	d[b] (cm)	h[c] (cm)	S/V[d] ratio
73	G.4	2,521	5	0,126	1,8	1,0	0,42
74	G.5	2,547	5	0,127	1,8	1,0	0,42
75	G.6	2,581	5	0,129	1,8	1,0	0,42
76	G.7	2,543	10	0,254	1,8	1,0	0,42
77	G.8	2,564	10	0,256	1,8	1,0	0,42
78	G.9	2,587	10	0,259	1,8	1,0	0,42

a) Given in Table A6

b) Diameter of pellet

c) Thickness of pellet

d) Surface area: volume ratio of pellet

TABLE B12. Compositions and dimensions of rubber-SLS pellets used in Experiment 13

Sample number	Formulation number[a]	Mass of pellet (g)	Mass % SLS	Mass of SLS (g)	S/V[b] ratio	pH of eluent
79	A.5	2,514	25	0,629	0,42	4,5
80	A.5	2,516	25	0,629	0,42	4,0
81	A.5	2,533	25	0,633	0,42	3,5
82	A.5	2,522	25	0,631	0,42	3,0
83	A.5	2,523	25	0,631	0,42	2,5
84	A.5	2,533	25	0,633	0,42	2,0
85	A.5	2,569	25	0,642	0,42	1,5

a) Given in Table 3.2

b) Surface area: volume ratio of pellet

TABLE B13. Compositions and dimensions of rubber-SLS pellets used in Experiment 14

Sample number	Formulation number[a]	Mass of pellet (g)	Mass % SLS	Mass of SLS (g)	S/V[b] ratio	pH of eluent
86	A.7	2,541	45	1,144	0,42	4,5
87	A.7	2,555	45	1,150	0,42	4,0
88	A.7	2,544	45	1,145	0,42	3,5
89	A.7	2,568	45	1,156	0,42	3,0
90	A.7	2,547	45	1,146	0,42	2,5
91	A.7	2,562	45	1,153	0,42	2,0
92	A.7	2,611	45	1,175	0,42	1,5

a) Given in Table 3.2

b) Surface area: volume ratio of pellet

TABLE B14. Compositions and dimensions of rubber-SLS pellets used in Experiment 15

Sample number	Formulation number[a]	Mass of pellet (g)	Mass % SLS	Mass of SLS (g)	S/V[b] ratio	pH of eluent
93	F.5	2,494	25	0,624	0,42	4,5
94	F.5	2,522	25	0,631	0,42	4,0
95	F.5	2,485	25	0,621	0,42	3,5
96	F.5	2,498	25	0,625	0,42	3,0
97	F.5	2,500	25	0,625	0,42	2,5
98	F.5	2,476	25	0,619	0,42	2,0
99	F.5	2,484	25	0,621	0,42	1,5

a) Given in Table A5

b) Surface area: volume ratio of pellet

TABLE B15. Compositions and dimensions of rubber-SLS pellets used in Experiment 16

Sample number	Formulation number[a]	Mass of pellet (g)	Mass % SLS	Mass of SLS (g)	S/V[b] ratio	pH of eluent
100	D.3	2,683	45	1,207	0,42	4,5
101	D.3	2,673	45	1,203	0,42	4,0
102	D.3	2,670	45	1,202	0,42	3,5
103	D.3	2,670	45	1,202	0,42	3,0
104	D.3	2,605	45	1,172	0,42	2,5
105	D.3	2,667	45	1,200	0,42	2,0
106	D.3	2,613	45	1,176	0,42	1,5

a) Given in Table A3

b) Surface area: volume ratio of pellet

TABLE B16. Compositions and dimensions of rubber-SLS pellets used in Experiment 17

Sample number	Formulation number[a]	Mass of pellet (g)	Mass % SLS	Mass of SLS (g)	S/V[b] ratio	pH of eluent
107	D.12	2,575	45	1,159	0,42	4,5
108	D.12	2,606	45	1,173	0,42	4,0
109	D.12	2,588	45	1,165	0,42	3,5
110	D.12	2,608	45	1,174	0,42	3,0
111	D.12	2,605	45	1,172	0,42	2,5
112	D.12	2,605	45	1,172	0,42	2,0
113	D.12	2,607	45	1,173	0,42	1,5

a) Given in Table A3

b) Surface area: volume ratio of pellet

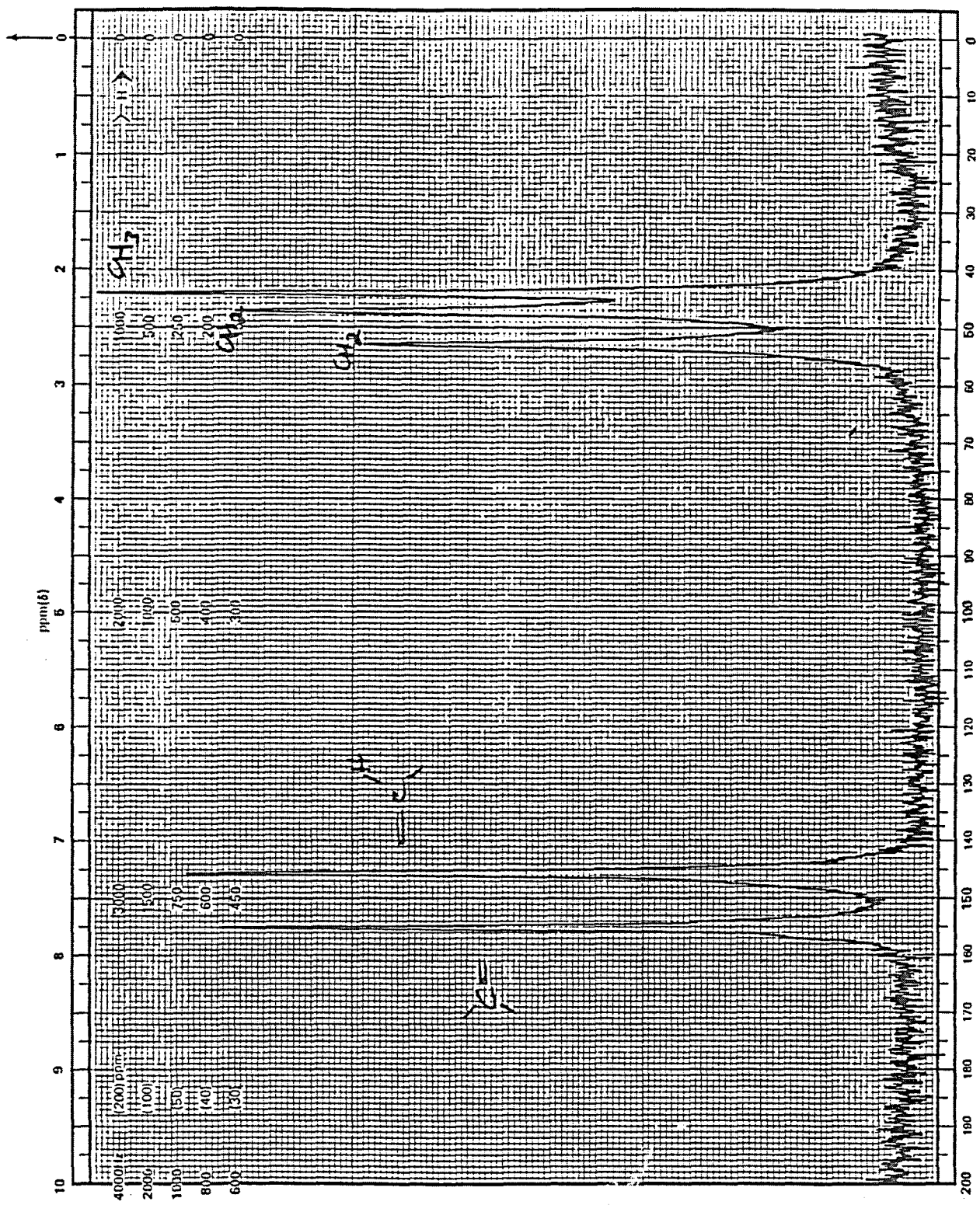

FIGURE 2A.1 ^{13}C NMR spectrum of natural rubber which contained no SLS.

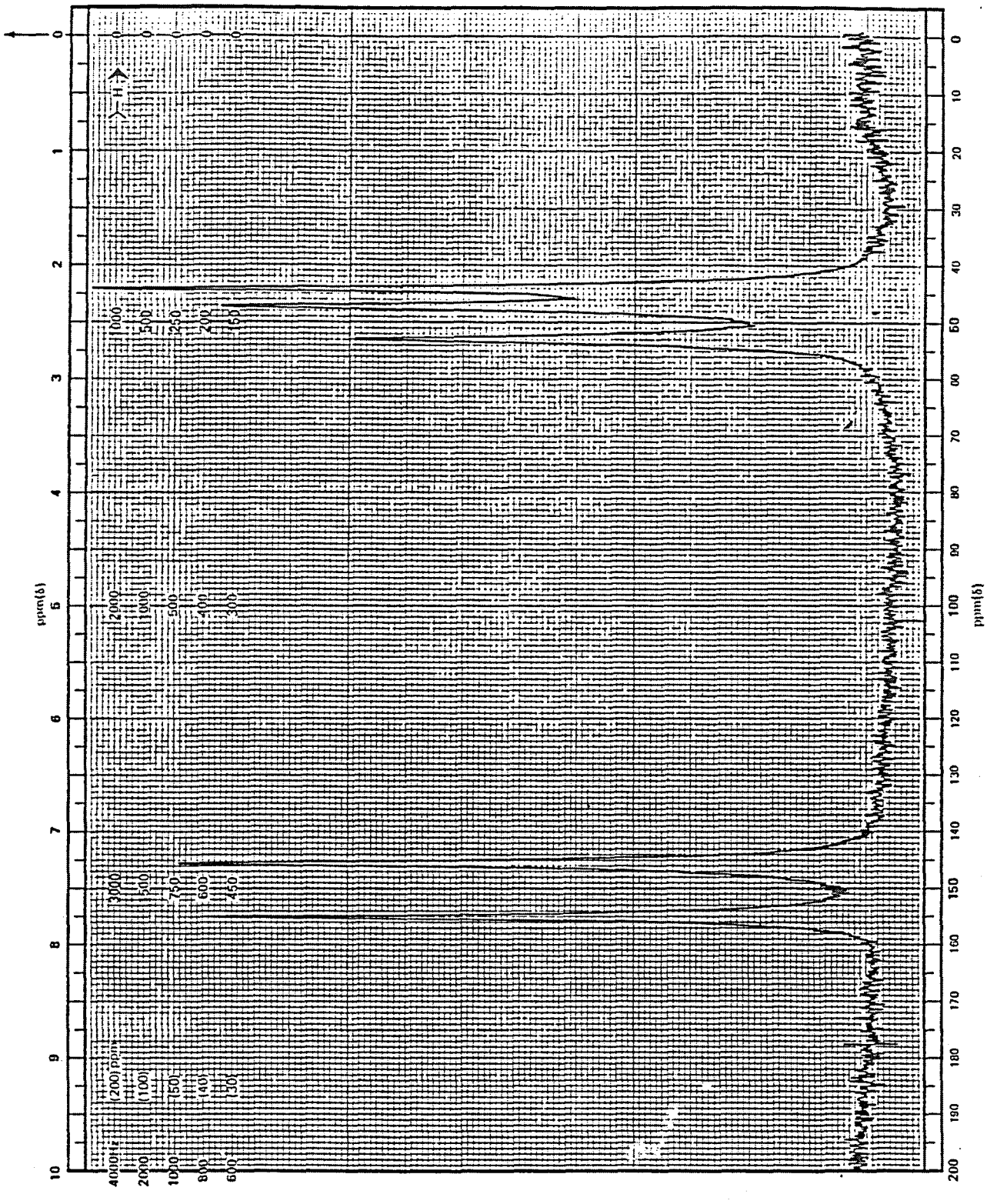

FIGURE 2A.2 ^{13}C NMR spectrum of natural rubber which contained 15% SLS.

APPENDIX 3A

THE CHEMISTRY OF ACCELERATED SULPHUR VULCANIZATION OF RUBBERS

The chemistry of accelerated sulphur vulcanization is so complex that it is only within the last few years that a coherent theoretical treatment has been possible. Even today, only the main stages are understood and there is still much to be learned about the effect of various additives[1].

Sulphur is combined in the vulcanization network in a number of ways, as shown in Figure 3A.1.

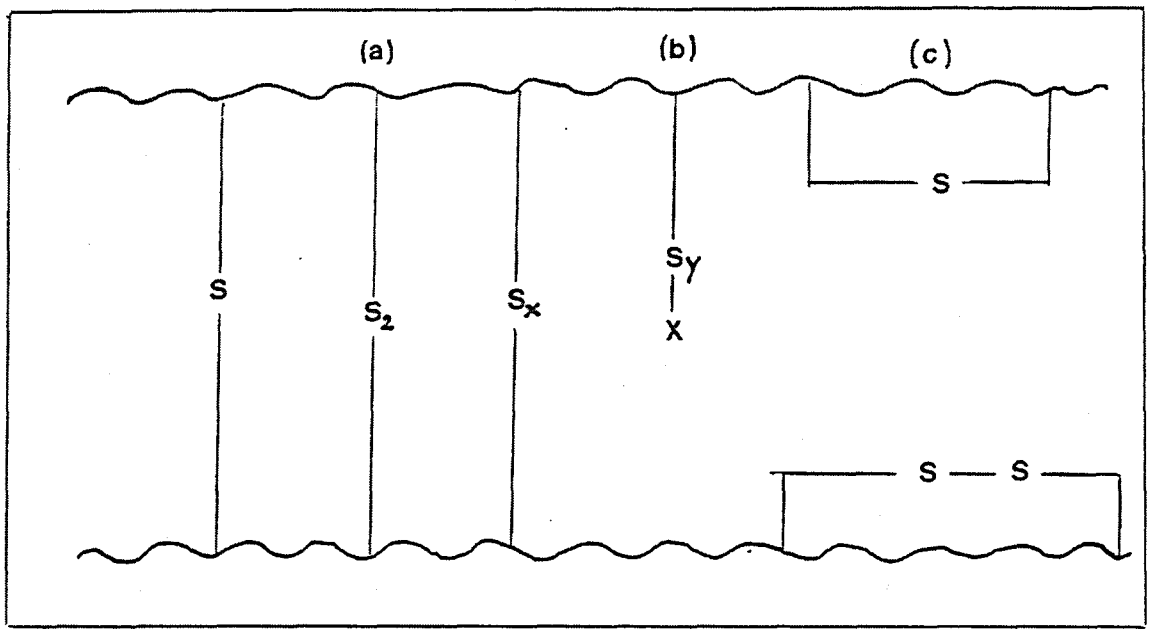

FIGURE 3A.1 Structural features of vulcanization network[1]

As crosslinks, sulphur may be present as monosulphide, disulphide, or polysulphide[a], but it may also be present as pendent sulphides[b], or cyclic mono- and disulphides[c].

The normal recipes used industrially for the vulcanization of olefinic rubbers include, in addition to sulphur, organic accelerators, zinc oxide, and long-chain fatty acids (stearic or lauric acids) or the zinc salts of these acids. Elemental sulphur can also be replaced in these mixtures with organosulphur compounds, such as tetramethylthiuram disulphide and dithiobisamines[2]. Typical organic accelerators are 2-mercaptobenzothiazole (and its disulphide, zinc salt, and sulphenamide derivatives), and zinc dimethyldithiocarbamate. The organic accelerators alone increase the rate of sulphur combination and crosslinking, but provide only marginal improvement in the crosslinking efficiency[2]. The presence of both zinc oxide and a fatty acid is essential if the crosslinking efficiency is to be improved markedly.

Network structures formed by accelerated sulphur vulcanization reactions have a preponderance of alkenyl mono- and disulphide crosslinks and little or no cyclic monosulphide units. The greatly-reduced tendency to form cyclic monosulphides in this type of reaction is evident in the mercaptobenzothiazole-accelerated reaction of sulphur with 2,6-dimethylocta-2,6-diene at 140°C[2].

The initial step in vulcanization seems to be the reaction of sulphur with the zinc salt of the accelerator to give a zinc perthiosalt, XS_xZnS_xX, where X is a group derived from the accelerator (e.g., thiocarbamate or benzthiazyl groups). This salt reacts with the rubber hydrocarbon, RH, to give a rubber-bound intermediate, (a)[1]:

$$XS_x ZnS_x X + RH \longrightarrow \underset{(a)}{XS_xR} + \underset{(b)}{ZnS} + \underset{(c)}{HS_{x-1}X}$$

and a perthio-accelerator group (c) which, with further zinc oxide will form a zinc perthio-salt of lower sulphur content. This may, nevertheless, again be an active sulphurating agent, forming intermediates $XS_{x-1}R$. In this way, each molecule of accelerator gives rise to a series of intermediates of various "degrees of polysulphidity".

The hydrogen atom which is removed is likely to be attached to a methylene group in the α-position to the double bond, i.e., in natural rubber, the hydrogen atoms at positions 4 and 5 are the most labile in this type of reaction[1]:

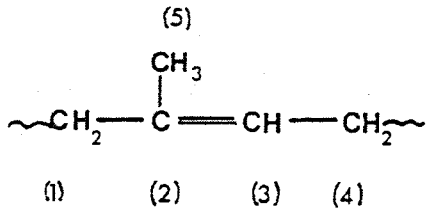

The rubber-bound intermediate, XS_xR, then reacts with a molecule of rubber hydrocarbon, RH, to give a crosslink, and more accelerator is regenerated:

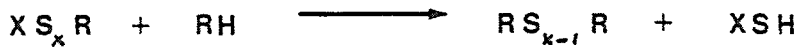

Even this is not the whole story, for, on further heating, the degree of polysulphidity of the crosslinks declines. This process is catalyzed by XS_xZnS_xX, and can result in additional crosslinks. It is also evident that the crosslinks which were initially at positions 4 and 5 undergo an allylic shift, with the result that new configurations appear[1]:

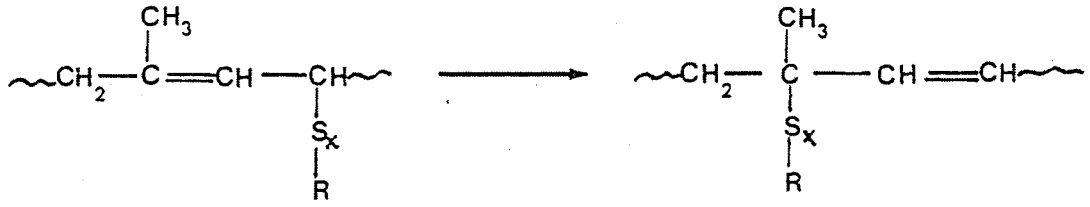

and

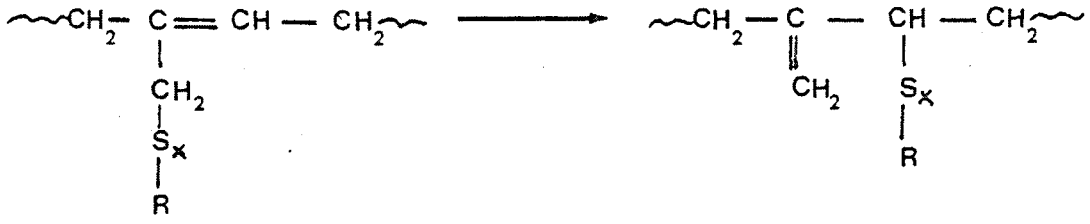

At the same time, disappearance of crosslinks of the disulphide and polysulphide types occurs, with the formation of conjugated trienes:

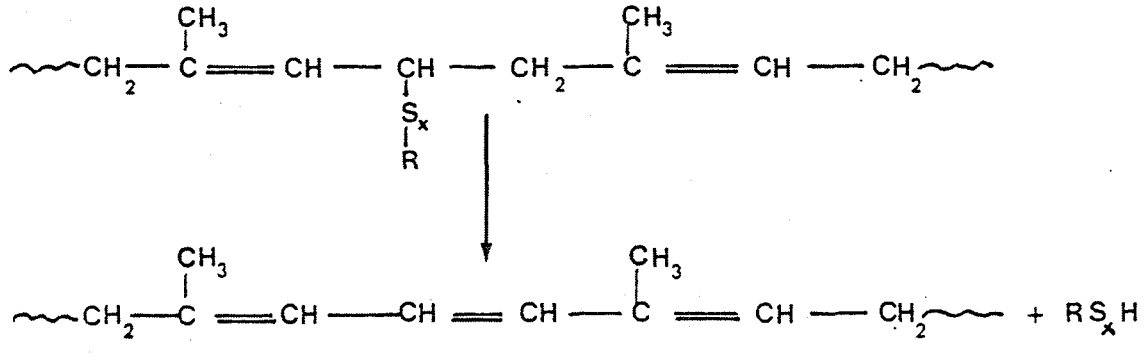

The destruction of crosslinks is apparently associated with the formation of cyclic sulphides, but this has not been investigated in detail[1].

A consideration of the above reactions leads to the conclusion that, if desulphuration proceeds rapidly, the final network will be highly crosslinked, with mainly monosulphidic bonds, and there will be relatively few modifications of the cyclic sulphide or conjugated triene type. Such a network is referred to as being "efficiently crosslinked".

On the other hand, if desulphuration proceeds slowly, there will be opportunities for thermal decomposition, leading to reversion or loss of crosslinks and to networks containing modifications. Further, the crosslinks which do survive will be di- or polysulphidic and, hence, will be liable to further decomposition. These networks are inefficiently crosslinked.

REFERENCES

1. **Morrell, S.H.**, The chemistry and technology of vulcanisation, in Blow, C.M., Ed., **Rubber Technology and Manufacture**, Newnes-Butterworths, London, 1978, 147.

2. **Lenz, R.W., Organic Chemistry of Synthetic High Polymers**, Interscience Publishers, New York, 1967, 709.

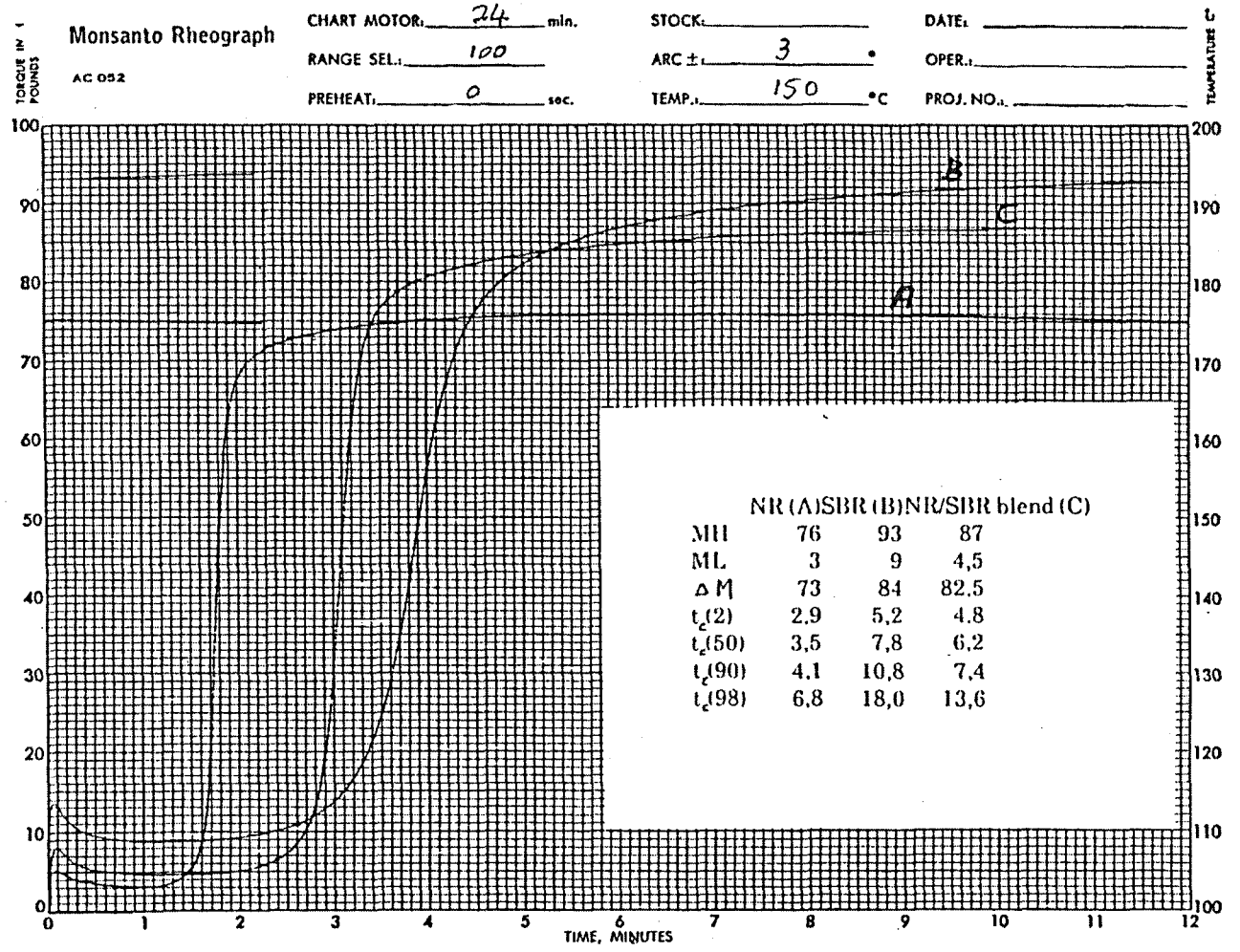

FIGURE 3B.1 Monsanto rheographs of masterbatch formulations A (NR), B (SBR) and C (NR/SBR blend).

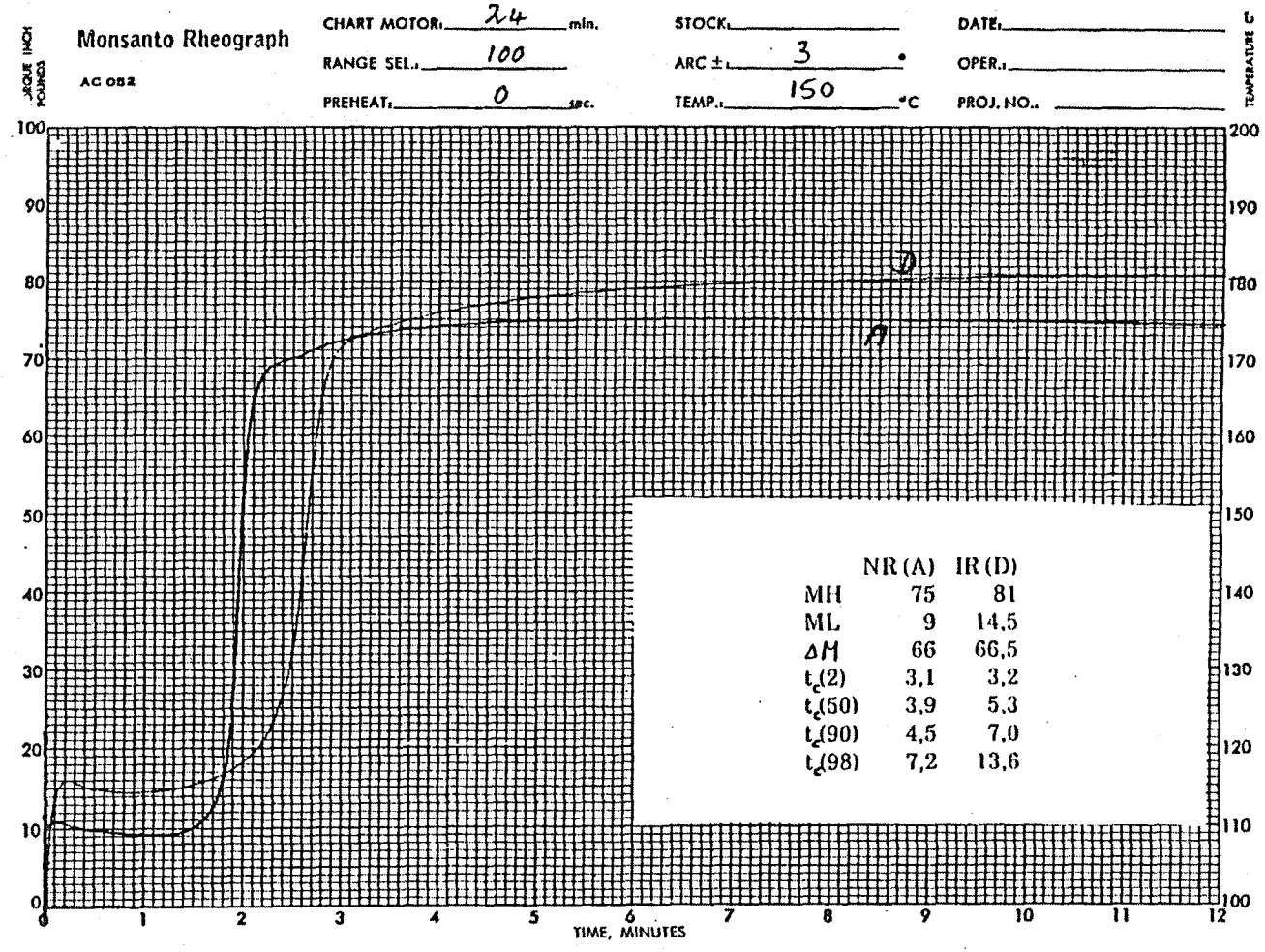

FIGURE 3B.2 Monsanto rheographs of masterbatch formulations A (NR) and D (IR)

APPENDIX 3C

Linear Expansion Coefficients of Rubber-SLS Formulations

TABLE 3C Coefficient of linear expansion, α, for a series of natural-rubber formulations which contained different loadings of SLS.

SLS loading (Mass %)	α [a] (μm/m °C)
0	228,5
	250,5
0,5	238,7
1	241,0
2	224,0
3	278,8
4	332,3
5	280,5
	230,4
6	322,1
7	209,5
8	243,7
9	263,7
10	174,5
	245,0
15	242,1
	202,5
25	190,0
35	179,9
45	133,0
55	88,4

(a) α was calculated from the linear portion of the TMA scan over the temperature range 80°-120°C

APPENDIX 3D

DSC Analysis of Rubber-SLS Formulations

TABLE 3D.1. Information obtained from analysis of curing exotherms for NR-SLS formulations

% SLS	Information obtained from DSC kinetics data analysis				Information obtained from DSC scans		
	Heat of reaction ΔH (J/g)	Activation energy, E (kJ/mole)	log Z_1 (min^{-1})	Reaction order, n	Heat of reaction ΔH(J/g)	Onset temperature (°C)	Peak temperature (°C)
	9,4	748	93,6	3,2	7,0	140,2	147,9
0	9,2	765	95,7	3,3	7,3	139,8	147,7
	9,4	616	77,3	2,6	7,6	138,3	147,3
	10,9	615	76,9	2,7	8,2	139,9	148,0
2	10,8	785	98,1	3,5	8,5	141,3	148,9
	11,0	746	93,0	3,3	8,7	141,6	149,2
	11,1	640	80,0	2,7	8,7	140,7	148,0
4	10,7	846	105,4	3,7	8,6	142,6	149,7
	10,6	782	97,4	3,2	8,6	142,2	149,6
	11,0	779	97,1	3,5	9,9	141,1	148,9
5	10,2	847	105,7	3,8	9,7	141,0	148,7
	11,4	766	95,5	3,4	10,1	141,8	149,4
	11,8	605	75,5	2,5	8,9	141,5	148,8
6	11,2	787	98,0	3,5	8,8	142,5	150,1
	11,2	796	99,3	3,7	8,9	141,3	148,7
	13,0	386	47,9	1,2	9,5	141,7	149,0
8	10,6	812	101,2	3,8	9,9	141,8	149,6
	10,7	784	97,7	3,8	9,4	141,7	149,7
	11,8	668	83,4	3,4	9,4	141,0	149,4
10	11,5	736	91,9	3,9	9,4	140,5	148,6
	11,0	663	82,8	3,3	9,2	140,2	148,6
11	11,8	849	106,0	4,6	9,4	141,4	149,2
12	11,2	751	93,8	4,0	8,6	141,0	148,7
13	11,7	703	87,8	4,1	9,3	140,5	148,4
14	10,9	872	109,0	5,0	9,3	140,9	148,3
15	10,0	950	118,9	5,4	8,0	140,9	147,4
25					0,9	137,7	143,8

TABLE 3D.2. Information obtained from analysis of curing exotherms for IR-SLS formulations

% SLS	Information obtained from DSC kinetics data analysis				Information obtained from DSC scans		
	Heat of reaction ΔH (J/g)	Activation energy, E (kJ/mole)	log Z (min^{-1})	Reaction order n	Heat of reaction ΔH(J/g)	Onset Temperature (°C)	Peak Temperature (°C)
	9,9	1287	157,9	3,5	7,8	150,8	155,2
0	9,3	1245	152,9	3,2	7,3	150,5	154,7
	9,7	1191	146,4	3,4	7,6	150,0	154,6
	9,4	1348	164,8	2,9	7,4	152,8	156,7
2	9,9	1271	155,6	2,9	7,8	152,2	156,2
	9,8	1033	126,6	2,5	7,7	151,1	155,9
	9,7	1009	124,2	2,9	7,7	148,5	154,4
3	14,0	1120	137,5	3,9	10,9	150,1	155,2
	9,8	1049	129,1	3,0	7,7	148,9	154,1
	9,7	1237	150,9	2,7	7,6	153,5	157,6
4	8,9	1203	147,0	2,5	7,0	153,0	157,2
	8,8	1251	152,9	2,6	6,9	152,8	156,8
	9,6	975	119,0	2,2	7,6	152,8	157,7
6	9,7	1097	133,8	2,5	7,6	153,1	157,9
	9,4	1164	142,1	2,8	7,4	153,0	157,8
	7,0	841	102,7	1,4	5,5	152,8	157,0
8	7,2	641	78,2	0,4	5,6	153,2	157,3
	7,4	845	103,2	1,5	5,8	152,8	157,2
	7,3	1053	130,2	3,7	5,8	146,9	152,5
10	7,4	1046	129,4	3,8	5,8	146,6	151,8
	7,8	1009	124,2	3,2	6,1	148,7	154,1
11	7,0	1180	145,1	3,7	5,5	149,5	154,6
12	7,3	730	89,9	2,1	5,8	148,2	154,1
13	6,7	1017	124,7	2,8	5,3	150,6	155,8
14	6,7	1004	123,2	2,8	5,3	150,5	155,6
15	6,0	981	120,2	2,6	4,7	151,3	156,5
25	2,2	1346	166,6	4,0	1,6	147,2	151,6

APPENDIX 4A

Data Obtained from Elution Experiments

TABLE 4A.1 Sodium concentrations in eluates (μg/ml)

Exp. No.	S/N	Day 1.	Day 3.	Day 5.	Day 7.	Day 14.	Day 21.	Day 28.	Day 35.	Day 42.	Day 49.	Day 56.
1	1	5	1	1	1	1	1	1	1	1	1	1
	2	8	2	2	1	1	1	1	1	2	1	1
	3	54	23	22	25	60	40	40	40	40	30	29
	4	500	320	320	280	500	230	70	12	6	4	3
	5	600	300	300	300	400	330	320	250	110	70	50
2	6	2	1	1	1	1	1	1	1	1	1	1
	7	12	3	2	2	2	2	2	1	1.5	1	1
	8	180	80	68	64	170	120	110	90	80	60	60
	9	900	450	330	310	445	33	3	2	2	1	2
	10	1300	500	450	290	120	12	4	3	2	1	1
3	11	3	1	1	1	1	1	1	1	1	1	1
	12	13	4	4	3	3	3	3	2	2	2	2
	13	120	52	36	32	80	50	50	50	40	31	30
	14	600	320	260	260	500	210	40	9	4	3	2
	15	1400	600	450	290	90	6	2	2	1	1	1
4	16	700	450	350	260	300	50	7	4	2	2	2
	17	800	480	330	270	320	32	9	3	2	2	2
	18	700	470	390	310	330	35	6	3	2	2	2
	19	700	490	280	250	300	70	13	5	2	2	2
	20	700	480	320	250	300	60	13	4	2	2	2
	21	800	500	380	280	310	34	5	2	2	1	2
	22	500	390	270	200	400	250	120	60	20	7	4
	23	700	500	330	280	400	70	14	5	2	2	2
	24	600	420	270	200	400	140	40	10	3	2	2
	25	600	430	260	260	400	160	50	15	6	3	2
	26	600	400	260	260	400	240	80	20	7	4	3
	27	600	410	300	280	400	150	50	11	5	2	2
	28	400	240	200	220	400	330	140	100	40	17	9
	29	600	360	270	230	400	220	80	23	8	4	3
	30	700	400	280	240	400	180	70	20	7	3	3
	31	500	250	200	180	400	320	240	110	50	21	11
	32	600	340	260	250	400	270	120	40	11	5	3
	33	500	250	250	230	500	330	220	60	21	9	6
5	34	3	1	1	1	1	1	1	1	1	1	1
	35	7	1	1	1	1	1	1	1	1	1	1
	36	36	8	8	8	16	9	10	9	8	8	7
	37	400	170	170	190	400	300	300	100	80	30	15
	38	1000	430	550	320	340	27	4	3	3	2	2
6	39	2	1	1	1	1	1	1	1	1	1	1
	40	3	1	1	1	1	1	1	1	1	1	1
	41	2	1	1	1	1	1	1	1	1	1	1
	42	3	1	1	1	1	1	1	1	1	1	1
7	43	56	24	24	25	70	50	40	40	40	30	31
	44	34	18	20	20	40	32	30	26	22	19	18
	45	50	24	25	24	70	40	40	40	32	27	26
	46	64	29	30	27	70	40	40	40	40	29	27
	47	120	60	54	42	110	60	60	70	60	50	50
	48	150	72	62	54	130	70	60	60	50	50	40
8	49	9	2	2	2	2	2	2	1	1	1	1
	50	17	5	4	3	6	4	3	3	2	2	2
	51	20	5	4	3	4	3	3	2	2	1	1
	52	23	7	5	3	6	4	4	3	2	2	2
	53	46	12	7	6	11	6	5	4	3	3	2
	54	52	13	10	7	14	8	7	5	4	4	3

9	55	600	370	300	230	500	150	40	8	4	2	2
	56	650	350	260	190	300	60	10	4	2	2	2
	57	800	410	280	220	320	31	5	3	2	2	2
	58	900	440	320	210	130	13	3	3	2	2	2
	59	1100	490	310	70	23	4	2	2	2	2	2
	60	1400	540	210	40	10	3	2	3	2	2	2
10	61	27	7	7	7	14	10	10	10	9	8	7
	62	33	9	8	8	15	10	10	9	9	8	7
	63	42	11	9	9	17	11	10	10	10	8	9
	64	52	14	12	12	26	17	15	13	12	10	11
	65	74	24	19	18	35	23	21	22	19.5	16	18
	66	80	27	22	21	43	27	24	24	21	16	18
11	67	3	1	1	1	1	1	1	1	1	1	1
	68	3	1	1	1	1	1	1	1	1	1	1
	69	2	1	1	1	1	1	1	1	1	1	1
	70	2	1	1	1	1	1	1	1	1	1	1
	71	4	1	1	1	1	1	1	1	1	1	1
	72	4	1	1	1	1	1	1	1	1	1	1
12	73	3	1	1	1	1	1	1	1	1	1	1
	74	2	1	1	1	1	1	1	1	1	1	1
	75	2	1	1	1	1	1	1	1	1	1	1
	76	5	1	1	1	1	1	1	1	1	1	1
	77	4	1	1	1	1	1	1	1	1	1	1
	78	5	1	1	1	1	1	1	1	1	1	1
13	79	7	1	1	1	1	1	1	1	2	1	1
	80	11	1	1	1	1	1	2	2	2	1	1
	81	10	2	2	2	2	2	2	2	2	1	1
	82	9	2	2	2	2	2	2	2	2	1	1
	83	11	2	2	2	2	2	2	2	2	2	2
	84	10	2	1	2	2	2	2	3	2	2	2
	85	10	1	2	2	2	2	2	2	2	2	2
14	86	18	7	7	6	16	13	13	13	13	11	13
	87	20	8	8	7	19	15	15	14	15	13	15
	88	21	7	7	8	21	16	16	16	15	14	15
	89	27	9	8	8	20	16	16	16	16	14	16
	90	32	11	9	9	23	18	18	18	19	19	21
	91	22	8	8	8	24	22	25	27	29	27	32
	92	700	440	320	250	400	90	23	9	6	4	3
15	93	10	1	1	1	1	1	1	1	1	1	1
	94	8	1	1	1	2	2	1	1	1	1	1
	95	8	1	1	1	1	1	1	1	2	1	1
	96	8	1	1	1	2	2	1	1	1	1	1
	97	8	1	1	1	1	1	1	1	1	1	1
	98	9	1	2	1	1	2	1	2	1	1	1
	99	8	1	1	1	2	2	1	1	1	1	1
16	100	800	400	350	260	300	32	7	3	3	2	2
	101	800	400	380	270	260	29	5	3	2	2	2
	102	800	400	320	280	400	60	11	4	3	2	2
	103	800	500	360	290	300	34	5	3	3	2	2
	104	700	400	280	250	400	120	25	8	6	4	4
	105	700	400	300	300	400	120	16	9	6	4	4
	106	800	400	320	280	400	100	20	8	5	3	3
17	107	700	400	260	260	400	80	17	6	3	2	2
	108	260	140	100	100	330	250	200	210	170	120	95
	109	180	110	80	80	290	230	200	200	160	120	120
	110	210	140	90	90	320	250	220	220	170	120	100
	111	180	110	80	80	250	190	170	180	140	110	90
	112	290	190	120	115	300	260	240	220	140	100	80
	113	290	200	140	120	300	290	260	230	150	100	80

TABLE 4A.2 SLS concentrations in eluates (μg/ml)

Exp. No.	S/N	Day 1.	Day 3.	Day 5.	Day 7.	Day 14.	Day 21.	Day 28.	Day 35.	Day 42.	Day 49.	Day 56.
1	1	62.7	12.5	12.5	12.5	12.5	12.5	12.5	12.5	12.5	12.5	12.5
	2	100.4	25.1	25.1	12.5	12.5	12.5	12.5	12.5	25.1	12.5	12.5
	3	677.6	288.6	276.1	313.7	752.9	501.9	501.9	501.9	501.9	376.5	363.9
	4	6274.2	4015.5	4015.5	3513.6	6274.2	2886.2	878.4	150.6	75.3	50.2	37.6
	5	7529.1	3764.5	3764.5	3764.5	5019.4	4141.0	4015.5	3137.1	1380.3	878.4	627.4
2	6	25.1	12.5	12.5	12.5	12.5	12.5	12.5	12.5	12.5	12.5	12.5
	7	150.6	37.6	25.1	25.1	25.1	25.1	25.1	12.5	18.8	12.5	12.5
	8	2258.7	1003.9	853.3	803.1	2133.2	1505.8	1380.3	1129.4	1003.9	752.9	752.9
	9	11293.6	5646.8	4141.0	3890.0	5584.1	414.1	37.6	25.1	25.1	12.5	25.1
	10	16313.0	6274.2	5646.8	3639.1	1505.8	150.6	50.2	37.6	25.1	12.5	12.5
3	11	37.6	12.5	12.5	12.5	12.5	12.5	12.5	12.5	12.5	12.5	12.5
	12	163.1	50.2	50.2	37.6	37.6	37.6	37.6	25.1	25.1	25.1	25.1
	13	1505.8	652.5	451.7	401.6	1003.9	627.4	627.4	627.4	501.9	389.0	376.5
	14	7529.1	4015.5	3262.6	3262.6	6274.2	2635.2	501.9	112.9	50.2	37.6	25.1
	15	17567.9	7529.1	5646.8	3639.1	1129.4	75.3	25.1	25.1	12.5	12.5	12.5
4	16	8783.9	5646.8	4392.0	3262.6	3764.5	627.4	87.8	50.2	25.1	25.1	25.1
	17	10038.8	6023.3	4141.0	3388.1	4015.5	401.6	112.9	37.6	25.1	25.1	25.1
	18	8783.9	5897.8	4893.9	3890.0	4141.0	439.2	75.3	37.6	25.1	25.1	25.1
	19	8783.9	6148.8	3513.6	3137.1	3764.5	878.4	163.1	62.7	25.1	25.1	25.1
	20	8783.9	6023.3	4015.5	3137.1	3764.5	752.9	163.1	50.2	25.1	25.1	25.1
	21	10038.8	6274.2	4768.4	3513.6	3890.0	426.6	62.7	25.1	25.1	12.5	25.1
	22	6274.2	4893.9	3388.1	2509.7	5019.4	3137.1	1505.8	752.9	251.0	87.8	50.2
	23	8783.9	6274.2	4141.0	3513.6	5019.4	878.4	175.7	62.7	25.1	25.1	25.1
	24	7529.1	5270.4	3388.1	3513.6	5019.4	1756.8	501.9	125.5	37.6	25.1	25.1
	25	7529.1	5395.9	3262.6	3262.6	5019.4	2007.8	627.4	188.2	75.3	37.6	25.1
	26	7529.1	5019.4	3262.6	3262.6	5019.4	3011.6	1003.9	251.0	87.8	50.2	37.6
	27	7529.1	5144.9	3764.5	3513.6	5019.4	1882.3	627.4	138.0	62.7	25.1	25.1
	28	5019.4	3011.6	2509.7	2760.7	5019.4	4141.0	1756.8	1254.8	501.9	213.3	112.9
	29	7529.1	4517.5	3388.1	2886.2	5019.4	2760.7	1003.9	288.6	100.4	50.2	37.6
	30	8783.9	5019.4	3513.6	3011.6	5019.4	2258.7	878.4	251.0	87.8	37.6	37.6
	31	6274.2	3137.1	2509.7	2258.7	5019.4	4015.5	3011.6	1380.3	627.4	263.5	138.0
	32	7529.1	4266.5	3262.6	3137.1	5019.4	3388.1	1505.8	501.9	138.0	62.7	37.6
	33	6274.2	3137.1	3137.1	2886.2	6274.2	4141.0	2760.7	752.9	263.5	112.9	75.3
5	34	37.6	12.5	12.5	12.5	12.5	12.5	12.5	12.5	12.5	12.5	12.5
	35	87.8	12.5	12.5	12.5	12.5	12.5	12.5	12.5	12.5	12.5	12.5
	36	451.7	100.4	100.4	100.4	200.8	112.9	125.5	112.9	100.4	100.4	87.8
	37	5019.4	2133.2	2133.2	2384.2	5019.4	3764.5	3764.5	2258.7	1003.9	376.5	188.2
	38	12548.5	5395.9	6901.7	4015.5	4266.5	338.8	50.2	37.6	37.6	25.1	25.1
6	39	25.1	12.5	12.5	12.5	12.5	12.5	12.5	12.5	12.5	12.5	12.5
	40	37.6	12.5	12.5	12.5	12.5	12.5	12.5	12.5	12.5	12.5	12.5
	41	25.1	12.5	12.5	12.5	12.5	12.5	12.5	12.5	12.5	12.5	12.5
	42	37.6	12.5	12.5	12.5	12.5	12.5	12.5	12.5	12.5	12.5	12.5
7	43	702.7	301.2	301.2	313.7	878.4	627.4	501.9	501.9	501.9	376.5	389.0
	44	426.6	225.9	251.0	251.0	501.9	401.6	376.5	326.3	276.1	238.4	225.9
	45	627.4	301.2	313.7	301.2	878.4	501.9	501.9	501.9	401.6	338.8	326.3
	46	803.1	363.9	376.5	338.8	878.4	501.9	501.9	501.9	501.9	363.9	338.8
	47	1505.8	752.9	677.6	527.0	1380.3	752.9	752.9	878.4	752.9	627.4	627.4
	48	1882.3	903.5	778.0	677.6	1631.3	878.4	752.9	752.9	627.4	627.4	501.9
8	49	112.9	25.1	25.1	25.1	25.1	25.1	25.1	12.5	12.5	12.5	12.5
	50	213.3	62.7	50.2	37.6	75.3	50.2	37.6	37.6	25.1	25.1	25.1
	51	251.0	62.7	50.2	37.6	50.2	37.6	37.6	25.1	25.1	12.5	12.5
	52	288.6	87.8	62.7	37.6	75.3	50.2	50.2	37.6	25.1	25.1	25.1
	53	577.2	150.6	87.8	75.3	138.0	75.3	62.7	50.2	37.6	37.6	25.1
	54	652.5	163.1	125.5	87.8	175.7	100.4	87.8	62.7	50.2	50.2	37.6

9	55	7529.1	4642.9	3764.5	2886.2	6274.2	1882.3	501.9	100.4	50.2	25.1	25.1
	56	8156.5	4392.0	3262.6	2384.2	3764.5	752.9	125.5	50.2	25.1	25.1	25.1
	57	10038.8	5144.9	3513.6	2760.7	4015.5	389.0	62.7	37.6	25.1	25.1	25.1
	58	11293.6	5521.3	4015.5	2635.2	1631.3	163.1	37.6	37.6	25.1	25.1	25.1
	59	13803.3	6148.8	3890.0	878.4	288.6	50.2	25.1	25.1	25.1	25.1	25.1
	60	17567.9	6776.2	2635.2	501.9	125.5	37.6	25.1	37.6	25.1	25.1	25.1
10	61	338.8	87.8	87.8	87.8	175.7	125.5	125.5	125.5	112.9	100.4	87.8
	62	414.1	112.9	100.4	100.4	188.2	125.5	125.5	112.9	112.9	100.4	87.8
	63	527.0	138.0	112.9	112.9	213.3	138.0	125.5	125.5	125.5	100.4	112.9
	64	652.5	175.7	150.6	150.6	326.3	213.3	188.2	163.1	150.6	125.5	138.0
	65	928.6	301.2	238.4	225.9	439.2	288.6	263.5	276.1	244.7	200.8	225.9
	66	1003.9	338.8	276.1	263.5	539.6	338.8	301.2	301.2	263.5	200.8	225.9
11	67	37.6	12.5	12.5	12.5	12.5	12.5	12.5	12.5	12.5	12.5	12.5
	68	37.6	12.5	12.5	12.5	12.5	12.5	12.5	12.5	12.5	12.5	12.5
	69	25.1	12.5	12.5	12.5	12.5	12.5	12.5	12.5	12.5	12.5	12.5
	70	25.1	12.5	12.5	12.5	12.5	12.5	12.5	12.5	12.5	12.5	12.5
	71	50.2	12.5	12.5	12.5	12.5	12.5	12.5	12.5	12.5	12.5	12.5
	72	50.2	12.5	12.5	12.5	12.5	12.5	12.5	12.5	12.5	12.5	12.5
12	73	37.6	12.5	12.5	12.5	12.5	12.5	12.5	12.5	12.5	12.5	12.5
	74	25.1	12.5	12.5	12.5	12.5	12.5	12.5	12.5	12.5	12.5	12.5
	75	25.1	12.5	12.5	12.5	12.5	12.5	12.5	12.5	12.5	12.5	12.5
	76	62.7	12.5	12.5	12.5	12.5	12.5	12.5	12.5	12.5	12.5	12.5
	77	50.2	12.5	12.5	12.5	12.5	12.5	12.5	12.5	12.5	12.5	12.5
	78	62.7	12.5	12.5	12.5	12.5	12.5	12.5	12.5	12.5	12.5	12.5
13	79	87.8	12.5	12.5	12.5	12.5	12.5	12.5	12.5	25.1	12.5	12.5
	80	138.0	12.5	12.5	12.5	12.5	12.5	25.1	25.1	25.1	12.5	12.5
	81	125.5	25.1	25.1	25.1	25.1	25.1	25.1	25.1	25.1	12.5	12.5
	82	112.9	25.1	25.1	25.1	25.1	25.1	25.1	25.1	25.1	12.5	12.5
	83	138.0	25.1	25.1	25.1	25.1	25.1	25.1	25.1	25.1	25.1	25.1
	84	125.5	25.1	12.5	25.1	25.1	25.1	25.1	37.6	25.1	25.1	25.1
	85	125.5	12.5	25.1	25.1	25.1	25.1	25.1	25.1	25.1	25.1	25.1
14	86	225.9	87.8	87.8	75.3	200.8	163.1	163.1	163.1	163.1	138.0	163.1
	87	251.0	100.4	100.4	87.8	238.4	188.2	188.2	175.7	188.2	163.1	188.2
	88	263.5	87.8	87.8	100.4	263.5	200.8	200.8	200.8	188.2	175.7	188.2
	89	338.8	112.9	100.4	100.4	251.0	200.8	200.8	200.8	200.8	175.7	200.8
	90	401.6	138.0	112.9	112.9	288.6	225.9	225.9	225.9	238.4	238.4	263.5
	91	276.1	100.4	100.4	100.4	301.2	276.1	313.7	338.8	363.9	338.8	401.6
	92	8783.9	5521.3	4015.5	3137.1	5019.4	1129.4	288.6	112.9	75.3	50.2	37.6
15	93	125.5	12.5	12.5	12.5	12.5	12.5	12.5	12.5	12.5	12.5	12.5
	94	100.4	12.5	12.5	12.5	25.1	25.1	12.5	12.5	12.5	12.5	12.5
	95	100.4	12.5	12.5	12.5	12.5	12.5	12.5	12.5	25.1	12.5	12.5
	96	100.4	12.5	12.5	12.5	25.1	25.1	12.5	12.5	12.5	12.5	12.5
	97	100.4	12.5	12.5	12.5	12.5	12.5	12.5	12.5	12.5	12.5	12.5
	98	112.9	12.5	25.1	12.5	12.5	25.1	12.5	25.1	12.5	12.5	12.5
	99	100.4	12.5	12.5	12.5	25.1	25.1	12.5	12.5	12.5	12.5	12.5
16	100	10038.8	5019.4	4392.0	3262.6	3764.5	401.6	87.8	37.6	37.6	25.1	25.1
	101	10038.8	5019.4	4768.4	3388.1	3262.6	363.9	62.7	37.6	25.1	25.1	25.1
	102	10038.8	5019.4	4015.5	3513.6	5019.4	752.9	138.0	50.2	37.6	25.1	25.1
	103	10038.8	6274.2	4517.5	3639.1	3764.5	426.6	62.7	37.6	37.6	25.1	25.1
	104	8783.9	5019.4	3513.6	3137.1	5019.4	1505.8	313.7	100.4	75.3	50.2	50.2
	105	8783.9	5019.4	3764.5	3764.5	5019.4	1505.8	200.8	112.9	75.3	50.2	50.2
	106	10038.8	5019.4	4015.5	3513.6	5019.4	1254.8	251.0	100.4	62.7	37.6	37.6
17	107	8783.9	5019.4	3262.6	3262.6	5019.4	1003.9	213.3	75.3	37.6	25.1	25.1
	108	3262.6	1756.8	1254.8	1254.8	4141.0	3137.1	2509.7	2635.2	2133.2	1505.8	1192.1
	109	2258.7	1380.3	1003.9	1003.9	3639.1	2886.2	2509.7	2509.7	2007.8	1505.8	1505.8
	110	2635.2	1756.8	1129.4	1129.4	4015.5	3137.1	2760.7	2760.7	2133.2	1505.8	1254.8
	111	2258.7	1380.3	1003.9	1003.9	3137.1	2384.2	2133.2	2258.7	1756.8	1380.3	1129.4
	112	3639.1	2384.2	1505.8	1443.1	3764.5	3262.6	3011.6	2760.7	1756.8	1254.8	1003.9
	113	3639.1	2509.7	1756.8	1505.8	3764.5	3639.1	3262.6	2886.2	1882.3	1254.8	1003.9

TABLE 4A.3 Cumulative concentrations of SLS released (μg/ml)

Exp. No.	S/N	Day 1.	Day 3.	Day 5.	Day 7.	Day 14.	Day 21.	Day 28.	Day 35.	Day 42.	Day 49.	Day 56.
1	1	62.7	75.3	87.8	100.4	112.9	125.5	138.0	150.6	163.1	175.7	188.2
	2	100.4	125.5	150.6	163.1	175.7	188.2	200.8	213.3	238.4	251.0	263.5
	3	677.6	966.2	1242.3	1556.0	2300.9	2810.9	3312.8	3814.7	4316.7	4693.1	5057.0
	4	6274.2	10289.8	14305.3	17818.9	24093.1	26979.3	27857.7	28008.3	28083.5	28133.7	28171.4
	5	7529.1	11293.6	15058.2	18822.7	23842.1	27983.2	31998.7	35135.8	36516.1	37394.5	38022.0
2	6	25.1	37.6	50.2	62.7	75.3	87.8	100.4	112.9	125.5	138.0	150.6
	7	150.6	188.2	213.3	238.4	263.5	288.6	313.7	326.3	345.1	357.6	370.2
	8	2258.7	3262.6	4115.9	4919.0	7052.3	8558.1	9938.4	11067.8	12071.7	12824.6	13577.5
	9	11293.6	16940.5	21081.5	24971.5	30555.6	30969.7	31007.3	31032.4	31057.5	31070.1	31095.2
	10	16313.0	22587.3	28234.1	31873.2	33379.0	33529.6	33579.8	33617.4	33642.5	33655.1	33667.6
3	11	37.6	50.2	62.7	75.3	87.8	100.4	112.9	125.5	138.0	150.6	163.1
	12	163.1	213.3	263.5	301.2	338.8	376.5	414.1	439.2	464.3	489.4	514.5
	13	1505.8	2158.3	2610.1	3011.6	4015.5	4642.9	5270.4	5897.8	6399.7	6788.7	7165.2
	14	7529.1	11544.6	14807.2	18069.8	24344.1	26979.3	27481.2	27594.2	27644.3	27682.0	27707.1
	15	17567.9	25097.0	30743.8	34302.9	35512.3	35587.5	35612.6	35637.7	35650.3	35662.8	35675.4
4	16	8783.9	14430.8	18822.7	22085.4	25849.9	26477.3	26565.2	26615.4	26640.5	26665.6	26690.7
	17	10038.8	16062.1	20203.1	23591.2	27606.7	28008.3	28121.2	28158.8	28183.9	28209.0	28234.1
	18	8783.9	14681.7	19575.7	23465.7	27606.7	28045.9	28121.2	28158.8	28183.9	28209.0	28234.1
	19	8783.9	14932.7	18446.3	21583.4	25348.0	26226.4	26389.5	26452.2	26477.3	26502.4	26527.5
	20	8783.9	14807.2	18822.7	21959.9	25724.4	26477.3	26640.5	26690.7	26715.8	26740.9	26765.9
	21	10038.8	16313.0	21081.5	24595.1	28485.1	28911.7	28974.5	20999.6	29024.7	29037.2	29062.3
	22	6274.2	11168.2	14556.3	17066.0	22085.4	25222.5	26728.3	27401.2	27732.2	27820.0	27870.2
	23	8783.9	15058.2	19199.2	22712.8	27732.2	28610.6	28786.3	28849.0	28874.1	28899.2	28924.3
	24	7529.1	12799.5	16187.6	19701.1	24720.5	26477.3	26979.3	27104.8	27142.4	27167.5	27192.6
	25	7529.1	12925.0	16187.6	19450.2	24469.6	26477.3	27104.8	27293.0	27368.3	27405.9	27431.0
	26	7529.1	12548.5	15811.1	19073.7	24093.1	27104.8	28108.6	28359.6	28447.4	28497.6	28535.3
	27	7529.1	12674.0	16438.5	19952.1	24971.5	26853.8	27481.2	27619.2	27682.0	27707.1	27732.2
	28	5019.4	8031.0	10540.7	13301.4	18320.8	22461.8	24218.6	25473.5	25975.4	26188.7	26301.7
	29	7529.1	12046.6	15434.7	18320.8	23340.2	26100.9	27104.8	27393.4	27493.8	27544.0	27581.6
	30	8783.9	13803.3	17316.9	20328.6	25348.0	27606.7	28485.1	28736.1	28823.9	28861.5	28899.2
	31	6274.2	9411.4	11921.1	14179.8	19199.2	23214.7	26226.4	27606.7	28234.1	28497.6	28635.7
	32	7529.1	11795.6	15058.2	18195.3	23214.7	26602.8	28108.6	28610.6	28748.6	28811.4	28849.0
	33	6274.2	9411.4	12548.5	15434.7	21708.9	25049.9	28610.6	29363.5	29627.0	29739.9	29815.2
5	34	37.6	50.2	62.7	75.3	87.8	100.4	112.9	125.5	138.0	150.6	163.1
	35	87.8	100.4	112.9	125.5	138.0	150.6	163.1	175.7	188.2	200.8	213.3
	36	451.7	552.1	652.5	752.9	953.7	1066.6	1192.1	1305.0	1405.4	1505.8	1593.7
	37	5019.4	7152.6	9285.9	11670.1	16689.5	20454.1	24218.6	26477.3	27481.2	27857.7	28045.9
	38	12548.5	17944.4	24846.0	28861.5	33128.0	33466.8	33517.0	33554.7	33592.3	33617.4	33642.5
6	39	25.1	37.6	50.2	62.7	75.3	87.8	100.4	112.9	125.5	138.0	150.6
	40	37.6	50.2	62.7	75.3	87.8	100.4	112.9	125.5	138.0	150.6	163.1
	41	25.1	37.6	50.2	62.7	75.3	87.8	100.4	112.9	125.5	138.0	150.6
	42	37.6	50.2	62.7	75.3	87.8	100.4	112.9	125.5	138.0	150.6	163.1
7	43	702.7	1003.9	1305.0	1618.8	2497.2	3124.6	3626.5	4128.5	4630.4	5006.9	5395.9
	44	426.6	652.5	903.5	1154.5	1656.4	2058.0	2434.4	2760.7	3036.7	3275.2	3501.0
	45	627.4	928.6	1242.3	1543.5	2421.9	2923.8	3425.7	3927.7	4329.2	4668.0	4994.3
	46	803.1	1167.0	1543.5	1882.3	2760.7	3262.6	3764.5	4266.5	4760.4	5132.3	5471.1
	47	1505.8	2258.7	2936.3	3463.4	4843.7	5596.6	6349.5	7227.9	7980.8	8608.3	9235.7
	48	1882.3	2785.8	3563.8	4241.4	5872.7	6751.1	7504.0	8256.9	8884.3	9511.8	10013.7
8	49	112.9	138.0	163.1	188.2	213.3	238.4	263.5	276.1	288.6	301.2	313.7
	50	213.3	276.1	326.3	363.9	439.2	489.4	527.0	564.7	589.8	614.9	640.0
	51	251.0	313.7	363.9	401.6	451.7	489.4	527.0	552.1	577.2	589.8	602.3
	52	288.6	376.5	439.2	476.8	552.1	602.3	652.5	690.2	715.3	740.4	765.5
	53	577.2	727.8	815.7	890.9	1029.0	1104.3	1167.0	1217.2	1254.8	1292.5	1317.6
	54	652.5	815.7	941.1	1029.0	1204.7	1305.0	1392.9	1455.6	1505.8	1556.0	1593.7

9	55	7529.1	12172.0	15936.6	18822.7	25097.0	26979.3	27481.2	27581.6	27631.8	27656.9	27682.0
	56	8156.5	12540.5	15811.1	18195.3	21959.9	22712.8	22838.3	22888.5	22913.6	22938.7	22963.8
	57	10038.8	15183.7	18697.3	21457.9	25473.5	25862.5	25925.2	25962.8	25987.9	26013.0	26038.1
	58	11293.6	16815.0	20830.5	23465.7	25097.0	25260.1	25297.8	25335.4	25360.5	25385.6	25410.7
	59	13803.3	19952.1	23842.1	24720.5	25009.2	25059.4	25084.5	25109.5	25134.6	25159.7	25184.8
	60	17567.9	24344.1	26979.3	27481.2	27606.7	27644.3	27669.4	27707.1	27732.2	27757.3	27782.4
10	61	338.8	426.6	514.5	602.3	778.0	903.5	1029.0	1154.5	1267.4	1367.8	1455.6
	62	414.1	527.0	627.4	727.8	916.0	1041.5	1167.0	1279.9	1392.9	1493.3	1581.1
	63	527.0	665.1	778.0	890.9	1104.3	1242.3	1367.8	1493.3	1618.8	1719.1	1832.1
	64	652.5	828.2	978.8	1129.4	1455.6	1669.0	1857.2	2020.3	2170.9	2296.4	2434.4
	65	928.6	1229.8	1468.2	1694.0	2133.2	2421.9	2685.4	2961.4	3206.1	3406.9	3632.8
	66	1003.9	1342.7	1618.8	1882.3	2421.9	2760.7	3061.8	3363.0	3626.5	3827.3	4053.2
11	67	37.6	50.2	62.7	75.3	87.8	100.4	112.9	125.5	138.0	150.6	163.1
	68	37.6	50.2	62.7	75.3	87.8	100.4	112.9	125.5	138.0	150.6	163.1
	69	25.1	37.6	50.2	62.7	75.3	87.8	100.4	112.9	125.5	138.0	150.6
	70	25.1	37.6	50.2	62.7	75.3	87.8	100.4	112.9	125.5	138.0	150.6
	71	50.2	62.7	75.3	87.8	100.4	112.9	125.5	138.0	150.6	163.1	175.7
	72	50.2	62.7	75.3	87.8	100.4	112.9	125.5	138.0	150.6	163.1	175.7
12	73	37.6	50.2	62.7	75.3	87.8	100.4	112.9	125.5	138.0	150.6	163.1
	74	25.1	37.6	50.2	62.7	75.3	87.8	100.4	112.9	125.5	138.0	150.6
	75	25.1	37.6	50.2	62.7	75.3	87.8	100.4	112.9	125.5	138.0	150.6
	[illegible]	62.7	75.3	87.8	100.4	112.9	125.5	138.0	150.6	163.1	175.7	188.2
	[illegible]	50.2	62.7	75.3	87.8	100.4	112.9	125.5	138.0	150.6	163.1	175.7
	78	62.7	75.3	87.8	100.4	112.9	125.5	138.0	150.6	163.1	175.7	188.2
13	79	87.8	100.4	112.9	125.5	138.0	150.6	163.1	175.7	200.8	213.3	225.9
	80	138.0	150.6	163.1	175.7	188.2	200.8	225.9	251.0	276.1	288.6	301.2
	81	125.5	150.6	175.7	200.8	225.9	251.0	276.1	301.2	326.3	338.8	351.4
	82	112.9	138.0	163.1	188.2	213.3	238.4	263.5	288.6	313.7	326.3	338.8
	83	138.0	163.1	188.2	213.3	238.4	263.5	288.6	313.7	338.8	363.9	389.0
	84	125.5	150.6	163.1	188.2	213.3	238.4	263.5	301.2	326.3	351.4	376.5
	85	125.5	138.0	163.1	188.2	213.3	238.4	263.5	288.6	313.7	338.8	363.9
14	86	225.9	313.7	401.6	476.8	677.6	840.7	1003.9	1167.0	1330.1	1468.2	1631.3
	87	251.0	351.4	451.7	539.6	778.0	966.2	1154.5	1330.1	1518.4	1681.5	1869.7
	88	263.5	351.4	439.2	539.6	803.1	1003.9	1204.7	1405.4	1593.7	1769.3	1957.6
	89	338.8	451.7	552.1	652.5	903.5	1104.3	1305.0	1505.8	1706.6	1882.3	2083.1
	90	401.6	539.6	652.5	765.5	1054.1	1279.9	1505.8	1731.7	1970.1	2208.5	2472.1
	91	276.1	376.5	476.8	577.2	878.4	1154.5	1468.2	1807.0	2170.9	2509.7	2911.3
	92	8783.9	14305.3	18320.8	21457.9	26477.3	27606.7	27895.3	28008.3	28083.5	28133.7	28171.4
15	93	125.5	138.0	150.6	163.1	175.7	188.2	200.8	213.3	225.9	238.4	251.0
	94	100.4	112.9	125.5	138.0	163.1	188.2	200.8	213.3	225.9	238.4	251.0
	95	100.4	112.9	125.5	138.0	150.6	163.1	175.7	188.2	213.3	225.9	238.4
	96	100.4	112.9	125.5	138.0	163.1	188.2	200.8	213.3	225.9	238.4	251.0
	97	100.4	112.9	125.5	138.0	150.6	163.1	175.7	188.2	200.8	213.3	225.9
	98	112.9	125.5	150.6	163.1	175.7	200.8	213.3	238.4	251.0	263.5	276.1
	99	100.4	112.9	125.5	138.0	163.1	188.2	200.8	213.3	225.9	238.4	251.0
16	100	10038.8	15058.2	19450.2	22712.8	26477.3	26870.9	26966.7	27004.4	27042.0	27067.1	27092.2
	101	10038.8	15058.2	19826.6	23214.7	26477.3	26841.2	26904.0	26941.6	26966.7	26991.8	27016.9
	102	10038.8	15058.2	19073.7	22587.3	27606.7	28359.6	28497.6	28547.8	28585.5	28610.6	28635.7
	103	10038.8	16313.0	20830.5	24469.6	28234.1	28660.8	28723.5	28761.2	28798.8	28823.9	28849.0
	104	8783.9	13803.3	17316.9	20454.1	25473.5	26979.3	27293.0	27393.4	27468.7	27518.9	27569.1
	105	8783.9	13803.3	17567.9	21332.4	26351.8	27857.7	28050.4	28171.4	28246.7	28296.9	28347.1
	106	10038.8	15058.2	19073.7	22587.3	27606.7	28861.5	29112.5	29212.9	29275.6	29313.3	29350.9
17	107	8783.9	13803.3	17066.0	20328.6	25348.0	26351.8	26565.2	26640.5	26678.1	26703.2	26728.3
	108	3262.6	5019.4	6274.2	7529.1	11670.1	14807.2	17316.9	19952.1	22085.4	23591.2	24783.3
	109	2258.7	3639.1	4642.9	5646.8	9285.9	12172.0	14681.7	17191.4	19199.2	20705.0	22210.8
	110	2635.2	4392.0	5521.3	6650.7	10666.2	13803.3	16564.0	19324.7	21457.9	22963.8	24218.6
	111	2258.7	3639.1	4642.9	5646.8	8783.9	11160.2	13301.4	15560.1	17316.9	18697.3	19826.6
	112	3639.1	6023.3	7529.1	8972.2	12736.7	15999.3	19011.0	21771.6	23528.4	24783.3	25787.2
	113	3639.1	6148.8	7905.6	9411.4	13175.9	16815.0	20077.6	22963.8	24846.0	26100.9	27104.8

TABLE 4A.4 Cumulative amounts of SLS released (μg)

Exp. No.	S/N	Day 1.	Day 3.	Day 5.	Day 7.	Day 14.	Day 21.	Day 28.	Day 35.	Day 42.	Day 49.	Day 56.
1	1	3137	3765	4392	5019	5647	6274	6902	7529	8157	8784	9411
	2	5019	6274	7529	8157	8784	9411	10039	10666	11921	12548	13176
	3	33881	48312	62115	77001	115446	140543	165640	190737	215834	234657	252852
	4	313712	514488	715264	890943	1204656	1348964	1392883	1400413	1404177	1406687	1408569
	5	376455	564682	752910	941137	1192107	1399158	1599934	1756790	1825807	1869726	1901098
2	6	1255	1882	2510	3137	3765	4392	5019	5647	6274	6902	7529
	7	7529	9411	10666	11921	13176	14431	15686	16313	17254	17882	18509
	8	112936	163130	205795	245951	352613	427904	496921	553389	603583	641228	678874
	9	564682	847024	1054074	1248576	1527780	1548485	1550367	1551622	1552877	1553504	1554759
	10	815652	1129365	1411706	1593659	1668950	1676480	1678989	1680871	1682126	1682754	1683381
3	11	1882	2510	3137	3765	4392	5019	5647	6274	6902	7529	8157
	12	8157	10666	13176	15058	16940	18823	20705	21960	23215	24470	25724
	13	75291	107917	130504	150582	200776	232147	263518	294890	319987	339437	358260
	14	376455	577231	740361	903492	1217204	1348964	1374061	1379708	1382217	1384099	1385354
	15	878395	1254850	1537191	1719144	1775613	1779377	1780632	1781887	1782514	1783142	1783769
4	16	439197	721539	941137	1104268	1292495	1323867	1328259	1330768	1332023	1333278	1334533
	17	501940	803104	1010154	1179559	1380335	1400413	1406059	1407942	1409196	1410451	1411706
	18	439197	734087	978783	1173285	1380335	1402295	1406059	1407942	1409196	1410451	1411706
	19	439197	746636	922315	1079171	1267398	1311318	1319475	1322612	1323867	1325122	1326376
	20	439197	740361	941137	1097994	1286221	1323867	1332023	1334533	1335788	1337043	1338297
	21	501940	815652	1054074	1229753	1424255	1445587	1448724	1449979	1451234	1451861	1453116
	22	313712	558408	727813	853298	1104268	1261124	1336415	1374061	1386609	1391001	1393511
	23	439197	752910	959960	1135639	1386609	1430529	1439313	1442450	1443705	1444960	1446215
	24	376455	639973	809378	985057	1236027	1323867	1348964	1355238	1357120	1358375	1359630
	25	376455	646248	809378	972509	1223479	1323867	1355238	1364649	1368414	1370296	1371551
	26	376455	627425	790555	953686	1204656	1355238	1405432	1417980	1422372	1424882	1426764
	27	376455	633699	821927	997606	1248576	1342689	1374061	1380962	1384099	1385354	1386609
	28	250970	401552	527037	665070	916040	1123091	1210930	1273673	1298770	1309436	1315083
	29	376455	602328	771733	916040	1167010	1305044	1355238	1369669	1374688	1377198	1379080
	30	439197	690167	865846	1016428	1267398	1380335	1424255	1436803	1441195	1443077	1444960
	31	313712	470569	596054	708990	959960	1160736	1311318	1380335	1411706	1424882	1431784
	32	376455	589779	752910	909766	1160736	1330141	1405432	1430529	1437431	1440568	1442450
	33	313712	470569	627425	771733	1005445	1292495	1430529	1468174	1481350	1486997	1490762
5	34	1882	2510	3137	3765	4392	5019	5647	6274	6902	7529	8157
	35	4392	5019	5647	6274	6902	7529	8157	8784	9411	10039	10666
	36	22587	27607	32626	37645	47684	53331	59605	65252	70272	75291	79683
	37	250970	357632	464294	583505	834475	1022703	1210930	1323867	1374061	1392883	1402295
	38	627425	897218	1242301	1443077	1656402	1673342	1675852	1677734	1679617	1680871	1682126
6	39	1255	1882	2510	3137	3765	4392	5019	5647	6274	6902	7529
	40	1882	2510	3137	3765	4392	5019	5647	6274	6902	7529	8157
	41	1255	1882	2510	3137	3765	4392	5019	5647	6274	6902	7529
	42	1882	2510	3137	3765	4392	5019	5647	6274	6902	7529	8157
7	43	35136	50194	65252	80938	124858	156229	181326	206423	231520	250343	269793
	44	21332	32626	45175	57723	82820	102898	121720	138033	151837	163758	175052
	45	31371	46429	62115	77173	121093	146190	171287	196384	216462	233402	249715
	46	40155	58351	77173	94114	138033	163130	188227	213324	238421	256617	273557
	47	75291	112936	146817	173169	242186	279832	317477	361397	399042	430414	461785
	48	94114	139288	178189	212070	293635	337555	375200	412846	444217	475588	500685
8	49	5647	6902	8157	9411	10666	11921	13176	13803	14431	15058	15686
	50	10666	13803	16313	18195	21960	24470	26352	28234	29489	30744	31999
	51	12548	15686	18195	20078	22587	24470	26352	27607	28862	29489	30116
	52	14431	18823	21960	23842	27607	30116	32626	34508	35763	37018	38273
	53	28862	36391	40783	44547	51449	55213	58351	60860	62742	64625	65880
	54	32626	40783	47057	51449	60233	65252	69644	72781	75291	77801	79683

9	55	376455	608602	796830	941137	1254850	1348964	1374061	1379080	1381590	1382845	1384099
	56	407826	627425	790555	909766	1097994	1135639	1141913	1144423	1145678	1146933	1148188
	57	501940	759184	934863	1072897	1273673	1293123	1296260	1298142	1299397	1300652	1301907
	58	564682	840749	1041525	1173285	1254850	1263006	1264889	1266771	1268026	1269281	1270536
	59	690167	997606	1192107	1236027	1250458	1252968	1254223	1255477	1256732	1257987	1259242
	60	878395	1217204	1348964	1374061	1380335	1382217	1383472	1385354	1386609	1387864	1389119
10	61	16940	21332	25724	30116	38900	45175	51449	57723	63370	68389	72781
	62	20705	26352	31371	36391	45802	52076	58351	63997	69644	74664	79056
	63	26352	33254	38900	44547	55213	62115	68389	74664	80938	85957	91604
	64	32626	41410	48939	56468	72781	83448	92859	101015	108545	114819	121720
	65	46429	61488	73409	84702	106662	121093	134269	148072	160307	170346	181640
	66	50194	67134	80938	94114	121093	138033	153092	168150	181326	191365	202658
11	67	1882	2510	3137	3765	4392	5019	5647	6274	6902	7529	8157
	6	1882	2510	3137	3765	4392	5019	5647	6274	6902	7529	8157
	69	1255	1882	2510	3137	3765	4392	5019	5647	6274	6902	7529
	70	1255	1882	2510	3137	3765	4392	5019	5647	6274	6902	7529
	71	2510	3137	3765	4392	5019	5647	6274	6902	7529	8157	8784
	72	2510	3137	3765	4392	5019	5647	6274	6902	7529	8157	8784
12	73	1882	2510	3137	3765	4392	5019	5647	6274	6902	7529	8157
	74	1255	1882	2510	3137	3765	4392	5019	5647	6274	6902	7529
	75	1255	1882	2510	3137	3765	4392	5019	5647	6274	6902	7529
	76	3137	3765	4392	5019	5647	6274	6902	7529	8157	8784	9411
	77	2510	3137	3765	4392	5019	5647	6274	6902	7529	8157	8784
	78	3137	3765	4392	5019	5647	6274	6902	7529	8157	8784	9411
13	79	4392	5019	5647	6274	6902	7529	8157	8784	10039	10666	11294
	80	6902	7529	8157	8784	9411	10039	11294	12548	13803	14431	15058
	81	6274	7529	8784	10039	11294	12548	13803	15058	16313	16940	17568
	82	5647	6902	8157	9411	10666	11921	13176	14431	15686	16313	16940
	83	6902	8157	9411	10666	11921	13176	14431	15686	16940	18195	19450
	84	6274	7529	8157	9411	10666	11921	13176	15058	16313	17568	18823
	85	6274	6902	8157	9411	10666	11921	13176	14431	15686	16940	18195
14	86	11294	15686	20078	23842	33881	42037	50194	58351	66507	73409	81565
	87	12548	17568	22587	26979	38900	48312	57723	66507	75918	84075	93486
	88	13176	17568	21960	26979	40155	50194	60233	70272	79683	88467	97878
	89	16940	22587	27607	32626	45175	55213	65252	75291	85330	94114	104153
	90	20078	26979	32626	38273	52704	63997	75291	86585	98506	110427	123603
	91	13803	18823	23842	28862	43920	57723	73409	90349	108545	125485	145563
	92	439197	715264	916040	1072897	1323867	1380335	1394766	1400413	1404177	1406687	1408569
15	93	6274	6902	7529	8157	8784	9411	10039	10666	11294	11921	12548
	94	5019	5647	6274	6902	8157	9411	10039	10666	11294	11921	12548
	95	5019	5647	6274	6902	7529	8157	8784	9411	10666	11294	11921
	96	5019	5647	6274	6902	8157	9411	10039	10666	11294	11921	12548
	97	5019	5647	6274	6902	7529	8157	8784	9411	10039	10666	11294
	98	5647	6274	7529	8157	8784	10039	10666	11921	12548	13176	13803
	99	5019	5647	6274	6902	8157	9411	10039	10666	11294	11921	12548
16	100	501940	752910	972509	1135639	1323867	1343944	1348336	1350219	1352101	1353356	1354611
	101	501940	752910	991331	1160736	1323867	1342062	1345199	1347081	1348336	1349591	1350846
	102	501940	752910	953686	1129365	1380335	1417980	1424882	1427392	1429274	1430529	1431784
	103	501940	815652	1041525	1223479	1411706	1433039	1436176	1438058	1439940	1441195	1442450
	104	439197	690167	865846	1022703	1273673	1348964	1364649	1369669	1373433	1375943	1378453
	105	439197	690167	878395	1066622	1317592	1392883	1402922	1408569	1412334	1414843	1417353
	106	501940	752910	953686	1129365	1380335	1443077	1455626	1460645	1463782	1465665	1467547
17	107	439197	690167	853298	1016428	1267398	1317592	1328259	1332023	1333905	1335160	1336415
	108	163130	250970	313712	376455	583505	740361	865846	997606	1104268	1179559	1239164
	109	112936	181953	232147	282341	464294	608602	734087	859572	959960	1035251	1110542
	110	131759	219599	276067	332535	533311	690167	828201	966234	1072897	1148188	1210930
	111	112936	181953	232147	282341	439197	558408	665070	778007	865846	934863	991331
	112	181953	301164	376455	448609	636836	799967	950549	1080582	1176422	1239164	1289358
	113	181953	307438	395278	470569	658796	840749	1003080	1148188	1242301	1305044	1355238

APPENDIX 4B

The Pascal Source Code POLI

```
program poli;
const ns = 113; nm = 11; half = 0.5; zero=0.0; izero=0;
type points = array[1..nm] of real;

var datafil                          : text;
    dbeg,dend                        : integer;
    q,i,j,k                          : integer;
    pg0,pg1                          : byte;
    x,logx,sqrtx                     : points;
    logy,sf,sf1,xl,xr,yr,sdx,sdy     : real;
    y                                : array[1..ns] of points;
    sx,sx2,sy,sy2,sxy,ax,ax2         : real;
    lx,lx2,ly,ly2,lxy                : real;
    sam,sm,sc,lm,lc,ccl,ccs,cca      : array[1..ns] of real;
    sam1,sm1,sc1,lm1,lc1             : real;

{$i HGCprs.pas}
procedure Setup;
var x,y : integer;
    mes : string[255];

begin
Gmode;
disp(pg1);
gpage(pg1);
ClrScr;
x :=  10;
y :=   0;
move(x,y);
y := 300;
dline(x,y);
x := 720;
dline(x,y);
x :=  10;
y := 340;
mes := 'Type RETURN to continue';
textst(x,y,mes);
end;

procedure Model(a,b,c:real);
var i,x,y : integer;
    x1,y1 : real;

begin
x := 10;
y := 300;
move(x,y);
for i:=1 to 20 do begin
  x1 := i*xl/700.0;
  y1 := a*exp(b*ln(x1)) + c;
  x  := i + 10;
  y  := trunc(300*(1 - y1/sf));
  dline(x,y);
  end;
for i:=3 to 70 do begin
  x1 := i*xl/70.0;
  y1 := a*exp(b*ln(x1)) + c;
  x  := 10*i + 10;
  y  := trunc(300*(1 - y1/sf));
  if y>347 then y:=347;
  if y<0   then y:=0;
  dline(x,y);
  end;
end;
```

```
procedure Plotpoints(i:integer);
var x0,y0,x1,y1,j : integer;
begin
for j:=1 to nm do begin
  x0 := 10 + trunc(700*x[j]/x1);
  y0 := trunc(300*(1 - y[i,j]/sf));
  x1 := x0 - 2;
  y1 := y0 - 2;
  move(x1,y1);
  x1 := x0 + 2;
  y1 := y0 + 2;
  dline(x1,y1);
  x1 := x0 + 2;
  y1 := y0 - 2;
  move(x1,y1);
  x1 := x0 - 2;
  y1 := y0 + 2;
  dline(x1,y1);
  end;
end;

procedure writedays;
var k : integer;
begin
for k:=dbeg to dend do
  write(datafil,' ',k);
writeln(datafil);
end;

procedure writemeas;
var k,l : integer;
begin
l := 1;
while x[l] < dbeg do l:=l+1;
for k:=dbeg to dend do
  if k = x[l] then begin
    write(datafil,y[i,l]:12:2);
    l := l+1;
    end
  else write(datafil,' "" ');
writeln(datafil);
end;

procedure writeav;
var k : integer;
begin
for k:=dbeg to dend do
  write(datafil,sam[i]*sqrt(k):12:2);
writeln(datafil);
end;

procedure writesqrt;
var k : integer;
begin
for k:= dbeg to dend do
  write(datafil,sm[i]*sqrt(k) + sc[i]:12:2);
writeln(datafil);
end;

procedure writelog;
var k : integer;
begin
for k:=dbeg to dend do
  write(datafil,lc[i]*exp(lm[i]*ln(k)):12:2);
writeln(datafil);
end;

begin
pg0 := 0;
pg1 := 1;
x[1]  := 1;
x[2]  := 3;
x[3]  := 5;
x[4]  := 7;
x[5]  := 14;
```

```
x[6]  := 21;
x[7]  := 28;
x[8]  := 35;
x[9]  := 42;
x[10] := 49;
x[11] := 56;
xl  := x[nm];
sx  := 0;
sx2 := 0;
lx  := 0;
lx2 := 0;
for i:=1 to nm do
  begin
  sqrtx[i] := sqrt(x[i]);
  sx       := sx  + sqrtx[i];
  sx2      := sx2 + x[i];
  logx[i]  := ln(x[i]);
  lx       := lx  + logx[i];
  lx2      := lx2 + logx[i]*logx[i];
  end;

assign(datafil,'CUMSLSPG.DAT');
reset(datafil);
sf := 0;
for i:=1 to ns do
begin
  read(datafil,k);
  if i<>k then writeln('Error in line ',i,'.  Sample number is ',k);
  for j:=1 to nm do
    read(datafil,y[i,j]);
  readln(datafil);
  writeln('Reading sample ',i);
  ax  := 0;
  ax2 := 0;
  sy  := 0;
  sy2 := 0;
  sxy := 0;
  ly  := 0;
  ly2 := 0;
  lxy := 0;
  for j:=1 to nm do
    begin
    if sf < y[i,j] then sf := y[i,j];
    ax   := ax  + y[i,j]/sqrtx[j];
    ax2  := ax2 + y[i,j]*y[i,j]/x[j];
    sy   := sy  + y[i,j];
    sy2  := sy2 + y[i,j]*y[i,j];
    sxy  := sxy + y[i,j]*sqrtx[j];
    logy := ln(y[i,j]);
    ly   := ly  + logy;
    ly2  := ly2 + logy*logy;
    lxy  := lxy + logy*logx[j];
  end;
  sam[i] := ax/nm;
  sm[i]  := (sxy - sx*sy/nm)/(sx2 - sx*sx/nm);
  sc[i]  := (sy - sm[i]*sx)/nm;
  lm[i]  := (lxy - lx*ly/nm)/(lx2 - lx*lx/nm);
  lc[i]  := (ly - lm[i]*lx)/nm;
  lc[i]  := exp(lc[i]);
  cca[i] := sqrt((ax2 - ax*ax/nm)/(nm-1)) / sam[i];
  sdx    := sqrt((sx2 - sx*sx/nm)/(nm-1));
  sdy    := sqrt((sy2 - sy*sy/nm)/(nm-1));
  ccs    := sm[i]*sdx/sdy;
  sdx    := sqrt((lx2 - lx*lx/nm)/(nm-1));
  sdy    := sqrt((ly2 - ly*ly/nm)/(nm-1));
  ccl[i] := lm[i]*sdx/sdy;
  end;
  sf := 10.0 * trunc(sf/10 + 1);
close(datafil);
repeat
  writeln; writeln;
  writeln('Do you want to:');
  writeln('    0 - Stop');
  writeln('    1 - Compare models');
  writeln('    2 - Compare samples');
  writeln('    3 - Print parameters');
  writeln('    4 - Print day datafile');
```

```
readln(q);
if q=1 then begin
  writeln('Compare models selected');
  repeat
  writeln('Enter sample no (0 to stop, <0 for average)');
  readln(i);
  j := i;
  if (i<=-1) and (i>=-ns) then begin
    i := -i;
    writeln('Enter end of averaging range sample no');
    readln(j);
    end;
  if (i>=1) and (i<=ns) and (j>=1) and (j<=ns) and (i<=j) then begin
    sam1 := 0;
    sm1  := 0;
    sc1  := 0;
    lm1  := 0;
    lc1  := 0;
    for k:=i to j do begin
      sam1 := sam1 + sam[k];
      sm1  := sm1  + sm[k];
      sc1  := sc1  + sc[k];
      lm1  := lm1  + lm[k];
      lc1  := lc1  + lc[k];
      end;
    k := j - i + 1;
    sam1 := sam1 / k;
    sm1  := sm1  / k;
    sc1  := sc1  / k;
    lm1  := lm1  / k;
    lc1  := lc1  / k;
    sf  := sqrt(x1)*sam1;
    sf1 := sqrt(x1)*sm1 + sc1;
    if sf<sf1 then sf := sf1;
    sf1 := lc1*exp(lm1*ln(x1));
    if sf<sf1 then sf := sf1;
    Setup;
    if i=j then Plotpoints(i);
    Model(sam1,half,zero);
    Model(sm1,half,sc1);
    Model(lc1,lm1,zero);
    read(k);
    Tmode;
    if i=j then writeln('Sample ',i)
           else writeln('Samples ',i,' to ',j);
    writeln('Maximum value ',sf:7:1);
    writeln('Av  S',cca[i]:7:3,sam1:16:2,' x^ ',0.5:5:3);
    writeln('Sq  R',ccs[i]:7:3, sm1:16:2,' x^ ',0.5:5:3,' + ',sc1:16:2);
    writeln('Ln  R',ccl[i]:7:3, lc1:16:2,' x^ ',lm1:5:3);
    end;
    until i=0;
    end;
  if q=2 then begin
  writeln('Compare samples selected');
  repeat
    writeln('Which model?:  1  -  Averaging');
    writeln('               2  -  Square root');
    writeln('               3  -  Logarithmic');
    readln(j);
    until j in [1,2,3];
  repeat
  writeln('Enter sample no (0 to stop, <0 for overlay)');
  readln(i);
  if (-ns<=i) and (i<=ns) and (i<>0) then begin
    k := abs(i);
    sam1 := sam[k];
    sm1  := sm[k];
    sc1  := sc[k];
    lm1  := lm[k];
    lc1  := lc[k];
    if i>0 then begin
      sf  := sqrt(x1)*sam1;
      sf1 := sqrt(x1)*sm1 + sc1;
      if sf<sf1 then sf := sf1;
      sf1 := lc1*exp(lm1*ln(x1));
      if sf<sf1 then sf := sf1;
      Setup;
      end
```

```
    else begin i:=-i; Gmode; disp(pg1); gpage(pg1); end;
    case j of
    1 : Model(sam1,half,zero);
    2 : Model(sm1,half,sc1);
    3 : Model(lc1,lm1,zero);
    end;
    read(k);
    disp(pg0);
    Tmode;
    writeln('Sample ',i);
    writeln('Av  S',cca[i]:7:3,sam1:16:2,' x^ ',0.5:5:3);
    writeln('Sq  R',ccs[i]:7:3, sm1:16:2,' x^ ',0.5:5:3,' + ',sc1:16:2);
    writeln('Ln  R',ccl[i]:7:3, lc1:16:2,' x^ ',lm1:5:3);
    end;
  until i=0;
  end;
if q=3 then begin
    writeln(lst,'Parameters');
    writeln(lst);
    writeln(lst,' No       Average                ',
            'Square Root                Logarithmic');
    writeln(lst,'              a      S/a          a          ',
            '  c     R             a     b      R');
    for i:=1 to ns do
      writeln(lst,i:3,sam[i]:12:2,cca[i]:8:3,sm[i]:12:2,sc[i]:12:2,
                  ccs[i]:7:3,lc[i]:12:2,lm[i]:7:3,ccl[i]:7:3);
    end;
if q=4 then begin
    writeln;
    writeln('Place disk containing space for');
    writeln('files SLS*.PRN in default drive.');
    writeln('Type RETURN to continue.');
    readln(i);

    assign(datafil,'SLS1.PRN');
    writeln('SLS1.PRN');
    rewrite(datafil);

    dbeg := 1;
    dend := 18;
    write(datafil,'"Day"',izero:12);
    Writedays;
    for i:=1 to 60 do begin
      writeln('Sample ',i);
      write(datafil,i:5,zero:12:2);
      Writemeas;
      write(datafil,'"Av"  ',zero:12:2);
      Writeav;
      write(datafil,'"Sqrt"',sc[i]:12:2);
      Writesqrt;
      write(datafil,'"Log" ',zero:12:2);
      Writelog;
      end;
    close(datafil);

    assign(datafil,'SLS2.PRN');
    writeln('SLS2.PRN');
    rewrite(datafil);

    dbeg := 19;
    dend := 37;
    Writedays;
    for i:=1 to 60 do begin
      writeln('Sample ',i);
      Writemeas;
      Writeav;
      Writesqrt;
      Writelog;
      end;
    close(datafil);

    assign(datafil,'SLS3.PRN');
    writeln('SLS3.PRN');
    rewrite(datafil);
```

```
        dbeg := 38;
        dend := 56;
        Writedays;
      for i:=1 to 60 do begin
        writeln('Sample ',i);
        Writemeas;
        Writeav;
        Writesqrt;
        Writelog;
        end;
      close(datafil);

      assign(datafil,'SLS4.PRN');
      writeln('SLS4.PRN');
      rewrite(datafil);

      dbeg := 1;
      dend := 18;
      write(datafil,'"Day" ',izero:12);
      Writedays;
      for i:=61 to ns do begin
        writeln('Sample ',i);
        write(datafil,i:5,zero:12:2);
        Writemeas;
        write(datafil,'"Av"  ',zero:12:2);
        Writeav;
        write(datafil,'"Sqrt"',sc[i]:12:2);
        Writesqrt;
        write(datafil,'"Log" ',zero:12:2);
        Writelog;
        end;
      close(datafil);

      assign(datafil,'SLS5.PRN');
      writeln('SLS5.PRN');
      rewrite(datafil);

      dbeg := 19;
      dend := 37;
      Writedays;
      for i:=61 to ns do begin
        writeln('Sample ',i);
        Writemeas;
        Writeav;
        Writesqrt;
        Writelog;
        end;
      close(datafil);

      assign(datafil,'SLS6.PRN');
      writeln('SLS6.PRN');
      rewrite(datafil);

        dbeg := 38;
        dend := 56;
        Writedays;
      for i:=61 to ns do begin
        writeln('Sample ',i);
        Writemeas;
        Writeav;
        Writesqrt;
        Writelog;
        end;
      close(datafil);
      end;
    until q=0;
end .
```

APPENDIX 4C

Standard Deviations and Correlation Coefficients

Sample Number	AVERAGE MODEL		SQUARE-ROOT MODEL			LOGARITHMIC MODEL		
	a_1[a]	S/a_1[b]	a_2[c]	C[d]	R[e]	a_3[f]	b[g]	R[e]
1	33.45	0.352	18.43	44.86	0.996	58.19	0.272	0.990
2	51.97	0.406	22.71	88.91	0.987	100.14	0.226	0.989
3	626.62	0.072	692.25	-231.59	0.998	586.57	0.524	0.995
4	5435.45	0.196	3363.33	7109.65	0.922	7355.33	0.378	0.966
5	6220.03	0.118	4898.47	4357.45	0.989	7668.47	0.418	0.996
6	20.87	0.100	18.43	7.22	0.996	24.61	0.436	0.997
7	76.95	0.410	32.21	136.91	0.992	149.61	0.222	0.999
8	1895.70	0.065	1805.43	253.43	0.999	2061.70	0.467	0.998
9	7214.22	0.347	2691.84	14688.31	0.861	13429.96	0.242	0.938
10	8799.23	0.462	2025.07	21513.91	0.784	19549.01	0.160	0.891
11	25.06	0.208	18.43	19.77	0.996	35.57	0.360	0.995
12	95.77	0.314	51.16	137.86	0.993	163.66	0.281	0.997
13	1095.60	0.150	877.69	658.23	1.000	1425.26	0.396	0.999
14	5620.01	0.235	3091.45	8423.08	0.918	8511.29	0.332	0.968
15	9470.56	0.473	2010.20	23674.57	0.761	21432.41	0.151	0.875
16	6143.02	0.336	2325.81	12521.22	0.850	11109.75	0.254	0.924
17	6634.53	0.356	2346.16	13958.57	0.847	12493.47	0.236	0.925
18	6418.93	0.324	2532.87	12837.35	0.845	11257.31	0.267	0.921
19	6107.73	0.339	2304.43	12436.76	0.860	11131.92	0.251	0.929
20	6160.82	0.337	2327.34	12560.15	0.854	11174.12	0.252	0.926
21	6817.37	0.352	2424.45	14353.06	0.838	12698.84	0.241	0.918
22	5342.09	0.198	3264.40	6995.90	0.946	7491.16	0.364	0.975
23	6460.83	0.310	2695.72	12430.83	0.867	11132.58	0.275	0.934
24	5761.12	0.268	2801.83	9836.94	0.899	9224.33	0.307	0.953
25	5767.19	0.264	2851.45	9678.12	0.907	9193.59	0.310	0.957
26	5798.86	0.239	3127.42	8877.25	0.926	8879.47	0.327	0.969
27	5824.59	0.262	2896.08	9755.55	0.902	9196.28	0.313	0.955
28	4485.66	0.117	3484.73	3471.22	0.969	5323.25	0.432	0.989
29	5623.69	0.244	3004.97	8665.59	0.928	8721.22	0.322	0.971
30	6150.27	0.282	2933.36	10533.62	0.917	10238.67	0.292	0.966
31	4952.07	0.140	3691.69	4163.13	0.978	6362.98	0.401	0.994
32	5683.22	0.220	3293.22	7917.10	0.943	8454.49	0.340	0.978
33	5251.90	0.137	3893.71	4641.68	0.962	6523.45	0.414	0.986
34	25.06	0.208	18.43	19.77	0.996	35.57	0.360	0.995
35	41.84	0.439	18.43	69.96	0.996	81.48	0.220	0.986
36	265.94	0.269	176.36	267.93	0.999	408.43	0.326	0.994
37	4332.44	0.078	3938.64	1351.40	0.987	4691.23	0.469	0.994
38	7961.20	0.365	2758.84	16908.37	0.835	15131.70	0.232	0.920
39	20.87	0.100	18.43	7.22	0.996	24.61	0.436	0.997
40	25.06	0.208	18.43	19.77	0.996	35.57	0.360	0.995
41	20.87	0.100	18.43	7.22	0.996	24.61	0.436	0.997
42	25.06	0.208	18.43	19.77	0.996	35.57	0.360	0.995
43	669.18	0.079	748.20	-268.67	0.999	606.82	0.536	0.996
44	442.41	0.068	487.77	-146.11	0.999	394.00	0.543	0.998
45	627.40	0.076	697.90	-231.21	0.999	559.31	0.543	0.997
46	723.73	0.046	734.79	-48.06	0.999	731.71	0.495	0.998
47	1278.64	0.067	1184.57	274.30	0.999	1432.22	0.456	0.999
48	1510.17	0.107	1255.47	806.14	0.998	1837.85	0.423	0.999
49	61.06	0.354	30.40	94.06	0.993	109.17	0.260	0.997
50	121.80	0.323	64.29	177.42	0.994	209.95	0.277	0.999
51	129.17	0.409	52.26	236.89	0.986	252.77	0.219	0.999
52	156.36	0.375	70.01	266.47	0.989	292.46	0.240	0.999
53	290.50	0.429	108.97	559.23	0.982	585.30	0.206	0.999
54	337.90	0.401	140.45	608.62	0.986	653.14	0.225	0.999
55	5742.02	0.250	2972.10	9234.86	0.906	8915.31	0.321	0.960
56	5294.64	0.344	2000.01	10700.63	0.871	9807.29	0.244	0.941
57	6202.04	0.374	2099.02	13241.58	0.855	12069.27	0.222	0.933
58	6491.37	0.437	1645.85	15488.23	0.796	13925.64	0.176	0.894
59	7027.63	0.523	1099.03	18653.24	0.696	17034.53	0.117	0.826
60	8123.23	0.580	898.85	22457.12	0.654	21007.02	0.084	0.795

61	220.28	0.197	173.98	133.42	0.999	298.76	0.378	0.993
62	256.60	0.239	179.30	231.12	1.000	379.00	0.343	0.995
63	310.27	0.278	197.81	338.37	0.999	488.22	0.316	0.996
64	402.66	0.241	276.61	380.44	0.999	597.71	0.341	0.996
65	591.73	0.230	410.08	549.03	0.999	872.32	0.344	0.998
66	659.93	0.211	468.42	584.22	0.999	946.95	0.356	0.998
67	25.06	0.208	18.43	19.77	0.996	35.57	0.360	0.995
68	25.06	0.208	18.43	19.77	0.996	35.57	0.360	0.995
69	20.87	0.100	18.43	7.22	0.996	24.61	0.436	0.997
70	20.87	0.100	18.43	7.22	0.996	24.61	0.436	0.997
71	29.26	0.290	18.43	32.31	0.996	46.77	0.309	0.992
72	29.26	0.290	18.43	32.31	0.996	46.77	0.309	0.992
73	25.06	0.208	18.43	19.77	0.996	35.57	0.360	0.995
74	20.87	0.100	18.43	7.22	0.996	24.61	0.436	0.997
75	20.87	0.100	18.43	7.22	0.996	24.61	0.436	0.997
76	33.45	0.352	18.43	44.86	0.996	58.19	0.272	0.990
77	29.26	0.290	18.43	32.31	0.996	46.77	0.309	0.992
78	33.45	0.352	18.43	44.86	0.996	58.19	0.272	0.990
79	42.33	0.425	20.38	64.87	0.990	79.98	0.233	0.977
80	60.69	0.495	25.26	103.97	0.986	123.00	0.199	0.957
81	66.43	0.360	34.67	95.90	0.997	117.82	0.263	0.994
82	62.24	0.332	34.67	83.35	0.997	106.27	0.280	0.995
83	71.10	0.377	36.87	102.27	0.996	127.92	0.256	0.989
84	65.19	0.361	37.70	80.36	0.993	112.20	0.275	0.980
85	63.85	0.367	36.03	81.97	0.995	110.53	0.273	0.982
86	195.57	0.086	216.02	-77.80	0.994	190.96	0.508	0.992
87	222.36	0.085	248.66	-97.34	0.994	212.58	0.516	0.993
88	229.63	0.105	264.50	-126.69	0.993	213.11	0.527	0.990
89	262.49	0.107	267.93	-36.75	0.994	284.33	0.468	0.990
90	307.49	0.114	312.26	-40.13	0.991	337.95	0.462	0.989
91	279.72	0.217	397.29	-409.73	0.975	205.46	0.610	0.981
92	6233.68	0.307	2665.79	11726.70	0.882	10759.87	0.275	0.945
93	54.42	0.519	18.43	107.60	0.996	117.19	0.172	0.982
94	48.64	0.412	23.49	75.21	0.999	90.35	0.241	0.988
95	46.53	0.457	20.38	77.42	0.990	91.68	0.214	0.974
96	48.64	0.412	23.49	75.21	0.999	90.35	0.241	0.988
97	46.03	0.470	18.43	82.51	0.996	93.30	0.201	0.984
98	54.46	0.426	24.86	88.62	0.996	104.03	0.229	0.986
99	48.64	0.412	23.49	75.21	0.999	90.35	0.241	0.988
100	6388.91	0.362	2236.64	13471.31	0.848	12161.32	0.231	0.928
101	6415.73	0.367	2188.71	13725.44	0.837	12283.54	0.228	0.921
102	6536.58	0.335	2562.99	12936.07	0.871	11899.05	0.252	0.943
103	6775.27	0.354	2396.02	14293.75	0.839	12672.46	0.239	0.919
104	6051.46	0.303	2654.42	11122.78	0.894	10434.91	0.276	0.954
105	6186.19	0.296	2764.70	11255.31	0.889	10487.97	0.283	0.951
106	6594.81	0.324	2705.70	12665.55	0.885	11796.79	0.260	0.950
107	5965.48	0.314	2505.16	11315.84	0.883	10491.36	0.267	0.949
108	3172.48	0.070	3504.25	-1117.90	0.998	2901.17	0.533	0.997
109	2570.66	0.145	3235.20	-2182.83	0.997	1956.80	0.600	0.996
110	2931.03	0.116	3522.85	-1935.06	0.998	2364.64	0.579	0.997
111	2408.32	0.099	2833.33	-1406.26	0.998	2022.03	0.565	0.997
112	3514.55	0.031	3585.94	-248.85	0.998	3477.75	0.504	0.999
113	3666.62	0.035	3806.35	-448.53	0.998	3522.29	0.515	0.999

(a) See Equation (4.8)

(b) Standard deviation / a_1

(c) See Equation (4.9)

(d) See Equation (4.9)

(e) Correlation coefficient

(f) See Equation (4.10)

APPENDIX 5A

Plots of the Fraction of SLS Released as a Function of Time

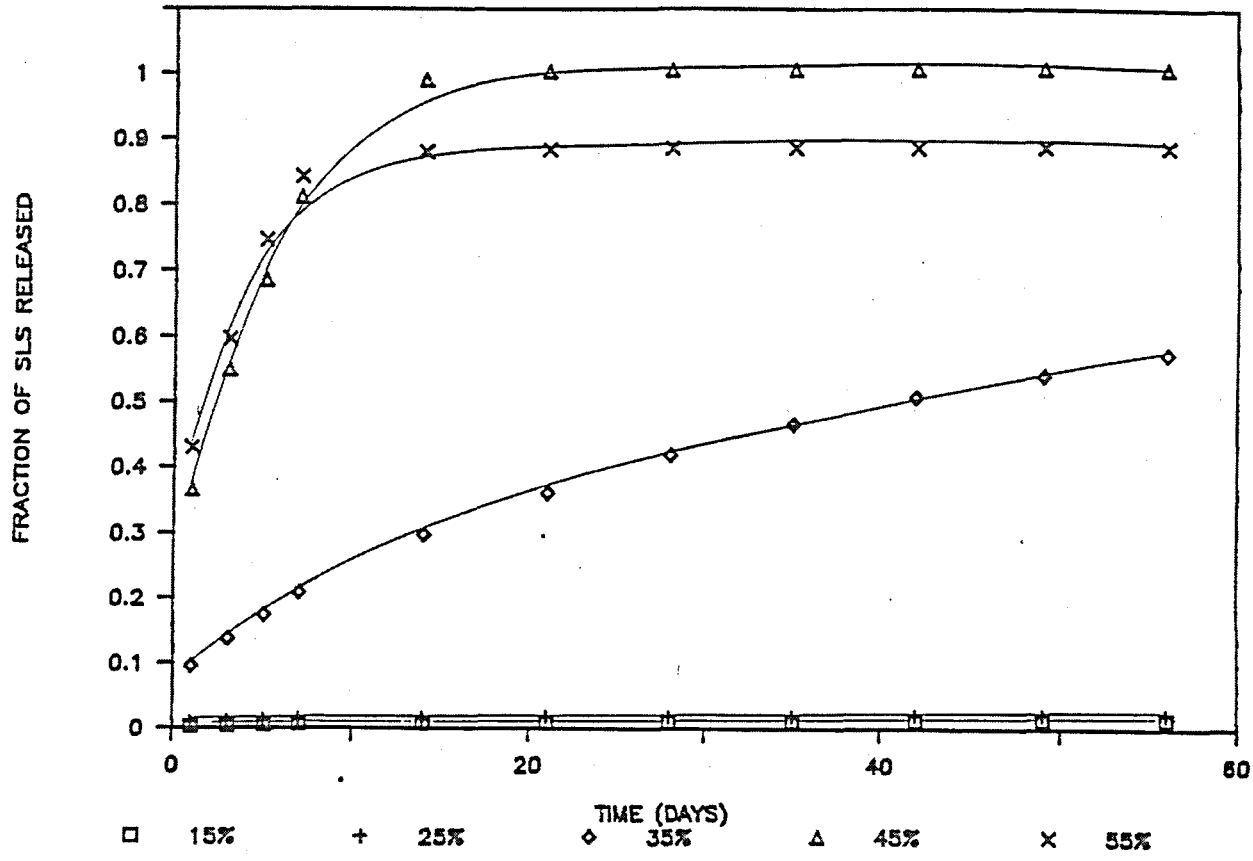

FIGURE 5A.1 The effect of the initial SLS loading on the release of SLS from SBR matrices.

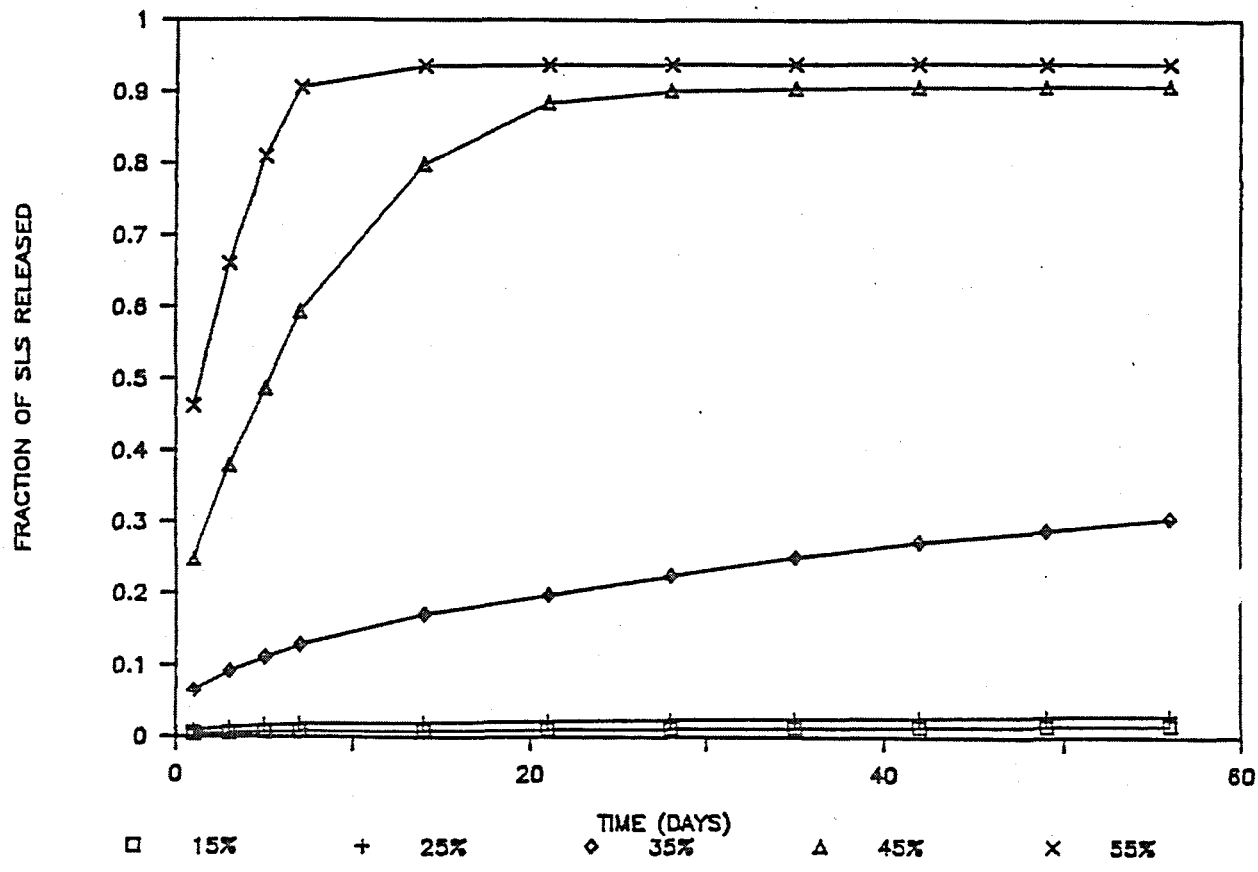

FIGURE 5A.2 The effect of the initial SLS loading on the release of SLS from NR/SBR matrices.

APPENDIX 6A

The Pascal Source Code DIFFCALC

```
program diffcalc;
label interrupt,next,exit;
const ns=13; nm=11; bz=60; np=1000; pi=3.1415927; tol=0.0001;
const net : integer = 88;
var i,j,k,n,ne          : integer;
    t,t0,y,f            : array[1..nm] of real;
    j0,alfa2            : array[1..np] of real;
    beta2               : array[0..np] of real;
    jtj,jtyfj,fj,dfj,d  : real;
    alfa,beta,a,l,a212  : real;
    d0,norm             : real;
    datafil,resfil      : text;
    filename            : string[30];
    convert,tfact       : real;
    intr                : boolean;

function intreq : boolean;
var ch : char;
begin
  if keypressed then begin
    read(kbd,ch);
    intr := (ch=#27);
    end;
  intreq := intr;
  end;

procedure test8087;
var r1,r2 : real;
begin
  if (ofs(r2)-ofs(r1))=8 then
    net := 200;
  end;

function lexp(x:real) : real;
begin
  if x<-net then
    lexp := 0
  else if abs(x)<0.01 then
    lexp := 1 + x
  else
    lexp := exp(x);
  end;

procedure lsq(t:real);
label con1,con2;
var i,j : integer;
    dt  : real;
    f1,f2,f3,f4   : real;
    expdat,expdbt : real;
begin
  dt := d*t;
  f1 := 0;
  f3 := 0;
  for i:=1 to np do begin
    expdat := lexp(-dt*alfa2[i]);
    if expdat=0 then goto con1;
    f1 := f1 + expdat/alfa2[i];
    f3 := f3 + expdat;
    end;
  i := np;
con1:
  f2 := 0;
  f4 := 0;
  for j:=0 to np do begin
```

```
    expdbt := lexp(-dt*beta2[j]);
    if expdbt=0 then goto con2;
    f2 := f2 + expdbt/beta2[j];
    f4 := f4 + expdbt;
    end;
  j := np;
con2:
  ne := (i + j) div 2;
  fj  := 1 - 8/a212*f1*f2;
  dfj := 8*t/a212*(f1*f4 + f2*f3);
  end;

begin

test8087;

t0[1] :=  1; t0[2] :=  3; t0[3] :=  5; t0[4]  :=  7; t0[5]  := 14; t0[6] := 21;
t0[7] := 28; t0[8] := 35; t0[9] := 42; t0[10] := 49; t0[11] := 56;

j0[1]  :=  2.4048255577; j0[2]  :=  5.5200781103; j0[3]  :=  8.6537279129;
j0[4]  := 11.7915344391; j0[5]  := 14.9309177086; j0[6]  := 18.0710639679;
j0[7]  := 21.2116366299; j0[8]  := 24.3524715308; j0[9]  := 27.4934791320;
j0[10] := 30.6346064684; j0[11] := 33.7758202136; j0[12] := 36.9170983537;
j0[13] := 40.0584257646; j0[14] := 43.1997917132; j0[15] := 46.3411883717;
j0[16] := 49.4826098974; j0[17] := 52.6240518411; j0[18] := 55.7655107550;
j0[19] := 58.9069839261; j0[20] := 62.0484691902;

j0[21] :=  65.18996; j0[22] :=  68.33147; j0[23] :=  71.47298;
j0[24] :=  74.61450; j0[25] :=  77.75603; j0[26] :=  80.89756;
j0[27] :=  84.03909; j0[28] :=  87.18063; j0[29] :=  90.32217;
j0[30] :=  93.46372; j0[31] :=  96.60527; j0[32] :=  99.74682;
j0[33] := 102.88837; j0[34] := 106.02993; j0[35] := 109.17149;
j0[36] := 112.31305; j0[37] := 115.45461; j0[38] := 118.59618;
j0[39] := 121.73774; j0[40] := 124.87931;

j0[41] := 128.0209; j0[42] := 131.1624; j0[43] := 134.3040; j0[44] := 137.4456;
j0[45] := 140.5872; j0[46] := 143.7287; j0[47] := 146.8703; j0[48] := 150.0119;
j0[49] := 153.1535; j0[50] := 156.2950; j0[51] := 159.4366; j0[52] := 162.5782;
j0[53] := 165.7198; j0[54] := 168.8613; j0[55] := 172.0029; j0[56] := 175.1445;
j0[57] := 178.2861; j0[58] := 181.4277; j0[59] := 184.5692; j0[60] := 187.7108;

for j:=bz+1 to np do
  j0[j] := j0[bz] + (j-bz)*pi;

d := 0.5;

repeat
  writeln('Enter name of input data file');
  readln(filename);
  assign(datafil,filename);
  {$I-} reset(datafil); {$I+}
  until IOresult=0;
repeat
  writeln('Enter name of result file');
  readln(filename);
  assign(resfil,filename);
  {$I-} rewrite(resfil); {$I+}
  until IOresult=0;

write(resfil,'"S#"','"a,l"','"d,e"','"Time in days" 0');
for i:=1 to nm do
  write(resfil,' ',t0[i]);
writeln(resfil);
read(datafil,n,a,l);
repeat
  writeln; writeln;
  writeln('Sample ',n,'   a = ',a:5:1,'   l = ',l:5:1);
  for j:=1 to nm do
    read(datafil,y[j]);
  for j:=1 to nm do
    write(y[j]:10:4);
  readln(datafil);
  writeln; writeln;
  writeln('Hit ESC to interrupt and modify  D  for next iteration');
```

```
  intr := false;
  a212 := a*a*l*l;
  for j:=1 to np do begin
    alfa     := j0[j]/a;
    alfa2[j] := alfa*alfa;
    end;
  for j:=0 to np do begin
    beta     := (2*j + 1)*pi/(2*l);
    beta2[j] := beta*beta;
    end;

  if y[nm]<0.1 then
    tfact := 24
  else
    tfact := 1;
  convert := 8.64E6/tfact;
  for j:=1 to nm do
    t[j] := tfact*t0[j];

  repeat
    jtj   := 0;
    jtyfj := 0;
    norm  := 0;
    for j:=1 to nm do begin
      if intreq then goto interrupt;
      write(j,'-');
      lsq(t[j]);
      if intreq then goto interrupt;
      write(ne,' ');
      f[j]  := fj;
      jtj   := jtj   + dfj*dfj;
      jtyfj := jtyfj + dfj*(y[j]-fj);
      norm  := norm  + (y[j]-fj)*(y[j]-fj);
      end;
    d0 := d;
    d  := d + jtyfj/jtj;
    if d<0 then
      d := d0/10;
interrupt:
    writeln;
    if intr or (d<1.0e-10) or (d>2) then begin
      if intr then
        writeln(#7,'D = ',d)
      else
        writeln(#7,#7,#7,'Warning D = ',d,#7,#7,#7);
      writeln('Enter new initial value:  (0 to skip this sample, -1 to stop)');
      readln(d);
      d0 := 10*d;
      if d=0 then begin
        d := 0.5;
        goto next;
        end;
      if d<0 then goto exit;
      end;
    writeln('D  = ',d); writeln;
    intr := false;
    until abs(d0-d)/d<tol;

  writeln('Sample ',n:3,'  D = ',d/convert:12,'  Norm = ',norm:10:6);
  writeln(resfil);
  write(resfil,n:3,a:6:2,' ',d/convert:12,' "Experimental" 0');
  for j:=1 to nm do
    write(resfil,y[j]:10:7);
  writeln(resfil);
  write(resfil,'"" ',1:6:2,' ',norm:12,' "Theoretical" 0');
  for j:=1 to nm do
    write(resfil,f[j]:10:7);
  writeln(resfil);
next:
  read(datafil,n,a,l);
  until eof(datafil);
exit:
  close(datafil);
  close(resfil);
end .
```

APPENDIX 6B

Lotus 1-2-3 Worksheet File ALSLS.WK1

Sodium concentration

SN	a	l	Day 1.	Day 3.	Day 5.	Day 7.	Day 14.	Day 21.	Day 28.	Day 35.	Day 42.	Day 49.	Day 56.	Mass Rubber gram	Mass SLS gram
1	9.0	5.0	5	1	1	1	1	1	1	1	1	1	1	2.50	0.3749
2	9.0	5.0	8	2	2	1	1	1	1	2	1	1	1	2.56	0.6390
3	9.0	5.0	54	23	22	25	60	40	40	40	40	30	29	2.60	0.9093
4	9.0	5.0	500	320	320	280	500	230	70	12	6	4	3	2.63	1.1822
5	9.0	5.0	600	300	300	300	400	330	320	250	110	70	50	2.68	1.4724
6	9.0	5.0	2	1	1	1	1	1	1	1	1	1	1	2.56	0.3837
7	9.0	5.0	12	3	2	2	2	2	2	1	2	1	1	2.58	0.6455
8	9.0	5.0	180	80	68	64	170	120	110	90	80	60	60	2.60	0.9093
9	9.0	5.0	900	450	330	310	445	33	3	2	2	1	2	2.64	1.1858
10	9.0	5.0	1300	500	450	290	120	12	4	3	2	1	1	2.65	1.4570
11	9.0	5.0	3	1	1	1	1	1	1	1	1	1	1	2.55	0.3828
12	9.0	5.0	13	4	4	3	3	3	3	2	2	2	2	2.59	0.6470
13	9.0	5.0	120	52	36	32	80	50	50	50	40	31	30	2.58	0.9016
14	9.0	5.0	600	320	260	260	500	210	40	9	4	3	2	2.60	1.1718
15	9.0	5.0	1400	600	450	290	90	6	2	2	1	1	1	2.65	1.4592
16	9.0	5.0	700	450	350	260	300	50	7	4	2	2	2	2.62	1.1790
17	9.0	5.0	800	480	330	270	320	32	9	3	2	2	2	2.65	1.1912
18	9.0	5.0	700	470	390	310	330	35	6	3	2	2	2	2.67	1.2024
19	9.0	5.0	700	490	280	250	300	70	13	5	2	2	2	2.63	1.1817
20	9.0	5.0	700	480	320	250	300	60	13	4	2	2	2	2.65	1.1907
21	9.0	5.0	800	500	380	280	310	34	5	2	2	1	2	2.69	1.2119
22	9.0	5.0	500	390	270	200	400	250	120	60	20	7	4	2.62	1.1808
23	9.0	5.0	700	500	330	280	400	70	14	5	2	2	2	2.66	1.1948
24	9.0	5.0	600	420	270	280	400	140	40	10	3	2	2	2.56	1.1529
25	9.0	5.0	600	430	260	260	400	160	50	15	6	3	2	2.61	1.1736
26	9.0	5.0	600	400	260	260	400	240	80	20	7	4	3	2.63	1.1831
27	9.0	5.0	600	410	300	280	400	150	50	11	5	2	2	2.66	1.1984
28	9.0	5.0	400	240	200	220	400	330	140	100	40	17	9	2.64	1.1867
29	9.0	5.0	600	360	270	230	400	220	80	23	8	4	3	2.64	1.1889
30	9.0	5.0	700	400	280	240	400	180	70	20	7	3	3	2.69	1.2119
31	9.0	5.0	500	250	200	180	400	320	240	110	50	21	11	2.64	1.1894
32	9.0	5.0	600	340	260	250	400	270	120	40	11	5	3	2.68	1.2047
33	9.0	5.0	500	250	250	230	500	330	220	60	21	9	6	2.69	1.2083
34	9.0	5.0	3	1	1	1	1	1	1	1	1	1	1	2.51	0.3759
35	9.0	5.0	7	1	1	1	1	1	1	1	1	1	1	2.52	0.6288
36	9.0	5.0	36	8	8	8	16	9	10	9	8	8	7	2.56	0.8964
37	9.0	5.0	400	170	170	190	400	300	300	180	80	30	15	2.60	1.1682
38	9.0	5.0	1000	430	550	320	340	27	4	3	3	2	2	2.63	1.4438
39	9.0	5.0	2	1	1	1	1	1	1	1	1	1	1	2.43	0.1236
40	9.0	5.0	3	1	1	1	1	1	1	1	1	1	1	2.47	0.2474
41	9.0	5.0	2	1	1	1	1	1	1	1	1	1	1	2.48	0.1241
42	9.0	5.0	3	1	1	1	1	1	1	1	1	1	1	2.50	0.2496
43	9.0	5.0	56	24	24	25	70	50	40	40	40	30	31	2.57	0.8988
44	6.0	5.0	34	18	20	20	40	32	30	26	22	19	18	2.31	0.8099
45	5.0	5.0	50	24	25	24	70	40	40	40	32	27	26	2.40	0.8400
46	4.0	5.0	64	29	30	27	70	40	40	40	40	29	27	2.56	0.8964
47	4.0	2.5	120	60	54	42	110	60	60	70	60	50	50	2.60	0.9104
48	3.0	2.5	150	72	62	54	130	70	60	60	50	50	40	2.64	0.9254
49	9.0	5.0	9	2	2	2	2	2	2	1	1	1	1	2.59	0.6463
50	6.0	5.0	17	5	4	3	6	4	3	3	2	2	2	2.31	0.5780
51	5.0	5.0	20	5	4	3	4	3	3	2	2	1	1	2.40	0.5990

52	4.0	5.0	23	7	5	3	6	4	4	3	2	2	2	2.56	0.6395
53	4.0	2.5	46	12	7	6	11	6	5	4	3	3	2	2.62	0.6553
54	3.0	2.5	52	13	10	7	14	8	7	5	4	4	3	2.67	0.6670
55	9.0	5.0	600	370	300	230	500	150	40	8	4	2	2	2.61	1.1745
56	6.0	5.0	650	350	260	190	300	60	10	4	2	2	2	2.33	1.0489
57	5.0	5.0	800	410	280	220	320	31	5	3	2	2	2	2.42	1.0890
58	4.0	5.0	900	440	320	210	130	13	3	3	2	2	2	2.58	1.1628
59	4.0	2.5	1100	490	310	70	23	4	2	2	2	2	2	2.61	1.1745
60	3.0	2.5	1400	540	210	40	10	3	2	3	2	2	2	2.65	1.1943
61	9.0	5.0	27	7	7	7	14	10	10	10	9	8	7	2.57	0.9978
62	6.0	5.0	33	9	8	8	15	10	10	9	9	8	7	2.29	0.8005
63	5.0	5.0	42	11	9	9	17	11	10	10	10	8	9	2.37	0.8302
64	4.0	5.0	52	14	12	12	26	17	15	13	12	10	11	2.54	0.8876
65	4.0	2.5	74	24	19	18	35	23	21	22	20	16	18	2.55	0.8918
66	3.0	2.5	80	27	22	21	43	27	24	24	21	16	18	2.60	0.9083
67	9.0	5.0	3	1	1	1	1	1	1	1	1	1	1	2.53	0.1265
68	9.0	5.0	3	1	1	1	1	1	1	1	1	1	1	2.59	0.1293
69	9.0	5.0	2	1	1	1	1	1	1	1	1	1	1	2.59	0.1297
70	9.0	5.0	2	1	1	1	1	1	1	1	1	1	1	2.57	0.2565
71	9.0	5.0	4	1	1	1	1	1	1	1	1	1	1	2.60	0.2597
72	9.0	5.0	4	1	1	1	1	1	1	1	1	1	1	2.60	0.2603
73	9.0	5.0	3	1	1	1	1	1	1	1	1	1	1	2.52	0.1261
74	9.0	5.0	2	1	1	1	1	1	1	1	1	1	1	2.55	0.1274
75	9.0	5.0	2	1	1	1	1	1	1	1	1	1	1	2.58	0.1291
76	9.0	5.0	5	1	1	1	1	1	1	1	1	1	1	2.54	0.2543
77	9.0	5.0	4	1	1	1	1	1	1	1	1	1	1	2.56	0.2564
78	9.0	5.0	5	1	1	1	1	1	1	1	1	1	1	2.59	0.2587
79	9.0	5.0	7	1	1	1	1	1	1	1	2	1	1	2.51	0.6285
80	9.0	5.0	11	1	1	1	1	1	2	2	2	1	1	2.52	0.6290
81	9.0	5.0	10	2	2	2	2	2	2	2	2	1	1	2.53	0.6333
82	9.0	5.0	9	2	2	2	2	2	2	2	2	1	1	2.52	0.6305
83	9.0	5.0	11	2	2	2	2	2	2	2	2	2	2	2.52	0.6308
84	9.0	5.0	10	2	1	2	2	2	2	3	2	2	2	2.53	0.6333
85	9.0	5.0	10	1	2	2	2	2	2	2	2	2	2	2.57	0.6423
86	9.0	5.0	18	7	7	6	16	13	13	13	13	11	13	2.54	1.1435
87	9.0	5.0	20	8	8	7	19	15	15	14	15	13	15	2.56	1.1498
88	9.0	5.0	21	7	7	8	21	16	16	16	15	14	15	2.54	1.1448
89	9.0	5.0	27	9	8	8	20	16	16	16	16	14	16	2.57	1.1556
90	9.0	5.0	32	11	9	9	23	18	18	18	19	19	21	2.55	1.1462
91	9.0	5.0	22	8	8	8	24	22	25	27	29	27	32	2.56	1.1529
92	9.0	5.0	700	440	320	250	400	90	23	9	6	4	3	2.61	1.1750
93	9.0	5.0	10	1	1	1	1	1	1	1	1	1	1	2.49	0.6235
94	9.0	5.0	8	1	1	1	2	2	1	1	1	1	1	2.52	0.6305
95	9.0	5.0	8	1	1	1	1	1	1	1	2	1	1	2.49	0.6213
96	9.0	5.0	8	1	1	1	2	2	1	1	1	1	1	2.50	0.6245
97	9.0	5.0	8	1	1	1	1	1	1	1	1	1	1	2.50	0.6250
98	9.0	5.0	9	1	2	1	1	2	1	2	1	1	1	2.48	0.6190
99	9.0	5.0	8	1	1	1	2	2	1	1	1	1	1	2.48	0.6210
100	9.0	5.0	800	400	350	260	300	32	7	3	3	2	2	2.68	1.2074
101	9.0	5.0	800	400	380	270	260	29	5	3	2	2	2	2.67	1.2029
102	9.0	5.0	800	400	320	280	400	60	11	4	3	2	2	2.67	1.2015
103	9.0	5.0	800	500	360	290	300	34	5	3	3	2	2	2.67	1.2015
104	9.0	5.0	700	400	280	250	400	120	25	8	6	4	4	2.61	1.1723
105	9.0	5.0	700	400	300	300	400	120	16	9	6	4	4	2.67	1.2002
106	9.0	5.0	800	400	320	280	400	100	20	8	5	3	3	2.61	1.1759
107	9.0	5.0	700	400	260	260	400	80	17	6	3	2	2	2.58	1.1588

108	9.0	5.0	260	140	100	100	330	250	200	210	170	120	95	2.61	1.1727
109	9.0	5.0	180	110	80	80	290	230	200	200	160	120	120	2.59	1.1646
110	9.0	5.0	210	140	90	90	320	250	220	220	170	120	100	2.61	1.1736
111	9.0	5.0	180	110	80	80	250	190	170	180	140	110	90	2.61	1.1723
112	9.0	5.0	290	190	120	115	300	260	240	220	140	100	80	2.61	1.1723
113	9.0	5.0	290	200	140	120	300	290	260	230	150	100	80	2.61	1.1732

[Na] to SLS in ug conversion factor 627.42

Cumulative SLS fraction released

SN	a	l	Day 1.	Day 3.	Day 5.	Day 7.	Day 14.	Day 21.	Day 28.	Day 35.	Day 42.	Day 49.	Day 56.	Content (ug)
1	9.0	5.0	0.0064	0.0077	0.0090	0.0103	0.0116	0.0129	0.0142	0.0154	0.0167	0.0180	0.0193	487370
2	9.0	5.0	0.0060	0.0076	0.0091	0.0098	0.0106	0.0113	0.0121	0.0128	0.0144	0.0151	0.0159	830700
3	9.0	5.0	0.0287	0.0409	0.0525	0.0658	0.0977	0.1189	0.1401	0.1614	0.1826	0.1985	0.2139	1182090
4	9.0	5.0	0.2041	0.3348	0.4654	0.5797	0.7838	0.8777	0.9063	0.9112	0.9137	0.9153	0.9165	1536860
5	9.0	5.0	0.1967	0.2950	0.3933	0.4917	0.6228	0.7310	0.8359	0.9178	0.9539	0.9768	0.9932	1914120
6	9.0	5.0	0.0025	0.0038	0.0050	0.0063	0.0075	0.0088	0.0101	0.0113	0.0126	0.0138	0.0151	498810
7	9.0	5.0	0.0090	0.0112	0.0127	0.0142	0.0157	0.0172	0.0187	0.0194	0.0206	0.0213	0.0221	839150
8	9.0	5.0	0.0955	0.1380	0.1741	0.2081	0.2983	0.3620	0.4204	0.4681	0.5106	0.5425	0.5743	1182090
9	9.0	5.0	0.3663	0.5495	0.6838	0.8100	0.9911	1.0045	1.0057	1.0065	1.0074	1.0078	1.0086	1541540
10	9.0	5.0	0.4306	0.5963	0.7453	0.8414	0.8811	0.8851	0.8864	0.8874	0.8881	0.8884	0.8887	1894100
11	9.0	5.0	0.0038	0.0050	0.0063	0.0076	0.0088	0.0101	0.0113	0.0126	0.0139	0.0151	0.0164	497640
12	9.0	5.0	0.0097	0.0127	0.0157	0.0179	0.0201	0.0224	0.0246	0.0261	0.0276	0.0291	0.0306	841100
13	9.0	5.0	0.0642	0.0921	0.1113	0.1285	0.1713	0.1981	0.2248	0.2516	0.2730	0.2896	0.3057	1172080
14	9.0	5.0	0.2471	0.3789	0.4860	0.5931	0.7990	0.8855	0.9020	0.9057	0.9074	0.9086	0.9094	1523340
15	9.0	5.0	0.4631	0.6615	0.8103	0.9063	0.9360	0.9380	0.9387	0.9393	0.9397	0.9400	0.9403	1896960
16	9.0	5.0	0.2866	0.4708	0.6140	0.7205	0.8433	0.8637	0.8666	0.8683	0.8691	0.8699	0.8707	1532700
17	9.0	5.0	0.3241	0.5186	0.6523	0.7617	0.8914	0.9043	0.9080	0.9092	0.9100	0.9108	0.9116	1548560
18	9.0	5.0	0.2810	0.4696	0.6262	0.7506	0.8831	0.8971	0.8995	0.9007	0.9015	0.9023	0.9031	1563120
19	9.0	5.0	0.2859	0.4860	0.6004	0.7025	0.8250	0.8536	0.8589	0.8610	0.8618	0.8626	0.8634	1536210
20	9.0	5.0	0.2[illegible]7	0.4783	0.6080	0.7093	0.8309	0.8553	0.8605	0.8622	0.8630	0.8638	0.8646	1547910
21	9.0	5.0	0.3[illegible]	0.5177	0.6691	0.7806	0.9040	0.9176	0.9196	0.9203	0.9211	0.9215	0.9223	1575470
22	9.0	5.0	0.2044	0.3638	0.4741	0.5559	0.7194	0.8216	0.8706	0.8951	0.9033	0.9062	0.9078	1535040
23	9.0	5.0	0.2828	0.4847	0.6180	0.7311	0.8927	0.9210	0.9267	0.9287	0.9295	0.9303	0.9311	1553240
24	9.0	5.0	0.2512	0.4270	0.5400	0.6572	0.8247	0.8833	0.9000	0.9042	0.9055	0.9063	0.9072	1498770
25	9.0	5.0	0.2467	0.4236	0.5305	0.6374	0.8019	0.8677	0.8883	0.8945	0.8969	0.8982	0.8990	1525680
26	9.0	5.0	0.2448	0.4079	0.5140	0.6201	0.7832	0.8812	0.9138	0.9219	0.9248	0.9264	0.9277	1538030
27	9.0	5.0	0.2416	0.4068	0.5276	0.6403	0.8014	0.8618	0.8820	0.8864	0.8884	0.8892	0.8900	1557920
28	9.0	5.0	0.1627	0.2603	0.3416	0.4311	0.5938	0.7280	0.7849	0.8256	0.8419	0.8488	0.8524	1542710
29	9.0	5.0	0.2436	0.3897	0.4993	0.5927	0.7551	0.8444	0.8769	0.8862	0.8894	0.8911	0.8923	1545570
30	9.0	5.0	0.2788	0.4381	0.5496	0.6452	0.8045	0.8761	0.9040	0.9120	0.9148	0.9160	0.9172	1575470
31	9.0	5.0	0.2029	0.3043	0.3855	0.4585	0.6208	0.7507	0.8481	0.8927	0.9130	0.9215	0.9260	1546220
32	9.0	5.0	0.2404	0.3766	0.4808	0.5809	0.7412	0.8493	0.8974	0.9134	0.9178	0.9198	0.9210	1566110
33	9.0	5.0	0.1997	0.2996	0.3994	0.4913	0.6910	0.8228	0.9107	0.9347	0.9431	0.9467	0.9491	1570790
34	9.0	5.0	0.0039	0.0051	0.0064	0.0077	0.0090	0.0103	0.0116	0.0128	0.0141	0.0154	0.0167	488670
35	9.0	5.0	0.0054	0.0061	0.0069	0.0077	0.0084	0.0092	0.0100	0.0107	0.0115	0.0123	0.0130	817440
36	9.0	5.0	0.0194	0.0237	0.0280	0.0323	0.0409	0.0458	0.0511	0.0560	0.0603	0.0646	0.0684	1165320
37	9.0	5.0	0.1653	0.2355	0.3057	0.3842	0.5495	0.6734	0.7974	0.8717	0.9048	0.9172	0.9234	1518660
38	9.0	5.0	0.3343	0.4780	0.6619	0.7688	0.8825	0.8915	0.8929	0.8939	0.8949	0.8955	0.8962	1876940
39	9.0	5.0	0.0078	0.0117	0.0156	0.0195	0.0234	0.0273	0.0312	0.0351	0.0390	0.0430	0.0469	160680
40	9.0	5.0	0.0059	0.0078	0.0098	0.0117	0.0137	0.0156	0.0176	0.0195	0.0215	0.0234	0.0254	321620
41	9.0	5.0	0.0078	0.0117	0.0156	0.0194	0.0233	0.0272	0.0311	0.0350	0.0389	0.0428	0.0467	161330
42	9.0	5.0	0.0058	0.0077	0.0097	0.0116	0.0135	0.0155	0.0174	0.0193	0.0213	0.0232	0.0251	324480
43	9.0	5.0	0.0301	0.0430	0.0558	0.0693	0.1069	0.1337	0.1552	0.1767	0.1981	0.2143	0.2309	1168440
44	6.0	5.0	0.0203	0.0310	0.0429	0.0548	0.0787	0.0977	0.1156	0.1311	0.1442	0.1555	0.1663	1052870
45	5.0	5.0	0.0287	0.0425	0.0569	0.0707	0.1109	0.1339	0.1569	0.1798	0.1982	0.2137	0.2287	1092000
46	4.0	5.0	0.0345	0.0501	0.0662	0.0808	0.1185	0.1400	0.1615	0.1831	0.2046	0.2202	0.2347	1165320
47	4.0	2.5	0.0636	0.0954	0.1241	0.1463	0.2046	0.2364	0.2682	0.3054	0.3372	0.3637	0.3902	1183520
48	3.0	2.5	0.0782	0.1150	0.1481	0.1763	0.2441	0.2806	0.3119	0.3432	0.3693	0.3953	0.4162	1203020
49	9.0	5.0	0.0067	0.0082	0.0097	0.0112	0.0127	0.0142	0.0157	0.0164	0.0172	0.0179	0.0187	840190
50	6.0	5.0	0.0142	0.0184	0.0217	0.0242	0.0292	0.0326	0.0351	0.0376	0.0392	0.0409	0.0426	751400
51	5.0	5.0	0.0161	0.0201	0.0234	0.0258	0.0290	0.0314	0.0338	0.0355	0.0371	0.0379	0.0387	778700

52	4.0	5.0	0.0174	0.0226	0.0264	0.0287	0.0332	0.0362	0.0392	0.0415	0.0430	0.0445	0.0460	831350
53	4.0	2.5	0.0339	0.0427	0.0479	0.0523	0.0604	0.0648	0.0685	0.0714	0.0737	0.0759	0.0773	851890
54	3.0	2.5	0.0376	0.0470	0.0543	0.0593	0.0695	0.0753	0.0803	0.0839	0.0868	0.0897	0.0919	867100
55	9.0	5.0	0.2466	0.3986	0.5219	0.6164	0.8219	0.8835	0.8999	0.9032	0.9049	0.9057	0.9065	1526850
56	6.0	5.0	0.2991	0.4601	0.5798	0.6672	0.8052	0.8328	0.8374	0.8393	0.8402	0.8411	0.8420	1363570
57	5.0	5.0	0.3546	0.5363	0.6604	0.7579	0.8997	0.9134	0.9156	0.9170	0.9178	0.9187	0.9196	1415700
58	4.0	5.0	0.3736	0.5562	0.6890	0.7762	0.8301	0.8355	0.8368	0.8380	0.8388	0.8397	0.8405	1511640
59	4.0	2.5	0.4520	0.6534	0.7808	0.8095	0.8190	0.8206	0.8214	0.8223	0.8231	0.8239	0.8247	1526850
60	3.0	2.5	0.5658	0.7840	0.8688	0.8850	0.8891	0.8903	0.8911	0.8923	0.8931	0.8939	0.8947	1552590
61	9.0	5.0	0.0145	0.0183	0.0220	0.0258	0.0333	0.0387	0.0441	0.0495	0.0543	0.0586	0.0624	1167140
62	6.0	5.0	0.0199	0.0253	0.0301	0.0350	0.0440	0.0500	0.0561	0.0615	0.0669	0.0717	0.0760	1040650
63	5.0	5.0	0.0244	0.0308	0.0360	0.0413	0.0512	0.0576	0.0634	0.0692	0.0750	0.0796	0.0849	1079260
64	4.0	5.0	0.0283	0.0359	0.0424	0.0489	0.0631	0.0723	0.0805	0.0875	0.0941	0.0995	0.1055	1153880
65	4.0	2.5	0.0400	0.0530	0.0633	0.0731	0.0920	0.1044	0.1158	0.1277	0.1383	0.1469	0.1567	1159340
66	3.0	2.5	0.0425	0.0569	0.0685	0.0797	0.1026	0.1169	0.1297	0.1424	0.1536	0.1621	0.1716	1180790
67	9.0	5.0	0.0114	0.0153	0.0191	0.0229	0.0267	0.0305	0.0343	0.0382	0.0420	0.0458	0.0496	164450
68	9.0	5.0	0.0112	0.0149	0.0187	0.0224	0.0261	0.0299	0.0336	0.0373	0.0411	0.0448	0.0485	168090
69	9.0	5.0	0.0074	0.0112	0.0149	0.0186	0.0223	0.0260	0.0298	0.0335	0.0372	0.0409	0.0447	168610
70	9.0	5.0	0.0038	0.0056	0.0075	0.0094	0.0113	0.0132	0.0151	0.0169	0.0188	0.0207	0.0226	333450
71	9.0	5.0	0.0074	0.0093	0.0112	0.0130	0.0149	0.0167	0.0186	0.0204	0.0223	0.0242	0.0260	337610
72	9.0	5.0	0.0074	0.0093	0.0111	0.0130	0.0148	0.0167	0.0185	0.0204	0.0222	0.0241	0.0260	338390
73	9.0	5.0	0.0115	0.0153	0.0191	0.0230	0.0268	0.0306	0.0344	0.0383	0.0421	0.0459	0.0498	163930
74	9.0	5.0	0.0076	0.0114	0.0152	0.0189	0.0227	0.0265	0.0303	0.0341	0.0379	0.0417	0.0455	165620
75	9.0	5.0	0.0075	0.0112	0.0150	0.0187	0.0224	0.0262	0.0299	0.0336	0.0374	0.0411	0.0449	167830
76	9.0	5.0	0.0095	0.0114	0.0133	0.0152	0.0171	0.0190	0.0209	0.0228	0.0247	0.0266	0.0285	330590
77	9.0	5.0	0.0075	0.0094	0.0113	0.0132	0.0151	0.0169	0.0188	0.0207	0.0226	0.0245	0.0264	333320
78	9.0	5.0	0.0093	0.0112	0.0131	0.0149	0.0168	0.0187	0.0205	0.0224	0.0243	0.0261	0.0280	336310
79	9.0	5.0	0.0054	0.0061	0.0069	0.0077	0.0084	0.0092	0.0100	0.0108	0.0123	0.0131	0.0138	817050
80	9.0	5.0	0.0084	0.0092	0.0100	0.0107	0.0115	0.0123	0.0138	0.0153	0.0169	0.0176	0.0184	817700
81	9.0	5.0	0.0076	0.0091	0.0107	0.0122	0.0137	0.0152	0.0168	0.0183	0.0198	0.0206	0.0213	823290
82	9.0	5.0	0.0069	0.0084	0.0100	0.0115	0.0130	0.0145	0.0161	0.0176	0.0191	0.0199	0.0207	819650
83	9.0	5.0	0.0084	0.0099	0.0115	0.0130	0.0145	0.0161	0.0176	0.0191	0.0207	0.0222	0.0237	820040
84	9.0	5.0	0.0076	0.0091	0.0099	0.0114	0.0130	0.0145	0.0160	0.0183	0.0198	0.0213	0.0229	823290
85	9.0	5.0	0.0075	0.0083	0.0098	0.0113	0.0128	0.0143	0.0158	0.0173	0.0188	0.0203	0.0218	834990
86	9.0	5.0	0.0076	0.0106	0.0135	0.0160	0.0228	0.0283	0.0338	0.0393	0.0447	0.0494	0.0549	1486550
87	9.0	5.0	0.0084	0.0118	0.0151	0.0180	0.0260	0.0323	0.0386	0.0445	0.0508	0.0562	0.0625	1494740
88	9.0	5.0	0.0089	0.0118	0.0148	0.0181	0.0270	0.0337	0.0405	0.0472	0.0535	0.0594	0.0658	1488240
89	9.0	5.0	0.0113	0.0150	0.0184	0.0217	0.0301	0.0368	0.0434	0.0501	0.0568	0.0626	0.0693	1502280
90	9.0	5.0	0.0135	0.0181	0.0219	0.0257	0.0354	0.0429	0.0505	0.0581	0.0661	0.0741	0.0830	1490060
91	9.0	5.0	0.0092	0.0126	0.0159	0.0193	0.0293	0.0385	0.0490	0.0603	0.0724	0.0837	0.0971	1498770
92	9.0	5.0	0.2875	0.4683	0.5997	0.7024	0.8667	0.9037	0.9131	0.9168	0.9193	0.9209	0.9221	1527500
93	9.0	5.0	0.0077	0.0085	0.0093	0.0101	0.0108	0.0116	0.0124	0.0132	0.0139	0.0147	0.0155	810550
94	9.0	5.0	0.0061	0.0069	0.0077	0.0084	0.0100	0.0115	0.0122	0.0130	0.0138	0.0145	0.0153	819650
95	9.0	5.0	0.0062	0.0070	0.0078	0.0085	0.0093	0.0101	0.0109	0.0117	0.0132	0.0140	0.0148	807690
96	9.0	5.0	0.0062	0.0070	0.0077	0.0085	0.0100	0.0116	0.0124	0.0131	0.0139	0.0147	0.0155	811850
97	9.0	5.0	0.0062	0.0069	0.0077	0.0085	0.0093	0.0100	0.0108	0.0116	0.0124	0.0131	0.0139	812500
98	9.0	5.0	0.0070	0.0078	0.0094	0.0101	0.0109	0.0125	0.0133	0.0148	0.0156	0.0164	0.0172	804700
99	9.0	5.0	0.0062	0.0070	0.0078	0.0085	0.0101	0.0117	0.0124	0.0132	0.0140	0.0148	0.0155	807300
100	9.0	5.0	0.3198	0.4797	0.6196	0.7235	0.8434	0.8562	0.8590	0.8602	0.8614	0.8622	0.8630	1569620
101	9.0	5.0	0.3210	0.4815	0.6339	0.7423	0.8466	0.8582	0.8602	0.8614	0.8622	0.8630	0.8638	1563770
102	9.0	5.0	0.3214	0.4820	0.6106	0.7230	0.8837	0.9078	0.9122	0.9139	0.9151	0.9159	0.9167	1561950
103	9.0	5.0	0.3214	0.5222	0.6668	0.7833	0.9038	0.9175	0.9195	0.9207	0.9219	0.9227	0.9235	1561950
104	9.0	5.0	0.2882	0.4529	0.5681	0.6711	0.8357	0.8852	0.8954	0.8987	0.9012	0.9029	0.9045	1523990
105	9.0	5.0	0.2815	0.4423	0.5630	0.6836	0.8445	0.8927	0.8992	0.9020	0.9052	0.9068	0.9084	1560260
106	9.0	5.0	0.3284	0.4925	0.6239	0.7388	0.9030	0.9440	0.9522	0.9555	0.9576	0.9588	0.9600	1520670
107	9.0	5.0	0.2915	0.4581	0.5664	0.6747	0.8413	0.8746	0.8817	0.8842	0.8855	0.8863	0.8871	1506440

108	9.0	5.0	0.1070	0.1646	0.2058	0.2469	0.3827	0.4856	0.5680	0.6544	0.7243	0.7737	0.8128	1524510
109	9.0	5.0	0.0746	0.1202	0.1533	0.1865	0.3067	0.4020	0.4849	0.5678	0.6341	0.6838	0.7335	1513980
110	9.0	5.0	0.0864	0.1439	0.1809	0.2180	0.3496	0.4524	0.5428	0.6333	0.7032	0.7526	0.7937	1525680
111	9.0	5.0	0.0741	0.1194	0.1523	0.1853	0.2882	0.3664	0.4364	0.5105	0.5681	0.6134	0.6505	1523990
112	9.0	5.0	0.1194	0.1976	0.2470	0.2944	0.4179	0.5249	0.6237	0.7143	0.7719	0.8131	0.8460	1523990
113	9.0	5.0	0.1193	0.2016	0.2592	0.3085	0.4320	0.5513	0.6582	0.7528	0.8145	0.8557	0.8886	1525160

APPENDIX 6C

Lotus 1-2-3 Worksheet File DIFFSLS.WK1

Controlled Release of Sodium Lauryl Sulphate [SLS] from Rubber

S#	a,l	D,e	Time in days	0	1	3	5	7	14	21	28	35	42	49	56
1	9.0	3.86E-12	Experimental	0.0000	0.0064	0.0077	0.0090	0.0103	0.0116	0.0129	0.0142	0.0154	0.0167	0.0180	0.0193
	5.0	4.57E-05	Theoretical	0.0000	0.0028	0.0048	0.0061	0.0073	0.0103	0.0126	0.0145	0.0162	0.0177	0.0192	0.0205
2	9.0	2.85E-12	Experimental	0.0000	0.0060	0.0076	0.0091	0.0098	0.0106	0.0113	0.0121	0.0128	0.0144	0.0151	0.0159
	5.0	6.31E-05	Theoretical	0.0000	0.0024	0.0041	0.0053	0.0062	0.0088	0.0108	0.0125	0.0139	0.0153	0.0165	0.0176
3	9.0	4.27E-10	Experimental	0.0000	0.0287	0.0409	0.0525	0.0658	0.0977	0.1189	0.1401	0.1614	0.1826	0.1985	0.2139
	5.0	6.58E-04	Theoretical	0.0000	0.0287	0.0494	0.0635	0.0748	0.1048	0.1274	0.1461	0.1625	0.1771	0.1903	0.2026
4	9.0	3.69E-08	Experimental	0.0000	0.2041	0.3348	0.4654	0.5797	0.7838	0.8777	0.9063	0.9112	0.9137	0.9153	0.9165
	5.0	2.21E-02	Theoretical	0.0000	0.2474	0.4023	0.4967	0.5664	0.7233	0.8157	0.8755	0.9153	0.9422	0.9605	0.9730
5	9.0	2.80E-08	Experimental	0.0000	0.1967	0.2950	0.3933	0.4917	0.6228	0.7310	0.8359	0.9178	0.9539	0.9768	0.9932
	5.0	2.02E-02	Theoretical	0.0000	0.2179	0.3574	0.4440	0.5089	0.6595	0.7534	0.8184	0.8652	0.8995	0.9249	0.9438
6	9.0	2.01E-12	Experimental	0.0000	0.0025	0.0038	0.0050	0.0063	0.0075	0.0088	0.0101	0.0113	0.0126	0.0138	0.0151
	5.0	2.35E-06	Theoretical	0.0000	0.0020	0.0034	0.0044	0.0053	0.0074	0.0091	0.0105	0.0117	0.0128	0.0139	0.0148
7	9.0	6.06E-12	Experimental	0.0000	0.0090	0.0112	0.0127	0.0142	0.0157	0.0172	0.0187	0.0194	0.0206	0.0213	0.0221
	5.0	1.43E-04	Theoretical	0.0000	0.0034	0.0060	0.0077	0.0091	0.0128	0.0157	0.0181	0.0203	0.0222	0.0240	0.0256
8	9.0	4.43E-09	Experimental	0.0000	0.0955	0.1380	0.1741	0.2081	0.2983	0.3620	0.4204	0.4681	0.5106	0.5425	0.5743
	5.0	2.09E-03	Theoretical	0.0000	0.0906	0.1537	0.1955	0.2286	0.3130	0.3737	0.4224	0.4633	0.4987	0.5300	0.5581
9	9.0	9.78E-08	Experimental	0.0000	0.3663	0.5495	0.6838	0.8100	0.9911	1.0045	1.0057	1.0065	1.0074	1.0078	1.0086
	5.0	9.45E-03	Theoretical	0.0000	0.3817	0.5943	0.7107	0.7883	0.9247	0.9726	0.9900	0.9963	0.9987	0.9995	0.9998
10	9.0	1.02E-07	Experimental	0.0000	0.4306	0.5963	0.7453	0.8414	0.8811	0.8851	0.8864	0.8874	0.8881	0.8884	0.8887
	5.0	7.52E-02	Theoretical	0.0000	0.3888	0.6038	0.7207	0.7980	0.9311	0.9760	0.9916	0.9971	0.9990	0.9996	0.9999
11	9.0	2.53E-12	Experimental	0.0000	0.0038	0.0050	0.0063	0.0076	0.0088	0.0101	0.0113	0.0126	0.0139	0.0151	0.0164
	5.0	9.64E-06	Theoretical	0.0000	0.0022	0.0039	0.0050	0.0059	0.0083	0.0102	0.0117	0.0131	0.0144	0.0155	0.0166
12	9.0	1.08E-11	Experimental	0.0000	0.0097	0.0127	0.0157	0.0179	0.0201	0.0224	0.0246	0.0261	0.0276	0.0291	0.0306
	5.0	1.47E-04	Theoretical	0.0000	0.0046	0.0079	0.0102	0.0121	0.0171	0.0209	0.0241	0.0270	0.0295	0.0318	0.0340
13	9.0	1.11E-09	Experimental	0.0000	0.0642	0.0921	0.1113	0.1285	0.1713	0.1981	0.2248	0.2516	0.2730	0.2896	0.3057
	5.0	8.49E-04	Theoretical	0.0000	0.0459	0.0787	0.1009	0.1186	0.1651	0.1998	0.2283	0.2529	0.2747	0.2945	0.3125
14	9.0	3.95E-08	Experimental	0.0000	0.2471	0.3789	0.4860	0.5931	0.7990	0.8855	0.9020	0.9057	0.9074	0.9086	0.9094
	5.0	1.93E-02	Theoretical	0.0000	0.2553	0.4141	0.5105	0.5812	0.7392	0.8307	0.8885	0.9261	0.9509	0.9673	0.9783
15	9.0	1.46E-07	Experimental	0.0000	0.4631	0.6615	0.8103	0.9063	0.9360	0.9380	0.9387	0.9393	0.9397	0.9400	0.9403
	5.0	2.43E-02	Theoretical	0.0000	0.4512	0.6844	0.8020	0.8729	0.9719	0.9937	0.9986	0.9997	0.9999	1.0000	1.0000
34	9.0	2.62E-12	Experimental	0.0000	0.0039	0.0051	0.0064	0.0077	0.0090	0.0103	0.0116	0.0128	0.0141	0.0154	0.0167
	5.0	9.97E-06	Theoretical	0.0000	0.0023	0.0039	0.0051	0.0060	0.0085	0.0104	0.0120	0.0134	0.0146	0.0158	0.0169
35	9.0	1.88E-12	Experimental	0.0000	0.0054	0.0061	0.0069	0.0077	0.0084	0.0092	0.0100	0.0107	0.0115	0.0123	0.0130
	5.0	3.93E-05	Theoretical	0.0000	0.0019	0.0033	0.0043	0.0051	0.0072	0.0088	0.0101	0.0113	0.0124	0.0134	0.0143
36	9.0	4.97E-11	Experimental	0.0000	0.0194	0.0237	0.0280	0.0323	0.0409	0.0458	0.0511	0.0560	0.0603	0.0646	0.0684

	5.0	2.66E-04	Theorctical	0.0000	0.0098	0.0170	0.0219	0.0259	0.0365	0.0446	0.0514	0.0574	0.0627	0.0677	0.0722
37	9.0	2.08E-08	Experimental	0.0000	0.1653	0.2355	0.3057	0.3842	0.5495	0.6734	0.7974	0.8717	0.9048	0.9172	0.9234
	5.0	3.42E-02	Theoretical	0.0000	0.1899	0.3139	0.3921	0.4515	0.5929	0.6848	0.7516	0.8024	0.8420	0.8733	0.0981
38	9.0	6.66E-08	Experimental	0.0000	0.3343	0.4780	0.6619	0.7688	0.8825	0.8915	0.8929	0.8939	0.8949	0.8955	0.8962
	5.0	5.20E-02	Theoretical	0.0000	0.3228	0.5128	0.6224	0.6995	0.8551	0.9278	0.9637	0.9817	0.9908	0.9954	0.9977
39	9.0	1.97E-11	Experimental	0.0000	0.0078	0.0117	0.0156	0.0195	0.0234	0.0273	0.0312	0.0351	0.0390	0.0430	0.0469
	5.0	2.26E-05	Theoretical	0.0000	0.0062	0.0107	0.0138	0.0164	0.0231	0.0283	0.0326	0.0364	0.0398	0.0430	0.0459
40	9.0	6.10E-12	Experimental	0.0000	0.0059	0.0078	0.0098	0.0117	0.0137	0.0156	0.0176	0.0195	0.0215	0.0234	0.0254
	5.0	2.31E-05	Theoretical	0.0000	0.0035	0.0060	0.0077	0.0091	0.0129	0.0158	0.0182	0.0203	0.0223	0.0240	0.0257
41	9.0	1.96E-11	Experimental	0.0000	0.0078	0.0117	0.0156	0.0194	0.0233	0.0272	0.0311	0.0350	0.0389	0.0428	0.0467
	5.0	2.23E-05	Theoretical	0.0000	0.0062	0.0107	0.0138	0.0163	0.0230	0.0282	0.0325	0.0363	0.0397	0.0428	0.0457
42	9.0	5.97E-12	Experimental	0.0000	0.0058	0.0077	0.0097	0.0116	0.0135	0.0155	0.0174	0.0193	0.0213	0.0232	0.0251
	5.0	2.23E-05	Theoretical	0.0000	0.0034	0.0059	0.0076	0.0090	0.0128	0.0156	0.0180	0.0201	0.0220	0.0238	0.0254
43	9.0	5.11E-10	Experimental	0.0000	0.0301	0.0430	0.0558	0.0693	0.1049	0.1337	0.1552	0.1767	0.1981	0.2143	0.2309
	5.0	7.50E-04	Theoretical	0.0000	0.0314	0.0539	0.0693	0.0816	0.1142	0.1388	0.1591	0.1768	0.1926	0.2069	0.2202
44	6.0	1.67E-10	Experimental	0.0000	0.0203	0.0310	0.0429	0.0548	0.0787	0.0977	0.1156	0.1311	0.1442	0.1555	0.1663
	5.0	2.21E-04	Theoretical	0.0000	0.0227	0.0391	0.0502	0.0593	0.0832	0.1012	0.1163	0.1295	0.1413	0.1520	0.1619
45	5.0	2.56E-10	Experimental	0.0000	0.0287	0.0425	0.0569	0.0707	0.1109	0.1339	0.1569	0.1798	0.1982	0.2137	0.2287
	5.0	6.13E-04	Theoretical	0.0000	0.0315	0.0542	0.0696	0.0820	0.1147	0.1393	0.1597	0.1775	0.1933	0.2076	0.2209
46	4.0	2.03E-10	Experimental	0.0000	0.0345	0.0501	0.0662	0.0808	0.1185	0.1400	0.1615	0.1831	0.2046	0.2202	0.2347
	5.0	2.08E-04	Theoretical	0.0000	0.0328	0.0563	0.0724	0.0853	0.1192	0.1448	0.1659	0.1843	0.2007	0.2157	0.2294
47	4.0	3.81E-10	Experimental	0.0000	0.0636	0.0954	0.1241	0.1463	0.2046	0.2364	0.2682	0.3054	0.3372	0.3637	0.3902
	2.5	4.27E-04	Theoretical	0.0000	0.0572	0.0978	0.1251	0.1469	0.2036	0.2455	0.2797	0.3091	0.3350	0.3583	0.3795
48	3.0	3.53E-10	Experimental	0.0000	0.0782	0.1158	0.1481	0.1763	0.2441	0.2806	0.3119	0.3432	0.3693	0.3953	0.4162
	2.5	6.83E-04	Theoretical	0.0000	0.0651	0.1110	0.1419	0.1664	0.2298	0.2764	0.3143	0.3466	0.3750	0.4004	0.4235
49	9.0	4.16E-12	Experimental	0.0000	0.0067	0.0082	0.0097	0.0112	0.0127	0.0142	0.0157	0.0164	0.0172	0.0179	0.0187
	5.0	6.78E-05	Theoretical	0.0000	0.0029	0.0049	0.0064	0.0075	0.0107	0.0130	0.0151	0.0168	0.0184	0.0199	0.0212
50	6.0	1.37E-11	Experimental	0.0000	0.0142	0.0184	0.0217	0.0242	0.0292	0.0326	0.0351	0.0376	0.0392	0.0409	0.0426
	5.0	2.99E-04	Theoretical	0.0000	0.0065	0.0113	0.0146	0.0172	0.0243	0.0297	0.0342	0.0382	0.0418	0.0451	0.0482
51	5.0	9.83E-12	Experimental	0.0000	0.0161	0.0201	0.0234	0.0258	0.0290	0.0314	0.0338	0.0355	0.0371	0.0379	0.0387
	5.0	4.97E-04	Theoretical	0.0000	0.0062	0.0108	0.0139	0.0164	0.0232	0.0283	0.0327	0.0365	0.0399	0.0431	0.0460
52	4.0	9.79E-12	Experimental	0.0000	0.0174	0.0226	0.0264	0.0287	0.0332	0.0362	0.0392	0.0415	0.0430	0.0445	0.0460
	5.0	5.51E-04	Theoretical	0.0000	0.0073	0.0125	0.0162	0.0191	0.0270	0.0330	0.0380	0.0424	0.0464	0.0501	0.0535
53	4.0	1.83E-11	Experimental	0.0000	0.0339	0.0427	0.0479	0.0523	0.0604	0.0648	0.0685	0.0714	0.0737	0.0759	0.0773
	2.5	2.27E-03	Theoretical	0.0000	0.0127	0.0220	0.0283	0.0335	0.0471	0.0575	0.0662	0.0739	0.0807	0.0870	0.0928
54	3.0	1.80E-11	Experimental	0.0000	0.0376	0.0470	0.0543	0.0593	0.0695	0.0753	0.0803	0.0839	0.0868	0.0897	0.0919
	2.5	2.57E-03	Theoretical	0.0000	0.0150	0.0258	0.0333	0.0393	0.0553	0.0674	0.0776	0.0865	0.0945	0.1018	0.1086

55	9.0	4.23E-08	Experimental	0.0000	0.2466	0.3986	0.5219	0.6164	0.8219	0.8835	0.8999	0.9032	0.9049	0.9057	0.9065
	5.0	2.18E-02	Theoretical	0.0000	0.2633	0.4260	0.5242	0.5961	0.7549	0.8450	0.9006	0.9360	0.9586	0.9732	0.9827
56	6.0	2.57E-08	Experimental	0.0000	0.2991	0.4601	0.5798	0.6672	0.8052	0.8328	0.8374	0.8393	0.8402	0.8411	0.8420
	5.0	7.43E-02	Theoretical	0.0000	0.2593	0.4193	0.5157	0.5861	0.7418	0.8312	0.8880	0.9254	0.9502	0.9667	0.9778
57	5.0	3.78E-08	Experimental	0.0000	0.3546	0.5363	0.6604	0.7579	0.8997	0.9134	0.9156	0.9170	0.9178	0.9187	0.9196
	5.0	2.90E-02	Theoretical	0.0000	0.3420	0.5385	0.6495	0.7261	0.8753	0.9416	0.9726	0.9871	0.9939	0.9971	0.9987
58	4.0	2.37E-08	Experimental	0.0000	0.3736	0.5562	0.6890	0.7762	0.8301	0.8355	0.8368	0.8380	0.8388	0.8397	0.8405
	5.0	1.31E-01	Theoretical	0.0000	0.3197	0.5080	0.6167	0.6931	0.8481	0.9223	0.9599	0.9793	0.9893	0.9945	0.9971
59	4.0	2.25E-08	Experimental	0.0000	0.4520	0.6534	0.7808	0.8095	0.8190	0.8206	0.8214	0.8223	0.8231	0.8239	0.8247
	2.5	1.98E-01	Theoretical	0.0000	0.3882	0.6020	0.7178	0.7945	0.9281	0.9743	0.9908	0.9967	0.9988	0.9996	0.9998
60	3.0	3.36E-08	Experimental	0.0000	0.5658	0.7840	0.8688	0.8850	0.8891	0.8903	0.8911	0.8923	0.8931	0.8939	0.8947
	2.5	8.38E-02	Theoretical	0.0000	0.5243	0.7669	0.8748	0.9316	0.9917	0.9990	0.9999	1.0000	1.0000	1.0000	1.0000
61	9.0	3.81E-11	Experimental	0.0000	0.0145	0.0183	0.0220	0.0258	0.0333	0.0387	0.0441	0.0495	0.0543	0.0586	0.0624
	5.0	6.92E-05	Theoretical	0.0000	0.0086	0.0149	0.0192	0.0227	0.0320	0.0392	0.0451	0.0504	0.0551	0.0594	0.0634
62	6.0	3.79E-11	Experimental	0.0000	0.0199	0.0253	0.0301	0.0350	0.0440	0.0500	0.0561	0.0615	0.0669	0.0717	0.0760
	5.0	2.43E-04	Theoretical	0.0000	0.0109	0.0188	0.0242	0.0286	0.0402	0.0491	0.0566	0.0631	0.0690	0.0744	0.0794
63	5.0	3.85E-11	Experimental	0.0000	0.0244	0.0308	0.0360	0.0413	0.0512	0.0576	0.0634	0.0692	0.0750	0.0796	0.0849
	5.0	4.87E-04	Theoretical	0.0000	0.0123	0.0213	0.0274	0.0323	0.0456	0.0556	0.0640	0.0714	0.0781	0.0842	0.0898
64	4.0	4.44E-11	Experimental	0.0000	0.0283	0.0359	0.0424	0.0489	0.0631	0.0723	0.0805	0.0875	0.0941	0.0995	0.1055
	5.0	5.18E-04	Theoretical	0.0000	0.0154	0.0266	0.0342	0.0404	0.0569	0.0694	0.0799	0.0890	0.0973	0.1048	0.1118
65	4.0	5.97E-11	Experimental	0.0000	0.0400	0.0530	0.0633	0.0731	0.0920	0.1044	0.1158	0.1277	0.1383	0.1469	0.1567
	2.5	1.00E-03	Theoretical	0.0000	0.0229	0.0394	0.0507	0.0599	0.0840	0.1023	0.1175	0.1308	0.1427	0.1535	0.1635
66	3.0	5.26E-11	Experimental	0.0000	0.0425	0.0569	0.0685	0.0797	0.1026	0.1169	0.1297	0.1424	0.1536	0.1621	0.1716
	2.5	1.05E-03	Theoretical	0.0000	0.0255	0.0438	0.0564	0.0665	0.0932	0.1133	0.1301	0.1447	0.1578	0.1697	0.1807

```
C*****************************************************************C
C                                                                 C
C                            PELLET                               C
C                                                                 C
C*****************************************************************C

C                  COMPILER:  VAX-11 FORTRAN V4.2


      INCLUDE 'PELLET.INC /LIST'

      CALL INPUT
      CALL GRID
      CALL INIT
      CALL BOUND
      CALL HEAD(7)
      CALL OUTPUT(7,0)
      CALL PLTDAT(9)
      WRITE(6,100)  CSUM0
      WRITE(11,100) CSUM0
100   FORMAT(' INITIAL CONTENT ',1PE9.2E1/
     :       '  TIME  SCANS NRSCMAX   FLUX    CUM REL     % REL')


C *** TIME STEPS ***

      IT = 0
10    T  = T + DT
      DT = DTINC*DT
      IT = IT + 1
      CALL TPREP

C *** SCAN THE DOMAIN ***

      DO 60 M = 1,MAXSCN

      CALL CPREP

      RSCMAX = 0.0

      DO 20 I=2,INM
      CALL TDMANS(I,1)
20    CONTINUE

      DO 30 J=2,JNM
      CALL TDMAEW(J,1)
30    CONTINUE

      DO 40 I=INM,2,-1
      CALL TDMANS(I,-1)
40    CONTINUE

      DO 50 J=JNM,2,-1
      CALL TDMAEW(J,-1)
50    CONTINUE

      IF (CMAX-CMIN.GT.TINY) THEN
         NRSCMX = RSCMAX / (CMAX-CMIN)
      ELSE
         NRSCMX = -RSCMAX
      ENDIF

      CALL BOUND
      CALL DPREP
```

```
      IF (NRSCMX.LE.TOL .OR. NRSCMX.GT.DIVFCT) GOTO 70
60    CONTINUE

      M = -MAXSCN

70    CALL OVACON

      IF (MOD(IT,MOUT).EQ.0) THEN
         CALL OUTPUT(7,0)
         CALL PLTDAT(9)
      ENDIF

      WRITE(6,101)  T,M,NRSCMX,DCSUM,CSUM0-CSUM,100*(CSUM0-CSUM)/CSUM0
      WRITE(11,101) T,M,NRSCMX,DCSUM,CSUM0-CSUM,100*(CSUM0-CSUM)/CSUM0
101   FORMAT(F8.2,I4,1P3E9.2E1,0PF9.2)

      IF (T.LT.T0+TIME) GOTO 10

C *** TERMINATION ***

      CALL PLTDAT(8)

      IF (.NOT.FULL .AND. MOD(IT,MOUT).NE.0) THEN
         FULL = .TRUE.
         CALL OUTPUT(7,0)
      ENDIF

      WRITE(6,*)  'PROGRAM STOP.  ERRORS:',IERROR,' WARNINGS:',IWARN
      WRITE(7,*)  'PROGRAM STOP.  ERRORS:',IERROR,' WARNINGS:',IWARN
      WRITE(11,*) 'PROGRAM STOP.  ERRORS:',IERROR,' WARNINGS:',IWARN

      STOP
      END


C ***********************************************************************
      SUBROUTINE INPUT
C ***********************************************************************

C *** PROVIDE INPUT DATA AND SPECIFICATIONS ***

      INCLUDE 'PELLET.INC'

      DATA TINY,RMAX,ZERO /1.0E-20,1.0E38,0.0/
      DATA UNDEF  /0.0/
      CHARACTER*80 FILNAM

      WRITE(5,*) 'DATA FILE?'
      READ(5,100) FILNAM
      WRITE(11,101) FILNAM
      OPEN(10,FILE=FILNAM,STATUS='OLD')

      READ(10,*,END=99) IN,XDIM,JN,YDIM,DT,TIME

      IF (IN.GT.ID .OR. JN.GT.JD) THEN
         WRITE(6,103)  ID,JD
         WRITE(7,103)  ID,JD
         WRITE(11,103) ID,JD
         STOP
      ENDIF

      READ(10,*,END=99) RDINIT,D0,CINIT,CALFA,CK
      READ(10,*,END=99) TOL,DIVFCT,MAXSCN,RELAX,THETA,DTINC
      READ(10,*,END=99) FULL,MOUT
      READ(10,*,END=99) (DX(I),I=2,IN-1)
```

```
      READ(10,*,END=99) (DY(J),J=2,JN-1)
      CLOSE(10)

      IF (IN.LE.15) FULL = .TRUE.
      RETURN

99    WRITE(6,*) '***ERROR: PREMATURE END OF FILE DETECTED'
      WRITE(6,*) 'PROGRAM ABORTED.'
      STOP

100   FORMAT(A80)
101   FORMAT(' DATA FILE: ',A30)
103   FORMAT(' ***ERROR: GRID TOO LARGE.  MAXIMUM SIZE IS ',I4,' X ',I4/
     :       ' PROGRAM ABORTED'///)
      END


C *************************************************************************
      SUBROUTINE GRID
C *************************************************************************

C *** FIX GRID GEOMETRY  ***

      INCLUDE 'PELLET.INC'
      REAL*8 YN(JD)

      INM  = IN - 1
      INM2 = IN - 2

      SUM = 0.0

      DO 10 I=2,INM
      SUM = SUM + DX(I)
10    CONTINUE

      FACT = SUM/XDIM

      DO 15 I=2,INM
      DX(I) = DX(I)/FACT
15    CONTINUE

      DKSI(1)   = 0.5*DX(2)

      DO 20 I=2,INM2
      DKSI(I) = 0.5*DX(I) + 0.5*DX(I+1)
20    CONTINUE

      DKSI(INM)  = 0.5*DX(INM)
      FX(1) = 0.0

      DO 25 I=2,INM2
      FX(I) = 0.5*DX(I)/DKSI(I)
25    CONTINUE

      FX(INM) = 1.0

      DO 30 I=2,IN
      GX(I) = 1 - FX(I-1)
30    CONTINUE

      X(1) = 0.0

      DO 35 I=2,IN
      X(I) = X(I-1) + DKSI(I-1)
35    CONTINUE
```

```
      JNM  = JN - 1
      JNM2 = JN - 2
      SUM = 0.0

      DO 50 J=2,JNM
      SUM = SUM + DY(J)
50    CONTINUE

      FACT = SUM/YDIM

      DO 55 J=2,JNM
      DY(J) = DY(J)/FACT
55    CONTINUE

      DETA(1)   = 0.5*DY(2)

      DO 60 J=2,JNM2
      DETA(J) = 0.5*DY(J) + 0.5*DY(J+1)
60    CONTINUE

      DETA(JNM)  = 0.5*DY(JNM)
      FY(1) = 0.0

      DO 65 J=2,JNM2
      FY(J) = 0.5*DY(J)/DETA(J)
65    CONTINUE

      FY(JNM) = 1.0

      DO 70 J=2,JN
      GY(J) = 1 - FY(J-1)
70    CONTINUE

      Y(1)  = 0.0
      YN(1) = 0.0

      DO 75 J=2,JN
      Y(J)  = Y(J-1)  + DETA(J-1)
      YN(J) = YN(J-1) + DY(J)
75    CONTINUE

      DO 90 I=2,INM
      DO 90 J=1,JNM
      AREAX(I,J) = DX(I)*YN(J)
90    CONTINUE

      DO 95 J=2,JNM
      AREAY(J) = 0.5*(YN(J)*YN(J) - YN(J-1)*YN(J-1))
95    CONTINUE

      DO 99 I=2,INM
      DO 99 J=2,JNM
      VOLUME(I,J) = DX(I)*AREAY(J)
99    CONTINUE

      END


C *************************************************************************
      SUBROUTINE INIT
C *************************************************************************

C *** INITIALIZE VARIABLES AND CONSTANTS ***

      INCLUDE 'PELLET.INC'
```

```
      IERROR = 0
      IWARN  = 0

      IF (RDINIT) THEN
         WRITE(6,*) 'INIT FILE?'
         READ(5,100) FILNAM
         WRITE(11,101) FILNAM
         OPEN(10,FILE=FILNAM,STATUS='OLD',ERR=99)

         READ(10,103,END=99,ERR=99) INREAD,JNREAD
         IF (IN.NE.INREAD  .OR.  JN.NE.JNREAD) THEN
            WRITE(6,*) '*** ERROR:  INIT FILE DIMENSIONS DOES NOT',
     :                 ' CORRESPOND TO PRESENT DIMENSIONS'
            WRITE(6,*) 'PROGRAM ABORTED'
            STOP
         ENDIF

         READ(10,104,END=99,ERR=99) T0,CINIT
         READ(10,102,END=99,ERR=99) (DUMMY,I=2,INM)
         READ(10,102,END=99,ERR=99) (DUMMY,J=2,JNM)
         READ(10,102,END=99,ERR=99) (DUMMY,I=1,INM)
         READ(10,102,END=99,ERR=99) (DUMMY,J=1,JNM)
         READ(10,102,END=99,ERR=99) ((C(I,J),J=1,JN),I=1,IN)
         READ(10,102,END=99,ERR=99) ((D(I,J),J=1,JN),I=1,IN)

         CLOSE(10)

      ELSE

         M0 = 0

         DO 10 I=1,IN
         DO 10 J=1,JN
         C(I,J) = CINIT
10       CONTINUE

      ENDIF

C *** INITIALIZE BOUNDARIES AND DIFFUSIVITY ***

      CALL BOUND
      CALL DPREP
      CALL OVACON

      IF (RDINIT) THEN
         CSUM0 = CINIT*0.5*XDIM*YDIM*YDIM
      ELSE
         CSUM0 = CSUM
      ENDIF

      SRSPPS = IN*JN
      RETURN

99    WRITE(6,*) '***ERROR: INITIALIZATION FILE READ ERROR'
      WRITE(6,*) 'PROGRAM ABORTED.'
      STOP

100   FORMAT(A30)
101   FORMAT(' INIT FILE: ',A30)
102   FORMAT(99(5E15.8/))
103   FORMAT(2I5)
104   FORMAT(F6.1)
      END

C ***************************************************************************
```

```
      SUBROUTINE HEAD(LU)
C ***********************************************************************

C *** PRINT HEADING AND PROBLEM SPECIFICATION ***

      INCLUDE 'PELLET.INC'
      CHARACTER*18 IFMT

      WRITE(LU,100)
100   FORMAT('1',20X,'PELLET'/
     :           21X,'======'//)

      WRITE(LU,102) XDIM,IN,YDIM,JN,TIME,DT,CSUM0
102   FORMAT(' PHYSICAL DIMENSIONS:'/
     : 5X,'HORISONTAL (X): ',F20.3/
     : 5X,'NODES IN HOR:   ',I20/
     : 5X,'VERTICAL (Y):   ',F20.3/
     : 5X,'NODES IN VERT:  ',I20/
     : 5X,'TIME:           ',F20.3/
     : 5X,'TIME STEP:      ',F20.3/1P
     : 5X,'INITIAL CONTENTS',E20.3E1)

      WRITE(LU,106) TOL,RELAX,DIVFCT,MAXSCN

106   FORMAT('1NUMERICAL CONTROL PARAMETERS:'/1P,
     : 5X,'ERROR TOLLERANCE:       ',E11.1/0P,
     : 5X,'RELAX FACTOR:           ',F11.3/
     : 5X,'DIVERGENCE FACTOR:      ',E11.1/
     : 5X,'MAXIMUM SCANS:          ',I11/)

      WRITE(LU,109)
109   FORMAT('1'20X,'GRID VARIABLE VALUES:'/
     1          21X,'====================='//)

      DO 20 K=1,IN,10
      IB = K
      IBP = MAX0(2,K)
      IE = MIN0(IN,K+9)
      IEM = MIN0(INM,K+9)

      IF (K.EQ.1) THEN
         IFMT = '(1X,A6,10X,9F10.4)'
      ELSE
         IFMT = '(1X,A6,10F10.4)   '
      ENDIF

      WRITE(LU,110) 'VAR/I=',(I,I=IB,IE)
      WRITE(LU,111,IOSTAT=IOERR)  'X     ',(X(I),I=IB,IE)
      WRITE(LU,IFMT,IOSTAT=IOERR) 'DX    ',(DX(I),I=IBP,IEM)
      WRITE(LU,111,IOSTAT=IOERR)  'DKSI  ',(DKSI(I),I=IB,IEM)
      WRITE(LU,111)  'FX    ',(FX(I),I=IB,IEM)
      WRITE(LU,IFMT) 'GX    ',(GX(I),I=IBP,IE)
20    CONTINUE

      DO 40 K=1,JN,10
      JB = K
      JBP = MAX0(2,K)
      JE = MIN0(JN,K+9)
      JEM = MIN0(JNM,K+9)

      IF (K.EQ.1) THEN
         IFMT = '(1X,A6,10X,9F10.4)'
      ELSE
         IFMT = '(1X,A6,10F10.4)   '
      ENDIF
```

```
      WRITE(LU,110) 'VAR/J=',(J,J=JB,JE)
      WRITE(LU,111,IOSTAT=IOERR)  'Y      ',(Y(J),J=JB,JE)
      WRITE(LU,IFMT,IOSTAT=IOERR) 'DY     ',(DY(J),J=JBP,JEM)
      WRITE(LU,111,IOSTAT=IOERR)  'DETA   ',(DETA(J),J=JB,JEM)
      WRITE(LU,111)  'FY     ',(FY(J),J=JB,JEM)
      WRITE(LU,IFMT) 'GY     ',(GY(J),J=JBP,JE)
40    CONTINUE

110   FORMAT(/1X,A6,I7,10I10)
111   FORMAT(1X,A6,10F10.4)
112   FORMAT(1X,A6,10F10.1)
      END


C *************************************************************************
      SUBROUTINE BOUND
C *************************************************************************

C *** PROVIDE BOUNDARY CONDITIONS ***

      INCLUDE 'PELLET.INC'

C *** SOUTHERN BOUNDARY ***

      DO 10 I=1,IN
      C(I,1) = C(I,2)
10    CONTINUE

C *** NORTHERN BOUNDARY ***

      DO 20 I=1,IN
      C(I,JN) = 0.0
20    CONTINUE

C *** EASTERN BOUNDARY ***

      DO 30 J=1,JN
      C(IN,J) = 0.0
30    CONTINUE

C *** WESTERN BOUNDARY ***

C *** MOVING SIDE BOX ***

      DO 40 J=1,JN
      C(1,J) = C(2,J)
40    CONTINUE

      END


C *************************************************************************
      SUBROUTINE TPREP
C *************************************************************************

C *** PREPARE FOR NEXT TIME STEP ***

      INCLUDE 'PELLET.INC'

      DO 10 I=1,IN
      DO 10 J=1,JN
      C0(I,J) = C(I,J)
10    CONTINUE

      END
```

```
C ***********************************************************************
      SUBROUTINE CPREP
C ***********************************************************************

C *** PREPARE FOR C-SWEEP ***

      INCLUDE 'PELLET.INC'
      REAL*8 DE(JD),DW(JD)

      DO 10 J=2,JNM
      DE(J) = DEW(1,J)*AREAY(J)/DKSI(1)
10    CONTINUE

      DO 20 I=2,INM
      DN    = 0.0
      DO 20 J=2,JNM
      DS    = DN
      DN    = DNS(I,J)*AREAX(I,J)/DETA(J)
      DW(J) = DE(J)
      DE(J) = DEW(I,J)*AREAY(J)/DKSI(I)
      AN(I,J) = DN
      AS(I,J) = DS
      AE(I,J) = DE(J)
      AW(I,J) = DW(J)
      AP0     = VOLUME(I,J)/DT
      SC(I,J) = AP0*C0(I,J)
      AP = (AN(I,J) + AS(I,J) + AE(I,J) + AW(I,J) + AP0) / RELAX

      IF (AP.LE.TINY) THEN
         IWARN = IWARN + 1
         WRITE(6,*)  '--- WARNING: C AVERAGED AT ',I,J
         WRITE(7,*)  '--- WARNING: C AVERAGED AT ',I,J
         WRITE(11,*) '--- WARNING: C AVERAGED AT ',I,J

         AN(I,J) = 0.25*RELAX
         AS(I,J) = 0.25*RELAX
         AE(I,J) = 0.25*RELAX
         AW(I,J) = 0.25*RELAX
         AP0     = 0.0
         SC(I,J) = C(I,J)*(1-RELAX)

      ELSE

         AN(I,J) = AN(I,J)/AP
         AS(I,J) = AS(I,J)/AP
         AE(I,J) = AE(I,J)/AP
         AW(I,J) = AW(I,J)/AP
         AP0     = AP0/AP
         SC(I,J) = SC(I,J)/AP + C(I,J)*(1-RELAX)

      ENDIF

      IF (.FALSE.) WRITE(7,110) I,J,AE(I,J),AW(I,J),AN(I,J),AS(I,J),
     :                          AP0,SC(I,J),AP

20    CONTINUE

100   FORMAT('1FD COEFFICIENTS CPREP'/
     :       4X,'I',3X,'J',4X,'AE',6X,'AW',6X,'AN',6X,'AS',5X,'AP0',
     :       8X,'SC',11X,'AP')
110   FORMAT(1X,2I4,5F8.5,1P,2E13.5)

      END
```

```
C ***********************************************************************
      SUBROUTINE DPREP
C ***********************************************************************

C *** CALCULATE THE VALUES OF D ***

      INCLUDE 'PELLET.INC'

      DMAX = 0.0
      DMIN = RMAX

      DO 10 I=1,IN
      DO 10 J=1,JN

      IF (C(I,J).GE.CALFA) THEN
         D(I,J) = D0
      ELSE
         ALFA = (CALFA-C(I,J))/CALFA
         D(I,J) = (1 + ALFA*(CK - 1))*D0
      ENDIF

      DMAX   = DMAX1(DMAX , D(I,J))
      DMIN   = DMIN1(DMIN , D(I,J))
10    CONTINUE

      END


C ***********************************************************************
      FUNCTION DNS(I,J)
C ***********************************************************************

C *** CALCULATE D AT NORTHERN AND SOUTHERN P CELL BOUNDARIES ***

      INCLUDE 'PELLET.INC'

      IF (J.EQ.1) THEN
         DNS  = D(I,1)
      ELSE IF (J.EQ.JNM) THEN
         DNS  = D(I,JN)
      ELSE IF (D(I,J).LT.TINY  .OR.  D(I,J+1).LT.TINY) THEN
         DNS  = 0.0
      ELSE
         DNS  = 1 / (FY(J)/D(I,J) + GY(J+1)/D(I,J+1))
      ENDIF

      END


C ***********************************************************************
      FUNCTION DEW(I,J)
C ***********************************************************************

C *** CALCULATE D AT EASTERN AND WESTERN P CELL BOUNDARIES ***

      INCLUDE 'PELLET.INC'

      IF (I.EQ.1) THEN
         DEW  = D(1,J)
      ELSE IF (I.EQ.INM) THEN
         DEW  = D(IN,J)
      ELSE IF (D(I,J).LT.TINY  .OR.  D(I+1,J).LT.TINY) THEN
         DEW  = 0.0
      ELSE
         DEW  = 1 / (FX(I)/D(I,J) + GX(I+1)/D(I+1,J))
      ENDIF
```

```
      END

C *************************************************************************
      SUBROUTINE TDMANS(I,DIR)
C *************************************************************************

C *** PERFORM TDMA NORTH-SOUTH ***

      INCLUDE 'PELLET.INC'
      INTEGER DIR
      REAL*8 ALFA(JD),BETA(JD)

      IF (DIR.EQ.1) THEN
         ATERM = THETA*AE(I,2)
      ELSE
         ATERM = THETA*AW(I,2)
      ENDIF

      AFACT = 1/(1 - ATERM)
      ALFA(2) = AFACT*AN(I,2)
      BETA(2) = AFACT*(AE(I,2)*C(I+1,2) + AW(I,2)*C(I-1,2) +
     :                 AS(I,2)*C(I,1)   + ATERM*C(I,2)     + SC(I,2))

      DO 10 J=3,JNM

      IF (DIR.EQ.1) THEN
         ATERM = THETA*AE(I,J)
      ELSE
         ATERM = THETA*AW(I,J)
      ENDIF

      AFACT = 1/(1 - ATERM)

      IF (DABS(1 - AFACT*AS(I,J)*ALFA(J-1)).LE.TINY) THEN
         IERROR = IERROR + 1
         WRITE(6,100)  I,J,AE(I,J),AW(I,J),AN(I,J),AS(I,J),
     :                 SC(I,J),ALFA(J-1)
         WRITE(7,100)  I,J,AE(I,J),AW(I,J),AN(I,J),AS(I,J),
     :                 SC(I,J),ALFA(J-1)
         WRITE(11,100) I,J,AE(I,J),AW(I,J),AN(I,J),AS(I,J),
     :                 SC(I,J),ALFA(J-1)
      ENDIF

100   FORMAT(' *** ERROR: IMMINENT TDMANS FAILURE AT I =',
     :       I4,' J =',I4/6F12.7)

      FACT    = AFACT / (1 - AFACT*AS(I,J)*ALFA(J-1))
      ALFA(J) = FACT * AN(I,J)
      BETA(J) = FACT * (AS(I,J)*BETA(J-1) + AE(I,J)*C(I+1,J) +
     :                  AW(I,J)*C(I-1,J)  - ATERM*C(I,J)     + SC(I,J))
10    CONTINUE

      DO 20 J=JNM,2,-1
      C1 = ALFA(J)*C(I,J+1) + BETA(J)
      RSCMAX = DMAX1(RSCMAX,DABS(C1-C(I,J)))
      CMAX   = DMAX1(CMAX , C1)
      CMIN   = DMIN1(CMIN , C1)
      C(I,J) = C1
20    CONTINUE

      END

C *************************************************************************
```

```
      SUBROUTINE TDMAEW(J,DIR)
C ***********************************************************************

C *** PERFORM TDMA EAST-WEST ***

      INCLUDE 'PELLET.INC'
      INTEGER DIR
      REAL*8 ALFA(ID),BETA(ID)

      IF (DIR.EQ.1) THEN
         ATERM = THETA*AN(2,J)
      ELSE
         ATERM = THETA*AS(2,J)
      ENDIF

      AFACT = 1/(1 - ATERM)
      ALFA(2) = AFACT*AE(2,J)
      BETA(2) = AFACT*(AN(2,J)*C(2,J+1) + AS(2,J)*C(2,J-1) +
     :                 AW(2,J)*C(1,J)   - ATERM*C(2,J)     + SC(2,J))

      DO 10 I=3,INM

      IF (DIR.EQ.1) THEN
         ATERM = THETA*AN(I,J)
      ELSE
         ATERM = THETA*AS(I,J)
      ENDIF

      AFACT = 1/(1 - ATERM)

      IF (DABS(1 - AFACT*AW(I,J)*ALFA(I-1)).LE.TINY) THEN
         IERROR = IERROR + 1
         WRITE(6,100)  I,J,AE(I,J),AW(I,J),AN(I,J),AS(I,J),
     :                 SC(I,J),ALFA(I-1)
         WRITE(7,100)  I,J,AE(I,J),AW(I,J),AN(I,J),AS(I,J),
     :                 SC(I,J),ALFA(I-1)
         WRITE(11,100) I,J,AE(I,J),AW(I,J),AN(I,J),AS(I,J),
     :                 SC(I,J),ALFA(I-1)
      ENDIF

100   FORMAT(' *** ERROR: IMMINENT TDMAEW FAILURE SCAN AT I =',
     :       I4,' J =',I4/6F12.7)

      FACT    = AFACT / (1 - AFACT*AW(I,J)*ALFA(I-1))
      ALFA(I) = FACT * AE(I,J)
      BETA(I) = FACT * (AW(I,J)*BETA(I-1) + AN(I,J)*C(I,J+1) +
     :                  AS(I,J)*C(I,J-1) - ATERM*C(I,J) + SC(I,J))
10    CONTINUE

      DO 20 I=INM,2,-1
      C1 = ALFA(I)*C(I+1,J) + BETA(I)
      RSCMAX = DMAX1(RSCMAX,DABS(C1-C(I,J)))
      CMAX   = DMAX1(CMAX , C1)
      CMIN   = DMIN1(CMIN , C1)
      C(I,J) = C1
20    CONTINUE

      END


C ***********************************************************************
      SUBROUTINE OVACON
C ***********************************************************************

C *** CALCULATE OVERALL CONTENTS ***
```

```
      INCLUDE 'PELLET.INC'

      CSUM1 = CSUM
      CSUM  = 0.0

      DO 10 I=2,INM
      DO 10 J=2,JNM
      CSUM = CSUM + C(I,J)*VOLUME(I,J)
10    CONTINUE

      DCSUM = (CSUM1 - CSUM)/DT

      END


C *************************************************************************
      SUBROUTINE OUTPUT(LU,NUM)
C *************************************************************************

C *** PRINT RESULTS ***

      INCLUDE 'PELLET.INC'
      CHARACTER*18 CFMT,DFMT
      CHARACTER*30 WHERE

      IF (NUM.EQ.0) THEN
         WHERE = 'END'
      ENDIF

      IF (FULL .OR. NUM.NE.0) THEN
         IX = 1
      ELSE
         IX = (IN-1)/15+1
      ENDIF

      MS = 0

      DO 40 K=1,IN,IX*15
      MS = MS + 1
      IB = K
      IE = MIN0(K+IX*15-1,IN)
      OCMAX = 0.0
      ODMAX = 0.0

      DO 10 I=IB,IE
      DO 10 J=1,JN
      OCMAX=DMAX1(OCMAX,C(I,J))
      ODMAX=DMAX1(ODMAX,D(I,J))
10    CONTINUE

      IF (OCMAX.GE.0.01 .AND. OCMAX.LT.100.0) THEN
         CFMT = '(1X,I2,15F8.4)     '
      ELSE
         CFMT = '(1X,I2,1P15E8.1E2)'
      ENDIF

      IF (ODMAX.GE.0.01 .AND. ODMAX.LT.100.0) THEN
         DFMT = '(1X,I2,15F8.4)     '
      ELSE
         DFMT = '(1X,I2,1P15E8.1E2)'
      ENDIF

      WRITE(LU,100) T,WHERE,MS
      WRITE(LU,101) RSCMAX,NRSCMX
      WRITE(LU,102) (I,I=IB,IE,IX)
```

```
      DO 20 J=JN,1,-1
      WRITE(LU,103) J,(C(I,J),I=IB,IE,IX)
20    CONTINUE

      WRITE(LU,104) DMIN,DMAX
      WRITE(LU,102) (I,I=IB,IE,IX)

      DO 30 J=JN,1,-1
      WRITE(LU,103) J,(D(I,J),I=IB,IE,IX)
30    CONTINUE

40    CONTINUE

100   FORMAT('1VARIABLE VALUES ',F6.1,1X,A30,'*',I1/)
101   FORMAT(//'1CONCENTRATION:   RSCMAX ',1PE9.2,' NRSCMX ',E9.2/)
102   FORMAT(1X,'J / I  ',15(I2,6X))
103   FORMAT(1X,I2,15F8.3)
104   FORMAT(//'1DIFFUSIVITY:   DMIN ',1PE9.2,' DMAX ',E9.2/)

      END


C *************************************************************************
      SUBROUTINE PLTDAT(LOGUNT)
C *************************************************************************

C *** SUPPLY RESTART DATA ***

      INCLUDE 'PELLET.INC'
      CHARACTER*1 BELL
      DATA BELL/7/

      IF (LOGUNT.LT.0) THEN
         LU = -LOGUNT
         OPEN(LU,STATUS='UNKNOWN')
      ELSE
         LU = LOGUNT
         OPEN(LU,STATUS='NEW')
      ENDIF

      WRITE(LU,100) IN,JN,XDIM,YDIM
      WRITE(LU,102) T,CINIT
      WRITE(LU,103) (DX(I),I=2,INM)
      WRITE(LU,103) (DY(J),J=2,JNM)
      WRITE(LU,103) (DKSI(I),I=1,INM)
      WRITE(LU,103) (DETA(J),J=1,JNM)
      WRITE(LU,103) ((C(I,J),J=1,JN),I=1,IN)
      WRITE(LU,103) ((D(I,J),J=1,JN),I=1,IN)

      CLOSE(LU)
      WRITE(6,104) BELL

100   FORMAT(2I5,1P,2E10.4E1)
102   FORMAT(F6.2,E15.5)
103   FORMAT(1P,99(5E15.8/))
104   FORMAT('+',A1)

      END
```

```
C ************************************************************************C
C                                                                        C
C       A program to read arbitrary results for a 2 dimensional structure C
C             (i.e. X- and Y-coordinates) and to plot these with         C
C                   UNIRAS functions. The user may choose:               C
C                                                                        C
C      i.           colour (DEFAULT) / black-and-white plots            C
C     ii.  automatic scaling (DEFAULT) / manual scale override option    C
C    iii.        1/4 th (DEFAULT) / whole AXISYMMETRIC structure         C
C     iv.     heading-, text- and unit strings and character height      C
C                                                                        C
C ************************************************************************C


      PARAMETER ID=50,JD=50,NCL=20

      REAL*4 DX(ID),DY(JD),C(ID,JD),CC(ID,JD),D(ID,JD)

      CHARACTER*13  FILNAM
      CHARACTER*60  HDGSTR,TXTSTR
      CHARACTER*10  UNTSTR
      CHARACTER*3   ONOFF,BLKWHT
      CHARACTER*7   WHOLE
      CHARACTER*132 LINE
      CHARACTER*1   CH

      LOGICAL       XYCORR,BLWH,WHOL,SELECT


      COMMON /LIM/ XMIN,XMAX,YMIN,YMAX,ZMIN,ZMAX,VMIN,VMAX
     :       /SCA/ SCALE,ISCALE,XDEV0,YDEV0
     :       /WRT/ UNTSTR,UNTHGT,HDGSTR,HDGHGT,TXTSTR,TXTHGT
     :       /DEV/ XSIZ,YSIZ,XYCORR,ESIZ
     :       /TYP/ ILUM,IHUE(12),ISAT(12),KOLOR,BLWH,WHOL

      COMMON /DIM/ IN,JN,XDIM,YDIM,SX(ID),SY(JD)

C *** HUE coordinate counterclockwise around cone ***

      DATA IHUE /0,30,60,90,120,150,180,210,240,270,300,330/

C *** 100 % saturation (i.e. outside of cone) ***

      DATA ISAT /100,100,100,100,100,100,100,100,100,100,100,100/


1000  FORMAT(A80)
1010  FORMAT(1X,A,I5)
1020  FORMAT( 7X,'X-MIN',7X,'X-MAX',7X,'Y-MIN',7X,
     :           'Y-MAX',7X,'Z-MIN',7X,'Z-MAX')
1030  FORMAT(1X,6(F'1.5,1X))
1040  FORMAT( 5X,'V-MIN',10X,'V-MAX',10X,'SCALE')
1050  FORMAT ('1 ,


C *** set default values ***

      KOLOR   = 1
      ONOFF   = 'OFF'
      WHOLE   = 'QUARTER'
      BLKWHT  = 'NO '
      UNTSTR  = '$'
      TXTSTR  = '$'
      HDGSTR  = '$'
      UNTHGT  = 3.0
```

```
      TXTHGT  = 3.5
      HDGHGT  = 3.5
      FILNAM  = ' '
      SELECT  = .FALSE.
      VECTOR  = .FALSE.
      PREVNT  = .FALSE.
      XYCORR  = .FALSE.
      BLWH    = .FALSE.
      WHOL    = .FALSE.

C *** extreme plotting values ***

      XMIN = 0.0
      XMAX = 0.0
      YMIN = 0.0
      YMAX = 0.0
      ZMIN = 0.0
      ZMAX = 0.0
      VMIN = 0.0
      VMAX = 0.0

C *** display options ***

10    CALL BELL

      WRITE(6,1050)
      WRITE(6,1050)
      WRITE(6,*) 'TIME',TIME
      WRITE(6,*) ' '
      WRITE(6,1020)
      WRITE(6,1030) XMIN,XMAX,YMIN,YMAX,ZMIN,ZMAX
      WRITE(6,*) ' '
      WRITE(6,1040)
      WRITE(6,  * )VMIN,VMAX,SCALE
      WRITE(6,*) ' '

C *** enter options ***

      WRITE(6,*)
     :'   FILENAME   -  Read result file FILENAME          ',FILNAM
      WRITE(6,*)
     :'   /HDG  "" h -  Enter hdg and charcter height   ',HDGHGT
      WRITE(6,*)
     :'    HDG       -  ',HDGSTR
      WRITE(6,*)
     :'   /TEXT "" h -  Enter text and chrtr height     ',TXTHGT
      WRITE(6,*)
     :'    TEXT      -  ',TXTSTR
      WRITE(6,*)
     :'   /UNIT "" h -  Enter units and chrtr height    ',UNTHGT
      WRITE(6,*)
     :'    UNIT      -  ',UNTSTR
      WRITE(6,*)
     :'   /SCALE     -  Scale override option             ',ONOFF
      WRITE(6,*)
     :'   /WHOLE     -  Plot whole / quarter structure     ',WHOLE
      WRITE(6,*)
     :'                 (repeat to return to 1/4-th again)'
      WRITE(6,*)
     :'   /BW        -  Black & White spectrum             ',BLKWHT
      WRITE(6,*)
     :'                 (repeat to return to colour again)'
      WRITE(6,*) '   /DRAW      -  Draw structure/resultant'
      WRITE(6,*) '   /REDRAW    -  Draw on previuosly selected device'
      WRITE(6,*) '   /STOP      -  End ADRAS program execution'
```

```
C *** read option ***

      READ(5,1000,ERR=10) LINE

C *** test option ***

      CALL UPCASE(LINE)

      IF (LINE(1:5).NE.'/STOP') GO TO 20'
      CALL BELL
      STOP

20    IF (LINE(1:3).EQ.'/BW') THEN
          IF(BLWH) THEN
             BLWH   = .FALSE.
             BLKWHT = 'NO '
          ELSE
             BLWH   = .TRUE.
             BLKWHT = 'YES'
          ENDIF
      GOTO 10
      ENDIF

      IF (LINE(1:5).EQ.'/WHOLE') THEN
          IF(WHOL) THEN
             WHOL   = .FALSE.
             WHOLE  = 'QUARTER'
          ELSE
             WHOL   = .TRUE.
             WHOLE  = 'WHOLE  '
             XMIN   = -XMAX
             YMIN   = -YMAX
          ENDIF
      GOTO 10
      ENDIF

      IF (LINE(1:5).EQ.'/DRAW') THEN
        IF (VMAX.GT.VMIN) GOTO 100
        WRITE(6,*) ' CONSTANT VALUE',VMAX
        GOTO 10
      ENDIF

      IF (LINE(1:7).EQ.'/REDRAW') THEN
        IF (VMAX.GT.VMIN) THEN
          IF (SELECT) THEN
            GOTO 110
          ELSE
            GOTO 100
          ENDIF
        ELSE
        WRITE(6,*) ' CONSTANT VALUE',VMAX
        GOTO 10
        ENDIF
      ENDIF

      IF (LINE(1:6).EQ.'/SCALE') THEN
30       CALL BELL
         WRITE(6,*) 'Give overall expected VMIN and VMAX'
         READ(5,*,ERR=30) VMIN, VMAX
            IF (VMIN .GT. VMAX) GOTO 30
            IF (SCALE .EQ. 0) GOTO 40
         VMIN = VMIN/SCALE
         VMAX = VMAX/SCALE
40       ONOFF= 'ON '
         GOTO 10
      ENDIF
```

```
      IF (LINE(1:4).EQ.'/HDG') THEN
         CALL POS('"',LINE,1,I)
         CALL POS('"',LINE,I+1,J)
         IF (J.GT.I+1) THEN
            HDGSTR = LINE(I+1:J-1)//'$'
            J = J+1
            CALL RGET(LINE,J,HDGHGT,IERR)
               IF (HDGHGT.GT.10.0) HDGHGT = 10.0
         ELSE
            WRITE(6,*) 'Error in string'
         ENDIF
      GOTO 10
      ENDIF

      IF (LINE(1:5).EQ.'/TEXT') THEN
         CALL POS('"',LINE,1,I)
         CALL POS('"',LINE,I+1,J)
         IF (J.GT.I+1) THEN
            TXTSTR = LINE(I+1:J-1)//'$'
            J = J+1
            CALL RGET(LINE,J,TXTHGT,IERR)
               IF (TXTHGT.GT.10.0) TXTHGT = 10.0
         ELSE
            WRITE(6,*) 'Error in string'
         ENDIF
      GOTO 10
      ENDIF

      IF (LINE(1:5).EQ.'/UNIT') THEN
         CALL POS('"',LINE,1,I)
         CALL POS('"',LINE,I+1,J)
         IF (J.GT.I+1) THEN
            UNTSTR = LINE(I+1:J-1)//'$'
            J = J+1
            CALL RGET(LINE,J,UNTHGT,IERR)
               IF (UNTHGT.GT.5.0) UNTHGT = 5.0
         ELSE
            WRITE(6,*) 'Error in string'
         ENDIF
      GOTO 10
      ENDIF

C *** define data file to plot ***

      OPEN(10,FILE=LINE,STATUS='OLD',ERR=10)
      FILNAM = LINE(1:30)

C *** read data from selected plot file ***

      READ(10,*) IN,JN,XDIM,YDIM
      READ(10,*) TIME,C0
      VMAX = C0
      READ(10,*) (DX(I),I=2,IN-1)
      READ(10,*) (DY(J),J=2,JN-1)
      READ(10,*) (DUMMY,I=1,IN-1)
      READ(10,*) (DUMMY,J=1,JN-1)
      READ(10,*) ((C(I,J),J=1,JN),I=1,IN)
      READ(10,*) ((D(I,J),J=1,JN),I=1,IN)
      CLOSE(10)

C *** override automatic scaling ***

      ISCALE = 0
      SCALE = AMAX1(VMAX,-VMIN)
      IF (SCALE .EQ. 0) GOTO 70
```

```
      ISCALE = LOG10(SCALE)
         IF (ISCALE .EQ. 1) THEN
            ISCALE = 0
            SCALE = 1.0
            GOTO 50
         ENDIF
      IF (ISCALE .LT. 0) ISCALE = ISCALE-1
      SCALE  = 10.0**ISCALE

50    VMIN = VMIN/SCALE
      VMAX = VMAX/SCALE

      DO 60 I=1,IN
         DO 60 J=1,JN
            CC(I,J) = C(I,J)/SCALE
60    CONTINUE


70    SX(1) = 0.0
      DO 80 I=2,IN
         SX(I) = SX(I-1) + DX(I)
         XMIN = AMIN1(XMIN,SX(I))
         XMAX = AMAX1(XMAX,SX(I))
80    CONTINUE

      SY(1) = 0.0
      DO 90 J=2,JN
         SY(J) = SY(J-1) + DY(J)
         YMIN = AMIN1(YMIN,SY(J))
         YMAX = AMAX1(YMAX,SY(J))
90    CONTINUE

      GOTO 10

C *** UNIRAS routines ***

100    CALL GROUTE(' ')
      SELECT=.TRUE.

110   CALL GOPEN

      CALL GINIT(NCL)
      CALL SHOW(CC,0.0,C0)
      CALL GCLOSE

      CALL BELL
      READ(5,'(A1)') CH

      GOTO 10

      END



C ***********************************************************************
      SUBROUTINE RGET(LINE,I,AREAL,IERR)
C ***********************************************************************

      CHARACTER*132 LINE

      RVAL  = 0
      RSIGN = 1
      IEXP  = 0
      ISIGN = 1
```

```
C *** preceding blanks ***

      DO 10 J=I,132
      IF (LINE(J:J).NE.' ' .AND. LINE(J:J).NE.',') GOTO 20
10    CONTINUE

      GOTO 90
20    IF (LINE(J:J).EQ.'+' .OR. LINE(J:J).EQ.'-') THEN
         IF (LINE(J:J).EQ.'-') RSIGN = -1
         J = J+1
      ENDIF

      I = J

      DO 30 J=I,132
         IF (LINE(J:J).EQ.' ' .OR. LINE(J:J).EQ.',') GOTO 80
         IF (LINE(J:J).EQ.'.') GOTO 40
         IF (LINE(J:J).EQ.'E') GOTO 60
         IF (LINE(J:J).LT.'0' .OR. LINE(J:J).GT.'9') GOTO 100
         RVAL = 10*RVAL + ICHAR(LINE(J:J)) - ICHAR('0')
30    CONTINUE

      J = 132
      GOTO 80

40    RDEC = 1.0
      I = J+1

      DO 50 J=I,132
         IF (LINE(J:J).EQ.' ' .OR. LINE(J:J).EQ.',') GOTO 80
         IF (LINE(J:J).EQ.'E') GOTO 60
         IF (LINE(J:J).LT.'0' .OR. LINE(J:J).GT.'9') GOTO 100
         RDEC = RDEC/10
         RVAL = RVAL + RDEC*(ICHAR(LINE(J:J))-ICHAR('0'))
50    CONTINUE

      J = 132
      GOTO 80
60    J = J+1

      IF (LINE(J:J).EQ.'+' .OR. LINE(J:J).EQ.'-') THEN
         IF (LINE(J:J).EQ.'-') ISIGN = -1
         J = J+1
      ENDIF
      I = J

      DO 70 J=I,132
         IF (LINE(J:J).EQ.' ' .OR. LINE(J:J).EQ.',') GOTO 80
         IF (LINE(J:J).LT.'0' .OR. LINE(J:J).GT.'9') GOTO 100
         IEXP = 10*IEXP + ICHAR(LINE(J:J)) - ICHAR('0')
70    CONTINUE

      J = 132
80    IERR  = 0
      IF (RVAL.EQ.0) THEN
         AREAL = 0.0
      ELSE
         IF (LOG10(RVAL)+ISIGN*IEXP.GT.38) GOTO 100
         AREAL = RSIGN*RVAL*10.**(ISIGN*IEXP)
      ENDIF

      GOTO 110

90    J = 132
      IERR  = -1
      GOTO 110
```

```
100   IERR = 1

110   I = J+1

      RETURN
      END


C *********************************************************************
      SUBROUTINE UPCASE(LINE)
C *********************************************************************

      CHARACTER*132 LINE
      LOGICAL QUOTE

      QUOTE = .FALSE.
      IOFS  = ICHAR('a') - ICHAR('A')

      DO 10 I=1,132
      IF (LINE(I:I).EQ.'"') QUOTE = .NOT. QUOTE
      IF (LINE(I:I).LT.'a' .OR. LINE(I:I).GT.'z' .OR. QUOTE) GOTO 10
      LINE(I:I) = CHAR(ICHAR(LINE(I:I)) - IOFS)
10    CONTINUE

      END


C *********************************************************************
      SUBROUTINE POS(FC,LINE,I,IPOS)
C *********************************************************************

      CHARACTER*1   FC
      CHARACTER*132 LINE

      DO 10 J=I,132
      IF (FC.EQ.LINE(J:J)) GOTO 20
10    CONTINUE

      IPOS = 0
      RETURN
20    IPOS = J
      END


C *********************************************************************
      SUBROUTINE GINIT(NCL)
C *********************************************************************

      LOGICAL BLWH
      LOGICAL HP7550,LT410X,GT4695,XYCORR

      CHARACTER*60  HDGSTR,TXTSTR
      CHARACTER*10  UNTSTR

      REAL*4  ZCL(100)

      COMMON /LIM/ XMIN,XMAX,YMIN,YMAX,ZMIN,ZMAX,VMIN,VMAX
     :       /SCA/ SCALE,ISCALE,XDEV0,YDEV0
     :       /WRT/ UNTSTR,UNTHGT,HDGSTR,HDGHGT,TXTSTR,TXTHGT
     :       /DEV/ XSIZ,YSIZ,XYCORR,ESIZ
     :       /TYP/ ILUM,IHUE(12),ISAT(12),KOLOR,BLWH,WHOL

      DIMENSION XX(10), YX(10), IPEN(10)
```

```
      DATA XX   /297.,297.,297.,297.,287., 10.,  0.,  0.,  0.,  0./
      DATA YX   / 40., 50.,200.,210.,210.,210.,210.,200., 50., 40./
      DATA IPEN /   0,   1,   0,   1,   1,   0,   1,   1,   0,   1/

1000  FORMAT('1')

      HP7550 = .FALSE.
      GT4695 = .FALSE.
      LT410X = .FALSE.

      ESIZ = 70.0

      CALL GRPSIZ(XSIZ,YSIZ)
      XSIZE = XSIZ
      YSIZE = YSIZ


C *** test for device type to adjust origin of plotting frame ***

      IF (XSIZ.GT.395.00 .AND. XSIZ.LT.397.00) THEN
         XDEV0=23.00                                  ! ... HP7550 (size B) /
         YDEV0= 4.00                                  !      ... PHP7550B
         HP7550 = .TRUE.
      ELSE
         IF (XSIZ.GT.420.00 .AND. XSIZ.LT.424.00) THEN
            XDEV0=40.00                               ! ... TEKTRONIX 4695  /
            YDEV0= 0.00                               !       ... GT4695
            GT4695 = .TRUE.

C *** The Paper-Roll on your GT4695 should  be as far RIGHT as possible. ***

            IF (XYCORR) GOTO 20
            WRITE(*,1000)
10          CALL BELL
            WRITE(6,*) ' Enter Horizontal and Vertical Corrections for '
            WRITE(6,*) 'exact A4-Frame Size (mm) on your GT4695 Plotter'
            WRITE(6,*) '          (-) Decrease, (+) Increase           '
            READ(5,*,ERR=10) XCORR, YCORR
            IF (ABS(XCORR) .GT. 50.0 .OR. ABS(YCORR) .GT. 50.0) GOTO 10
            XYCORR = .TRUE.
         ELSE
            XDEV0=0.0                                 ! ... TEKTRONIX 4105/6/7
            YDEV0=0.0                                 !       ... LT410X
            LT410X = .TRUE.
         ENDIF

20       CONTINUE

      ENDIF


      XSIZ = AMIN1(254.,XSIZ)
      YSIZ = AMIN1(170.,YSIZ)



C *** draw frame around the complete plotting - frame ***

      CALL RRECT(XDEV0+0.0,YDEV0+0.0, 234.0+XDEV0, 169.0+YDEV0, 0, 0.1)
      CALL GVECT(  0.0+XDEV0, 155.0+YDEV0, 0)
      CALL GVECT(234.0+XDEV0, 155.0+YDEV0, 1)

C *** indicators on where to cut paper to A4-format ***

      IF (LT410X) GOTO 50
         IF (HP7550) THEN
```

```
            DO 30 ITER=1,5
30          CALL GVECT (XX(ITER)-20.00,YX(ITER)-13.00,IPEN(ITER))
            CALL GVECT (50.0    -20.00, 210.0  -13.00, 0         )
            CALL GVECT (40.0    -20.00, 210.0  -13.00, 1         )
         ELSE
            DO 40 ITER=1,10
               IF (ITER .LT. 6) THEN
                  CALL GVECT ((XX(ITER)+XCORR),
     :                        (YX(ITER)+YCORR),IPEN(ITER))
               ELSE
                  CALL GVECT ( XX(ITER),
     :                        (YX(ITER)+YCORR),IPEN(ITER))
               ENDIF
40          CONTINUE
         ENDIF

C *** define size of viewport ***

50    CALL GPRINT(0)

      CALL GVPORT(5.0+XDEV0,20.0+YDEV0,XSIZ-85.0,YSIZ-50.0)

      CALL GLIMIT(XMIN,XMAX,YMIN,YMAX,0.0,0.0)

      CALL GEOWID(FRAME)

      DO 60 I=0,NCL
         ZCL(I+1) = I*(VMAX-VMIN)/NCL + VMIN
60    CONTINUE

C *** draw color scale legend ***

      CALL GCHARF('SOFT')
      CALL GCHARF('ITAL')
      CALL GCHARC(1)
      CALL GCONA(2.,1,50.,3)

      CALL GCMODE(4,ZIAMODE)

C *** Black & White spectrum ***

         IF (BLWH) THEN
            CALL GSHADE(3,0)

C *** Colour spectrum ***

         ELSE
            CALL GSHADE(6,0)
         ENDIF

      CALL GZCL(ZCL,NCL,0)
      CALL GSCSCO('^<s^>$s',4.0,2,0,1)
      CALL GCOSCL(XSIZ+XDEV0-ESIZ,0.065*YSIZ+YDEV0)
      CALL GCHARJ(0)
      X0 = XSIZ+XDEV0-ESIZ
      Y0 = 0.065*YSIZ+YDEV0+110.0

C *** write units above color scale legend ***

      CALL GSCAMM
      CALL GCHARF('SOFT')
      CALL GCHARF('ITAL')
      CALL GCHARC(1)
      CALL GCHARJ(7)
      CALL GCHAR(UNTSTR,X0+4.0,Y0,UNTHGT)
```

```
C *** write scale factor above color scale legend ***

      CALL GCHARF('SOFT')
      CALL GCHARF('ITAL')
      CALL GCHARC(1)
      CALL GCHAR('  * 10$',X0+28.5,Y0,3.0)
      CALL GNUMB(1.0*ISCALE,X0+39.5,Y0+3.0,2.0,0)

C *** write heading above drawing ***

      CALL GCHARF('ITAL')
      CALL GCHARC(1)
      CALL GCHARJ(7)
      CALL GCHAR(HDGSTR,117.0+XDEV0,164.0+YDEV0,HDGHGT)

C *** write text below drawing ***

      CALL GCHARF('ITAL')
      CALL GCHARC(1)
      CALL GCHARJ(1)
      CALL GCHAR(TXTSTR, 92.0+XDEV0,YDEV0+2.0*TXTHGT,TXTHGT)

      END



C ***********************************************************************
      SUBROUTINE BELL
C ***********************************************************************

      DATA IBELL /7/
      WRITE(*,'(1X,2A1,$)') IBELL,IBELL
      END



C ***********************************************************************
      SUBROUTINE SHOW(FI,FIMIN,FIMAX)
C ***********************************************************************

      PARAMETER ID=50,JD=50

      REAL*4 FI(ID,JD),X(4),Y(4),Z(4)

      LOGICAL WHOL

      COMMON /LIM/ XMIN,XMAX,YMIN,YMAX,ZMIN,ZMAX,VMIN,VMAX
     :       /SCA/ SCALE,ISCALE,XDEV0,YDEV0
     :       /WRT/ UNTSTR,UNTHGT,HDGSTR,HDGHGT,TXTSTR,TXTHGT
     :       /DEV/ XSIZ,YSIZ,XYCORR,ESIZ
     :       /TYP/ ILUM,IHUE(12),ISAT(12),KOLOR,BLWH,WHOL

      COMMON /DIM/ IN,JN,XDIM,YDIM,SX(ID),SY(JD)


      CALL GVPORT(20.0+XDEV0,25.0+YDEV0,XSIZ-85.0,YSIZ-50.0)
      CALL GLIMIT(XMIN,XMAX,YMIN,YMAX,0.0,0.0)
      CALL GSCALE


C *** Draw 1st Quarter ***

      DO 10 I=1,IN-1
      DO 10 J=1,JN-1
      X(1) = SX(I)
      Y(1) = SY(J)
```

```
      Z(1) = FI(I,J)
      X(2) = SX(I+1)
      Y(2) = SY(J)
      Z(2) = FI(I+1,J)
      X(3) = SX(I+1)
      Y(3) = SY(J+1)
      Z(3) = FI(I+1,J+1)
      X(4) = SX(I)
      Y(4) = SY(J+1)
      Z(4) = FI(I,J+1)
      CALL GSURF4(X,Y,Z)
10    CONTINUE

C *** Duplicate remaining 3/4 th of axisymmetric structure, if requested ***

      IF (WHOL) THEN
      DO 20 I=1,IN-1
      DO 20 J=1,JN-1
      X(1) = -SX(I)
      Y(1) = SY(J)
      Z(1) = FI(I,J)
      X(2) = -SX(I+1)
      Y(2) = SY(J)
      Z(2) = FI(I+1,J)
      X(3) = -SX(I+1)
      Y(3) = SY(J+1)
      Z(3) = FI(I+1,J+1)
      X(4) = -SX(I)
      Y(4) = SY(J+1)
      Z(4) = FI(I,J+1)
      CALL GSURF4(X,Y,Z)
20    CONTINUE

      DO 30 I=1,IN-1
      DO 30 J=1,JN-1
      X(1) = SX(I)
      Y(1) = -SY(J)
      Z(1) = FI(I,J)
      X(2) = SX(I+1)
      Y(2) = -SY(J)
      Z(2) = FI(I+1,J)
      X(3) = SX(I+1)
      Y(3) = -SY(J+1)
      Z(3) = FI(I+1,J+1)
      X(4) = SX(I)
      Y(4) = -SY(J+1)
      Z(4) = FI(I,J+1)
      CALL GSURF4(X,Y,Z)
30    CONTINUE

      DO 40 I=1,IN-1
      DO 40 J=1,JN-1
      X(1) = -SX(I)
      Y(1) = -SY(J)
      Z(1) = FI(I,J)
      X(2) = -SX(I+1)
      Y(2) = -SY(J)
      Z(2) = FI(I+1,J)
      X(3) = -SX(I+1)
      Y(3) = -SY(J+1)
      Z(3) = FI(I+1,J+1)
      X(4) = -SX(I)
      Y(4) = -SY(J+1)
      Z(4) = FI(I,J+1)
      CALL GSURF4(X,Y,Z)
40    CONTINUE
```

SAMPLE: NATURAL RUBBER (INITIAL SLS CONTENT 55%)

DATA FILE: d.dat
INITIAL CONTENT 1.11E+4

TIME	SCANS	NRSCMAX	FLUX	CUM REL	% REL
0.10	6	4.90E-4	6.16E+3	6.47E+2	5.81
0.21	7	6.55E-4	3.55E+3	1.04E+3	9.33
0.32	28	9.11E-4	2.31E+3	1.31E+3	11.73
0.43	10	6.15E-4	1.82E+3	1.53E+3	13.71
0.55	24	9.84E-4	1.51E+3	1.72E+3	15.44
0.68	10	7.13E-4	1.22E+3	1.88E+3	16.91
0.81	19	9.54E-4	9.64E+2	2.02E+3	18.13
0.95	12	7.27E-4	8.02E+2	2.14E+3	19.19
1.10	11	8.36E-4	7.19E+2	2.25E+3	20.20
1.26	21	9.19E-4	6.70E+2	2.36E+3	21.18
1.42	17	9.44E-4	6.40E+2	2.47E+3	22.16
1.59	12	7.28E-4	6.39E+2	2.58E+3	23.19
1.77	19	9.92E-4	6.73E+2	2.71E+3	24.33
1.96	10	8.10E-4	7.22E+2	2.85E+3	25.61
2.16	18	8.29E-4	7.56E+2	3.01E+3	27.02
2.37	15	9.02E-4	7.61E+2	3.18E+3	28.51
2.58	9	6.72E-4	7.37E+2	3.34E+3	30.03
2.81	19	9.52E-4	6.96E+2	3.51E+3	31.53
3.05	16	9.80E-4	6.44E+2	3.67E+3	33.00
3.31	12	9.15E-4	5.89E+2	3.83E+3	34.40
3.57	14	9.67E-4	5.42E+2	3.98E+3	35.75
3.85	18	9.78E-4	5.09E+2	4.13E+3	37.09
4.14	15	8.83E-4	4.91E+2	4.28E+3	38.44
4.45	9	7.00E-4	4.81E+2	4.44E+3	39.84
4.77	16	7.25E-4	4.69E+2	4.60E+3	41.26
5.11	16	9.06E-4	4.54E+2	4.76E+3	42.72
5.47	18	7.88E-4	4.34E+2	4.92E+3	44.17
5.84	13	7.75E-4	4.12E+2	5.08E+3	45.62
6.23	16	9.17E-4	3.91E+2	5.24E+3	47.07
6.64	19	9.20E-4	3.73E+2	5.40E+3	48.52
7.08	13	7.00E-4	3.57E+2	5.57E+3	49.97
7.53	16	8.89E-4	3.43E+2	5.73E+3	51.44
8.01	15	9.34E-4	3.28E+2	5.89E+3	52.91
8.51	18	8.19E-4	3.13E+2	6.06E+3	54.39
9.03	15	9.40E-4	2.98E+2	6.22E+3	55.87
9.58	14	9.53E-4	2.84E+2	6.39E+3	57.34
10.16	18	8.08E-4	2.71E+2	6.55E+3	58.83
10.77	16	9.32E-4	2.59E+2	6.72E+3	60.31
11.41	14	7.31E-4	2.46E+2	6.88E+3	61.79
12.08	15	8.39E-4	2.34E+2	7.05E+3	63.27
12.78	13	8.17E-4	2.22E+2	7.21E+3	64.75
13.52	17	7.93E-4	2.12E+2	7.38E+3	66.22
14.30	16	8.87E-4	2.01E+2	7.54E+3	67.70
15.11	15	7.14E-4	1.91E+2	7.70E+3	69.16
15.97	14	7.33E-4	1.80E+2	7.86E+3	70.62
16.87	13	7.65E-4	1.70E+2	8.03E+3	72.05
17.81	15	9.84E-4	1.62E+2	8.19E+3	73.49
18.80	17	9.37E-4	1.53E+2	8.34E+3	74.92
19.84	13	8.95E-4	1.42E+2	8.50E+3	76.32
20.93	16	7.87E-4	1.36E+2	8.66E+3	77.71
22.08	13	9.49E-4	1.25E+2	8.81E+3	79.06
23.29	14	8.83E-4	1.18E+2	8.95E+3	80.40
24.55	14	9.85E-4	1.10E+2	9.10E+3	81.70
25.88	15	9.09E-4	1.03E+2	9.24E+3	82.99
27.27	16	8.44E-4	9.59E+1	9.38E+3	4.25
28.73	16	9.22E-4	8.84E+1	9.52E+3	85.47
30.27	16	9.99E-4	8.12E+1	9.65E+3	86.64
31.89	17	9.31E-4	7.50E+1	9.78E+3	87.79
33.58	18	8.79E-4	6.90E+1	9.90E+3	88.89
35.36	18	9.55E-4	6.24E+1	1.00E+4	89.94
37.23	19	8.96E-4	5.68E+1	1.01E+4	90.94
39.19	19	9.16E-4	5.08E+1	1.02E+4	91.88
41.25	19	9.11E-4	4.51E+1	1.03E+4	92.75
43.41	18	9.72E-4	3.92E+1	1.04E+4	93.55
45.68	18	9.28E-4	3.43E+1	1.05E+4	94.28
48.06	17	9.46E-4	2.93E+1	1.06E+4	94.94
50.57	16	9.49E-4	2.48E+1	1.06E+4	95.53
53.20	15	9.41E-4	2.09E+1	1.07E+4	96.05
55.96	13	9.87E-4	1.68E+1	1.07E+4	96.48
58.85	12	9.65E-4	1.38E+1	1.08E+4	96.86

PROGRAM STOP. ERRORS: 0 WARNINGS: 0

SAMPLE: STYRENE-BUTADIENE RUBBER (INITIAL SLS CONTENT 35%)

DATA FILE: d.dat
INITIAL CONTENT 7.09E+3

TIME	SCANS	NRSCMAX	FLUX	CUM REL	% REL
0.10	5	2.77E-4	1.09E+3	1.14E+2	1.61
0.21	5	2.31E-4	9.39E+2	2.18E+2	3.07
0.32	4	9.91E-4	8.08E+2	3.11E+2	4.39
0.43	4	8.51E-4	6.95E+2	3.96E+2	5.59
0.55	4	7.72E-4	5.98E+2	4.72E+2	6.66
0.68	4	7.42E-4	5.15E+2	5.41E+2	7.64
0.81	4	7.93E-4	4.43E+2	6.04E+2	8.52
0.95	4	8.53E-4	3.81E+2	6.60E+2	9.31
1.10	4	9.10E-4	3.28E+2	7.11E+2	10.03
1.26	4	9.61E-4	2.83E+2	7.57E+2	10.68
1.42	5	3.24E-4	2.44E+2	7.99E+2	11.27
1.59	5	3.47E-4	2.11E+2	8.36E+2	11.80
1.77	5	3.67E-4	1.82E+2	8.71E+2	12.28
1.96	5	3.90E-4	1.58E+2	9.02E+2	12.73
2.16	5	7.38E-4	1.38E+2	9.31E+2	13.13
2.37	6	6.43E-4	1.22E+2	9.57E+2	13.51
2.58	6	7.58E-4	1.12E+2	9.83E+2	13.87
2.81	6	6.19E-4	1.06E+2	1.01E+3	14.23
3.05	6	5.48E-4	1.05E+2	1.03E+3	14.60
3.31	6	5.15E-4	1.08E+2	1.06E+3	15.01
3.57	6	3.77E-4	1.13E+2	1.10E+3	15.45
3.85	5	7.70E-4	1.16E+2	1.13E+3	15.93
4.14	5	5.54E-4	1.16E+2	1.16E+3	16.43
4.45	5	9.52E-4	1.13E+2	1.20E+3	16.95
4.77	7	7.74E-4	1.06E+2	1.24E+3	17.45
5.11	7	7.86E-4	9.75E+1	1.27E+3	17.94
5.47	6	8.90E-4	8.78E+1	1.30E+3	18.41
5.84	6	4.58E-4	7.82E+1	1.34E+3	18.84
6.23	7	9.37E-4	6.95E+1	1.36E+3	19.24
6.64	8	7.03E-4	6.30E+1	1.39E+3	19.63
7.08	7	8.75E-4	5.99E+1	1.42E+3	20.01
7.53	6	9.48E-4	6.04E+1	1.45E+3	20.42
8.01	6	5.74E-4	6.30E+1	1.48E+3	20.86
8.51	6	9.00E-4	6.63E+1	1.51E+3	21.35
9.03	6	7.18E-4	6.92E+1	1.55E+3	21.89
9.58	9	9.04E-4	7.16E+1	1.59E+3	22.48
10.16	9	6.99E-4	7.38E+1	1.64E+3	23.11
10.77	9	8.39E-4	7.62E+1	1.69E+3	23.80
11.41	8	7.70E-4	7.91E+1	1.74E+3	24.54
12.08	7	4.13E-4	8.23E+1	1.80E+3	25.36
12.78	11	8.52E-4	8.51E+1	1.86E+3	26.25
13.52	9	6.37E-4	8.67E+1	1.93E+3	27.20
14.30	7	9.54E-4	8.65E+1	2.00E+3	28.19
15.11	11	6.91E-4	8.46E+1	2.07E+3	29.22
15.97	10	9.63E-4	8.12E+1	2.14E+3	30.25
16.87	7	9.63E-4	7.69E+1	2.22E+3	31.27
17.81	11	7.70E-4	7.25E+1	2.29E+3	32.28
18.80	13	7.75E-4	6.80E+1	2.36E+3	33.28
19.84	11	8.26E-4	6.37E+1	2.43E+3	34.26
20.93	10	7.69E-4	5.99E+1	2.50E+3	35.23
22.08	13	9.00E-4	5.69E+1	2.57E+3	36.20
23.29	9	8.73E-4	5.52E+1	2.64E+3	37.18
24.55	13	8.85E-4	5.42E+1	2.71E+3	38.20
25.88	13	9.28E-4	5.38E+1	2.78E+3	39.26
27.27	8	8.98E-4	5.32E+1	2.86E+3	40.36
28.73	14	7.46E-4	5.23E+1	2.94E+3	41.49
30.27	10	8.29E-4	5.08E+1	3.02E+3	42.65
31.89	12	8.07E-4	4.91E+1	3.11E+3	43.82
33.58	14	9.93E-4	4.70E+1	3.19E+3	45.00
35.36	9	7.36E-4	4.49E+1	3.27E+3	46.19
37.23	15	9.15E-4	4.31E+1	3.36E+3	47.38
39.19	11	8.27E-4	4.15E+1	3.44E+3	48.58
41.25	13	9.07E-4	4.01E+1	3.53E+3	49.81
43.41	14	8.12E-4	3.88E+1	3.62E+3	51.05
45.68	12	9.52E-4	3.74E+1	3.71E+3	52.31
48.06	11	7.04E-4	3.60E+1	3.80E+3	53.58
50.57	15	8.86E-4	3.46E+1	3.89E+3	54.86
53.20	11	9.99E-4	3.31E+1	3.98E+3	56.15
55.96	14	9.32E-4	3.18E+1	4.07E+3	57.45
58.85	12	9.34E-4	3.05E+1	4.16E+3	58.76

PROGRAM STOP. ERRORS: 0 WARNINGS: 0

APPENDIX 7D

Concentration Distribution of SLS in an SBR Pellet at Different Intervals During the Elution Period

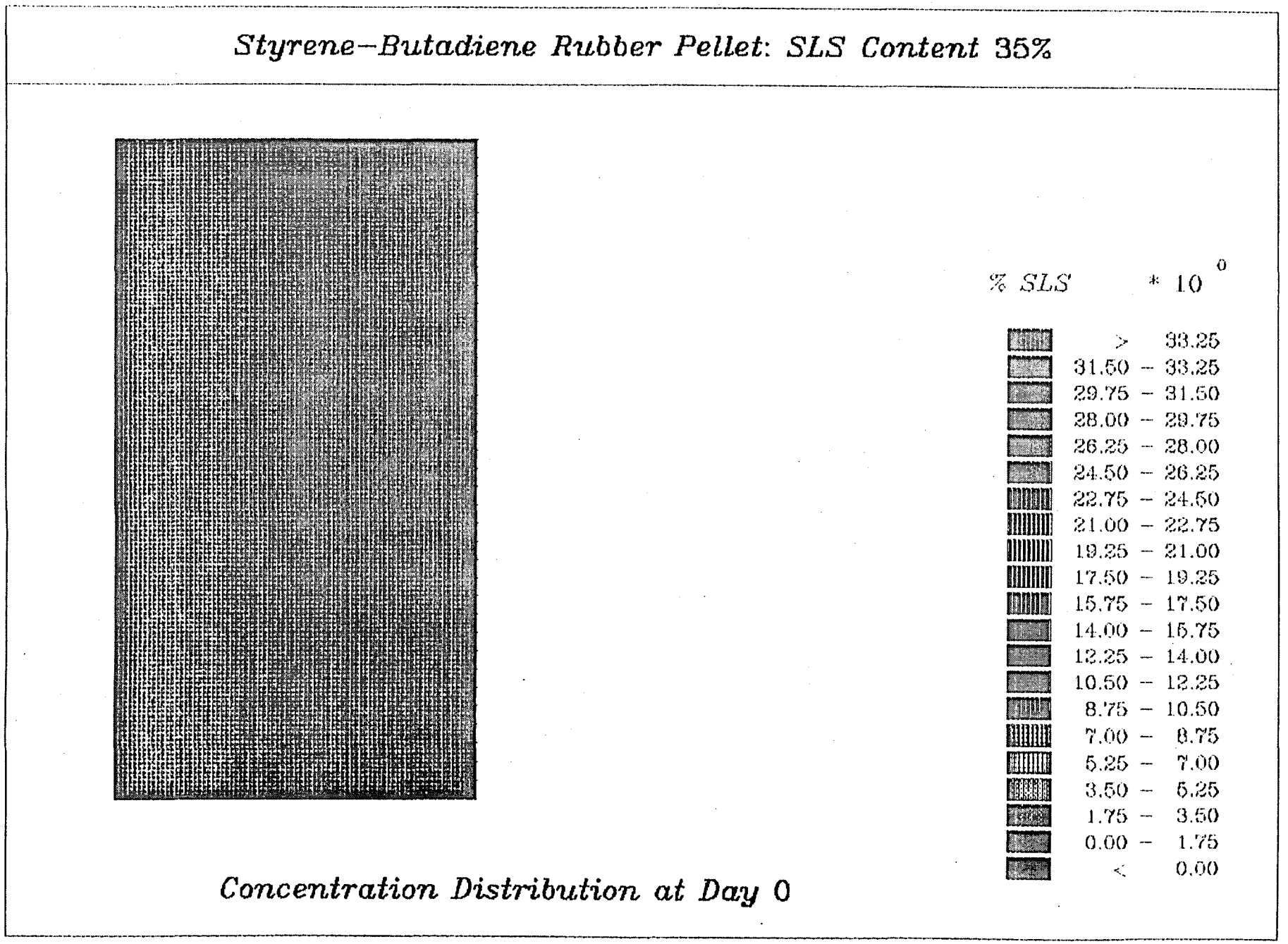

FIGURE 7D(a). Concentration distribution of SLS in a styrene-butadiene-rubber pellet before elution

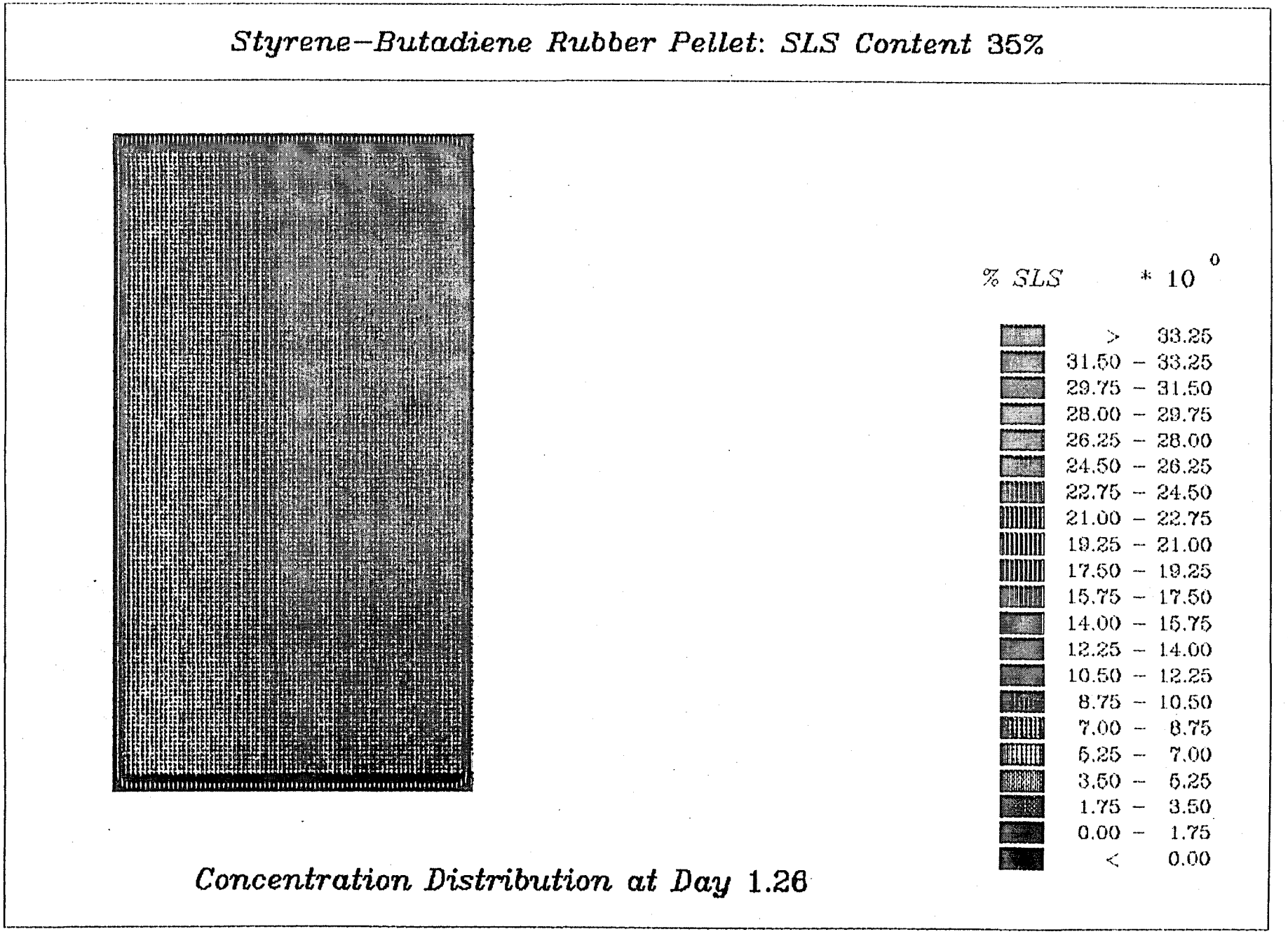

FIGURE 7D(b). Concentration distribution of SLS in a styrene-butadiene-rubber pellet after 1,26 days elution

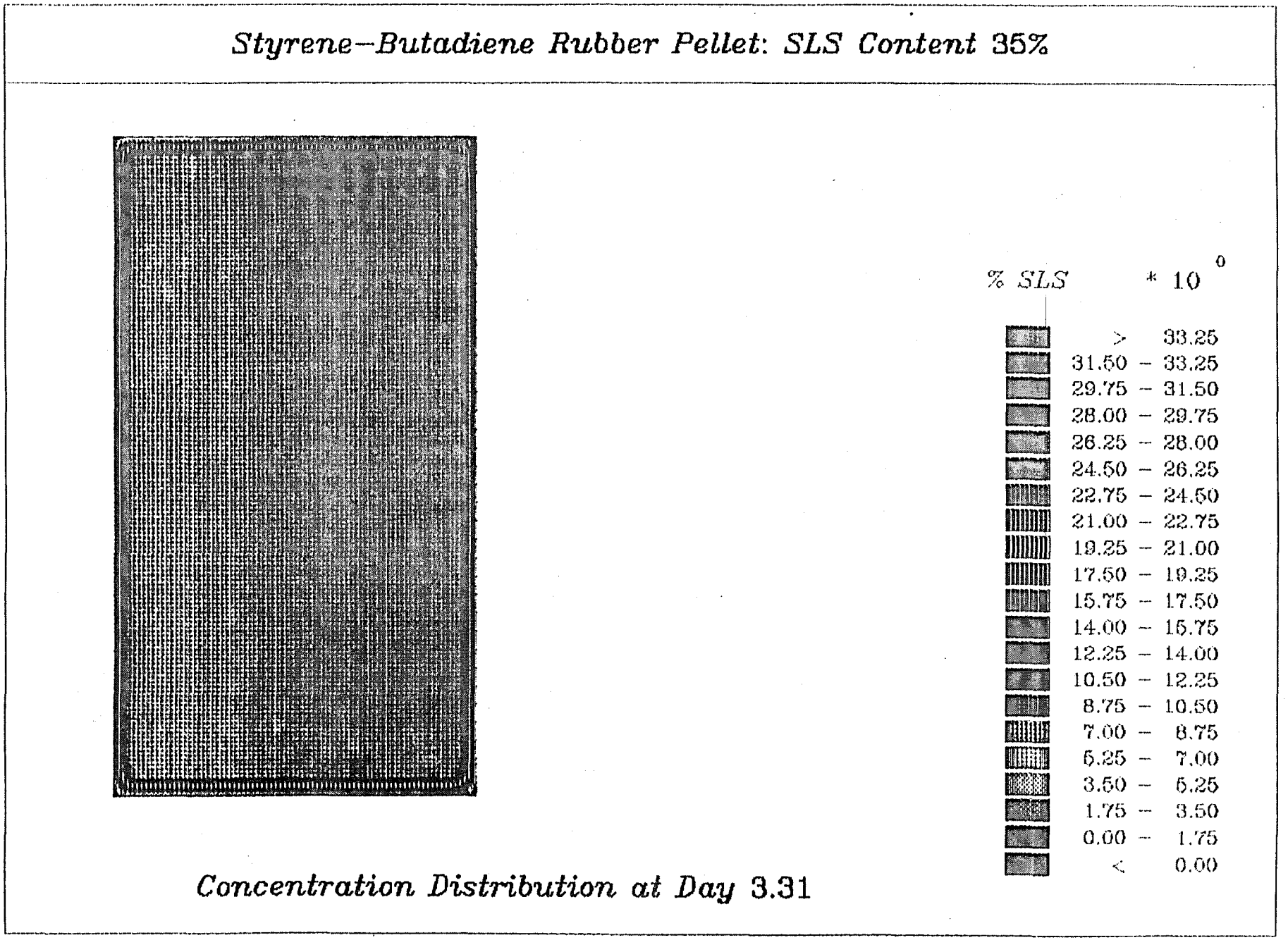

FIGURE 7D(c). Concentration distribution of SLS in a styrene-butadiene-rubber pellet after 3,31 days elution

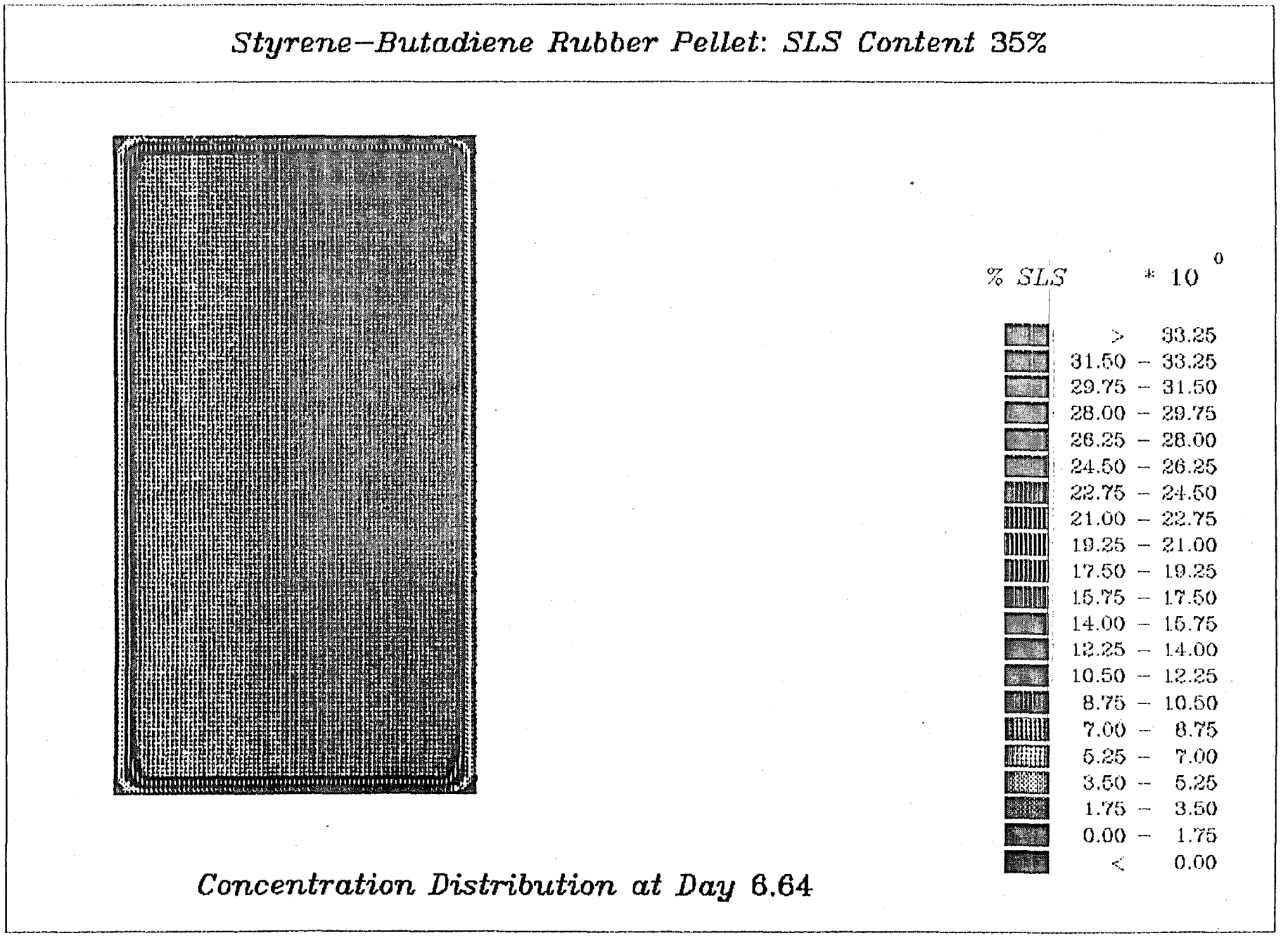

FIGURE 7D(d). Concentration distribution of SLS in a styrene-butadiene-rubber pellet after 6,64 days elution

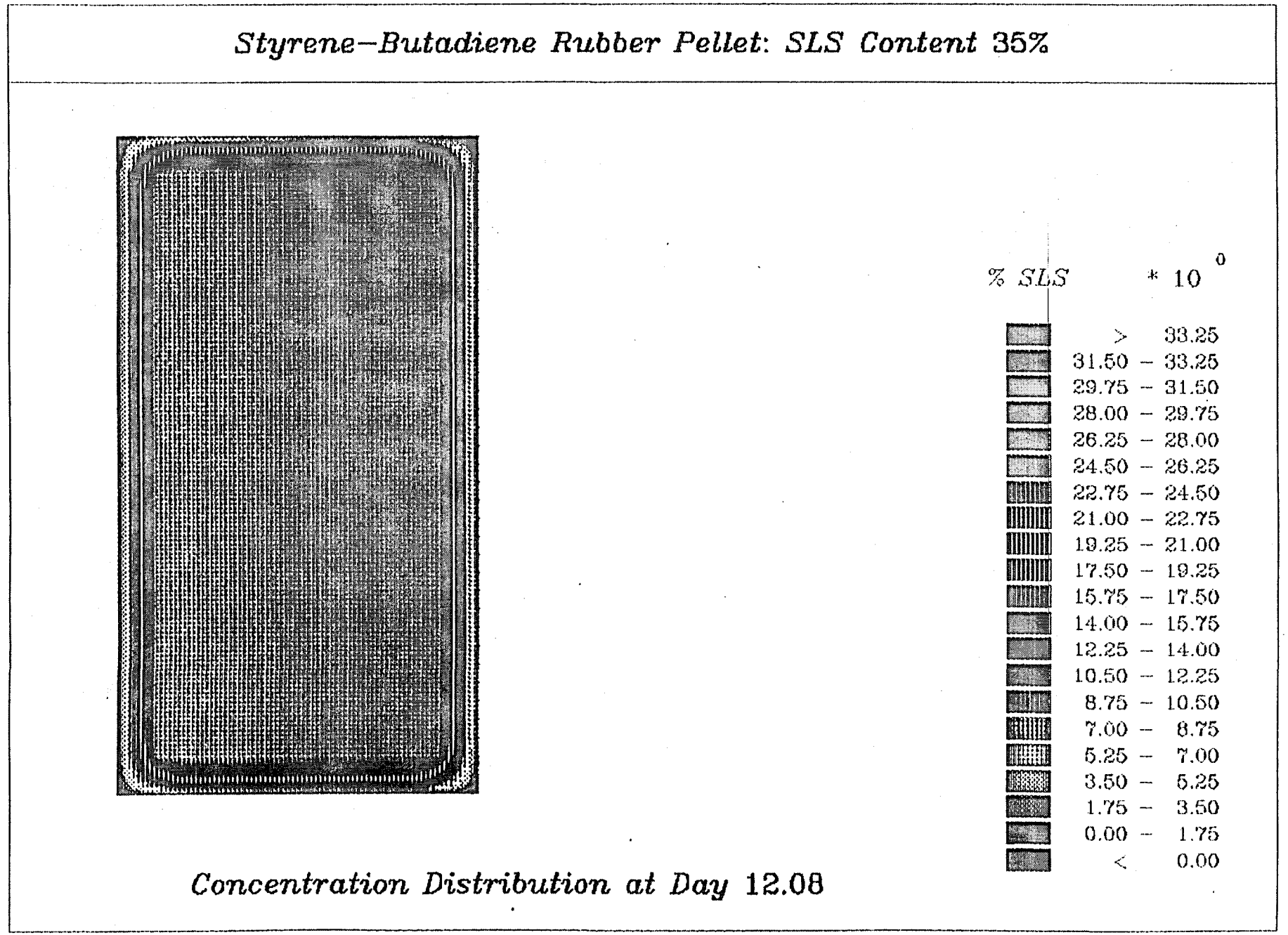

FIGURE 7D(e). Concentration distribution of SLS in a styrene-butadiene-rubber pellet after 12,08 days elution

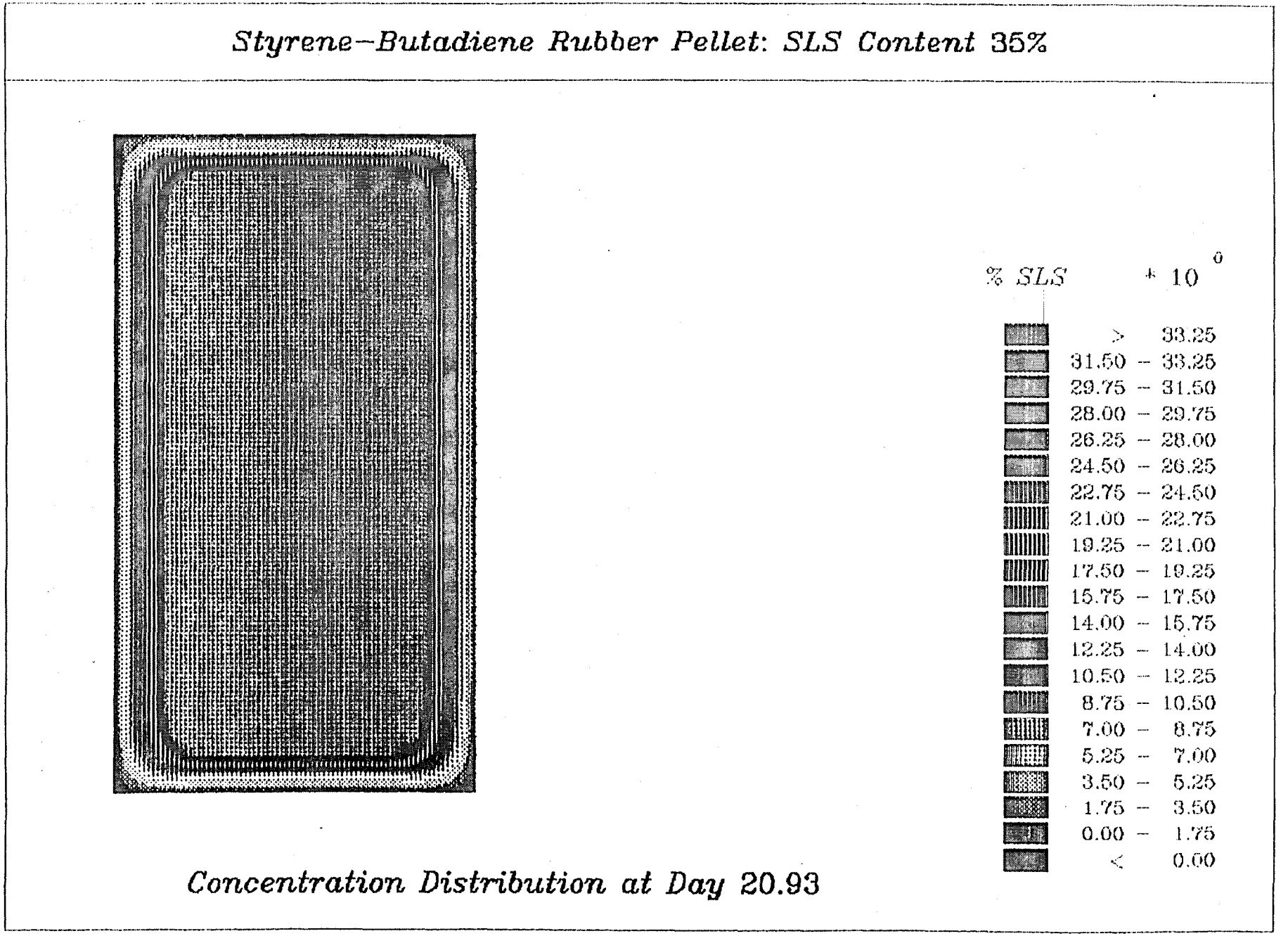

FIGURE 7D(f). Concentration distribution of SLS in a styrene-butadiene-rubber pellet after 20,93 days elution

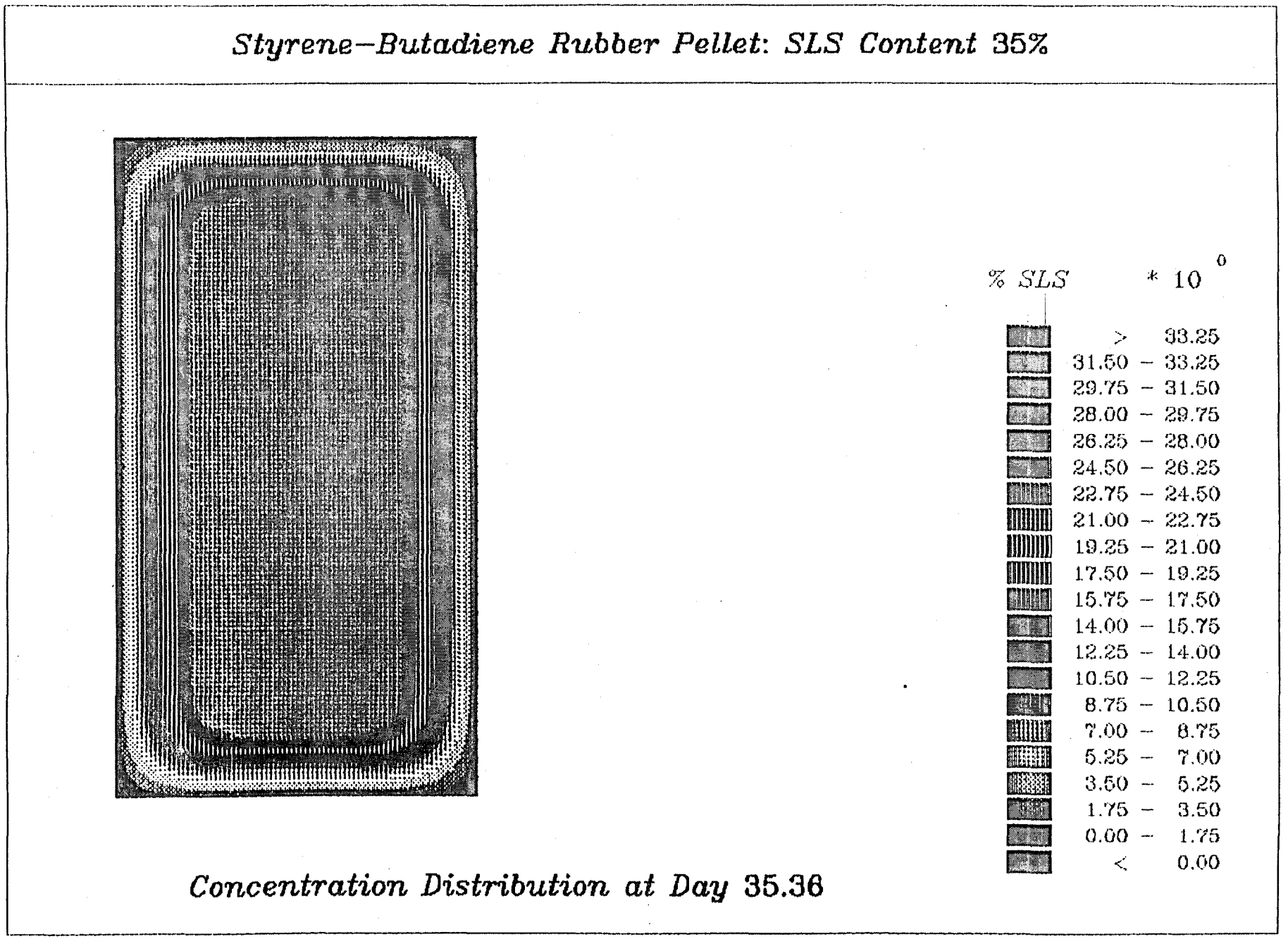

FIGURE 7D(g). Concentration distribution of SLS in a styrene-butadiene-rubber pellet after 35,36 days elution

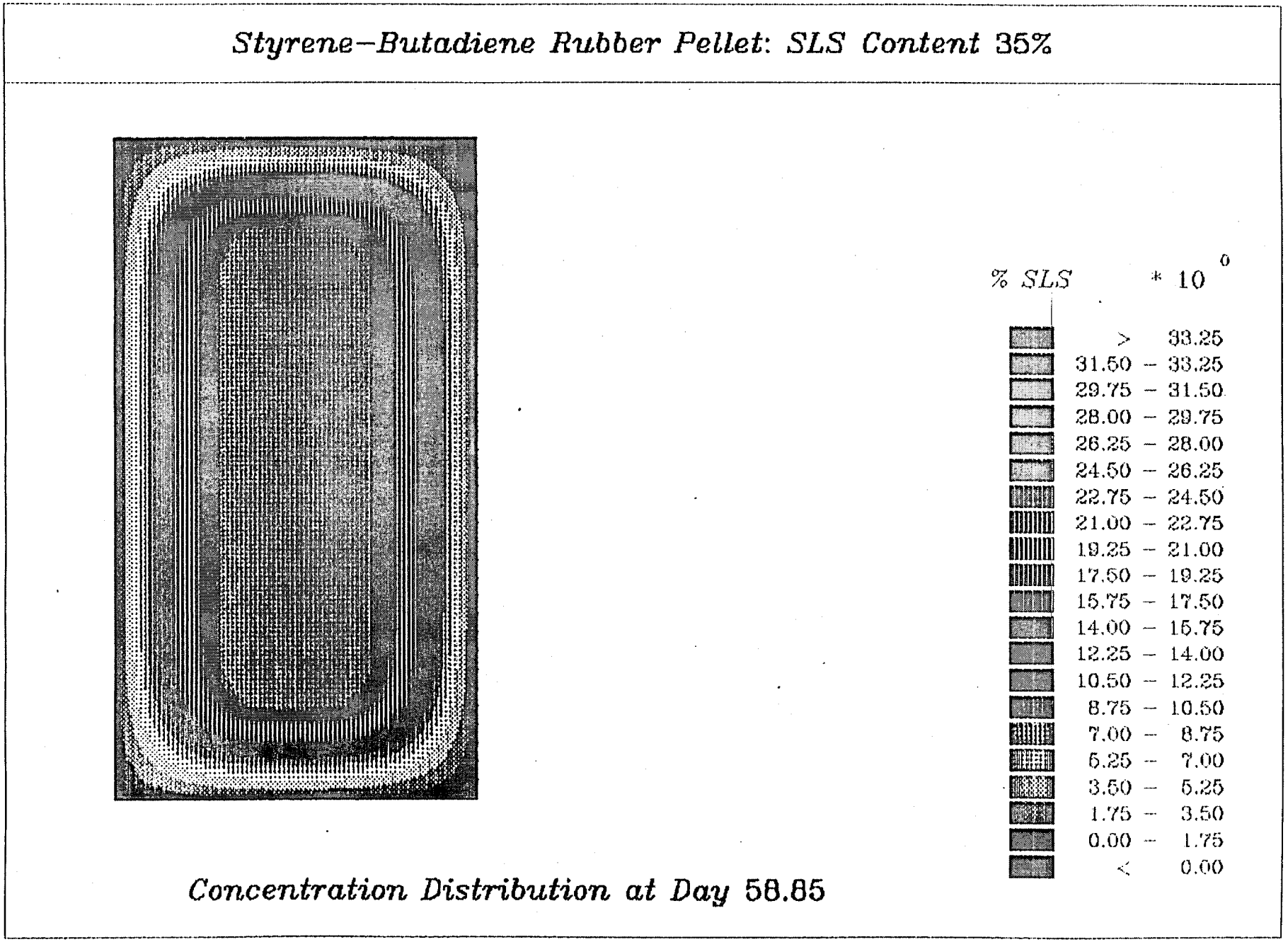

FIGURE 7D (h). Concentration distribution of SLS in a styrene-butadiene-rubber pellet after 58,85 days elution

APPENDIX 8A

THE BEHAVIOUR OF SURFACTANTS IN SOLUTION

Surfactants have two very important properties, namely, surface activity, i.e., the ability to adsorb strongly to air-water and oil-water interfaces and to surfaces of hydrophobic solids (e.g. carbon) or to macromolecules (e.g. proteins), and the tendency to form micellar aggregates in solution.

Over the years, an enormous amount of research has gone into studying the surface-active properties of surfactants, the phenomenon of micelle formation, and the solubilization of otherwise insoluble substances by micellar solutions. The literature on surfactants and micelle formation is immense, and a reasonably complete overview would be far beyond the scope of this thesis. References 1 to 8 are convenient sources for review of this extremely wide and diverse field.

In this section, the behaviour of surfactants in solution is discussed briefly, with emphasis on aspects such as general structural features of surfactants, formation of micelles in aqueous media, the critical micelle concentration, the structure and shape of micelles, and the formation of reverse micelles in apolar media.

1. General Structural Features of Surfactants

Surfactants have a characteristic molecular structure consisting of a structural group that has very little attraction for the solvent, known as a lyophobic group (or hydrophobic group,if the solvent is water), together with a group that has strong attraction for the solvent, called the lyophilic group (or hydrophilic group in aqueous media). This is known as an amphipathic structure[6,9]. An immense number of amphipathic monomers are known[6,10].

The hydrophobic group is usually a long-chain hydrocarbon residue, and less often a halogenated or oxygenated hydrocarbon or siloxane chain. The hydrophobic par can be of different chain lengths (usually between C_8 and C_{16}), it can contain unsaturated portions or aromatic moieties, and it can be branched or consist of two or more chains[9]. The hydrophilic group is an ionic or highly polar group. Depending on the nature of the hydrophilic group, surfactants are classified as anionic, cationic, zwitterionic, and non-ionic[6]. The ionic surfactants are, of course, always associated with counterions, and their properties are often modified markedly by different counterions[9].

2. The Formation of Micelles in Aqueous Media

Amphipathic molecules, such as sodium lauryl sulphate [$CH_3 (CH_2)_{11} SO_4^- Na^+$], have the tendency to associate in water to form a colloidal particle, called a micelle, as shown in Figure 8A.1.

The structure of this micelle is such that the hydrocarbon chains are inside, remote from the water, and the polar head groups are on the outside of the spherical particle. Micelles may be defined as aggregates of colloidal dimensions existing in equilibrium with the molecules or ions from which they are formed. Micelle formation by surfactants has been well discussed by several authors[1,5,7,9]. The thermodynamics and kinetics of micellization in aqueous media, and the formation of micelles in non-aqueous media have also been thoroughly investigated[8].

3. The Critical Micelle Concentration

Almost from the beginning of the study of the properties of surfactant solutions, it has been recognized that their bulk properties were unusual and indicated the presence of colloidal particles in the solution.

When the equivalent conductivity (specific conductance per gram-equivalent of solute) of an anionic surfactant of the type Na^+R^- in water is plotted against the square root of the normality of the solution, the curve obtained, instead of being the smoothly decreasing curve characteristic of ionic electrolytes of this type, has a sharp break in it at low concentrations[6], as shown in Figure 8A.2.

This break in the curve, with its sharp reduction in the conductivity of the solution, indicates a sharp increase in the mass per unit charge of the material in solution. This is interpreted as evidence that, at this point, micelles are formed from the unassociated molecules of the surfactant, with part of the charge of the micelle neutralized by the associated counterions[6]. The concentration at which this phenomenon occurs is called the critical micelle concentration (CMC).

Similar breaks in almost every measurable physical property that depends on size or number of particles in solution are shown by all types of surfactants - non-ionic, anionic, cationic, and zwitterionic. The determination of the value of the CMC can be made by using the breaks in the electrical conductivity-, surface tension-, light scattering-, or refractive index-concentration curves[6].

The critical micelle concentration of surfactants and the factors which influence the value of the CMC have been discussed by several authors[5,6,9]. The large number of methods which have been applied to the determination of the CMC of surfactants have been discussed in detail by Shinoda et al.[5]. A comprehensive list of the CMCs of some surfactants in aqueous media has been presented in Reference 6.

4. The Structure and Shape of Micelles

The exact structure of micelles and some details of the process of micellization are still disputed matters[6]. In spite of this, it is generally accepted that the structure of the micelle in an aqueous medium, at concentrations not too far above the CMC, can be considered to be roughly spherical[1,5,6,9]

The interior region of the spherical micelle contains the hydrophobic groups of the surfactant molecules and the radius of this interior region is approximately equal to the length of a fully-extended hydrophobic group. The hydrophobic interior region is surrounded by an outer region containing the hydrated hydrophilic groups and bound water[6]. Partial molar volume determinations have indicated that the hydrophobic alkyl chains in the interior of the micelle are more expanded than those in the normal liquid state[6].

The interior region of ionic micelles is surrounded by a region that contains the ionic head groups. A large number of the counterions are bound to the micelle, while the remaining counterions form the diffuse electrical double layer, which extends further into the aqueous phase[9].

In concentrated solutions, ten times the CMC or more, micelles are generally non-spherical. At least in some cases, the surfactant molecules are believed to form extended parallel sheets two molecules thick (lamellar micelles), with the individual molecules orientated perpendicular to the plane of the sheet. In aqueous solution, the hydrophilic heads of the surfactant molecules form the two parallel surfaces of the sheets, and the hydrophobic tails comprise the interior region[6]. Water molecules occupy the region between parallel sheets of surfactant molecules. In concentrated solutions, surfactant micelles may also take the form of long cylinders packed together, for example, in hexagonal array and surrounded by solvent[6]. The lyophilic groups constitute the surface of the cylinders and the lyophobic groups comprise their interior. These ordered arrangements of extended micellar structures are called lyotropic mesomorphs or liquid crystalline phases[6].

Some of the models which have been proposed for the structure and shape of micelles are shown in Figure 8A.3 (from Shinoda et al.[5]). The wide variety of structures and mesophases which have been identified in concentrated surfactant solutions are shown in Figure 8A.4 (from Mittal et al.[9]).

5. Reverse Micelles in Apolar Media

Micelle formation also occurs in non-polar solvents. In a hydrocarbon medium, the structure of the micelles is similar to that described in Section 4, but it is reversed. For the spherical micelle, the hydrophilic heads comprise the interior region, which is surrounded by an outer region containing the hydrophobic groups and hydrocarbon solvent. In concentrated solutions of surfactant in non-polar solvents, where lamellar micelles are believed to form, the hydrophobic groups of the surfactant molecules comprise the surfaces of the sheets and the hydrophilic groups comprise the interior. The possible structure of a reverse micelle is shown in Figure 8A.5. Reverse micelles have been discussed in detail by Luisi et al.[11].

REFERENCES

1. **Hartley, G.S., Aqueous Solutions of Paraffin-Chain Salts: A Study in Micelle Formation,** Hermann & Cie, Paris, 1936.

2. **Surface Active Agents,** A symposium held at Nottingham University, England, by the Society of Chemical Industry, 1979.

3. **Robb, I.D., Ed., Microemulsions,** Plenum Press, New York, 1982.

4. **Moilliet, J.L., Collie, B., and Black, W., Surface Activity,** Second Edition, E. & F.N. Spon Ltd., London, 1961.

5. **Shinoda, K., Nakagawa, T., Tamamushi, B., and Isemura, T., Colloidal Surfactants: Some Physicochemical Properties,** Academic Press, New York, 1963.

6. **Rosen, M.J., Surfactants and Interfacial Phenomena,** John Wiley and Sons, New York, 1978.

7. **Elworthy, P.H., Florence, A.T., and Macfarlane, C.B., Solubilization by Surface-Active Agents and its Applications in Chemistry and the Biological Sciences,** Chapman and Hall, London, 1968.

8. **Mittal, K.L., Ed., Micellization, Solubilization, and Microemulsions,** Volumes 1 and 2, Plenum Press, New York, 1977.

9. **Mittal, K.L. and Mukerjee, P.,** The wide world of micelles, in Mittal, K.L., Ed., **Micellization, Solubilization, and Microemulsions,** Vol. 1, Plenum Press, New York, 1977, 1.

10. **Garrett, H.E., Surface Active Chemicals,** Pergamon Press, Oxford, 1975.

11. **Luisi, P.L. and Straub, B.E., Eds., Reverse Micelles: Biological and Technological Relevance of Amphiphilic Structures in Apolar Media,** Plenum Press, New York, 1984.

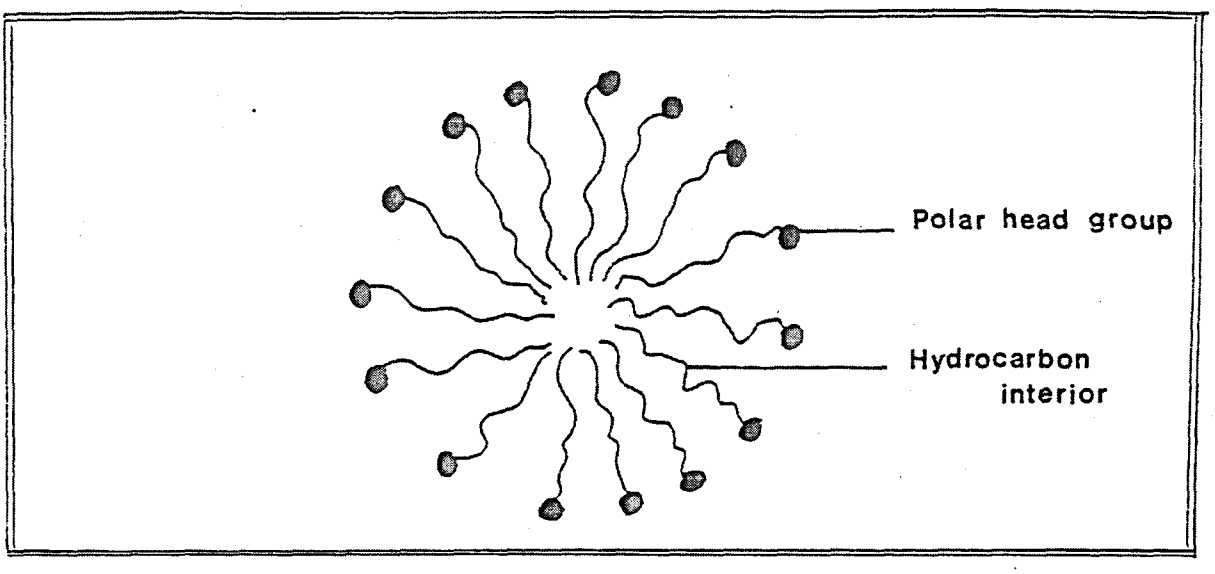

FIGURE 8A.1 Suggested structure of a cross-section of a spherical micelle in aqueous media.

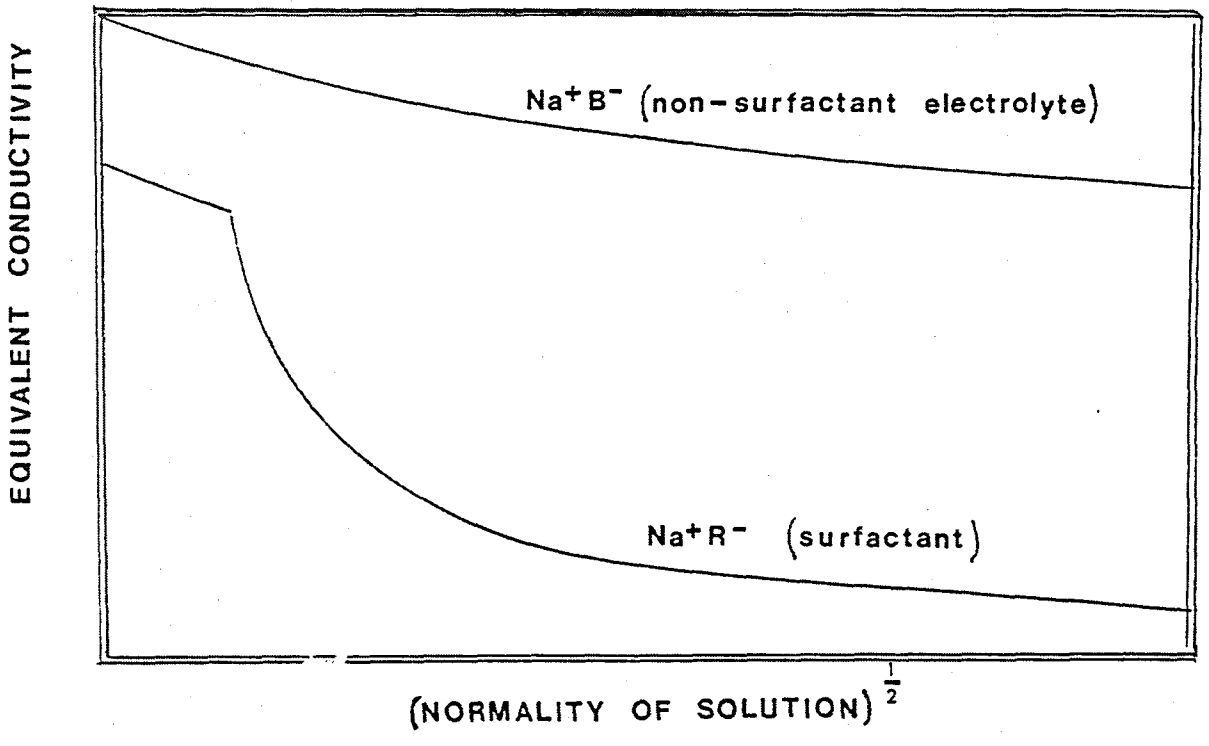

FIGURE 8A.2 Plot of equivalent conductivity versus the square root of the normality of the solution for an aqueous solution of a surfactant of the type Na^+R^-.

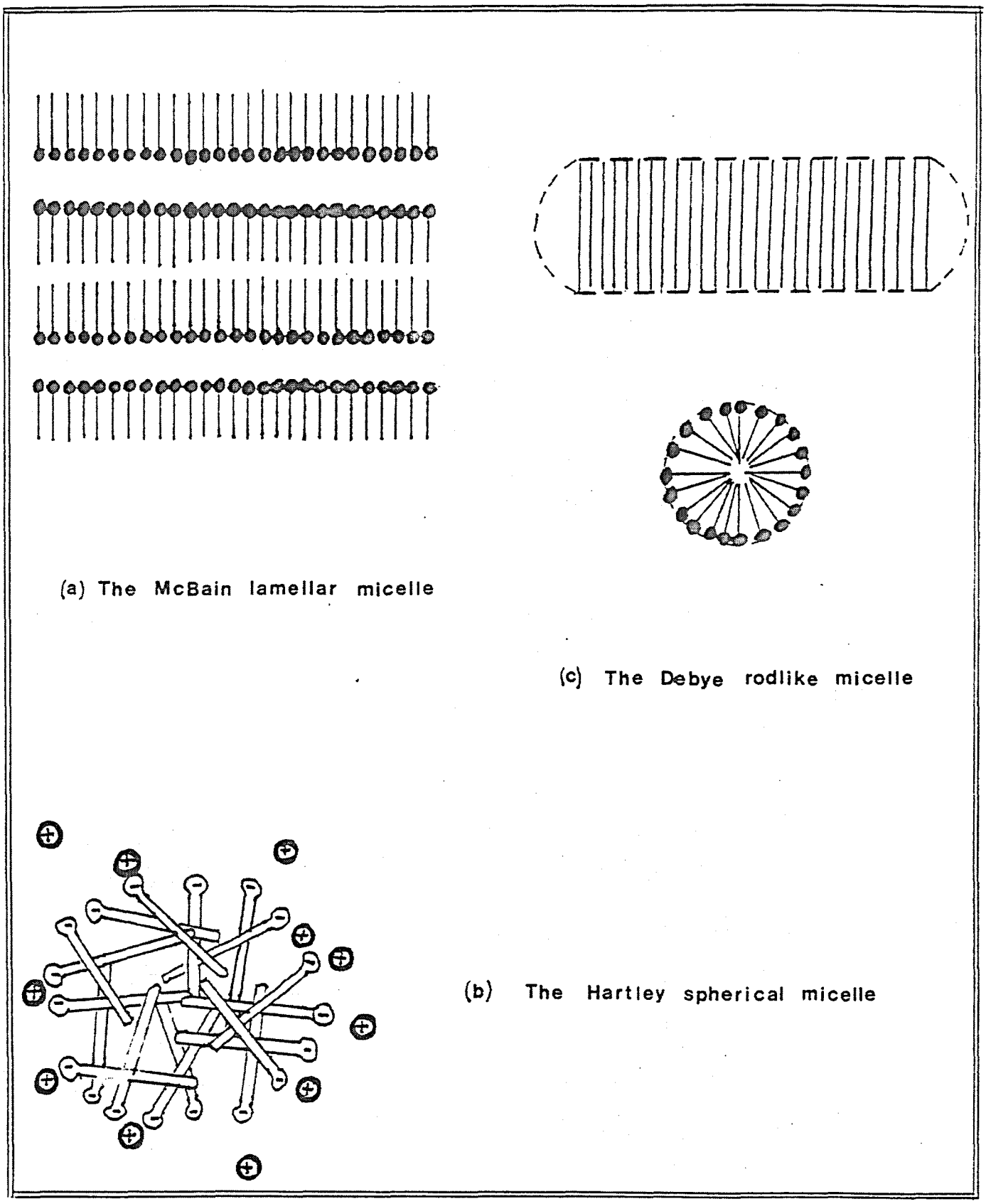

FIGURE 8A.3 Some of the proposed models for the structure and shape of micelles.

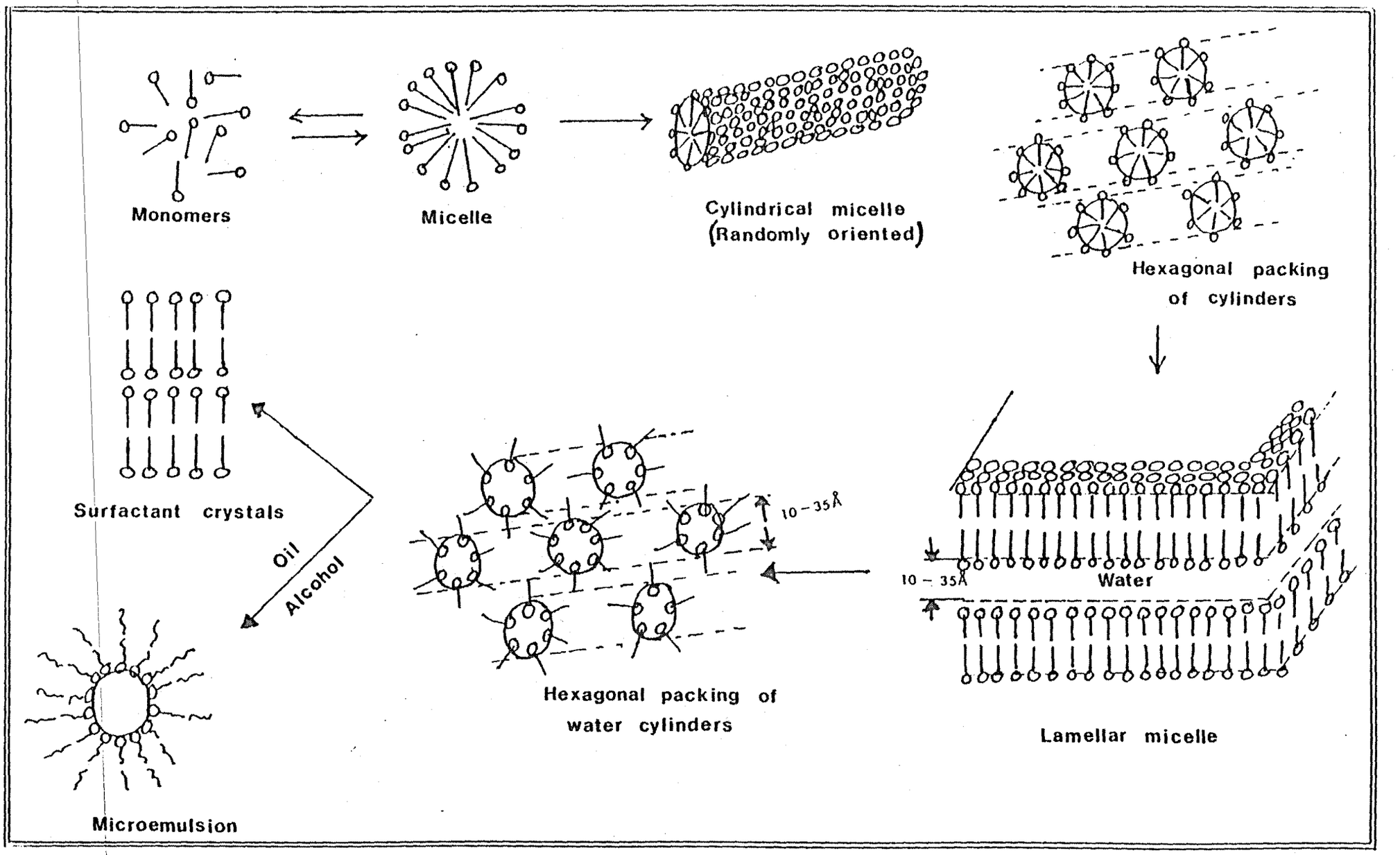

FIGURE 8A.4 Different structures of micelles and mesophase.

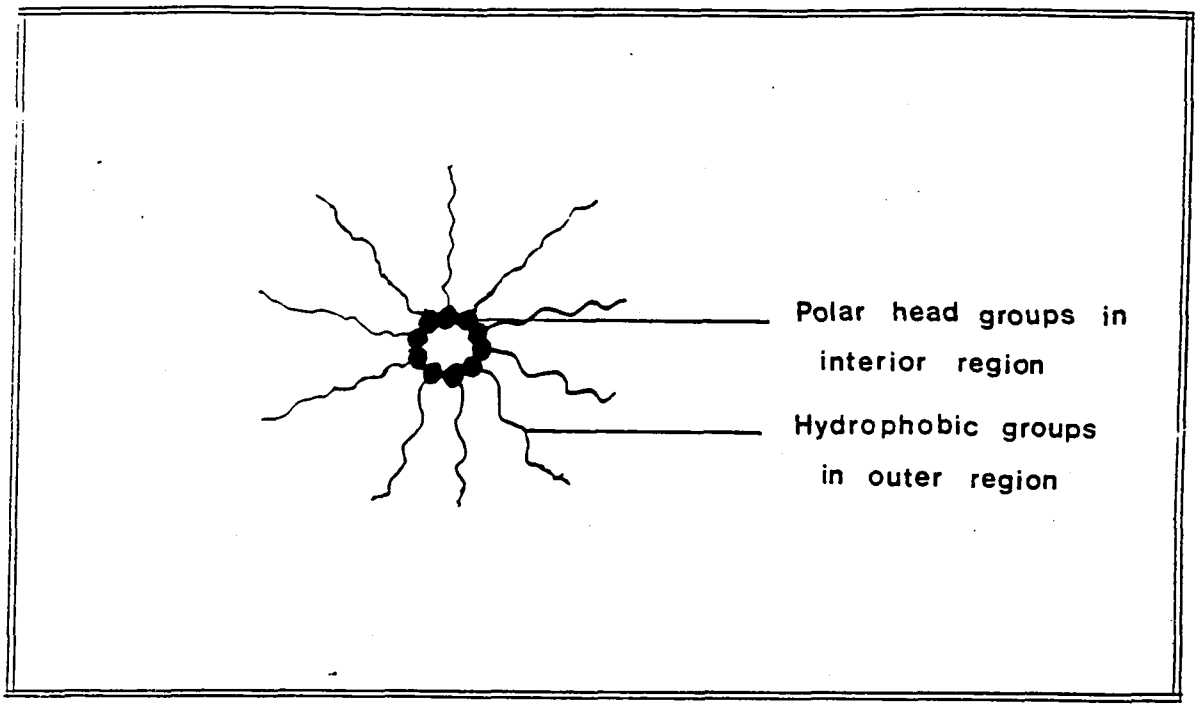

FIGURE 8A.5 Schematic representation of the possible structure of a reverse micelle in non-polar media.